



The
University
Of
Sheffield.

Evaluation of Quantitative Imaging Biomarkers in Interstitial Lung Disease

Dr James Anthony Eaden

A thesis submitted in partial fulfilment of the requirements for the degree of
Doctor of Philosophy

Supervised by:

Prof J.M. Wild

Dr S.M. Bianchi

The University of Sheffield
Faculty of Medicine
Department of Infection, Immunity and Cardiovascular Sciences
Academic Unit of Radiology

Submission Date: October 2021

Contents

Acknowledgements	7
Thesis Synopsis	8
List of Figures.....	9
List of Tables.....	13
List of Abbreviations	18
Chapter 1: Classification and Clinical Assessment of Interstitial Lung Disease	20
1.1 Interstitial Lung Disease	21
1.1.1 Classification of Interstitial Lung Disease.....	21
1.1.2 Idiopathic Pulmonary Fibrosis.....	26
1.1.3 Idiopathic Non-specific Interstitial Pneumonia.....	28
1.1.4 Connective Tissue Disease associated ILD	28
1.1.5 Hypersensitivity pneumonitis	29
1.1.6 Drug Induced ILD.....	31
1.2 Current methods for diagnosis and longitudinal assessment of ILD.....	32
1.2.1 Multidisciplinary team assessment.....	32
1.2.2 High-resolution computed tomography	33
1.2.3 Pulmonary function tests.....	35
1.3 Summary	36
Chapter 2: Precision Medicine in Interstitial Lung Disease: Quantitative Imaging and Prognostic Biomarkers	37
1.1 Precision medicine in ILD	38
2.1 Quantitative computed tomography.....	38
2.1.1 Lung density / histogram analysis.....	39
2.1.2 Adaptive Multiple Features Method (AMFM)	42
2.1.3 Gaussian Histogram Normalised Correlation system	42
2.1.4 Quantitative Lung Fibrosis score / Quantitative ILD score	43
2.1.5 Computer-Aided Lung Informatics for Pathology Evaluation and Rating.....	44
2.1.6 Data-driven Textural Analysis (DTA)	45
2.1.7 Other texture analysis software.....	45
2.1.8 Functional respiratory imaging (FRI).....	46
2.1.9 Deep learning algorithms.....	46
2.2 Magnetic resonance imaging.....	47
2.2.1 Proton MRI	47
2.2.2 Dynamic contrast enhanced and vascular MRI.....	49
2.2.3 Other functional proton MRI methods	53

2.2.3.1	Oxygen enhanced MRI	53
2.2.3.2	Magnetic resonance elastography.....	54
2.2.4	Hyperpolarised ¹²⁹ Xenon MRI	55
2.2.4.1	¹²⁹ Xe MR spectroscopy	56
2.2.4.2	Diffusion-weighted MRI	59
2.2.4.3	Ventilation imaging	60
2.3	CT and PFT biomarkers predicting mortality and/or disease progression in ILD ...	61
2.3.1	Computed tomography (quantitative CT and visual CT scores)	61
2.3.2	Pulmonary function tests	65
2.4	Summary	68
Chapter 3: The Assessment of Interstitial Lung Disease Using Imaging Biomarkers – Methods of Two Longitudinal Studies.....		69
3.1	Development of imaging biomarkers for the detection and monitoring of drug induced interstitial lung disease (TRISTAN-ILD study): Aims/objectives of the study, eligibility criteria and study design	70
3.1.1	Brief overview of the study.....	70
3.1.2	Study aims and objectives.....	70
3.1.3	Eligibility criteria.....	71
3.1.4	Study design	72
3.2	Investigation into prognostic indicators of idiopathic pulmonary fibrosis using structural-functional pulmonary MRI assessment (IPF study): Aims/objectives of the study, eligibility criteria and study design	75
3.2.1	Brief overview of the study.....	75
3.2.2	Study aims and objectives.....	75
3.2.3	Eligibility criteria.....	76
3.2.4	Study design	76
3.3	CT acquisition and analysis	77
3.3.1	CALIPER analysis.....	77
3.3.2	Semi-quantitative visual CT scoring	78
3.4	MRI protocol	79
3.5	Pulmonary function tests	83
3.6	Statistics	83
3.6.1	Power calculation for TRISTAN-ILD study	83
3.6.2	Power calculation for IPF study	84
3.6.3	Statistical analyses	85
3.7	Summary	86
Chapter 4: The Assessment of Interstitial Lung Disease Using Imaging Biomarkers: TRISTAN-ILD Study Results		87

4.1	Recruitment and demographic data	88
4.1.1	Recruitment	88
4.1.2	Study visits	89
4.1.3	Days between diagnostic CT scan and first study visit.....	90
4.1.4	Subject demographics.....	90
4.1.5	Co-morbidities.....	91
4.1.6	Treatment approach	91
4.2	Pulmonary function tests	92
4.2.1	Visit 1 (baseline).....	92
4.2.2	Visit 2 (6 weeks or 6 months depending on ILD subtype)	94
4.2.3	Visit 3 (6 months or 12 months depending on ILD subtype)	95
4.2.4	Visits 1, 2, and 3	98
4.3	Dissolved ¹²⁹ Xe MRI	99
4.3.1	Study visits and examples of images / spectra	99
4.3.2	Visit 1 (baseline).....	101
4.3.2.1	High-resolution dissolved phase spectroscopy.....	101
4.3.2.2	IDEAL spectroscopic imaging technique	102
4.3.3	Visit 2 (6 weeks or 6 months depending on ILD subtype)	103
4.3.3.1	High-resolution dissolved phase spectroscopy.....	103
4.3.3.2	IDEAL spectroscopic imaging technique	106
4.4	¹²⁹ Xe Diffusion-weighted MRI (airway microstructure).....	108
4.4.1	Study visits and examples of images.....	108
4.4.2	Visit 1 (baseline).....	110
4.4.3	Visit 2 (6 weeks or 6 months depending on ILD subtype)	117
4.5	¹²⁹ Xe Ventilation MRI	120
4.5.1	Study visits and examples of images.....	120
4.5.2	Visit 1 (baseline).....	121
4.5.3	Visit 2 (6 weeks or 6 months depending on ILD subtype)	121
4.6	Dynamic contrast enhanced MRI	122
4.6.1	Study visits and examples of images.....	122
4.6.2	Visit 1 (baseline).....	124
4.6.3	Visit 2 (6 weeks or 6 months depending on ILD subtype)	125
4.7	CALIPER CT analysis	127
4.7.1	Study visits and examples of images.....	127
4.7.2	Visit 1 (baseline).....	128
4.7.3	Visit 2 (6 weeks or 6 months depending on ILD subtype)	131

4.7.4	Visit 3 (6 months or 12 months depending on ILD subtype)	136
4.8	Visual CT scoring	145
4.8.1	Visit 1 (baseline).....	145
4.8.2	Visit 2 (6 weeks or 6 months depending on ILD subtype)	148
4.8.3	Visit 3 (6 months or 12 months depending on ILD subtype)	150
4.9	The effect of steroids on pulmonary function tests and imaging measurements in the drug induced ILD subjects	152
4.10	Summary of the imaging outcomes from the TRISTAN-ILD study	156
4.11	Correlations	158
4.11.1	Strong correlations ($r = 0.60 - 0.79$)	158
4.11.2	Moderate correlations ($r = 0.40 - 0.59$).....	159
4.12	Variables that predict disease progression.....	164
4.13	Summary	166
Chapter 5: The Assessment of Interstitial Lung Disease Using Imaging Biomarkers – IPF Study Results		167
5.1	Recruitment and demographic data	168
5.1.1	Study visits	169
5.1.2	Days between baseline and follow-up study visits	170
5.1.3	Days between diagnostic CT scan and first study visit.....	171
5.1.4	Subject demographics.....	171
5.1.5	Co-morbidities.....	172
5.2	Pulmonary function tests	172
5.2.1	Baseline visit.....	172
5.2.2	3-month visit	173
5.2.3	6-month visit	174
5.2.4	12-month visit	178
5.2.5	Baseline, 3-month, 6-month and 12-month visits	179
5.2.6	Baseline, 6-month and 12-month visits in the total cohort.....	182
5.3	Dissolved ^{129}Xe MRI	186
5.3.1	Study visits	186
5.3.2	Baseline visit.....	187
5.3.2.1	High-resolution dissolved phase spectroscopy.....	187
5.7.2.2	IDEAL spectroscopic imaging technique	187
5.7.3	3-month visit	189
5.7.3.1	High-resolution dissolved phase spectroscopy.....	189
5.7.3.2	IDEAL spectroscopic imaging technique	189
5.3.4	6-month visit	189

5.3.4.1	High-resolution dissolved phase spectroscopy.....	189
5.3.4.2	IDEAL spectroscopic imaging technique	190
5.3.5	12-month visit	191
5.3.5.1	High-resolution dissolved phase spectroscopy.....	191
5.3.5.2	IDEAL spectroscopic imaging technique	192
5.3.6	Baseline, 3-month, 6-month and 12-month visits	192
5.3.7	Baseline, 6-month and 12-month visits in the total cohort.....	193
5.4	Diffusion-weighted MRI (airway microstructure).....	194
5.4.1	Baseline visit.....	194
5.4.2	3-month visit	196
5.4.4	12-month visit	198
5.4.5	Baseline, 3-month, 6-month and 12-month visits	204
5.4.6	Baseline, 6-month and 12-month visits in the total cohort.....	204
5.5	Dynamic contrast enhanced MRI	205
5.5.1	Baseline visit.....	206
5.5.2	3-month visit	209
5.5.3	6-month visit	209
5.5.4	12-month visit	210
5.5.5	Baseline, 3-month, 6-month and 12-month visits	212
5.5.6	Baseline, 6-month and 12-month visits in the total cohort.....	212
5.6	CALIPER CT analysis	213
5.6.1	Study visits	213
5.6.2	Baseline visit.....	214
5.6.3	12-month visit	218
5.7	Visual CT scoring	222
5.7.1	Study visits	222
5.7.2	Baseline visit.....	222
5.7.3	12-month visit	224
5.8	Summary of the imaging outcomes in the IPF study	225
5.9	Correlations	226
5.9.1	Very strong correlations ($r = 0.80 - 0.99$)	226
5.9.2	Strong correlations ($r = 0.60 - 0.79$)	228
5.9.3	Moderate correlations ($r = 0.40 - 0.59$).....	231
5.10	Variables that predict disease progression.....	234
5.11	Summary	237

Chapter 6: The Assessment of Interstitial Lung Disease Using Imaging Biomarkers – Discussion of Two Longitudinal Studies	238
6.1 Imaging outcomes	239
6.1.1 Summary of the imaging outcomes in the TRISTAN-ILD study	239
6.1.2 Summary of the imaging outcomes in the IPF study	242
6.1.3. Dissolved ¹²⁹ Xe MRI	244
6.1.4. Diffusion weighted MRI	245
6.1.5. Dynamic contrast enhanced MRI	245
6.1.6. CALIPER CT analysis	246
6.1.7. Visual CT scores	247
6.1.8 Correlations – TRISTAN-ILD study	248
6.1.9 Correlations – IPF study	249
6.1.10. Predictors of disease progression	250
6.2. Limitations	251
6.2.1 Sample size	251
6.2.2 Timing of follow-up study visits	253
6.2.3 Imaging methodology and biomarkers	253
6.2.4 Treatment effects	256
6.2.5 Confounding effects of emphysema and pulmonary hypertension	256
6.2.6 Interpretation of findings when multiple outcome measures are used	257
6.3. Future work	257
6.4. Conclusion	258
References	260
Appendix 1: Differences in DCE-MRI calculations between TRISTAN-ILD study and IPF study data (written by Paul Hughes)	280
Appendix 2: Research Output	282
Research papers published as first author in peer reviewed journals during the PhD (not directly related to this thesis)	282
Research papers published as second author in peer reviewed journals during the PhD	282
Conference abstract proceedings and presentations as first author during the PhD	283
Awards	283
Appendix 3: Participant Information Sheets	284
TRISTAN-ILD study: DI-ILD, HP or iNSIP patients	284
TRISTAN-ILD study: CTD-ILD or IPF patients	290
IPF study	296

Acknowledgements

I would first like to thank my PhD supervisors, Prof. Jim Wild and Dr Stephen Bianchi for their tremendous help and support over the last three years, and for giving me the opportunity to perform this research. Their commitment and hard work are admirable.

The work that is presented in this thesis would not have been possible without the help from a large group of colleagues in the academic radiology department at the University of Sheffield. I would like to thank Nick for his guidance at the start of my PhD and for his suggestions with the writing of the thesis. Andy and Smitha spent a lot of time performing the visual CT scoring and I am very grateful for this. I would like to thank Fung, Guilhem and Paul for their work associated with the MRI sequences and help with the analysis. I would also like to thank Alberto and Martin for providing IT assistance. Thanks to Laurie and Matt who performed the pulmonary function tests and ensured that the results were valid. Several colleagues (Graham, Guilhem, Jimmy, Madhwesha, Olly and Ryan) were involved with providing the hyperpolarised gas for the MRI scans and I appreciate all their hard work. I would also like to thank the radiographers in the University of Sheffield MRI department (Anna, Dave, Debbie, Jody, Julia and Sarah) who helped perform the MRI scans. Leanne and Jen were integral to ensuring that study visits could be booked and their help with the general organisation of the studies is much appreciated. Thanks to the research co-ordinators Lisa Watson and Jim Lithgow who were valuable in keeping the studies running smoothly. I would like to acknowledge the staff in the clinical research facility who helped with the TRISTAN-ILD study.

I would like to thank Brian Bartholmai and Ron Karwoski at the Mayo clinic for processing the quantitative CT (CALIPER) data. I am very appreciative of all the members of the TRISTAN-ILD study work package 3 for setting up the study and their ongoing support, as well as the wider IMI TRISTAN consortium. The physicians from Manchester deserve much credit for their recruitment of subjects into the study. I would like to thank Dr Sarah Skeoch and Dr Nazia Chaudhuri in particular. Bioxydyn Ltd deserve acknowledgement for their MRI analysis.

My parents, Debbie and Tony deserve a lot of thanks for their continued support over the years. Finally, I would like to thank my amazing wife Claire and my wonderful son Oliver. They have kept me motivated and helped me get through all the hard work.

Thesis Synopsis

Despite evidence that hyperpolarised ^{129}Xe MRI, combined with proton MRI, is able to provide useful structural and functional data, its clinical application has been relatively limited in the field of interstitial lung disease (ILD). However, the insensitivity of pulmonary function tests (PFTs) in early disease, and the ability of hyperpolarised ^{129}Xe MRI to assess regional lung function makes it an appealing tool to explore the diagnosis and monitoring of ILD.

CT involves ionising radiation and is unable to provide functional data. It has some advantages over MRI in terms of its speed, image contrast and spatial resolution. Various automated, computer based, quantitative CT (QCT) analysis methods have been reported in ILD.

The findings reported in this thesis represent the first known longitudinal data combining hyperpolarised ^{129}Xe MRI and dynamic contrast enhanced (DCE) MRI with QCT alongside PFTs in various ILD subtypes. It also expands upon previous work involving these novel MRI techniques in idiopathic pulmonary fibrosis (IPF).

^{129}Xe spectroscopy derived red blood cell / tissue plasma ratio (RBC:TP) was used in the assessment of alveolar gas exchange, showing a statistically significant change over 6 and 12 months in IPF subjects, despite relatively stable PFTs. ^{129}Xe diffusion-weighted (DW) MRI techniques demonstrate increased Brownian gas diffusion in fibrotic ILD. This is likely due to microstructural changes in the distal airways and alveoli as a result of honeycombing and/or traction bronchiectasis. There was also evidence that DW-MRI measurements may have utility in the monitoring and prediction of disease progression. Changes in pulmonary perfusion over short time periods were found using DCE-MRI in subjects with hypersensitivity pneumonitis, suggesting potential value in demonstrating an early inflammation response to steroid therapy. As new drug treatments are developed, the ability to quantify subtle changes using QCT and functional lung MRI could be particularly valuable.

List of Figures

Figure 1.1. CT features of UIP..	22
Figure 1.2. CT features of NSIP.	23
Figure 1.3. Classification of ILD (progressive fibrosing ILDs are indicated in bold)	25
Figure 1.4. Schematic representation of different possible clinical courses of IPF	27
Figure 1.5. CT features of non-fibrotic HP.	30
Figure 2.1. Example of differences in kurtosis and skewness between two patients with mild and severe IPF.	40
Figure 2.2. CALIPER quantitative analysis results from one patient with rows a-c and d-f corresponding to two separate time points.	44
Figure 2.4. Example of a time series of perfusion images and the MTT parametric map generated from them in an IPF patient.	51
Figure 2.5. Representation of FWHM in DCE-MRI.	52
Figure 2.6. Diagram of the spin-exchange optical pumping process.	55
Figure 2.7. Diagram of ^{129}Xe transfer from alveoli into capillary RBCs (A). ^{129}Xe spectrum exhibits three distinct resonances in the lung (B).	56
Figure 2.8. Central and posterior coronal slices of ventilation (red=ventilation defects, blue=high), barrier uptake (red=low, plum/orchid=high) and RBC transfer (red=low, blue=high), binning maps and CT images in 1 healthy volunteer and 4 IPF patients.	58
Figure 2.9. RBC signal amplitude and frequency shift in various diseases	59
Figure 2.10. Schematic of ^{129}Xe gas diffusion (white arrows) in a healthy lung and an IPF lung.	60
Figure 3.1. Schedule of study visits for each ILD subtype (visit 1A highlighted in red).	74
Figure 3.2. A schematic representation of the MRI sequences used in the TRISTAN-ILD study and the metrics generated from each sequence. The same ^{129}Xe MRI and DCE-MRI sequences were used in the IPF study.	81
Figure 3.3. DCE-MRI sequences used in the TRISTAN-ILD and IPF studies.	82
Figure 3.4. Photos of the ^{129}Xe spin-exchange optical polariser (A) and the polariser cell (B) used at the University of Sheffield MRI department.	82
Figure 3.5. Photo of the University of Sheffield 1.5T MRI scanner and the ^{129}Xe MRI coil used in the studies (A). Photo of an example of the 1L Tedlar bag used for the inhalation of ^{129}Xe (B).	83
Figure 4.1. Summary of subject numbers at each study visit and reasons for not completing the study.	89
Figure 4.2. Co-morbidities in the total cohort and ILD subtypes. Other was defined as any co-morbidity that occurred in only one subject out of the total cohort.	91
Figure 4.3. D_{LCO} at visit 1 versus visit 3 for the IPF group (a-b). $D_{\text{LCO}}\%$ at visit 1 versus visit 3 for the IPF group (c-d) (n=13).	98
Figure 4.4. FVC % predicted (a) and D_{LCO} % predicted (b) at visits 1, 2 and 3 in subjects stratified into fibrotic (n=21) and inflammation (n=14) groups.	99
Figure 4.5. Summary of the number of subjects that had dissolved ^{129}Xe spectroscopy performed at each study visit.	100
Figure 4.6. Example of a ^{129}Xe RBC:TP spectra in an IPF subject.	100
Figure 4.7. Example of ^{129}Xe ratio maps in an IPF subject.	101
Figure 4.8. ^{129}Xe RBC:TP at visit 1 versus visit 2 in the IPF group (a-b) and the fibrotic group (c-d)	104
Figure 4.9. ^{129}Xe RBC:TP (a), FVC % predicted (b), and D_{LCO} % predicted (c) at visit 1 versus visit 2 in the fibrotic and inflammation groups.	105
Figure 4.10. Summary of the number of subjects that had ^{129}Xe DW-MRI performed at each study visit.	108
Figure 4.11. Example of a ^{129}Xe ADC map (a), ^{129}Xe L_{mD} map (b) and corresponding coronal HRCT image (c) in an IPF subject.	109
Figure 4.12. Difference between ILD subtypes at visit 1 in global ^{129}Xe ADC (a) and L_{mD} (b).	110
Figure 4.13. Difference between fibrotic (n=31) and inflammation (n=23) groups at visit 1 in global ^{129}Xe ADC (a) and L_{mD} (b).	110
Figure 4.14. ^{129}Xe ADC and L_{mD} in the upper, middle and lower zones in the DI-ILD group (a-b), the HP group (c-d) and the IPF group (e-f) at visit 1.	112

Figure 4.15. ^{129}Xe ADC in the central and peripheral zones for the HP group (a) and the IPF group (b).	113
Figure 4.16. ^{129}Xe Lm_D in the central and peripheral zones for the DI-ILD group (a), HP group (b) and the IPF group (c).	113
Figure 4.17. ^{129}Xe ADC for the fibrotic group in the upper, middle and lower zones (a), and in the central and peripheral zones (b). ^{129}Xe ADC for the inflammation group in the upper, middle and lower zones (c), and in the central and peripheral zones (d).	115
Figure 4.18. ^{129}Xe Lm_D in the upper, middle and lower zones (a), and in the central and peripheral zones (b) in the fibrotic group. ^{129}Xe Lm_D in the upper, middle and lower zones (c), and in the central and peripheral zones (d) in the inflammation group.	116
Figure 4.19. Global ^{129}Xe ADC (a-b) and Lm_D (c-d) at visit 1 versus visit 2 in the DI-ILD group (n=10).	117
Figure 4.20. Example of a ^{129}Xe ventilation image (a) and the corresponding coronal HRCT image (b) in a DI-ILD subject. VV%: 82.3%, CV%: 20.8%, FVC % predicted: 60.5%, DLCO % predicted: 28.6%. Example of a ^{129}Xe ventilation image (c) and the corresponding coronal HRCT image (d) in an IPF subject. VV%: 93.9%, CV%: 14.1%, FVC % predicted: 70.2%, DLCO % predicted: 22.1%.	120
Figure 4.21. The number of subjects that had DCE-MRI performed at each study visit.	122
Figure 4.22. Example of DCE-MRI images of MTT (a), PBF (b), PBV (c), and corresponding coronal HRCT image (d) and UTE-MRI image in a subject with DI-ILD.	123
Figure 4.23. Example of DCE-MRI images of MTT (a), PBF (b), PBV (c), and corresponding coronal HRCT image (d) and UTE-MRI image in an IPF subject.	124
Figure 4.24. MTT (a-b) and PBF (c-d) in the HP group at visit 1 versus visit 2.	125
Figure 4.25. Example of a coronal HRCT image (a) and corresponding CALIPER CT texture analysis (b) in an IPF subject.	127
Figure 4.26. Global CALIPER VRS % at visit 1 versus visit 2 for the IPF group (n=11).	131
Figure 4.27. Global CALIPER fibrosis % (a), ground glass % (b), ILD % (c) and reticular % (d) at visit 1 versus visit 2 in the inflammation group.	133
Figure 4.28. Global CALIPER honeycomb % at visit 1 versus visit 3 in the DI-ILD group (n=8).	136
Figure 4.29. Global CALIPER VRS % at visit 1 versus visit 3 in the IPF group (n=11).	136
Figure 4.30. Difference between the fibrotic and inflammation groups in global CALIPER fibrosis % (a), ground glass % (b), honeycomb % (c), ILD % (d), reticular % (e) and VRS % (f) at visit 3.	138
Figure 4.31. Global CALIPER VRS % at visit 1 versus visit 3 in the fibrotic group (n=19).	139
Figure 4.32. Global CALIPER fibrosis % (a), ground glass % (b), honeycomb % (c), ILD % (d), reticular % (e) and VRS % (f) at visit 1 vs visit 3 in the inflammation group (n=12).	140
Figure 4.33. Global CALIPER fibrosis % (a), ground glass % (b), honeycomb % (c), ILD % (d), reticular % (e), VRS % (f), FVC % predicted (g), and DLCO % predicted (h) at visits 1, 2 and 3 for the fibrotic and inflammation groups.	142
Figure 4.34. Difference between ILD subgroups at visit 1 in global visual CT fibrosis score (a) and ground glass score (b).	145
Figure 4.35. Global visual CT ground glass score at visit 1 versus visit 3 in the inflammation group.	151
Figure 4.36. FVC % predicted (a) and DLCO % predicted (b) at visit 1 versus visit 2 in the DI-ILD group (n=11). FVC % predicted (c) and DLCO % predicted (d) at visits 1, 2 and 3 in the DI-ILD group (n=9).	152
Figure 4.37. ^{129}Xe RBC:TP (a), ADC (b) and Lm_D (c) at visit 1 versus visit 2 in the DI-ILD group (n=11).	153
Figure 4.38. Mean transit time (a), blood flow (b) and blood volume (c) at visit 1 versus visit 2 in the DI-ILD group (n=11).	154
Figure 4.39. CALIPER fibrosis % (a), ground glass % (b), honeycomb % (c), ILD % (d), reticular % (e) and VRS % (f) at visit 1 versus visit 2 in the DI-ILD group (n=11).	155
Figure 4.40. CALIPER fibrosis % (a), ground glass % (b), ILD % (c) and VRS % (d) at visits 1, 2 and 3 in the DI-ILD group (n=9).	156
Figure 5.1. Longitudinal change in FVC, DLCO and RBC:TP in IPF patients (A–C). Individual patients' measurements of FVC, DLCO and RBC:TP at baseline, 6 and 12 months are plotted in (D), (E) and (F), respectively.	169

Figure 5.2. Summary of subject numbers at each study visit and reasons for not completing study visits for the total study cohort (n=49).	169
Figure 5.3. Number of days between the baseline and follow-up study visits.	170
Figure 5.4. Co-morbidities in the total cohort (n=49). Other was defined as any co-morbidity that occurred in only one subject out of the total cohort.	172
Figure 5.5. FVC at baseline visit versus 3-month visit (n=22).	173
Figure 5.6. FVC (a-b) and FVC% (c-d) at baseline visit versus 6-month visit in the total study cohort (n=30).	175
Figure 5.7. DL _{CO} (a-b) and DL _{CO} % (c-d) at baseline visit versus 6-month visit in the total study cohort (n=30).	176
Figure 5.8. K _{CO} (a-b) and K _{CO} % (c-d) at baseline visit versus 6-month visit in the total study cohort (n=30).	177
Figure 5.9. FVC (a-b) and FVC % predicted (c-d) at baseline, 3-month, 6-month and 12-month visits (n=12).	180
Figure 5.10. DL _{CO} (a-b) and DL _{CO} % predicted (c-d) at baseline, 3-month, 6-month and 12-month visits (n=12).	181
Figure 5.11. K _{CO} (a-b) and K _{CO} % predicted (c-d) at baseline, 3-month, 6-month and 12-month visits (n=12).	182
Figure 5.12. FVC (a-b) and FVC % predicted (c-d) at baseline, 6-month and 12-month visits (n=27).	183
Figure 5.13. FVC (a-b) and FVC % predicted (c-d) at baseline, 6-month and 12-month visits in five subjects taking antifibrotic therapy during the study.	183
Figure 5.14. DL _{CO} (a-b) and DL _{CO} % predicted (c-d) at baseline, 6-month and 12-month visits (n=27).	184
Figure 5.15. DL _{CO} (a-b) and DL _{CO} % predicted (c-d) at baseline, 6-month and 12-month visits in five subjects taking antifibrotic therapy during the study.	184
Figure 5.16. K _{CO} (a-b) and K _{CO} % predicted (c-d) at baseline, 6-month and 12-month visits (n=27).	185
Figure 5.17. K _{CO} (a-b) and K _{CO} % predicted (c-d) at baseline, 6-month and 12-month visits in five subjects taking antifibrotic therapy during the study.	185
Figure 5.18. Bland-Altman statistical analysis of the manual versus the automated method of ¹²⁹ Xe RBC:TP analysis.	186
Figure 5.19. ¹²⁹ Xe RBC:TP (a) and RBC:Gas (b) in the upper, middle and lower zones.	188
Figure 5.20. ¹²⁹ Xe RBC:TP at baseline visit versus 6-month visit for the total study cohort (n=28).	190
Figure 5.21. ¹²⁹ Xe RBC:TP at baseline visit versus 12-month visit for the total study cohort (n=31).	191
Figure 5.22. ¹²⁹ Xe RBC:TP at baseline, 3-month, 6-month and 12-month visits (n=10).	192
Figure 5.23. ¹²⁹ Xe RBC:TP (a-b), K _{CO} (c) and K _{CO} % (d) at baseline, 6-month and 12-month visits (n=22).	193
Figure 5.24. Bland-Altman statistical analysis of ¹²⁹ Xe versus ³ He Lm _D .	194
Figure 5.25. ¹²⁹ Xe ADC (a) and Lm _D (b) in the upper, middle and lower zones. ¹²⁹ Xe ADC (c) and Lm _D (d) in the central and peripheral zones.	195
Figure 5.26. Global Lm _D at baseline visit versus 6-month visit for the total study cohort (n=30).	197
Figure 5.27. ¹²⁹ Xe Lm _D at the baseline visit versus the 6-month visit in the middle zone (a-b) and central zone (c-d).	198
Figure 5.28. Example of ¹²⁹ Xe ADC maps at the baseline visit (a) and 12-month visit (b) in the same IPF subject.	199
Figure 5.29. Example of ¹²⁹ Xe Lm _D maps at the baseline visit (a) and 12-month visit (b) in the same IPF subject.	200
Figure 5.30. Global ¹²⁹ Xe ADC at the baseline visit versus the 12-month visit (n=20).	201
Figure 5.31. Global Lm _D at baseline visit versus 12-month visit for the total study cohort (n=33).	202
Figure 5.32. ¹²⁹ Xe ADC at the baseline visit versus the 12-month visit in the lower zone (a-b) and peripheral zone (c-d) (n=20).	203
Figure 5.33. ¹²⁹ Xe Lm _D at the baseline visit versus the 12-month visit in the lower zone (n=20).	203
Figure 5.34. ¹²⁹ Xe ADC at baseline, 3-month, 6-month and 12-month visits in the middle zone (n=12).	204
Figure 5.35. Lm _D at baseline, 6-month and 12-month visits (n=27).	205
Figure 5.36. Regional differences in MTT (a-b) and FWHM (c-d) at the baseline visit.	207

Figure 5.37. Regional differences in PBF (a-b) and PBV (c-d) at the baseline visit.	208
Figure 5.38. Example of FWHM maps at the baseline visit (a) and 12-month visit (b) in the same IPF subject.	210
Figure 5.39. Example of MTT maps at the baseline visit (a) and 12-month visit (b) in the same IPF subject.	210
Figure 5.40. Example of PBF maps at the baseline visit (a) and 12-month visit (b) in the same IPF subject.	211
Figure 5.41. Example of PBV maps at the baseline visit (a) and 12-month visit (b) in the same IPF subject.	211
Figure 5.42. PBV at baseline, 6-month and 12-month visits in the lower zone (n=20).	213
Figure 5.43. CALIPER fibrosis % (a), ground glass % (b), honeycomb % (c), ILD % (d), reticular % (e), VRS % (f) in the upper, middle and lower zones at baseline visit.	215
Figure 5.44. CALIPER fibrosis % (a), ground glass % (b), honeycomb % (c), ILD % (d), reticular % (e), VRS % (f) in the central and peripheral zones at the baseline visit.	216
Figure 5.45. Upper zone ground glass % (a-b), honeycomb % (c-d) and VRS % (e-f) change between the baseline and 12-month visits in the total study cohort (n=12).	219
Figure 5.46. Central zone ground glass % (a-b) and ILD % (c-d) change between the baseline and 12-month visits in the total study cohort (n=12).	220
Figure 5.47. Visual CT fibrosis score, ILD score (b) and reticular score (c) in the upper, middle and lower zones at the baseline visit in the total study cohort (n=49).	223
Figure 5.48. Correlation between K_{CO} and ^{129}Xe ADC (a), and between K_{CO} and ^{129}Xe L_{mD} (b) at the 12-month visit.	226
Figure 5.49. Correlations between the change in CALIPER honeycomb % and the change in ^{129}Xe ADC (a) and L_{mD} (b) between the baseline and 12-month visits.	227

List of Tables

Table 1.1. Radiological findings in fibrotic and/or non-fibrotic HP.....	31
Table 2.1. First pass semi-quantitative metrics used in DCE-MRI.....	50
Table 2.2. Mortality risk prediction models incorporating CALIPER.....	63
Table 2.3. Semi-quantitative visual CT variables with utility to predict mortality in ILD.	64
Table 2.4. Pulmonary function tests with utility to predict mortality in ILD.	67
Table 2.5. Pulmonary function tests with utility to predict disease progression in ILD.....	68
Table 3.1. Data collected at each visit of TRISTAN-ILD study.....	73
Table 3.2. Data collected at the ILD clinic appointment and at each study visit.	77
Table 3.3. Semi-quantitative visual CT scoring system.....	78
Table 3.4. Technical details of the MRI sequences.....	81
Table 4.1. Number of subjects with each ILD subtype that completed each study visit.	90
Table 4.2. Demographic data for the total cohort and each ILD subtype.....	91
Table 4.3. Summary of the treatment received by subjects during the study.	92
Table 4.4. PFT results at visit 1 for the total cohort and ILD subtypes.....	93
Table 4.5. PFT results at visit 1 for the fibrotic and inflammation groups.	93
Table 4.6. FVC and FVC% results at visit 2 , and the longitudinal change in FVC and FVC% between visit 1 and visit 2 for the total cohort and the ILD subtypes.	94
Table 4.7. DLCO and DLCO% at visit 2 , and the longitudinal change in DLCO and DLCO% between visit 1 and visit 2 for the total cohort and the ILD subtypes.....	94
Table 4.8. FVC and FVC% results at visit 2 , and the longitudinal change in FVC and FVC% between visit 1 and visit 2 in the fibrotic and inflammation groups.....	95
Table 4.9. DLCO and DLCO% at visit 2 , and the longitudinal change in DLCO and DLCO% between visit 1 and visit 2 in the fibrotic and inflammation groups.....	95
Table 4.10. FVC and FVC% results at visit 3 , and the longitudinal change in FVC and FVC% between visit 1 and visit 3 for the total cohort and the ILD subtypes.....	96
Table 4.11. DLCO and DLCO% at visit 3 , and the longitudinal change in DLCO and DLCO% between visit 1 and visit 3 for the total cohort and the ILD subtypes.....	96
Table 4.12. FVC and FVC% results at visit 3 , and the longitudinal change in FVC and FVC% between visit 1 and visit 3 in the fibrotic and inflammation groups.	97
Table 4.13. DLCO and DLCO% at visit 3 , and the longitudinal change in DLCO and DLCO% between visit 1 and visit 3 in the fibrotic and inflammation groups.....	97
Table 4.14. Global ¹²⁹ Xe RBC:TP at visit 1 for the total cohort and ILD subtypes.	101
Table 4.15. Global ¹²⁹ Xe RBC:TP at visit 1 in the fibrotic and inflammation groups	101
Table 4.16. Regional ¹²⁹ Xe RBC:TP, TP:Gas and RBC:Gas results at visit 1 for the total cohort and each ILD subtype.	102
Table 4.17. Regional ¹²⁹ Xe RBC:TP, TP:Gas and RBC:Gas results at visit 1 in the fibrotic and inflammation groups.....	103
Table 4.18. ¹²⁹ Xe RBC:TP at visit 2 , and the longitudinal change in ¹²⁹ Xe RBC:TP between visit 1 and visit 2 for the total cohort and the ILD subtypes.....	104
Table 4.19. ¹²⁹ Xe RBC:TP at visit 2 , and the longitudinal change in ¹²⁹ Xe RBC:TP between visit 1 and visit 2 in the fibrotic and inflammation groups.	105
Table 4.20. % change in regional ¹²⁹ Xe RBC:TP, TP:Gas and RBC:Gas results between visit 1 and visit 2 for the total cohort and each ILD subtype.....	106
Table 4.21. % change in regional ¹²⁹ Xe RBC:TP, TP:Gas and RBC:Gas results between visit 1 and visit 2 in the fibrotic and inflammation groups.	107
Table 4.22. Global ¹²⁹ Xe ADC and Lm _D at visit 1 for the total cohort and ILD subtypes. Results are presented as median (inter-quartile range).....	111
Table 4.23. Global ¹²⁹ Xe ADC and Lm _D at visit 1 in the fibrotic and inflammation groups.	111
Table 4.24. Regional ¹²⁹ Xe ADC and Lm _D results at visit 1 for the total cohort and each ILD subtype.	114
Table 4.25. Regional ¹²⁹ Xe ADC and Lm _D results at visit 1 in the fibrotic and inflammation groups.	116
Table 4.26. Global ¹²⁹ Xe ADC and Lm _D results at visit 2 , and the longitudinal change in global ¹²⁹ Xe ADC and Lm _D between visit 1 and visit 2 for the total cohort and each ILD subtype.	118

Table 4.27. Global ¹²⁹ Xe ADC and LmD results at visit 2 , and the longitudinal change in global ¹²⁹ Xe ADC and LmD between visit 1 and visit 2 in the fibrotic and inflammation groups.....	118
Table 4.28. % change in regional ¹²⁹ Xe ADC and LmD results between visit 1 and visit 2 for the total cohort and each ILD subtype.	119
Table 4.29. % change in regional ¹²⁹ Xe ADC and LmD results between visit 1 and visit 2 in the fibrotic and inflammation groups.....	119
Table 4.30. ¹²⁹ Xe VV% and CV% at visit 1 for the total cohort and each ILD subtype.	121
Table 4.31. ¹²⁹ Xe VV% and CV% at visit 1 in the fibrotic and inflammation groups.....	121
Table 4.32. ¹²⁹ Xe VV% and CV% results at visit 2 , and the longitudinal change in ¹²⁹ Xe VV% and CV% between visit 1 and visit 2 for the total cohort and each ILD subtype.	121
Table 4.33. ¹²⁹ Xe VV% and CV% results at visit 2 , and the change in ¹²⁹ Xe VV% and CV% between visit 1 and visit 2 in the fibrotic and inflammation groups.....	122
Table 4.34. MTT, PBF and PBV at visit 1 for the total cohort and ILD subtypes.	124
Table 4.35. MTT, PBF and PBV at visit 1 in the fibrotic and inflammation groups.....	125
Table 4.36. DCE-MRI results at visit 2 , and the longitudinal change in MTT, PBF and PBV between visit 1 and visit 2 for the total cohort and each ILD subtype.	126
Table 4.37. DCE-MRI results at visit 2 , and the longitudinal change in MTT, PBF and PBV between visit 1 and visit 2 in the fibrotic and inflammation groups.....	126
Table 4.38. Global CALIPER CT results at visit 1 for the total cohort and ILD subtypes.....	128
Table 4.39. Global CALIPER CT results at visit 1 in the fibrotic and inflammation groups.....	128
Table 4.40. Regional CALIPER fibrosis %, ground glass %, ILD % and VRS % results at visit 1 for the total cohort and each ILD subtype.	129
Table 4.41. Regional CALIPER CT fibrosis %, ground glass %, ILD % and VRS % results at visit 1 in the fibrotic and inflammation groups.	130
Table 4.42. Global CALIPER CT results at visit 2 , and the longitudinal change in global CALIPER CT measurements between visit 1 and visit 2 for the total cohort and each ILD subtype.....	132
Table 4.43. Global CALIPER CT results at visit 2 , and the longitudinal change in global CALIPER CT measurements between visit 1 and visit 2 in the fibrotic and inflammation groups.....	133
Table 4.44. Change in regional CALIPER CT fibrosis %, ground glass %, ILD % and VRS % results between visit 1 and visit 2 for the total cohort and each ILD subtype. Results are presented as median.....	134
Table 4.45. Change in regional CALIPER CT fibrosis %, ground glass %, ILD % and VRS % results between visit 1 and visit 2 in the fibrotic and inflammation groups.....	135
Table 4.46. Global CALIPER CT results at visit 3 , and the longitudinal change in global CALIPER CT measurements between visit 1 and visit 3 in the total cohort and each ILD subtype.	137
Table 4.47. Global CALIPER CT results at visit 3 , and the longitudinal change in global CALIPER CT measurements between visit 1 and visit 3 in the fibrotic and inflammation groups.....	141
Table 4.48. Change in regional CALIPER CT fibrosis %, ground glass %, ILD % and VRS % results between visit 1 and visit 3 in the total cohort and each ILD subtype.	143
Table 4.49. Change in regional CALIPER CT fibrosis %, ground glass %, ILD % and VRS % results between visit 1 and visit 3 in the fibrotic and inflammation groups.....	144
Table 4.50. Global visual CT score results at visit 1 for the total cohort and ILD subtypes.	146
Table 4.51. Global visual CT score results at visit 1 in the fibrotic and inflammation groups.	146
Table 4.52. Regional visual CT fibrosis, ground glass and ILD scores at visit 1 for the total cohort and each ILD subtype.	147
Table 4.53. Regional CT fibrosis, ground glass and ILD scores at visit 1 in the fibrotic and inflammation groups.....	148
Table 4.54. Global visual CT scores at visit 2 , and the longitudinal change in global visual CT scores between visit 1 and visit 2 for the total cohort and each ILD subtype.....	148
Table 4.55. Global visual CT scores at visit 2 , and the longitudinal change in global visual CT scores between visit 1 and visit 2 in the fibrotic and inflammation groups.....	149
Table 4.56. Global visual CT scores at visit 3 , and the longitudinal change in global visual CT scores between visit 1 and visit 3 for the total cohort and each ILD subtype.....	150
Table 4.57. Global visual CT scores at visit 3 , and the longitudinal change in global visual CT scores between visit 1 and visit 3 in the fibrotic and inflammation groups.....	150

Table 4.58. Change between visits 1 and 2 in the various biomarkers in the DI-ILD, HP and IPF groups, as well as the DI-ILD and HP subjects in the inflammation group.....	157
Table 4.59. Strong correlations between global ¹²⁹ Xe DW-MRI measurements and visual CT fibrosis score.....	158
Table 4.60. Strong correlations between global CALIPER CT measurements and PFT.....	158
Table 4.61. Strong correlations between global CALIPER CT measurements and visual CT scores.	158
Table 4.62. Strong correlations between regional ¹²⁹ Xe DW-MRI measurements and visual CT scores in the lower zone.	159
Table 4.63. Moderate correlations between MRI measurements.....	159
Table 4.64. Moderate correlations between global ¹²⁹ Xe MRI and PFTs.....	159
Table 4.65. Moderate correlations between global ¹²⁹ Xe MRI and visual CT scores.....	159
Table 4.66. Moderate correlations between global MRI and CALIPER honeycomb %.	160
Table 4.67. Moderate correlations between global CALIPER CT and PFTs.	160
Table 4.68. Moderate correlations between global CALIPER CT and visual CT scores.	161
Table 4.69. Moderate correlations between global visual CT scores and PFTs.	161
Table 4.70. Moderate correlations between the change in global DCE-MRI measurements and the change in PFTs.	161
Table 4.71. Moderate correlations between the change in global DCE-MRI measurements and the change in global visual CT scores.	162
Table 4.72. Moderate correlations between the change in global CALIPER CT measurements and the change in global visual CT scores (visits 1-3).....	162
Table 4.73. Moderate correlations between the change in global visual CT scores and the change in PFTs (visits 1-2).....	162
Table 4.74. Moderate correlations between regional ¹²⁹ Xe IDEAL spectroscopic imaging measurements and ¹²⁹ Xe DW-MRI measurements.	163
Table 4.75. Moderate correlations between regional ¹²⁹ Xe IDEAL spectroscopic imaging measurements and CALIPER CT measurements.	163
Table 4.76. Moderate correlations between regional ¹²⁹ Xe IDEAL spectroscopic imaging measurements and visual CT scores.....	163
Table 4.77. Moderate correlations between regional ¹²⁹ Xe DW-MRI measurements and CALIPER CT measurements.	164
Table 4.78. Moderate correlations between regional ¹²⁹ Xe DW-MRI measurements and visual CT scores.....	164
Table 4.79. Variables with a statistically significant odds ratio for predicting disease progression using univariate logistic regression analysis.....	165
Table 4.80. Variables that had odds ratios with p values 0.05 – 0.10 for predicting disease progression using univariate logistic regression analysis.	166
Table 4.81. Variables for predicting disease progression with age added to the logistic regression model.....	166
Table 5.1. Number of days between the baseline and follow-up study visits.....	170
Table 5.2. Demographic data for the total study cohort (n=49) and subjects 19-49 (n=31).....	171
Table 5.3. PFT results at the baseline visit for the total study cohort (n=49) and subjects 19-49 (n=31).....	172
Table 5.4. FVC and FVC% results at the 3-month visit , and the longitudinal change in FVC and FVC% between the baseline and 3-month visits (n=22).....	173
Table 5.5. DLCO and DLCO% results at the 3-month visit , and the longitudinal change in DLCO and DLCO% between the baseline and 3-month visits (n=22).....	174
Table 5.6. KCO and KCO% results at the 3-month visit , and the longitudinal change in KCO and KCO% between the baseline and 3-month visits (n=22).	174
Table 5.7. FVC and FVC% results at the 6-month visit , and the longitudinal change in FVC and FVC% between the baseline and 6-month visits in the total study cohort (n=30) and subjects 19-49 (n=16).....	175
Table 5.8. DLCO and DLCO% results at the 6-month visit , and the longitudinal change in DLCO and DLCO% between the baseline and 6-month visits in the total study cohort (n=30) and subjects 19-49 (n=16).....	176

Table 5.9. K _{CO} and K _{CO} % results at the 6-month visit , and the longitudinal change in K _{CO} and K _{CO} % between the baseline and 6-month visits in the total study cohort (n=30) and subjects 19-49 (n=16).	177
Table 5.10. FVC and FVC% results at the 12-month visit , and the longitudinal change in FVC and FVC% between the baseline and 12-month visits in the total study cohort (n=33) and subjects 19-49 (n=20).	178
Table 5.11. DL _{CO} and DL _{CO} % results at the 12-month visit , and the longitudinal change in DL _{CO} and DL _{CO} % between the baseline and 12-month visits in the total study cohort (n=33) and subjects 19-49 (n=20).	178
Table 5.12. K _{CO} and K _{CO} % results at the 12-month visit , and the longitudinal change in K _{CO} and K _{CO} % between the baseline and 12-month visits for the total study cohort (n=33) and subjects 19-49 (n=20).	179
Table 5.13. The number of subjects in which dissolved ¹²⁹ Xe spectroscopy data was available for each study visit.	187
Table 5.14. Regional ¹²⁹ Xe RBC:TP, TP:Gas and RBC:Gas results at the baseline visit (n=15).	188
Table 5.15. ¹²⁹ Xe RBC:TP at the 3-month visit (n=21), and the longitudinal change in ¹²⁹ Xe RBC:TP between the baseline and 3-month visits (n=20).	189
Table 5.16. % change in regional ¹²⁹ Xe RBC:TP, TP:Gas and RBC:Gas between the baseline and 3-month visits (n=12).	189
Table 5.17. ¹²⁹ Xe RBC:TP at the 6-month visit , and the longitudinal change in ¹²⁹ Xe RBC:TP between the baseline and 6-month visits for the total study cohort (n=28) and subjects 19-49 (n=15).	189
Table 5.18. % change in regional ¹²⁹ Xe RBC:TP, TP:Gas and RBC:Gas between the baseline and 6-month visits (n=5).	190
Table 5.19. ¹²⁹ Xe RBC:TP at the 12-month visit , and the longitudinal change in ¹²⁹ Xe RBC:TP between the baseline and 12-month visits for the total study cohort (n=31) and subjects 19-49 (n=18).	191
Table 5.20. % change in regional ¹²⁹ Xe RBC:TP, TP:Gas and RBC:Gas between the baseline and 12-month visits (n=9).	192
Table 5.21. Global ¹²⁹ Xe ADC and L _{mD} at the baseline visit in subjects 19-49 (n=31).	194
Table 5.22. Regional ¹²⁹ Xe ADC and L _{mD} results at the baseline visit in subjects 19-49 (n=31).	195
Table 5.23. Global ¹²⁹ Xe ADC and L _{mD} at the 3-month visit (n=22), and the longitudinal change in global ¹²⁹ Xe ADC and L _{mD} between the baseline and 3-month visits (n=22).	196
Table 5.24. % change in regional ¹²⁹ Xe ADC and L _{mD} between the baseline and 3-month visits (n=22).	196
Table 5.25. Global ADC and L _{mD} at the 6-month visit and the longitudinal change in global ADC and L _{mD} between the baseline and 6-month visits.	196
Table 5.26. % change in regional ¹²⁹ Xe ADC and L _{mD} between the baseline and 6-month visits (n=16).	197
Table 5.27. Global ADC and L _{mD} at the 12-month visit and the longitudinal change in global ADC and L _{mD} between the baseline and 12-month visits.	201
Table 5.28. % change in regional ¹²⁹ Xe ADC and L _{mD} between the baseline and 12-month visits (n=20).	202
Table 5.29. The number of subjects in which DCE-MRI data was available for each study visit in the total study cohort and subjects 19-49.	205
Table 5.30. Global DCE-MRI results at the baseline visit in the total cohort (n=40) and subjects 19-49 (n=28).	206
Table 5.31. Regional DCE-MRI results at the baseline visit in the total cohort (n=40) and subjects 19-49 (n=28).	206
Table 5.32. Global DCE-MRI results at the 3-month visit , and the longitudinal change in global FWHM, MTT, PBF and PBV between the baseline and 3-month visits (n=20).	209
Table 5.33. Global DCE-MRI results at the 6-month visit , and the longitudinal change in global FWHM, MTT, PBF and PBV between the baseline and 6-month visits in the total study cohort (n=27) and subjects 19-49 (n=16).	209

Table 5.34. Global DCE-MRI results at the 12-month visit , and the longitudinal change in global FWHM, MTT, PBF and PBV between the baseline and 12-month visits in the total study cohort (n=25) and subjects 19-49 (n=16).	212
Table 5.35. Global CALIPER CT results at the baseline visit in the total study cohort (n=43) and subjects 19-49 (n=27).	214
Table 5.36. Regional CALIPER CT results at the baseline visit in the total study cohort (n=43) and subjects 19-49 (n=27).	217
Table 5.37. Global CALIPER CT results at the 12-month visit and the change in the global CALIPER CT measurements between the baseline and 12-month visits in the total study cohort (n=12) and subjects 19-49 (n=8).	218
Table 5.38. Change in regional CALIPER CT measurements between the baseline visit and the 12-month visit in the total study cohort (n=12) and subjects 19-49 (n=8).	221
Table 5.39. Global visual CT scores at the baseline visit in the total study cohort (n=49) and subjects 19-49 (n=31).	222
Table 5.40. Regional visual CT scores at the baseline visit in the total study cohort (n=49) and subjects 19-49 (n=31).	224
Table 5.41. Global visual CT scores at the 12-month visit and the change in the global visual CT scores between the baseline and 12-month visits in the total study cohort (n=20) and subjects 19-49 (n=10).	225
Table 5.42. Very strong correlations between global CALIPER CT measurements and visual CT scores.	227
Table 5.43. Strong correlations between global ¹²⁹ Xe MRI measurements and PFTs.	228
Table 5.44. Strong correlations between global CALIPER CT measurements and global visual CT scores.	228
Table 5.45. Strong correlations between global CALIPER CT measurements and PFT.	229
Table 5.46. Strong correlations between global visual CT scores and PFTs.	229
Table 5.47. Strong correlations between regional ¹²⁹ Xe IDEAL spectroscopic imaging measurements and other regional MRI measurements.	230
Table 5.48. Strong correlations between regional MRI measurements and regional CALIPER CT measurements.	230
Table 5.49. Strong correlations between regional MRI measurements and regional visual CT measurements.	230
Table 5.50. Moderate correlations between different global MRI measurements.	231
Table 5.51. Moderate correlations between global MRI measurements and PFTs.	231
Table 5.52. Moderate correlations between global CALIPER CT measurements and global visual CT scores.	231
Table 5.53. Moderate correlations between global CALIPER CT measurements and PFTs.	232
Table 5.54. Moderate correlations between global visual CT scores and PFTs.	232
Table 5.55. Moderate correlations between regional ¹²⁹ Xe IDEAL spectroscopic imaging measurements and CALIPER CT measurements at the baseline visit.	233
Table 5.56. Moderate correlations between regional ¹²⁹ Xe MRI measurements and visual CT scores at the baseline visit.	233
Table 5.57. Moderate correlations between regional ¹²⁹ Xe DW-MRI measurements and other regional MRI measurements.	234
Table 5.58. Moderate correlations between the change in regional ¹²⁹ Xe DW-MRI measurements and the change in regional DCE-MRI measurements between the baseline and 6-month visits.	234
Table 5.59. Variables with a statistically significant odds ratio for predicting disease progression using univariate logistic regression analysis.	236
Table 5.60. Imaging variables that had odds ratios with p values 0.05 – 0.10 for predicting disease progression using univariate logistic regression analysis.	237
Table 6.1. Summary of the global MRI results in the TRISTAN-ILD study.	240
Table 6.2. Summary of the global CT results in the TRISTAN-ILD study.	241
Table 6.3. Summary of the global MRI results in the IPF study.	243
Table 6.4. Summary of the global CT results in the IPF study.	244

List of Abbreviations

6MWD	Six-minute walk distance	FRC	Functional residual capacity
ALAT	Latin American Thoracic Society	FRI	Functional respiratory imaging
AMFM	Adaptive Multiple Features Method	FVC	Forced vital capacity
ATS	American Thoracic Association	FWHM	Full width of half maximum
BMI	Body mass index	GAP	Gender-age-physiology
CA	Contrast agent	GGO	Ground glass opacity
CALIPER	Computer-Aided Lung Informatics for Pathology Evaluation and Rating	GHNC	Gaussian Histogram Normalised Correlation
COPD	Chronic obstructive pulmonary disease	GLI	Global Lung Function Initiative
CPI	Composite physiologic index	¹ H	Proton
CT	Computed tomography	HAA%	High attenuation area percent
CTD	Connective tissue disease	³ He	Helium
CV	Coefficient of variation	HP	Hypersensitivity pneumonitis
DCE	Dynamic contrast enhanced	HR	Hazard ratio
DI	Drug induced	HRCT	High resolution computed tomography
D _{LCO}	Diffusing capacity of the lung for carbon monoxide	HU	Hounsfield unit
DTA	Data-driven Textural Analysis	ICI	Immune checkpoint inhibitors
DW	Diffusion weighted	IDEAL	Iterative decomposition of water and fat with echo asymmetry and least-squares estimation
ERS	European Respiratory Society	K _{CO}	Carbon monoxide transfer coefficient
F _{ACO}	Fractional concentration of carbon monoxide in the alveolar space	L _{mD}	Mean diffusive length scale
FEV ₁	Forced expiratory volume in one second	MCTD	Mixed connective tissue disease

MLA	Mean lung attenuation	RBC	Red blood cell
MLD	Mean lung density	SI	Signal intensity
MRE	Magnetic resonance elastography	siRADaw	Specific image-based airway radius
MRI	Magnetic resonance imaging	siV	Specific airway volume
MRS	Magnetic resonance spectroscopy	SLE	Systemic lupus erythematosus
MTT	Mean transit time	SLS	Scleroderma Lung Study
N ₂	Nitrogen	SNR	Signal to noise ratio
NICE	National Institute for Health and Care Excellence	SPGR	Spoiled gradient echo
NSIP	Non-specific interstitial pneumonia	SpO ₂	Oxygen saturation
OE	Oxygen enhanced	SSc	Systemic sclerosis
P _{ACO}	Partial pressure of carbon monoxide	TLC	Total lung capacity
PBF	Pulmonary blood flow	TP	Tissue plasma
PBV	Pulmonary blood volume	TR	Repetition time
PC	Phase contrast	UIP	Usual interstitial pneumonia
PFT	Pulmonary function test	UK	United Kingdom
PH	Pulmonary hypertension	USA	United States of America
PVV	Pulmonary vessel volume		
QA	Quality assurance	UTE	Ultra-short echo time
QCT	Quantitative computed tomography	V _A	Alveolar volume
QILD	Quantitative interstitial lung disease	VDP	Ventilation defect percentage
QLF	Quantitative Lung Fibrosis	VRS	Vessel related structures
QOL	Quality of life	VV	Ventilation volume
RA	Rheumatoid arthritis	¹²⁹ Xe	¹²⁹ -xenon

Chapter 1: Classification and Clinical Assessment of Interstitial Lung Disease

1.1 Interstitial Lung Disease

The term interstitial lung disease (ILD) includes a group of heterogeneous diseases of the lung parenchyma of various causes, although many are idiopathic (cause unknown). The predominant pathological feature is variable inflammation and/or fibrosis of the lung interstitium, the anatomic space interposed between the cells of the alveolar membrane and the endothelial cells of the interstitial capillaries. Many ILD subtypes share similar clinical, pathophysiological and radiological features but the response to treatment and prognosis can differ significantly. Accurate diagnosis of a specific ILD subtype is often difficult, with up to 15% of patients being categorised as having unclassifiable ILD (1).

1.1.1 Classification of Interstitial Lung Disease

Fibrotic ILD can largely be differentiated radiologically (through computed tomography (CT) imaging) and pathologically into two distinct patterns; usual interstitial pneumonia (UIP) and non-specific interstitial pneumonia (NSIP). UIP pattern fibrosis is classically located in the sub-pleural areas of the lower lobes and comprises honeycombing, reticulation and traction bronchiectasis (Figure 1.1) (2). Honeycombing generally appears as several rows of small (3-10mm diameter) subpleural cysts, but can also present as a single layer only (3). Traction bronchiectasis is identified as irregular bronchial dilatation due to retractile fibrosis in the adjacent lung parenchyma (4). On CT, NSIP is widely distributed throughout the lung parenchyma but is usually lower zone predominant with sparing of the sub-pleural regions (Figure 1.2) (5). Bilateral ground glass opacification (GGO) is seen, often in association with evidence of fibrosis such as reticulation, traction bronchiectasis and lower-lobe volume loss, but honeycombing is rare (6, 7). The majority of cases of UIP pattern on CT are due to IPF, whereas other causes include asbestosis, hypersensitivity pneumonitis (HP), connective tissue disease (CTD) and drug toxicity. NSIP is usually idiopathic or secondary to CTD.

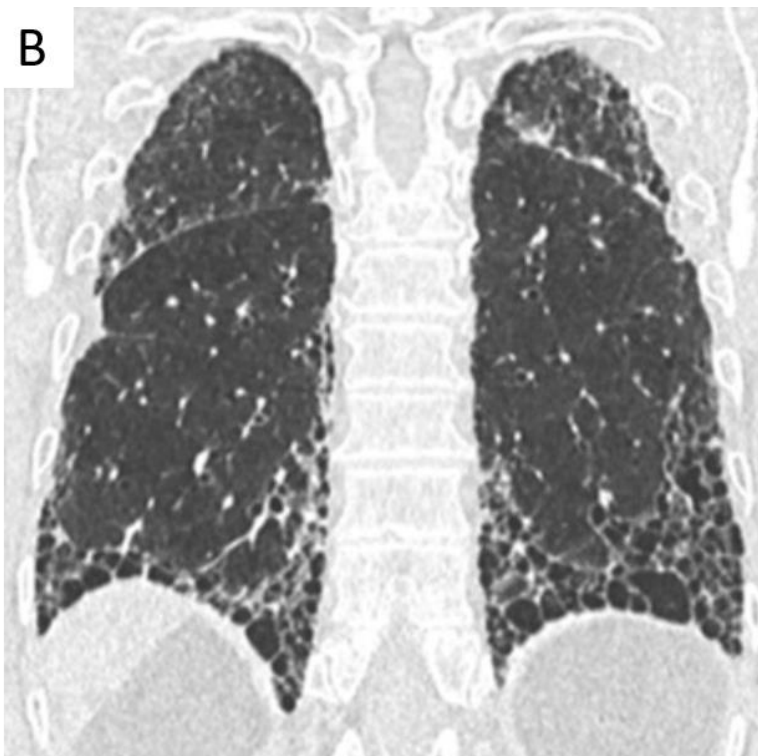
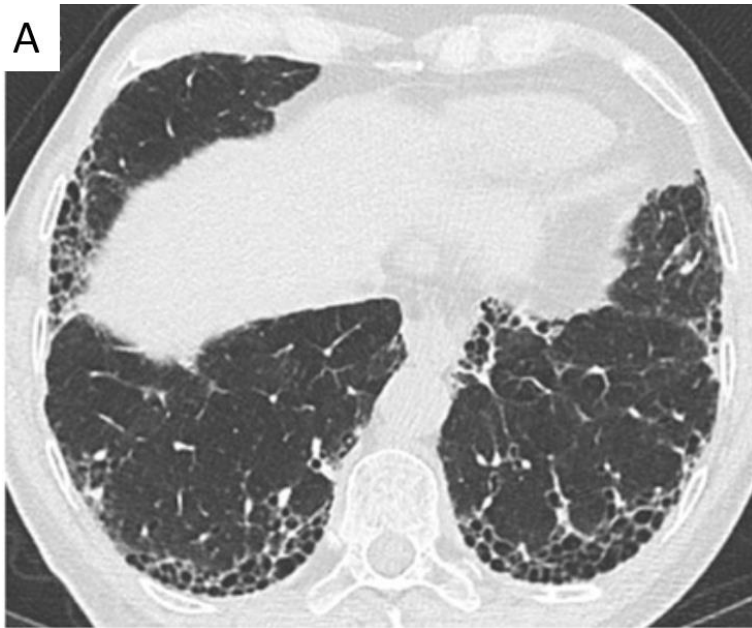


Figure 1.1. CT features of UIP. Axial (A) and coronal (B) images demonstrate subpleural distribution of honeycombing, reticulation and traction bronchiectasis in the lower zones.

Adapted with permission of the American Thoracic Society. Copyright © 2020 American Thoracic Society. All rights reserved. Raghu G et al / 2018 / Diagnosis of Idiopathic Pulmonary Fibrosis. An Official ATS/ERS/JRS/ALAT Clinical Practice Guideline / 198(5):e44-e68. The American Journal of Respiratory and Critical Care Medicine is an official journal of the American Thoracic Society. Readers are encouraged to read the entire article for the correct context at <https://www.atsjournals.org/doi/full/10.1164/rccm.201807-1255ST>. The authors, editors, and The American Thoracic Society are not responsible for errors or omissions in adaptations.

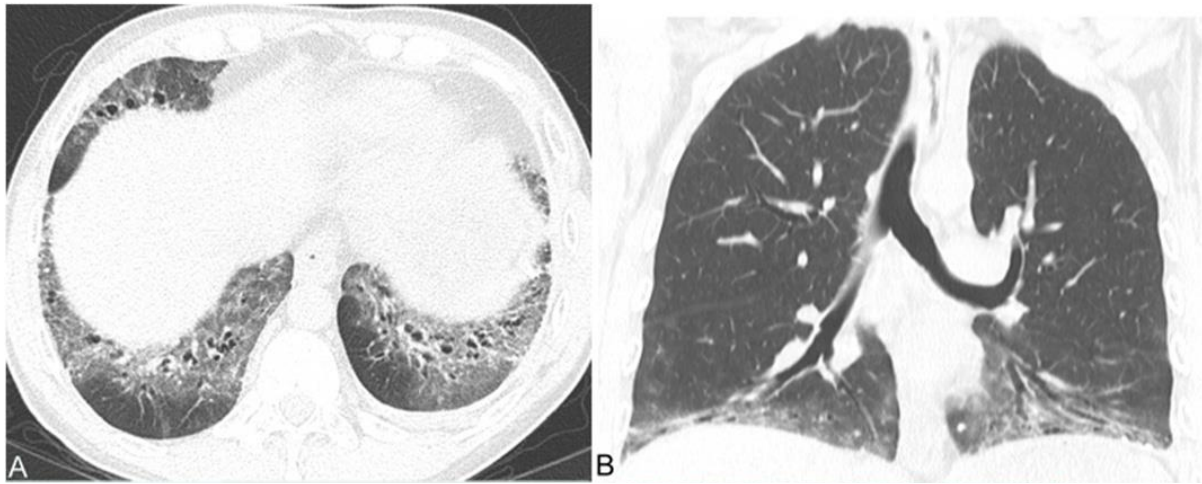


Figure 1.2. CT features of NSIP. Axial (A) and coronal (B) images show bilateral and central GGO in the lower zones with traction bronchiectasis.

Adapted with permission of the American Thoracic Society. Copyright © 2020 American Thoracic Society. All rights reserved. Travis WD et al / 2013 / An official American Thoracic Society/European Respiratory Society statement: Update of the international multidisciplinary classification of the idiopathic interstitial pneumonias / 188(6):733-48. The American Journal of Respiratory and Critical Care Medicine is an official journal of the American Thoracic Society. Readers are encouraged to read the entire article for the correct context at <https://www.atsjournals.org/doi/full/10.1164/rccm.201308-1483ST>. The authors, editors, and The American Thoracic Society are not responsible for errors or omissions in adaptations.

A recent term “progressive-fibrosing ILD” has been used to describe a combination of fibrotic ILD subtypes with similar clinical and radiological presentations, that are likely to progress despite treatment (8, 9). The consequence of progressive-fibrosing ILD is usually a decline in lung function with subsequent worsening breathlessness resulting in deterioration in a patient’s quality of life (QOL) and increased likelihood of early mortality (10). By definition, idiopathic pulmonary fibrosis (IPF) is a chronic progressive-fibrosing ILD, while only a proportion of other ILD subtypes develop a progressive-fibrosing phenotype. The non-IPF ILD subtypes that are most likely to demonstrate this phenotype include asbestosis, HP, idiopathic NSIP (iNSIP), rheumatoid arthritis (RA) associated ILD, silicosis, stage IV sarcoidosis, systemic sclerosis (SSc) associated ILD and unclassifiable ILD (10).

Progressive-fibrosing ILD appears more common in older adults although the incidence and prevalence of these various diseases is poorly defined (11). The advantage of applying the progressive-fibrosing ILD phenotype, rather than considering specific disease entities, is its practical value in predicting disease

behaviour. This has been demonstrated by a recent multicentre, randomised, placebo-controlled drug trial (the INBUILD study) reporting the efficacy of nintedanib in slowing the decline of forced vital capacity (FVC) by approximately 50% in patients with non-IPF progressive-fibrosing ILD (12). The INBUILD study used specific criteria to define disease progression over the previous 24 months, with any one of the following three scenarios being accepted:

1. Relative decline in FVC of $\geq 10\%$ predicted
2. Relative decline in FVC of 5% to $< 10\%$ predicted plus worsening respiratory symptoms or increased extent of fibrosis on CT
3. Worsening respiratory symptoms and increased extent of fibrosis on CT

ILD tends to be classified based on the underlying aetiology (e.g. CTD) and many ILD subtypes with no known aetiology are grouped under the term idiopathic interstitial pneumonia (IIP) (Figure 1.3). The American Thoracic Association (ATS) / European Respiratory Society (ERS) IIP classification published in 2002 (13) used the combination of clinical, histopathological and radiological data, differing from prior classification which relied mainly on histopathology. This classification has since been updated by the ATS/ERS IIP consensus statement of 2013 (14) . The main changes made to the revision were:

1. iNSIP was accepted as a specific ILD subtype.
2. The disease course in IPF was recognised to be heterogenous.
3. Acute exacerbations were more clearly defined and acknowledged to occur in chronic fibrotic IIPs.

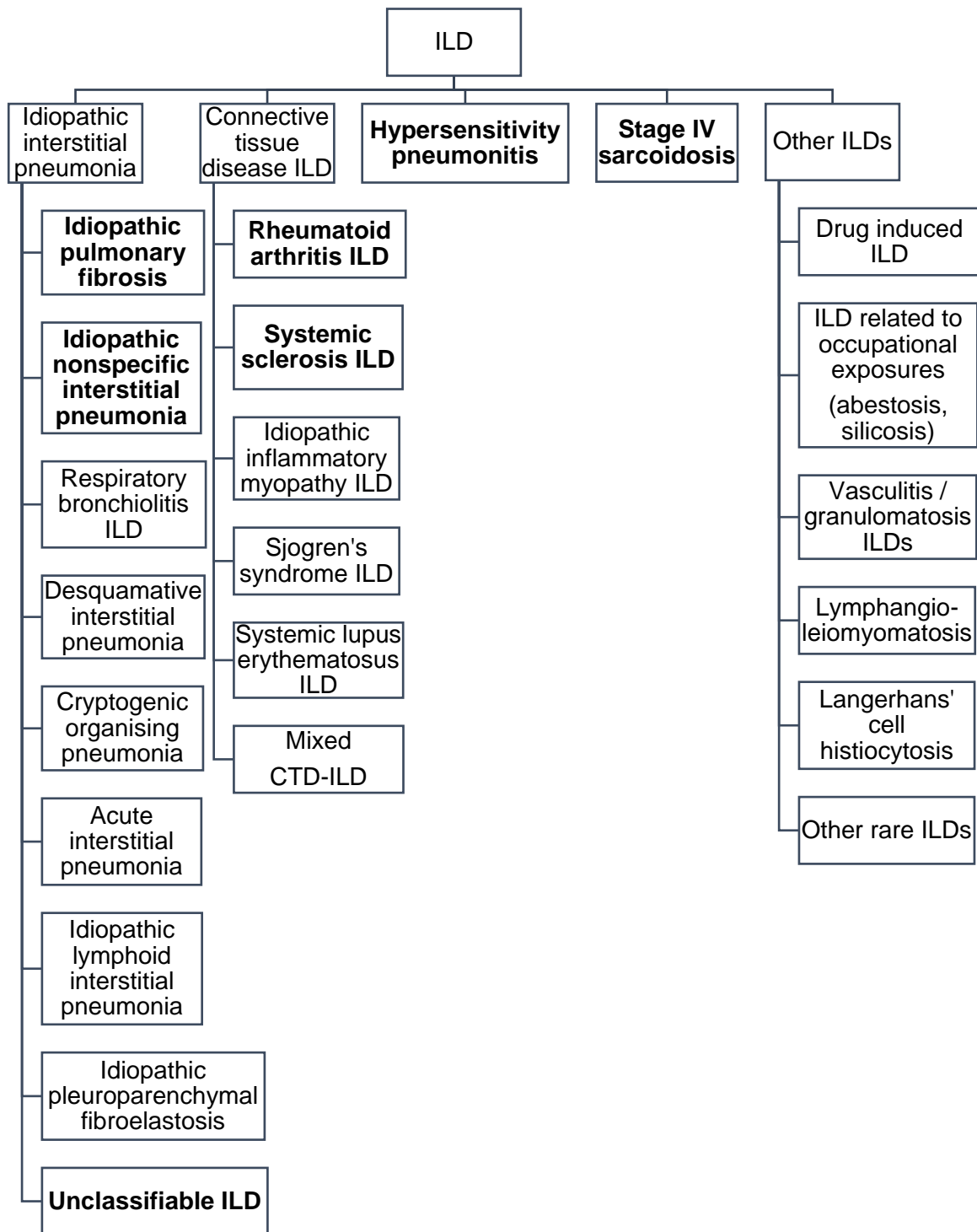


Figure 1.3. Classification of ILD (progressive fibrosing ILDs are indicated in bold).

Modified with permission of the © ERS 2020: European Respiratory Review 27 (150) 180076; DOI: 10.1183/16000617.0076-2018 Published 21 December 2018.

1.1.2 Idiopathic Pulmonary Fibrosis

IPF is a progressive, irreversible fibrotic ILD of unknown aetiology. It is more common in males, usually over 60 years of age. Risk factors linked to IPF include environmental exposures, genetic variants, microbial pathogens and cigarette smoking (3). It is rare for patients under the age of 50 to be diagnosed with IPF, with such patients likely to have familial IPF or who subsequently develop CTD features that were not apparent at the time of diagnosis (15). The histopathological and/or radiological pattern of IPF is UIP, with honeycombing being the characteristic feature (3). Multidisciplinary team (MDT) discussion incorporating clinical, radiological and possibly histopathological information is acknowledged as the current diagnostic reference standard in IPF (16).

IPF is the most common IIP. The prevalence of IPF has been reported to be increasing, although this may be due to improved recognition of the disease (17). The prognosis of IPF is generally poor, with a recent systematic review reporting a mean survival of four years in patients not receiving antifibrotic therapy (18). However, the use of antifibrotics over the last several years has led to improved survival as reported in IPF registries (19, 20). In the European IPF registry, the median survival of patients taking antifibrotics was 123.1 months, compared to a median survival of 68.3 months in those not receiving antifibrotic treatment (20).

The unpredictable progression of IPF means that providing a reliable prognosis in individual patients at diagnosis is challenging (21). Most patients with IPF experience a steady deterioration in symptoms and pulmonary function, some demonstrate relative stability while others die prematurely, often within the first 12 months as a result of rapidly progressive disease (Figure 1.4) (22).

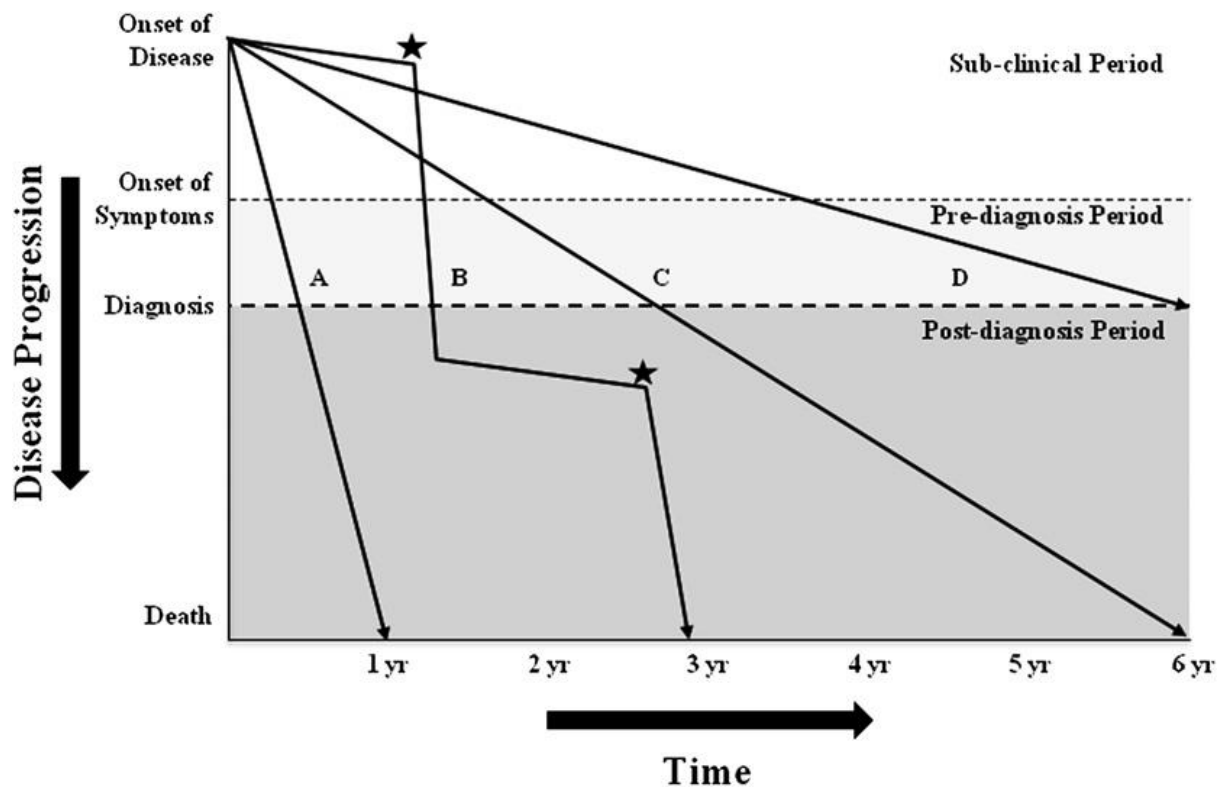


Figure 1.4. Schematic representation of different possible clinical courses of IPF (22).

Reprinted with permission of the American Thoracic Society. Copyright © 2020 American Thoracic Society. All rights reserved. Ley B, Collard HR, King TE, Jr./2011/ Clinical course and prediction of survival in idiopathic pulmonary fibrosis / *Am J Respir Crit Care Med* /183(4)/431-40. The American Journal of Respiratory and Critical Care Medicine is an official journal of the American Thoracic Society.

In 2013, the National Institute for Health and Care Excellence (NICE) in the UK approved the use of pirfenidone in IPF patients with a FVC of 50-80% predicted (23). Nintedanib, a tyrosine kinase inhibitor, was approved by NICE for the treatment of IPF in 2016 (24). In placebo-controlled, randomised clinical trials, both anti-fibrotic medications were found to reduce the rate of decline in FVC by approximately 50% over a 12-month period (25, 26). Therefore, an accurate and consistent diagnosis of IPF is crucial in order to attain the greatest benefit for patients with ILD (27).

It has previously been suggested by an expert panel that all-cause mortality and all-cause non-elective hospitalisation are the most robust and meaningful primary endpoints for IPF drug studies (28). However, trials with all-cause mortality as the primary outcome require a large number of subjects and a long duration of follow-up with substantial associated costs which would likely prohibit such a study from being feasible (29). It has been reported that the addition of hospitalisation to all-cause

mortality as a composite endpoint would potentially reduce the required sample size by 50-75% (30). Currently, FVC is the most recommended and validated tool to monitor the progression of IPF and is considered to be an acceptable surrogate endpoint in IPF therapeutic trials, despite being relatively insensitive to longitudinal change (31). Studies have suggested that weekly home-based measurements of FVC could potentially improve endpoint efficiency of future IPF drug trials by reducing the number of subjects required (32, 33).

1.1.3 Idiopathic Non-specific Interstitial Pneumonia

NSIP can be categorised by radiology and histopathology as either cellular or fibrotic. In cellular NSIP, the GGO is not accompanied by traction bronchiectasis; however, in fibrotic NSIP the GGO is associated with traction bronchiectasis and reticulation which tends to signify fine fibrosis rather than inflammation (34). It can often be difficult to confidently distinguish fibrotic NSIP from IPF radiologically. However, on CT, NSIP is characterised by its spatial and temporal homogeneity and often demonstrates subpleural sparing (10). In contrast to IPF, iNSIP is more common in never smokers and women (35). iNSIP tends to have a superior prognosis compared to IPF (7), although mortality has been found to be influenced more by lung function than histopathology (36).

1.1.4 Connective Tissue Disease associated ILD

Approximately 15% of all patients with CTD will develop ILD, and those with RA or SSc are most likely to be affected (37). In contrast to IPF, CTD-ILD is more common in younger patients (less than 50 years of age) and women (38). Overall, CTD-ILD tends to demonstrate NSIP on histopathology and CT (39). ILD associated with SSc, systemic lupus erythematosus (SLE), idiopathic inflammatory myopathy (IIM), Sjogren's syndrome and mixed CTD (MCTD) are most likely to show a NSIP pattern, whereas UIP pattern is most common in RA-ILD (40). CTD-ILD has a heterogenous clinical course with variation in the severity of ILD within and between the different CTDs.

1.1.5 Hypersensitivity pneumonitis

HP (previously known as extrinsic allergic alveolitis) is an immune-mediated ILD, caused by the repeated inhalation of low molecular weight substances or specific organic antigens in genetically susceptible individuals (41, 42). It involves inflammation and/or fibrosis of the small airways and lung parenchyma (43). Historically, exposure to moulds and bird feathers was characteristically associated with HP, but more recently, exposure to mycobacteria identified in coolant used in metal cutting and exposure to *Mycobacterium avium* (hot tub lung) has been reported (44). Over 300 different agents associated with the development of HP have been identified, with many being linked to specific occupations (42, 45). HP is more likely to occur in females, and smoking is reported as being protective against the development of the disease (46). Compared to IPF, patients with HP tend to be younger (47).

The radiological features of HP (Figure 1.5 and Table 1.1) are dependent on the stage of the disease, although fibrotic HP is considered to have a variable appearance on CT (43). In non-smokers, the HRCT features of GGO with poorly-defined centrilobular nodules or mosaic attenuation on inspiration and/or air trapping on expiration are highly suggestive of HP (46). In fibrotic HP, the fibrosis is bilateral and is usually dispersed equally in the three lung zones with relative basal sparing, or predominantly affects the middle lung zone; however, the CT abnormalities in non-fibrotic HP tend to be bilateral and diffuse (43). In the advanced stage of fibrotic HP, it is often difficult to differentiate the disease pattern on CT from UIP or fibrotic NSIP (48). Upper zone-predominant fibrosis has been reported as a radiological feature to differentiate HP from IPF (49), but less than 10% of fibrotic HP presents with this distribution of fibrosis (50-52). A study involving 66 patients with fibrotic ILD found that HRCT was able to differentiate between fibrotic HP and other fibrotic ILDs in only 53% of cases (49). A radiological diagnostic model for HP demonstrated that diffuse axial distribution in combination with the extent of mosaic attenuation or air trapping being more than that of reticulation resulted in a false-positive rate of less than 10% (53).

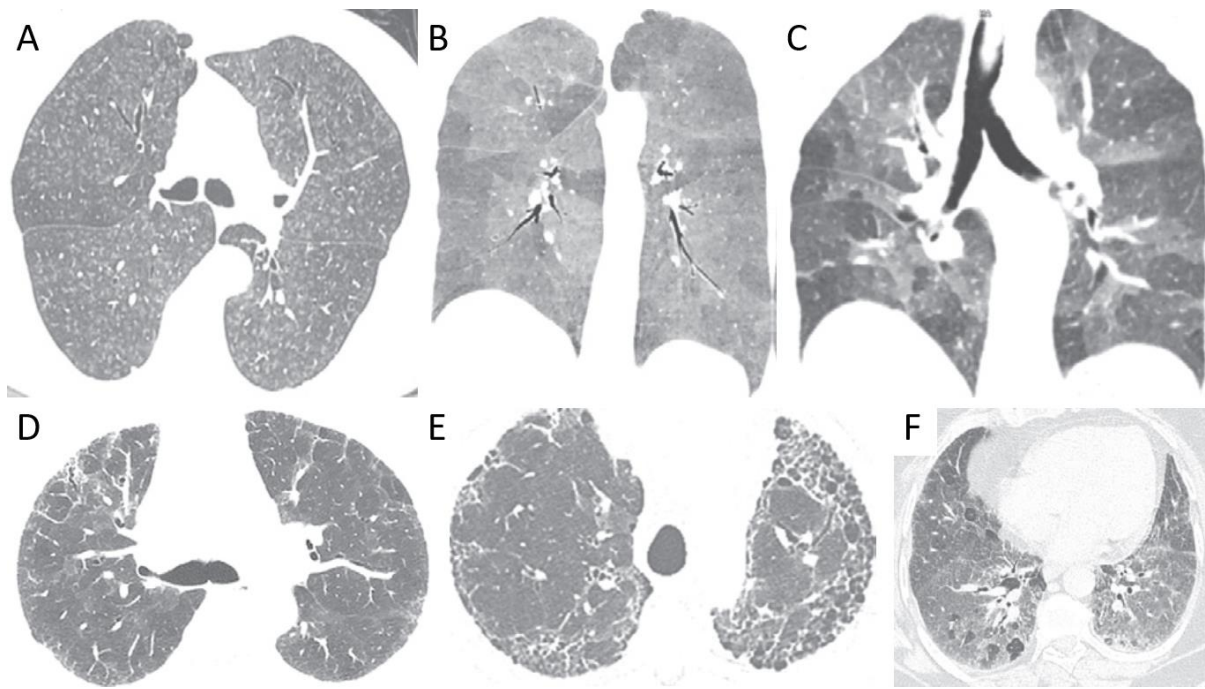


Figure 1.5. CT features of non-fibrotic HP characterised by centrilobular nodules (A), mosaic attenuation on inspiration (B), and air trapping on expiration (C). CT features of fibrotic HP including reticulation with no zonal predominance (D), upper zone reticulation with architectural lung distortion (E), and fibrotic GGO with small airway disease (F).

Adapted with permission of the American Thoracic Society. Copyright © 2020 American Thoracic Society. All rights reserved. Raghu G et al / 2020 / Diagnosis of Hypersensitivity Pneumonitis in Adults. An Official ATS/JRS/ALAT Clinical Practice Guideline / 202(3):e36-e69. The American Journal of Respiratory and Critical Care Medicine is an official journal of the American Thoracic Society. Readers are encouraged to read the entire article for the correct context at <https://www.atsjournals.org/doi/full/10.1164/rccm.202005-2032ST>. The authors, editors, and The American Thoracic Society are not responsible for errors or omissions in adaptations.

Radiological findings	Fibrotic HP	Non-fibrotic HP
“Three-density pattern” or “headcheese sign” (combining ground glass opacity, lobules of decreased attenuation / vascularity & normal lung)	Highly specific	No
Mosaic attenuation (regions of variable attenuation within the lung parenchyma on inspiratory CT)	Typical	Typical
Features of small airways disease: air trapping (focal hypoattenuation in the background of normal lung on expiratory CT) and/or small, poorly-defined centrilobular nodules on inspiratory CT	Typical	Typical
Irregular, fine or coarse reticulation with architectural lung distortion	Typical	No
Traction bronchiectasis	Typical	No
Honeycombing	Often	No
Ground glass opacity	Often	Typical
Airspace consolidation	No	Occasionally
Lung cysts	No	Occasionally

CT: Computed tomography; HP: Hypersensitivity pneumonitis

Table 1.1. Radiological findings in fibrotic and/or non-fibrotic HP.

1.1.6 Drug Induced ILD

Although the exact number is unknown, at least 450 drugs have been reported to cause ILD (54). This number will likely continue to rise as new medications are developed. The main categories of medications associated with drug induced (DI) ILD include antimicrobial (e.g. nitrofurantoin), anti-inflammatory (e.g. methotrexate), biological (e.g. rituximab), cardiovascular (e.g. amiodarone), chemotherapeutic (e.g. bleomycin) and miscellaneous agents (55). A UK population-based study published in 2012 estimated that the incidence of drug/radiation induced ILD between 1997-2008 was 4.1 per million person-years (56). However, this is likely to be underestimated due to the increased use of biologics and immune checkpoint inhibitors (ICI) over the past decade (57, 58).

Currently there are no general guidelines regarding the diagnostic and management approach for suspected DI-ILD. The diagnosis initially involves excluding infection and is particularly challenging due to the non-specific clinical, histological and radiological findings which can overlap with other ILD subtypes. Diagnosis of DI-ILD is supported by a temporal link between an exposure to the offending drug and the development of new respiratory symptoms, signs and/or radiological changes; however, DI-ILD may

develop within the first few days or even several years after the drug was commenced (59). Furthermore, drugs used to treat CTDs can themselves cause DI-ILD, making it difficult to determine if the development of ILD is due to the underlying CTD or the drug in question. Likewise, ICIs may be used in patients with lung cancer who may already have respiratory symptoms. Improvement of symptoms and radiology usually occurs following discontinuation of the suspected drug. However, irreversible fibrosis may occur especially if the diagnosis of DI-ILD is delayed.

Several risk factors are associated with the development of DI-ILD in patients treated for cancer including older age, reduced FVC, pre-existing ILD, male gender, poor performance status, smoking and HRCT fibrosis score (60-64). DI-ILD secondary to ICIs is more likely to occur in patients with non-small cell lung cancer compared to melanoma (65), and the risk is higher in cancer patients treated with more than one ICI (66). Future studies are needed to identify predictive biomarkers for DI-ILD and help determine what biological factors are associated with the variable clinical presentations (58).

1.2 Current methods for diagnosis and longitudinal assessment of ILD

The main aim in the diagnosis of a specific ILD subtype is to enable a confident diagnosis by using an approach that is the least invasive (43). Current diagnostic investigations in ILD mainly consist of HRCT and PFTs. Imaging interpretation alone is often not enough to confidently make a definitive diagnosis and a combination of the HRCT with functional and clinical data is usually required by a MDT with expertise in ILD (14).

1.2.1 Multidisciplinary team assessment

MDT assessment has been considered to be the gold standard for the diagnosis of ILD since the publication of the ATS/ERS IIP classification in 2002 (13, 14). In order to maximise diagnostic accuracy, close consultation is needed between the members of the MDT, which usually involves at least one respiratory physician, a radiologist and when appropriate, a pathologist (13). Often a definitive diagnosis cannot be achieved by the MDT, but instead a “working diagnosis” of high probability can be reached by

combining the key information available to increase or decrease the diagnostic probability of a specific ILD subtype (16).

A number of studies have demonstrated the importance of a MDT diagnosis, reporting that it results in improved diagnostic confidence and superior interobserver agreement when compared to diagnosis by individual clinicians (27, 67, 68). A study involving 70 ILD cases and seven international ILD MDTs reported high levels of inter-MDT meeting agreement for an IPF diagnosis (kappa (κ) coefficient of agreement = 0.60) and a CTD-ILD diagnosis ($\kappa=0.64$); however, inter-MDT meeting agreement was low for the diagnosis of iNSIP ($\kappa=0.25$) and HP ($\kappa=0.24$) (27). Even though a MDT diagnosis of specific ILD subtypes may have a good level of diagnostic agreement, this doesn't always mean superior diagnostic accuracy, with the success of MDT meeting being dependent on the expertise of the individuals participating (69). A small study involving 39 IIP cases, found superior diagnostic agreement between academic clinicians ($\kappa=0.71$) compared to community clinicians ($\kappa=0.44$), with the clinicians based in the community more likely to make a diagnosis of IPF than their academic colleagues (70).

1.2.2 High-resolution computed tomography

HRCT has the ability to accurately characterise the morphologic patterns which are associated with the various types of ILD. The presence of honeycombing is key in the radiological classification of definite UIP (3), and the extent of honeycombing on HRCT is a useful discriminator between NSIP and UIP patterns (71). In the absence of honeycombing on HRCT, the likelihood of an IPF diagnosis has been reported as approximately 80% in patients at least 60 years of age with one-third or more of the lung volume consisting of reticulation (72). The degree of the imaging abnormalities on HRCT in ILD has been shown to correlate with the amount of pathological involvement and the extent of PFT abnormality (73). HRCT is the preferred method for pulmonary imaging in ILD due to its superior resolution when compared to nuclear imaging techniques and magnetic resonance imaging (MRI) (74). However, the resolution on HRCT scans is still limited in the assessment of GGOs which could signify either reversible inflammation or fine intra-lobular fibrosis (75). Fibrotic disease is more likely if the GGO is accompanied with reticulation and traction bronchiectasis

(76, 77). The 2018 official ATS/ERS/JRS/ALAT clinical practice guideline for the diagnosis of IPF recommends volumetric acquisition at full inspiration with sub-millimetric collimation with contiguous or overlapping reconstruction of thin-section CT images (3).

Despite HRCT being crucial in the diagnosis of ILD, it does have some limitations. A multicentre HRCT study involving 11 thoracic radiologists reported moderate levels of agreement ($\kappa=0.48$) between observers for the first choice diagnosis of ILD subtype, with NSIP being the associated with 55% of disagreements (78). Higher levels of agreement were seen between radiologists based in a tertiary referral centre ($\kappa=0.60$) compared to those from regional centres ($\kappa=0.34$), suggesting that interobserver variability may increase among radiologists working in less specialist centres. However, a more recent study found that the interobserver agreement for the radiological diagnosis of UIP was not significantly different between radiologist subgroups of variable levels of experience (79).

It has been reported that the characteristic features on HRCT to confidently differentiate between HP, IPF and NSIP are present in approximately half of these patients (49). The accuracy of HRCT in identifying NSIP may be particularly limited, with multiple studies finding that a significant proportion (32-44%) of patients with a UIP pattern on histopathology have HRCT scans suggestive of NSIP (71, 80-83). Radiological abnormalities may evolve over time, as a study demonstrated that 28% of patients initially having CT features in keeping with NSIP progressed to a pattern more consistent with UIP over a follow-up period of at least 3 years (83). Lower lobe honeycombing on HRCT was the strongest predictor of histopathological UIP pattern in a study of 91 subjects with suspected IPF and the finding of a UIP pattern on HRCT was accurate in 96% of cases (84). Other studies using histopathology as the diagnostic gold standard have also shown that the identification of a UIP pattern on HRCT has a positive predictive value of at least 90% (81, 85-88). However, a study found that 94.7% of patients with a HRCT scan inconsistent with UIP had histopathology classified as definite or probable UIP (89).

1.2.3 Pulmonary function tests

The standard spirometry measurements used in ILD are forced expiratory volume in one second (FEV₁), FVC and FEV₁/FVC ratio. FVC is the volume of air exhaled as completely and forcefully as possible after full inspiration. FEV₁ is the volume of air exhaled in the first second of the FVC manoeuvre. Reduced lung compliance secondary to fibrosis leads to a restrictive ventilatory defect, defined by a decreased FVC and/or total lung capacity (TLC) (90). The diffusing capacity of the lung for carbon monoxide (D_{LCO}) is a measure of gas exchange across the alveolar-capillary interface in the lung. It is decreased in ILD as a consequence of the thickened alveolar capillary membrane and reduced capillary bed (91). PFTs are useful to determine the severity of ILD but generally have limited diagnostic value, as reduced FVC and D_{LCO} is common to all ILD subtypes (92).

In 1957, Ogilvie *et al* described a standardised clinical method of measuring D_{LCO} using the alveolar concentration and alveolar volume of carbon monoxide at the start of breath-holding (93). D_{LCO} is dependent on the alveolar volume (V_A), the fractional concentration of carbon monoxide in the alveolar space (F_{ACO}) and the partial pressure of carbon monoxide (P_{ACO}) as illustrated in the equation: $D_{LCO} = V_A \cdot \Delta F_{ACO} / \Delta t / P_{ACO}$.

The carbon monoxide transfer coefficient (K_{CO}) represents gas exchange per unit of lung volume and can be calculated as D_{LCO} divided by alveolar volume. However, it should not be used as a simple technique to normalise D_{LCO} for lung volume as full lung inflation may not be possible in ILD due to fibrotic restriction (90, 94). K_{CO} increases at low lung volumes in subjects without lung disease, therefore K_{CO} predicted values are insufficient in the assessment of patients with restrictive lung diseases such as ILD (95). A study reported that K_{CO} was in the normal range in 33.4% of fibrotic IIP patients despite almost all subjects (97.5%) having a reduced D_{LCO} (96).

There is no specific definition of ILD progression but the majority of clinical trials and observational studies use the decline in FVC, measured either as a change in millilitres (mL) or percent (%) predicted (97). Other definitions of ILD progression use categorical change over 12 months (usually $\geq 10\%$ predicted FVC and/or $\geq 15\%$ predicted D_{LCO}), or as a combination of categorical change in pulmonary function and death (97). Longitudinal changes in FVC and D_{LCO} are used in clinical practice to monitor disease severity in ILD and the response to treatment.

Standard PFTs are limited by several factors in the monitoring of ILD. Firstly, they lack disease specificity as they measure the global function of the lungs only. Secondly, comorbidities such as emphysema and pulmonary hypertension (PH) can have a confounding effect on FVC and DLCO respectively (97). Emphysema can result in a normal or increased FVC and/or TLC, even when there is significant fibrosis (98). DLCO is dependent on membrane and vascular conductance, with the latter being affected by PH as a result of a reduction in the pulmonary capillary volume (90). Thirdly, changes in FVC of less than 10% and changes in DLCO of less than 15% can be difficult to interpret as they are often identified as measurement variation or felt to be due to sub-maximal effort (99). However, this is less likely to be the case if there is a similar change in both FVC and DLCO and/or corresponding change in breathlessness. Fourthly, IPF studies have reported that previous FVC decline is inaccurate in predicting future changes in FVC (31, 100). Finally, PFTs are relatively insensitive to early ILD and progression of disease as a result of the wide range (80-120%) of normal values (75). Therefore, a new approach to investigate regional lung structure-function, which is sensitive in early disease is required. A method to stage the various types of ILD at clinical presentation and estimate the prognosis accurately is also urgently needed, especially in the new era of precision medicine.

Wells *et al* developed the composite physiologic index (CPI) in order to account for the confounding effect of emphysema on FVC and DLCO in IPF (101). It correlates with disease extent on CT better than the individual PFTs and combines DLCO, FVC and FEV₁ into the formula: $CPI = 91.0 - (0.65 \times DLCO \% \text{ predicted}) - (0.53 \times FVC \% \text{ predicted}) + (0.34 \times FEV_1 \% \text{ predicted})$.

1.3 Summary

The predominant feature of ILD is variable inflammation and/or fibrosis of the lung interstitium. Current methods for diagnosis and longitudinal assessment of ILD mainly consists of HRCT and PFTs. However, there are limitations associated with these investigations and the following chapter will describe various novel imaging methods that have been studied in ILD over the last few decades.

Chapter 2: Precision Medicine in Interstitial Lung Disease: Quantitative Imaging and Prognostic Biomarkers

1.1 Precision medicine in ILD

Precision (personalised) medicine refers to the customised approach of clinical decision making for individual patients in order to achieve a superior outcome (102). It involves the use of quantitative biomarkers such as proteins (e.g. blood, fluid or tissue), physiological values (e.g. FVC) or imaging measurements, that enables the clinician to accurately determine the severity of disease and the most favourable treatment options for each patient (103). Most of the biomarker studies in ILD have focused on IPF, with small numbers of subjects, and the majority have not been independently validated (14).

Novel imaging methods such as quantitative CT (QCT) and functional lung MRI hold great potential for addressing some of the unmet needs within ILD. Numerous ILD observational studies have reported various different predictors of disease progression and/or mortality. However, the ability to accurately predict the disease course for individual patients with ILD is currently a great challenge. The following chapter will cover the background of these imaging techniques including relevant studies that have been published to date.

2.1 Quantitative computed tomography

QCT involves either lung density and/or histogram analysis, or more complex automated texture analysis such as the Adaptive Multiple Features Method (AMFM), Gaussian Histogram Normalised Correlation (GHNC) system, Quantitative Lung Fibrosis (QLF), Computer-Aided Lung Informatics for Pathology Evaluation and Rating (CALIPER) and Data-driven Textural Analysis (DTA). QCT offers a rapid, non-invasive method to characterise and quantify anatomic structures and may be used for diagnostic, predictive and prognostic purposes (104). The last two decades have seen progressive development and validation of sophisticated QCT software in ILD which now enables clinicians to objectively measure disease progression on consecutive scans and identify features on CT that are not detectable visually by humans (105).

Visual scoring of the degree of ILD on CT is time-consuming, poorly standardised, and its sensitivity in longitudinal assessment is not well validated (106). Significant inter-observer variability in the qualitative visual assessment of ILD abnormalities,

especially honeycombing by radiologists is well known (70, 107-112). Therefore, the application of automated QCT technology into routine clinical practice in the future is desirable. Automated QCT is currently limited to the research environment as the majority of the texture analysis software used in studies are not commercially available and require significant computational power (105). If QCT is to be used routinely as a surrogate endpoint in future ILD multicentre drug trials (using different scanners under various conditions), a system that is fully optimised with standardised imaging acquisition and post-processing protocols will be necessary (113, 114). Inspiratory volume can have a significant effect on the characterisation of QCT features, therefore standardised breathing instructions or the use of spirometric control may be required in order to improve reproducibility (21). Adjustment for lung volume may be a solution for this limitation (115).

2.1.1 Lung density / histogram analysis

The majority of QCT studies in ILD have involved the use of lung density and/or histogram analysis. Lung density is measured using the Hounsfield unit (HU) scale which is based on the extent of air, blood and soft tissue in each voxel. The CT histogram represents the distribution of HU values for each CT image or for the whole lung (21). ILD is typically associated with an increase in mean lung density (MLD) and mean lung attenuation (MLA) but a decrease in kurtosis (the amount a histogram is peaked) and skewness (the degree of histogram asymmetry) (116). Patients with severe IPF have increased positive skewness (skewed to the right) and reduced kurtosis (less peaked) (Figure 2.1). The challenge of using lung density analysis in ILD is that, unlike emphysema, it lacks a standard HU threshold that can differentiate between normal and diseased lung parenchyma (117).

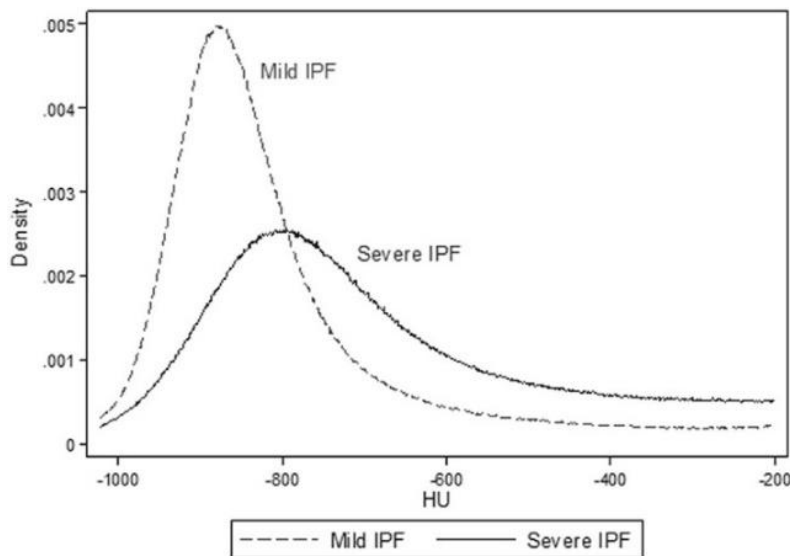


Figure 2.1. Example of differences in kurtosis and skewness between two patients with mild and severe IPF. Reproduced with permission from Elsevier (118).

MLD was found to be a useful quantitative variable in IPF in two studies by Beinert *et al* (119, 120). However, subpleural lung density was superior to MLD in differentiating between IPF patients and healthy volunteers (120). A statistically significant difference in kurtosis, skewness and MLA has been demonstrated between patients with IPF and healthy volunteers (121, 122). MLA has also been found to be significantly greater in SSc patients with ILD compared to those without ILD (123). Another study investigating patients with SSc showed that in those with ILD, the median percentage of lower lobe volume was significantly lower than in those without ILD (41.5% vs 47.1% respectively, $p=0.041$) (124).

The ability of lung density and/or histogram analysis to differentiate between IPF and other ILD subtypes is debatable. Do *et al* demonstrated significant differences in kurtosis ($p=0.02$) and skewness ($p=0.01$) between NSIP and UIP pattern (125). However, two studies by Sverzellati *et al* did not identify a significant difference in kurtosis, skewness or MLA between IPF patients and patients with HP and/or unclassifiable IIP (121, 122). Entropy (126), cystic areas % (127) and H-pattern (128) have been found to differentiate between NSIP and UIP pattern. Therefore, one could argue that lung density and/or histogram analysis could be a valuable tool in the diagnosis of ILDs, especially in cases of NSIP versus UIP pattern, which is known to be challenging for radiologists.

A number of studies involving patients with IPF have shown a correlation between different lung density and/or histogram values and PFTs (127, 129-134), visual CT score (127, 130, 132, 135, 136), and CPI (130). Several other studies involving patients with CTD-ILD have also demonstrated an association between various lung density and/or histogram values and PFTs (124, 137-147), visual CT score (137, 139-141, 143, 144, 148-150), six minute walk distance (6MWD) (138, 145) and QOL questionnaires (138). MLD (137), MLA (138), kurtosis (137, 138), skewness (137, 138) and pulmonary fibrosis % (144) have been found to be better correlated with PFTs than visual CT score in patients with SSc-ILD.

A number of longitudinal studies have investigated lung density and/or histogram values in patients with IPF (136, 151) and SSc-ILD (152-155). In the monitoring of IPF progression, a promising quantitative variable is the change in the density values of the 40th and the 80th percentile of the HRCT attenuation frequency histogram (136). A recent study comparing a computer aided method of histogram CT analysis versus a visual CT score to detect response to one-year immunosuppressive treatment in 45 patients with SSc-ILD found that the QCT analysis was superior to assess disease progression and response to therapy (155).

Three studies have investigated the use of lung density analysis pre- and post-autologous stem cell transplantation (SCT) in SSc-ILD (152-154). Compared to qualitative visual CT analysis, the QCT analysis of the change in the amount of GGO demonstrated greater correlation with the therapeutic response post treatment (152). Yabuuchi *et al*/found that 24 months after autologous SCT, in the group that responded to treatment, there was a statistically significant improvement in total lung volume and high attenuation values compared to the group that did not respond to treatment (153). In a study involving 23 SSc-ILD patients receiving autologous SCT, significantly lower mean intensity and entropy of skewness and higher uniformity of skewness was reported in responders compared to non-responders at baseline, whereas there was no significant difference in visual CT score between the two groups (154). At 6-months follow-up, changes in QCT measurements and a decrease in the visual CT fibrosis score was seen in both responders and non-responders; however, at 12-months, only the responder group demonstrated further improvement.

The type of reconstruction algorithm used has been shown to have an impact on the histogram values and the correlation with PFTs (156). Two studies have assessed the consequence of low dose versus standard dose CT on lung density and/or histogram analysis with conflicting results (121, 150). Sverzellati *et al* found no significant difference in kurtosis, skewness or MLA between low dose and standard dose CT (121). However, Nguyen-Kim *et al* demonstrated significantly increased kurtosis and skewness when low dose CT with reduced slices was used (150).

2.1.2 Adaptive Multiple Features Method (AMFM)

AMFM is an automated HRCT analysis programme which can be trained to identify and quantify a range of radiologic lung tissue patterns using a combination of various mathematical texture features (157). In 1999, Uppaluri *et al* published two articles using AMFM in 19 patients with IPF, as well as in healthy volunteers and patients with emphysema or sarcoidosis (158, 159). When the radiologists were blinded to the diagnosis, the correct outcome of the AMFM result versus the radiologists was 44.4% and 47.3% respectively (158). In the diagnosis of IPF versus normal, the accuracy of AMFM was 99%, whereas the accuracy of MLD and histogram analysis was 87% and 71% respectively (159). In IPF, longitudinal change in the AMFM features post baseline HRCT scan was shown to be correlated with change in PFTs and this was also the case with the visual CT score (157).

2.1.3 Gaussian Histogram Normalised Correlation system

The GHNC system combines local histograms and the degree of CT attenuation to separate the lungs into five categories. Using the GHNC system, Iwasawa *et al* showed a smaller increase in fibrosis score and F-pattern volume on the follow-up CTs in 38 IPF patients treated with pirfenidone compared to 40 age matched controls with IPF (160). There were no significant differences in the sensitivity, specificity, and accuracy, between GHNC analysis, visual CT score and radiologist interpretation. The authors concluded that GHNC analysis was comparable to radiologist scoring when comparing serial HRCT scans and changes in fibrosis measurement values.

2.1.4 Quantitative Lung Fibrosis score / Quantitative ILD score

A computer aided diagnosis system for quantitative scoring of ILD abnormalities has been developed by Kim *et al* and used to investigate patients with IPF (118) and SSc-ILD (161-164). The QLF score uses a support vector machine classifier to assess the amount of reticulation in a CT scan. The quantitative ILD (QILD) score represents the sum of fibrosis, GGO and honeycombing. At baseline, the QLF score and kurtosis have been found to correlate with PFTs in a study involving 57 patients with IPF (118). Compared to CT histogram analysis, the QLF score was superior in the assessment of structural status and IPF progression.

The QLF score has been shown to correlate significantly with the visual CT score and PFTs in 129 patients with SSc-ILD from the Scleroderma Lung Study (SLS) (161). The mean difference in QLF score between the placebo (n=42) and cyclophosphamide (n=41) groups after 12 months was 5% in the whole lung and 12% in the most severely affected zone (162). In the patients from the SLS that were in the placebo group, as the QLF scores increased there was a significant decrease in the quantitative ground glass scores in the most severely affected zone (163). The authors concluded that GGO may signify early fibrosis which develops into reticulation over a period of several months if patients do not receive effective treatment.

The QLF score and the QILD score have been used to investigate changes in lung abnormalities over 24 months in 97 SSc-ILD patients that participated in the SLS II (164). There was a significant decrease in the QILD score (-2.51%, p=0.001) in the total cohort, whereas the QLF score remained stable (-0.003%, p>0.05). No significant difference in the QILD score was observed between the cyclophosphamide and mycophenolate groups (-2.66% vs -2.38%; p=0.88). Over 24 months, changes in the QILD score correlated significantly with changes in FVC % predicted (r=-0.37, p<0.001) and DL_{CO} % predicted (r=-0.22, p=0.04). Changes in the QLF score correlated significantly with changes in FVC % predicted (r=-0.43, p<0.001) but not DL_{CO} % predicted (r=-0.09, p=0.42).

2.1.5 Computer-Aided Lung Informatics for Pathology Evaluation and Rating

CALIPER is a CT image analysis software that was developed by the Mayo Clinic, Rochester, USA. It uses training sets acquired through the Lung Tissue Research Consortium to quantify various radiological parenchymal features based on histogram signature mapping techniques trained by expert radiologist consensus (165). The initial pre-processing stage involves segmentation and extraction of the anatomic regions before the lung parenchyma is characterised and quantified (166). CALIPER has been used retrospectively in several types of ILD including IPF (165, 167-172), CTD-ILD (172-174), HP (172, 175-177) and iNSIP (171). An example of the results of the CALIPER quantitative analysis in IPF is shown in Figure 2.2.

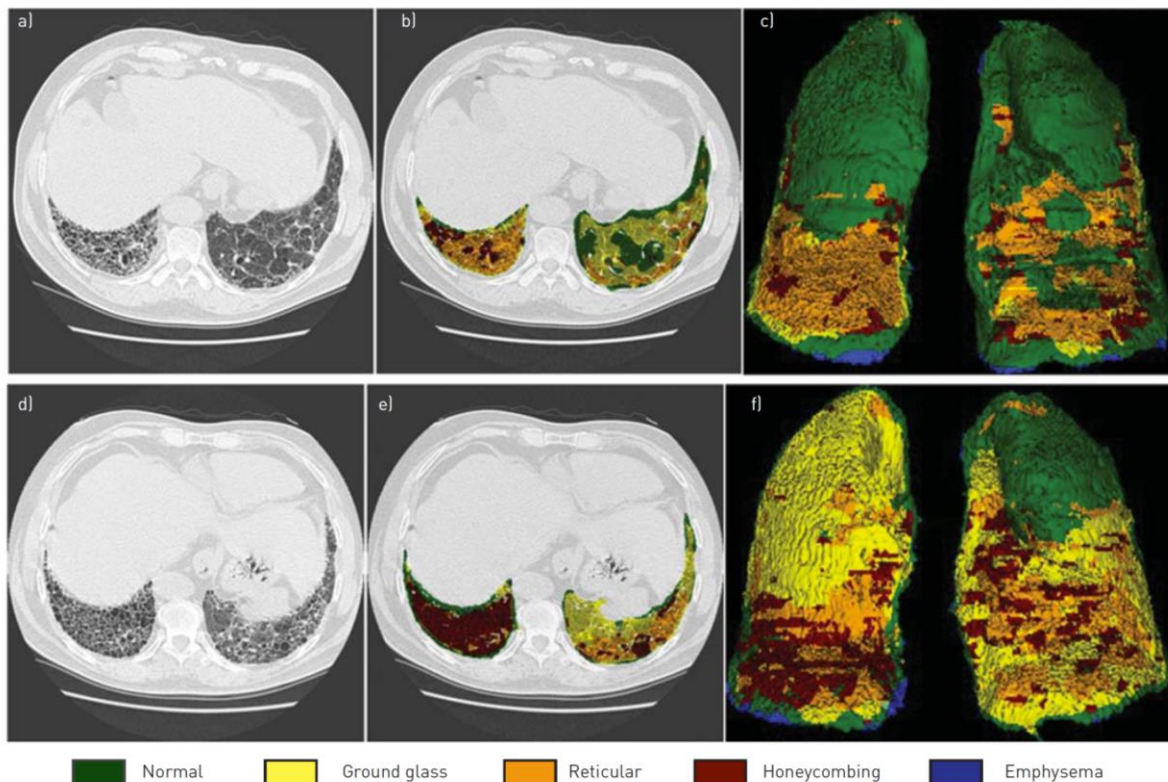


Figure 2.2. CALIPER quantitative analysis results from one patient with rows a-c and d-f corresponding to two separate time points.

Reproduced with permission of the © ERS 2020: European Respiratory Journal 43 (1) 204-212; DOI: 10.1183/09031936.00071812 Published 31 December 2013.

A correlation between CALIPER variables and visual CT score has been demonstrated in IPF (165). Following this study, *Jacob et al* showed that assessment of IPF severity using CALIPER was superior than visual CT scores for predicting CPI, FEV₁ and FVC, but not DLCO (167). IIM has been studied using CALIPER, demonstrating a significant correlation between DLCO and total interstitial abnormalities at baseline (174). A recent study of 225 patients with various ILD subtypes reported increased peripheral reticulation in those with IPF compared to either CTD-ILD (p=0.033) or chronic HP (p=0.004) (172). CALIPER has demonstrated utility as a predictor of mortality and disease progression in several studies involving various ILD subtypes, which is discussed in detail in section 2.3.1.

2.1.6 Data-driven Textural Analysis (DTA)

DTA involves an unsupervised machine-learning technique which uses a group of unidentified images to perform initial clustering analysis. In an IPF study, DTA fibrosis score was found to correlate with PFTs and visual CT fibrosis score at baseline, and change in DTA fibrosis score correlated with change in DLCO and FVC % predicted over 15 months (178). On multivariate analysis, a DTA score of 5.5% was able to predict a FVC decrease $\geq 5\%$. Another IPF study demonstrated a significant correlation between change in DTA fibrosis score and changes in FVC, DLCO, 6MWD and St George's Respiratory Questionnaire total score (179).

2.1.7 Other texture analysis software

A number of studies have investigated ILD using various types of automated texture analysis software that have not already been discussed above. Using a texture based automated system, *Park et al* were able to successfully differentiate radiologically between histologically proven NSIP and UIP pattern with an accuracy of 82%, which was superior to the radiologists (180). Texture analysis software has been shown to be comparable to visual CT score in assessing the disease extent of CTD-ILD (181, 182), as well as NSIP and UIP pattern (183). Texture analysis software has also been found to correlate with PFTs in IPF (183, 184), NSIP (183) and SSc-ILD (185).

2.1.8 Functional respiratory imaging (FRI)

FRI is a novel simulation technique to measure airway volume and resistance. Specific image-based airway radius (siRADaw) and specific airway volume (siVaw) are the airway measurements that have been investigated in previous FRI studies (186-188). A study involving 66 IPF patients treated with pamrevlumab for 48 weeks found a significant negative correlation between siRADaw at TLC and FVC, and change in FVC was significantly correlated with changes in FRI lung volumes and siRADaw at weeks 24 and 48 (186). siRADaw demonstrated increased sensitivity to longitudinal change than FVC, suggesting that it could be superior in identifying early disease progression.

A recent study used FRI to distinguish between IPF patients with evidence of disease progression, defined using a cut off of 10% absolute FVC decline between two HRCT scans at various time points (188). There was a larger decrease in FRI lung volume in the progressive group compared to the stable group (-740 mL vs -270 mL, $p=0.03$). A significant increase in siVaw was seen in the progressive group compared to the stable group (6ml/L vs -0.57ml/L, $p=0.0002$). A significant correlation was found between change in siVaw and change in FVC ($r^2=0.39$, $p=0.001$). Further prospective studies are needed, but FRI appears to be a useful QCT method in the assessment of IPF.

2.1.9 Deep learning algorithms

Deep learning, a subcategory of machine learning, has been used to train an algorithm to classify HRCT scans from patients with fibrotic ILD and this algorithm has been validated against an independent group of 91 thoracic radiologists (189). The algorithm was slightly more accurate than the thoracic radiologists at distinguishing between UIP and non-UIP cases (C-index: 0.85 vs 0.79). The authors suggested that the algorithm could be useful for the stratification of patients in clinical studies and to provide diagnostic support to centres with a lack of expertise in thoracic imaging. The advantage of this deep learning approach is that the algorithm automatically learns the important features of the HRCT scans which might not be apparent to humans.

2.2 Magnetic resonance imaging

Pulmonary MRI has historically been limited by the low signal to noise ratio (SNR) in the lungs which is mainly due to low proton density, motion artefacts and fast T2 decay secondary to air-tissue interfaces (190, 191). However, improvements in image reconstruction and gradient performance with the introduction of ultra-short echo time (UTE) proton (^1H) MRI have led to advances in the structural image quality and reduced scan time (191). Most of the MRI studies in ILD are limited by a small number of patients and a lack of validation. The use of hyperpolarised 129-xenon (^{129}Xe) MRI has demonstrated an exciting opportunity to develop MRI as a valuable tool to monitor ILD longitudinally due to the lack of radiation and the ability to quantify functional impairment as well as abnormal morphology simultaneously. Another key advantage of pulmonary MRI is its ability to provide regional functional information that is not possible with the use of PFTs which enable a global assessment of lung function only.

2.2.1 Proton MRI

MRI technology has advanced significantly since McFadden *et al* first published the use of ^1H MRI to stage activity of ILD in 1987 (192). They found no correlation between any MRI values and chest radiograph or gallium scan scores in 34 patients with different types of ILD using 0.15T MRI. Over the subsequent three decades, a number of ^1H MRI studies have investigated its value in the assessment of various ILD subtypes. An early study suggested that when compared to thoracic HRCT imaging, 1.5T spin-echo MRI is inferior at identifying pulmonary fibrosis as well as in the anatomic assessment of the lung parenchyma of patients with chronic infiltrative lung diseases (193).

With the introduction of UTE MRI, the diagnostic accuracy of ^1H MRI in ILD has been found to be almost comparable with that of HRCT (194-196). The majority of ^1H MRI studies in ILD have used 1.5T MRI. However, studies have also reported the utility of 3T ^1H MRI in the evaluation of ILD (195-198). One such study found that 93% of the segments showing abnormalities on CT were also identified by MRI, and that by using respiratory gating, motion artefacts were reduced (197). Another study using 3T ^1H MRI with a T2-weighted turbo spin echo sequence suggested that high field MRI may be useful to determine the activity of ILD (198). ILD was defined as active if the signal

intensity in the lung was twice or higher in high signal areas (e.g. pleural fluid, cerebrospinal fluid) compared to intermediate signal areas (e.g. muscle). Using this definition 12 out of 21 cases were felt to represent active disease on MRI, whereas 14 of the 21 cases were felt to represent active disease when using histology, blood tests and PFTs. Patterns of disease using 1.5T ^1H MRI have been shown to correlate with histopathology on lung biopsies in patients with chronic infiltrative lung disease, including IPF and HP (199).

A recent prospective study reported significantly reduced mean lung T_1 in 19 IPF patients compared to 10 healthy volunteers (1.08 ± 0.09 vs 1.21 ± 0.14 ; $p=0.028$) when acquired during free breathing but not when using breath-hold manoeuvres (200). There was no significant longitudinal change in mean lung T_1 in the patients with IPF when assessed at a six-month study visit. Using 3D-UTE MRI and T_2 BLADE at 1.5T, a study recently found significantly higher T_2 signal-intensity volume in 21 patients with IPF compared to four control subjects without ILD (201). T_2 signal-intensity volume was significantly correlated with CPI ($r=0.48$; $p<0.05$) and FVC ($r=0.50$; $p<0.05$).

Two studies investigating the utility of ^1H MRI in the assessment of CTD-ILD have been published (194, 195). Using UTE 3T MRI, Ohno *et al* found a statistically significant difference in the mean T_2^* value between 18 consecutive patients with CTD-ILD and eight healthy volunteers (195). There was a moderate correlation between the mean T_2^* value and visual CT disease severity score in the CTD-ILD group ($r=0.57$; $p=0.01$) with the authors suggesting that UTE MRI can be considered as a potential imaging biomarker in the management of patients with CTD-ILD. A retrospective study using a T_2 -weighted ultrafast SE sequence on a 1.5T MRI scanner in 18 patients with SSc also demonstrated a strong correlation between median MRI extent values and visual extent of ILD measured by HRCT ($r=0.85$; $p<0.001$) (194). In addition, there was a negative correlation between median MRI extent values and both FVC ($r=-0.60$; $p=0.01$) and D_{Lco} ($r=-0.79$; $p=0.04$).

A major difficulty in the diagnosis of ILD is confidently differentiating between UIP and NSIP pattern. This has been investigated in a small study of six patients with NSIP and six patients with UIP pattern (202). A correlation was found between T_2 relaxation time and fibrotic tissue concentration which the authors explained was due to the proportion of the regional water molecules motion restriction and the level of tissue

density resulting in higher T2 relaxation values in honeycomb areas of the lung. A larger study by the same group published two years later confirmed a strong positive correlation between T2 relaxation and ^1H density in NSIP ($r=0.64$; $p<0.001$) but this correlation was weak in UIP ($r=0.20$; $p=0.01$) (203). In the NSIP group, those with suspected inflammatory activity had statistically significant increased T2 relaxation times compared to those with suspected stable disease. Unfortunately, the difference in T2 relaxation times between UIP and NSIP was not statistically significant, thereby suggesting that T2 weighted ^1H MRI is not a reliable method to differentiate between these two important radiological patterns of ILD. Ongoing development of ^1H MRI sequences is likely to be necessary before highly accurate identification of the radiographic pattern of ILD is possible (204).

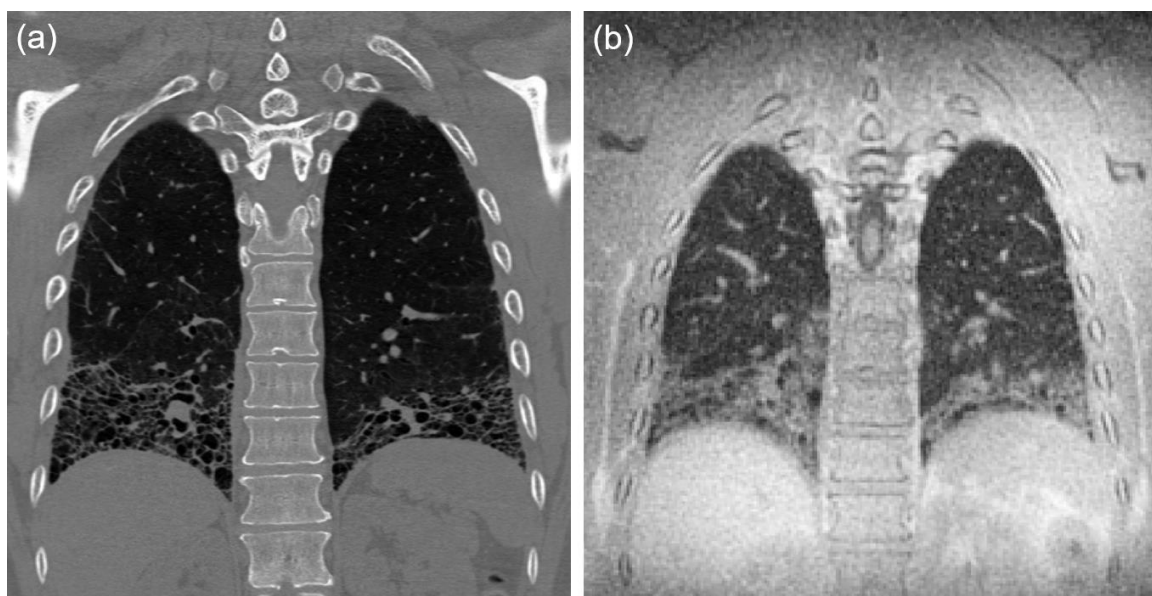


Figure 2.3. Examples of HRCT (a) and ^1H UTE-MRI (b) images in an IPF patient.

2.2.2 Dynamic contrast enhanced and vascular MRI

Dynamic contrast enhanced (DCE) MRI enables the enhancement pattern of a tissue to be analysed, resulting in quantifiable measurements of microvascular function and lung perfusion at the capillary level. Images are acquired at baseline without contrast, then during and after the injection of a paramagnetic contrast agent (CA) into the bloodstream, thereby generating positive enhanced T1 weighted images. As the CA travels through the tissue, it changes the MR signal intensity (SI) of the tissue and the

signal that is acquired is used to produce a time intensity curve which can be analysed to generate measurements of microvascular blood flow (205).

Semi-quantitative values are generated directly from the SI curve and do not involve demanding data acquisition (206). Table 2.1 lists the first pass semi-quantitative metrics most commonly used in DCE-MRI. The disadvantage of using these semi-quantitative metrics is that it is unclear to what extent they contribute to the MR-signal (207). Another issue is that they are dependent on several factors including the CA properties, injection protocol, hardware settings, scan duration, sequence parameters and volume of CA injected, thereby making a comparison of semi-quantitative studies difficult (205). However, these semi-quantitative metrics reflect physiological mechanisms and measurements of the relative changes in an individual or a group of patients are useful.

Parameter	Definition
Initial area under the curve	A calculation of the area under the concentration time curve of a tissue
Maximum (relative) enhancement (%)	Maximum signal difference (difference between the maximum SI and the signal baseline) / signal baseline
Maximum rate of change of enhancement (%/min)	Maximal intensity change per time
Rate of enhancement (%/min)	$[(SI_{max} - SI_{base}) / (SI_{base} \times T_{max})] \times 100$
Rate of peak enhancement (%/min)	$[(SI_{end} - SI_{prior}) / (SI_{base} \times T)] \times 100$
T90 (sec)	Time taken to attain 90% of the subsequent maximal enhancement of a tissue
Time to maximum signal intensity (sec)	Time between the arterial peak enhancement and the end of the steepest portion of signal intensity
Time to peak enhancement (sec)	Time between the arterial peak enhancement and the end of the steepest portion of enhancement

SI: Signal intensity; T: Time

Table 2.1. First pass semi-quantitative metrics used in DCE-MRI. Modified with permission from AME Publishing Company (205).

First pass methods, which assume that the early enhancement pattern represents the CA kinetics has also been utilised semi-quantitatively in DCE-MRI, especially in myocardial perfusion studies (208). Using the first pass perfusion signal enhancement, parametric maps of pulmonary blood flow (PBF), pulmonary blood volume (PBV) and mean transit time (MTT) can be generated (209). An example of a time series of perfusion images and the MTT parametric map generated from them in an IPF patient is shown in Figure 2.4. Significant changes in pulmonary perfusion during breath-hold at different inspiratory levels have been reported, with increased PBF and PBV, but reduced MTT seen during expiration compared to inspiration (210).

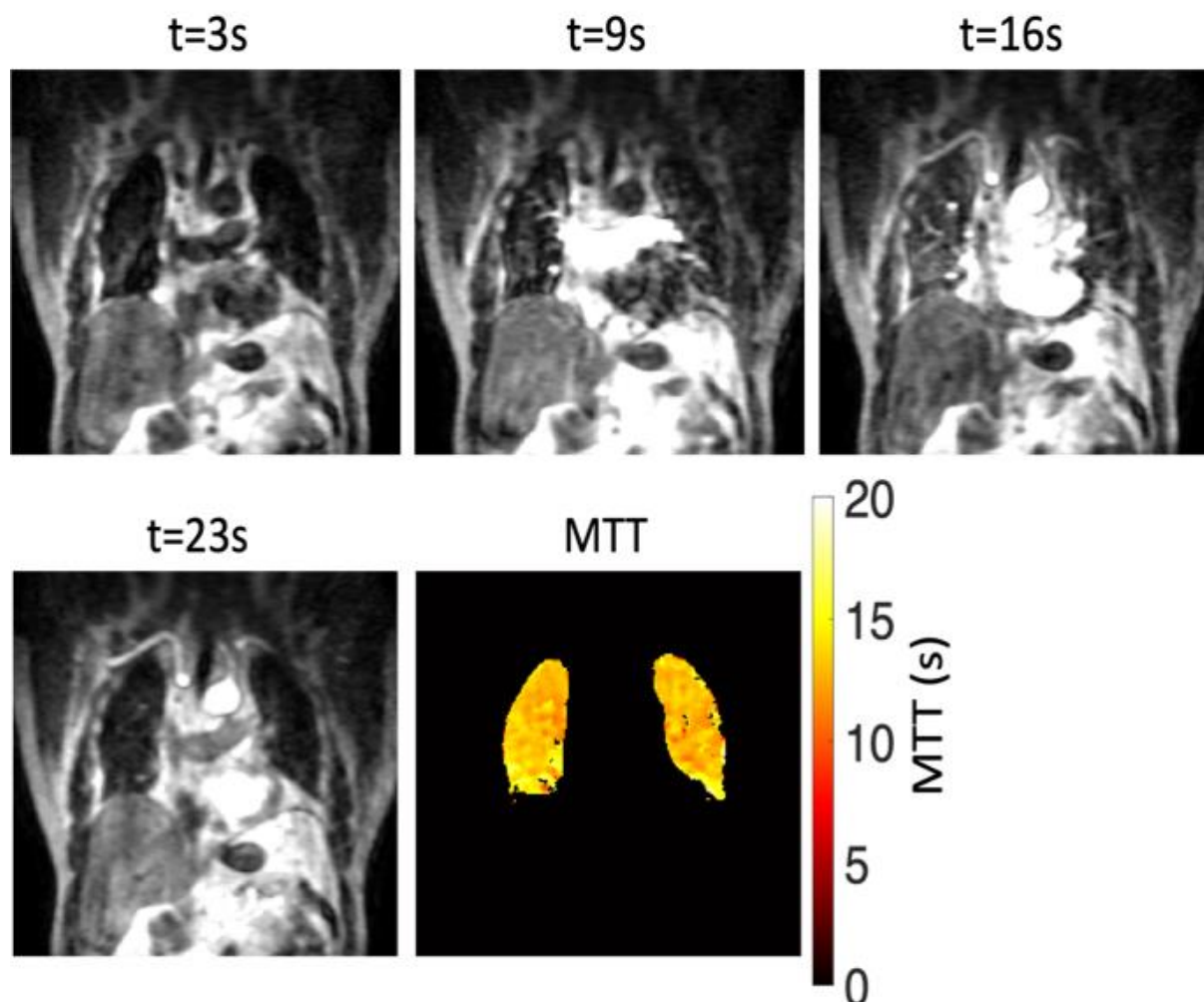


Figure 2.4. Example of a time series of perfusion images and the MTT parametric map generated from them in an IPF patient.

The full width of half maximum (FWHM) of the first pass perfusion signal enhancement (Figure 2.5) is similar to MTT but has the advantage of standardising for the amplitude of contrast. This approach was used in a recent publication by Weatherley *et al*, which reported a statistically significant increase in mean FWHM ($p=0.040$) over a 6-month period, with a decrease in FVC ($p=0.040$) and K_{CO} ($p=0.014$), but no significant change in D_{LCO} ($p=0.090$) (211).

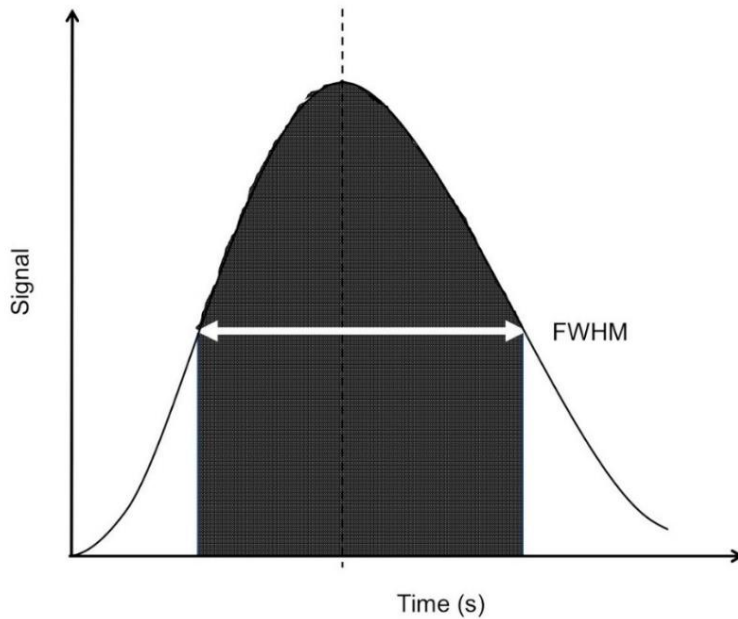


Figure 2.5. Representation of FWHM in DCE-MRI.

Quantitative DCE-MRI analysis, involving mathematical curve-fitting methods, are able to generate parameters that reflect the physiological properties of the vasculature directly and its main advantage over the semi-quantitative metrics is that it creates absolute numbers enabling comparability between studies (205).

T1-weighted DCE-MRI has been shown to be of value in distinguishing between inflammation and fibrosis predominant lesions with the majority (82%) of inflammation predominant lesions having an early enhancement pattern (212). There were significant differences in the quantitative analysis of DCE-MRI when comparing the inflammatory and fibrotic lung regions, with the areas of inflammation predominant lesions showing a faster slope of enhancement, shorter time to peak enhancement and a greater percentage signal intensity at one minute.

A small pilot study demonstrated that pre-gadolinium administration, when compared to normal lung tissue in ten healthy volunteers and ten patients with IPF, the T1 value of fibrotic lung regions was significantly increased ($p=0.02$) (213). Ten minutes post-gadolinium, the T1 value in both normal and fibrotic lung tissue in the IPF patients was significantly higher than in the healthy volunteers ($p=0.001$). However, from 20 minutes after the administration of gadolinium the T1 values from areas of fibrotic lung was significantly reduced compared to normal lung in patients with IPF ($p<0.05$), indicating continuous uptake of contrast in the fibrotic tissue. Another study also demonstrated that late enhanced (10-12 minutes post gadolinium administration) MRI signal was significantly increased in 20 IPF patients compared to 12 healthy volunteers (10.5 ± 1.6 vs 8.5 ± 1.5 ; $p=0.01$) (214). There was a strong correlation ($r=0.78$; $p<0.001$) between the degree of pulmonary fibrosis on late enhanced MRI and HRCT. These two studies suggest that MRI using delayed gadolinium contrast enhancement techniques may have a role in detecting early fibrotic changes in patients with IPF as well as quantifying the extent of lung fibrosis. Gadofosveset-enhanced MRI in IPF subjects has demonstrated increased vascular leak by directly imaging albumin extravasation when compared to healthy controls (215).

Velocity sensitised imaging, using phase contrast (PC) MRI has been investigated by Tsuchiya *et al* (216, 217). An initial study found that in 11 patients with ILD, both pulmonary and systemic blood flow was decreased compared to 15 healthy volunteers (216). A larger study published three years later in 30 patients with ILD showed that PBF had a positive correlation with lung volume on CT and a negative correlation with visual CT score of fibrosis severity (217).

2.2.3 Other functional proton MRI methods

2.2.3.1 Oxygen enhanced MRI

With the use of T1 weighted pulse sequences, oxygen enhanced (OE) MRI of the lungs involves image acquisition while the subject is breathing room air, then high flow oxygen. Oxygen acts as a weak paramagnetic T1 shortening contrast agent, resulting in SI changes in areas of the lungs in which oxygen diffuses from the alveoli into the

interstitial tissue and capillaries (218). The potential advantages of OE-MRI over hyperpolarised gas MRI techniques are that it doesn't require any hardware modifications to the MRI scanner and oxygen is cheap and readily available. However, the disadvantages are its relatively low SNR and the possibility of changing lung physiology with the administration of high flow oxygen (219). Also, the requirement of respiratory gating and the lengthy acquisition times results in lengthy scan times of up to 20 minutes (74).

Muller *et al*/reported a statistically significant difference in the SI changes and SI slopes between 17 patients with various pulmonary diseases (including 12 with IPF and one with HP) and 11 healthy volunteers (218). A strong correlation was seen between the SI slope values and D_{LCO} but the correlation was weak between SI change values and D_{LCO} . The number of oxygen activated pixels over the total number of pixels in the regions of interest has been shown to be significantly lower in ten consecutive patients with ILD (eight IPF, one NSIP, one sarcoidosis) compared to 12 healthy volunteers (36.7% vs 81.7%, $p=0.001$) (220).

OE-MRI, using the mean relative enhancement ratio (MRER) has been compared to a visual CT disease severity score in the assessment of CTD-ILD (221). A statistically significant difference between patients with CTD-ILD ($n=36$) and those with CTD but no evidence of ILD ($n=9$) was seen with both OE-MRI and HRCT. In the patients with CTD-ILD there was a strong correlation between MRER and K_{CO} ($r=0.75$; $p<0.0001$), and a moderate correlation between MRER and visual CT disease severity score ($r=0.42$; $p<0.05$). There were no significant differences in the sensitivity, specificity or accuracy between MRER and visual CT disease severity score.

2.2.3.2 Magnetic resonance elastography

A study by Marinelli *et al* used magnetic resonance elastography (MRE) to quantify the difference in topographical distribution of shear stiffness between 15 patients with ILD (including eight with IPF) compared to 11 healthy volunteers (222). They found that with increasing transpulmonary pressure (from residual volume to total lung capacity) the lung stiffness increased. It would be interesting to see if future studies using MRE in ILD can demonstrate this as a valuable tool in monitoring of disease progression and providing dynamic lung function data.

2.2.4 Hyperpolarised ^{129}Xe MRI

Significant advances have been made over the last decade in the development of hyperpolarised gas MRI. Due to the limited availability and increasing cost of helium (^3He), the last few years have seen a transition to the use of ^{129}Xe as the preferred noble gas (223).

Polarisation is performed using a technique called spin-exchange optical pumping (Figure 2.6) which involves the use of an optical cell containing a small volume of the noble gas, buffer gases and an alkali metal such as rubidium (224). Following polarisation, the MR signal can be increased by up to 100,000 times above thermal equilibrium levels (225). Hyperpolarised ^{129}Xe is usually mixed with nitrogen (N_2) to produce a standardised one litre volume. Once inhaled, it acts as a contrast agent resulting in increased SNR in the airways and lung parenchyma (226). Scans are performed within a single breath-hold, usually lasting less than 15 seconds and patients can have supplemental oxygen delivered via a nasal cannula if required.

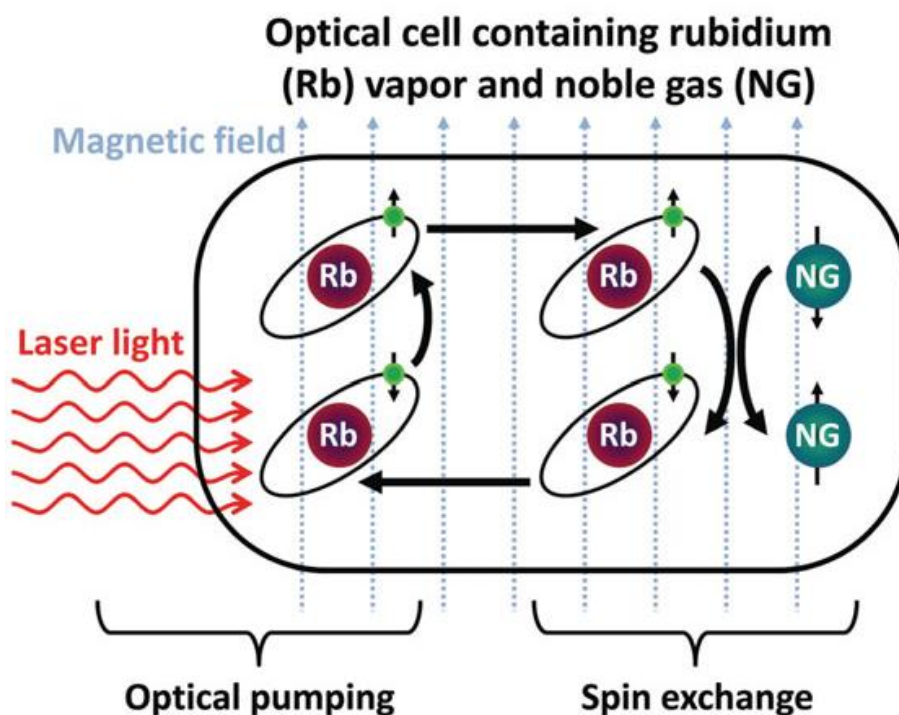


Figure 2.6. Diagram of the spin-exchange optical pumping process. Reproduced with permission from John Wiley and Sons (227).

2.2.4.1 ^{129}Xe MR spectroscopy

Hyperpolarised ^{129}Xe MRI is an ideal imaging modality for the assessment of gas exchange in ILD. ^{129}Xe is soluble in lung tissue and blood and exhibits distinct resonances as it dissolves from the airways through the tissue plasma (TP) barrier into the red blood cells (RBCs) in the pulmonary capillaries (74). Compared to the gas phase in the alveoli, the resonance of ^{129}Xe in the TP shifts by 197 ppm then by 218 ppm in the RBCs (Figure 2.7), thus allowing the uptake of ^{129}Xe in these compartments to be measured separately (228).

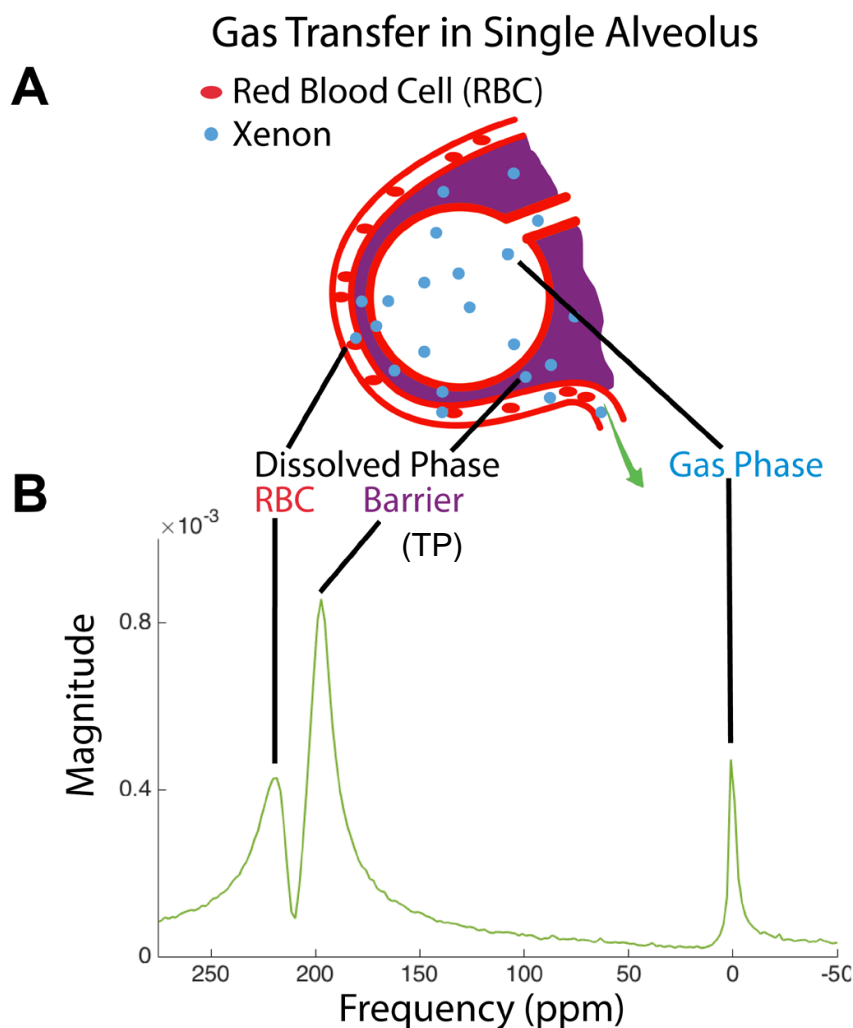


Figure 2.7. Diagram of ^{129}Xe transfer from alveoli into capillary RBCs (A). ^{129}Xe spectrum exhibits three distinct resonances in the lung (B). Reproduced with permission from BMJ Publishing Group Ltd (229).

Using hyperpolarised ^{129}Xe magnetic resonance spectroscopy (MRS) as a global measure of gas exchange, Kaushik *et al* demonstrated that the ratio of the ^{129}Xe signal in the RBCs versus the TP barrier (RBC:TP) was significantly reduced in six patients with IPF compared to 11 healthy volunteers (0.16 ± 0.03 vs 0.55 ± 0.13 ; $p < 0.0002$) (230). There was a very strong correlation between the RBC:TP and DLco ($r = 0.89$; $p < 0.0001$) in all subjects. In the healthy volunteers, the RBC:TP was highly reproducible when repeated on the same day but there was a mean difference of 8.25% ($p = 0.01$) in RBC:TP when repeated on different days. The RBC:TP is dependent on the flip angle and repetition time (TR) which need to be standardised to be able to compare measurements between studies (223).

A preliminary study using the hyperpolarised ^{129}Xe chemical shift saturation recovery technique compared ten healthy volunteers with four IPF patients and four patients with SSc (231). There was a statistically significant difference in RBC:TP between the healthy volunteers (0.42 ± 0.18) and the eight patients. No statistically significant difference was seen between the patients with IPF (0.13 ± 0.04) and SSc (0.18 ± 0.04).

A study evaluating the sensitivity of ^{129}Xe MRS to longitudinal change in patients with IPF demonstrated statistically significant median changes over 12 months in RBC:TP ($p = 0.001$) and FVC ($p = 0.048$) but not DLco ($p = 0.881$) (232). There was a statistically significant correlation between baseline RBC:TP and DLco ($r = 0.677$), but not FVC ($r = 0.336$). MRS repeated on the same day in ten subjects demonstrated highly reproducible RBC:TP (intraclass correlation coefficient (ICC): 0.96). This is consistent with a study using a 3D radial 1-point Dixon ^{129}Xe MRS method in 14 healthy volunteers which reported that mean RBC:TP is reproducible (ICC: 0.92) over an approximately one month interval (233).

Hyperpolarised ^{129}Xe MRS has been developed further to investigate regional gas exchange impairment in IPF by using a single, UTE one-point Dixon acquisition (229, 234, 235). Using this method, Kaushik *et al* were able to produce isotropic 3D images showing defects in focal gas exchange in three subjects with IPF (234). The regions of reduced RBC:TP were seen at the bases and periphery of the lungs where fibrotic changes were present on CT. However, 28% of the ^{129}Xe MRS abnormalities were identified in areas of normal lung on CT suggesting that this imaging technique may be able to detect subtle regions of inflammation.

Semi-quantitative binning maps have been developed to allow visualisation of increased TP uptake and reduced RBC transfer in IPF patients (235). Following on from this, Wang *et al* compared the spatial distribution of ^{129}Xe gas transfer MRI with PFTs and visual CT fibrosis scores in 12 subjects with IPF and 13 healthy volunteers (229). Overall, when compared with healthy volunteers the patients with IPF had a 188% higher mean TP barrier uptake, which suggests impairment of gas exchange. In the IPF cohort, RBC transfer was reduced significantly in the peripheral and basal lung regions (Figure 2.8), which corresponds with a UIP pattern seen on CT. There was a weak correlation between the visual CT fibrosis score and all mean ^{129}Xe MRI values including global RBC:TP ($r=-0.05$; $p=0.88$). Significant correlations were found between all ^{129}Xe MRI values and PFTs (except ventilated volume (VV) and D_{LCO}), with the strongest correlation seen between global RBC:TP and D_{LCO} ($r=0.94$; $p<0.01$).

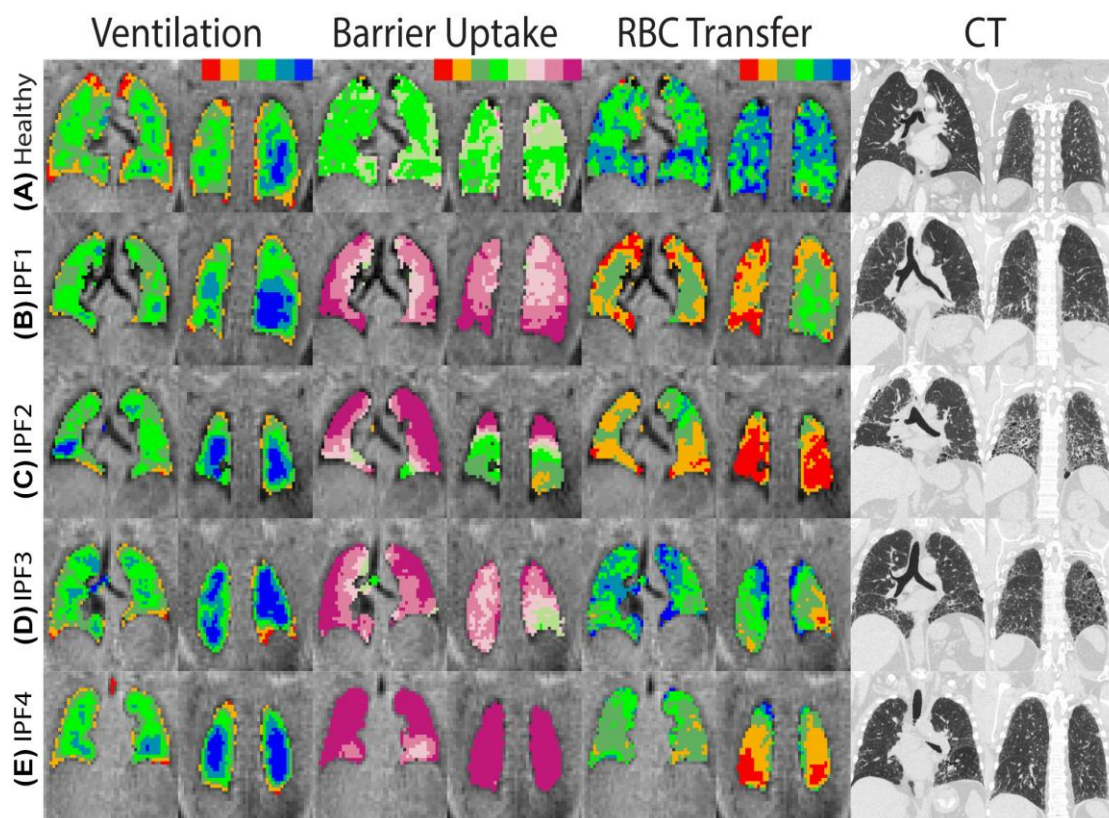


Figure 2.8. Central and posterior coronal slices of ventilation (red=ventilation defects, blue=high), barrier uptake (red=low, plum/orchid=high) and RBC transfer (red=low, blue=high), binning maps and CT images in 1 healthy volunteer and 4 IPF patients. Reproduced with permission from BMJ Publishing Group Ltd (229).

^{129}Xe MR spectra can be acquired dynamically every 20ms to quantify cardiogenic oscillations in the RBC signal amplitude and frequency shift, with studies demonstrating significantly increased ^{129}Xe RBC amplitude and shift in IPF patients compared to healthy volunteers and other diseases (Figure 2.9) (236, 237). Increased RBC amplitude oscillations were also found in patients with left heart failure, which suggests that this could be due to changes in capillary blood volume during the cardiac cycle and secondary to post-capillary PH (237).

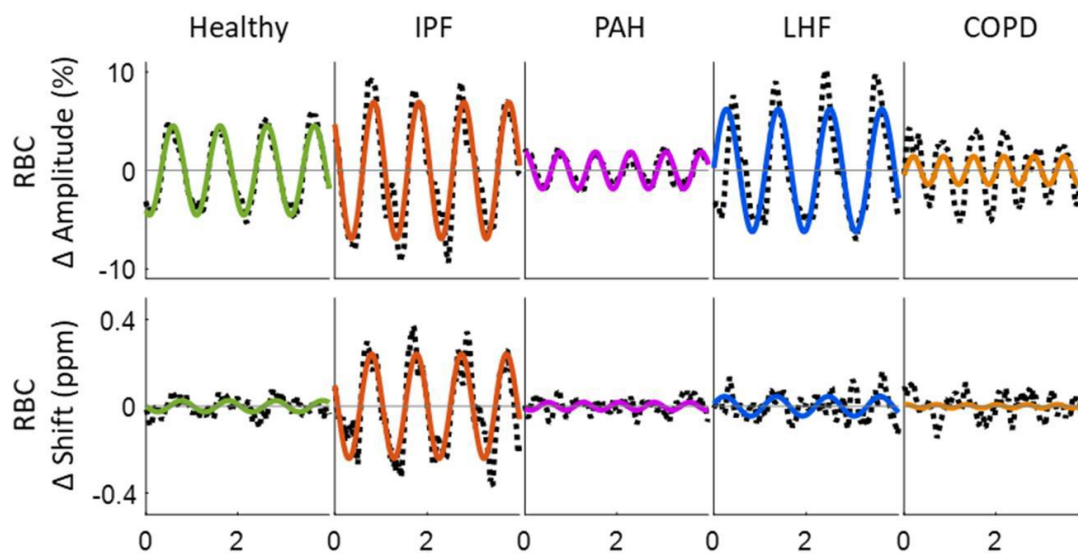


Figure 2.9. RBC signal amplitude and frequency shift in various diseases (237).

Reproduced with permission of the © ERS 2020: European Respiratory Journal 54 (6) 1900831; DOI: 10.1183/13993003.00831-2019 Published 12 December 2019.

2.2.4.2 Diffusion-weighted MRI

Apparent diffusion coefficient (ADC) is a measure of Brownian diffusion of gas in airspaces, where restrictions by tissue boundaries provide novel information about lung microstructure down to the alveolar level (Figure 2.10). ADC values are proportional to the average alveolar dimensions and are dependent on MRI factors such as the degree of diffusion weighting and the time delay (191). The size of the alveoli is related to the lung inflation volume and the volume of gas inhaled, and thus can affect the ADC values obtained (238). ^{129}Xe diffusion weighted (DW) MRI of the lung in emphysema patients shows increased ADC as a result of damage to the alveolar wall (239).

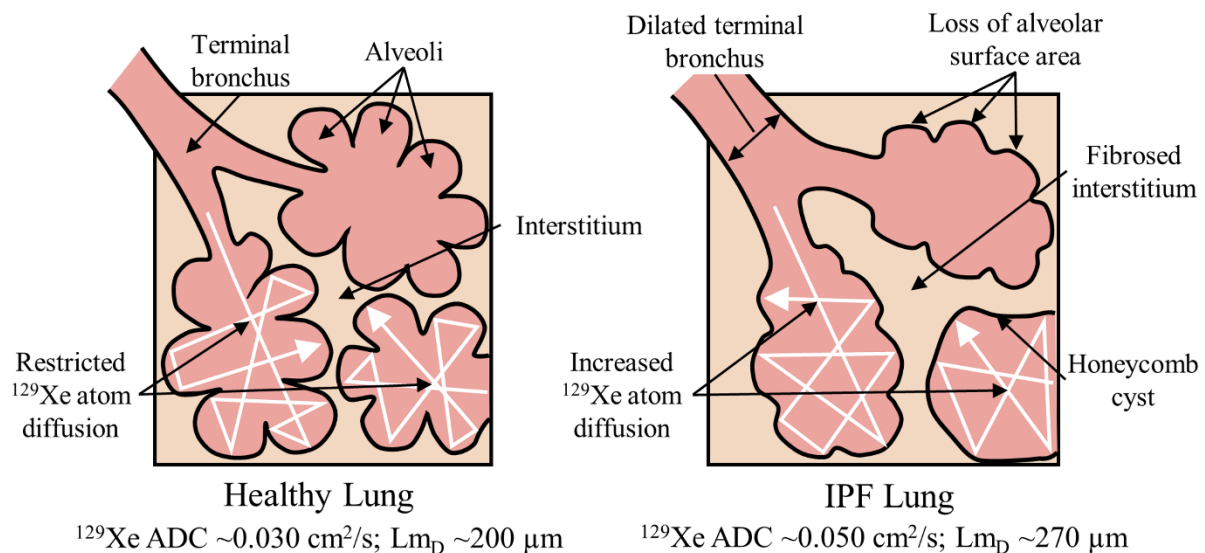


Figure 2.10. Schematic of ^{129}Xe gas diffusion (white arrows) in a healthy lung and an IPF lung. Reproduced with permission from RSNA publications (240).

The mean diffusive length scale (L_{mD}), is a DW-MRI lung microstructure measurement calculated using a stretched exponential fit method (241). A DW-MRI study using hyperpolarised ^3He in patients with IPF demonstrated that both ADC and L_{mD} correlate with D_{LCO} , K_{CO} and regional fibrosis on CT (240). There was no significant longitudinal change in ADC, FVC or D_{LCO} , although L_{mD} increased significantly over 12-months ($p=0.001$). DW-MRI repeated on the same day in 11 subjects demonstrated that ADC and L_{mD} values are highly reproducible. The authors suggested that the increased ADC and L_{mD} measurements seen in IPF are due to the reduced acinar integrity as a consequence of microstructural changes in the lung secondary to fibrosis. Significant correlation has been found between ^3He ADC and ^{129}Xe ADC (242). To date, no data are available on the utility of ^{129}Xe diffusion in ILD.

2.2.4.3 Ventilation imaging

Hyperpolarised gas MRI is commonly used to visualise the distribution and homogeneity of lung ventilation. Ventilation defects, due to the absence of hyperpolarised gas in affected regions of the lung can be caused by constriction or obstruction of the airway (238). The $VV\%$ can be calculated quantitatively by co-registering the ^1H lung images and hyperpolarised gas MRI ventilation images (243).

The ventilation defect percentage (VDP), a quantitative measurement of unventilated lung volume, has been shown to be greater using ^{129}Xe when compared to ^3He in patients with asthma, suggesting that ^{129}Xe is more sensitive to airway abnormalities than ^3He (244). In IPF patients, ^{129}Xe VDP has been reported to be significantly increased compared to healthy volunteers ($p \leq 0.01$), but significantly reduced compared to patients with chronic obstructive pulmonary disease (COPD) ($p \leq 0.02$) (237). ^{129}Xe ventilation has been shown to be significantly correlated with FVC ($r=0.39$, $p=0.04$) but not D_{LCO} ($r=0.35$, $p=0.06$) when IPF patients and healthy volunteers were combined into one group (229).

2.3 CT and PFT biomarkers predicting mortality and/or disease progression in ILD

The following section lists the CT and PFT biomarkers that have been found to predict mortality and/or disease progression in ILD. It will focus on the following ILD subtypes: CTD-ILD, DI-ILD, HP, iNSIP and IPF.

2.3.1 Computed tomography (quantitative CT and visual CT scores)

Numerous studies have evaluated various lung density and/or histogram measurements to predict mortality in IPF (127, 128, 133, 135, 151, 245), NSIP (127, 128) and SSc-ILD (246). H-pattern volumes in the subpleural area within 2 mm under the pleura (128), kurtosis (127, 133, 246), skewness (133), MLD (133), high attenuation area percent (HAA%) (133) and honeycomb (F2) pattern volume by GHNC (135) have all been shown to be significant predictors of mortality. A study including 70 IPF patients reported that a novel CT histogram parameter, the area right of the inflection point was the only prognostic factor (among age, sex, D_{LCO} , FVC, kurtosis and skewness) that demonstrated significance on multivariate regression analysis (245). In an IPF study, increased HAA% was found to be associated with the highest risk of death when compared to MLD, kurtosis and skewness (133). In a study involving 167 patients with IPF, kurtosis and skewness were not superior to a visual CT score in prediction of survival over a median follow-up period of 18 months (151).

CALIPER is the most extensively studied QCT texture analysis software that has demonstrated prognostic utility in ILD. In the first study using CALIPER in IPF, changes in CALIPER measurements, including volumes of reticular opacity and honeycombing over a period of 3-15 months were predictive of survival (165). Following this study, Jacob *et al* showed that in 283 IPF patients, CALIPER values were better at predicting death than visual CT scores, and using a combination of CALIPER and CPI was superior than the gender-age-physiology (GAP) index (168). Out of all the CALIPER derived variables investigated, the best predictor of mortality was pulmonary vessel volume (PVV) which quantifies the volume of pulmonary veins and arteries (excluding the lung hilum vessels) as a percentage of total lung volume. The pathophysiological mechanism is not yet fully understood; however various hypotheses have been proposed (105). In another IPF study by Jacob *et al*, CALIPER derived vessel related structures (VRS) in the upper zone was the strongest predictor of death and/or 10% FVC decline at 12 months, outperforming CPI, GAP score, GAP index and PFTs (169). An IPF study, using a QCT model based on CALIPER identified parenchymal damage and vessel percentage as independent predictors of mortality, but they were inferior compared to the GAP index (247). Using CALIPER, ILD score (combining GGO, reticulation and honeycombing) $\geq 20\%$, and VRS $\geq 5\%$ have been found to predict 3-year mortality in a recent study involving 105 patients with IPF (248).

Jacob *et al*, have also used CALIPER to investigate its prognostic utility in CTD-ILD and HP. In a study involving 203 patients with various types of CTD-ILD, PVV was found to be the most superior CALIPER measurement in predicting survival and when CALIPER variables were combined with the ILD-GAP model, it was better at predicting death than the original model (173). In a study of 116 HP patients, PVV was a better predictor of mortality than CPI and PFTs, with a significant quantity of patients having an outcome similar to that of IPF (176). As in the CTD-ILD study (173), the prognostic accuracy of the ILD-GAP model was improved when CALIPER variables were combined with it in a study involving 98 patients with HP (177). The independent prognostic value of CALIPER VRS was demonstrated in a recent study involving 225 subjects with various ILD subtypes including CTD-ILD, chronic HP and IPF (172).

CALIPER has been incorporated into mortality risk prediction models in two recent IPF studies (Table 2.2) (249, 250). In a multicentre prospective study of 185 IPF patients, a revised version of the CPI using CALIPER was found to be a superior predictor of

18-month survival compared to the original CPI and the GAP index (249). A small (n=58) multicentre Italian IPF study reported that a combination of FVC decrease $\geq 10\%$ and relative increase of CALIPER-total lung fibrosis $\geq 20\%$ over 12 months was a useful predictor of mortality, but it was slightly inferior to a combination of GAP score and pack-years of smoking (250).

Variables	C-statistic (95% CI)	
	Hosein <i>et al</i> (249)	Sverzellati <i>et al</i> (250)
CALIPER-revised CPI >28	0.75 (0.68-0.82)	
CALIPER-revised CPI increase over 6 months	0.65 (0.55-0.74)	
CPI >54	0.66 (0.58-0.72)	
CPI increase over 6 months	0.61 (0.51-0.70)	
FVC decrease $\geq 10\%$ and disease progression visually on CT over 12 months		0.64
FVC decrease $\geq 10\%$ and relative increase of CALIPER-total lung fibrosis $\geq 20\%$ over 12 months		0.69
FVC% decrease and disease progression visually on CT over 24 months		0.60
FVC% decrease and relative increase of CALIPER-VRS $\geq 20\%$ over 24 months		0.65
GAP score + pack-years of smoking		0.71
GAP score + pack-years of smoking + reticular pattern on CT (visual scoring)		0.60
GAP + pack-years of smoking + reticular pattern (CALIPER) + VRS		0.64
GAP stage 3	0.74 (0.67-0.80)	
GAP stage increase over 6 months	0.57 (0.48-0.67)	

CALIPER: Computer-Aided Lung Informatics for Pathology Evaluation and Rating; CPI: composite physiology index; FVC: forced vital capacity; GAP: gender-age-physiology; VRS: vessel related structures.

Table 2.2. Mortality risk prediction models incorporating CALIPER.

Using data from the PANTHER-IPF trial, AMFM ground glass reticulation score was shown to be independently related to an increased risk of disease progression, either as a categorical variable per 10% increase (OR 1.36; 95% CI 1.01-1.84; p=0.04) or using a cut of value $\geq 10\%$ (OR 2.60; 95% CI 1.24-5.45; p=0.01) (157). A study in the USA involving 134 patients with IPF found a link between decline in FVC $\geq 10\%$ and

an increase in QLF score $\geq 4\%$ over 6 months (OR 3.32; $p=0.021$), as well as increase in QLF score $\geq 4\%$ over 6 months in the most severe lobe (OR 5.92; $p=0.001$) (251).

Multiple variables have been described in studies using semi-quantitative visual CT scoring performed by radiologists, and those that have demonstrated utility as independent predictors of mortality in ILD are shown in Table 2.3.

Semi-quantitative CT variable	ILD subtype
Consolidation	IPF (168)
Cross-sectional area of erector spinae muscles (relative % decline over 6 months)	IPF (252)
Extent of lung disease	HP (253), SSc-ILD (254, 255)
Fibrosis / fibrosis score	Fibrotic NSIP pattern (256, 257), HP (258-262), iNSIP (259), IPF (107, 258, 259, 263-266), SSc-ILD (267), UIP pattern (256, 257)
Fibrosis coarseness	iNSIP (268)
Fibrosis score 11-30%	IPF (264)
Fibrosis score >30%	IPF (264)
Fibrosis score increase >7	IPF (269)
Fibrosis score increase >6.7 over 6 months	IPF (270)
Fibrosis score increase >13.5 over 12 months	IPF (270)
Ground glass	IPF (168, 271)
Ground glass + reticulation	Fibrotic NSIP pattern (257), UIP pattern (257)
Honeycombing	CTD-ILD (111, 272), DI-ILD (273), HP (253, 262), IPF (168, 271, 272, 274, 275)
Interstitial score ≥ 3	IPF (276)
Mediastinal lymph node enlargement	IPF (266)
Mediastinal lymph node $\geq 10\text{mm}$	CTD-ILD (277), HP (277), IPF (277)
Mosaic perfusion / air trapping	HP (47, 261)
Normal lung area $\leq 50\%$	DI-ILD (273)
Oesophageal diameter	SSc-ILD (278)
Pulmonary artery / aorta ratio	IPF (279)
Pulmonary artery / aorta ratio >1	IPF (280)
Reticulation	IPF (168, 271), SS-ILD (281)
Total ILD extent	IPF (271)
Total parenchymal score	IPF (282)
Traction bronchiectasis	CTD-ILD (111), HP (253), IPF (263, 271)
T4 level muscle index	IPF (283)

CTD-ILD: Connective tissue disease associated interstitial lung disease; DI-ILD: Drug induced interstitial lung disease; HP: Hypersensitivity pneumonitis; iNSIP: Idiopathic non-specific interstitial pneumonia; IPF: Idiopathic pulmonary fibrosis; NSIP: Non-specific interstitial pneumonia; SSc-ILD: Systemic sclerosis associated interstitial lung disease; UIP: Usual interstitial pneumonia.

Table 2.3. Semi-quantitative visual CT variables with utility to predict mortality in ILD.

The amount of traction bronchiectasis appears to be most strongly associated with survival in ILD when compared to other CT features. A UK study involving 168 patients with CTD-ILD found that the CT variables that were associated with an increased risk of death were severity of honeycombing (HR 1.08; 95% CI 1.04-1.17; p=0.022) and increasing extent of traction bronchiectasis (HR 1.10; 95% CI 1.02-1.13; p=0.001) (111). Similar findings were demonstrated by the same research group in a study of 92 HP patients, in which reduced survival was linked to severity of macroscopic honeycombing (HR 1.06; 95% CI 1.01-1.10; p<0.01) and increasing extent of traction bronchiectasis (HR 1.10; 95% CI 1.04-1.16; p<0.001), as well as the extent of lung disease (HR 1.02; 95% CI 1.00-1.03; p=0.02) (253). In this study, traction bronchiectasis severity was also reported to be a stronger predictor of mortality when compared with PFTs. The amount of traction bronchiectasis has been shown to be most predictive of survival in IPF when compared to other CT variables including fibrosis score, GGO, honeycombing, reticulation and total ILD extent (263, 271).

In IPF, fibrosis score has been associated with progression free survival (time to FVC decline $\geq 10\%$, DLCO decline $\geq 15\%$ or death) (284) and visual ground glass reticulation score has been found to be predictive of disease progression (decline in FVC $> 10\%$, hospitalisation or death within 60 weeks) (157).

Although semi-quantitative visual CT assessment by radiologists seems to be valuable for prognostic purposes, it is considered as impractical for widespread clinical use due to time limitations and the inconsistent expertise among radiologists causing inter- and intra-observer variability (285). However, the accuracy, sensitivity and speed of QCT make it an attractive alternative compared to semi-quantitative visual CT assessment.

2.3.2 Pulmonary function tests

PFTs are the most extensively studied prognostic biomarkers in ILD, mainly as a continuous variable at baseline, but also using various cut-off values and longitudinal change of varying amounts over different time periods (Table 2.4). Baseline DLCO % predicted and FVC % predicted, as well their longitudinal change, have been found to be independently predictive of survival in multiple ILD studies and are used routinely in the ILD clinic.

Both absolute and relative decline in DLCO % predicted and FVC % predicted have been studied, and it has been reported that using relative rather than absolute FVC % change in IPF patients does not affect prognostic accuracy (286). In IPF, FVC decline is now widely accepted as a surrogate endpoint for death and it was the primary endpoint in the antifibrotic drug trials (25, 26, 287).

Pulmonary function test	ILD subtype
D _{LCO}	IPF (288, 289), SSc-ILD (290, 291)
D _{LCO} % predicted	ASS (292), CTD-ILD (111, 293), iNSIP (36, 293), IPF (36, 107, 293-301), RA-ILD (40, 302)
D _{LCO} <35% predicted	iNSIP (303), IPF (303)
D _{LCO} ≤36% predicted	IPF (304)
D _{LCO} <40% predicted	IPF (305, 306), RA-ILD (307), SSc-ILD (308)
D _{LCO} <43.6% predicted	IPF (309)
D _{LCO} <55% predicted	IPF (310)
D _{LCO} decrease ≥10% over 6 months	IPF (311, 312)
D _{LCO} decrease ≥10% over 12 months	IPF (311)
D _{LCO} decrease ≥15% over 6 months	IPF (311)
D _{LCO} decrease ≥15% over 12 months	IPF (276, 311)
D _{LCO} decrease ≥20% over 6 months	IPF (311)
D _{LCO} decrease ≥20% over 12 months	IPF (311)
D _{LCO} decrease ≥25% over 6 months	IPF (311)
D _{LCO} decrease ≥25% over 12 months	IPF (311)
FEV ₁ decrease ≥5% over 6 months	IPF (311)
FEV ₁ decrease ≥5% over 12 months	IPF (311)
FEV ₁ decrease ≥10% over 12 months	IPF (311)
FEV ₁ decrease ≥15% over 12 months	IPF (311)
FEV ₁ decrease ≥20% over 12 months	IPF (311)
FEV ₁ /FVC ratio	HP (258), IPF (258, 313-315)
FEV ₁ /FVC ratio >0.89	IPF (305)
FVC	SSc-ILD (267, 291)
FVC% predicted	CTD-ILD (293, 316), HP (258, 262, 317-319), IIM-ILD (320), iNSIP (293), IPF (258, 262, 264, 270, 275, 284, 293, 296, 299-301, 316, 321-328)
FVC ≤50% predicted	IPF (329-331)
FVC 51-65% predicted	IPF (330, 331)
FVC ≤63% predicted	IPF (304)
FVC ≤65% predicted	IPF (264)
FVC 66-79% predicted	IPF (330)
FVC <70% predicted	IPF (305)
FVC <80% predicted	IPF (310)
FVC% decrease over 3 months	IPF (32)
FVC% decrease over 6 months	Fibrotic iNSIP (332), IPF (32, 332)

FVC% decrease over 12 months	Fibrotic iNSIP (333), IPF (32, 333)
FVC decrease $\geq 5\%$ over 6 months	IPF (311)
FVC decrease $\geq 5\%$ over 12 months	IPF (311)
FVC decrease 5-9.9% over 6 months	IPF (330, 331, 334)
FVC decrease $\geq 10\%$ over 12-16 weeks	IPF (335)
FVC decrease $\geq 10\%$ over 6 months	IPF (312, 330, 331, 334)
FVC decrease $> 10\%$ over 6 months	IPF (336)
FVC decrease $\geq 10\%$ over 6-12 months	HP (319)
FVC decrease $\geq 10\%$ over 12 months	IPF (311)
FVC decrease $\geq 15\%$ over 12 months	IPF (311)
FVC decrease $\geq 20\%$ over 12 months	IPF (311)
FVC decrease $\geq 100\text{ml}$ over 14 weeks	IPF (337)
FVC/ D_{LCO} ratio	SSc-ILD (291)
Inability to perform D_{LCO}	IPF (289)
K_{CO}	SSc-ILD (291)
$K_{\text{CO}}\%$ predicted decrease over 6 months	Fibrotic iNSIP (333), IPF (333)
K_{CO} decrease $\geq 10\%$ over 24 months	SSc-ILD (291)
Positive vascular index (baseline $K_{\text{CO}}\% \leq 50\%$ and/or K_{CO} decrease $\geq 15\%$ over 6 months)	Fibrotic iNSIP (332), IPF (332)
TLC% predicted	CTD-ILD (272), IPF (272, 294, 313, 338)

ASS: Antisynthetase syndrome; CTD-ILD: Connective tissue disease associated interstitial lung disease; D_{LCO} : Diffusing capacity of the lung for carbon monoxide; FEV_1 : Forced expiratory volume in one second; FVC: Forced vital capacity; HP: Hypersensitivity pneumonitis; IIM-ILD: Idiopathic inflammatory myopathy associated interstitial lung disease; iNSIP: Idiopathic non-specific interstitial pneumonia; IPF: Idiopathic pulmonary fibrosis; K_{CO} : Carbon monoxide transfer coefficient; RA-ILD: Rheumatoid arthritis associated interstitial lung disease; SSc-ILD: Systemic sclerosis associated interstitial lung disease; TLC: Total lung capacity.

Table 2.4. Pulmonary function tests with utility to predict mortality in ILD.

The majority of the PFT cut off values presented in Table 2.4 have demonstrated independent prognostic value in only one study, with most of them involving IPF patients only. However, $D_{\text{LCO}} < 40\%$ predicted (305, 306) and FVC $\leq 50\%$ predicted (329-331) have both demonstrated an independent association with increased risk of death in more than one IPF study. In terms of longitudinal change, D_{LCO} decrease $\geq 10\%$ over 6 months (311, 312), D_{LCO} decrease $\geq 15\%$ over 12 months (276, 311), FVC decrease 5-9.9% over 6 months (330, 331, 334) and FVC decrease $\geq 10\%$ over 6 months (330, 331, 334) have each been reported as an independent predictor of increased mortality in at least two IPF studies.

Using data from two large drug trials, du Bois *et al* identified independent predictors of one-year mortality in 1,099 IPF patients (330). Of the PFTs investigated, the strongest prognostic factor was baseline FVC $\leq 50\%$ predicted (HR 3.90; 95% CI 1.49-10.19; $p=0.006$), followed by FVC decrease $\geq 10\%$ over 24 weeks (HR 3.65; 95% CI 2.03-6.57; $p<0.001$), DLCO decrease $\geq 15\%$ over 24 weeks (HR 2.41; 95% CI 1.19-4.87; $p=0.015$), FVC 51-65% predicted (HR 2.35; 95% CI 1.18-4.78; $p=0.016$), FVC decrease 5-9.9% over 24 weeks (HR 1.95; 95% CI 1.24-3.09; $p=0.004$) and baseline DLCO $\leq 35\%$ predicted (HR 1.74; 95% CI 1.01-2.99; $p=0.046$).

Several ILD studies have also reported that PFTs have utility in the prediction of disease progression (Table 2.5). FVC is considered as the most reliable clinical biomarker of disease progression in IPF and is widely used for this purpose in routine clinical practice (339). However, it has been suggested that decline in FVC should not be used to assess IPF progression if there is $\geq 15\%$ emphysema on HRCT, and that CPI or DLCO should be used instead (340).

Pulmonary function test	ILD subtype
DLCO % predicted	SSc-ILD (341)
FVC % predicted	IIP (327), RA-ILD (UIP) (342)
FVC $<76\%$ predicted	IPF (309)
FVC decrease 5-10% over 6 months	IPF (343)
FVC decrease $\geq 100\text{ml}$ over 14 weeks	IPF (337)
TLC % predicted	IPF (344)

DLCO: Diffusing capacity of the lung for carbon monoxide; FVC: Forced vital capacity; IIP: Idiopathic interstitial pneumonia; IPF: Idiopathic pulmonary fibrosis; RA-ILD: Rheumatoid arthritis associated interstitial lung disease; SSc-ILD: Systemic sclerosis associated interstitial lung disease; TLC: Total lung capacity; UIP: Usual interstitial pneumonia.

Table 2.5. Pulmonary function tests with utility to predict disease progression in ILD.

2.4 Summary

Hyperpolarised ^{129}Xe MRI, combined with ^1H MRI, is able to provide useful regional data of lung structure and function which makes it an appealing tool to explore the diagnosis and monitoring of ILD. CT has some advantages over MRI in terms of its speed, image contrast and spatial resolution but is unable to provide functional data. Various QCT analysis methods have been reported in ILD and there is evidence that texture analysis techniques are superior to visual CT scores performed by radiologists.

Chapter 3: The Assessment of Interstitial Lung Disease Using Imaging Biomarkers – Methods of Two Longitudinal Studies

3.1 Development of imaging biomarkers for the detection and monitoring of drug induced interstitial lung disease (TRISTAN-ILD study): Aims/objectives of the study, eligibility criteria and study design

3.1.1 Brief overview of the study

The TRISTAN-ILD study is a prospective, multicentre, observational, imaging study of patients presenting with suspected DI-ILD and other ILD subtypes including CTD-ILD, HP, iNSIP and IPF from two large tertiary ILD centres: Sheffield and Manchester. The diagnosis of the ILD subtype was established in ILD MDT meetings involving respiratory physicians, thoracic radiologists and pathologists. Recruitment of patients into the study started in February 2018. Recruitment was paused in March 2020 due to COVID-19 restrictions.

The hypothesis is that pulmonary MRI and CT measurements correlate with FVC and/or D_{LCO} in patients with ILD and can provide superior information regarding diagnosis and prognosis when compared with current measurements used in ILD.

The study was given ethical approval by the North West-Liverpool Central NHS Research Ethics Committee under reference 17/NW/0631. It is sponsored by the University of Manchester and is registered with the National Institute for Health Research (NIHR) Clinical Research Network Portfolio, with UK Clinical Research Network (UKCRN) ID 36546. The study received funding from the Innovative Medicines Initiatives 2 Joint Undertaking under grant agreement No 116106. This Joint Undertaking received support from the European Union's Horizon 2020 research and innovation programme and the European Federation of Pharmaceutical Industries and Associations.

3.1.2 Study aims and objectives

The primary aims of the study were to compare pulmonary MRI and CT measurements with FVC and D_{LCO} in ILD patients, and to assess whether these imaging measurements can detect early signs of progression or resolution of disease.

Primary objectives:

- 1) To compare pulmonary MRI and CT measurements with FVC and D_{LCO} in patients with a new diagnosis of ILD or patients with a previous diagnosis of ILD (excluding DI-ILD) who were identified as having a recent significant decline in pulmonary function ($>10\%$ reduction in FVC or $>15\%$ reduction in D_{LCO} within the prior 12 months)
- 2) To compare longitudinal changes in pulmonary MRI and CT measurements with changes in FVC and D_{LCO} in ILD patients.

The secondary aim was to determine if any of the imaging measurements have the ability to discriminate between DI-ILD and the other ILD subtypes.

The secondary objectives were:

- 1) To evaluate the ability of pulmonary MRI and CT measurements at baseline to distinguish between the ILD subtypes.
- 2) To determine the association of changes in MRI measurements with changes on CT between visits 1 and 2.

3.1.3 Eligibility criteria

Inclusion criteria:

- New radiological abnormalities on CT suggesting ILD, or worsening of respiratory symptoms, decline in PFTs (decline in FVC $\geq 10\%$ or $D_{LCO} \geq 15\%$ within 12 months) and progression of radiological abnormalities on CT in a patient known to have non-drug induced ILD
- Age ≥ 18 years
- Ability to provide informed consent
- Ability to perform PFTs

Exclusion criteria:

- Contra-indication to MRI scan
- Renal impairment (Glomerular filtration rate < 30 ml/min)
- Previous allergy to MRI contrast agent (gadolinium)
- Weight >150kg (maximum safe weight for MRI scanner)
- Significant cardio-pulmonary disease (e.g. congestive cardiac failure, bronchiectasis) which could compromise the ability of the imaging measurements to detect abnormalities related to ILD
- Radiotherapy to the lungs within six months of baseline visit
- Clinical, microbiological or radiological evidence of lower respiratory tract infection
- Previous thoracic surgery (e.g. lobectomy) or embolization which could result in distorted pulmonary architecture
- Estimated survival less than six months
- Suspected or confirmed lung malignancy
- MDT concerns regarding the radiation exposure associated with research CT scans if frequent CTs are performed or planned due to other condition(s)
- Pregnancy

3.1.4 Study design

Potential subjects were identified by respiratory physicians during ILD MDT meetings where patients' cases were discussed as part of routine clinical care. During the patient's clinic visit, a patient information sheet (PIS) was provided and the study was briefly discussed with them. Further contact was made by telephone at least 24 hours after issuing the PIS to allow the patient to ask any additional questions. If the patient agreed to participate in the study, a baseline visit was arranged, when informed consent was obtained and a number of initial assessments were performed. For patients recruited in Sheffield, the assessments were performed on the same day as the MRI scan. The assessments were performed within a week prior to the MRI scan in the Manchester subjects. I was responsible for the recruitment and study visits of the Sheffield patients, as well as the ¹²⁹Xe MRI analysis for all subjects. A summary of the data that were collected during the study visits is presented in Table 3.1.

Data/activity	Visit 1	Visit 1A	Visit 2	Visit 3
Consent	X			
Clinical history	X		X	X
Clinical examination	X		X	X
Height	X		X	X
Weight	X		X	X
Questionnaires				
MRC chronic dyspnoea questionnaire	X		X	X
Dyspnoea 12 questionnaire	X		X	X
Leicester cough questionnaire	X		X	X
Short form 36	X		X	X
Patient global assessment	X		X	X
MRI satisfaction survey	X			
Blood tests				
FBC	X		X	X
U&Es	X		X	X
LFTs	X		X	X
CRP	X		X	X
Serum and plasma sample for storage	X		X	X
Whole blood sample for DNA analysis	X		X	X
In patients with RA only:				
Rheumatoid factor	X			
Anti-citrullinated peptide	X			
In CTD patients only:				
Anti-nuclear antibody	X			
Extractable nuclear antigen	X			
Creatinine kinase	X			
In SLE patients only:				
Double stranded DNA levels	X		X	X
Complement levels (C3, C4)	X		X	X
Pulmonary physiology assessments				
FEV ₁	X	X	X	X
FVC	X	X	X	X
D _{LCO}	X	X	X	X
Pulse oximetry	X	X	X	X
Imaging				
HRCT Thorax			X	X
¹ H/ ¹²⁹ Xe MRI	X	X	X	

CRP: C-reactive protein; D_{LCO}: Diffusing capacity of the lung for carbon monoxide; DNA: Deoxyribonucleic acid; FBC: Full blood count; FEV₁: Forced expiratory volume in one second; FVC: Forced vital capacity; ¹H: Proton; HRCT: High resolution computed tomography; LFTs: Liver function test; MRC: Medical Research Council; MRI: Magnetic resonance imaging; U&Es: Urea and electrolytes; ¹²⁹Xe: 129-xenon.

Table 3.1. Data collected at each visit of TRISTAN-ILD study.

The diagnostic HRCT scan was used as the baseline HRCT scan in the study. This scan was de-identified and uploaded via secure server to Bioxydyn Limited where a quality assurance (QA) process was performed within three days of upload. If the CT images failed QA participants were asked to undertake a repeat HRCT scan either on the day that they attended for their MRI scan (Sheffield participants), or alternatively at their local site on another day within two weeks of their MRI scan (non-Sheffield participants).

The timings of the follow-up visits varied by ILD subtype (Figure 3.1). Patients with DI-ILD, HP or iNSIP were expected to clinically and physiologically improve or progress within a six months window; whereas improvements or progression of disease in CTD-ILD and IPF tend to occur over longer periods of time. Therefore, subjects with DI-ILD, HP or iNSIP attended for their second visit at six weeks and their third visit at six months; whereas, the CTD-ILD and IPF subjects attended for their second visit at six months and their third visit at 12 months. In June 2019 an amendment to the study was made to include patients with iNSIP. The amendment also added a study visit between visit 1 and 2 (visit 1A), which took place at two weeks after visit 1 for the subjects with DI-ILD, HP and iNSIP, and at three months after visit 1 for the CTD-ILD and IPF subjects.

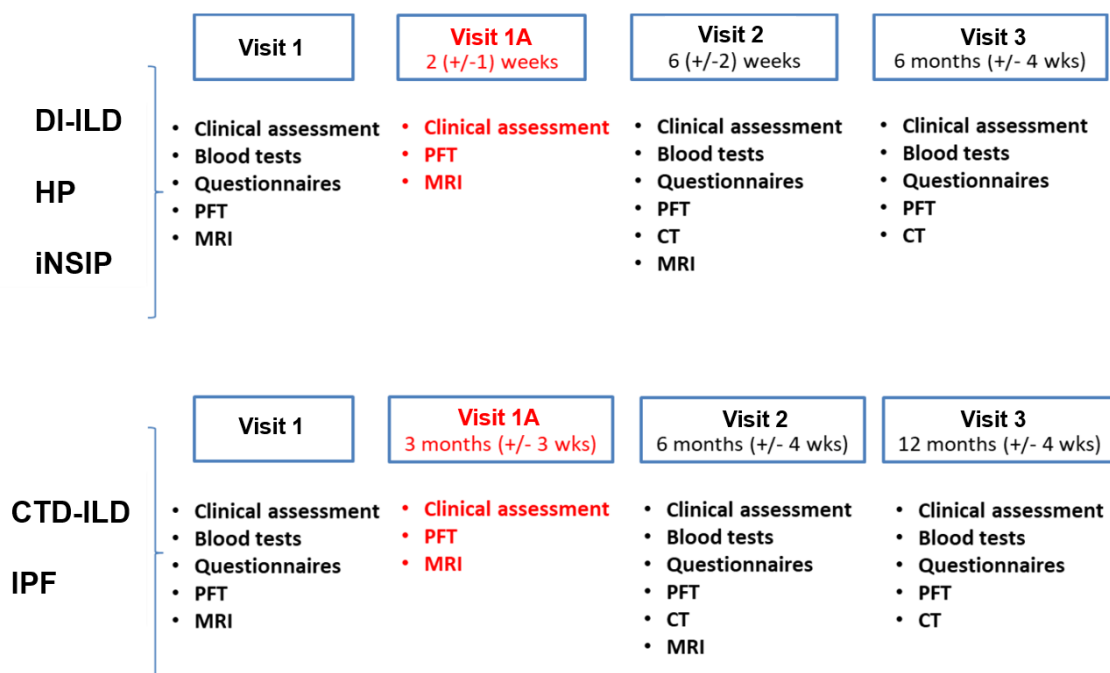


Figure 3.1. Schedule of study visits for each ILD subtype (visit 1A highlighted in red).

3.2 Investigation into prognostic indicators of idiopathic pulmonary fibrosis using structural-functional pulmonary MRI assessment (IPF study): Aims/objectives of the study, eligibility criteria and study design

3.2.1 Brief overview of the study

This is a prospective, single centre, observational, imaging study of patients presenting with IPF to Northern General Hospital, Sheffield. The diagnosis of IPF was based on the most recent official ATS / ERS / JRS / ALAT clinical practice guideline for the diagnosis of IPF (3) and established in ILD MDT meetings involving respiratory physicians and thoracic radiologists. The hypothesis of the study was that longitudinal pulmonary MRI measurements can provide detailed information regarding progression of disease in IPF.

The study was given ethical approval by the North West-Liverpool Central NHS Research Ethics Committee under reference 15/NW/0750. It is sponsored by Sheffield Teaching Hospitals Research and Development (STH18876) and is registered with the NIHR Clinical Research Network Portfolio, with UKCRN ID 20468.

I am continuing the work of Dr Nicholas Weatherley, who recruited 21 IPF patients into the study between February 2016 and February 2018. ^3He DW-MRI, ^{129}Xe RBC:TP and DCE-MRI data from subjects 1-18 of this cohort has been published (211, 232, 240).

3.2.2 Study aims and objectives

The aim of the study was to evaluate the ability of pulmonary MRI measurements to assess prognosis in IPF patients. The primary objectives were to compare the MRI measurements with PFTs, and to assess whether the MRI measurements can detect early signs of disease progression. The secondary objective was to compare changes in pulmonary MRI measurements with changes in CT measurements.

3.2.3 Eligibility criteria

Inclusion criteria:

- Diagnosis of IPF (as determined by the Sheffield ILD MDT)
- SpO₂ ≥90% in room air
- Age 18-80

Exclusion criteria:

- Patients on immunosuppressive treatment (excluding prednisolone at a dose of ≤ 20mg/day or N-acetylcysteine)
- Pregnancy
- Renal impairment (Glomerular filtration rate < 30 ml/min)
- SpO₂ <90% in room air
- Age >80 years old, or <18 years old at the onset of the study
- Inability to lie supine comfortably for at least 60 minutes
- Malignancy with a life expectancy of less than one year
- Significant co-morbidity likely to reduce life expectancy to less than one year
- Severe ischaemic heart disease or symptoms of angina not fully controlled
- Significant congestive cardiac failure
- Any contraindication(s) to MRI scanning
- Previous allergy to MRI contact agent (gadolinium)

3.2.4 Study design

Potential subjects were identified during ILD MDT meetings where patients' cases are discussed as part of routine clinical care at Northern General Hospital, Sheffield. Upon clinical contact during the ILD clinic, patients were provided with a PIS and the study was briefly discussed with them. Further contact was made by telephone at least 24 hours after issuing the PIS to allow the patient to ask any additional questions. If the patient agreed to participate in the study, a baseline visit was arranged, upon which informed consent was obtained. The diagnostic HRCT thorax was used as the baseline CT in the study and patients with significant emphysema were not recruited. PH screening was performed using echocardiography.

	ILD clinic (screening)	Baseline visit	3-month visit	6-month visit	12-month visit
HRCT thorax	X				X
Echocardiography	X				
Offer participant information sheet	X				
MRI safety check review	X	X	X	X	X
Eligibility checked	X	X	X	X	X
Informed consent		X			
Brief clinical review		X	X	X	X
Resting pulse oximetry		X	X	X	X
MRI scan		X	X	X	X
PFTs		X	X	X	X

HRCT: High resolution computed tomography; MRI: Magnetic resonance imaging; PFT: Pulmonary function test.

Table 3.2. Data collected at the ILD clinic appointment and at each study visit.

3.3 CT acquisition and analysis

The acquisition criteria include an unenhanced volumetric HRCT thorax with full lung coverage, <1mm slice thickness and contiguous slices. HRCT scans were performed on various scanners (mainly Siemens or Toshiba).

3.3.1 CALIPER analysis

QCT analysis was performed on all scans using CALIPER software at the Mayo clinic, Rochester, Massachusetts, USA. The CALIPER data included volumetric parenchymal pattern classification of each pixel into GGO, low attenuation areas (e.g. emphysema), honeycombing, reticulation or normal tissue (166). The global percentage of each of these parenchymal patterns was calculated by dividing the corresponding volume by the total lung volume. Honeycombing % and reticulation % was combined and identified as fibrosis %. GGO %, honeycombing % and reticulation % was combined and identified as ILD %. The CALIPER software also performs automated segmentation of the VRS in the lung excluding the large vessels at the hilum (169).

Regional data was also collected as the CALIPER software can classify the same volumetric data by distribution in the lungs, thereby producing analysis of central and

peripheral zones in the upper, middle and lower zones of each lung. The central vs peripheral zones for each region are approximately 50/50 with an additional 5cm sphere at each hilum that is considered central. The upper zone is classified as the region above the carina, and the middle / lower zones are based on 50% craniocaudal distance between the carina and the most inferior extent of the lungs. An overall central zone % value was produced by multiplying the individual central zones of the upper, middle and lower zones of each lung together. An overall peripheral zone % was calculated in a similar way using each peripheral region. Upper, middle and lower zone % values were produced by multiplying the right and left lung values together for each of the corresponding zones.

3.3.2 Semi-quantitative visual CT scoring

A semi-quantitative visual CT scoring system (Table 3.3) was used by two experienced consultant chest radiologists in Sheffield. Honeycombing and reticulation was combined and identified as fibrosis. GGO, honeycombing and reticulation was combined and identified as ILD. Upper, middle and lower zone values were produced by multiplying the right and left lung values together for each of the corresponding zones. In the TRISTAN-ILD study, this CT scoring system was used to distinguish between the fibrotic (IPF subjects or GGO score <2) and inflammation (non-IPF subjects with a GGO score ≥2) groups.

Abnormality	Grading for each abnormality		Anatomical regions scored
	Percentage disease extent	Score	
-GGO alone	0	0	Lobes are scored independently Lingula is considered a separate lobe Global score: summation of scores for each abnormality, in all lobes
-Mixed ground glass and reticular disease	1-25%	1	
-Reticular fibrosis alone	26-50%	2	
-Honeycombing	51-75%	3	
-Consolidation	>75%	4	

GGO: Ground glass opacity

Table 3.3. Semi-quantitative visual CT scoring system. Modified from Ooi *et al* (345) and Rossi *et al* (346).

3.4 MRI protocol

All pulmonary MRI was performed at 1.5T on a whole-body GE scanner at the University of Sheffield MRI department and included the following sequences:

¹H MRI

- UTE MRI was acquired using an 8-element cardiac array with a 3D radial sequence during free-breathing with prospective respiratory bellows gating on expiration (347).
- 3D DCE-MRI for quantitative assessment of first pass perfusion, vascular resistance, late enhancement assessment of endothelial permeability and capillary leakage. Half dose of MRI contrast agent (gadolinium) was used with the injection rate controlled via an activated pump injector (Spectris, MedRad, Pittsburgh, PA) via a vein in the antecubital fossa, followed by a 20ml flush of 0.9% saline. 3D spoiled gradient echo (SPGR) acquisitions were used. Perfusion was quantified using indicator dilution analysis of the first pass of contrast agent and capillary leakage was quantified using the extended Tofts tracer kinetic model (348). In the TRISTAN-ILD study, data analysis was performed by Bioxydyn Limited and MTT was calculated using singular value deconvolution with a threshold set at 0.01 (349). In the IPF study, data analysis was performed using in-house developed MATLAB (MathWorks, Natick, Massachusetts, USA) software at the University of Sheffield.
- 3D dynamic OE-MRI for quantitative assessment of gas transfer, perfusion and ventilation (TRISTAN-ILD study only). This was acquired during free breathing, using 100% oxygen delivered at 15 l/min via a non-rebreathing face mask (2 mins medical air, 8 mins 100% oxygen, 5 mins medical air). 3D SPGR acquisitions were used, with a baseline T₁ measurement provided by an inversion recovery approach (350). Oxygen delivery was quantified by change in partial pressure of oxygen, gas wash-in rate, wash-out rate and maximum pO₂ (351). Data analysis was performed by Bioxydyn Limited.

¹²⁹Xe MRI

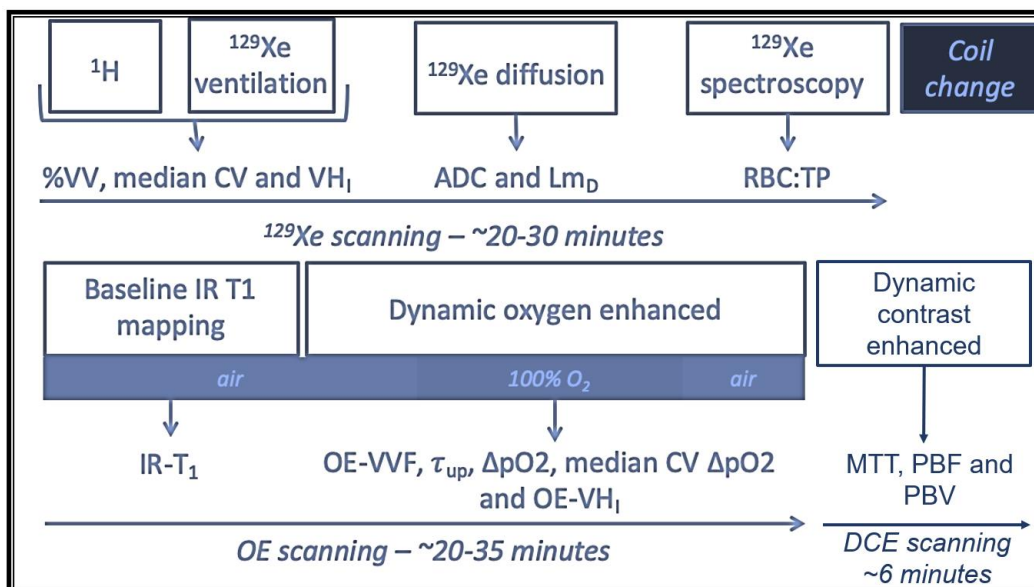
- Using a 3D steady-state free precession sequence, a ¹²⁹Xe gas phase MRI was performed to image the distribution of ventilation (352). This was acquired after the inhalation of a mixture of 500ml ¹²⁹Xe and 500ml N₂ from functional residual capacity (FRC). Prior to the ¹²⁹Xe acquisition a proton anatomical image was acquired using 1L of room air. ¹H anatomical images were co-registered to the same spatial domain as the ¹²⁹Xe ventilation image, and semi-automatic segmentation and manual editing (353) was performed at the University of Sheffield. VV% was calculated by dividing the ventilated volume (from the ventilation image) by the thoracic cavity volume (from the ¹H structural image). The median of the coefficient of variation percentage (CV%) of ventilated signal intensity was also calculated (354).
- A high-resolution dissolved phase spectroscopy sequence was used to acquire MR spectra of ¹²⁹Xe from the whole lungs and after zeroth-order phasing on the RBC and TP resonances, peak integrals were calculated to derive the RBC:TP. Subjects inhaled a mixture of 600ml ¹²⁹Xe and 400ml N₂ from FRC. A double Lorentzian, two peak method of calculating the RBC:TP was performed (230). Data analysis was performed using MATLAB (MathWorks, Natick, Massachusetts, USA) software at the University of Sheffield.
- Chemical shift imaging of ¹²⁹Xe gas/dissolved compartments used a 4-point iterative decomposition of water and fat with echo asymmetry and least-squares estimation (IDEAL) technique (355). Details of the theory and methodology of this chemical shift imaging, combined with a 3D radial SPGR sequence has recently been published (356). Global and regional values (central/peripheral regions, and upper/middle/lower zones of the lungs) were produced as per Collier *et al* (356). Data analysis was performed using MATLAB (MathWorks, Natick, Massachusetts, USA) software at the University of Sheffield.
- 3D gas phase DW-MRI was performed using a 3D SPGR multiple b-value sequence (b=0, 12, 20, 30 s/cm²). Subjects inhaled a mixture of 550ml ¹²⁹Xe and 450ml N₂ from FRC. Maps of ADC and L_{mD} were calculated for each imaging voxel using a mono-exponential fit of the first two DW b-values (b=0, 12 s/cm²) (241). Global and regional values (central/peripheral regions, and upper/middle/lower zones of the lungs) were calculated. Each of the central and

peripheral zones corresponded to approximately half the lung volume, and each of the upper, middle and lower zones corresponded to approximately a third of the total lung height. Data analysis was performed using MATLAB (MathWorks, Natick, Massachusetts, USA) software at the University of Sheffield.

	Acquisition matrix	Pixel size (mm)	Slice thickness	Flip angle (°)	TE/TR (ms)	Bandwidth (kHz)
¹ H SPGR	100x100	4x4	5	5	0.6/1.9	±83.3
¹ H UTE	256x256	~1.5x1.5	~1.5	4	0.078/2.9	±125
¹²⁹ Xe diffusion	64x64	6.25x6.25	15	3.1	14.0/17.4	±8.0
¹²⁹ Xe IDEAL	20x20x20	20x20	20	40/0.7	0.55/40	±15.625
¹²⁹ Xe spectroscopy	256	NA	NA	90	0/163	±1.8
¹²⁹ Xe ventilation	100x80	4x4	10	10	2.2/6.7	±8.0
Dynamic OE	96x96	4.2x4.2	10	5	0.4/1.5	±31.25
IR-T ₁ mapping	96x96	4.2x4.2	10	5	0.4/1.5	±31.25

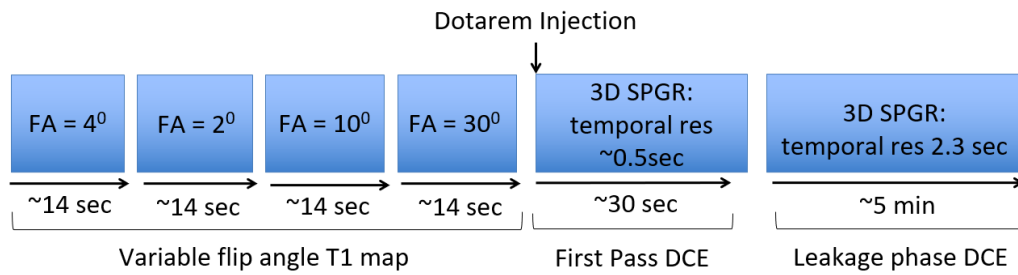
¹H: proton; IDEAL: Iterative decomposition of water and fat with echo asymmetry and least-squares estimation; IR: inversion recovery; NA: Not applicable; OE: oxygen enhanced; SPGR: steady-state free precession; TE: echo time; TR: repetition time; UTE: Ultra-short echo time; ¹²⁹Xe: 129-xenon

Table 3.4. Technical details of the MRI sequences.



ADC: apparent diffusion coefficient; CV: coefficient of variation; DCE: dynamic contrast enhanced; ¹H: proton; IR: inversion recovery; Lm_D: mean diffusive length scale; MTT: mean transit time; OE: oxygen enhanced; PBF: pulmonary blood flow; PBV: pulmonary blood volume; pO₂: partial pressure of oxygen; RBC:TP: red blood cell to tissue plasma ratio; VH₁: ventilation heterogeneity index; VV: ventilated volume; VVF: ventilated volume fraction; ¹²⁹Xe: 129-xenon; τ_{up}: oxygen wash in time.

Figure 3.2. A schematic representation of the MRI sequences used in the TRISTAN-ILD study and the metrics generated from each sequence. The same ¹²⁹Xe MRI and DCE-MRI sequences were used in the IPF study.



DCE: Dynamic contrast enhanced; FA: Flip angle; SPGR: Steady-state free precession.

Figure 3.3. DCE-MRI sequences used in the TRISTAN-ILD and IPF studies.

^{129}Xe was polarised on site at the University of Sheffield under regulatory licence to approximately 30% using a custom-made spin exchange optical polariser (Figure 3.4) capable of generating 500ml doses in less than 15 minutes (224).

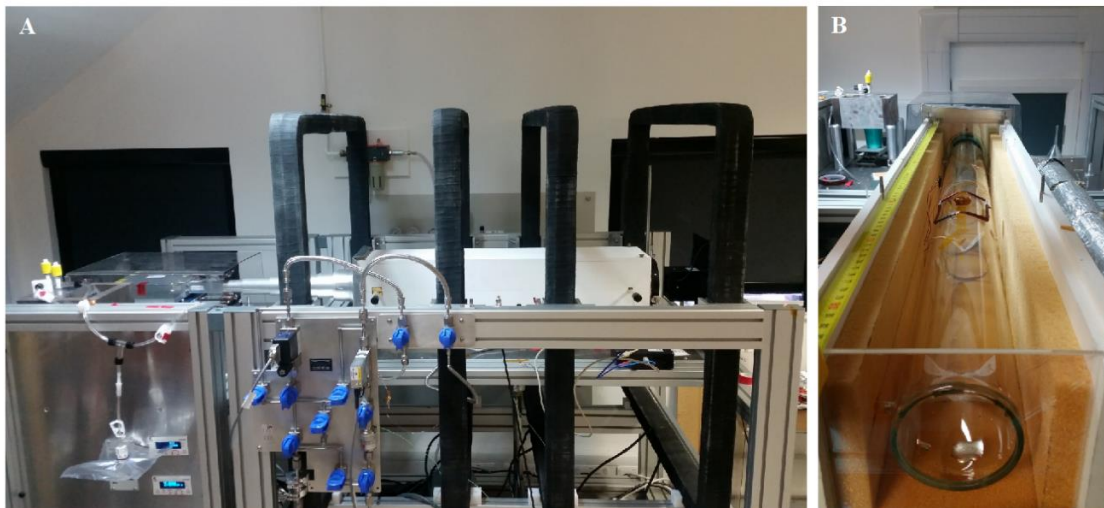


Figure 3.4. Photos of the ^{129}Xe spin-exchange optical polariser (A) and the polariser cell (B) used at the University of Sheffield MRI department.

An eight-channel cardiac array coil (General Electrics, Massachusetts, USA) was used for ^1H MRI. All ^{129}Xe images were acquired at FRC+1L in a flexible quadrature transmit/receive quadrature coil (Clinical MR solutions, Brookfield, Wisconsin, USA). ^{129}Xe was mixed with nitrogen and the subject inhaled the gas from a 1L Tedlar bag (Figure 3.5). Continuous monitoring of the patient's heart rate and oxygen saturations was performed during the ^{129}Xe MRI scans.

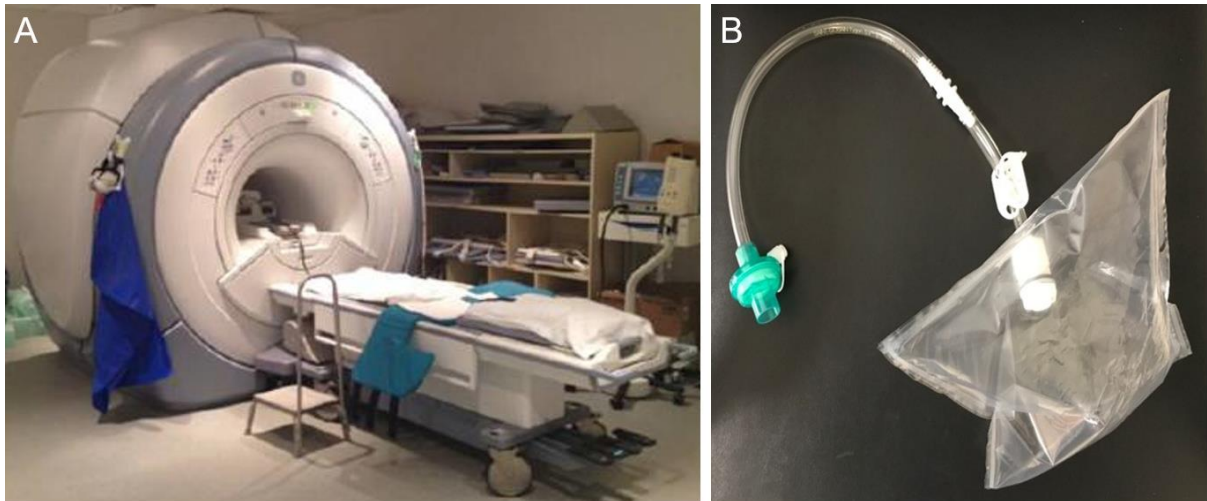


Figure 3.5. Photo of the University of Sheffield 1.5T MRI scanner and the ^{129}Xe MRI coil used in the studies (A). Photo of an example of the 1L Tedlar bag used for the inhalation of ^{129}Xe (B).

3.5 Pulmonary function tests

In the TRISTAN-ILD study, PFTs (FEV_1 , FVC, D_{LCO} and K_{CO}) were performed on the same day as the MRI scan for the Sheffield subjects, and within one week prior to the MRI scan for the Manchester subjects. PFTs were performed in the seated position and the Global Lung Function Initiative (GLI) 2012 reference equations (357) were used to calculate the % predicted values.

In the IPF study, all PFTs were performed on the same day as the MRI scan. Standard PFTs (FEV_1 , FVC, D_{LCO} and K_{CO}) were performed in the seated position. The GLI 2012 reference (357) equations were used to calculate the % predicted values.

3.6 Statistics

3.6.1 Power calculation for TRISTAN-ILD study

The power calculation to estimate the sample size was based on data derived from the ^{129}Xe MRI methods for the assessment of COPD that was developed in Sheffield. The following assumptions were made to calculate the sample size:

- The standard deviation of septal thickness between IPF subjects in the prospective study will be the same as that which has been measured previously (i.e. 1.1 μm (358)).
- Thus, the “Cohen’s d” effect size, $d = 1/1.1 = 0.909$.
- Assume a statistical significance criterion of $p < 0.05$.

Using a standard statistical power of $p=0.8$, the number of subjects required in order to meet the above criteria is $n=12$. However, if a statistical power of $p=0.95$ is used then the number of subjects required in order to meet the above criteria is $n=18$. Therefore, $n=15$ patients in each ILD subgroup was proposed as a compromise between the two statistical powers.

3.6.2 Power calculation for IPF study

The power calculation to estimate the sample size was based on data derived from the ^{129}Xe MRI methods for the assessment of COPD that was developed in Sheffield. The following assumptions were made to calculate the sample size:

- The standard deviation of septal thickness between IPF subjects will be the same as that which has been measured previously (i.e. 1.1 μm (358)).
- Thus, the “Cohen’s d” effect size, $d = 1/1.1 = 0.909$.
- Assume a statistical significance criterion of $p < 0.05$.

Using a standard statistical power of $p=0.8$, the number of subjects required in order to meet the above criteria is $n=12$. However, if a statistical power of $p=0.95$ is used then the number of subjects required in order to meet the above criteria is $n=18$. Therefore, as a compromise between the two statistical powers, and to allow for patient drop out, $n=15$ patients as a minimum and $n=30$ as a maximum was proposed. In the first phase of this study, as of April 2018, a total of 21 IPF patients had been recruited.

A further power calculation was performed, based on the data from the first phase of this study, using the formula: $n = f(\alpha, \beta) \cdot \frac{2s}{\delta^2}$. Where α is the two-sided significance, $1-\beta$ is the power of the test, $f(\alpha, \beta)$ is the function provided from these variables by standard statistical look up tables, s is the standard deviation of RBC:TP in the original

cohort and δ is the smallest difference required to measure. The value of δ was set at 0.02, half the observed difference seen over six months in the phase 1 cohort, rounded down to 2 decimal places, as per the accuracy of the test. Finally, this output was multiplied by 2, to allow for a 50% combined dropout and mortality rate. From this calculation, with $\alpha=0.05$ and $1-\beta=95\%$, $s=0.11$, and $\delta=0.02$; $n=32$. Therefore, the recruitment of a further 32 participants, which would result in a total recruitment of up to 53 patients (21 patients from the first cohort and 32 patients from the second cohort) was proposed.

3.6.3 Statistical analyses

Continuous variables were stated as mean \pm standard deviation or as median and inter-quartile range (IQR), as appropriate according to normal distribution of data. The Pearson correlation coefficient (non-parametric data – Spearman's rank correlation) was used to determine the strength of correlations. Paired data were analysed for variance using the paired sample t test (non-parametric data – Wilcoxon paired-sample test) for comparisons over two time points, whereas analysis of variance (ANOVA) (non-parametric data – Friedman test) was used for matched data comparisons over more than two time points. Independent data were analysed for variance using the independent samples t test (non-parametric data – Mann Whitney test) for comparisons over two time points or between two subgroups at a single time point. For comparisons over more than two time points or between more than two subgroups, independent data were analysed for variance using ANOVA (non-parametric data – Kruskal-Wallis test). When statistical analyses were performed for multiple comparisons, the p values were adjusted using the appropriate test (e.g. Holm-Sidak's or Tukey's for one-way ANOVA, Dunn's for Friedman test and Kruskal-Wallis test).

In the IPF study, disease progression was defined as $\geq 10\%$ absolute decline in FVC%, $\geq 15\%$ absolute decline in DLCO%, lung transplantation or all-cause mortality over 12 months. In the TRISTAN-ILD study, disease progression was defined as $\geq 10\%$ absolute decline in FVC%, $\geq 15\%$ absolute decline in DLCO%, lung transplantation or all-cause mortality over 6 months for the subjects with DI-ILD, HP or iNSIP. However, for those with CTD-ILD or IPF, disease progression was defined as $\geq 10\%$ absolute

decline in FVC%, $\geq 15\%$ absolute decline in DLco%, lung transplantation or all-cause mortality over 12 months. Univariate logistic regression analysis was performed to identify variables associated with disease progression. Logistic regression analysis was performed with age added to the model for variables that demonstrated statistical significance in the univariate logistic regression analysis.

Subjects who missed study visits were included for analysis with the available data. To determine regional variation within groups, or differences between groups, statistical analysis was not performed on groups containing less than 12 subjects (number of subjects required in power calculation using a standard statistical power of $p=0.8$). All tests were two-tailed and statistical significance was assumed at $p<0.05$. Data were analysed using GraphPad Prism (San Diego, USA) version 9.0.1.

3.7 Summary

The TRISTAN-ILD study is a prospective, multicentre, observational, imaging study of patients presenting with various ILD subtypes (CTD-ILD, DI-ILD, HP, iNSIP and IPF). The hypothesis is that pulmonary MRI and CT measurements correlate with FVC and/or DLco in patients with ILD and can provide superior information regarding diagnosis and prognosis when compared with current measurements used in ILD. The IPF study is a prospective, single centre, observational, imaging study of patients with IPF. The hypothesis is that longitudinal pulmonary MRI measurements can provide detailed information regarding progression of disease in IPF. The following two chapters will demonstrate the results of these studies.

Chapter 4: The Assessment of Interstitial Lung Disease Using Imaging Biomarkers: TRISTAN-ILD Study Results

4.1 Recruitment and demographic data

4.1.1 Recruitment

61 patients were recruited into the study over a two-year period, between February 2018 and March 2020. 55 participants completed at least one study visit. The data in this thesis refers to these subjects. Of these 55 participants, 38 were recruited from Sheffield, 16 from Manchester and one from Leeds (NB – although subsequently a two-centre study, Leeds acted as a partner site at the beginning of the study). Initially, the four ILD subtypes included in the study were CTD-ILD, DI-ILD, HP and IPF. However, in June 2019, due to a combination of slow recruitment and iterative protocol development, a decision was made to invite patients with iNSIP to participate. The number of subjects with each ILD subtype was as follows:

- 5 CTD-ILD (9.1%)
 - 4 incident cases, 1 prevalent case with significant progression
 - Type of CTD: 1 MCTD, 1 SLE, 1 SS, 1 SSc, 1 undifferentiated CTD
- 13 DI-ILD (23.6%)
 - Causes: 1 amiodarone, 1 bleomycin, 1 carbamazepine, 1 dasatinib, 1 etanercept, 1 hydroxycarbamide, 3 nitrofurantoin, 1 raltitrexed, 1 rituximab, 1 sertraline, 1 simvastatin
- 15 HP (27.3%)
 - 12 incident cases, 3 prevalent cases with significant progression
 - 5 classified as acute, 10 classified as chronic
- 3 iNSIP (5.5%)
 - All incident cases
- 19 IPF (34.5%)
 - 18 incident cases, 1 prevalent case with significant progression

Due to the heterogeneity of the groups and, following the publication of the INBUILD study, the total cohort was also divided into fibrotic and inflammation phenotypic groups. The fibrotic group included IPF subjects or those with a baseline GGO score <2 using the semi-quantitative visual CT scoring system as demonstrated in Table 3.3.

The inflammation group included non-IPF subjects with a baseline GGO score ≥ 2 . Out of a total cohort of 55 subjects, 32 (58.2%) were in the fibrotic group and 23 (41.8%) were in the inflammation group.

4.1.2 Study visits

A summary of the total number of subjects at each study visit and the reasons for not completing the study are presented in Figure 4.1. Table 4.1 shows the number of subjects (total cohort, fibrotic and inflammation groups) with each ILD subtype that completed each study visit. Figure 4.1 and Table 4.1 do not include the additional visit (visit 1A) which was introduced in November 2019. Only eight subjects participated in these visits (visit 1A occurred at two weeks for DI-ILD, HP and iNSIP subjects, and at three months for CTD-ILD and IPF subjects). Due to the small number of subjects and the subsequent lack of statistical power, the visit 1A data has not been included in the following sections of this chapter.

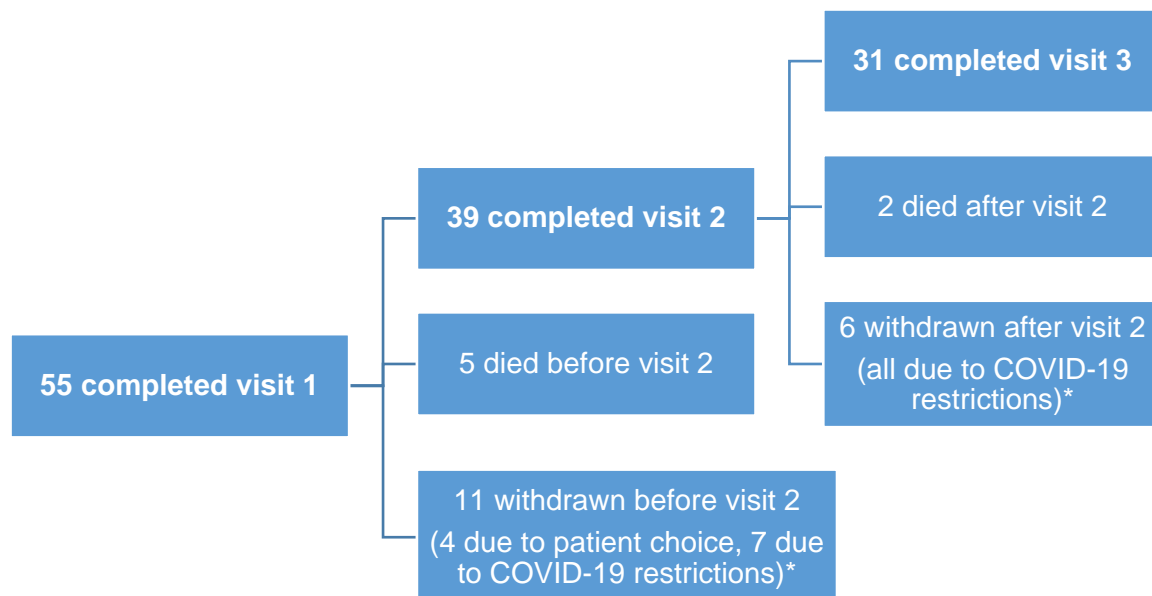


Figure 4.1. Summary of subject numbers at each study visit and reasons for not completing the study. *8 of the 10 subjects withdrawn due to COVID-19 restrictions had clinical PFT data available to use at visit 3 for research purposes.

	Total	CTD-ILD	DI-ILD	HP	iNSIP	IPF
Visit 1						
Total	55	5	13	15	3	19
Fibrotic	32	1	6	5	1	19
Inflammation	23	4	7	10	2	0
Visit 2						
Total	39	5	11	10	2	11
Fibrotic	22	1	5	4	1	11
Inflammation	17	4	6	6	1	0
Visit 3						
Total	31	5	8	7	0	11
Fibrotic	19	1	5	2	0	11
Inflammation	12	4	3	5	0	0

CTD-ILD: Connective tissue disease associated interstitial lung disease; DI-ILD: Drug induced interstitial lung disease; HP: Hypersensitivity pneumonitis; iNSIP: Idiopathic non-specific interstitial pneumonia; IPF: Idiopathic pulmonary fibrosis

Table 4.1. Number of subjects with each ILD subtype that completed each study visit.

4.1.3 Days between diagnostic CT scan and first study visit

The HRCT scan which was used in the ILD MDT meeting for diagnostic purposes was used as the baseline HRCT scan in the study. Therefore, a baseline HRCT scan was not acquired routinely for research purposes unless the CT images failed the QA process. As a result, there was a period of up to 12 months between the baseline HRCT scan and the first study visit.

13 out of 55 baseline CT scans failed the QA process and were therefore repeated for research purposes at the first study visit. The mean time between the baseline HRCT and the first study visit was 91 days, standard deviation 77 days, range 0 – 317 days.

4.1.4 Subject demographics

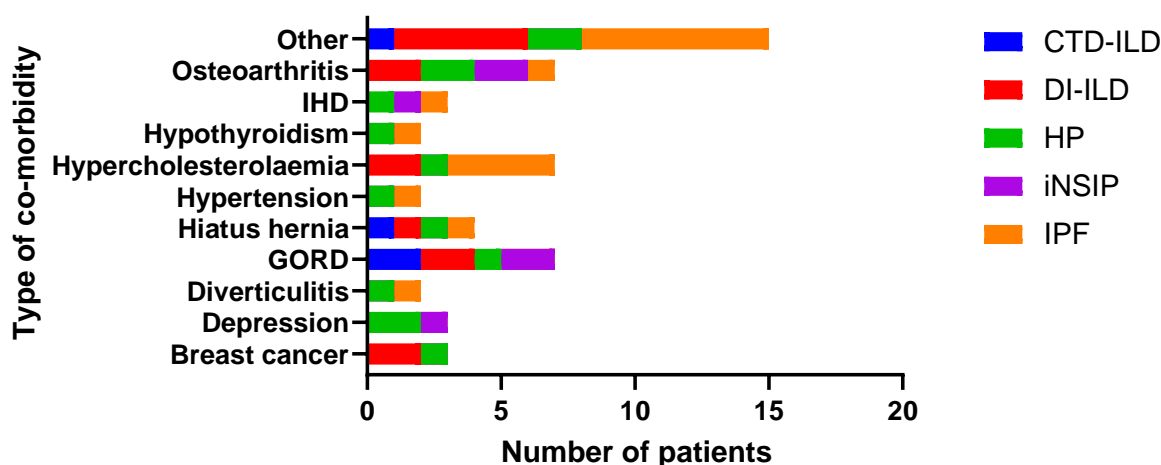
Baseline characteristics are presented in Table 4.2. Of the 24 ever smokers in the total cohort, only one was a current smoker. The IPF subjects in the TRISTAN-ILD study had similar baseline characteristics to the incident IPF subgroup in the INSIGHTS-IPF registry (359) which reported the following data: mean age 71.0, male gender 86.6%, ever smoker 67.8%, mean body mass index (BMI) 28.2.

	Total (n = 55)	CTD-ILD (n = 5)	DI-ILD (n = 13)	HP (n = 15)	iNSIP (n = 3)	IPF (n = 19)
Age (years), median (IQR)	69.0 (58.0 – 76.0)	55.0 (48.5 – 69.5)	64.0 (57.0 – 70.0)	63.0 (56.8 – 73.5)	76.0 (69.0 – 79.0)	74.0 (67.0 – 77.0)
Male gender, n (%)	30 (54.5)	2 (40.0)	7 (53.8)	5 (33.3)	0 (0)	16 (84.2)
Ever smoker, n (%)	24 (43.6)	2 (40.0)	4 (30.8)	7 (46.7)	0 (0)	12 (63.2)
Body mass index, median (IQR)	26.6 (25.0 – 31.1)	25.1 (19.6 – 30.8)	25.3 (23.0 – 27.4)	28.3 (26.1 – 33.6)	27.7 (27.6 – 31.2)	26.6 (25.4 – 31.1)

CTD-ILD: Connective tissue disease associated interstitial lung disease; DI-ILD: Drug induced interstitial lung disease; HP: Hypersensitivity pneumonitis; iNSIP: Idiopathic non-specific interstitial pneumonia; IPF: Idiopathic pulmonary fibrosis; IQR: interquartile range.

Table 4.2. Demographic data for the total cohort and each ILD subtype.

4.1.5 Co-morbidities



CTD-ILD: Connective tissue disease associated interstitial lung disease; DI-ILD: Drug induced interstitial lung disease; GORD: Gastroesophageal reflux disease; HP: Hypersensitivity pneumonitis; IHD: ischaemic heart disease; iNSIP: Idiopathic non-specific interstitial pneumonia; IPF: Idiopathic pulmonary fibrosis.

Figure 4.2. Co-morbidities in the total cohort and ILD subtypes. Other was defined as any co-morbidity that occurred in only one subject out of the total cohort.

4.1.6 Treatment approach

The treatment approach prior and during the study period varied (Table 4.3). All subjects with DI-ILD had the offending drug stopped and there were no occasions where the drug was restarted. An antigen was confidently identified (exposure to birds) in two of the 15 HP subjects. The management plan for both subjects was antigen avoidance and prednisolone.

Group	Treatment	Prior to visit 1, n (%)	Visits 1 – 2, n (%)	Visits 2 – 3, n (%)
CTD-ILD	Immunosuppressant	4 (80.0)	4 (80.0)	4 (80.0)
	Prednisolone + MMF	2 (40.0)	2 (40.0)	2 (40.0)
	Prednisolone + AZA	2 (40.0)	2 (40.0)	2 (40.0)
DI-ILD	Prednisolone	6 (46.2)	3 (27.3)	3 (37.5)
HP	Immunosuppressant	10 (66.7)	10 (100)	6 (85.6)
	Prednisolone	6 (40.0)	4 (40.0)	2 (28.6)
	Prednisolone + MMF	4 (26.7)	5 (50.0)	3 (42.9)
	AZA only	0	1 (10.0)	1 (14.3)
iNSIP	Prednisolone	0	2 (100)	NA
IPF	Nintedanib	3 (15.8)	2 (18.2)	2 (18.2)
Fibrotic	Immunosuppressant	8 (25.0)	7 (31.8)	4 (21.1)
	Prednisolone	4 (12.5)	2 (9.1)	1 (5.3)
	Prednisolone + MMF	4 (12.5)	5 (22.7)	3 (15.8)
	Nintedanib	3 (9.4)	2 (9.1)	2 (10.5)
Inflammation	Immunosuppressant	12 (52.2)	12 (70.6)	9 (75.0)
	Prednisolone	8 (34.8)	7 (41.2)	4 (33.3)
	Prednisolone + MMF	2 (8.7)	2 (11.8)	2 (16.7)
	Prednisolone + AZA	2 (8.7)	2 (11.8)	2 (16.7)
	AZA only	0	1 (5.9)	1 (8.3)

AZA: Azathioprine; CTD-ILD: Connective tissue disease associated interstitial lung disease; DI-ILD: Drug induced interstitial lung disease; HP: Hypersensitivity pneumonitis; iNSIP: Idiopathic non-specific interstitial pneumonia; IPF: Idiopathic pulmonary fibrosis; MMF: Mycophenolate mofetil.

Table 4.3. Summary of the treatment received by subjects during the study.

4.2 Pulmonary function tests

4.2.1 Visit 1 (baseline)

The IPF subjects in the TRISTAN-ILD study had higher PFT values when compared to the incident IPF subgroup in the INSIGHTS-IPF registry (359) which had the following results (mean): FEV₁ 76.9%, FVC 73.7%, DL_{CO} 37.7%.

	Total (n = 55)	CTD-ILD (n = 5)	DI-ILD (n = 13)	HP (n = 15)	iNSIP (n = 3)	IPF (n = 19)
FEV₁ (L)	2.26 (1.75 - 2.84)	2.29 (2.22 - 2.78)	2.26 (1.72 - 2.53)	1.77 (1.43 - 2.41)	1.86 (1.67 - 2.30)	2.45 (2.00 - 3.00)
FEV₁ (% predicted)	85.5 (63.9 - 103)	83.3 (78.7 - 102)	79.7 (62.9 - 99.4)	80.9 (58.0 - 102)	100.6 (99.5 - 106)	92.2 (73.3 - 111)
FVC (L)	2.84 (2.14 - 3.56)	2.87 (2.79 - 3.47)	2.90 (2.13 - 3.12)	2.14 (1.86 - 3.29)	2.23 (2.15 - 2.61)	3.29 (2.24 - 4.14)
FVC (% predicted)	84.7 (65.3 - 99.0)	85.4 (75.0 - 103)	86.1 (62.9 - 95.0)	77.8 (52.9 - 90.2)	94.5 (91.7 - 98.2)	90.1 (66.3 - 113)
FEV₁ / FVC (%)	79.8 (75.3 - 84.8)	78.4 (76.9 - 84.4)	76.9 (73.7 - 81.8)	81.9 (75.3 - 88.1)	83.4 (77.7 - 88.1)	79.4 (74.2 - 83.5)
D_{LCO} (mmol. min⁻¹.kPa⁻¹)	4.54 (2.72 - 5.27)	4.67 (3.32 - 5.08)	4.55 (2.62 - 5.82)	3.42 (2.72 - 4.92)	3.93 (3.88 - 6.29)	4.89 (2.63 - 5.41)
D_{LCO} (% predicted)	59.2 (40.1 - 72.3)	62.8 (37.3 - 74.8)	65.6 (39.2 - 76.7)	48.2 (40.1 - 70.9)	72.3 (71.3 - 93.9)	54.3 (35.2 - 72.4)

CTD-ILD: Connective tissue disease associated interstitial lung disease; DI-ILD: Drug induced interstitial lung disease; D_{LCO}: Diffusing capacity of the lung for carbon monoxide; FEV₁: Forced expiratory volume in one second; FVC: Forced vital capacity; HP: Hypersensitivity pneumonitis; iNSIP: Idiopathic non-specific interstitial pneumonia; IPF: Idiopathic pulmonary fibrosis

Table 4.4. PFT results at visit 1 for the total cohort and ILD subtypes. Results are presented as median (inter-quartile range).

	Fibrotic (n = 32)	Inflammation (n = 23)	p value
FEV₁ (L)	2.29 ± 0.76	2.29 ± 0.65	0.99
FEV₁ (% predicted)	85.1 ± 25.6	89.0 ± 20.9	0.56
FVC (L)	2.92 ± 1.06	2.91 ± 0.83	0.96
FVC (% predicted)	82.8 ± 26.7	87.8 ± 20.5	0.45
FEV₁ / FVC (%)	79.8 ± 7.3	79.1 ± 6.9	0.70
D_{LCO} (mmol. min⁻¹.kPa⁻¹)	4.03 ± 1.68	4.30 ± 1.35	0.52
D_{LCO} (% predicted)	54.0 ± 22.1	60.4 ± 16.7	0.25

D_{LCO}: Diffusing capacity of the lung for carbon monoxide; FEV₁: Forced expiratory volume in one second; FVC: Forced vital capacity

Table 4.5. PFT results at visit 1 for the fibrotic and inflammation groups. Results are presented as mean ± standard deviation.

4.2.2 Visit 2 (6 weeks or 6 months depending on ILD subtype)

	Total (n = 39)	CTD-ILD (n = 5)	DI-ILD (n = 11)	HP (n = 10)	iNSIP (n = 2)	IPF (n = 11)
FVC (L)	2.84 (2.25 – 3.83)	2.79 (2.74 – 3.61)	2.84 (2.09 – 3.85)	2.56 (1.61 – 3.53)	2.50 (2.34 – 2.65)	3.75 (2.25 – 4.34)
FVC change (L)	0.00 (-0.13 – 0.11)	0.00 (-0.09 – 0.14)	0.00 (-0.37 – 0.01)	0.065 (-0.11 – 0.15)	0.075 (0.04 – 0.11)	-0.13 (-0.28 – 0.11)
FVC change (%)	0.00 (-5.80 – 4.82)	0.00 (-2.98 – 3.42)	0.00 (-11.4 – 0.49)	1.61 (-5.68 – 5.72)	3.23 (1.53 – 4.93)	-3.28 (-6.95 – 2.60)
FVC (% predicted)	87.0 (69.6 – 100)	88.3 (73.0 – 102)	86.7 (60.8 – 93.0)	76.9 (53.5 – 105)	95.3 (92.9 – 97.8)	87.0 (71.6 – 110)
FVC% absolute change (%)	0.00 (-4.50 – 2.93)	0.82 (-6.44 – 4.38)	-0.10 (-10.9 – 0.59)	1.89 (-4.22 – 4.54)	2.22 (1.21 – 3.23)	-1.16 (-4.68 – 2.30)
FVC% relative change (%)	0.00 (-5.78 – 3.42)	0.80 (-8.52 – 5.37)	-0.18 (-11.3 – 0.69)	1.75 (-5.29 – 6.63)	2.37 (1.32 – 3.42)	-0.93 (-5.78 – 2.71)

CTD-ILD: Connective tissue disease associated interstitial lung disease; DI-ILD: Drug induced interstitial lung disease; FVC: Forced vital capacity; HP: Hypersensitivity pneumonitis; iNSIP: Idiopathic non-specific interstitial pneumonia; IPF: Idiopathic pulmonary fibrosis.

Table 4.6. FVC and FVC% results at **visit 2**, and the longitudinal change in FVC and FVC% between visit 1 and visit 2 for the total cohort and the ILD subtypes. Results are presented as median (inter-quartile range).

	Total (n = 39)	CTD-ILD (n = 5)	DI-ILD (n = 11)	HP (n = 10)	iNSIP (n = 2)	IPF (n = 11)
DLco (mmol. min⁻¹.kPa⁻¹)	4.43 (2.88 – 5.36)	4.87 (3.51 – 5.56)	4.75 (2.85 – 5.94)	3.79 (2.25 – 4.64)	5.63 (4.48 – 6.77)	4.43 (2.88 – 5.36)
DLco change (mmol. min⁻¹.kPa⁻¹)	-0.040 (-0.46 – 0.43)	0.37 (-0.02 – 0.61)	0.020 (-0.89 – 0.51)	-0.28 (-0.71 – 0.48)	0.47 (0.38 – 0.55)	-0.33 (-0.50 – -0.04)
DLco change (%)	-0.74 (-19.1 – 12.0)	7.02 (-0.32 – 18.7)	0.34 (-19.6 – 12.0)	-5.97 (-22.6 – 15.4)	9.97 (5.95 – 14.0)	-9.41 (-19.1 – -0.74)
DLco (% predicted)	56.8 (40.6 – 73.5)	62.3 (41.8 – 81.1)	66.5 (39.1 – 78.0)	52.2 (37.1 – 68.2)	90.1 (81.2 – 99.0)	53.8 (42.8 – 66.8)
DLco% absolute change (%)	-0.49 (-6.75 – 5.74)	4.36 (-0.26 – 8.60)	0.36 (-9.64 – 7.92)	-3.07 (-10.9 – 6.94)	7.03 (5.10 – 8.96)	-3.75 (-17.4 – 2.71)
DLco% relative change (%)	-0.78 (-20.2 – 12.1)	8.31 (-0.41 – 19.4)	0.42 (-19.7 – 12.1)	-5.41 (-22.5 – 16.4)	8.92 (5.43 – 12.4)	-8.02 (-24.2 – 4.07)

CTD-ILD: Connective tissue disease associated interstitial lung disease; DI-ILD: Drug induced interstitial lung disease; DLco: Diffusing capacity of the lung for carbon monoxide; HP: Hypersensitivity pneumonitis; iNSIP: Idiopathic non-specific interstitial pneumonia; IPF: Idiopathic pulmonary fibrosis.

Table 4.7. DLco and DLco% at **visit 2**, and the longitudinal change in DLco and DLco% between visit 1 and visit 2 for the total cohort and the ILD subtypes. Results are presented as median (inter-quartile range).

	Fibrotic (n = 22)	Inflammation (n = 17)	p value
FVC (L)	2.97 ± 1.17	3.04 ± 0.83	0.82
FVC change (L)	-0.04 ± 0.24	-0.03 ± 0.24	0.47
FVC change (%)	-2.09 ± 9.54	-0.43 ± 7.38	0.52
FVC (% predicted)	82.2 ± 25.8	91.3 ± 22.5	0.26
FVC% absolute change (%)	-2.24 ± 7.95	0.11 ± 6.85	0.27
FVC% relative change (%)	-2.56 ± 9.76	0.14 ± 7.39	0.35

FVC: Forced vital capacity

Table 4.8. FVC and FVC% results at **visit 2**, and the longitudinal change in FVC and FVC% between visit 1 and visit 2 in the fibrotic and inflammation groups. Results are presented as mean ± standard deviation.

	Fibrotic (n = 22)	Inflammation (n = 17)	p value
D_{LCO} (mmol.min⁻¹.kPa⁻¹)	4.15 ± 1.98	4.28 ± 1.27	0.82
D_{LCO} change (mmol.min⁻¹.kPa⁻¹)	-0.07 ± 0.63	-0.12 ± 0.78	0.83
D_{LCO} change (%)	-3.58 ± 19.0	-1.28 ± 16.8	0.70
D_{LCO} (% predicted)	54.2 ± 23.8	59.5 ± 17.6	0.45
D_{LCO}% absolute change (%)	-1.98 ± 9.69	-0.82 ± 11.1	0.73
D_{LCO}% relative change (%)	-3.94 ± 19.5	-0.73 ± 17.7	0.60

D_{LCO}: Diffusing capacity of the lung for carbon monoxide

Table 4.9. D_{LCO} and D_{LCO}% at **visit 2**, and the longitudinal change in D_{LCO} and D_{LCO}% between visit 1 and visit 2 in the fibrotic and inflammation groups. Results are presented as mean ± standard deviation.

There were no statistically significant changes in FVC, FVC%, D_{LCO} or D_{LCO}% between visit 1 and visit 2 when the groups were analysed separately.

4.2.3 Visit 3 (6 months or 12 months depending on ILD subtype)

Eight out of ten subjects that could not attend the final study visit due to COVID-19 restrictions had clinical PFT data available to use at visit 3 for research purposes. Therefore, PFT data was available for 39 subjects at visit 3, despite only 31 of them completing their final study visit.

	Total (n = 39)	CTD-ILD (n = 5)	DI-ILD (n = 9)	HP (n = 9)	iNSIP (n = 3)	IPF (n = 13)
FVC (L)	2.92 (2.44 – 3.67)	2.97 (2.72 – 3.72)	2.81 (2.43 – 3.53)	2.92 (1.94 – 4.05)	2.44 (2.13 – 2.70)	3.29 (2.31 – 3.98)
FVC change (L)	-0.02 (-0.18 – 0.13)	0.10 (-0.07 – 0.25)	-0.02 (-0.26 – 0.11)	0.06 (-0.24 – 0.26)	0.09 (-0.02 – 0.21)	-0.16 (-0.49 – -0.01)
FVC change (%)	-0.71 (-7.58 – 3.81)	3.48 (-2.51 – 7.25)	-0.67 (-7.82 – 4.54)	2.80 (-9.02 – 9.38)	3.45 (-0.93 – 9.42)	-7.14 (-10.9 – -0.09)
FVC (% predicted)	88.5 (74.0 – 103)	88.5 (77.3 – 106)	85.7 (70.4 – 97.2)	84.8 (64.2 – 106)	96.4 (94.2 – 102)	89.6 (63.8 – 110)
FVC% absolute change (%)	-1.20 (-5.40 – 5.67)	3.13 (-1.50 – 6.94)	-1.26 (-5.77 – 5.30)	3.50 (-6.15 – 7.94)	2.50 (-1.82 – 7.04)	-4.59 (-12.1 – 0.68)
FVC% relative change (%)	-1.42 (-8.14 – 5.13)	3.66 (-1.73 – 7.58)	-1.42 (-8.20 – 5.37)	3.54 (-9.10 – 10.6)	2.73 (-1.85 – 7.45)	-7.29 (-11.5 – 0.63)

CTD-ILD: Connective tissue disease associated interstitial lung disease; DI-ILD: Drug induced interstitial lung disease; FVC: Forced vital capacity; HP: Hypersensitivity pneumonitis; iNSIP: Idiopathic non-specific interstitial pneumonia; IPF: Idiopathic pulmonary fibrosis.

Table 4.10. FVC and FVC% results at **visit 3**, and the longitudinal change in FVC and FVC% between visit 1 and visit 3 for the total cohort and the ILD subtypes. Results are presented as median (inter-quartile range).

	Total (n = 39)	CTD-ILD (n = 5)	DI-ILD (n = 9)	HP (n = 9)	iNSIP (n = 3)	IPF (n = 13)
D_{LCO} (mmol. min⁻¹.kPa⁻¹)	4.55 (3.50 – 5.10)	4.93 (3.80 – 5.49)	4.97 (3.32 – 6.33)	4.29 (3.64 – 4.86)	4.12 (3.83 – 6.19)	4.35 (2.70 – 4.74)
D_{LCO} change (mmol. min⁻¹.kPa⁻¹)	0.00 (-0.59 – 0.25)	0.05 (0.03 – 0.97)	0.24 (-0.47 – 0.73)	0.00 (-0.48 – 0.30)	-0.05 (-0.20 – 0.19)	-0.54 (-0.72 – 0.10)
D_{LCO} change (%)	0.00 (-12.4 – 8.51)	1.02 (0.61 – 34.0)	5.07 (-12.8 – 17.6)	0.00 (-11.6 – 7.50)	-1.29 (-3.13 – 4.83)	-11.0 (-16.9 – 3.50)
D_{LCO} (% predicted)	62.7 (45.7 – 70.7)	63.1 (42.8 – 82.9)	69.5 (40.3 – 80.9)	62.7 (53.3 – 66.6)	75.0 (70.2 – 90.3)	47.7 (37.7 – 61.6)
D_{LCO}% absolute change (%)	-0.72 (-6.54 – 3.99)	1.13 (0.56 – 12.6)	2.82 (-5.26 – 10.7)	-1.80 (-7.79 – 7.51)	-1.16 (-3.56 – 2.70)	-5.39 (-13.7 – 1.45)
D_{LCO}% relative change (%)	-0.83 (-12.0 – 8.16)	1.54 (0.97 – 33.4)	4.15 (-12.3 – 17.4)	-2.48 (-11.9 – 15.4)	-1.63 (-3.79 – 3.74)	-10.2 (-23.5 – 4.02)

CTD-ILD: Connective tissue disease associated interstitial lung disease; DI-ILD: Drug induced interstitial lung disease; D_{LCO}: Diffusing capacity of the lung for carbon monoxide; HP: Hypersensitivity pneumonitis; iNSIP: Idiopathic non-specific interstitial pneumonia; IPF: Idiopathic pulmonary fibrosis.

Table 4.11. D_{LCO} and D_{LCO}% at **visit 3**, and the longitudinal change in D_{LCO} and D_{LCO}% between visit 1 and visit 3 for the total cohort and the ILD subtypes. Results are presented as median (inter-quartile range).

	Fibrotic (n = 23)	Inflammation (n = 16)	p value
FVC (L)	2.91 ± 1.11	3.11 ± 0.84	0.53
FVC change (L)	-0.13 ± 0.38	0.07 ± 0.24	0.063
FVC change (%)	-4.89 ± 15.2	3.00 ± 8.46	0.068
FVC (% predicted)	83.6 ± 26.3	94.5 ± 18.2	0.16
FVC% absolute change (%)	-4.05 ± 12.6	3.19 ± 7.04	0.045
FVC% relative change (%)	-4.48 ± 14.6	3.37 ± 8.53	0.017

FVC: Forced vital capacity

Table 4.12. FVC and FVC% results at **visit 3**, and the longitudinal change in FVC and FVC% between visit 1 and visit 3 in the fibrotic and inflammation groups. Results are presented as mean ± standard deviation.

	Fibrotic (n = 23)	Inflammation (n = 16)	p value
D_{LCO} (mmol.min⁻¹.kPa⁻¹)	4.08 ± 1.88	4.64 ± 0.83	0.27
D_{LCO} change (mmol.min⁻¹.kPa⁻¹)	-0.18 ± 0.69	0.08 ± 0.70	0.25
D_{LCO} change (%)	-5.22 ± 20.6	4.92 ± 17.0	0.17
D_{LCO} (% predicted)	54.0 ± 22.2	65.8 ± 10.9	0.057
D_{LCO}% absolute change (%)	-3.81 ± 11.0	2.38 ± 9.84	0.079
D_{LCO}% relative change (%)	-5.55 ± 20.6	5.81 ± 17.6	0.081

D_{LCO}: Diffusing capacity of the lung for carbon monoxide

Table 4.13. D_{LCO} and D_{LCO}% at **visit 3**, and the longitudinal change in D_{LCO} and D_{LCO}% between visit 1 and visit 3 in the fibrotic and inflammation groups. Results are presented as mean ± standard deviation.

There was a statistically significant difference in D_{LCO} and D_{LCO}% between visit 1 and visit 3 in the IPF group (mean D_{LCO} (mmol. min⁻¹.kPa⁻¹): 4.25 ± 1.35 vs 3.79 ± 1.38, p=0.017; mean D_{LCO} (% predicted): 58.1 ± 18.6 vs 50.3 ± 16.2, p=0.032), as presented in Figure 4.3. However, there was no statistically significant difference in FVC or FVC% between visit 1 and visit 3 in the IPF group. There were no statistically significant differences in FVC, FVC%, D_{LCO} or D_{LCO}% between visit 1 and visit 3 when the fibrotic and inflammation groups were analysed separately.

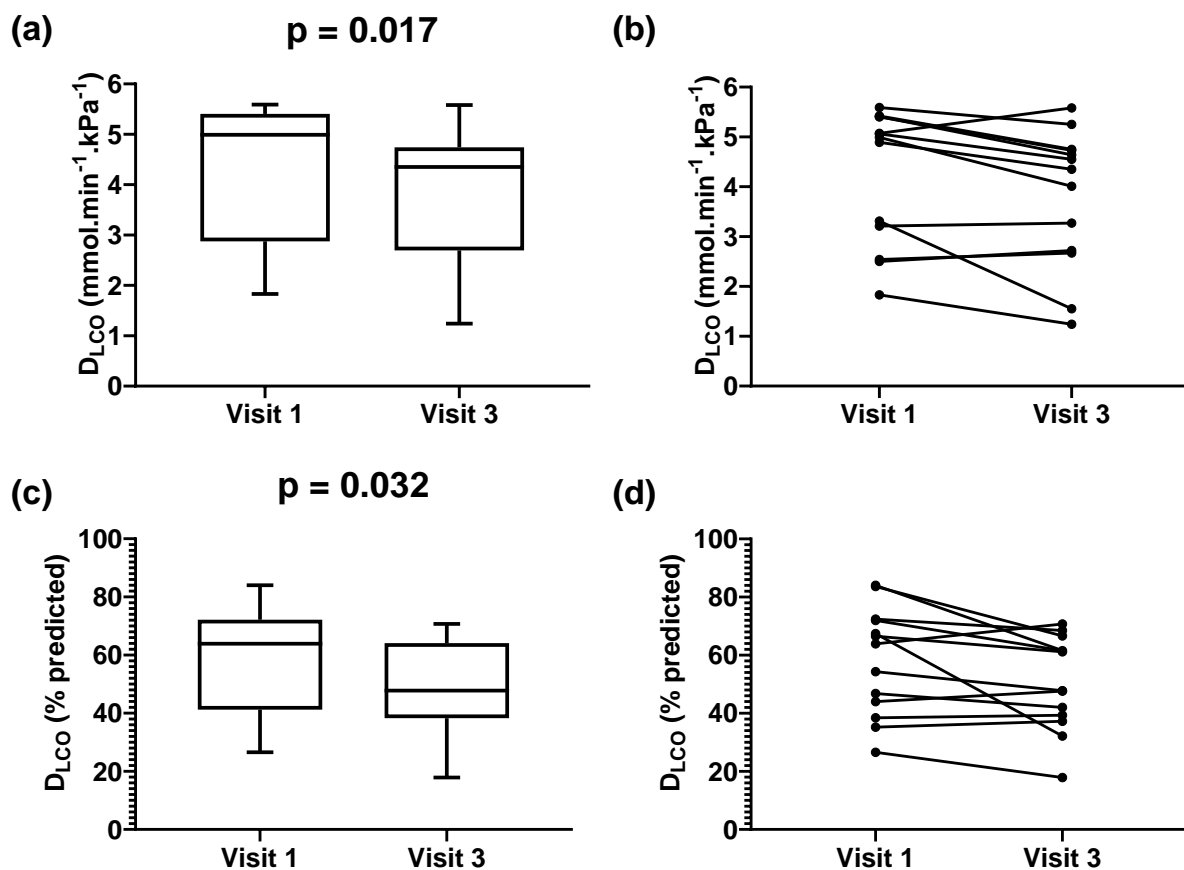


Figure 4.3. DLCO at visit 1 versus visit 3 for the IPF group (a-b). DLCO% at visit 1 versus visit 3 for the IPF group (c-d) (n=13). Statistical test: paired *t* test.

4.2.4 Visits 1, 2, and 3

35 subjects had PFT data available for visits 1, 2 and 3. This included 5 CTD-ILD, 9 DI-ILD, 8 HP, 2 iNSIP and 11 IPF subjects. There were 21 subjects in the fibrotic group and 14 in the inflammation group. Using two-way ANOVA statistical analysis, there was a statistically significant difference between visit 2 and visit 3 in FVC ($p=0.021$) and FVC% ($p=0.020$) in the inflammation group (Figure 4.4a). Of the 14 subjects in the inflammation group that completed the study, one received a two-week course of prednisolone between visits 1 and 2, one received a three-week course of prednisolone between visits 2 and 3, seven continued prednisolone and/or second line immunosuppressant treatment throughout the study and the remaining five subjects were not treated with immunosuppressants.

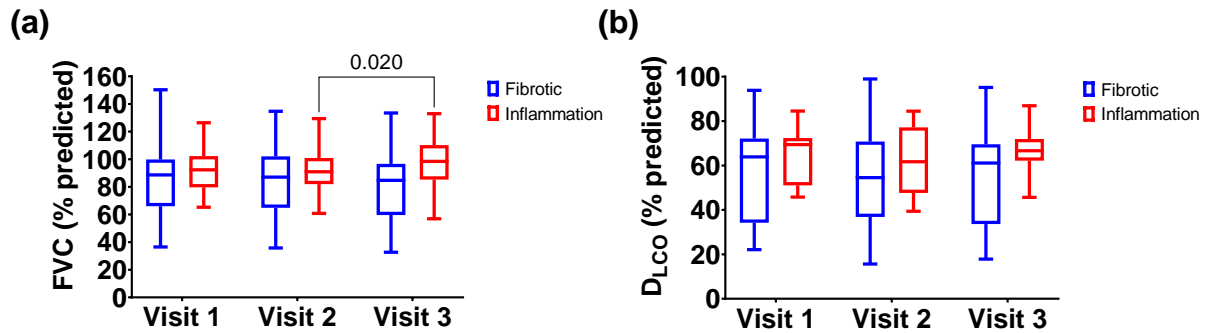


Figure 4.4. FVC % predicted (a) and DLco % predicted (b) at visits 1, 2 and 3 in subjects stratified into fibrotic (n=21) and inflammation (n=14) groups. Statistical test: two-way ANOVA.

4.3 Dissolved ¹²⁹Xe MRI

4.3.1 Study visits and examples of images / spectra

High-resolution dissolved phase spectroscopy was implemented from the beginning of the study which provided a global measure of ¹²⁹Xe RBC:TP. There was an error with the scan for this sequence in one of the visit 1 scans and therefore global ¹²⁹Xe RBC:TP data was available for 54 subjects at visit 1. Although 39 subjects had global ¹²⁹Xe RBC:TP data available at visit 2, one of these subjects did not have visit 1 data and therefore the longitudinal change in global ¹²⁹Xe RBC:TP between visit 1 and visit 2 could not be calculated. Figure 4.5 shows a summary of the number of subjects that had dissolved ¹²⁹Xe spectroscopy performed at each study visit. An IDEAL four-echo flyback 3D radial spectroscopic imaging technique was subsequently implemented in March 2019. This MRI sequence provided a regional measure of ¹²⁹Xe RBC:TP, RBC:Gas and TP:Gas, separated into upper / middle / lower zones, as well as central / peripheral zones. As demonstrated in Figure 4.5, 20 subjects had IDEAL spectroscopy performed at visit 1 and nine of these subjects returned for the visit 2 scan. Statistical analysis was not performed on the IDEAL spectroscopy data due to the small sample size.

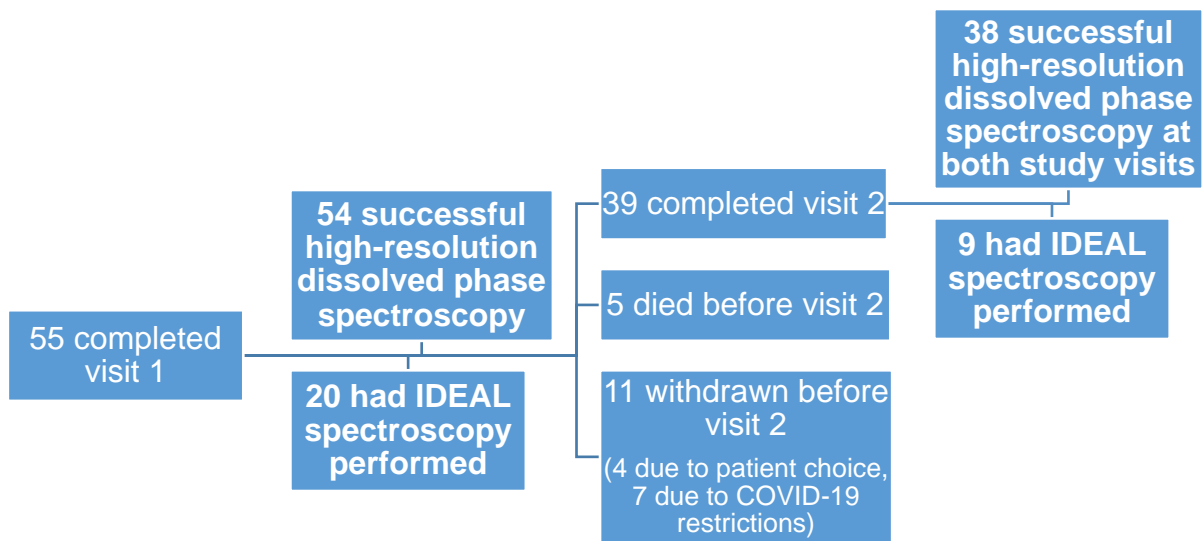


Figure 4.5. Summary of the number of subjects that had dissolved ^{129}Xe spectroscopy performed at each study visit.

An example of a ^{129}Xe RBC:TP spectra is presented in Figure 4.6. Figure 4.7 is an example of ^{129}Xe ratio maps using the IDEAL spectroscopic imaging technique. Both figures are from the same IPF subject.

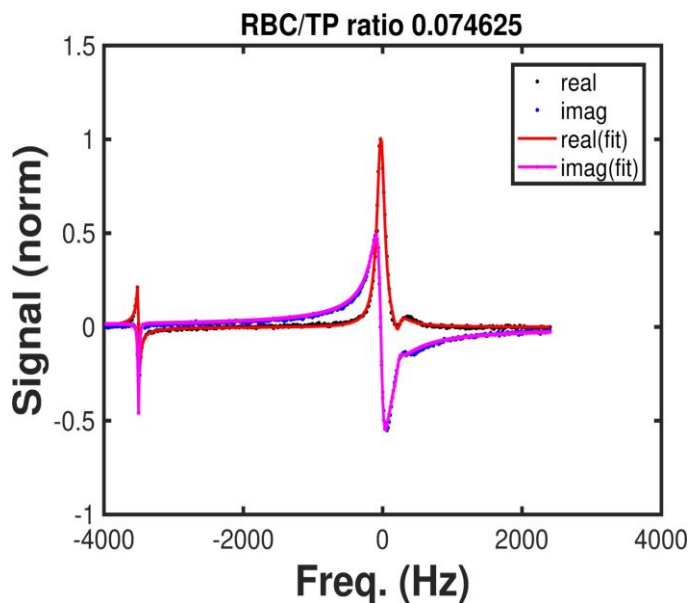


Figure 4.6. Example of a ^{129}Xe RBC:TP spectra in an IPF subject.

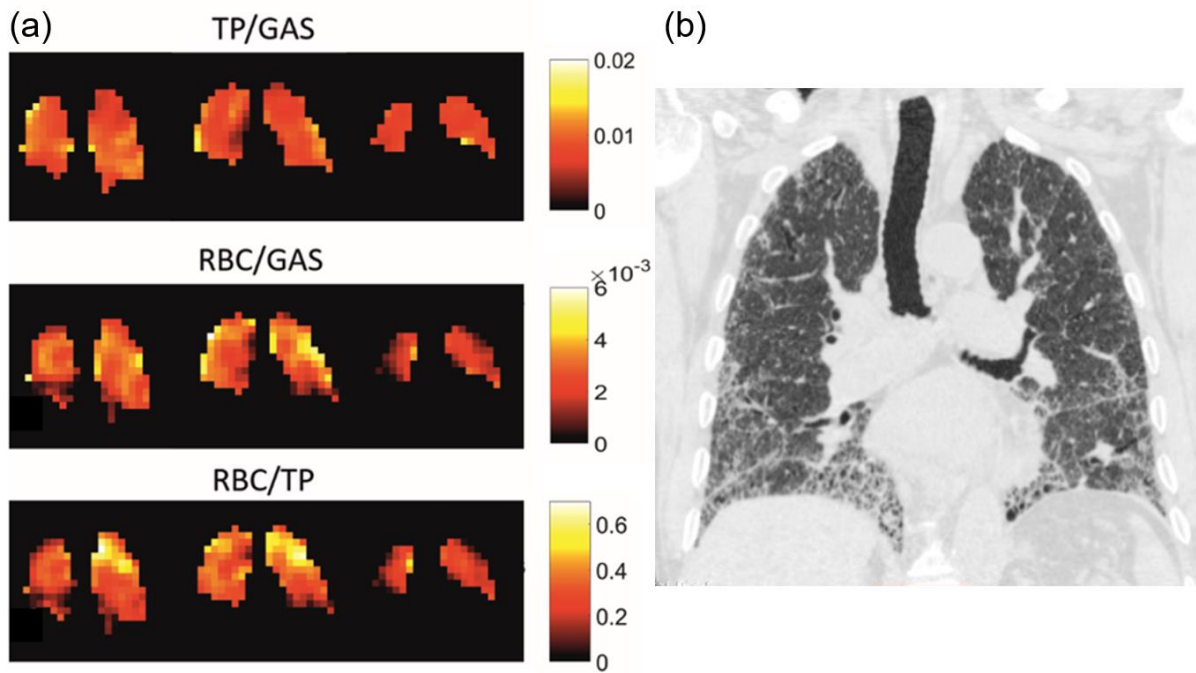


Figure 4.7. Example of ^{129}Xe ratio maps (a) and the corresponding HRCT thorax image (b) in an IPF subject.

4.3.2 Visit 1 (baseline)

4.3.2.1 High-resolution dissolved phase spectroscopy

	Total (n = 54)	CTD-ILD (n = 5)	DI-ILD (n = 13)	HP (n = 14)	iNSIP (n = 3)	IPF (n = 19)
RBC:TP	0.13 (0.11 – 0.19)	0.19 (0.11 – 0.20)	0.11 (0.10 – 0.19)	0.12 (0.10 – 0.16)	0.12 (0.10 – 0.19)	0.15 (0.13 – 0.19)

CTD-ILD: Connective tissue disease associated interstitial lung disease; DI-ILD: Drug induced interstitial lung disease; HP: Hypersensitivity pneumonitis; iNSIP: Idiopathic non-specific interstitial pneumonia; IPF: Idiopathic pulmonary fibrosis; RBC: Red blood cell; TP: Tissue plasma.

Table 4.14. Global ^{129}Xe RBC:TP at visit 1 for the total cohort and ILD subtypes. Results are presented as median (inter-quartile range).

	Fibrotic (n = 31)	Inflammation (n = 23)	p value
RBC:TP	0.16 ± 0.05	0.14 ± 0.05	0.18

RBC: Red blood cell; TP: Tissue plasma.

Table 4.15. Global ^{129}Xe RBC:TP at visit 1 in the fibrotic and inflammation groups. Results are presented as mean ± standard deviation.

4.3.2.2 IDEAL spectroscopic imaging technique

	Total (n = 20)	DI-ILD (n = 5)	HP (n = 7)	iNSIP (n = 3)	IPF (n = 5)
RBC:TP					
Upper zone	0.19 (0.16 – 0.22)	0.19 (0.17 – 0.24)	0.18 (0.16 – 0.22)	0.20 (0.19 – 0.22)	0.21 (0.13 – 0.22)
Middle zone	0.17 (0.15 – 0.20)	0.18 (0.14 – 0.22)	0.15 (0.14 – 0.22)	0.17 (0.16 – 0.21)	0.17 (0.12 – 0.19)
Lower zone	0.16 (0.14 – 0.21)	0.22 (0.14 – 0.25)	0.15 (0.13 – 0.21)	0.16 (0.15 – 0.21)	0.16 (0.12 – 0.20)
Central zone	0.18 (0.14 – 0.20)	0.19 (0.15 – 0.23)	0.15 (0.13 – 0.20)	0.17 (0.17 – 0.20)	0.19 (0.11 – 0.20)
Peripheral zone	0.18 (0.16 – 0.22)	0.21 (0.16 – 0.23)	0.18 (0.15 – 0.22)	0.18 (0.17 – 0.22)	0.18 (0.14 – 0.19)
TP:Gas					
Upper zone	0.010 (0.007 – 0.012)	0.010 (0.007 – 0.013)	0.010 (0.009 – 0.018)	0.0068 (0.006 – 0.009)	0.011 (0.007 – 0.012)
Middle zone	0.0093 (0.007 – 0.010)	0.0092 (0.006 – 0.011)	0.010 (0.008 – 0.016)	0.0075 (0.005 – 0.009)	0.0098 (0.007 – 0.010)
Lower zone	0.0085 (0.007 – 0.011)	0.0082 (0.006 – 0.011)	0.011 (0.007 – 0.014)	0.0083 (0.005 – 0.009)	0.0082 (0.007 – 0.010)
Central zone	0.0096 (0.007 – 0.011)	0.0096 (0.007 – 0.012)	0.011 (0.008 – 0.013)	0.0072 (0.005 – 0.009)	0.0096 (0.007 – 0.011)
Peripheral zone	0.0094 (0.007 – 0.011)	0.0093 (0.006 – 0.011)	0.011 (0.009 – 0.021)	0.0081 (0.006 – 0.009)	0.0094 (0.007 – 0.011)
RBC:Gas					
Upper zone	0.0019 (0.001 – 0.002)	0.0020 (0.001 – 0.003)	0.002 (0.001 – 0.003)	0.0014 (0.001 – 0.002)	0.0016 (0.001 – 0.002)
Middle zone	0.0014 (0.001 – 0.002)	0.0013 (0.001 – 0.002)	0.0017 (0.001 – 0.003)	0.0012 (0.001 – 0.002)	0.0014 (0.001 – 0.002)
Lower zone	0.0016 (0.001 – 0.002)	0.0015 (0.001 – 0.003)	0.0017 (0.001 – 0.003)	0.0013 (0.001 – 0.002)	0.0016 (0.001 – 0.002)
Central zone	0.0015 (0.001 – 0.002)	0.0014 (0.001 – 0.003)	0.0018 (0.001 – 0.003)	0.0012 (0.001 – 0.002)	0.0015 (0.001 – 0.002)
Peripheral zone	0.0017 (0.001 – 0.002)	0.0016 (0.001 – 0.003)	0.0017 (0.002 – 0.003)	0.0014 (0.001 – 0.002)	0.0014 (0.001 – 0.002)

CTD-ILD: Connective tissue disease associated interstitial lung disease; DI-ILD: Drug induced interstitial lung disease; HP: Hypersensitivity pneumonitis; iNSIP: Idiopathic non-specific interstitial pneumonia; IPF: Idiopathic pulmonary fibrosis; RBC: Red blood cell; TP: Tissue plasma.

Table 4.16. Regional ^{129}Xe RBC:TP, TP:Gas and RBC:Gas results at visit 1 for the total cohort and each ILD subtype. Results are presented as median (inter-quartile range).

	Fibrotic (n = 9)	Inflammation (n = 11)	p value
RBC:TP			
Upper zone	0.19 ± 0.039	0.20 ± 0.043	0.55
Middle zone	0.16 ± 0.035	0.17 ± 0.038	0.59
Lower zone	0.17 ± 0.042	0.18 ± 0.054	0.46
Central zone	0.17 ± 0.039	0.18 ± 0.040	0.48
Peripheral zone	0.18 ± 0.036	0.19 ± 0.042	0.43
TP:Gas			
Upper zone	0.0096 ± 0.0022	0.011 ± 0.0058	>0.99
Middle zone	0.0090 ± 0.0019	0.010 ± 0.0050	0.42
Lower zone	0.0086 ± 0.0017	0.010 ± 0.0043	0.31
Central zone	0.0091 ± 0.0020	0.010 ± 0.0051	0.47
Peripheral zone	0.0090 ± 0.0017	0.011 ± 0.0058	0.64
RBC:Gas			
Upper zone	0.0018 ± 0.0004	0.0021 ± 0.0010	0.38
Middle zone	0.0014 ± 0.0003	0.0019 ± 0.0010	0.23
Lower zone	0.0014 ± 0.0003	0.0019 ± 0.0008	0.16
Central zone	0.0015 ± 0.0004	0.0018 ± 0.0008	0.26
Peripheral zone	0.0016 ± 0.0003	0.0022 ± 0.0015	0.44

RBC: Red blood cell; TP: Tissue plasma.

Table 4.17. Regional ^{129}Xe RBC:TP, TP:Gas and RBC:Gas results at visit 1 in the fibrotic and inflammation groups. Results are presented as mean ± standard deviation.

4.3.3 Visit 2 (6 weeks or 6 months depending on ILD subtype)

4.3.3.1 High-resolution dissolved phase spectroscopy

There was a statistically significant decrease in ^{129}Xe RBC:TP between visits 1 and 2 in the IPF group (mean: 0.18 ± 0.06 vs 0.14 ± 0.03 ; $p=0.014$; $n=11$) (Figure 4.8a-b) and in the fibrotic group (mean: 0.17 ± 0.05 vs 0.14 ± 0.04 ; $p=0.006$; $n=21$) (Figure 4.8c-d). There was no statistically significant change in FVC, FVC%, DLCO or DLCO% between visits 1 and 2 in the IPF and fibrotic groups. This suggests that global ^{129}Xe RBC:TP is more sensitive to early disease progression in fibrotic ILD compared to PFTs. The repeatability coefficient of ^{129}Xe RBC:TP was 0.09 in ten healthy volunteers using the same MRI protocol and performed at the University of Sheffield. The repeatability coefficient is a measurement of precision, representing the value below which the absolute difference between two repeated measurements on the same subject is expected to lie with a 95% probability (95% limit of agreement) (360).

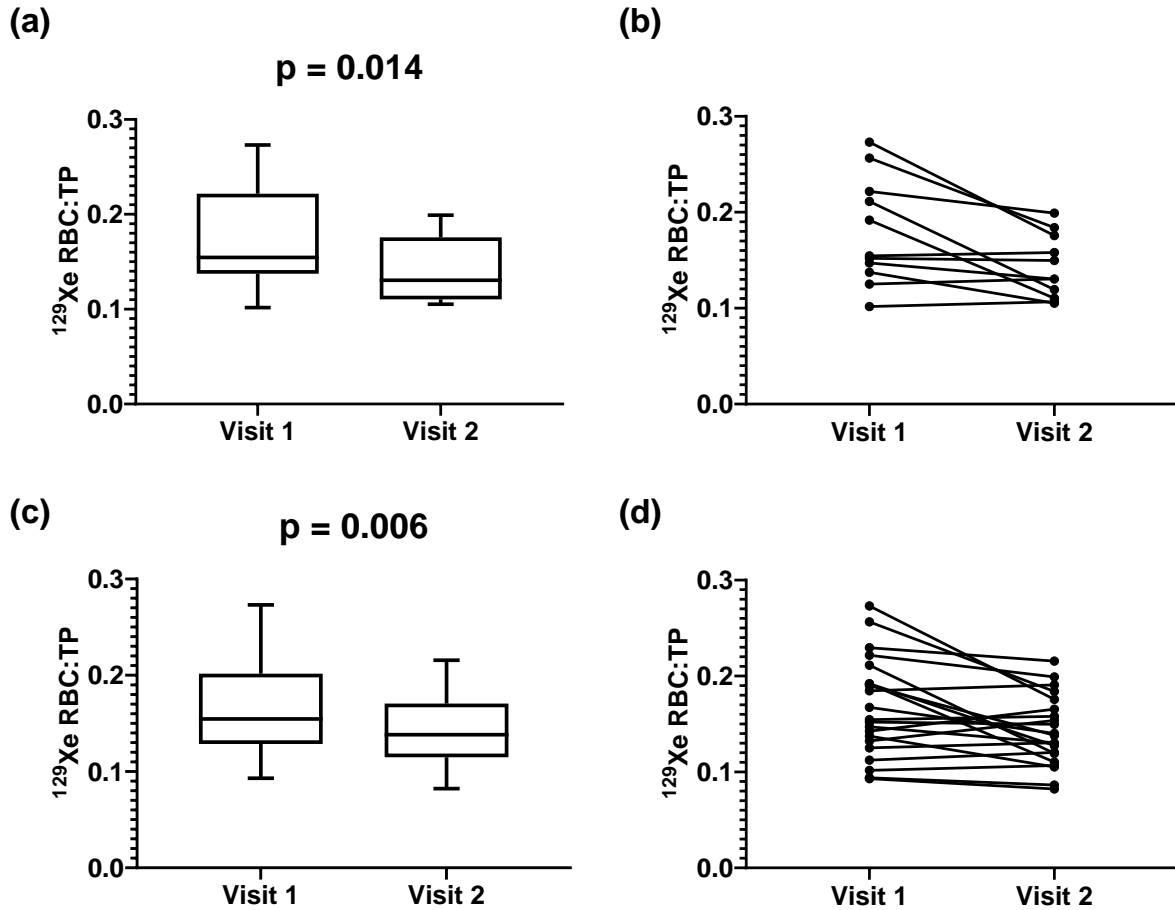


Figure 4.8. ^{129}Xe RBC:TP at visit 1 versus visit 2 in the IPF group (n=11; a-b) and the fibrotic group (n=21; c-d). Statistical test: paired *t* test.

	Total (n = 38)	CTD-ILD (n = 5)	DI-ILD (n = 11)	HP (n = 9)	iNSIP (n = 2)	IPF (n = 11)
RBC:TP	0.13 (0.11 – 0.17)	0.13 (0.12 – 0.20)	0.12 (0.09 – 0.19)	0.15 (0.11 – 0.16)	0.12 (0.10 – 0.14)	0.13 (0.11 – 0.18)
RBC:TP change	-0.003 (-0.02 – 0.01)	0.006 (-0.05 – 0.02)	-0.004 (-0.02 – 0.01)	0.003 (-0.01 – 0.02)	-0.027 (-0.05 – 0.00)	-0.023 (-0.08 – 0.00)
RBC:TP change (%)	-3.16 (-14.8 – 5.12)	5.73 (-24.0 – 13.8)	-3.60 (-11.6 – 3.96)	2.07 (-5.41 – 20.4)	-15.0 (-27.2 – -2.72)	-11.4 (-35.7 – 2.20)

CTD-ILD: Connective tissue disease associated interstitial lung disease; DI-ILD: Drug induced interstitial lung disease; HP: Hypersensitivity pneumonitis; iNSIP: Idiopathic non-specific interstitial pneumonia; IPF: Idiopathic pulmonary fibrosis; RBC: Red blood cell; TP: Tissue plasma.

Table 4.18. ^{129}Xe RBC:TP at **visit 2**, and the longitudinal change in ^{129}Xe RBC:TP between visit 1 and visit 2 for the total cohort and the ILD subtypes. Results are presented as median (inter-quartile range).

	Fibrotic (n = 21)	Inflammation (n = 17)	p value
RBC:TP	0.14 ± 0.04	0.14 ± 0.05	0.64
RBC:TP change	-0.025 ± 0.04	0.004 ± 0.02	0.007
RBC:TP change (%)	-11.7 ± 18.3	3.34 ± 17.5	0.015

RBC: Red blood cell; TP: Tissue plasma.

Table 4.19. ^{129}Xe RBC:TP at visit 2, and the longitudinal change in ^{129}Xe RBC:TP between visit 1 and visit 2 in the fibrotic and inflammation groups. Results are presented as mean ± standard deviation.

Two-way ANOVA statistical analysis confirmed a statistically significant difference in ^{129}Xe RBC:TP between visits 1 and 2 in the fibrotic group (Figure 4.9).

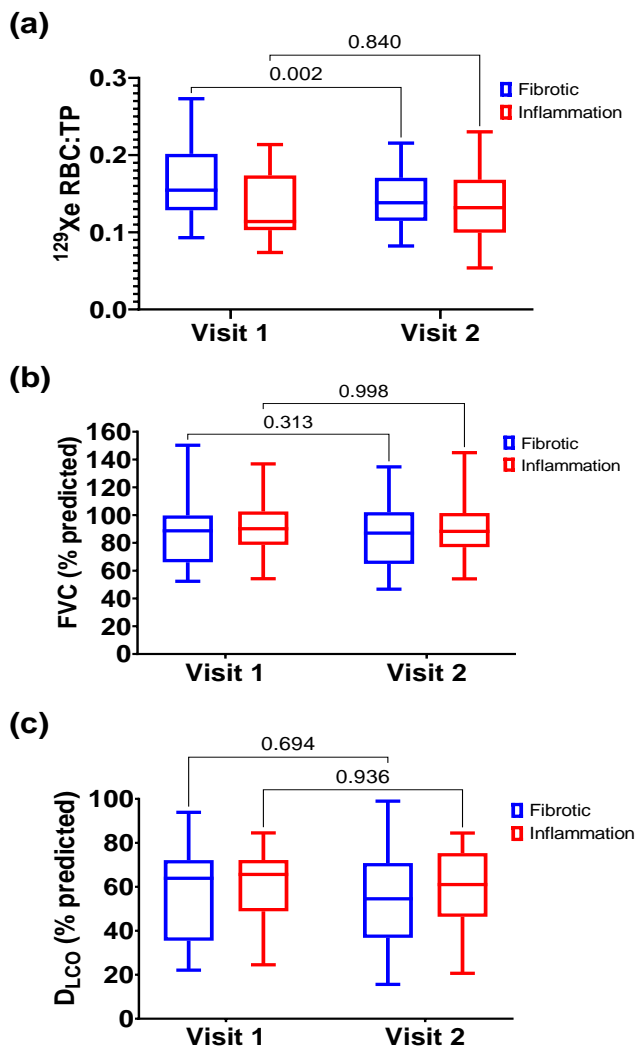


Figure 4.9. ^{129}Xe RBC:TP (a), FVC % predicted (b), and DLco % predicted (c) at visit 1 versus visit 2 in the fibrotic (n=21) and inflammation (n=17) groups. Statistical test: two-way ANOVA.

4.3.3.2 IDEAL spectroscopic imaging technique

	Total (n = 9)	DI-ILD (n = 4)	HP (n = 3)	iNSIP (n = 2)
RBC:TP change (%)				
Upper zone	-4.95 (-33.3 – 15.8)	-10.2 (-33.7 – 32.7)	-28.5 (-43.5 – 31.4)	-3.65 (-4.95 - -2.34)
Middle zone	2.88 (-20.0 – 15.2)	0.34 (-18.7 – 25.3)	-15.8 (-35.1 – 24.2)	5.59 (4.92 – 6.25)
Lower zone	0.010 (-14.0 – 8.36)	2.92 (0.23 – 10.1)	-13.9 (-36.2 – 22.8)	-7.70 (-14.2 - -1.21)
Central zone	0.72 (-7.05 – 19.5)	0.39 (-1.77 – 19.4)	-11.7 (-35.2 – 22.0)	10.2 (3.37 – 16.9)
Peripheral zone	-1.19 (-19.3 – 10.2)	0.30 (-8.23 – 14.4)	-22.9 (-35.8 – 36.8)	-7.38 (-15.7 – 0.96)
TP:Gas change (%)				
Upper zone	4.95 (-3.46 – 20.6)	8.20 (-2.33 – 12.3)	-1.44 (-9.85 – 44.9)	13.2 (-2.15 – 28.6)
Middle zone	4.12 (-1.12 – 13.4)	6.14 (3.27 – 10.7)	-3.79 (-10.8 – 35.1)	8.44 (1.55 – 15.3)
Lower zone	2.89 (-1.81 – 16.0)	2.30 (-1.49 – 9.80)	-1.17 (-18.6 – 34.2)	11.4 (2.89 – 20.0)
Central zone	4.69 (0.17 – 14.5)	5.51 (0.26 – 7.88)	1.10 (-13.9 – 34.7)	12.9 (4.69 – 21.1)
Peripheral zone	4.15 (-5.44 – 13.4)	5.11 (-0.76 – 10.2)	-6.88 (-13.3 – 34.4)	5.60 (-3.99 – 15.2)
RBC:Gas change (%)				
Upper zone	-4.47 (-7.24 – 20.4)	-3.92 (-7.73 – 47.0)	-5.66 (-26.7 – 20.3)	7.74 (-4.98 – 20.5)
Middle zone	9.96 (-4.78 – 17.4)	12.0 (4.06 – 33.6)	-11.6 (-18.2 – 11.0)	12.3 (3.68 – 20.8)
Lower zone	2.10 (-6.59 – 9.17)	9.17 (3.18 – 16.7)	-14.3 (-15.2 – 1.09)	2.15 (2.10 – 2.19)
Central zone	6.49 (-2.76 – 17.4)	7.99 (5.06 – 21.3)	-10.1 (-13.0 – 6.07)	23.1 (6.63 – 39.5)
Peripheral zone	-2.93 (-10.1 – 13.9)	3.54 (-4.10 – 23.6)	-14.6 (-27.4 – 21.1)	-3.70 (-4.46 - -2.93)

DI-ILD: Drug induced interstitial lung disease; HP: Hypersensitivity pneumonitis; iNSIP: Idiopathic non-specific interstitial pneumonia; RBC: Red blood cell; TP: Tissue plasma.

Table 4.20. % change in regional ¹²⁹Xe RBC:TP, TP:Gas and RBC:Gas results between visit 1 and visit 2 for the total cohort and each ILD subtype. Results are presented as median (inter-quartile range).

	Fibrotic (n = 3)	Inflammation (n = 6)	p value
RBC:TP change (%)			
Upper zone	31.4 (-2.34 – 43.6)	-24.6 (-39.5 - -3.69)	0.048
Middle zone	24.2 (4.92 – 32.7)	-8.99 (-27.0 – 3.72)	0.048
Lower zone	4.96 (-1.21 – 22.8)	-6.93 (-19.7 – 3.59)	0.26
Central zone	22.0 (3.37 – 25.6)	-1.16 (-17.6 – 4.77)	0.048
Peripheral zone	18.6 (0.96 – 36.8)	-13.2 (-26.1 - -0.45)	0.048
TP:Gas change (%)			
Upper zone	-2.15 (-9.85 – 12.6)	8.20 (-2.27 – 32.7)	0.38
Middle zone	1.55 (-10.8 – 4.12)	9.86 (1.29 – 20.3)	0.17
Lower zone	1.38 (-18.6 – 2.89)	7.60 (-1.49 – 23.5)	0.26
Central zone	-0.76 (-13.9 – 4.69)	7.82 (2.75 – 24.5)	0.10
Peripheral zone	-3.99 (-13.3 – 6.07)	7.84 (-3.52 – 20.0)	0.26
RBC:Gas change (%)			
Upper zone	20.3 (-4.98 – 63.7)	-5.07 (-13.3 – 2.59)	0.26
Middle zone	11.0 (3.68 – 40.1)	6.03 (-13.3 – 15.8)	0.38
Lower zone	2.19 (1.09 – 7.38)	1.94 (-14.5 – 12.9)	0.91
Central zone	6.63 (6.07 – 25.2)	5.54 (-10.8 – 17.0)	0.55
Peripheral zone	21.1 (-4.46 – 29.3)	-4.26 (-17.8 – 1.95)	0.17

RBC: Red blood cell; TP: Tissue plasma.

Table 4.21. % change in regional ¹²⁹Xe RBC:TP, TP:Gas and RBC:Gas results between visit 1 and visit 2 in the fibrotic and inflammation groups. Results are presented as median (inter-quartile range).

4.4 ¹²⁹Xe Diffusion-weighted MRI (airway microstructure)

4.4.1 Study visits and examples of images

There was an error with the ¹²⁹Xe DW-MRI sequence in one of the visit 1 scans, and therefore ¹²⁹Xe DW-MRI data was available for 54 subjects at visit 1. Although 39 subjects completed visit 2, there was an error with the scan for this sequence in two of the visit 2 scans. Therefore, the longitudinal change in ¹²⁹Xe ADC and L_{mD} between visit 1 and visit 2 could not be calculated in two of the 39 subjects that completed visit 2.

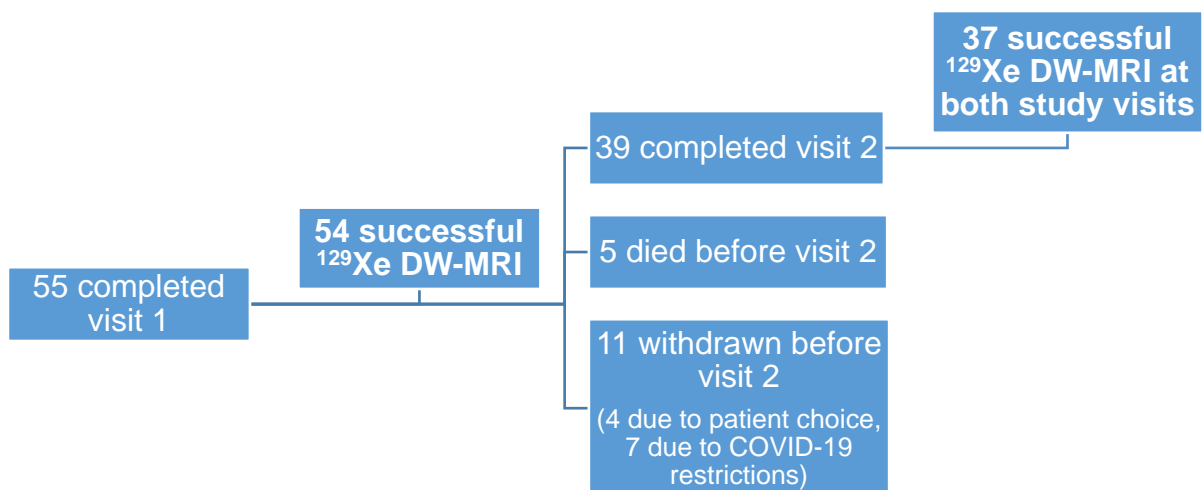


Figure 4.10. Summary of the number of subjects that had ¹²⁹Xe DW-MRI performed at each study visit.

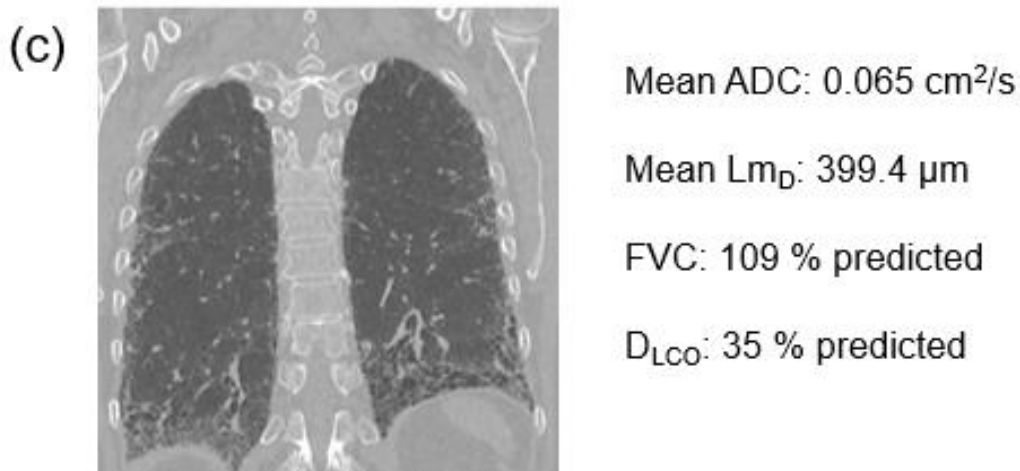
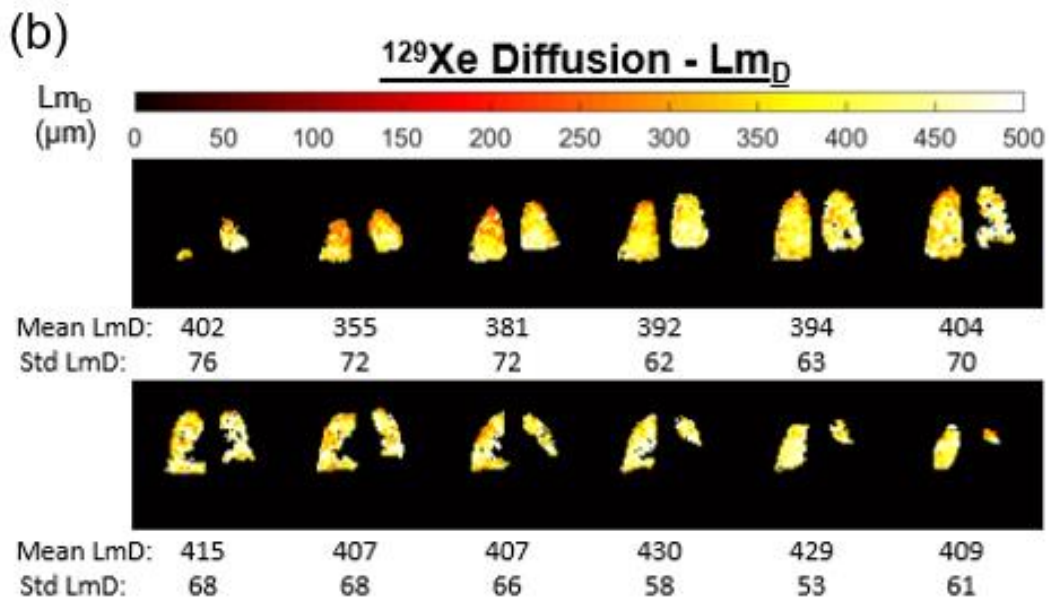
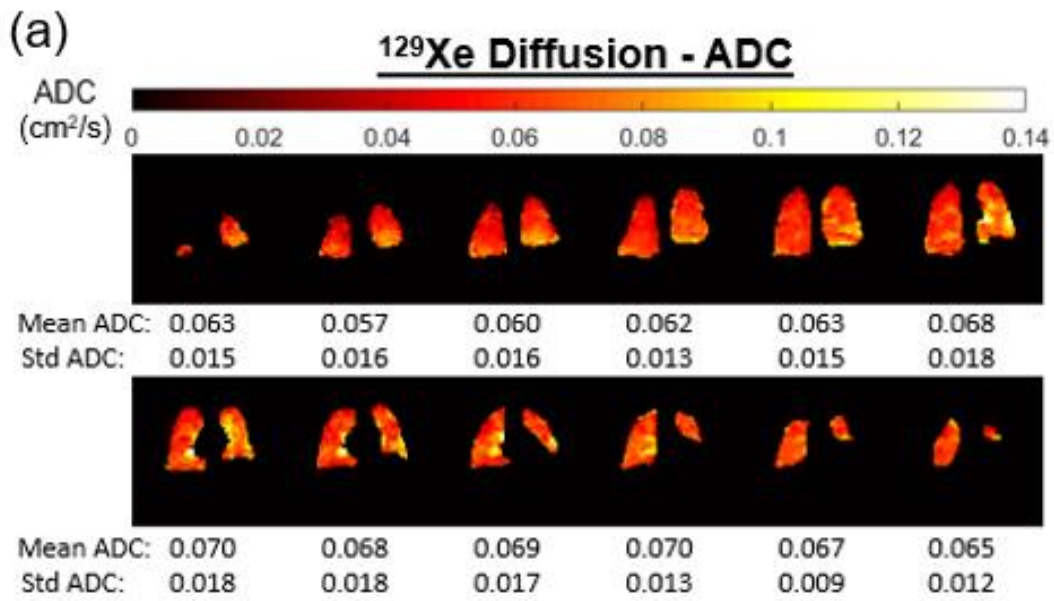


Figure 4.11. Example of a ^{129}Xe ADC map (a), ^{129}Xe Lm_D map (b) and corresponding coronal HRCT image (c) in an IPF subject.

4.4.2 Visit 1 (baseline)

There was a statistically significant difference between the five ILD subtypes at visit 1 in global ^{129}Xe ADC ($p=0.014$; HP vs IPF: $p=0.011$) and Lm_D ($p=0.015$; HP vs IPF: $p=0.013$) (Figure 4.12). There was a statistically significant difference between the fibrotic and inflammation groups at visit 1 in global ^{129}Xe ADC (mean (cm^2/s): 0.046 ± 0.008 vs 0.042 ± 0.006 ; $p=0.034$) and Lm_D (mean (μm): 333 ± 34 vs 316 ± 27 ; $p=0.046$) (Figure 4.13). These findings suggest that ^{129}Xe DW-MRI has value in differentiating between the pathological processes that cause the physiological abnormalities in the various ILD subtypes.

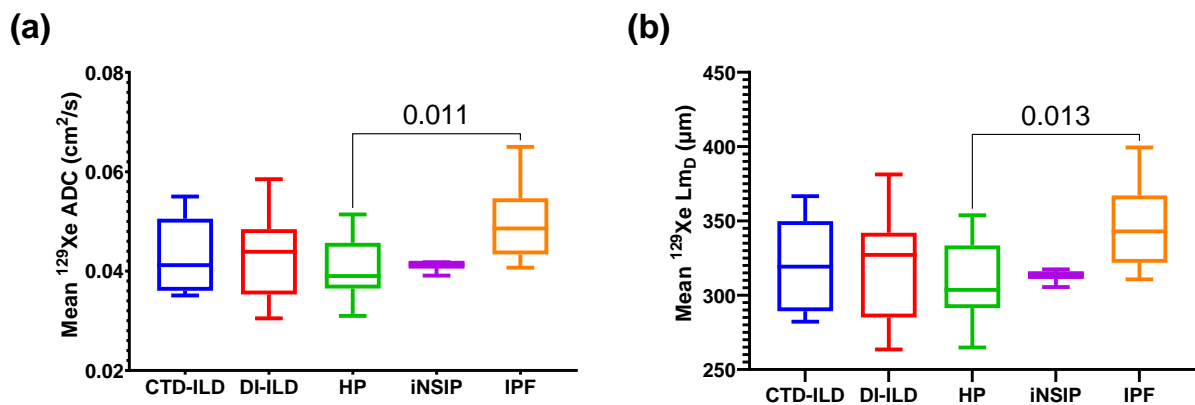


Figure 4.12. Difference between ILD subtypes at visit 1 in global ^{129}Xe ADC (a) and Lm_D (b). Statistical test: Kruskal-Wallis.

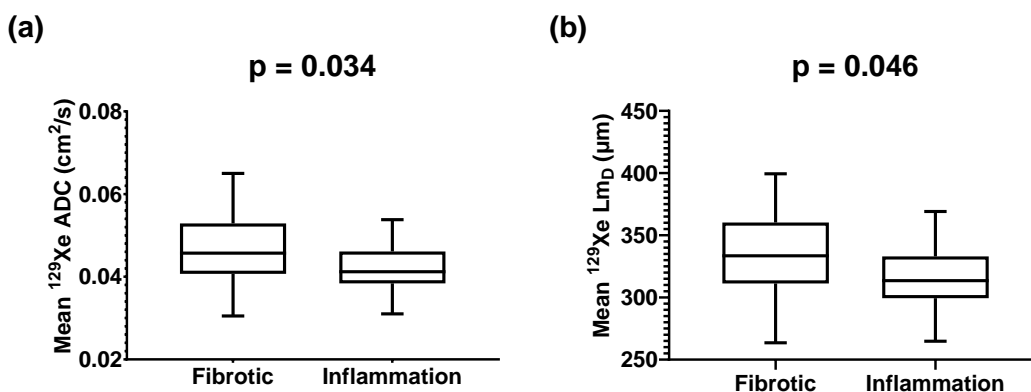


Figure 4.13. Difference between fibrotic ($n=31$) and inflammation ($n=23$) groups at visit 1 in global ^{129}Xe ADC (a) and Lm_D (b). Statistical test: independent samples t test.

	Total (n = 54)	CTD-ILD (n = 5)	DI-ILD (n = 13)	HP (n = 15)	iNSIP (n = 3)	IPF (n = 18)
ADC (cm²/s)	0.044 (0.039 – 0.050)	0.041 (0.036 – 0.051)	0.044 (0.035 – 0.048)	0.039 (0.037 – 0.046)	0.041 (0.039 – 0.042)	0.049 (0.043 – 0.055)
L_{mD} (μm)	323 (303 – 347)	319 (289 – 350)	327 (285 – 342)	304 (291 – 334)	314 (306 – 317)	343 (322 – 367)

ADC: Apparent diffusion coefficient; CTD-ILD: Connective tissue disease associated interstitial lung disease; DI-ILD: Drug induced interstitial lung disease; HP: Hypersensitivity pneumonitis; iNSIP: Idiopathic non-specific interstitial pneumonia; IPF: Idiopathic pulmonary fibrosis; L_{mD}: mean diffusive length scale.

Table 4.22. Global ¹²⁹Xe ADC and L_{mD} at visit 1 for the total cohort and ILD subtypes. Results are presented as median (inter-quartile range).

	Fibrotic (n = 31)	Inflammation (n = 23)	p value
ADC (cm²/s)	0.046 ± 0.008	0.042 ± 0.006	0.034
L_{mD} (μm)	333 ± 34	316 ± 27	0.046

ADC: Apparent diffusion coefficient; L_{mD}: mean diffusive length scale.

Table 4.23. Global ¹²⁹Xe ADC and L_{mD} at visit 1 in the fibrotic and inflammation groups. Results are presented as mean ± standard deviation.

In the DI-ILD group (n=13), there was a statistically significant difference between the upper and middle zone in ¹²⁹Xe ADC (median (cm²/s): 0.041 (0.035 – 0.044) vs 0.045 (0.037 – 0.047); p=0.018) (Figure 4.14a) and ¹²⁹Xe L_{mD} (median (μm): 311 (283 – 326) vs 324 (292 – 345); p=0.015) (Figure 4.14b). In the HP group (n=15), there was a statistically significant difference between the middle and lower zone in ¹²⁹Xe ADC (median (cm²/s): 0.042 (0.037 – 0.048) vs 0.037 (0.035 – 0.043); p<0.001) (Figure 4.14c) and ¹²⁹Xe L_{mD} (median (μm): 315 (292 – 350) vs 296 (280 – 318); p<0.001) (Figure 4.14d). In the IPF group (n=18), there was a statistically significant difference between the upper and middle zone in ¹²⁹Xe ADC (median (cm²/s): 0.045 (0.042 – 0.049) vs 0.050 (0.045 – 0.055); p<0.001) (Figure 4.14e) and ¹²⁹Xe L_{mD} (median (μm): 328 (316 – 349) vs 348 (322 – 374); p<0.001) (Figure 4.14f). There was also a statistically significant difference in ¹²⁹Xe L_{mD} between the upper and lower zone in the IPF group (median (μm): 328 (316 – 349) vs 344 (323 – 378); p=0.043) (Figure 4.14f). ¹²⁹Xe DW-MRI provides unique information regarding microstructural changes, especially in fibrotic ILD. This is supported by the regional variation found between ILD subtypes.

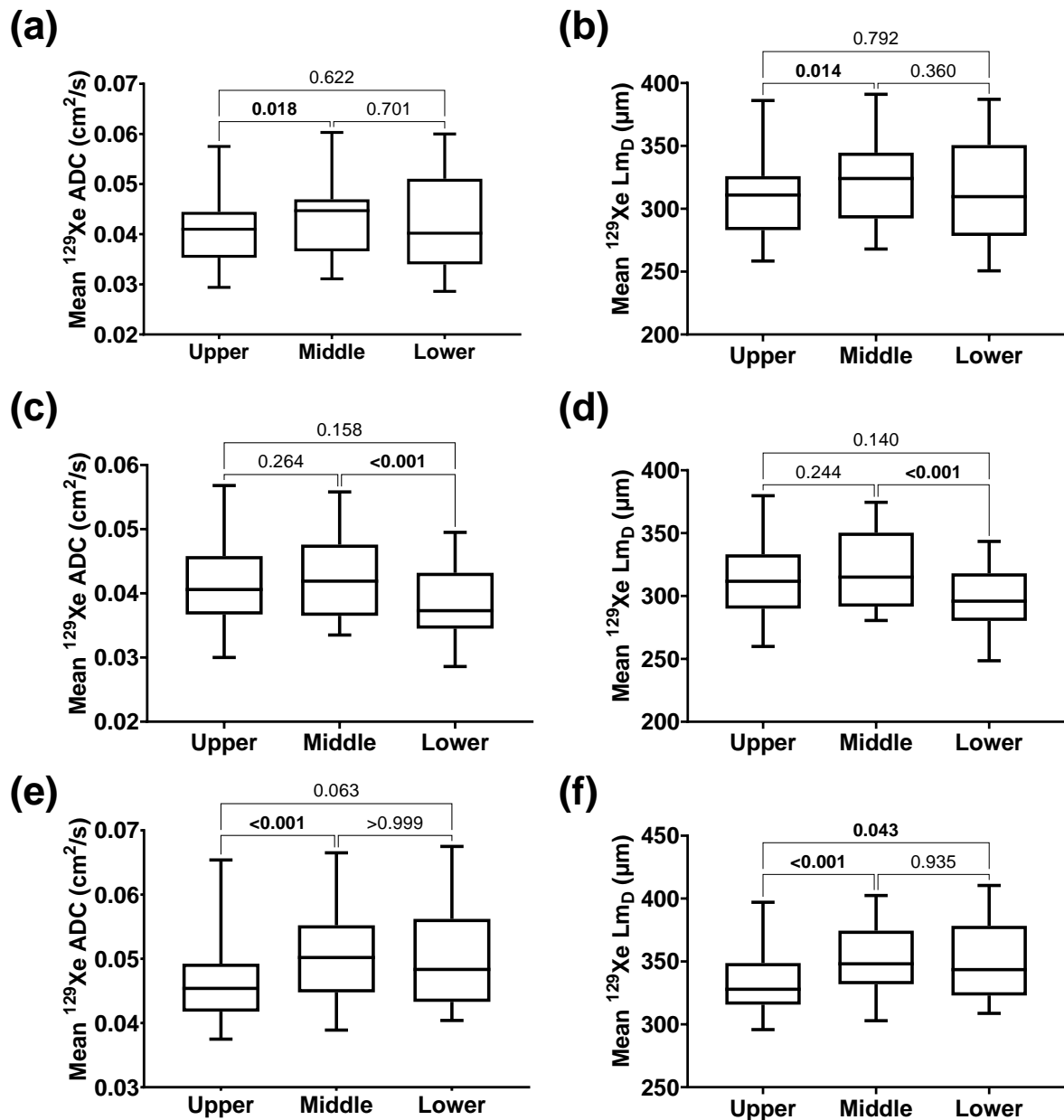


Figure 4.14. ^{129}Xe ADC and L_mD in the upper, middle and lower zones in the DI-ILD group (a-b), the HP group (c-d) and the IPF group (e-f) at visit 1. Statistical test: one-way ANOVA.

There was a statistically significant difference in ^{129}Xe ADC between the central zone and the peripheral zone in the HP group (median (cm^2/s): 0.041 (0.038 – 0.046) vs 0.038 (0.036 – 0.046); $p=0.020$; $n=15$) and the IPF group (median (cm^2/s): 0.050 (0.045 – 0.056) vs 0.048 (0.042 – 0.055); $p=0.005$; $n=18$) (Figure 4.15).

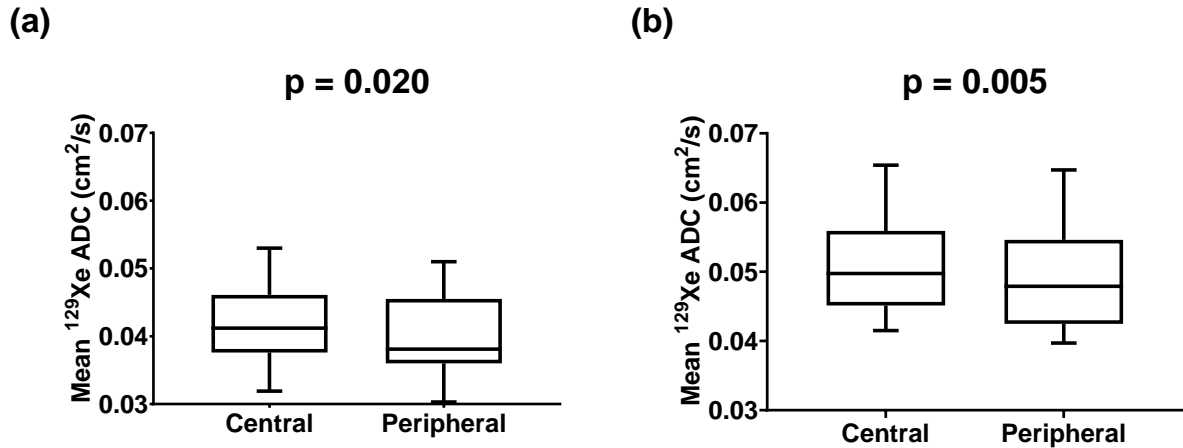


Figure 4.15. ^{129}Xe ADC in the central and peripheral zones for the HP group (a) and the IPF group (b). Statistical test: paired *t* test.

There was a statistically significant difference in ^{129}Xe L_{MD} between the central zone and the peripheral zone in the DI-ILD group (median (μm): 329 (293 – 346) vs 319 (279 – 341); $p=0.001$; $n=13$), HP group (median (μm): 314 (297 – 336) vs 297 (289 – 332); $p=0.001$; $n=15$), and the IPF group (median (μm): 351 (332 – 377) vs 338 (314 – 368); $p<0.001$; $n=18$) (Figure 4.16). It is likely that this finding is due to the higher density of large airways in the central zones when compared to the peripheral zone.

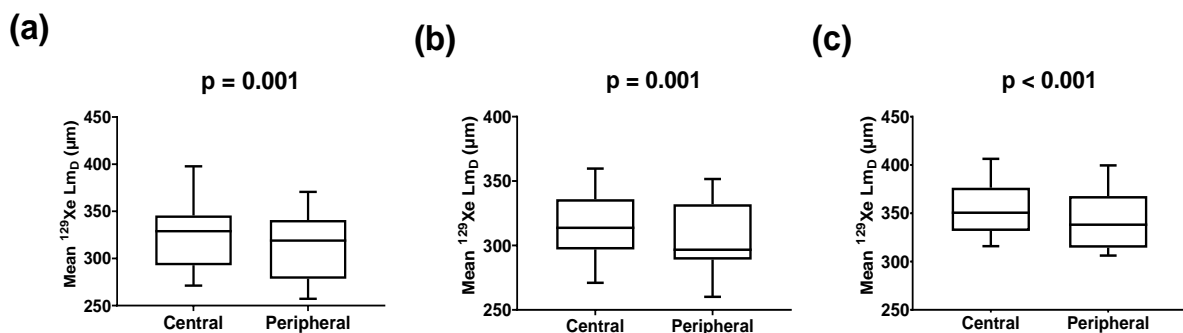


Figure 4.16. ^{129}Xe L_{MD} in the central and peripheral zones for the DI-ILD group (a), HP group (b) and the IPF group (c). Statistical test: paired *t* test.

	Total (n = 54)	CTD-ILD (n = 5)	DI-ILD (n = 13)	HP (n = 15)	iNSIP (n = 3)	IPF (n = 18)
ADC (cm²/s)						
Upper zone	0.042 (0.038 – 0.046)	0.038 (0.034 – 0.043)	0.041 (0.035 – 0.044)	0.041 (0.037 – 0.046)	0.039 (0.038 – 0.041)	0.045 (0.042 – 0.049)
Middle zone	0.045 (0.040 – 0.051)	0.041 (0.038 – 0.049)	0.045 (0.037 – 0.047)	0.042 (0.037 – 0.048)	0.043 (0.040 – 0.044)	0.050 (0.045 – 0.055)
Lower zone	0.043 (0.036 – 0.050)	0.043 (0.035 – 0.058)	0.040 (0.034 – 0.051)	0.037 (0.035 – 0.043)	0.039 (0.039 – 0.042)	0.048 (0.043 – 0.056)
Central zone	0.044 (0.041 – 0.050)	0.042 (0.038 – 0.049)	0.044 (0.037 – 0.048)	0.041 (0.038 – 0.046)	0.043 (0.041 – 0.044)	0.050 (0.045 – 0.056)
Peripheral zone	0.043 (0.038 – 0.049)	0.040 (0.035 – 0.051)	0.043 (0.034 – 0.049)	0.038 (0.036 – 0.046)	0.040 (0.038 – 0.040)	0.048 (0.042 – 0.055)
Lm_D (μm)						
Upper zone	317 (298 – 335)	300 (277 – 318)	311 (283 – 326)	312 (290 – 333)	307 (298 – 309)	328 (316 – 349)
Middle zone	329 (310 – 356)	322 (298 – 347)	324 (292 – 345)	315 (292 – 350)	314 (312 – 330)	348 (332 – 374)
Lower zone	319 (293 – 349)	326 (286 – 372)	310 (278 – 351)	296 (280 – 318)	306 (302 – 316)	344 (323 – 378)
Central zone	332 (313 – 358)	327 (302 – 352)	329 (293 – 346)	314 (297 – 336)	321 (316 – 331)	351 (332 – 377)
Peripheral zone	317 (297 – 343)	313 (280 – 349)	319 (279 – 341)	297 (289 – 332)	307 (298 – 309)	338 (314 – 368)

ADC: Apparent diffusion coefficient; CTD-ILD: Connective tissue disease associated interstitial lung disease; DI-ILD: Drug induced interstitial lung disease; HP: Hypersensitivity pneumonitis; iNSIP: Idiopathic non-specific interstitial pneumonia; IPF: Idiopathic pulmonary fibrosis; Lm_D: mean diffusive length scale.

Table 4.24. Regional ¹²⁹Xe ADC and Lm_D results at visit 1 for the total cohort and each ILD subtype. Results are presented as median (inter-quartile range).

In the fibrotic group (n=31), there was a statistically significant difference in ¹²⁹Xe ADC between the upper and middle zone (mean (cm²/s): 0.043 ± 0.007 vs 0.047 ± 0.008; p<0.001), between the upper and lower zone (mean (cm²/s): 0.043 ± 0.007 vs 0.047 ± 0.011; p=0.013), and between the central and peripheral zone (mean (cm²/s): 0.047 ± 0.008 vs 0.046 ± 0.009; p=0.002) (Figure 4.17a-b). In the inflammation group (n=23), there was a statistically significant difference in ¹²⁹Xe ADC between the upper zone and the middle zone (mean (cm²/s): 0.042 ± 0.007 vs 0.044 ± 0.006; p=0.019), between the middle zone and the lower zone (mean (cm²/s): 0.044 ± 0.006 vs 0.040 ± 0.007; p<0.001), and between the central zone and the peripheral zone (mean (cm²/s): 0.043 ± 0.006 vs 0.041 ± 0.006; p<0.001) (Figure 4.17c-d).

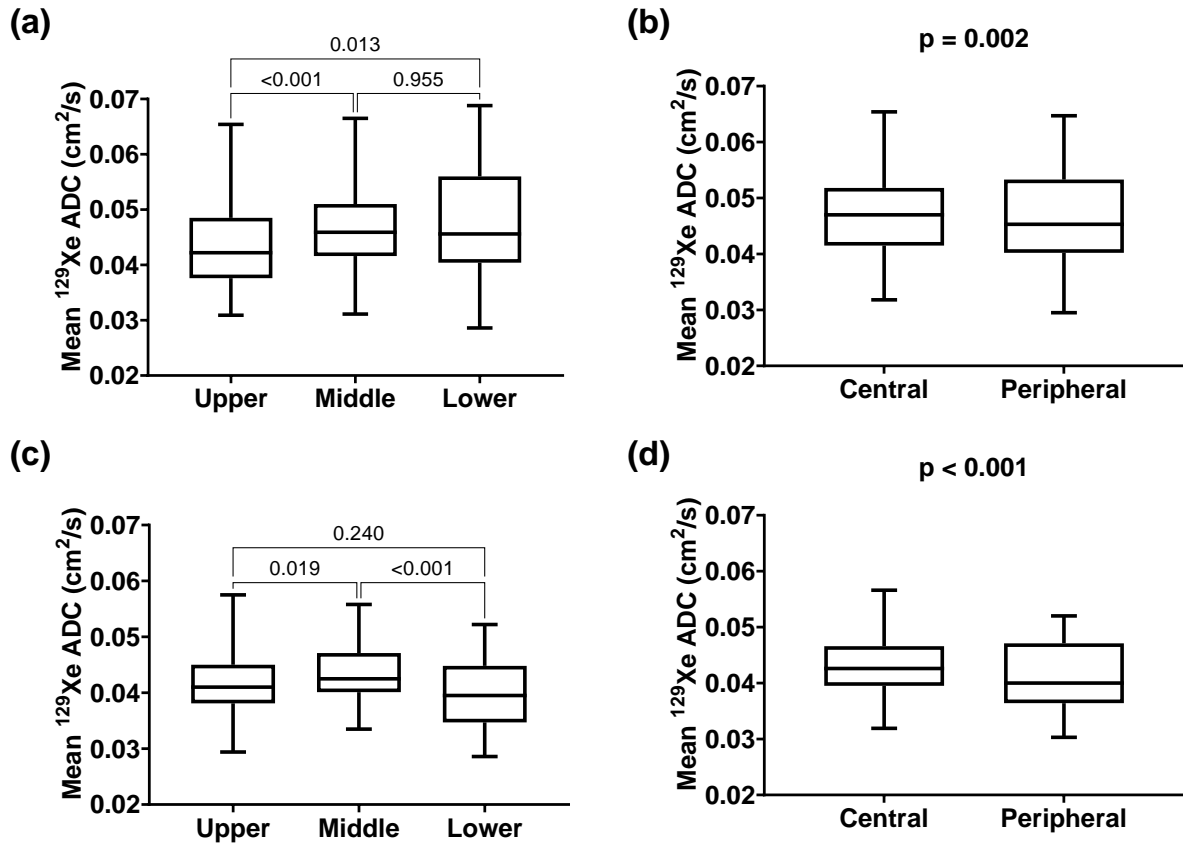


Figure 4.17. ^{129}Xe ADC for the fibrotic group (n=31) in the upper, middle and lower zones (a), and in the central and peripheral zones (b). ^{129}Xe ADC for the inflammation group (n=23) in the upper, middle and lower zones (c), and in the central and peripheral zones (d). Statistical test: one-way ANOVA.

In the fibrotic group (n=31), there was a statistically significant difference in ^{129}Xe L_{mD} between the upper and middle zone (mean (μm): 320 ± 32 vs 337 ± 34 ; $p < 0.001$), between the upper and lower zone (mean (μm): 320 ± 32 vs 336 ± 42 ; $p = 0.013$), and between the central and peripheral zone (mean (μm): 341 ± 35 vs 328 ± 34 ; $p < 0.001$) (Figure 4.18a-b). In the inflammation group (n=23), there was a statistically significant difference in ^{129}Xe L_{mD} between the upper and middle zone (mean (μm): 315 ± 33 vs 325 ± 28 ; $p = 0.014$), between the middle and lower zone (mean (μm): 325 ± 28 vs 305 ± 30 ; $p < 0.001$), and between the central and peripheral zone (mean (μm): 324 ± 28 vs 310 ± 28 ; $p < 0.001$) (Figure 4.18c-d).

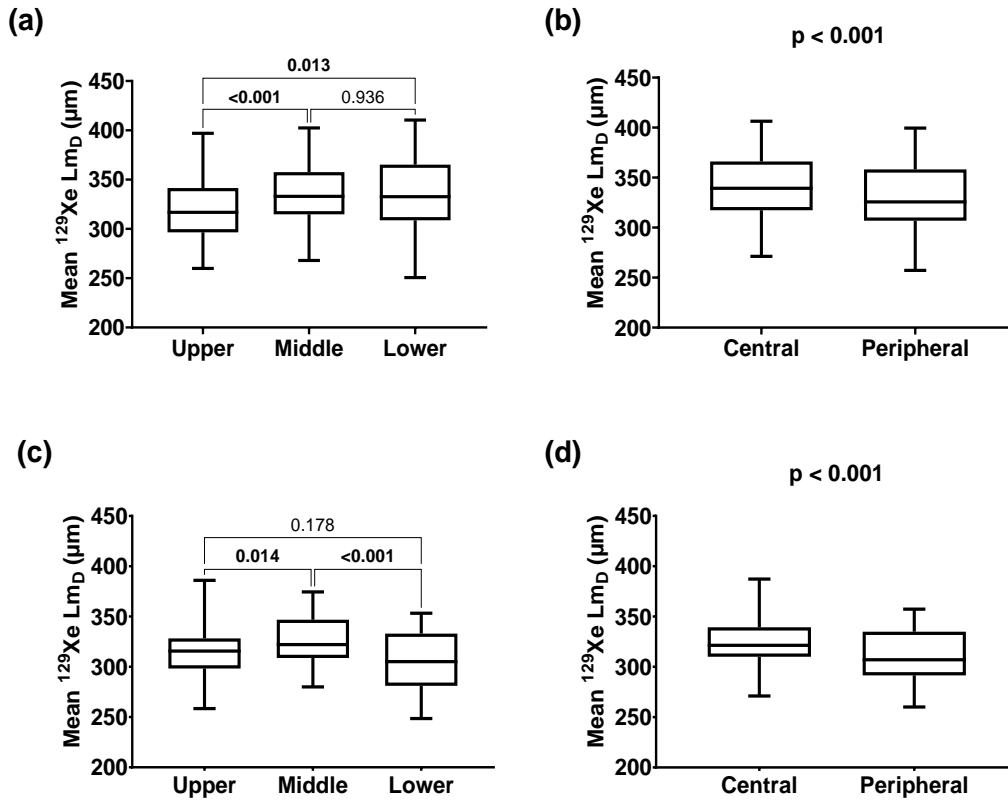


Figure 4.18. ^{129}Xe LmD in the upper, middle and lower zones (a), and in the central and peripheral zones (b) in the fibrotic group (n=31). ^{129}Xe LmD in the upper, middle and lower zones (c), and in the central and peripheral zones (d) in the inflammation group (n=23). Statistical test: one-way ANOVA.

	Fibrotic (n = 31)	Inflammation (n = 23)	p value
ADC (cm²/s)			
Upper zone	0.043 ± 0.007	0.042 ± 0.007	0.50
Middle zone	0.047 ± 0.008	0.044 ± 0.006	0.12
Lower zone	0.047 ± 0.011	0.040 ± 0.007	0.004
Central zone	0.047 ± 0.008	0.043 ± 0.006	0.047
Peripheral zone	0.046 ± 0.009	0.041 ± 0.006	0.030
LmD (μm)			
Upper zone	320 ± 31	315 ± 33	0.58
Middle zone	337 ± 34	325 ± 28	0.16
Lower zone	336 ± 42	305 ± 30	0.004
Central zone	341 ± 35	324 ± 28	0.063
Peripheral zone	328 ± 34	310 ± 28	0.040

ADC: Apparent diffusion coefficient; LmD: mean diffusible length scale.

Table 4.25. Regional ^{129}Xe ADC and LmD results at visit 1 in the fibrotic and inflammation groups. Results are presented as mean ± standard deviation.

4.4.3 Visit 2 (6 weeks or 6 months depending on ILD subtype)

In the DI-ILD group (n=10), there was a statistically significant increase in global ^{129}Xe ADC (mean (cm^2/s): 0.045 ± 0.007 vs 0.047 ± 0.008 ; $p=0.005$) and Lm_D (mean (μm): 329 ± 32 vs 333 ± 34 ; $p=0.017$) between visits 1 and 2 (Figure 4.19). The repeatability coefficient of ^{129}Xe ADC and Lm_D was 0.002 and 11.3 respectively in ten healthy volunteers using the same MRI protocol and performed at the University of Sheffield. Although the increase in ^{129}Xe ADC and Lm_D occurred over a short period of time, it is possible that these findings were due to fibrotic microstructural changes. Three out of the ten DI-ILD subjects were treated with prednisolone between visits 1 and 2. Four out of the ten DI-ILD subjects were in the fibrotic group (one was treated with prednisolone).

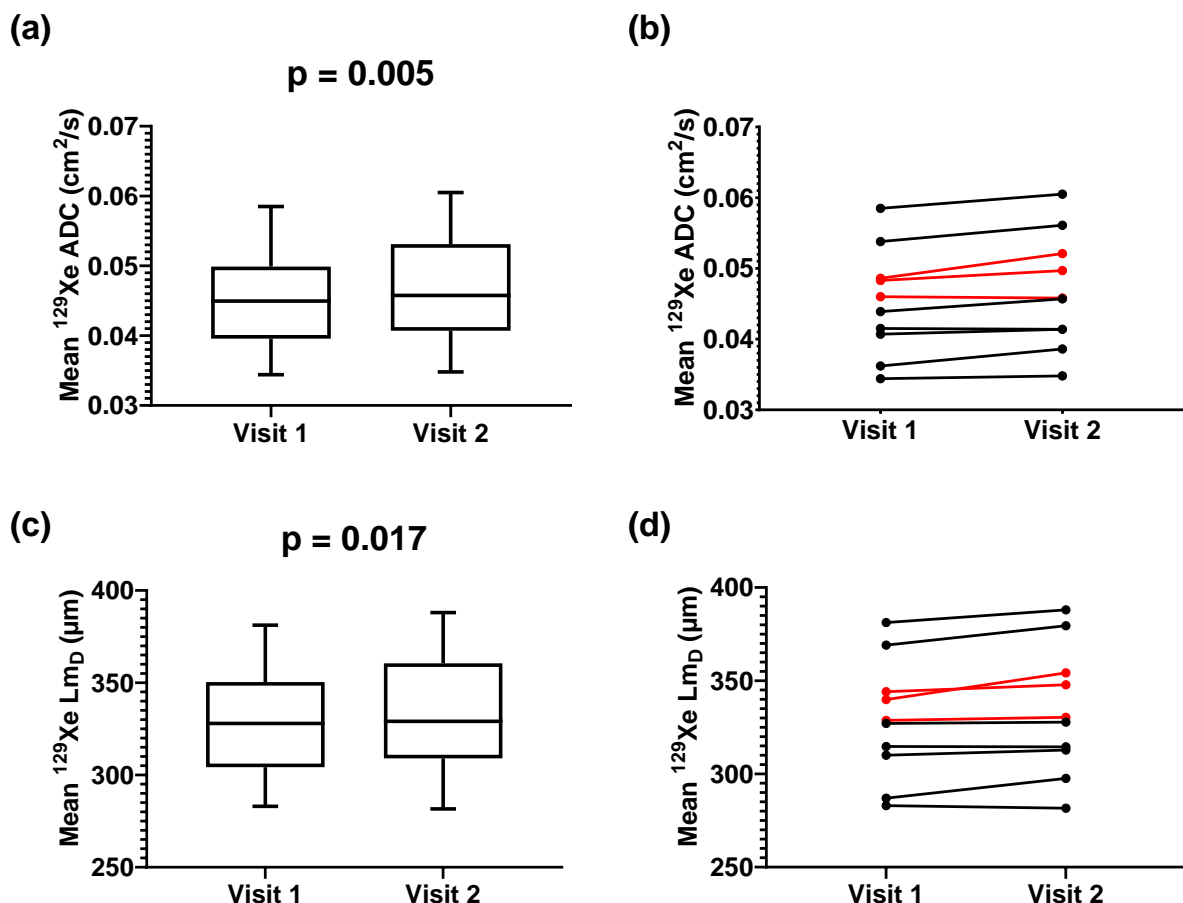


Figure 4.19. Global ^{129}Xe ADC (a-b) and Lm_D (c-d) at visit 1 versus visit 2 in the DI-ILD group (n=10). The three subjects were treated with prednisolone between visits 1 and 2 are highlighted in red. Statistical test: paired t test.

	Total (n = 37)	CTD-ILD (n = 5)	DI-ILD (n = 10)	HP (n = 9)	iNSIP (n = 2)	IPF (n = 11)
ADC (cm²/s)	0.044 (0.039 – 0.051)	0.041 (0.036 – 0.048)	0.046 (0.041 – 0.053)	0.040 (0.037 – 0.046)	0.040 (0.039 – 0.041)	0.051 (0.048 – 0.057)
ADC change (cm²/s)	0.0001 (-0.0015 – 0.0016)	-0.0006 (-0.002 – 0.0004)	0.0016 (0.0003 – 0.0023)	-0.0011 (-0.003 – 0.003)	0.0000	-0.0001 (-0.003 – 0.0009)
ADC change (%)	0.24 (-3.75 – 3.51)	-1.62 (-4.32 – 1.00)	3.16 (0.81 – 4.87)	-2.72 (-6.01 – 6.34)	0.12 (0.00 – 0.24)	-0.18 (-6.46 – 1.65)
Lm_D (µm)	328 (302 – 351)	319 (292 – 339)	329 (309 – 361)	306 (296 – 333)	310 (303 – 318)	328 (302 – 351)
Lm_D change (µm)	-0.30 (-7.15 – 5.75)	-6.10 (-10.7 – 5.20)	3.25 (0.48 – 10.5)	-0.90 (-13.5 – 11.5)	-1.10 (-3.00 – 0.80)	-1.30 (-15.2 – -0.30)
Lm_D change (%)	-0.090 (-2.29 – 1.67)	-2.06 (-3.02 – 1.85)	0.99 (0.14 – 3.04)	-0.30 (-4.07 – 3.71)	-0.37 (-0.98 – 0.25)	-0.35 (-4.26 – -0.08)

ADC: Apparent diffusion coefficient; CTD-ILD: Connective tissue disease associated interstitial lung disease; DI-ILD: Drug induced interstitial lung disease; HP: Hypersensitivity pneumonitis; iNSIP: Idiopathic non-specific interstitial pneumonia; IPF: Idiopathic pulmonary fibrosis; Lm_D: mean diffusive length scale.

Table 4.26. Global ¹²⁹Xe ADC and LmD results at **visit 2**, and the longitudinal change in global ¹²⁹Xe ADC and LmD between visit 1 and visit 2 for the total cohort and each ILD subtype. Results are presented as median (inter-quartile range).

	Fibrotic (n = 21)	Inflammation (n = 16)	p value
ADC (cm²/s)	0.048 ± 0.008	0.042 ± 0.005	0.031
ADC change (cm²/s)	0.0004 ± 0.0035	-0.0002 ± 0.0016	0.58
ADC change (%)	1.20 ± 8.19	-0.38 ± 3.48	0.48
Lm_D (µm)	338 ± 36	317 ± 24	0.049
Lm_D change (µm)	1.11 ± 16.5	-1.21 ± 7.33	0.60
Lm_D change (%)	0.45 ± 5.29	-0.37 ± 2.27	0.56

ADC: Apparent diffusion coefficient; Lm_D: mean diffusive length scale.

Table 4.27. Global ¹²⁹Xe ADC and LmD results at **visit 2**, and the longitudinal change in global ¹²⁹Xe ADC and LmD between visit 1 and visit 2 in the fibrotic and inflammation groups. Results are presented as mean ± standard deviation.

In the DI-ILD group, between visits 1 and 2, there was a statistically significant increase in ¹²⁹Xe ADC in the middle zone (mean (cm²/s): 0.046 ± 0.007 vs 0.047 ± 0.008; p=0.040), lower zone (mean (cm²/s): 0.045 ± 0.009 vs 0.047 ± 0.010; p=0.003), central zone (mean (cm²/s): 0.046 ± 0.008 vs 0.048 ± 0.008; p=0.009) and peripheral zone (mean (cm²/s): 0.045 ± 0.008 vs 0.046 ± 0.008; p=0.019), and a statistically significant increase in ¹²⁹Xe Lm_D in the lower zone (mean (µm): 325 ± 39 vs 333 ± 44; p=0.017) and the peripheral zone (mean (µm): 323 ± 32 vs 327 ± 34; p=0.027).

	Total (n = 37)	CTD-ILD (n = 5)	DI-ILD (n = 9)	HP (n = 8)	iNSIP (n = 2)	IPF (n = 11)
ADC change (%)						
Upper zone	1.02 (-4.03 – 5.48)	1.05 (-7.55 – 7.46)	3.41 (-2.33 – 6.65)	5.59 (-19.8 – 23.4)	1.83 (0.77 – 2.89)	-1.79 (-13.1 – 16.6)
Middle zone	-0.34 (-3.77 – 3.26)	-2.65 (-6.40 – -0.07)	2.77 (0.71 – 6.86)	2.85 (-11.1 – 15.7)	0.64 (-0.23 – 1.50)	1.50 (-9.92 – 5.35)
Lower zone	0.92 (-3.87 – 5.44)	-1.16 (-3.12 – -0.28)	2.28 (1.83 – 6.56)	4.09 (-19.0 – 13.6)	-2.86 (-6.75 – 1.03)	4.22 (-9.64 – 21.3)
Central zone	0.00 (-4.92 – 4.36)	-4.05 (-5.88 – -1.78)	3.76 (0.75 – 6.12)	5.02 (-6.99 – 15.8)	-0.09 (-0.92 – 0.74)	-4.12 (-6.63 – 8.01)
Peripheral zone	0.74 (-3.99 – 3.99)	-0.56 (-4.05 – 4.24)	3.46 (0.33 – 5.14)	-0.50 (-11.9 – 13.6)	-0.15 (-0.79 – 0.50)	7.73 (-12.1 – 14.1)
L_{mD} change (%)						
Upper zone	0.03 (-2.84 – 2.83)	0.56 (-5.30 – 6.18)	1.79 (-1.79 – 3.41)	-2.11 (-6.24 – 1.94)	0.90 (0.62 – 1.17)	-1.30 (-3.09 – 3.50)
Middle zone	-0.58 (-2.42 – 2.47)	-2.13 (-3.87 – 1.03)	0.96 (-0.64 – 3.49)	-1.55 (-5.93 – 3.04)	0.18 (-0.32 – 0.67)	-1.36 (-3.23 – -0.84)
Lower zone	-0.39 (-2.58 – 2.76)	-1.32 (-3.00 – 1.04)	1.74 (0.37 – 4.74)	-2.10 (-5.55 – 2.36)	-2.65 (-4.90 – -0.39)	-1.48 (-5.23 – 2.68)
Central zone	-0.60 (-2.79 – 2.69)	-2.79 (-3.15 – -0.71)	1.12 (-0.31 – 3.15)	-0.59 (-4.05 – 3.18)	-0.51 (-0.60 – -0.41)	-0.77 (-5.10 – 0.29)
Peripheral zone	-0.33 (-2.18 – 2.60)	-1.29 (-3.13 – 4.06)	1.29 (-0.64 – 3.13)	-2.86 (-4.78 – 1.75)	-0.50 (-1.61 – 0.61)	-0.33 (-2.43 – 1.72)

ADC: Apparent diffusion coefficient; CTD-ILD: Connective tissue disease associated interstitial lung disease; DI-ILD: Drug induced interstitial lung disease; HP: Hypersensitivity pneumonitis; iNSIP: Idiopathic non-specific interstitial pneumonia; IPF: Idiopathic pulmonary fibrosis; L_{mD}: mean diffusive length scale.

Table 4.28. % change in regional ¹²⁹Xe ADC and L_{mD} results between visit 1 and visit 2 for the total cohort and each ILD subtype. Results are presented as median (inter-quartile range).

	Fibrotic (n = 21)	Inflammation (n = 16)	p value
ADC change (%)			
Upper zone	0.68 ± 10.8	0.32 ± 5.72	0.012
Middle zone	0.17 ± 8.30	-0.96 ± 4.12	0.007
Lower zone	1.90 ± 9.17	-0.14 ± 5.85	0.072
Central zone	1.07 ± 8.83	-0.58 ± 4.19	0.011
Peripheral zone	1.34 ± 8.22	-0.31 ± 4.09	0.017
L_{mD} change (%)			
Upper zone	0.29 ± 6.96	-0.12 ± 3.88	0.83
Middle zone	-0.17 ± 5.27	-0.82 ± 2.55	0.65
Lower zone	0.85 ± 6.01	0.03 ± 3.66	0.63
Central zone	0.30 ± 6.15	-0.59 ± 2.25	0.59
Peripheral zone	0.61 ± 5.13	-0.30 ± 3.23	0.54

ADC: Apparent diffusion coefficient; L_{mD}: mean diffusive length scale.

Table 4.29. % change in regional ¹²⁹Xe ADC and L_{mD} results between visit 1 and visit 2 in the fibrotic and inflammation groups. Results are presented as mean ± standard deviation.

4.5 ^{129}Xe Ventilation MRI

4.5.1 Study visits and examples of images

^{129}Xe ventilation MRI was implemented from the beginning of the study. Following an interim analysis in September 2019, a decision was made to remove the ^{129}Xe ventilation MRI sequence from the protocol. The reason for this was its inability to demonstrate any statistically significant differences between groups and a lack of sensitivity to longitudinal change between visits. ^{129}Xe ventilation MRI data was available for 41 subjects at visit 1 and 34 subjects at visit 2.

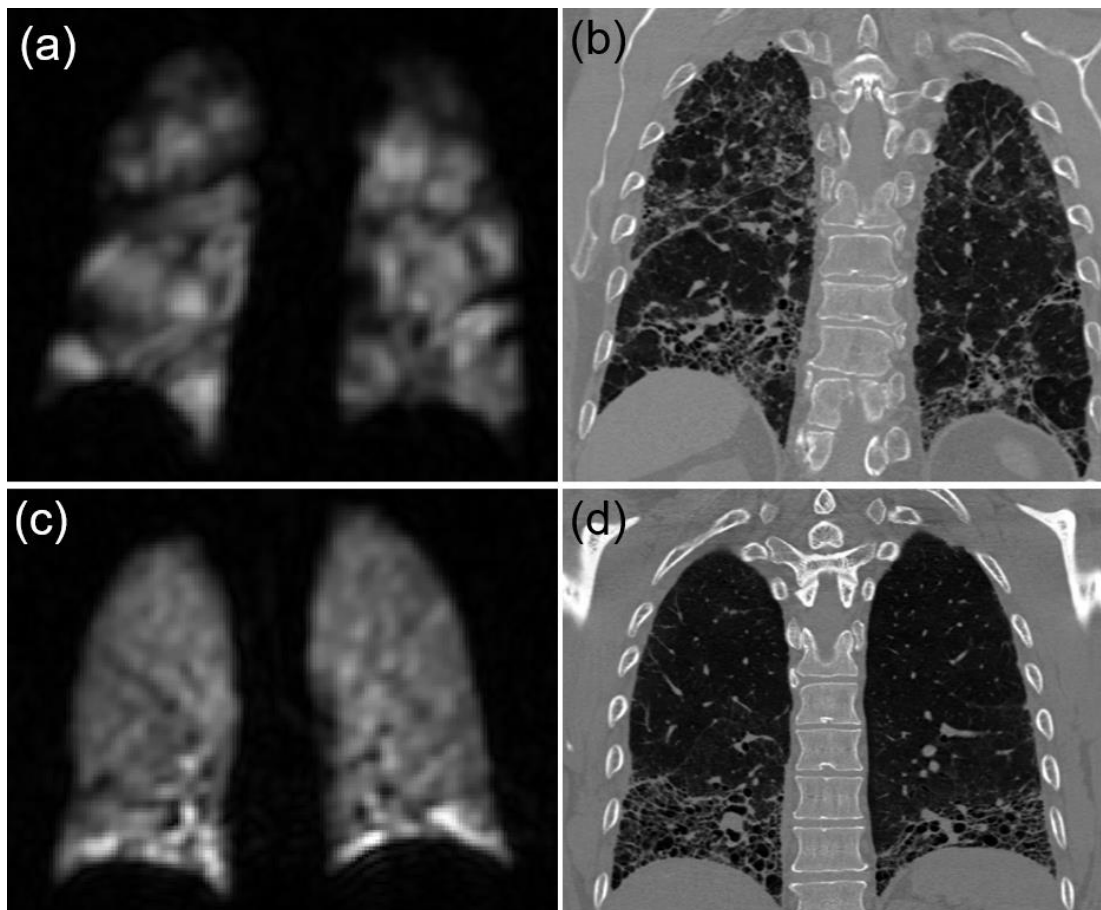


Figure 4.20. Example of a ^{129}Xe ventilation image (a) and the corresponding coronal HRCT image (b) in a DI-ILD subject. VV%: 82.3%, CV%: 20.8%, FVC % predicted: 60.5%, DLCO % predicted: 28.6%. Example of a ^{129}Xe ventilation image (c) and the corresponding coronal HRCT image (d) in an IPF subject. VV%: 93.9%, CV%: 14.1%, FVC % predicted: 70.2%, DLCO % predicted: 22.1%.

4.5.2 Visit 1 (baseline)

	Total (n = 41)	CTD-ILD (n = 5)	DI-ILD (n = 11)	HP (n = 11)	IPF (n = 14)
VV%	92.0 (87.5 – 93.8)	92.2 (86.6 – 94.8)	92.0 (89.2 – 94.6)	92.8 (89.6 – 96.8)	88.6 (86.2 – 93.0)
CV%	17.9 (14.6 – 20.7)	15.4 (13.9 – 17.2)	16.0 (14.5 – 20.8)	16.5 (13.0 – 20.3)	19.5 (18.9 – 21.0)

CTD-ILD: Connective tissue disease associated interstitial lung disease; CV: Coefficient of variation; DI-ILD: Drug induced interstitial lung disease; HP: Hypersensitivity pneumonitis; IPF: Idiopathic pulmonary fibrosis; VV: Ventilation volume.

Table 4.30. ^{129}Xe VV% and CV% at visit 1 for the total cohort and each ILD subtype. Results are presented as median (inter-quartile range).

	Fibrotic (n = 24)	Inflammation (n = 17)	p value
VV%	88.7 ± 7.06	92.3 ± 4.25	0.075
CV%	18.8 ± 3.32	16.7 ± 3.76	0.065

CV: Coefficient of variation; VV: Ventilation volume.

Table 4.31. ^{129}Xe VV% and CV% at visit 1 in the fibrotic and inflammation groups. Results are presented as mean ± standard deviation.

4.5.3 Visit 2 (6 weeks or 6 months depending on ILD subtype)

	Total (n = 34)	CTD-ILD (n = 5)	DI-ILD (n = 10)	HP (n = 8)	IPF (n = 11)
VV%	91.3 (87.2 – 93.4)	92.7 (86.2 – 96.3)	92.8 (88.2 – 97.0)	90.6 (88.0 – 93.4)	89.9 (86.2 – 91.8)
VV% absolute change (%)	-0.25 (-4.15 – 4.08)	-2.90 (-6.85 – 9.75)	1.20 (-4.33 – 5.80)	-1.40 (-3.48 – 2.25)	0.60 (-6.70 – 3.80)
VV% relative change (%)	-0.27 (-4.49 – 4.57)	-3.03 (-7.40 – 11.6)	1.29 (-4.64 – 7.04)	-1.51 (-3.78 – 2.56)	0.67 (-7.17 – 4.32)
CV%	19.1 (16.0 – 20.6)	15.1 (14.1 – 19.7)	17.6 (14.2 – 21.9)	18.2 (15.7 – 20.7)	19.4 (18.2 – 20.8)
CV% absolute change (%)	0.35 (-1.23 – 1.68)	1.00 (-0.45 – 2.50)	0.75 (-1.73 – 2.35)	0.90 (-1.03 – 2.20)	-0.60 (-1.60 – 0.50)
CV% relative change (%)	2.17 (-6.27 – 9.90)	7.09 (-2.76 – 14.6)	4.32 (-8.32 – 15.9)	5.45 (-5.18 – 13.7)	-3.00 (-7.37 – 2.65)

CTD-ILD: Connective tissue disease associated interstitial lung disease; CV: Coefficient of variation; DI-ILD: Drug induced interstitial lung disease; HP: Hypersensitivity pneumonitis; IPF: Idiopathic pulmonary fibrosis; VV: Ventilation volume.

Table 4.32. ^{129}Xe VV% and CV% results at **visit 2**, and the longitudinal change in ^{129}Xe VV% and CV% between visit 1 and visit 2 for the total cohort and each ILD subtype. Results are presented as median (inter-quartile range).

	Fibrotic (n = 19)	Inflammation (n = 15)	p value
VV%	89.3 ± 5.10	91.3 ± 5.06	0.27
VV% absolute change (%)	0.62 ± 6.24	-0.52 ± 6.48	0.61
VV% relative change (%)	1.15 ± 7.57	-0.36 ± 7.36	0.56
CV%	18.9 ± 2.73	17.7 ± 3.23	0.24
CV% absolute change (%)	0.06 ± 1.47	0.39 ± 2.21	0.61
CV% relative change (%)	1.34 ± 8.64	3.13 ± 12.4	0.62

CV: Coefficient of variation; VV: Ventilation volume.

Table 4.33. ¹²⁹Xe VV% and CV% results at **visit 2**, and the change in ¹²⁹Xe VV% and CV% between visit 1 and visit 2 in the fibrotic and inflammation groups. Results are presented as mean ± standard deviation.

4.6 Dynamic contrast enhanced MRI

4.6.1 Study visits and examples of images

Accurate DCE-MRI analysis could not be performed in 12 of the visit 1 scans and therefore DCE-MRI data was available for only 43 subjects at visit 1. Although 39 subjects completed visit 2, accurate DCE-MRI analysis could not be performed in seven of the visit 2 scans. As a result, the longitudinal change in MTT, PBF and PBV between visit 1 and visit 2 could only be calculated in 28 subjects.

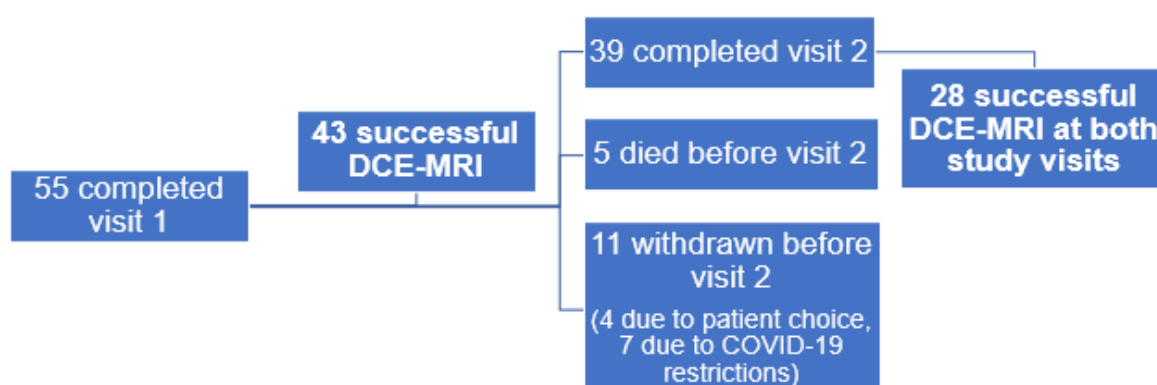


Figure 4.21. The number of subjects that had DCE-MRI performed at each study visit.

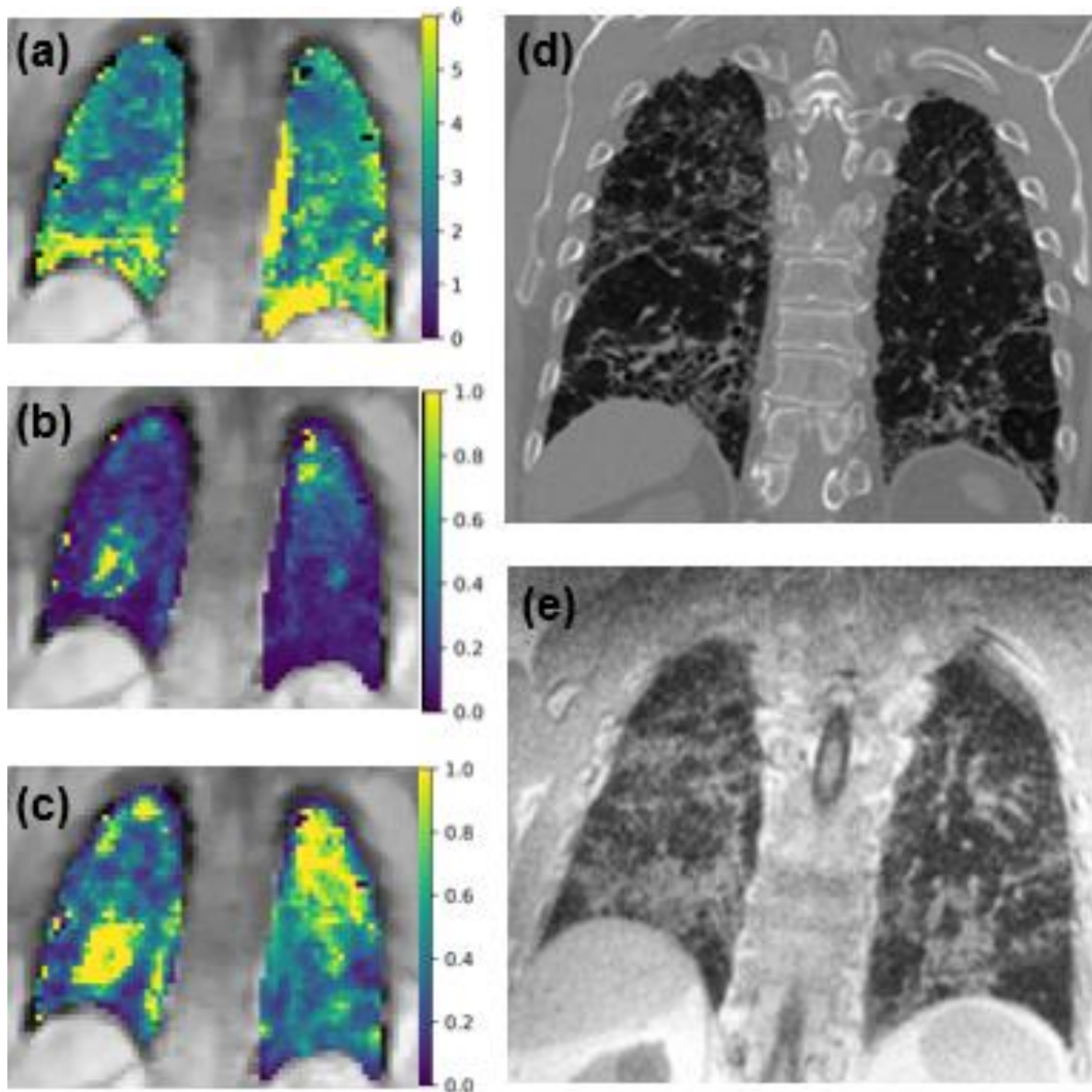


Figure 4.22. Example of DCE-MRI images of MTT (a), PBF (b), PBV (c), and corresponding coronal HRCT image (d) and UTE-MRI image in a subject with DI-ILD.

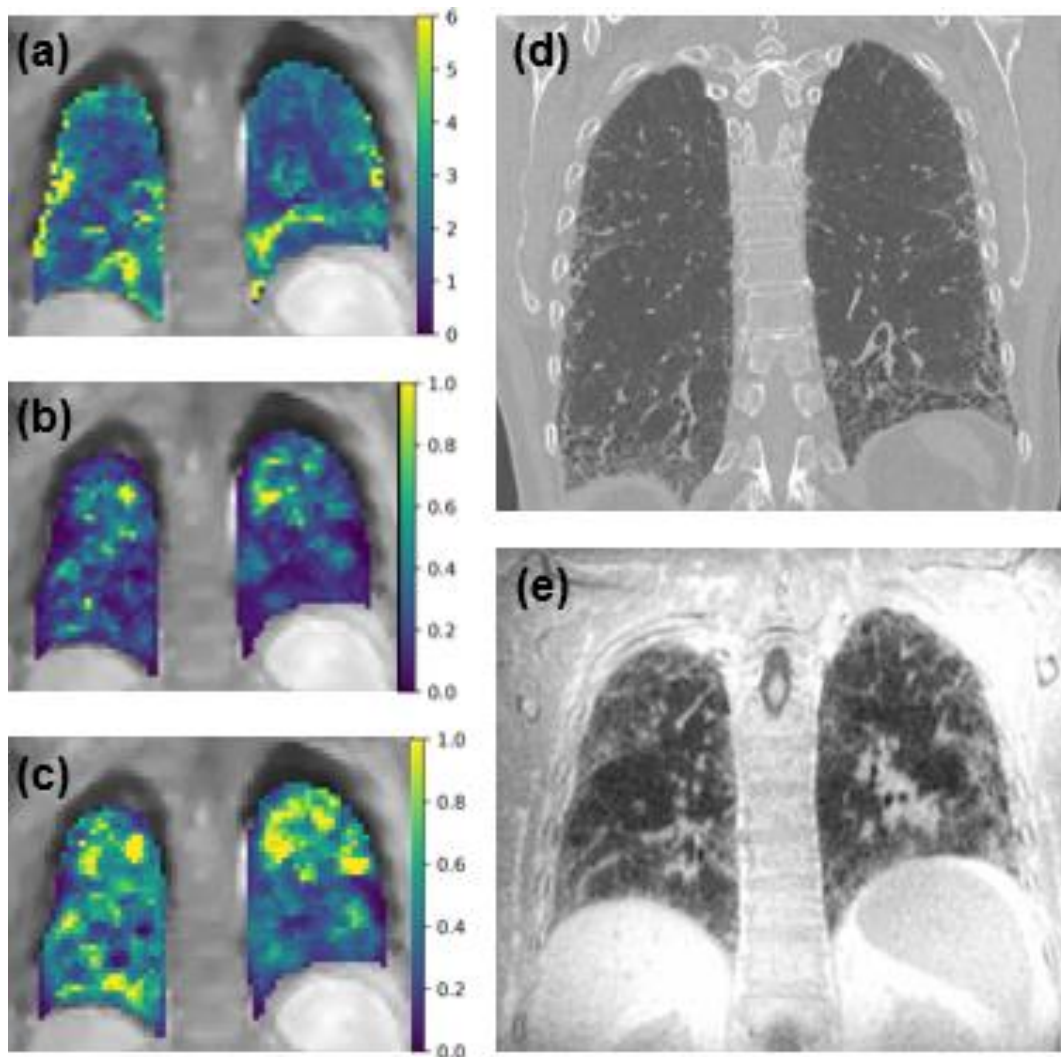


Figure 4.23. Example of DCE-MRI images of MTT (a), PBF (b), PBV (c), and corresponding coronal HRCT image (d) and UTE-MRI image in an IPF subject.

4.6.2 Visit 1 (baseline)

	Total (n = 42)	CTD-ILD (n = 3)	DI-ILD (n = 9)	HP (n = 13)	iNSIP (n = 3)	IPF (n = 14)
MTT (s)	1.83 (1.68 – 2.54)	1.82 (1.79 – 3.57)	1.84 (1.64 – 2.73)	1.94 (1.71 – 2.97)	1.74 (1.47 – 2.39)	1.81 (1.57 – 2.18)
PBF (ml.mm³.s⁻¹)	0.19 (0.13 – 0.27)	0.25 (0.08 – 0.28)	0.14 (0.12 – 0.32)	0.18 (0.13 – 0.22)	0.16 (0.10 – 0.20)	0.19 (0.13 – 0.27)
PBV (ml.mm³)	0.37 (0.28 – 0.48)	0.43 (0.27 – 0.49)	0.37 (0.23 – 0.54)	0.38 (0.27 – 0.46)	0.24 (0.24 – 0.34)	0.35 (0.30 – 0.51)

CTD-ILD: Connective tissue disease associated interstitial lung disease; DI-ILD: Drug induced interstitial lung disease; HP: Hypersensitivity pneumonitis; iNSIP: Idiopathic non-specific interstitial pneumonia; IPF: Idiopathic pulmonary fibrosis; MTT: Mean transit time; PBF: Pulmonary blood flow; PBV: Pulmonary blood volume.

Table 4.34. MTT, PBF and PBV at visit 1 for the total cohort and ILD subtypes. Results are presented as median (inter-quartile range).

	Fibrotic (n = 23)	Inflammation (n = 19)	p value
MTT (s)	1.96 ± 0.58	2.21 ± 0.73	0.33
PBF (ml.mm ³ .s ⁻¹)	0.22 ± 0.10	0.18 ± 0.09	0.23
PBV (ml.mm ³)	0.39 ± 0.13	0.37 ± 0.14	0.78

MTT: Mean transit time; PBF: Pulmonary blood flow; PBV: Pulmonary blood volume.

Table 4.35. MTT, PBF and PBV at visit 1 in the fibrotic and inflammation groups. Results are presented as mean ± standard deviation.

4.6.3 Visit 2 (6 weeks or 6 months depending on ILD subtype)

In the HP group (n=8), there was a statistically significant difference between visits 1 and 2 in MTT (mean (s): 2.58 ± 0.77 vs 1.97 ± 0.63; p=0.025) and PBF (mean (ml.mm³.s⁻¹): 0.16 ± 0.05 vs 0.24 ± 0.10; p=0.037) (Figure 4.24). Six out of the eight HP subjects were in the inflammation group and five of these six subjects were taking prednisolone at some point between visits 1 and 2. It is possible that the decrease in MTT and increase in PBF was associated with a reduction in inflammation due to a response to steroids in subjects with inflammation predominant HP.

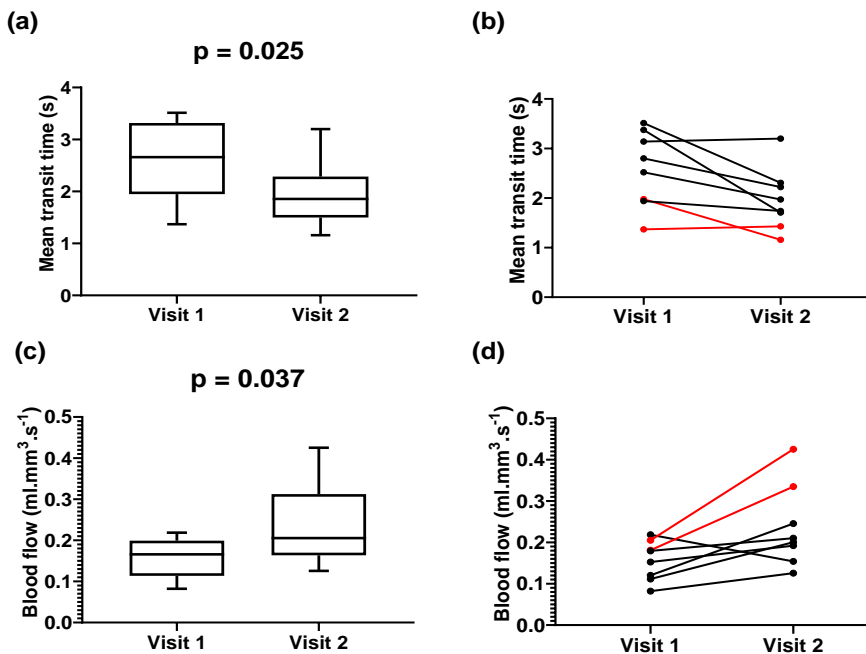


Figure 4.24. MTT (a-b) and PBF (c-d) in the HP group at visit 1 versus visit 2 (n=8). The two subjects highlighted red were in the fibrotic group (visual CT ground glass score <2). Statistical test: paired *t* test.

	Total (n = 28)	CTD-ILD (n = 2)	DI-ILD (n = 8)	HP (n = 8)	iNSIP (n = 2)	IPF (n = 8)
MTT (s)	2.04 (1.69 – 2.76)	1.31 (1.29 – 1.34)	2.43 (1.76 – 3.27)	1.86 (1.50 – 2.29)	2.36 (1.98 – 2.75)	2.27 (1.76 – 2.76)
MTT change (s)	-0.15 (-0.54 – 0.69)	-0.49 (-0.50 – -0.48)	-0.11 (-0.29 – 1.32)	-0.56 (-1.11 – -0.01)	0.76 (0.50 – 1.01)	0.58 (-0.25 – 0.89)
MTT change (%)	-6.44 (-25.2 – 40.0)	-27.2 (-28.1 – -26.3)	-4.39 (-12.1 – 73.5)	-21.2 (-39.7 – -1.13)	46.1 (34.0 – 58.3)	31.7 (-9.05 – 69.3)
PBF (ml.mm³.s⁻¹)	0.19 (0.15 – 0.25)	0.40 (0.40 – 0.41)	0.16 (0.12 – 0.25)	0.21 (0.16 – 0.31)	0.16 (0.10 – 0.22)	0.17 (0.15 – 0.20)
PBF change (ml.mm³.s⁻¹)	0.034 (-0.05 – 0.11)	0.14 (0.12 – 0.15)	0.025 (-0.07 – 0.09)	0.066 (0.03 – 0.15)	-0.013 (-0.09 – 0.07)	-0.038 (-0.21 – 0.07)
PBF change (%)	25.8 (-21.0 – 74.7)	51.2 (43.8 – 58.6)	24.4 (-21.1 – 78.0)	66.5 (19.4 – 99.3)	-2.39 (-47.2 – 42.5)	-18.7 (-52.3 – 23.2)
PBV (ml.mm³)	0.42 (0.35 – 0.46)	0.53 (0.51 – 0.54)	0.41 (0.35 – 0.44)	0.42 (0.38 – 0.46)	0.36 (0.29 – 0.43)	0.39 (0.31 – 0.48)
PBV change (ml.mm³)	0.047 (-0.09 – 0.12)	0.066 (0.05 – 0.08)	0.047 (-0.16 – 0.18)	0.052 (0.001 – 0.12)	0.073 (-0.05 – 0.20)	-0.026 (-0.20 – 0.11)
PBV change (%)	12.3 (-15.9 – 48.8)	14.5 (10.2 – 18.8)	12.3 (-27.0 – 73.3)	14.1 (0.66 – 43.4)	34.0 (-15.3 – 83.3)	-1.00 (-41.0 – 41.6)

CTD-ILD: Connective tissue disease associated interstitial lung disease; DI-ILD: Drug induced interstitial lung disease; HP: Hypersensitivity pneumonitis; iNSIP: Idiopathic non-specific interstitial pneumonia; IPF: Idiopathic pulmonary fibrosis; MTT: Mean transit time; PBF: Pulmonary blood flow; PBV: Pulmonary blood volume.

Table 4.36. DCE-MRI results at **visit 2**, and the longitudinal change in MTT, PBF and PBV between visit 1 and visit 2 for the total cohort and each ILD subtype. Results are presented as median (inter-quartile range).

	Fibrotic (n = 15)	Inflammation (n = 13)	p value
MTT (s)	2.06 ± 0.69	2.35 ± 1.01	0.39
MTT change (s)	0.046 ± 0.75	0.069 ± 1.25	0.95
MTT change (%)	9.10 ± 42.7	11.6 ± 61.5	0.62
PBF (ml.mm³.s⁻¹)	0.34 ± 0.11	0.20 ± 0.10	0.41
PBF change (ml.mm³.s⁻¹)	0.020 ± 0.16	0.014 ± 0.11	0.90
PBF change (%)	28.8 ± 66.3	21.1 ± 51.6	0.74
PBV (ml.mm³)	0.43 ± 0.09	0.40 ± 0.08	0.40
PBV change (ml.mm³)	0.032 ± 0.18	0.005 ± 0.14	0.66
PBV change (%)	21.2 ± 48.4	16.8 ± 51.2	0.82

MTT: Mean transit time; PBF: Pulmonary blood flow; PBV: Pulmonary blood volume.

Table 4.37. DCE-MRI results at **visit 2**, and the longitudinal change in MTT, PBF and PBV between visit 1 and visit 2 in the fibrotic and inflammation groups. Results are presented as mean ± standard deviation.

4.7 CALIPER CT analysis

4.7.1 Study visits and examples of images

CALIPER CT analysis was performed on all available HRCT scans which provided both a global and regional measure of ground glass, honeycomb, reticular and VRS. Honeycomb and reticular were combined and termed fibrosis. Also, ground glass, honeycomb and reticular were combined and termed ILD. CALIPER CT data were available for all subjects that completed each of visits 1 (n=55), 2 (n=39) and 3 (n=31).

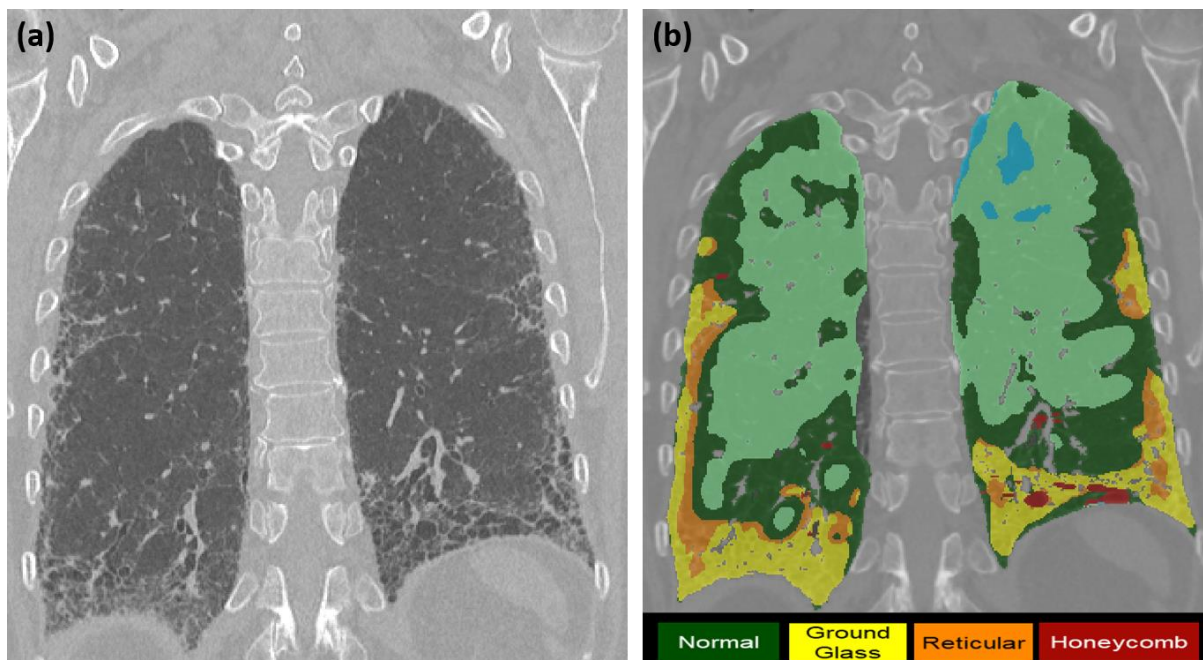


Figure 4.25. Example of a coronal HRCT image (a) and corresponding CALIPER CT texture analysis (b) in an IPF subject.

4.7.2 Visit 1 (baseline)

	Total (n = 55)	CTD-ILD (n = 5)	DI-ILD (n = 13)	HP (n = 15)	iNSIP (n = 3)	IPF (n = 19)
Fibrosis %	4.77 (2.46 – 7.81)	2.30 (0.85 – 5.14)	5.09 (2.34 – 10.9)	4.95 (4.33 – 6.43)	2.59 (1.64 – 4.85)	4.93 (1.96 – 7.04)
Ground glass %	8.07 (3.07 – 18.7)	7.44 (6.43 – 11.0)	9.09 (1.95 – 16.7)	14.8 (5.29 – 30.2)	15.5 (2.97 – 20.8)	4.89 (1.80 – 11.0)
Honeycomb %	0.10 (0.03 – 0.63)	0.02 (0.01 – 1.23)	0.04 (0.01 – 0.55)	0.09 (0.03 – 0.32)	0.08 (0.02 – 0.72)	0.24 (0.10 – 0.67)
ILD %	15.5 (7.43 – 26.8)	11.7 (7.27 – 15.2)	17.6 (7.48 – 25.9)	26.8 (11.4 – 35.6)	17.2 (7.82 – 23.4)	10.0 (5.73 – 19.8)
Reticular %	4.42 (2.30 – 6.50)	2.30 (0.83 – 3.91)	4.50 (2.31 – 10.8)	4.69 (4.32 – 6.40)	2.50 (1.63 – 4.12)	4.86 (1.80 – 6.50)
VRS %	3.49 (2.60 – 4.87)	2.82 (2.40 – 3.75)	3.79 (2.11 – 5.23)	4.02 (2.77 – 5.55)	3.47 (3.40 – 3.49)	3.82 (2.47 – 4.66)

CTD-ILD: Connective tissue disease associated interstitial lung disease; DI-ILD: Drug induced interstitial lung disease; HP: Hypersensitivity pneumonitis; ILD: Interstitial lung disease; iNSIP: Idiopathic non-specific interstitial pneumonia; IPF: Idiopathic pulmonary fibrosis; VRS: Vessel related structures.

Table 4.38. Global CALIPER CT results at visit 1 for the total cohort and ILD subtypes. Results are presented as median (inter-quartile range).

There was a statistically significant difference between the fibrotic and inflammation groups at visit 1 in global CALIPER ground glass % (median (%): 5.99 (1.96 – 10.9) vs 12.9 (6.68 – 22.7); p=0.004), honeycomb % (median (%): 0.14 (0.07 – 0.66) vs 0.03 (0.01 – 0.32); p=0.022) and ILD % (median (%): 11.7 (5.76 – 21.0) vs 22.7 (11.7 – 35.6); p=0.005).

	Fibrotic (n = 32)	Inflammation (n = 23)	p value
Fibrosis %	4.85 (2.60 – 7.62)	4.70 (2.30 – 9.35)	0.97
Ground glass %	5.99 (1.96 – 10.9)	12.9 (6.68 – 22.7)	0.004
Honeycomb %	0.14 (0.07 – 0.66)	0.03 (0.01 – 0.32)	0.022
ILD %	11.7 (5.76 – 21.0)	22.7 (11.7 – 35.6)	0.005
Reticular %	4.46 (2.13 – 6.48)	4.42 (2.30 – 9.35)	0.79
VRS %	3.81 (2.56 – 4.76)	3.33 (2.63 – 5.24)	0.80

ILD: Interstitial lung disease; VRS: Vessel related structures.

Table 4.39. Global CALIPER CT results at visit 1 in the fibrotic and inflammation groups. Results are presented as median (inter-quartile range).

	Total (n = 55)	CTD-ILD (n = 5)	DI-ILD (n = 13)	HP (n = 15)	iNSIP (n = 3)	IPF (n = 19)
Fibrosis %						
Upper zone	1.82	0.53	2.23	5.50	0.95	1.66
Middle zone	4.35	1.54	5.03	5.07	2.58	4.42
Lower zone	7.92	4.17	9.91	5.90	5.25	8.92
Central zone	2.31	1.43	3.06	2.90	1.08	1.46
Peripheral zone	6.79	3.21	7.93	6.63	2.76	8.62
Ground glass %						
Upper zone	2.13	0.20	1.31	8.87	1.44	0.85
Middle zone	6.40	2.66	6.43	12.5	8.95	3.79
Lower zone	16.6	25.0	16.6	8.94	36.9	12.8
Central zone	3.84	3.85	6.54	7.63	7.36	0.94
Peripheral zone	12.0	11.5	12.8	18.4	23.8	10.4
ILD %						
Upper zone	5.59	0.78	5.88	24.0	2.61	4.14
Middle zone	13.8	5.45	14.4	21.8	9.78	8.66
Lower zone	28.3	35.6	28.3	45.9	40.5	21.7
Central zone	6.70	5.43	10.5	16.0	8.01	2.49
Peripheral zone	22.8	19.4	20.6	35.0	26.5	19.4
VRS %						
Upper zone	2.37	2.05	1.96	3.98	2.28	2.32
Middle zone	3.86	3.08	4.20	3.92	3.85	4.05
Lower zone	3.92	3.77	3.50	3.24	4.05	4.28
Central zone	5.04	4.25	5.19	6.09	5.04	4.37
Peripheral zone	1.92	1.23	1.45	1.92	1.73	2.32

CTD-ILD: Connective tissue disease associated interstitial lung disease; DI-ILD: Drug induced interstitial lung disease; HP: Hypersensitivity pneumonitis; ILD: Interstitial lung disease; iNSIP: Idiopathic non-specific interstitial pneumonia; IPF: Idiopathic pulmonary fibrosis; VRS: Vessel related structures.

Table 4.40. Regional CALIPER fibrosis %, ground glass %, ILD % and VRS % results at visit 1 for the total cohort and each ILD subtype. Results are presented as median.

In the DI-ILD group (n=13), there were statistically significant regional differences between the upper and lower zone, and between the central and peripheral zone in CALIPER fibrosis %, ground glass % and ILD %. There were also statistically significant regional differences in CALIPER VRS % (upper vs lower zone: p=0.010; upper vs middle zone: p=0.001; central vs peripheral zone: p<0.001).

In the HP group (n=15), there were statistically significant regional differences in CALIPER fibrosis % (central vs peripheral zone: p<0.001), ILD % (central vs peripheral zone: p=0.015), and VRS % (upper vs middle zone: p=0.003; central vs peripheral zone: p<0.001).

In the IPF group (n=19), there were statistically significant regional differences in CALIPER fibrosis % (upper vs lower zone: p<0.001; upper vs middle zone: p=0.004; middle vs lower zone: p=0.017; central vs peripheral zone: p<0.001), ground glass % (upper vs lower zone: p<0.001; upper vs middle zone: p=0.006; middle vs lower zone: p=0.006; central vs peripheral zone: p<0.001), ILD % (upper vs lower zone: p<0.001; upper vs middle zone: p=0.004; middle vs lower zone: p=0.017; central vs peripheral zone: p<0.001), and VRS % (upper vs lower zone: p<0.001; upper vs middle zone: p<0.001; central vs peripheral zone: p<0.001).

	Fibrotic (n = 32)	Inflammation (n = 23)	p value
Fibrosis %			
Upper zone	1.64	2.99	0.25
Middle zone	4.19	4.45	0.69
Lower zone	8.89	5.90	0.36
Central zone	1.73	2.90	0.052
Peripheral zone	8.34	5.65	0.39
Ground glass %			
Upper zone	0.92	4.85	0.015
Middle zone	4.01	10.6	0.006
Lower zone	12.7	20.7	0.083
Central zone	1.52	7.63	<0.001
Peripheral zone	10.8	18.3	0.043
ILD %			
Upper zone	1.64	13.1	<0.001
Middle zone	4.19	17.1	<0.001
Lower zone	8.89	40.1	<0.001
Central zone	1.73	16.0	<0.001
Peripheral zone	8.34	27.3	<0.001
VRS %			
Upper zone	2.62	2.22	0.85
Middle zone	3.97	3.50	0.82
Lower zone	4.17	3.77	0.46
Central zone	4.99	5.04	0.44
Peripheral zone	2.33	1.45	0.13

ILD: Interstitial lung disease; VRS: Vessel related structures.

Table 4.41. Regional CALIPER CT fibrosis %, ground glass %, ILD % and VRS % results at visit 1 in the fibrotic and inflammation groups. Results are presented as median.

In the fibrotic group (n=32), there were statistically significant regional differences in CALIPER fibrosis % (upper vs lower zone: $p < 0.001$; upper vs middle zone: $p < 0.001$; middle vs lower zone: $p = 0.012$; central vs peripheral zone: $p < 0.001$), ground glass % (upper vs lower zone: $p < 0.001$; upper vs middle zone: $p = 0.003$; middle vs lower zone: $p = 0.002$; central vs peripheral zone: $p < 0.001$), ILD % (upper vs lower zone: $p < 0.001$; upper vs middle zone: $p = 0.004$; middle vs lower zone: $p = 0.026$; central vs peripheral zone: $p < 0.001$), and VRS % (upper vs lower zone: $p < 0.001$; upper vs middle zone: $p < 0.001$; central vs peripheral zone: $p < 0.001$).

In the inflammation group (n=23), there were statistically significant regional differences in CALIPER fibrosis % (upper vs lower zone: $p = 0.002$; middle vs lower zone: $p = 0.015$; central vs peripheral zone: $p < 0.001$), ground glass % (upper vs lower zone: $p < 0.001$; central vs peripheral zone: $p = 0.003$), ILD % (upper vs lower zone: $p < 0.001$; central vs peripheral zone: $p < 0.001$), and VRS % (upper vs lower zone: $p < 0.001$; upper vs middle zone: $p < 0.001$; central vs peripheral zone: $p < 0.001$).

4.7.3 Visit 2 (6 weeks or 6 months depending on ILD subtype)

In the IPF group (n=11), there was a statistically significant increase in global CALIPER VRS % between visits 1 and 2 (mean (%): 3.35 ± 0.94 vs 3.84 ± 1.30 ; $p = 0.010$) (Figure 4.26). In the same subjects, there was no statistically significant change in FVC, FVC%, DLCO or DLCO% over 6 months. This suggests that CALIPER VRS % is more sensitive to early disease progression in IPF compared to PFTs.

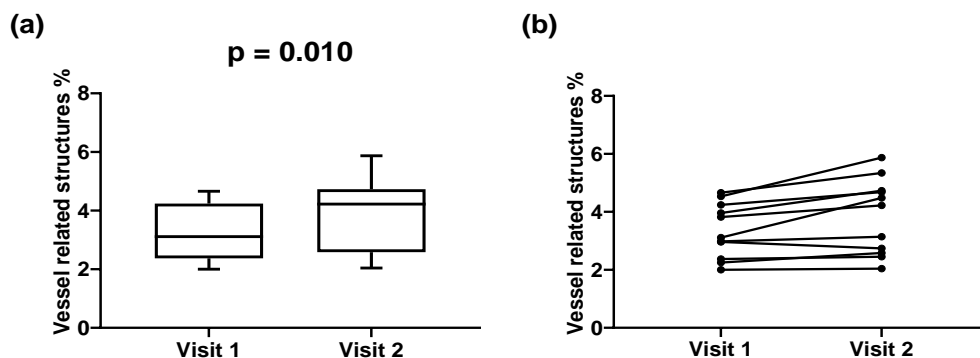


Figure 4.26. Global CALIPER VRS % at visit 1 versus visit 2 for the IPF group (n=11). Statistical test: paired *t* test.

	Total (n = 39)	CTD-ILD (n = 5)	DI-ILD (n = 11)	HP (n = 10)	iNSIP (n = 2)	IPF (n = 11)
Fibrosis %	2.72 (1.12 – 5.93)	0.74 (0.30 – 5.47)	4.24 (1.52 – 5.40)	4.44 (1.31 – 7.23)	1.28 (1.12 – 1.44)	4.12 (0.95 – 5.93)
Fibrosis % change	-0.48 (-1.82 – 0.70)	-0.48 (-1.32 - 0.57)	-0.86 (-4.65 – 1.29)	-1.56 (-4.48 – 0.97)	-0.84 (-1.47 - -0.20)	0.03 (-1.55 – 1.41)
Ground glass %	5.98 (2.12 – 14.7)	1.74 (0.24 – 6.08)	9.83 (4.44 – 16.1)	15.2 (4.05 – 38.0)	3.09 (0.19 – 5.98)	4.03 (2.83 – 8.55)
Ground glass % change	-0.04 (-5.99 – 1.98)	-6.08 (-9.98 - -0.99)	-0.04 (-4.84 – 1.87)	1.42 (-18.0 – 12.0)	-15.1 (-20.6 - -9.55)	0.95 (-0.83 – 1.98)
Honeycomb %	0.090 (0.03 – 0.24)	0.030 (0.02 – 1.94)	0.030 (0.02 – 0.29)	0.055 (0.01 – 0.16)	0.13 (0.07 – 0.19)	0.18 (0.10 – 0.39)
Honeycomb % change	0.00 (-0.03 – 0.10)	0.03 (-0.01 - 0.72)	0.01 (-0.01 – 0.10)	-0.03 (-0.27 – -0.01)	0.08 (0.05 - 0.11)	0.04 (-0.02 – 0.11)
ILD %	10.5 (3.71 – 21.2)	3.71 (0.55 – 10.9)	14.2 (8.67 – 28.2)	21.6 (5.24 – 53.0)	4.37 (1.31 – 7.42)	10.5 (4.99 – 15.4)
ILD % change	-0.86 (-1.80 – 0.24)	-6.94 (-11.1 - -0.42)	-3.08 (-16.8 – 1.68)	2.02 (-20.7 – 13.4)	-15.9 (-22.1 - -9.74)	0.55 (-1.30 – 2.96)
Reticular %	2.70 (0.92 – 5.82)	0.72 (0.29 – 3.53)	2.74 (1.48 – 5.39)	4.40 (1.24 – 7.20)	1.15 (0.92 – 1.38)	3.60 (0.87 – 5.82)
Reticular % change	-0.86 (-1.80 – 0.24)	-0.86 (-1.40 - 0.12)	-1.36 (-4.67 – 1.30)	-1.54 (-4.15 – 1.38)	-0.92 (-1.58 - -0.25)	0.03 (-1.02 – 0.69)
VRS %	3.36 (2.27 – 4.68)	2.27 (1.67 – 3.41)	3.58 (1.97 – 5.62)	4.09 (2.30 – 5.30)	2.43 (2.23 – 2.62)	4.22 (2.58 – 4.73)
VRS % change	0.08 (-0.81 – 0.73)	-0.39 (-0.92 - -0.23)	0.38 (-0.81 – 1.70)	-0.14 (-1.29 – 1.21)	-1.01 (-1.23 - -0.78)	0.40 (0.08 – 0.77)

CTD-ILD: Connective tissue disease associated interstitial lung disease; DI-ILD: Drug induced interstitial lung disease; HP: Hypersensitivity pneumonitis; ILD: Interstitial lung disease; iNSIP: Idiopathic non-specific interstitial pneumonia; IPF: Idiopathic pulmonary fibrosis; VRS: Vessel related structures.

Table 4.42. Global CALIPER CT results at **visit 2**, and the longitudinal change in global CALIPER CT measurements between visit 1 and visit 2 for the total cohort and each ILD subtype. Results are presented as median (inter-quartile range).

In the fibrosis group (n=22), between visit 1 and visit 2 there was a no statistically significant change in any CALIPER CT measurements. In the inflammation group (n=17), between visit 1 and visit 2 there was a statistically significant decrease in global CALIPER fibrosis % (median (%): 4.70 (2.00 – 7.89) vs 1.98 (0.77 – 4.59); p=0.008), ground glass % (median (%): 13.9 (7.95 – 22.2) vs 6.72 (1.26 – 14.6); p=0.023), ILD % (median (%): 22.7 (12.1 – 31.9) vs 8.34 (2.64 – 19.2); p=0.006) and reticular % (median (%): 4.63 (1.99 – 7.88) vs 1.48 (0.72 – 4.57); p=0.008) (Figure 4.27). There were no statistically significant changes in PFTs over the same study visit period. This suggests that CALIPER CT measurements may have the potential to identify early structural improvements in inflammation predominant ILD, before significant physiological changes are seen.

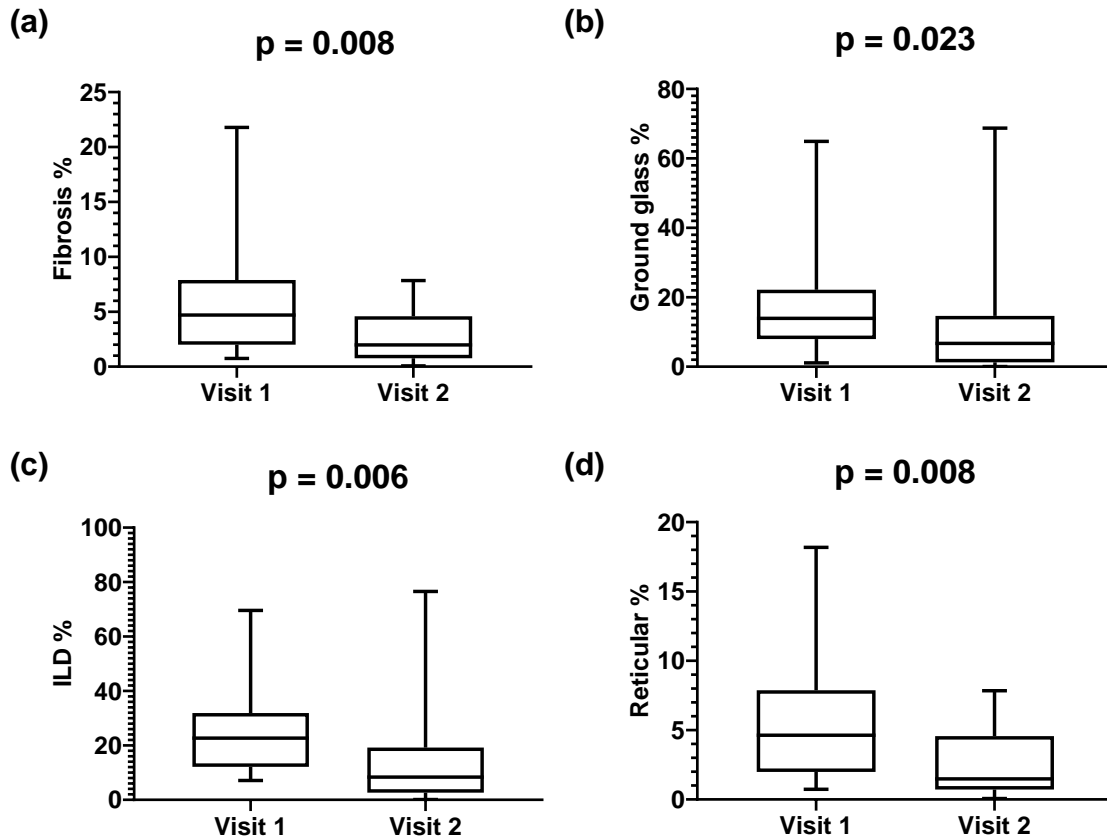


Figure 4.27. Global CALIPER fibrosis % (a), ground glass % (b), ILD % (c) and reticular % (d) at visit 1 versus visit 2 in the inflammation group (n=17). Statistical test: Wilcoxon test.

	Fibrotic (n = 22)	Inflammation (n = 17)	p value
Fibrosis %	4.25 (2.55 – 4.88)	2.62 (2.12 – 4.26)	0.081
Fibrosis % change	0.025 (-1.40 – 1.52)	-1.75 (-4.37 - -0.10)	0.019
Ground glass %	5.41 (2.65 – 15.9)	6.72 (1.26 – 14.6)	0.99
Ground glass % change	0.68 (-1.84 – 5.14)	-4.67 (-11.0 – 0.37)	0.031
Honeycomb %	0.19 (0.06 – 0.40)	0.03 (0.02 – 0.11)	0.012
Honeycomb % change	0.03 (-0.02 – 0.18)	-0.01 (-0.11 – 0.03)	0.13
ILD %	12.3 (4.67 – 22.7)	8.34 (2.64 – 19.2)	0.68
ILD % change	0.49 (-2.19 – 6.24)	-7.95 (-20.7 – 0.85)	0.007
Reticular %	3.91 (1.00 – 6.11)	1.48 (0.72 – 4.57)	0.091
Reticular % change	-0.01 (-1.37 – 0.84)	-1.72 (-4.37 - -0.10)	0.017
VRS %	4.25 (2.55 – 4.88)	2.62 (2.12 – 4.26)	0.10
VRS % change	0.37 (-0.18 – 1.35)	-0.39 (-1.11 – 0.38)	0.029

ILD: Interstitial lung disease; VRS: Vessel related structures.

Table 4.43. Global CALIPER CT results at **visit 2**, and the longitudinal change in global CALIPER CT measurements between visit 1 and visit 2 in the fibrotic and inflammation groups. Results are presented as median (interquartile range).

	Total (n = 39)	CTD-ILD (n = 5)	DI-ILD (n = 11)	HP (n = 10)	iNSIP (n = 2)	IPF (n = 11)
Fibrosis % change						
Upper zone	-0.23	-0.13	-0.25	-2.10	-0.58	-0.03
Middle zone	-0.55	-0.47	-0.55	-1.23	-1.10	0.03
Lower zone	-0.55	0.20	-1.25	-0.68	-0.61	-0.23
Central zone	-0.37	-0.41	-0.75	-1.02	-0.98	-0.09
Peripheral zone	-0.64	-0.41	-0.80	-2.06	-0.68	-0.10
Ground glass % change						
Upper zone	-0.05	-0.20	0.00	-2.98	-3.14	0.10
Middle zone	-1.14	-1.82	-1.63	2.07	-14.2	0.33
Lower zone	-0.13	-16.7	-0.13	0.25	-31.8	2.50
Central zone	-0.18	-2.57	-0.18	1.48	-8.83	0.10
Peripheral zone	-0.18	-11.4	-0.18	-0.72	-21.5	2.01
ILD % change						
Upper zone	-0.10	-0.32	0.01	-0.85	-3.71	0.03
Middle zone	-1.55	-1.93	-7.03	0.12	-15.3	-0.22
Lower zone	-1.38	-18.6	-8.09	-0.95	-32.4	0.93
Central zone	-0.49	-2.69	-5.55	1.16	-9.81	0.10
Peripheral zone	-1.19	-12.7	-2.3	-0.50	-22.2	1.06
VRS % change						
Upper zone	0.16	-0.28	0.20	-0.12	-0.50	0.32
Middle zone	0.11	-0.32	0.18	-0.18	-0.90	0.38
Lower zone	0.27	-0.68	0.55	0.39	-1.91	0.63
Central zone	0.09	-0.60	0.19	-0.15	-1.34	0.49
Peripheral zone	0.16	-0.22	0.32	-0.05	-0.69	0.41

CTD-ILD: Connective tissue disease associated interstitial lung disease; DI-ILD: Drug induced interstitial lung disease; HP: Hypersensitivity pneumonitis; ILD: Interstitial lung disease; iNSIP: Idiopathic non-specific interstitial pneumonia; IPF: Idiopathic pulmonary fibrosis; VRS: Vessel related structures.

Table 4.44. Change in regional CALIPER CT fibrosis %, ground glass %, ILD % and VRS % results between visit 1 and visit 2 for the total cohort and each ILD subtype. Results are presented as median.

In the IPF group (n=11), there was a statistically significant increase in CALIPER VRS % between visit 1 and visit 2 in the upper zone (median (%): 2.26 (1.37 – 3.27) vs 2.63 (1.42 – 3.85); p=0.017), middle zone (median (%): 3.67 (2.95 – 4.84) vs 5.20 (2.90 – 5.75); p=0.032), lower zone (median (%): 3.91 (3.44 – 4.96) vs 4.60 (3.72 – 5.74); p=0.007), central zone (median (%): 4.23 (3.18 – 5.09) vs 4.66 (3.45 – 6.34); p=0.016) and peripheral zone (median (%): 2.09 (1.31 – 3.45) vs 3.00 (1.45 – 3.87); p=0.008).

	Fibrotic (n = 22)	Inflammation (n = 17)	p value
Fibrosis % change			
Upper zone	-0.08	-0.84	0.036
Middle zone	-0.06	-1.43	0.025
Lower zone	-0.11	-1.96	0.036
Central zone	-0.005	-1.31	0.013
Peripheral zone	-0.28	-1.95	0.048
Ground glass % change			
Upper zone	0.05	-0.73	0.012
Middle zone	0.17	-4.11	0.007
Lower zone	1.61	-4.05	0.072
Central zone	0.05	-2.57	0.011
Peripheral zone	1.45	-4.77	0.017
ILD % change			
Upper zone	0.02	-0.94	0.016
Middle zone	-0.06	-8.05	0.002
Lower zone	0.72	-13.8	0.002
Central zone	0.10	-5.25	0.002
Peripheral zone	0.93	-12.7	0.005
VRS % change			
Upper zone	0.26	-0.28	0.031
Middle zone	0.33	-0.32	0.013
Lower zone	0.48	-0.57	0.030
Central zone	0.40	-0.60	0.023
Peripheral zone	0.31	-0.22	0.019

ILD: Interstitial lung disease; VRS: Vessel related structures.

Table 4.45. Change in regional CALIPER CT fibrosis %, ground glass %, ILD % and VRS % results between visit 1 and visit 2 in the fibrotic and inflammation groups. Results are presented as median.

In the inflammation group (n=17), between visits 1 and 2 there was a statistically significant decrease in regional CALIPER fibrosis % (upper zone: p=0.008; middle zone: p=0.002; lower zone: p=0.035; central zone: p=0.005; peripheral zone: p=0.013), ground glass % (middle zone: p=0.017; lower zone: p=0.018; central zone: p=0.027; peripheral zone: p=0.020), and ILD % (upper zone: p=0.045; middle zone: p=0.007; lower zone: p=0.002; central zone: p=0.008; peripheral zone: p=0.006). The treatment these subjects received is presented in Table 4.3.

4.7.4 Visit 3 (6 months or 12 months depending on ILD subtype)

In the DI-ILD group (n=8), there was a statistically significant increase in global CALIPER honeycomb % between visit 1 and visit 3 (median (%): 0.015 (0.00 – 0.085) vs 0.12 (0.005 – 0.63); p=0.031) (Figure 4.28). Five out of the eight DI-ILD subjects were in the fibrotic group. Two out of the eight DI-ILD subjects were taking prednisolone during the study.

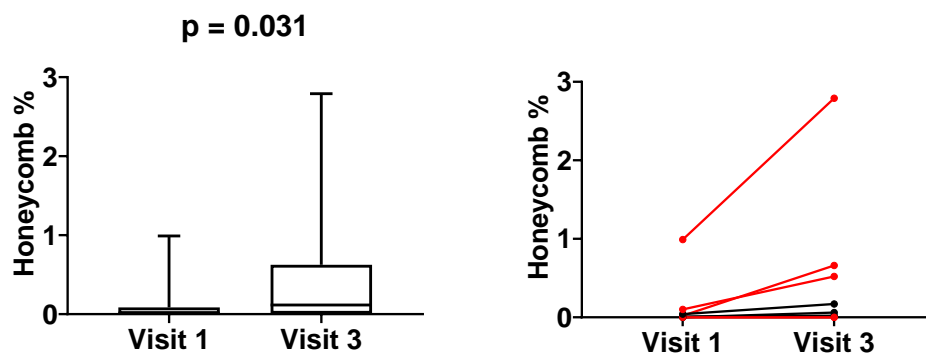


Figure 4.28. Global CALIPER honeycomb % at visit 1 versus visit 3 in the DI-ILD group (n=8). The five subjects highlighted in red were in the fibrotic group. Statistical test: Wilcoxon test.

In the IPF group (n=11), there was a statistically significant increase in global CALIPER VRS % between visit 1 and visit 3 (mean (%): 3.35 ± 0.94 vs 4.30 ± 1.30 ; p=0.010) (Figure 4.29).

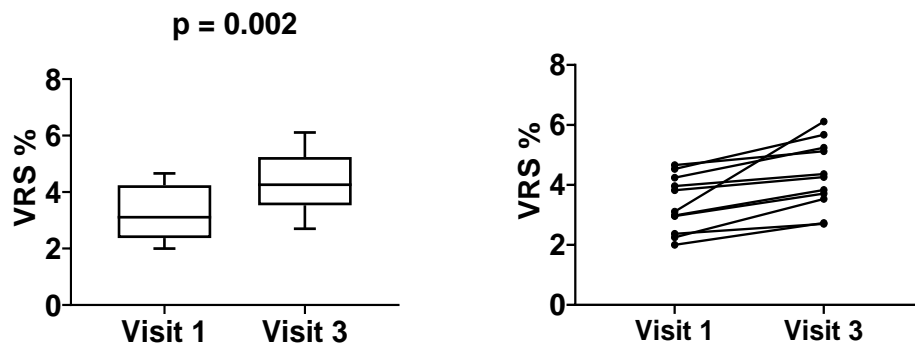


Figure 4.29. Global CALIPER VRS % at visit 1 versus visit 3 in the IPF group (n=11). Statistical test: paired *t* test.

	Total (n = 31)	CTD-ILD (n = 5)	DI-ILD (n = 8)	HP (n = 7)	IPF (n = 11)
Fibrosis %	3.29 (0.86 – 6.41)	0.64 (0.28 – 3.47)	2.42 (0.84 – 6.20)	3.17 (0.31 – 8.78)	5.13 (2.73 – 7.27)
Fibrosis % change	0.10 (-0.80 – 1.27)	0.06 (-2.39 – 0.29)	0.10 (-2.15 – 0.55)	-0.63 (-2.24 – 1.96)	0.93 (-0.20 – 1.88)
Ground glass %	6.60 (1.96 – 15.6)	1.24 (0.33 – 8.78)	3.64 (1.60 – 20.1)	13.3 (0.28 – 32.1)	7.05 (4.62 – 9.39)
Ground glass % change	-0.50 (-4.76 – 2.05)	-0.03 (-2.63 – 5.19)	-5.06 (-6.54 - -1.54)	-0.72 (-19.5 – 16.3)	1.06 (-2.15 – 3.81)
Honeycomb %	0.11 (0.03 – 0.52)	0.03 (0.02 – 0.79)	0.12 (0.01 – 0.63)	0.06 (0.02 – 0.08)	0.24 (0.12 – 0.76)
Honeycomb % change	0.01 (-0.01 – 0.08)	0.00 (-1.23 – 0.08)	0.08 (-0.01 – 0.30)	0.01 (-0.06 – 0.03)	0.04 (-0.01 – 0.08)
ILD %	10.6 (3.69 – 22.4)	2.39 (0.72 – 11.9)	7.27 (2.97 – 25.8)	15.2 (0.59 – 39.8)	10.8 (10.3 – 15.1)
ILD % change	-0.03 (-5.08 – 3.74)	0.04 (-2.56 – 3.01)	-5.13 (-9.18 - -0.43)	-1.35 (-21.6 – 18.9)	1.40 (-1.96 – 5.52)
Reticular %	3.23 (0.82 – 5.57)	0.61 (0.27 – 2.68)	2.31 (0.83 – 5.08)	3.11 (0.23 – 8.70)	4.05 (2.61 – 7.03)
Reticular % change	0.11 (-0.74 – 0.88)	0.07 (-1.18 – 0.22)	-0.05 (-2.17 – 0.33)	-0.57 (-2.31 – 1.92)	0.87 (0.10 – 1.81)
VRS %	3.71 (2.40 – 5.12)	2.19 (1.52 – 4.07)	3.01 (1.94 – 5.51)	3.99 (1.84 – 4.89)	4.26 (3.53 – 5.24)
VRS % change	0.03 (-0.36 – 0.69)	-0.04 (-0.28 – 0.77)	-0.12 (-0.48 – 0.32)	-0.55 (-1.51 – 0.61)	0.56 (-0.19 – 0.95)

CTD-ILD: Connective tissue disease associated interstitial lung disease; DI-ILD: Drug induced interstitial lung disease; HP: Hypersensitivity pneumonitis; ILD: Interstitial lung disease; iNSIP: Idiopathic non-specific interstitial pneumonia; IPF: Idiopathic pulmonary fibrosis; VRS: Vessel related structures.

Table 4.46. Global CALIPER CT results at **visit 3**, and the longitudinal change in global CALIPER CT measurements between visit 1 and visit 3 in the total cohort and each ILD subtype. Results are presented as median (inter-quartile range).

At visit 3, there was a statistically significant difference between the fibrotic and inflammation groups in all global CALIPER CT measurements with all of them being significantly higher in the fibrotic group (Figure 4.30). This is in contrast to the findings at visit 1 in which the inflammation group had a significantly higher CALIPER ground glass % ($p=0.004$) and ILD % ($p=0.005$) compared to the fibrotic group.

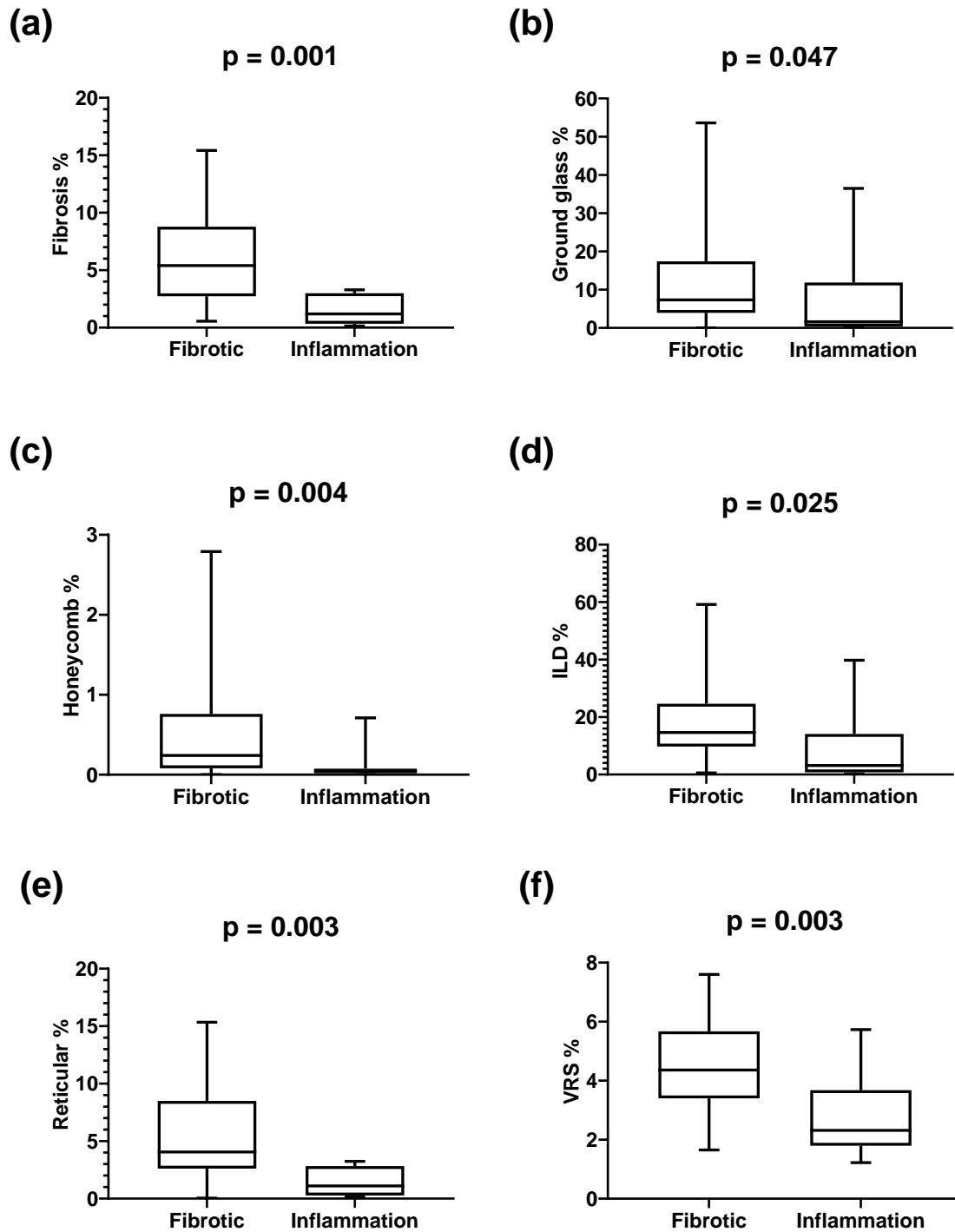


Figure 4.30. Difference between the fibrotic (n=19) and inflammation (n=12) groups in global CALIPER fibrosis % (a), ground glass % (b), honeycomb % (c), ILD % (d), reticular % (e) and VRS % (f) at visit 3. Statistical test: Mann-Whitney test.

In the fibrotic group (n=19), between visits 1 and 3 there was a statistically significant increase in global CALIPER VRS % (mean (%): 3.57 ± 1.30 vs 4.42 ± 1.51 ; $p=0.004$) (Figure 4.31). The treatment these subjects received is provided in Table 4.3.

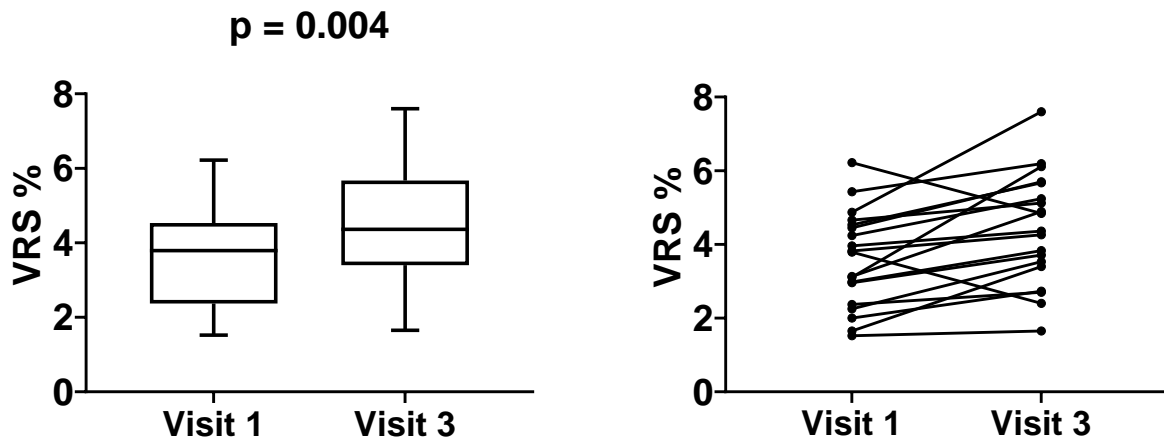


Figure 4.31. Global CALIPER VRS % at visit 1 versus visit 3 in the fibrotic group (n=19). Statistical test: paired *t* test.

In the inflammation group (n=12), between visits 1 and 3 there was a statistically significant decrease in global CALIPER fibrosis % (median (%): 4.59 (1.85 – 6.18) vs 1.19 (0.34 – 2.99); $p=0.005$), ground glass % (median (%): 13.4 (7.31 – 28.3) vs 1.60 (0.36 – 11.9); $p=0.003$), ILD % (median (%): 19.6 (8.61 – 33.8) vs 3.13 (0.75 – 14.1); $p<0.001$), reticular % (median (%): 4.53 (1.83 – 6.15) vs 1.10 (0.27 – 2.82); $p=0.004$) and VRS % (median (%): 2.75 (2.26 – 4.80) vs 2.32 (1.80 – 3.68); $p=0.033$) (Figure 4.32). The treatment these subjects received is shown in Table 4.3.

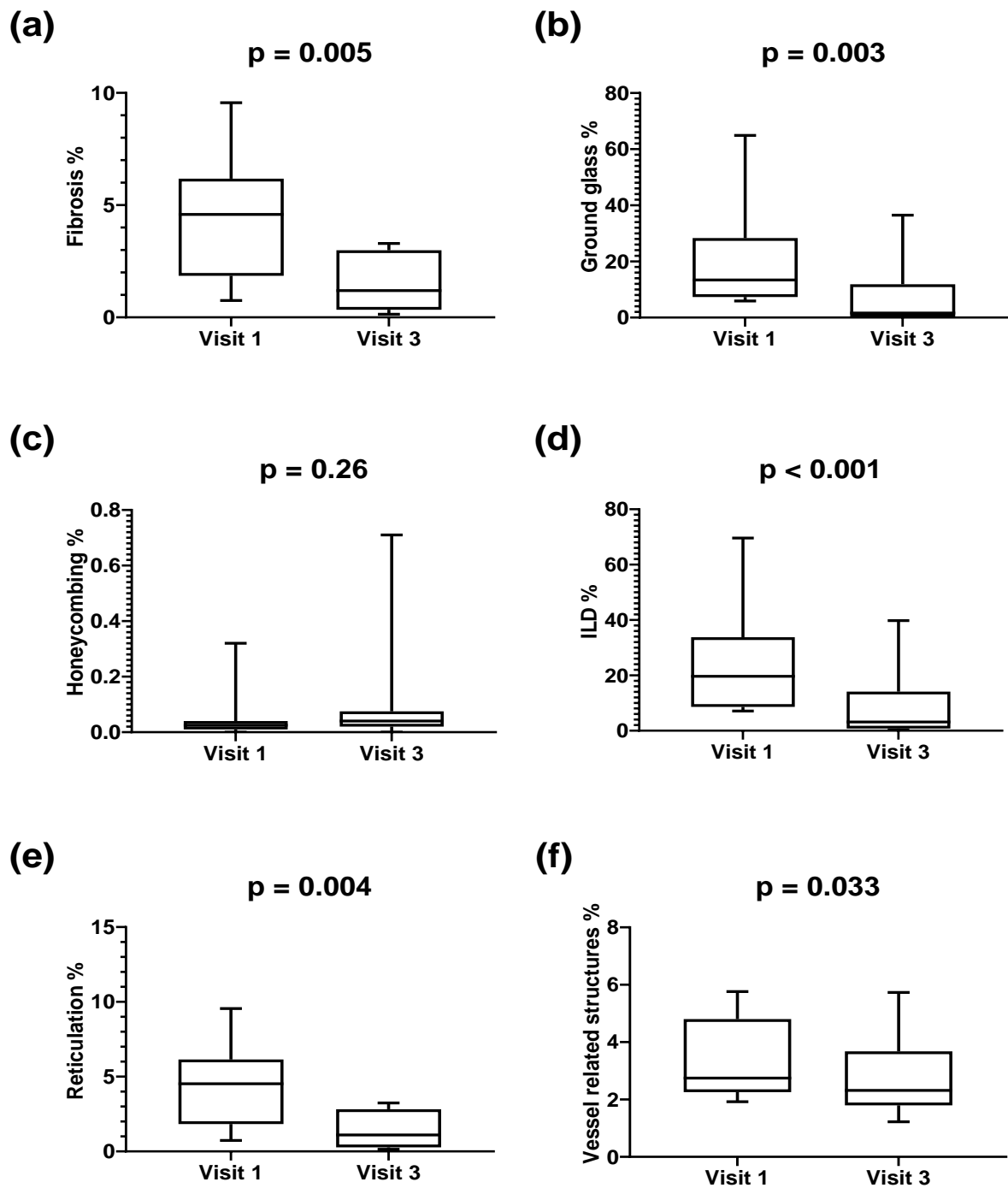


Figure 4.32. Global CALIPER fibrosis % (a), ground glass % (b), honeycomb % (c), ILD % (d), reticular % (e) and VRS % (f) at visit 1 vs visit 3 in the inflammation group (n=12). Statistical test: Wilcoxon test.

	Fibrotic (n = 19)	Inflammation (n = 12)	p value
Fibrosis %	5.40 (2.73 – 8.78)	1.19 (0.34 – 2.99)	0.001
Fibrosis % change	0.59 (-0.74 – 1.88)	-0.14 (-2.48 – 0.36)	0.055
Ground glass %	7.33 (3.95 – 17.4)	1.60 (0.36 – 11.9)	0.047
Ground glass % change	0.46 (-2.92 – 3.81)	-2.74 (-11.5 – 0.15)	0.071
Honeycomb %	0.24 (0.08 – 0.76)	0.04 (0.02 – 0.08)	0.004
Honeycomb % change	0.04 (-0.01 – 0.24)	0.005 (-0.01 – 0.03)	0.39
ILD %	14.6 (9.73 – 24.6)	3.13 (0.75 – 14.1)	0.025
ILD % change	1.02 (-2.67 – 5.52)	-3.22 (-14.3 – 0.24)	0.053
Reticular %	4.05 (2.61 – 8.49)	1.10 (0.27 – 2.82)	0.003
Reticular % change	0.47 (-0.28 – 1.74)	-0.22 (-2.49 – 0.27)	0.022
VRS %	4.36 (3.40 – 5.67)	2.32 (1.80 – 3.68)	0.003
VRS % change	0.42 (-0.19 – 0.74)	-0.14 (-1.03 – 0.08)	0.027

ILD: Interstitial lung disease; VRS: Vessel related structures.

Table 4.47. Global CALIPER CT results at **visit 3**, and the longitudinal change in global CALIPER CT measurements between visit 1 and visit 3 in the fibrotic and inflammation groups. Results are presented as median (interquartile range).

Two-way ANOVA statistical analysis was used in the 31 subjects that had CALIPER CT data at each of the three study visits (Figure 4.33). In the inflammation group (n=12), between visits 1 and 3 there was a statistically significant decrease in global CALIPER fibrosis % (p<0.001), ground glass % (p=0.029), ILD % (p=0.012) and reticular % (p=0.011). There was also a statistically significant decrease in global CALIPER fibrosis % between visits 1 and 2 (p=0.027), and a statistically significant decline in FVC% between visits 2 and 3 (p=0.024). In the fibrotic group (n=19), there was a statistically significant increase in global CALIPER VRS% between visits 1 and 3 (p=0.011), but not between visits 1 and 2. The treatment these subjects received is demonstrated in Table 4.3.

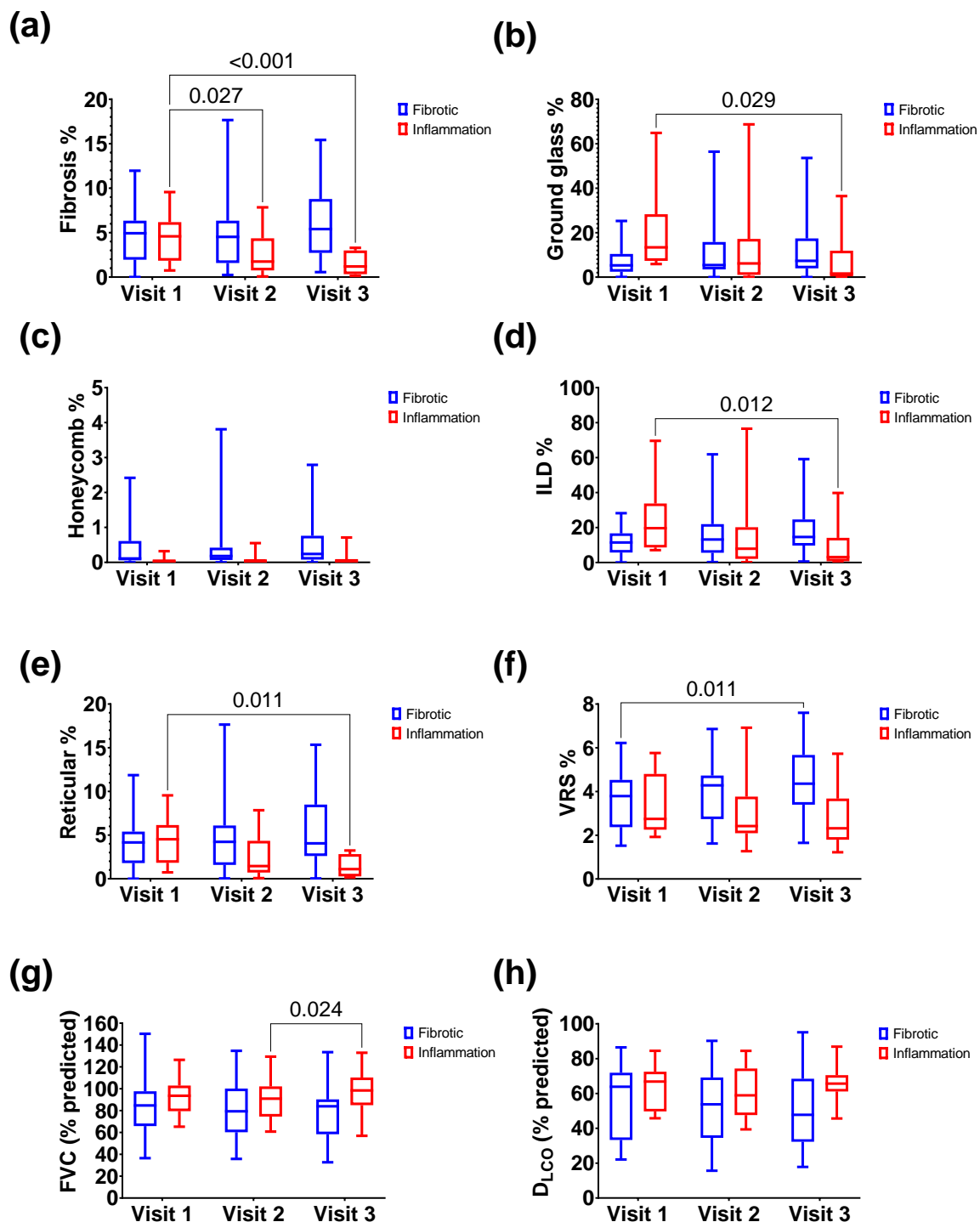


Figure 4.33. Global CALIPER fibrosis % (a), ground glass % (b), honeycomb % (c), ILD % (d), reticular % (e), VRS % (f), FVC % predicted (g), and DLCO % predicted (h) at visits 1, 2 and 3 for the fibrotic and inflammation groups. Statistical test: two-way ANOVA.

	Total (n = 31)	CTD-ILD (n = 5)	DI-ILD (n = 8)	HP (n = 7)	IPF (n = 11)
Fibrosis % change					
Upper zone	0.01	0.00	-0.41	-0.32	0.07
Middle zone	0.13	0.00	-0.20	-0.86	0.67
Lower zone	0.27	0.16	0.21	0.77	3.22
Central zone	0.00	0.00	-0.45	-0.26	0.41
Peripheral zone	0.20	0.14	-0.05	-1.01	1.48
Ground glass % change					
Upper zone	0.00	0.00	-2.40	-0.35	0.04
Middle zone	-0.23	0.00	-5.77	-0.87	1.00
Lower zone	0.32	-0.10	-1.14	-0.85	3.28
Central zone	-0.14	0.01	-2.97	-0.45	0.37
Peripheral zone	-0.52	-0.07	-5.90	-0.98	2.11
ILD % change					
Upper zone	-0.01	-0.01	-3.30	-0.67	0.11
Middle zone	0.03	0.03	-6.20	-1.74	2.28
Lower zone	0.96	0.59	0.85	-1.47	5.16
Central zone	0.01	0.02	-3.80	-0.71	0.76
Peripheral zone	-0.12	0.07	-6.83	-1.99	2.32
VRS % change					
Upper zone	-0.02	-0.03	-0.06	-0.2	0.28
Middle zone	0.06	-0.06	-0.16	-0.40	0.40
Lower zone	0.05	0.00	0.01	-0.76	0.88
Central zone	0.06	-0.11	-0.35	-0.81	0.41
Peripheral zone	0.05	-0.03	0.10	-0.34	0.33

CTD-ILD: Connective tissue disease associated interstitial lung disease; DI-ILD: Drug induced interstitial lung disease; HP: Hypersensitivity pneumonitis; ILD: Interstitial lung disease; iNSIP: Idiopathic non-specific interstitial pneumonia; IPF: Idiopathic pulmonary fibrosis; VRS: Vessel related structures.

Table 4.48. Change in regional CALIPER CT fibrosis %, ground glass %, ILD % and VRS % results between visit 1 and visit 3 in the total cohort and each ILD subtype. Results are presented as median.

In the IPF group (n=11), between visits 1 and 3 there was a statistically significant increase in CALIPER VRS % in the upper zone (mean (%): 2.30 ± 0.91 vs 2.92 ± 1.18 ; $p=0.003$), middle zone (mean (%): 3.86 ± 1.02 vs 4.90 ± 1.31 ; $p=0.002$), lower zone (mean (%): 4.21 ± 1.32 vs 5.68 ± 1.61 ; $p=0.011$), central zone (mean (%): 4.26 ± 1.01 vs 5.26 ± 1.15 ; $p=0.003$) and peripheral zone (mean (%): 2.28 ± 1.06 vs 3.23 ± 1.37 ; $p=0.002$). The treatment these subjects received is presented in Table 4.3.

	Fibrotic (n = 19)	Inflammation (n = 12)	p value
Fibrosis % change			
Upper zone	0.10	-0.09	0.053
Middle zone	0.63	-0.11	0.006
Lower zone	1.26	-0.23	0.053
Central zone	0.41	-0.29	0.10
Peripheral zone	0.61	-0.08	0.060
Ground glass % change			
Upper zone	0.01	-0.18	0.24
Middle zone	0.00	-1.27	0.14
Lower zone	2.67	-1.15	0.12
Central zone	0.15	-1.15	0.15
Peripheral zone	0.84	-4.23	0.12
ILD % change			
Upper zone	0.11	-0.33	0.16
Middle zone	0.63	-1.77	0.060
Lower zone	3.37	-0.71	0.069
Central zone	0.43	-1.53	0.087
Peripheral zone	1.04	-4.88	0.082
VRS % change			
Upper zone	0.16	-0.07	0.045
Middle zone	0.40	-0.16	0.059
Lower zone	0.52	-0.21	0.035
Central zone	0.33	-0.35	0.065
Peripheral zone	0.33	-0.07	0.007

ILD: Interstitial lung disease; VRS: Vessel related structures.

Table 4.49. Change in regional CALIPER CT fibrosis %, ground glass %, ILD % and VRS % results between visit 1 and visit 3 in the fibrotic and inflammation groups. Results are presented as median.

In the fibrotic group (n=19), between visits 1 and 3 there was a statistically significant increase in regional CALIPER fibrosis % (middle zone: p=0.024; peripheral zone: p=0.049), ILD % (middle zone: p=0.029), and VRS % (upper zone: p=0.009; middle zone: p=0.004; lower zone: p=0.005; central zone: p=0.013; peripheral zone: p=0.001). In the inflammation group (n=12), between visits 1 and 3 there was a statistically significant decrease in CALIPER fibrosis %, ground glass % and ILD % in all five zones. There was also a statistically significant decrease in CALIPER VRS % between visit 1 and visit 3 in the lower zone (p=0.004). The treatment these subjects received is provided in Table 4.3.

4.8 Visual CT scoring

Visual CT scoring was performed by two consultant thoracic radiologists on all available HRCT scans. This provided global and regional ground glass, honeycomb and reticular scores. As with the CALIPER CT data, honeycomb and reticular scores were combined and termed fibrosis score. Also, ground glass, honeycomb and reticular scores were combined and termed ILD score. Visual CT scoring data were available for all subjects that completed each of visits 1 (n=55), 2 (n=39) and 3 (n=31).

4.8.1 Visit 1 (baseline)

There was a statistically significant difference between the HP (n=15) and IPF (n=19) groups in global visual CT fibrosis score (median: 4.0 (0.0 – 12.0) vs 13.0 (8.0 – 17.0); p=0.022) and ground glass score (median: 10.0 (0.0 – 14.0) vs 0.0 (0.0 – 4.0); p=0.032) (Figure 4.34).

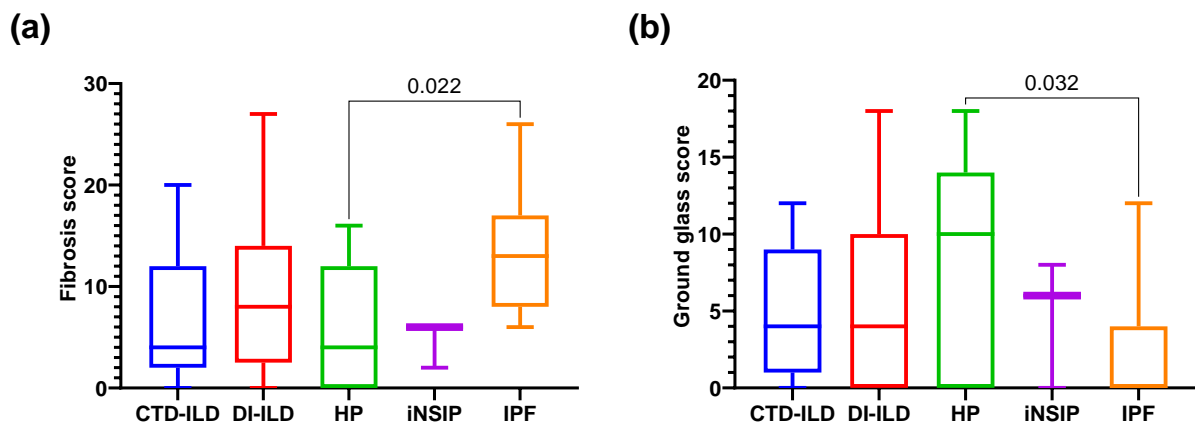


Figure 4.34. Difference between ILD subgroups at visit 1 in global visual CT fibrosis score (a) and ground glass score (b). Statistical test: Kruskal-Wallis test.

	Total (n = 55)	CTD-ILD (n = 5)	DI-ILD (n = 13)	HP (n = 15)	iNSIP (n = 3)	IPF (n = 19)
Fibrosis score	10.0 (4.0 – 14.0)	4.0 (2.0 – 12.0)	8.0 (2.5 – 14.0)	4.0 (0.0 – 12.0)	6.0 (2.0 – 6.0)	13.0 (8.0 – 17.0)
Ground glass score	2.0 (0.0 – 9.0)	4.0 (1.0 – 9.0)	4.0 (0.0 – 10.0)	10.0 (0.0 – 14.0)	6.0 (0.0 – 8.0)	0.0 (0.0 – 4.0)
Honeycomb score	0.0 (0.0 – 2.0)	0.0 (0.0 – 6.0)	0.0 (0.0 – 0.5)	0.0 (0.0 – 0.0)	0.0 (0.0 – 0.0)	2.0 (0.0 – 6.0)
ILD score	14.0 (10.0 – 18.0)	10.0 (7.0 – 16.0)	13.0 (9.5 – 18.5)	14.0 (12.0 – 17.0)	10.0 (6.0 – 12.0)	15.0 (12.0 – 20.0)
Reticular score	8.0 (4.0 – 11.0)	4.0 (2.0 – 6.0)	7.0 (2.5 – 11.5)	4.0 (0.0 – 12.0)	6.0 (2.0 – 6.0)	10.0 (8.0 – 12.0)

CTD-ILD: Connective tissue disease associated interstitial lung disease; DI-ILD: Drug induced interstitial lung disease; HP: Hypersensitivity pneumonitis; iNSIP: Idiopathic non-specific interstitial pneumonia; IPF: Idiopathic pulmonary fibrosis.

Table 4.50. Global visual CT score results at visit 1 for the total cohort and ILD subtypes. Results are presented as median (inter-quartile range).

There was a statistically significant difference between the fibrotic (n=32) and inflammation (n=23) groups in global CT visual fibrosis score (median: 13.0 (8.5 – 17.0) vs 4.0 (0.0 – 6.0); p<0.001), ground glass score (median: 0.0 (0.0 – 1.0) vs 10.0 (6.0 – 12.0); p<0.001), honeycomb score (median: 1.0 (0.0 – 7.5) vs 0.0 (0.0 – 0.0); p<0.001) and reticular score (median: 10.0 (8.0 – 12.0) vs 4.0 (0.0 – 6.0); p<0.001).

	Fibrotic (n = 32)	Inflammation (n = 23)	p value
Fibrosis score	13.0 (8.5 – 17.0)	4.0 (0.0 – 6.0)	<0.001
Ground glass score	0.0 (0.0 – 1.0)	10.0 (6.0 – 12.0)	<0.001
Honeycomb score	1.0 (0.0 – 7.5)	0.0 (0.0 – 0.0)	<0.001
ILD score	14.0 (10.25 – 19.0)	13.0 (10.0 – 16.0)	0.44
Reticular score	10.0 (8.0 – 12.0)	4.0 (0.0 – 6.0)	<0.001

Table 4.51. Global visual CT score results at visit 1 in the fibrotic and inflammation groups. Results are presented as median (inter-quartile range).

In the DI-ILD group (n=13), there was a statistically significant difference between the middle and lower zone in visual CT fibrosis score (p=0.021) and ILD score (p=0.007), and between the upper and lower zone in visual CT ILD score (p=0.021).

In the IPF group (n=19), there was a statistically significant difference between the upper and lower zone in visual CT fibrosis score (p<0.001) and ILD score (p<0.001), and between the middle and lower zone in visual CT ILD score (p=0.045).

	Total (n = 55)	CTD-ILD (n = 5)	DI-ILD (n = 13)	HP (n = 15)	iNSIP (n = 3)	IPF (n = 19)
Fibrosis score						
Upper zone	2.0	0.0	2.0	2.0	2.0	3.0
Middle zone	3.0	1.0	2.0	2.0	2.0	4.0
Lower zone	4.0	3.0	4.0	0.0	2.0	5.0
Ground glass score						
Upper zone	0.0	0.0	0.0	2.0	2.0	0.0
Middle zone	0.0	1.0	1.0	3.0	2.0	0.0
Lower zone	2.0	3.0	2.0	3.0	2.0	0.0
ILD score						
Upper zone	4.0	0.0	4.0	5.0	2.0	4.0
Middle zone	4.0	4.0	4.0	4.0	2.0	4.0
Lower zone	6.0	6.0	6.0	4.0	4.0	7.0

CTD-ILD: Connective tissue disease associated interstitial lung disease; DI-ILD: Drug induced interstitial lung disease; HP: Hypersensitivity pneumonitis; iNSIP: Idiopathic non-specific interstitial pneumonia; IPF: Idiopathic pulmonary fibrosis.

Table 4.52. Regional visual CT fibrosis, ground glass and ILD scores at visit 1 for the total cohort and each ILD subtype. Results are presented as median.

In the fibrotic group, there was a statistically significant difference in visual CT fibrosis score between the upper and lower zone (p=0.003), and the middle and lower zone (p=0.031). There was also a statistically significant difference in visual CT ILD score between the upper and lower zone (p=0.001), and the middle and lower zone (p=0.012).

In the inflammation group, there was a statistically significant difference in visual CT ground glass score between the upper and lower zone (p<0.001).

	Fibrotic (n = 32)	Inflammation (n = 23)	p value
Fibrosis score			
Upper zone	4.0	0.0	<0.001
Middle zone	4.0	1.0	<0.001
Lower zone	5.0	2.0	<0.001
Ground glass score			
Upper zone	0.0	2.0	<0.001
Middle zone	0.0	3.0	<0.001
Lower zone	0.0	4.0	<0.001
ILD score			
Upper zone	4.0	4.0	0.57
Middle zone	4.0	4.0	0.99
Lower zone	6.0	6.0	0.51

Table 4.53. Regional CT fibrosis, ground glass and ILD scores at visit 1 in the fibrotic and inflammation groups. Results are presented as median

4.8.2 Visit 2 (6 weeks or 6 months depending on ILD subtype)

	Total (n = 39)	CTD-ILD (n = 5)	DI-ILD (n = 11)	HP (n = 10)	iNSIP (n = 2)	IPF (n = 11)
Fibrosis score	10.0 (4.0 – 16.0)	4.0 (1.0 – 12.0)	9.0 (6.0 – 14.0)	10.5 (0.0 – 13.25)	5.0 (2.0 – 8.0)	16.0 (8.0 – 20.0)
Fibrosis score change	0.0 (0.0 – 0.0)	0.0 (-1.0 – 0.0)	0.0 (0.0 – 3.0)	0.0 (0.0 – 0.0)	1.0 (0.0 – 2.0)	0.0 (0.0 – 0.0)
Ground glass score	1.0 (0.0 – 6.0)	1.0 (0.0 – 5.0)	3.0 (0.0 – 8.0)	1.5 (0.0 – 11.25)	7.0 (6.0 – 8.0)	0.0 (0.0 – 0.0)
Ground glass score change	0.0 (0.0 – 0.0)	0.0 (-6.5 – 0.0)	0.0 (-2.0 – 4.0)	0.0 (-1.5 – 0.0)	3.0 (0.0 – 6.0)	0.0 (0.0 – 0.0)
Honeycomb score	0.0 (0.0 – 3.0)	0.0 (0.0 – 6.0)	0.0 (0.0 – 1.0)	0.0 (0.0 – 2.25)	0.0 (0.0 – 0.0)	2.0 (0.0 – 8.0)
Honeycomb score change	0.0 (0.0 – 0.0)	0.0 (0.0 – 0.0)	0.0 (0.0 – 0.0)	0.0 (0.0 – 0.0)	0.0 (0.0 – 0.0)	0.0 (0.0 – 0.0)
ILD score	13.0 (10.0 – 20.0)	8.0 (1.5 – 15.0)	14.0 (11.0 – 25.0)	12.5 (8.75 – 19.25)	12.0 (10.0 – 14.0)	16.0 (10.0 – 20.0)
ILD score change	0.0 (0.0 – 0.0)	0.0 (-7.5 – 0.0)	0.0 (-1.0 – 5.0)	0.0 (-1.5 – 0.0)	4.0 (0.0 – 8.0)	0.0 (0.0 – 0.0)
Reticular score	8.0 (4.0 – 11.0)	4.0 (1.0 – 6.0)	9.0 (6.0 – 13.0)	8.0 (0.0 – 12.0)	5.0 (2.0 – 8.0)	10.0 (8.0 – 12.0)
Reticular score change	0.0 (0.0 – 0.0)	0.0 (-1.0 – 0.0)	0.0 (0.0 – 3.0)	0.0 (0.0 – 0.0)	1.0 (0.0 – 2.0)	0.0 (0.0 – 0.0)

CTD-ILD: Connective tissue disease associated interstitial lung disease; DI-ILD: Drug induced interstitial lung disease; HP: Hypersensitivity pneumonitis; iNSIP: Idiopathic non-specific interstitial pneumonia; IPF: Idiopathic pulmonary fibrosis.

Table 4.54. Global visual CT scores at **visit 2**, and the longitudinal change in global visual CT scores between visit 1 and visit 2 for the total cohort and each ILD subtype. Results are presented as median (inter-quartile range).

	Fibrotic (n = 22)	Inflammation (n = 17)	p value
Fibrosis score	12.5 (8.75 – 20.0)	4.0 (0.0 – 9.5)	<0.001
Fibrosis score change	0.0 (0.0 – 0.0)	0.0 (0.0 – 1.0)	0.45
Ground glass score	0.0 (0.0 – 0.0)	5.0 (2.0 – 11.5)	<0.001
Ground glass score change	0.0 (0.0 – 0.0)	0.0 (-4.5 – 0.0)	0.024
Honeycomb score	1.5 (0.0 – 8.0)	0.0 (0.0 – 0.0)	<0.001
Honeycomb score change	0.0 (0.0 – 0.0)	0.0 (0.0 – 0.0)	>0.99
ILD score	14.0 (11.0 – 20.0)	11.0 (5.0 – 18.5)	0.15
ILD score change	0.0 (0.0 – 0.0)	0.0 (-3.5 – 0.0)	0.15
Reticular score	10.0 (8.0 – 12.0)	4.0 (0.0 – 9.5)	0.005
Reticular score change	0.0 (0.0 – 0.0)	0.0 (0.0 – 1.0)	0.29

Table 4.55. Global visual CT scores at **visit 2**, and the longitudinal change in global visual CT scores between visit 1 and visit 2 in the fibrotic and inflammation groups. Results are presented as median (interquartile range).

There was a statistically significant difference between the fibrotic and inflammation groups at visit 2 in visual CT fibrosis score (median: 12.5 (8.75 – 20.0) vs 4.0 (0.0 – 9.5); $p < 0.001$), ground glass score (median: 0.0 (0.0 – 0.0) vs 5.0 (2.0 – 11.5); $p < 0.001$), honeycomb score (median: 1.5 (0.0 – 8.0) vs 0.0 (0.0 – 0.0); $p < 0.001$) and reticular score (median: 10.0 (8.0 – 12.0) vs 4.0 (0.0 – 9.5); $p = 0.005$).

Between visits 1 and 2, there was no statistically significant change in any of the regional visual CT scores in any of the ILD subtypes, or the fibrotic and inflammation groups.

4.8.3 Visit 3 (6 months or 12 months depending on ILD subtype)

	Total (n = 31)	CTD-ILD (n = 5)	DI-ILD (n = 8)	HP (n = 7)	IPF (n = 11)
Fibrosis score	9.0 (1.0 – 17.0)	4.0 (1.5 – 12.0)	9.0 (2.0 – 19.5)	0.0 (0.0 – 11.0)	16.0 (8.0 – 20.0)
Fibrosis score change	0.0 (0.0 – 0.0)	0.0 (0.0 – 0.5)	0.0 (0.0 – 0.75)	0.0 (0.0 – 0.0)	0.0 (0.0 – 0.0)
Ground glass score	0.0 (0.0 – 5.0)	1.0 (0.0 – 5.0)	1.0 (0.0 – 4.5)	5.0 (0.0 – 9.0)	0.0 (0.0 – 0.0)
Ground glass score change	0.0 (0.0 – 0.0)	0.0 (0.0 – 0.0)	0.0 (-1.5 – 0.0)	0.0 (-6.0 – 0.0)	0.0 (0.0 – 0.0)
Honeycomb score	0.0 (0.0 – 7.0)	0.0 (0.0 – 6.0)	0.0 (0.0 – 7.0)	0.0 (0.0 – 0.0)	2.0 (0.0 – 10.0)
Honeycomb score change	0.0 (0.0 – 0.0)	0.0 (0.0 – 0.0)	0.0 (0.0 – 0.0)	0.0 (0.0 – 0.0)	0.0 (0.0 – 0.0)
ILD score	12.0 (6.0 – 19.0)	8.0 (2.0 – 15.0)	12.0 (2.5 – 23.75)	11.0 (5.0 – 14.0)	16.0 (8.0 – 20.0)
ILD score change	0.0 (0.0 – 0.0)	0.0 (0.0 – 0.5)	0.0 (0.0 – 0.75)	0.0 (-6.0 – 0.0)	0.0 (0.0 – 0.0)
Reticular score	8.0 (1.0 – 10.0)	4.0 (1.5 – 6.0)	8.5 (2.0 – 12.75)	0.0 (0.0 – 10.0)	10.0 (8.0 – 10.0)
Reticular score change	0.0 (0.0 – 0.0)	0.0 (0.0 – 0.5)	0.0 (0.0 – 0.75)	0.0 (0.0 – 0.0)	0.0 (0.0 – 0.0)

CTD-ILD: Connective tissue disease associated interstitial lung disease; DI-ILD: Drug induced interstitial lung disease; HP: Hypersensitivity pneumonitis; iNSIP: Idiopathic non-specific interstitial pneumonia; IPF: Idiopathic pulmonary fibrosis.

Table 4.56. Global visual CT scores at **visit 3**, and the longitudinal change in global visual CT scores between visit 1 and visit 3 for the total cohort and each ILD subtype. Results are presented as median (inter-quartile range).

	Fibrotic (n = 19)	Inflammation (n = 12)	p value
Fibrosis score	12.0 (8.0 – 20.0)	1.5 (0.0 – 7.0)	<0.001
Fibrosis score change	0.0 (0.0 – 0.0)	0.0 (0.0 – 0.0)	0.65
Ground glass score	0.0 (0.0 – 0.0)	3.5 (0.25 – 6.0)	0.005
Ground glass score change	0.0 (0.0 – 0.0)	0.0 (-4.75 – 0.0)	0.15
Honeycomb score	2.0 (0.0 – 10.0)	0.0 (0.0 – 0.0)	0.002
Honeycomb score change	0.0 (0.0 – 0.0)	0.0 (0.0 – 0.0)	0.91
ILD score	14.0 (10.0 – 20.0)	7.0 (2.0 – 11.5)	0.008
ILD score change	0.0 (0.0 – 0.0)	0.0 (-4.75 – 0.0)	0.31
Reticular score	10.0 (8.0 – 12.0)	1.5 (0.0 – 7.0)	0.001
Reticular score change	0.0 (0.0 – 0.0)	0.0 (0.0 – 0.0)	0.65

Table 4.57. Global visual CT scores at **visit 3**, and the longitudinal change in global visual CT scores between visit 1 and visit 3 in the fibrotic and inflammation groups. Results are presented as median (interquartile range).

There was a statistically significant difference between the fibrotic (n=19) and inflammation (n=12) groups at visit 3 in visual CT fibrosis score (median: 12.0 (8.0 – 20.0) vs 1.5 (0.0 – 7.0); $p < 0.001$), ground glass score (median: 0.0 (0.0 – 0.0) vs 3.5 (0.25 – 6.0); $p = 0.005$), honeycomb score (median: 2.0 (0.0 – 10.0) vs 0.0 (0.0 – 0.0); $p = 0.002$), ILD score (median: 14.0 (10.0 – 20.0) vs 7.0 (2.0 – 11.5); $p = 0.008$) and reticular score (median: 10.0 (8.0 – 12.0) vs 1.5 (0.0 – 7.0); $p = 0.001$).

In the inflammation group (n=12), there was a statistically significant decrease in the global visual CT ground glass score between visit 1 and visit 3 (mean: 9.08 ± 5.04 vs 4.17 ± 4.22 ; $p = 0.023$) (Figure 4.35). There were no statistically significant changes in PFTs over the same study visit period. This suggests that the semi-quantitative assessment of GGO on HRCT by radiologists may be useful to determine response to immunosuppressant treatment in inflammation predominant ILD, before significant physiological changes are identified.

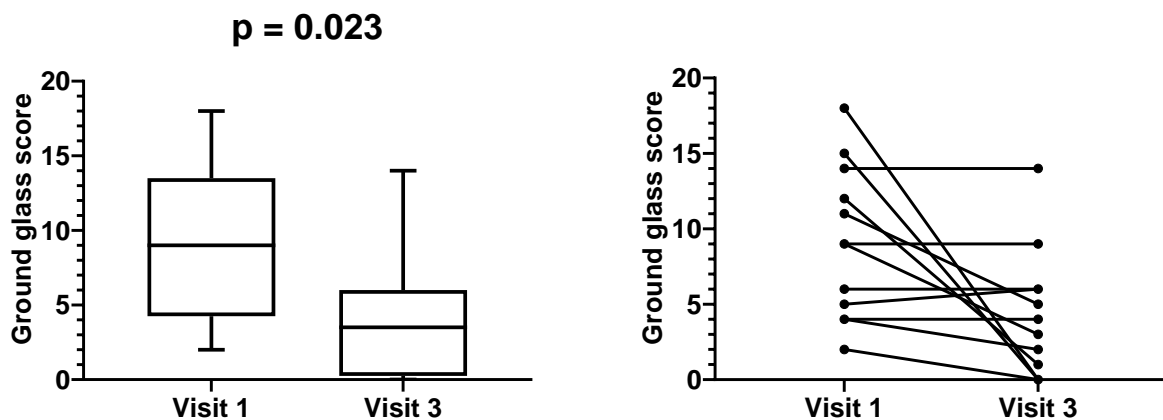


Figure 4.35. Global visual CT ground glass score at visit 1 versus visit 3 in the inflammation group. Statistical test: paired *t* test.

In the inflammation group (n=12), between visit 1 and visit 3 there was a statistically significant decrease in the visual CT ground glass score in the middle zone (median: 3.0 (2.0 – 4.0) vs 0.5 (0.0 – 2.0); $p = 0.031$) and the lower zone (mean: 3.67 ± 1.37 vs 2.08 ± 1.56 ; $p = 0.035$).

4.9 The effect of steroids on pulmonary function tests and imaging measurements in the drug induced ILD subjects

Of the 11 DI-ILD subjects that completed visit 1 and visit 2, two of them were taking prednisolone daily during the six-week period in addition to withholding the offending drug. One subject (highlighted in red in Figures 4.36 – 4.39) commenced prednisolone 113 days prior to visit 1, and was taking a dose of 10mg once daily between visit 1 and visit 2. This subject died four weeks after visit 2. The other subject (highlighted in blue in Figures 4.36 – 4.40) commenced prednisolone 40mg once daily 17 days prior to visit 1, with a reducing dose regimen of 5mg every two weeks until reaching a maintenance dose of 10mg once daily, which was the dose at visit 3. Another DI-ILD subject (highlighted in green in Figures 4.36 – 4.40) commenced prednisolone 20mg 14 days after visit 2 and the treatment duration was 21 days only.

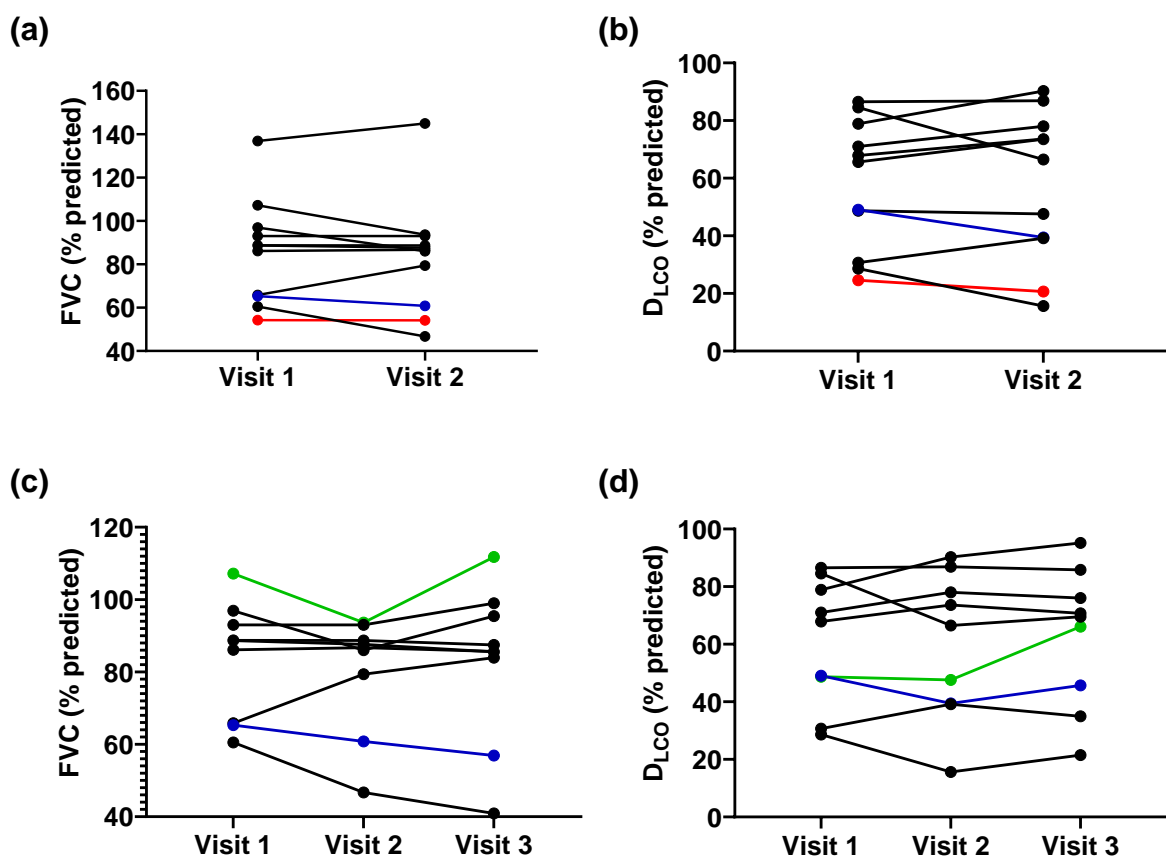


Figure 4.36. FVC % predicted (a) and DLCO % predicted (b) at visit 1 versus visit 2 in the DI-ILD group (n=11). FVC % predicted (c) and DLCO % predicted (d) at visits 1, 2 and 3 in the DI-ILD group (n=9).

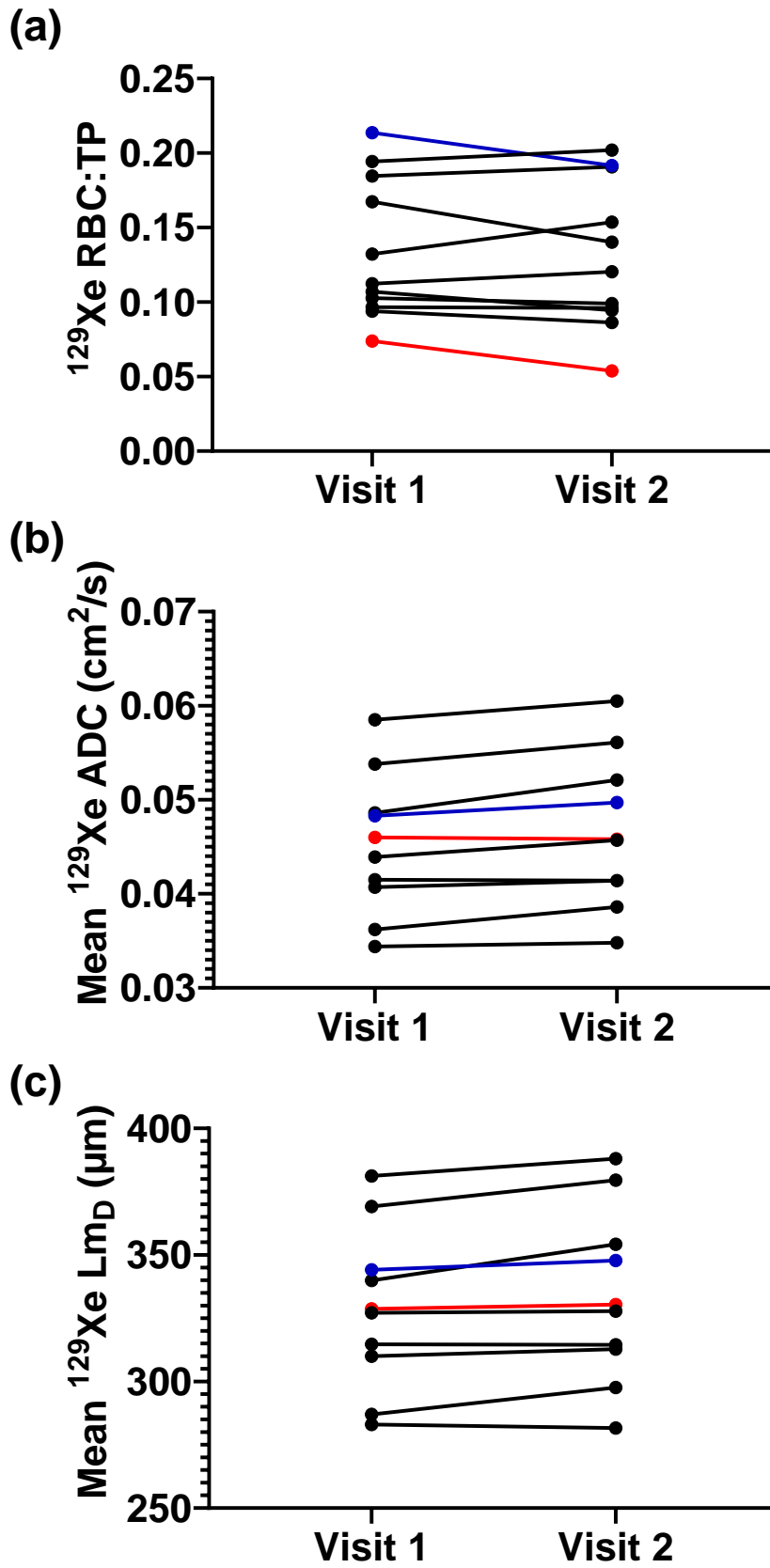


Figure 4.37. ^{129}Xe RBC:TP (a), ADC (b) and L_{mD} (c) at visit 1 versus visit 2 in the DL-ILD group (n=11).

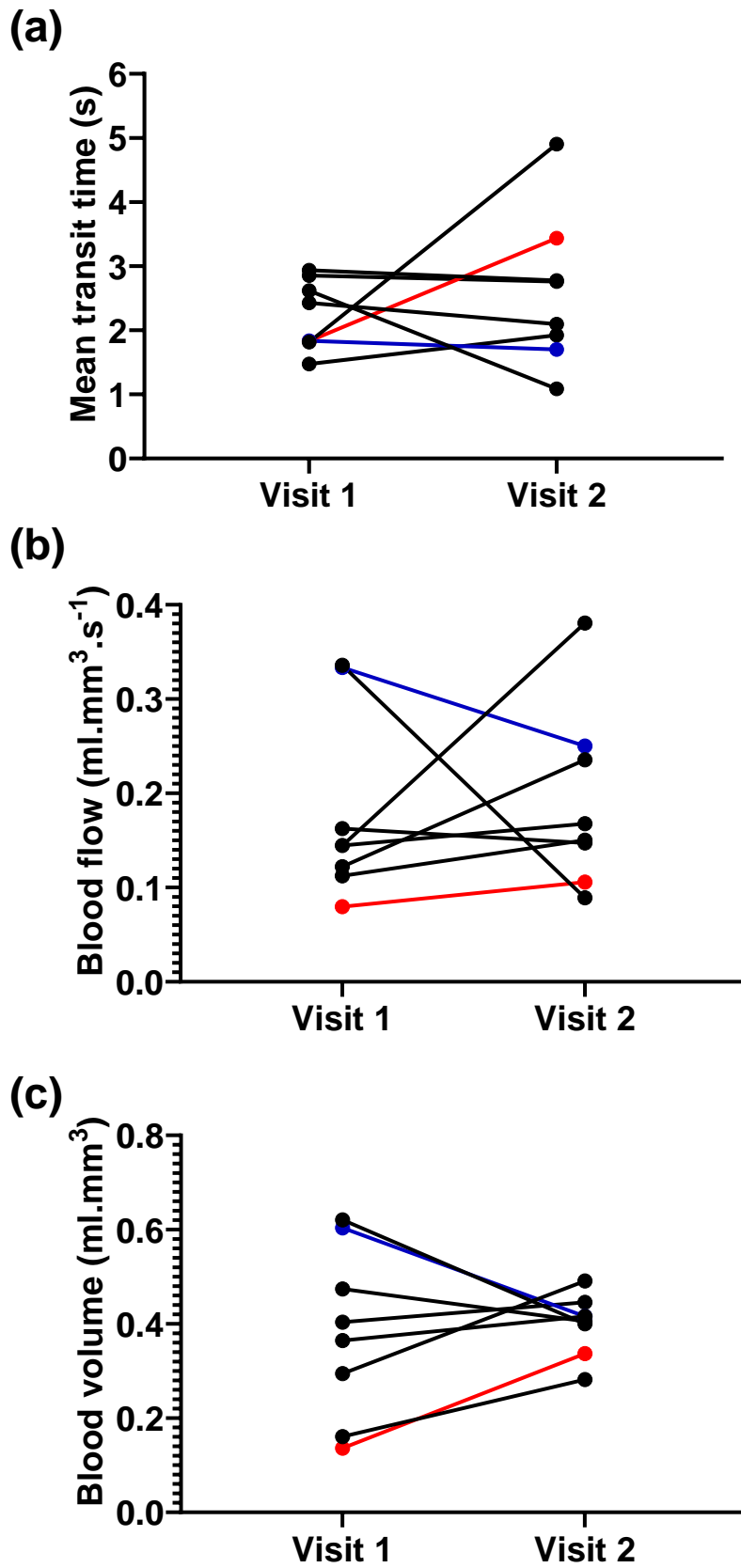


Figure 4.38. Mean transit time (a), blood flow (b) and blood volume (c) at visit 1 versus visit 2 in the DI-ILD group (n=11).

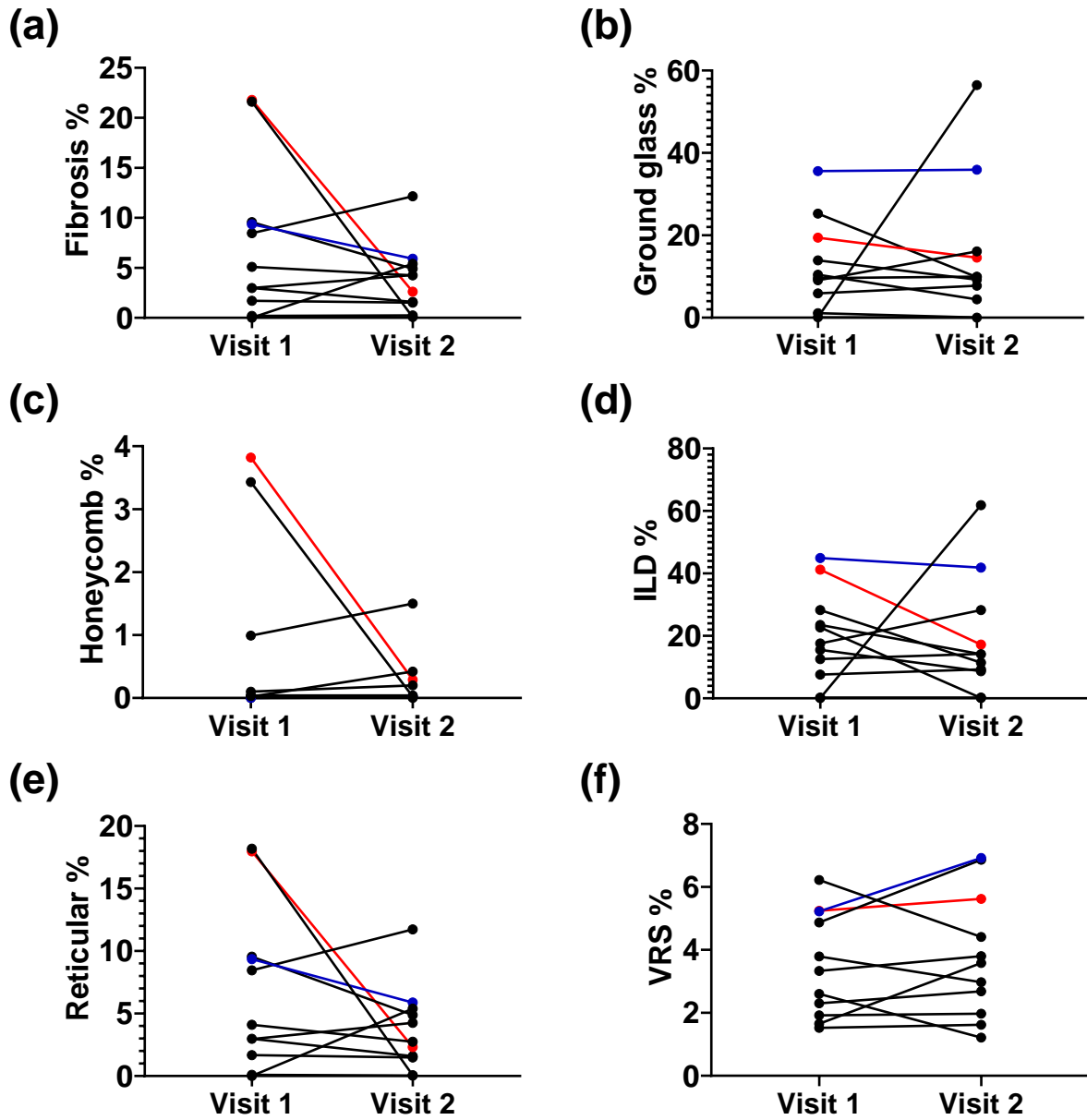


Figure 4.39. CALIPER fibrosis % (a), ground glass % (b), honeycomb % (c), ILD % (d), reticular % (e) and VRS % (f) at visit 1 versus visit 2 in the DI-ILD group (n=11).

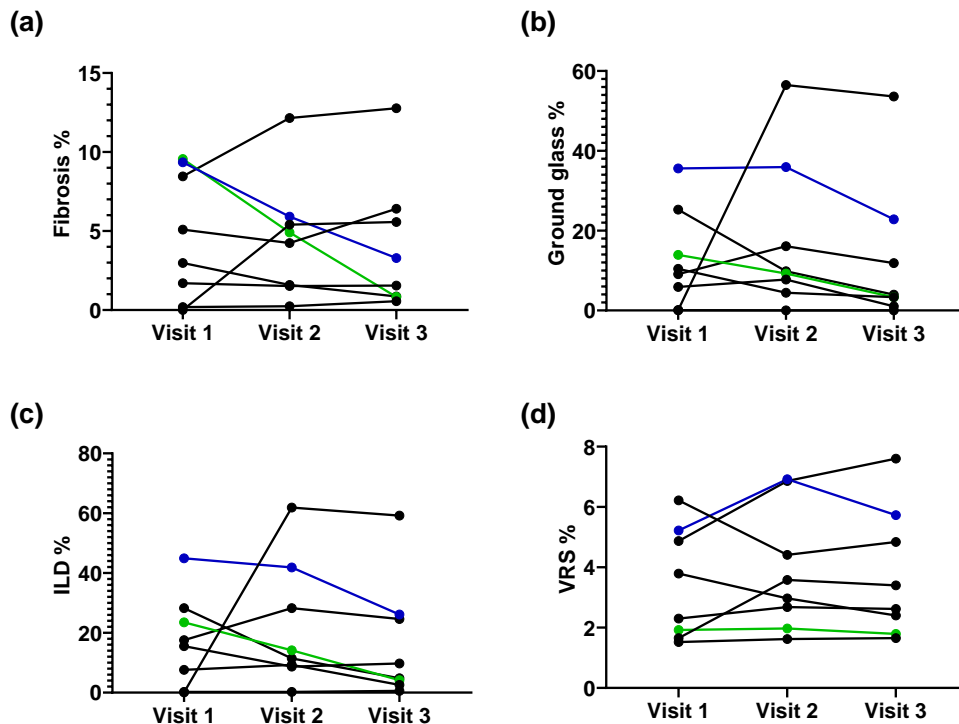


Figure 4.40. CALIPER fibrosis % (a), ground glass % (b), ILD % (c) and VRS % (d) at visits 1, 2 and 3 in the DI-ILD group (n=9).

4.10 Summary of the imaging outcomes from the TRISTAN-ILD study

The key imaging outcomes which demonstrated statistical significance were:

1. A difference in global ^{129}Xe ADC and Lm_D between the ILD subtypes, and between the fibrotic and inflammation groups, with higher values seen in IPF versus HP, and in the fibrotic versus inflammation groups.
2. A decrease in global ^{129}Xe RBC:TP and an increase in global CALIPER CT VRS % in the IPF group over six months, with no statistically significant PFT change over the same time period.
3. An increase in global ^{129}Xe ADC and Lm_D over six weeks in the DI-ILD group, with no statistically significant PFT change over the same time period.
4. A decrease in global MTT and increase in global PBF over six weeks in the HP group, with no statistically significant PFT change over the same time period.
5. A decrease in global CALIPER CT fibrosis %, ground glass %, ILD % and reticular % between visits 1 and 2 in the inflammation group, with no statistically significant PFT change over the same time period.

The change between visits 1 and 2 in some of the biomarkers differed between the DI-ILD, HP and IPF groups (Table 4.58). Statistical analysis was not performed due to the small sample sizes. The proportion of DI-ILD and HP subjects receiving prednisolone between visits 1 and 2 differed, with the majority of DI-ILD subjects being managed by withdrawal of the offending drug only.

	DI-ILD (n = 11)	HP (n = 9)	IPF (n = 11)	Inflammation group	
				DI-ILD (n = 6)	HP (n = 6)
Prednisolone treatment, n (%)	3 (27.3)	8 (88.9)	0	2 (33.3)	5 (83.3)
PFT					
FVC	↓	↑	↓	↓	↑
D _{LCO}	↑	↓	↓	↓	↓
MRI					
¹²⁹ Xe RBC:TP	↓	↑	↓	↓	↑
¹²⁹ Xe ADC / Lm _D	↑	↓	↓	↑	↓
MTT	↓	↓	↑	↑	↓
PBF	↑	↑	↓	↓	↑
PBV	↑	↑	↓	↓	↑
CALIPER CT					
Fibrosis %	↓	↓	↑	↓	↓
Ground glass %	↓	↓	↑	↓	↓
Honeycomb %	↑	↑	↑	↓	↑
ILD %	↓	↓	↑	↓	↓
Reticular %	↓	↓	↑	↓	↓
VRS %	↑	↓	↑	↑	↓
Visual CT score					
Fibrosis	↔	↔	↔	↑	↔
Ground glass	↔	↔	↔	↓	↓
Honeycomb	↔	↔	↑	↔	↔
ILD	↔	↔	↔	↓	↑
Reticular	↔	↔	↔	↑	↔

ADC: Apparent diffusion coefficient; CALIPER: Computer-Aided Lung Informatics for Pathology Evaluation and Rating; CT: Computed tomography; DI-ILD: Drug induced interstitial lung disease; D_{LCO}: Diffusing capacity of the lung for carbon monoxide; FVC: Forced vital capacity; HP: Hypersensitivity pneumonitis; ILD: Interstitial lung disease; IPF: Idiopathic pulmonary fibrosis; Lm_D: mean diffusive length scale; MTT: Mean transit time; PBF: Pulmonary blood flow; PBV: Pulmonary blood volume; RBC: Red blood cell; TP: Tissue plasma; VRS: Vessel related structures; ¹²⁹Xe: 129-xenon.

Table 4.58. Change between visits 1 and 2 in the various biomarkers in the DI-ILD, HP and IPF groups, as well as the DI-ILD and HP subjects in the inflammation group. The number and proportion of subjects in each group that were taking prednisolone between visits 1 and 2 is also displayed.

4.11 Correlations

Correlation analysis involving data from PFTs, global MRI measurements and global CT measurements were performed for each study visit. Data from each study visit for each type of measurement were also combined. The same approach was taken for the regional ¹²⁹Xe MRI and CT data to perform correlation analysis. In addition to this, correlation analysis of the longitudinal change in the various measurements was performed.

4.11.1 Strong correlations (r = 0.60 – 0.79)

¹²⁹ Xe DW-MRI measurement	Visual CT score	Visit(s)
ADC	Fibrosis	2; 1 & 2 (combined)
Lm _D	Fibrosis	2

ADC: Apparent diffusion coefficient; CT: Computed tomography; DW-MRI: Diffusion weighted magnetic resonance imaging; Lm_D: mean diffusive length scale; ¹²⁹Xe: 129-xenon.

Table 4.59. Strong correlations between global ¹²⁹Xe DW-MRI measurements and visual CT fibrosis score.

CALIPER CT measurement	PFT	Visit(s)
Fibrosis %	FEV ₁ & FVC	3
	FVC%; D _{LCO} ; D _{LCO} %	2 & 3
Reticular %	FEV ₁	3
	FVC; FVC%; D _{LCO} ; D _{LCO} %	2 & 3
Vessel related structures %	FVC%	2 & 3
	D _{LCO} & D _{LCO} %	2 & 3; 1 - 3 (combined)

CALIPER: Computer-Aided Lung Informatics for Pathology Evaluation and Rating; CT: Computed tomography; D_{LCO}: Diffusing capacity of the lung for carbon monoxide; FEV₁: Forced expiratory volume in one second; FVC: Forced vital capacity; ILD: Interstitial lung disease; PFT: Pulmonary function test.

Table 4.60. Strong correlations between global CALIPER CT measurements and PFT.

CALIPER CT measurement	Visual CT score(s)	Visit(s)
Honeycomb %	Fibrosis & ILD	3
	Honeycomb	2 & 3
Vessel related structures %	Fibrosis & ILD	3

CALIPER: Computer-Aided Lung Informatics for Pathology Evaluation and Rating; CT: Computed tomography.

Table 4.61. Strong correlations between global CALIPER CT measurements and visual CT scores.

¹²⁹ Xe DW-MRI measurement	Visual CT score(s)	Visit(s)
ADC	Fibrosis & reticular	2; 1 & 2 (combined)
	Honeycomb & ILD	2
Lm _D	Fibrosis	1; 2; 1 & 2 (combined)
	ILD & reticular	2

ADC: Apparent diffusion coefficient; CT: Computed tomography; DW-MRI: Diffusion weighted magnetic resonance imaging; Lm_D: mean diffusive length scale; ¹²⁹Xe: 129-xenon.

Table 4.62. Strong correlations between regional ¹²⁹Xe DW-MRI measurements and visual CT scores in the lower zone.

4.11.2 Moderate correlations (r = 0.40 – 0.59)

MRI measurements		Visit(s)
¹²⁹ Xe RBC:TP	Pulmonary blood volume	2; 1 & 2 (combined)
¹²⁹ Xe ADC	Ventilated volume %	1
¹²⁹ Xe Lm _D	Ventilated volume %	1

ADC: Apparent diffusion coefficient; MRI: Magnetic resonance imaging; Lm_D: mean diffusive length scale; RBC: Red blood cell; TP: Tissue plasma; ¹²⁹Xe: 129-xenon.

Table 4.63. Moderate correlations between MRI measurements.

¹²⁹ Xe MRI measurement	PFT	Visit(s)
RBC:TP	D _{LCO} & D _{LCO} %	1; 1 & 2 (combined)
ADC	D _{LCO} %	1
Lm _D	D _{LCO} %	1; 2; 1 & 2 (combined)

ADC: Apparent diffusion coefficient; D_{LCO}: Diffusing capacity of the lung for carbon monoxide; Lm_D: mean diffusive length scale; MRI: Magnetic resonance imaging; PFT: Pulmonary function test; RBC: Red blood cell; TP: Tissue plasma; ¹²⁹Xe: 129-xenon.

Table 4.64. Moderate correlations between global ¹²⁹Xe MRI and PFTs.

¹²⁹ Xe MRI measurement	Visual CT score(s)	Visit(s)
ADC	Fibrosis	1
	Honeycomb; ILD; reticular	1; 2; 1 & 2 (combined)
Lm _D	Fibrosis	1; 1 & 2 (combined)
	Honeycomb; ILD; reticular	1; 2; 1 & 2 (combined)

ADC: Apparent diffusion coefficient; CT: Computed tomography; ILD: Interstitial lung disease; Lm_D: mean diffusive length scale; MRI: Magnetic resonance imaging; ¹²⁹Xe: 129-xenon.

Table 4.65. Moderate correlations between global ¹²⁹Xe MRI and visual CT scores.

MRI measurement	CALIPER CT measurement	Visit
¹²⁹ Xe ADC & Lm _D	Honeycomb %	2
Pulmonary blood volume	Honeycomb %	1

ADC: Apparent diffusion coefficient; CALIPER: Computer-Aided Lung Informatics for Pathology Evaluation and Rating; CT: Computed tomography; Lm_D: mean diffusive length scale; MRI: Magnetic resonance imaging; ¹²⁹Xe: 129-xenon.

Table 4.66. Moderate correlations between global MRI and CALIPER honeycomb %.

CALIPER CT measurement	PFT	Visit(s)
Fibrosis %	FEV ₁ ; FVC	2; 1 - 3 (combined)
	FEV ₁ %	2; 3; 1 - 3 (combined)
	FVC%	1 - 3 (combined)
	D _{LCO} & D _{LCO} %	1; 1 - 3 (combined)
Ground glass %	FEV ₁ & FVC	2 & 3
Honeycomb %	D _{LCO}	1; 3; 1 - 3 (combined)
	D _{LCO} %	2; 3; 1 - 3 (combined)
ILD %	FEV ₁ ; FEV ₁ %; FVC; FVC%; D _{LCO}	2; 3; 1 - 3 (combined)
	D _{LCO} %	2; 1 - 3 (combined)
Reticular %	FEV ₁	2
	FEV ₁ %	2 & 3
	FVC & FVC%	1 - 3 (combined)
	D _{LCO} & D _{LCO} %	1; 1 - 3 (combined)
Vessel related structures %	FEV ₁	2 & 3
	FEV ₁ %	2; 1 - 3 (combined)
	FVC	2; 3; 1 - 3 (combined)
	FVC%	1; 1 - 3 (combined)
	D _{LCO} & D _{LCO} %	1

CALIPER: Computer-Aided Lung Informatics for Pathology Evaluation and Rating; CT: Computed tomography; D_{LCO}: Diffusing capacity of the lung for carbon monoxide; FEV₁: Forced expiratory volume in one second; FVC: Forced vital capacity; ILD: Interstitial lung disease; PFT: Pulmonary function test.

Table 4.67. Moderate correlations between global CALIPER CT and PFTs.

CALIPER CT measurement	Visual CT score(s)	Visit(s)
Fibrosis %	Fibrosis & honeycomb	2 & 3
	Reticular	3
Ground glass %	Ground glass	1
Honeycomb %	Fibrosis	2; 1 - 3 (combined)
	Honeycomb	1 - 3 (combined)
	ILD	1 & 2
	Reticular	3
ILD %	Ground glass	1
Reticular %	Fibrosis	3
Vessel related structures %	Fibrosis	2; 1 - 3 (combined)
	Honeycomb	2; 3; 1 - 3 (combined)
	ILD	1; 1 - 3 (combined)
	Reticular	3

CALIPER: Computer-Aided Lung Informatics for Pathology Evaluation and Rating; CT: Computed tomography; ILD: Interstitial lung disease.

Table 4.68. Moderate correlations between global CALIPER CT and visual CT scores.

Visual CT score	PFT	Visit(s)
Fibrosis	D _{LCO}	3
	D _{LCO} %	1 & 2
Honeycomb	D _{LCO}	1; 2; 3
	D _{LCO} %	1 & 2
ILD	D _{LCO}	1; 2; 3
	D _{LCO} %	2 & 3
Reticular	D _{LCO} %	3

CT: Computed tomography; D_{LCO}: Diffusing capacity of the lung for carbon monoxide; ILD: Interstitial lung disease; PFT: Pulmonary function test.

Table 4.69. Moderate correlations between global visual CT scores and PFTs.

DCE-MRI measurement	PFT
Mean transit time change	FEV ₁ change
Pulmonary blood flow change	D _{LCO} change

DCE-MRI: Dynamic contrast enhanced magnetic resonance imaging; D_{LCO}: Diffusing capacity of the lung for carbon monoxide; FEV₁: Forced expiratory volume in one second; PFT: Pulmonary function test.

Table 4.70. Moderate correlations between the change in global DCE-MRI measurements and the change in PFTs.

DCE-MRI measurement	Visual CT score(s)
Mean transit time change	Fibrosis change
Pulmonary blood flow change	Fibrosis & honeycomb change

CT: Computed tomography; DCE-MRI: Dynamic contrast enhanced magnetic resonance imaging.

Table 4.71. Moderate correlations between the change in global DCE-MRI measurements and the change in global visual CT scores.

CALIPER CT measurement	Visual CT score(s)
Fibrosis % change	Ground glass change
Ground glass % change	Ground glass change
ILD % change	Ground glass change
Reticular % change	Ground glass & ILD change

CALIPER: Computer-Aided Lung Informatics for Pathology Evaluation and Rating; CT: Computed tomography; ILD: Interstitial lung disease.

Table 4.72. Moderate correlations between the change in global CALIPER CT measurements and the change in global visual CT scores (visits 1-3).

Visual CT score	PFT
Fibrosis change	FEV ₁ & D _{LCO} change
ILD change	FVC change
Reticular change	FEV ₁ change

CT: Computed tomography; D_{LCO}: Diffusing capacity of the lung for carbon monoxide; FEV₁: Forced expiratory volume in one second; FVC: Forced vital capacity; ILD: Interstitial lung disease; PFT: Pulmonary function test.

Table 4.73. Moderate correlations between the change in global visual CT scores and the change in PFTs (visits 1-2).

Between visits 1 and 3, the change in CALIPER VRS % correlated moderately with the change in FEV₁% (r=-0.44; p=0.014) and FVC% (r=-0.41; p=0.024).

¹²⁹ Xe IDEAL spectroscopic imaging measurement	¹²⁹ Xe DW-MRI measurements	Zone(s)	Visit(s)
TP:Gas	ADC & Lm _D	Upper	1 & 2
RBC:Gas	ADC & Lm _D	Upper	1 & 2

ADC: Apparent diffusion coefficient; DW-MRI: Diffusion weighted magnetic resonance imaging; IDEAL: Iterative decomposition of water and fat with echo asymmetry and least-squares estimation Lm_D: mean diffusive length scale; RBC: Red blood cell; TP: Tissue plasma; ¹²⁹Xe: 129-xenon.

Table 4.74. Moderate correlations between regional ¹²⁹Xe IDEAL spectroscopic imaging measurements and ¹²⁹Xe DW-MRI measurements.

¹²⁹ Xe IDEAL spectroscopic imaging measurement	CALIPER CT measurement(s)	Zone(s)	Visit(s)
RBC:TP	Ground glass % & ILD %	Lower	1 & 2
RBC:Gas	Honeycomb %	Lower & peripheral	1

CALIPER: Computer-Aided Lung Informatics for Pathology Evaluation and Rating; CT: Computed tomography; IDEAL: Iterative decomposition of water and fat with echo asymmetry and least-squares estimation; ILD: Interstitial lung disease; RBC: Red blood cell; TP: Tissue plasma; ¹²⁹Xe: 129-xenon.

Table 4.75. Moderate correlations between regional ¹²⁹Xe IDEAL spectroscopic imaging measurements and CALIPER CT measurements.

¹²⁹ Xe IDEAL spectroscopic imaging measurement	Visual CT score(s)	Zone(s)	Visit(s)
RBC:TP	Fibrosis & reticular	Lower	1; 1 & 2 (combined)
	ILD	Lower	1
RBC:Gas	Fibrosis & reticular	Middle & lower	1 & 2 (combined)
	ILD	Lower	1 & 2 (combined)

CT: Computed tomography; IDEAL: Iterative decomposition of water and fat with echo asymmetry and least-squares estimation; ILD: Interstitial lung disease; RBC: Red blood cell; TP: Tissue plasma; ¹²⁹Xe: 129-xenon.

Table 4.76. Moderate correlations between regional ¹²⁹Xe IDEAL spectroscopic imaging measurements and visual CT scores.

¹²⁹ Xe DW-MRI measurement	CALIPER CT measurement(s)	Zone(s)	Visit(s)
ADC	Fibrosis %	Lower	1; 2; 1 & 2 (combined)
	Honeycomb %	Lower; central; peripheral	1; 2; 1 & 2 (combined)
		Middle	1; 1 & 2 (combined)
	Reticular %	Lower	1; 2; 1 & 2 (combined)
		Peripheral	1
VRS %	Lower & peripheral	1; 2; 1 & 2 (combined)	
Lm _D	Fibrosis % & reticular %	Lower	1; 2; 1 & 2 (combined)
		Peripheral	1
	Honeycomb %	Lower; central; peripheral	1; 2; 1 & 2 (combined)
		Middle	1; 1 & 2 (combined)
	VRS %	Lower & peripheral	1; 2; 1 & 2 (combined)

ADC: Apparent diffusion coefficient; CALIPER: Computer-Aided Lung Informatics for Pathology Evaluation and Rating; CT: Computed tomography; DW-MRI: Diffusion weighted magnetic resonance imaging; Lm_D: mean diffusive length scale; VRS: Vessel related structures; ¹²⁹Xe: 129-xenon.

Table 4.77. Moderate correlations between regional ¹²⁹Xe DW-MRI measurements and CALIPER CT measurements.

¹²⁹ Xe DW-MRI measurement	Visual CT score(s)	Zone(s)	Visit(s)
ADC	Fibrosis; ILD; reticular	Middle	1; 2; 1 & 2 (combined)
	Honeycomb	Middle	2; 1 & 2 (combined)
Lm _D	Fibrosis	Middle	1; 2; 1 & 2 (combined)
		Middle	2
	Honeycomb	Lower	1; 2; 1 & 2 (combined)
		Middle	1; 2; 1 & 2 (combined)
	ILD & reticular	Lower	1; 1 & 2 (combined)

ADC: Apparent diffusion coefficient; CT: Computed tomography; DW-MRI: Diffusion weighted magnetic resonance imaging; ILD: Interstitial lung disease; Lm_D: mean diffusive length scale; ¹²⁹Xe: 129-xenon.

Table 4.78. Moderate correlations between regional ¹²⁹Xe DW-MRI measurements and visual CT scores.

4.12 Variables that predict disease progression

Univariate logistic regression analysis was performed to identify any variables that were able to predict disease progression. The cohort included a total of 46 subjects in which data was available to determine whether disease progression had occurred between visit 1 (baseline) and visit 3 (6 months or 12 months depending on ILD subtype).

Disease progression was defined as death, lung transplantation, $\geq 10\%$ absolute reduction in FVC% and/or $\geq 15\%$ absolute reduction in DLCO%. The following variables were investigated:

- Age
- Gender
- Ever smoker
- BMI
- ILD subtype and fibrotic group
- Immunosuppressant treatment during study
- Antifibrotic therapy during study
- Visit 1 oxygen saturations
- Oxygen therapy during study
- Hospitalisation during study
- Visit 1 PFTs (including FEV₁, FEV₁%, FVC, FVC%, DLCO and DLCO%) and visit 1-2 change
- Visit 1 ¹²⁹Xe RBC:TP (global) and visit 1-2 change
- Visit 1 ¹²⁹Xe RBC:TP, TP:Gas and RBC:Gas (regional), and visit 1-2 change
- Visit 1 ¹²⁹Xe ADC and Lm_D (global and regional), and visit 1-2 change
- Visit 1 ¹²⁹Xe VV% and CV%, and visit 1-2 change
- Visit 1 MTT, PBF and PBV, and visit 1-2 change
- Visit 1 CALIPER CT measurements (global and regional) and visit 1-2 change
- Visit 1 visual CT scores (global and regional) and visit 1-2 change

Variable	Odds ratio	95% confidence interval	P value
Age	1.09	1.02 – 1.18	0.023
FVC change	0.0045	3.79e-005 – 0.18	0.010
FVC% absolute change	0.84	0.72 – 0.95	0.012
FVC% relative change	0.88	0.77 – 0.97	0.018
DLCO change	0.064	0.0066 – 0.30	0.003
DLCO% absolute change	0.82	0.70 – 0.91	0.003
DLCO% relative change	0.91	0.85 – 0.96	0.003

DLCO: Diffusing capacity of the lung for carbon monoxide; FVC: Forced vital capacity;

Table 4.79. Variables with a statistically significant odds ratio for predicting disease progression using univariate logistic regression analysis.

Variable	Odds ratio	95% confidence interval	P value
IPF	2.95	0.86 – 10.7	0.090
Antifibrotic therapy	5.63	1.05 – 43.3	0.057
FEV ₁ % absolute change	0.90	0.79 – 0.99	0.053
FEV ₁ % relative change	0.91	0.81 – 0.99	0.065
Visit 1 ¹²⁹ Xe RBC:TP	1.71e-06	1.64e-13 – 1.45	0.075
Visit 1 CALIPER VRS %	1.43	0.96 – 2.22	0.088
Visit 1 CALIPER VRS % upper zone	1.56	0.95 – 2.72	0.091
Visit 1 CALIPER VRS % middle zone	1.37	0.97 – 2.03	0.086
Visit 1 CALIPER VRS % peripheral zone	1.44	0.97 – 2.25	0.083

CALIPER: Computer-Aided Lung Informatics for Pathology Evaluation and Rating; FEV₁: Forced expiratory volume in one second; IPF: Idiopathic pulmonary fibrosis; RBC: Red blood cell; TP: Tissue plasma; VRS: Vessel related structures; ¹²⁹Xe: 129-xenon.

Table 4.80. Variables that had odds ratios with p values 0.05 – 0.10 for predicting disease progression using univariate logistic regression analysis.

When age was added to the logistic regression model, all the variables in Table 4.79 had a statistically significant odds ratio for predicting disease progression (Table 4.81).

Variable	Odds ratio	95% confidence interval	P value
FVC change	1.91e-05	2.23e-10 – 0.020	0.015
FVC% absolute change	0.73	0.51 – 0.92	0.034
FVC% relative change	0.75	0.54 – 0.92	0.030
D _{LCO} change	0.054	0.002 – 0.33	0.014
D _{LCO} % absolute change	0.82	0.66 – 0.93	0.015
D _{LCO} % relative change	0.92	0.84 – 0.98	0.017

D_{LCO}: Diffusing capacity of the lung for carbon monoxide; FVC: Forced vital capacity.

Table 4.81. Variables for predicting disease progression with age added to the logistic regression model.

4.13 Summary

The results reported in this chapter represent the first known longitudinal data combining hyperpolarised ¹²⁹Xe MRI and DCE-MRI with QCT alongside PFTs in various ILD subtypes. Novel findings include significant differences in ¹²⁹Xe DW-MRI measurements between HP and IPF subjects, and significant changes in pulmonary perfusion over short time periods were found using DCE-MRI in subjects with HP.

Chapter 5: The Assessment of Interstitial Lung Disease Using Imaging Biomarkers – IPF Study Results

5.1 Recruitment and demographic data

51 patients with IPF (diagnosed within 12 months) were recruited from ILD clinics at Northern General Hospital, Sheffield, between February 2016 and November 2019. 49 of them completed at least one study visit. 22 subjects were recruited by Dr Weatherley, as part of his PhD, between February 2016 and February 2018. The study visit time periods for these subjects were baseline, 6 months and 12 months. The remaining 29 subjects were recruited by myself, between November 2018 and November 2019. The study visit time periods for these subjects were baseline, 3 months, 6 months and 12 months with the 3-month visit added to assess rate of progression over a shorter time period.

Subjects 19-49 refers to the 31 subjects that completed at least one study visit and were not included in Dr Weatherley's thesis. I performed the MRI analysis for all 31 subjects. Subjects 1-18 refers to the 18 subjects recruited by Dr Weatherley and were included in his thesis. The total study cohort refers to the 49 subjects (subjects 1-49) that completed at least one study visit between February 2016 and November 2019.

The key MRI findings in IPF patients previously published from this study include:

1. A statistically significant median change over 12 months in RBC:TP ($p=0.001$) and FVC ($p=0.048$) but not D_{LCO} (-0.5% ; $p=0.881$), as shown in Figure 5.1 (232). There was a statistically significant correlation between baseline RBC:TP and D_{LCO} ($r=0.68$), but not FVC ($r=0.34$).
2. ^3He ADC and L_{mD} correlate with D_{LCO} , KCO and regional fibrosis on CT (240). There was no significant longitudinal change in ADC, FVC or D_{LCO} , although L_{mD} increased significantly over 12-months ($p=0.001$).
3. A statistically significant increase in mean FWHM ($p=0.040$) over a 6-month period, with a decrease in FVC ($p=0.040$) and KCO ($p=0.014$), but no significant change in D_{LCO} ($p=0.090$) (211).

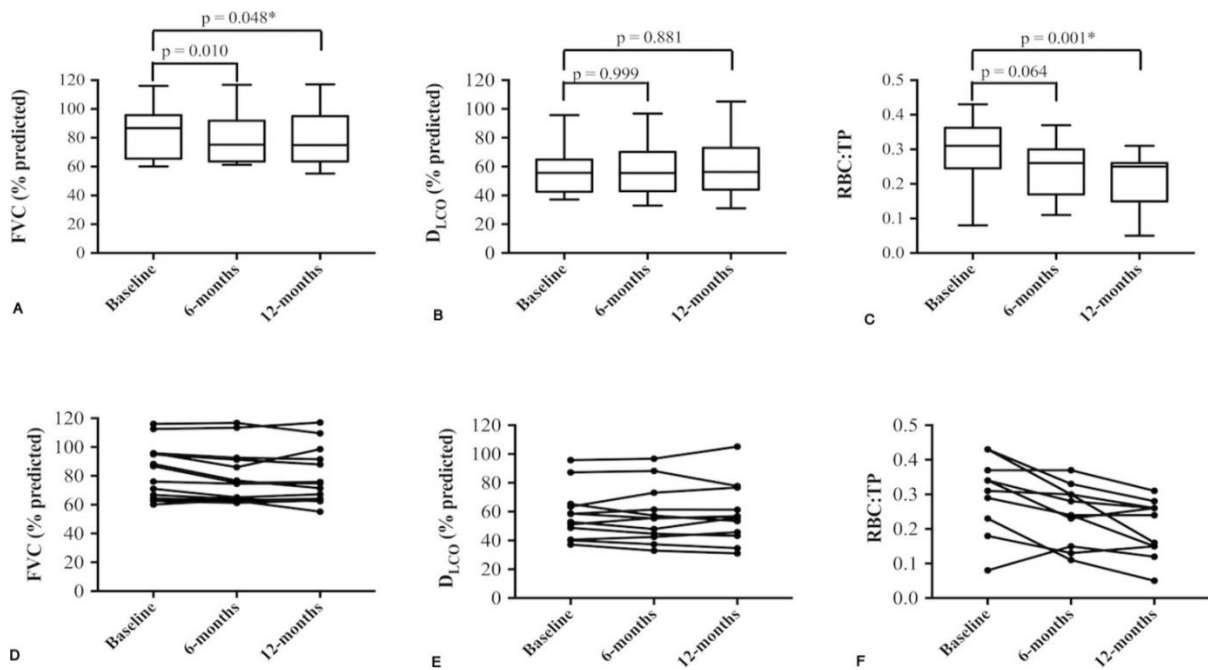


Figure 5.1. Longitudinal change in FVC, DLCO and RBC:TP in IPF patients (A–C). Individual patients’ measurements of FVC, DLCO and RBC:TP at baseline, 6 and 12 months are plotted in (D), (E) and (F), respectively (232).

5.1.1 Study visits

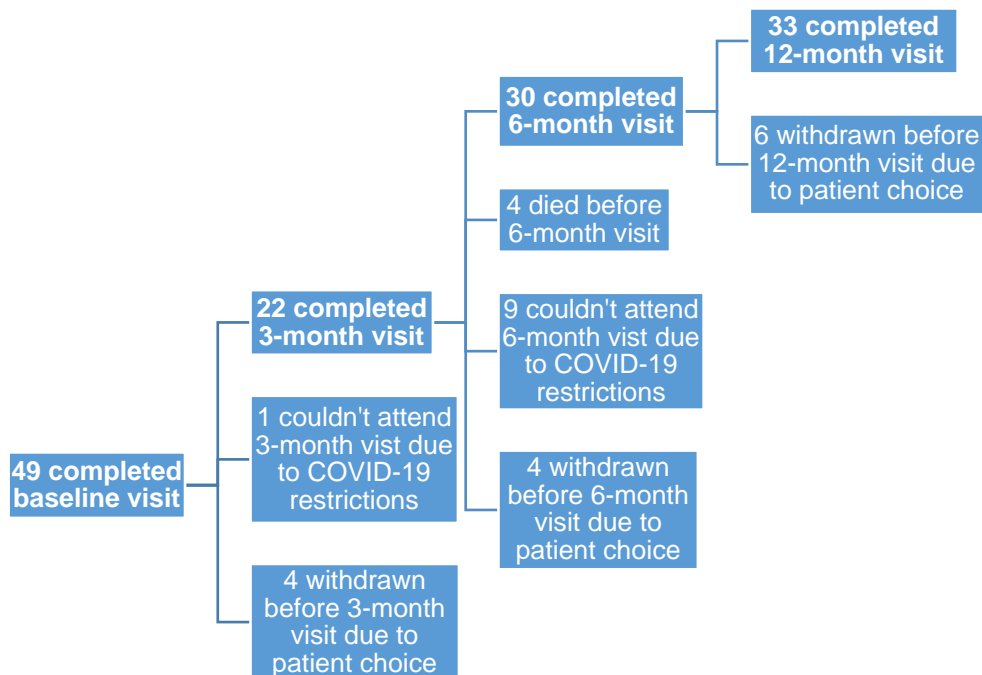


Figure 5.2. Summary of subject numbers at each study visit and reasons for not completing study visits for the total study cohort (n=49).

5.1.2 Days between baseline and follow-up study visits

Due to COVID-19 restrictions, seven of the 12-month study visits were delayed for 2 – 5 months, and several of the earlier study visits were missed (Figure 5.2). Once the impact of COVID-19 on the study was realised, the study protocol was amended and subsequently approved to allow the 12-month study visit to take place up to 18 months post baseline visit.

	0 - 3 months (n = 22)	0 - 6 months (n = 30)	0 - 12 months (n = 33)
Mean (days)	97	189	394
Standard deviation (days)	11	18	57
Range (days)	78 – 124	147 – 229	304 – 535

Table 5.1. Number of days between the baseline and follow-up study visits.

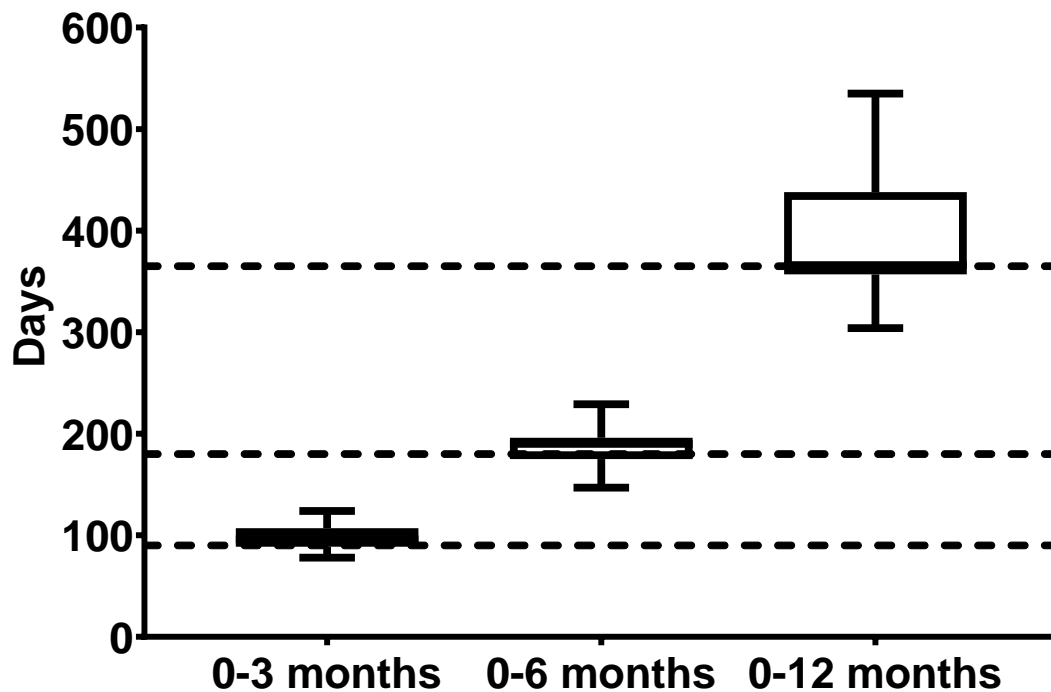


Figure 5.3. Number of days between the baseline and follow-up study visits. The dotted lines represent the ideal number of days between the baseline and follow-up study visits for each time point.

5.1.3 Days between diagnostic CT scan and first study visit

The CT scan which was used in the ILD MDT meeting for diagnostic purposes was used as the baseline CT scan in the study. Therefore, a baseline HRCT scan was not acquired routinely for research purposes unless the diagnostic CT scan was not a volumetric inspiratory non-contrast HRCT scan. As a result, there was a period of up to 12 months between the baseline HRCT scan and the first study visit.

13 out of 49 baseline CT scans failed the protocol requirements and were therefore repeated for research purposes at the first study visit. The median (IQR) time between the baseline HRCT and the first study visit was 101 days (0 – 195).

5.1.4 Subject demographics

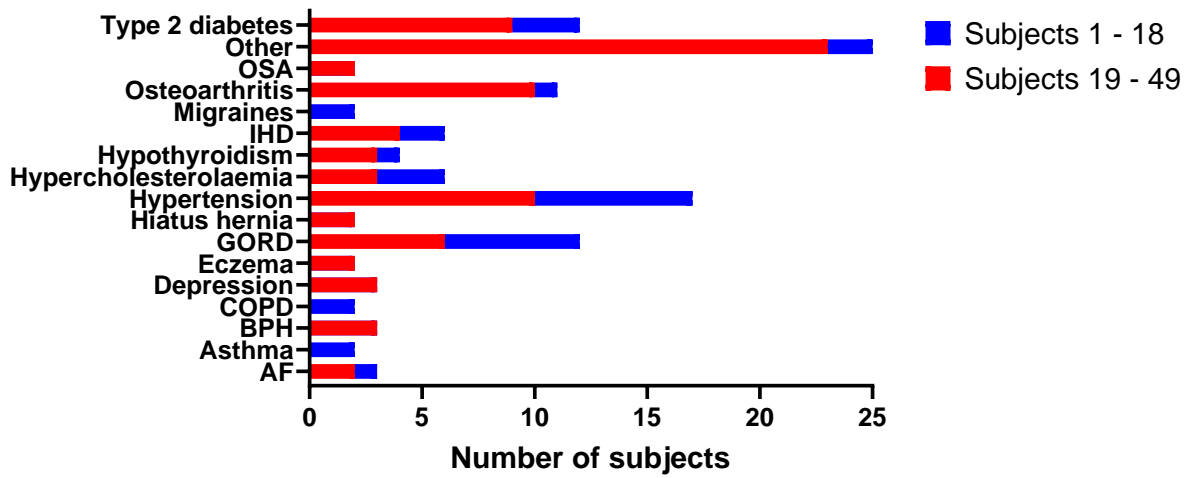
Baseline characteristics are presented in Table 5.2. Of the 28 ever smokers in the total cohort, only one was a current smoker. The subjects in the IPF study were of a similar age and BMI when compared to the incident IPF subgroup in the INSIGHTS-IPF registry (359) which reported the following data: mean age 71.0, male gender 86.6%, ever smoker 67.8%, mean BMI 28.2.

Subjects	Age (years), median (IQR)	Male gender, n (%)	Ever smoker, n (%)	Body mass index, mean (SD)
1 – 49	72.0 (67.5 – 75.8)	40 (81.6)	28 (57.1)	28.5 ± 4.38
19 – 49	73.3 (66.4 – 76.7)	24 (77.4)	16 (51.6)	28.0 ± 4.22

IQR: interquartile range; SD: standard deviation

Table 5.2. Demographic data for the total study cohort (n=49) and subjects 19-49 (n=31).

5.1.5 Co-morbidities



AF: Atrial fibrillation; BPH: Benign prostatic hypertrophy; COPD: Chronic obstructive pulmonary disease; GORD: Gastroesophageal reflux disease; IHD: ischaemic heart disease; OSA: Obstructive sleep apnoea.

Figure 5.4. Co-morbidities in the total cohort (n=49). Other was defined as any co-morbidity that occurred in only one subject out of the total cohort.

5.2 Pulmonary function tests

5.2.1 Baseline visit

	Subjects 1 – 49	Subjects 19 – 49
FEV₁ (L)	2.39 ± 0.51	2.44 ± 0.53
FEV₁ (% predicted)	85.1 ± 15.1	88.6 ± 15.1
FVC (L)	3.21 ± 0.79	3.28 ± 0.76
FVC (% predicted)	86.7 ± 17.1	90.5 ± 16.1
FEV₁ / FVC (%)	75.2 ± 7.13	75.0 ± 6.33
DL_{CO} (mmol. min⁻¹.kPa⁻¹)	4.83 ± 1.74	5.36 ± 1.60
DL_{CO} (% predicted)	61.9 ± 20.0	69.2 ± 16.3
K_{CO} (mmol.min⁻¹.kPa⁻¹L⁻¹)	1.08 ± 0.28	1.16 ± 0.24
K_{CO} (% predicted)	78.8 ± 19.9	84.8 ± 17.8

DL_{CO}: Diffusing capacity of the lung for carbon monoxide; FEV₁: Forced expiratory volume in one second; FVC: Forced vital capacity; K_{CO}: Carbon monoxide transfer coefficient.

Table 5.3. PFT results at the baseline visit for the total study cohort (n=49) and subjects 19-49 (n=31). Results are presented as mean ± standard deviation.

The subjects in the IPF study had higher PFT values when compared to the incident IPF subgroup in the INSIGHTS-IPF registry (359) which had the following results (mean): FEV₁ 76.9%, FVC 73.7%, DL_{CO} 37.7%.

5.2.2 3-month visit

	Mean	Standard deviation
FVC (L)	3.30	0.81
FVC change (L)	-0.07	0.16
FVC change (%)	-1.83	5.27
FVC (% predicted)	90.4	16.5
FVC% absolute change (%)	-1.59	4.17
FVC% relative change (%)	-1.58	5.20

FVC: Forced vital capacity.

Table 5.4. FVC and FVC% results at the **3-month visit**, and the longitudinal change in FVC and FVC% between the baseline and 3-month visits (n=22).

There was a statistically significant decrease in FVC between the baseline visit and the 3-month visit (mean (L): 3.37 ± 0.86 vs 3.30 ± 0.81; p=0.040) (Figure 5.5).

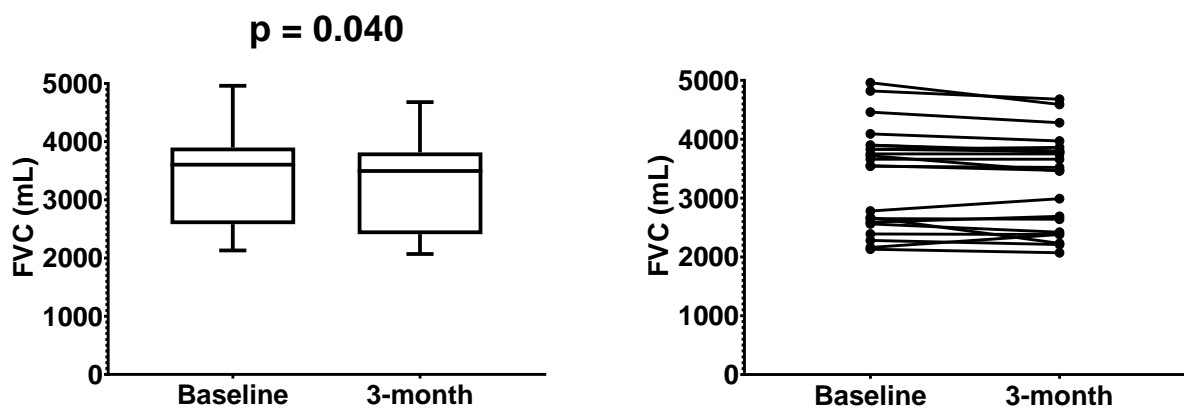


Figure 5.5. FVC at baseline visit versus 3-month visit (n=22).

	Mean	Standard deviation
DL_{CO} (mmol.min⁻¹.kPa⁻¹)	5.58	1.63
DL_{CO} change (mmol.min⁻¹.kPa⁻¹)	-0.006	0.35
DL_{CO} change (%)	0.34	5.91
DL_{CO} (% predicted)	71.3	16.4
DL_{CO}% absolute change (%)	0.17	4.56
DL_{CO}% relative change (%)	0.37	5.85

DL_{CO}: Diffusing capacity of the lung for carbon monoxide.

Table 5.5. DL_{CO} and DL_{CO}% results at the **3-month visit**, and the longitudinal change in DL_{CO} and DL_{CO}% between the baseline and 3-month visits (n=22).

	Mean	Standard deviation
K_{CO} (mmol.min⁻¹.kPa⁻¹L⁻¹)	1.19	0.24
K_{CO} change (mmol.min⁻¹.kPa⁻¹L⁻¹)	0.003	0.06
K_{CO} change (%)	0.37	4.99
K_{CO} (% predicted)	86.6	17.6
K_{CO}% absolute change (%)	0.22	4.68
K_{CO}% relative change (%)	0.46	5.07

K_{CO}: Carbon monoxide transfer coefficient.

Table 5.6. K_{CO} and K_{CO}% results at the **3-month visit**, and the longitudinal change in K_{CO} and K_{CO}% between the baseline and 3-month visits (n=22).

5.2.3 6-month visit

In the total cohort (n=30), between the baseline and 6-month visits there was a statistically significant decrease in FVC (mean (L): 3.41 ± 0.87 vs 3.32 ± 0.90; p=0.010), FVC% (mean (%): 89.0 ± 17.7 vs 86.8 ± 18.5; p=0.018), DL_{CO} (mean (mmol.min⁻¹.kPa⁻¹): 5.13 ± 1.70 vs 4.95 ± 1.68; p=0.016), K_{CO} (mean (mmol.min⁻¹.kPa⁻¹L⁻¹): 1.12 ± 0.24 vs 1.08 ± 0.23; p<0.001) and K_{CO}% (mean (%): 80.9 ± 17.7 vs 78.3 ± 16.9; p=0.001) (Figures 5.6 – 5.8).

In subjects 19-49 (n=16), over the six-month period there was a statistically significant decrease in DL_{CO} (mean (mmol.min⁻¹.kPa⁻¹): 5.77 ± 1.65 vs 5.51 ± 1.60; p=0.024), K_{CO} (mean (mmol.min⁻¹.kPa⁻¹L⁻¹): 1.18 ± 0.26 vs 1.13 ± 0.25; p=0.004) and K_{CO}% (mean (%): 85.5 ± 18.9 vs 82.1 ± 18.1; p=0.006).

	Subjects 1 – 49	Subjects 19 – 49
FVC (L)	3.32 ± 0.90	3.58 ± 0.78
FVC change (L)	-0.09 ± 0.18	-0.03 ± 0.15
FVC change (%)	-2.87 ± 5.50	-0.81 ± 4.01
FVC (% predicted)	86.8 ± 18.5	93.6 ± 16.1
FVC% absolute change (%)	-2.11 ± 4.61	-0.40 ± 3.93
FVC% relative change (%)	-2.47 ± 5.18	-0.38 ± 3.86

FVC: Forced vital capacity.

Table 5.7. FVC and FVC% results at the **6-month visit**, and the longitudinal change in FVC and FVC% between the baseline and 6-month visits in the total study cohort (n=30) and subjects 19-49 (n=16). Results are presented as mean ± standard deviation.

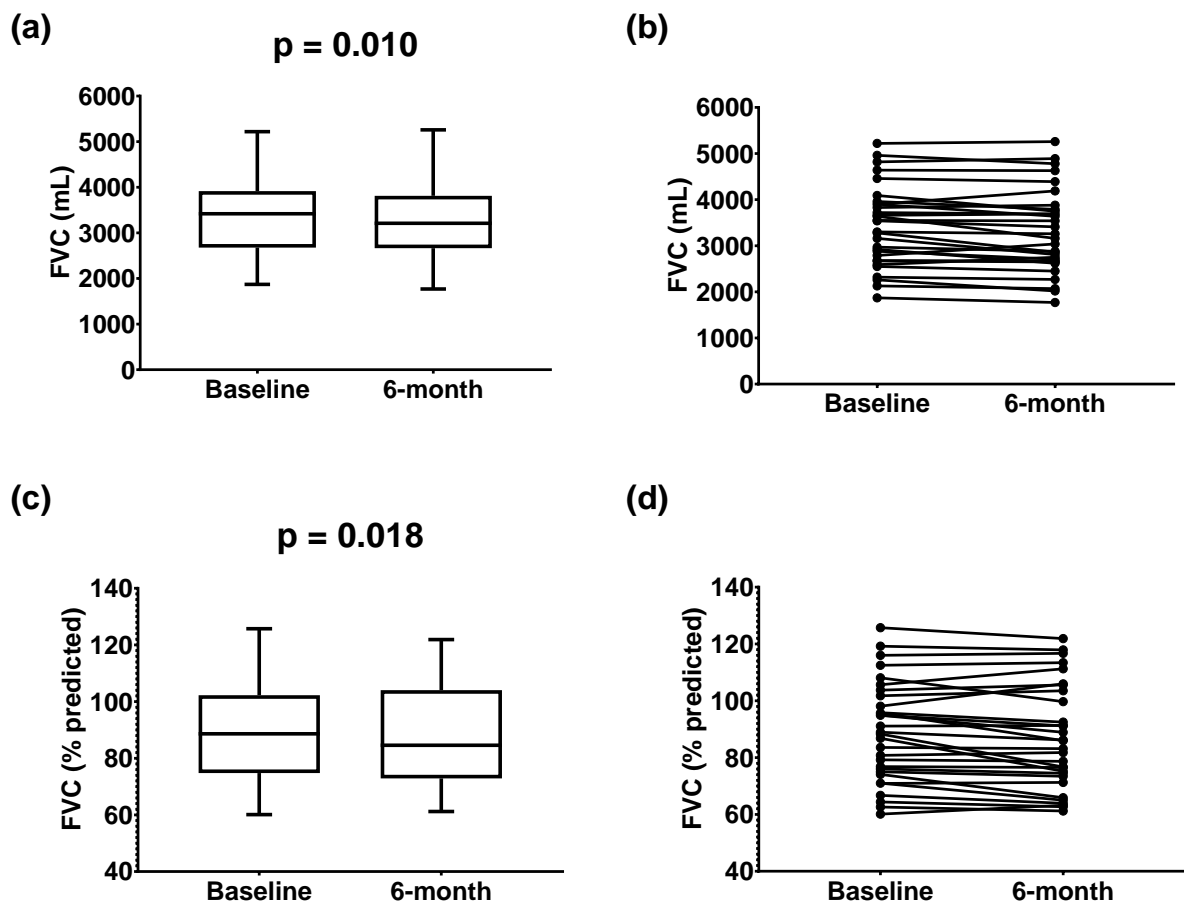


Figure 5.6. FVC (a-b) and FVC% (c-d) at baseline visit versus 6-month visit in the total study cohort (n=30). Statistical test: paired *t* test.

	Subjects 1 – 49	Subjects 19 – 49
D_{LCO} (mmol.min⁻¹.kPa⁻¹)	4.95 ± 1.68	5.51 ± 1.60
D_{LCO} change (mmol.min⁻¹.kPa⁻¹)	-0.18 ± 0.38	-0.25 ± 0.40
D_{LCO} change (%)	-3.33 ± 7.37	-4.02 ± 6.41
D_{LCO} (% predicted)	62.3 ± 19.0	68.8 ± 16.4
D_{LCO}% absolute change (%)	-1.49 ± 5.45	-2.05 ± 6.12
D_{LCO}% relative change (%)	-2.35 ± 9.12	-2.46 ± 9.89

D_{LCO}: Diffusing capacity of the lung for carbon monoxide.

Table 5.8. D_{LCO} and D_{LCO}% results at the **6-month visit**, and the longitudinal change in D_{LCO} and D_{LCO}% between the baseline and 6-month visits in the total study cohort (n=30) and subjects 19-49 (n=16). Results are presented as mean ± standard deviation.

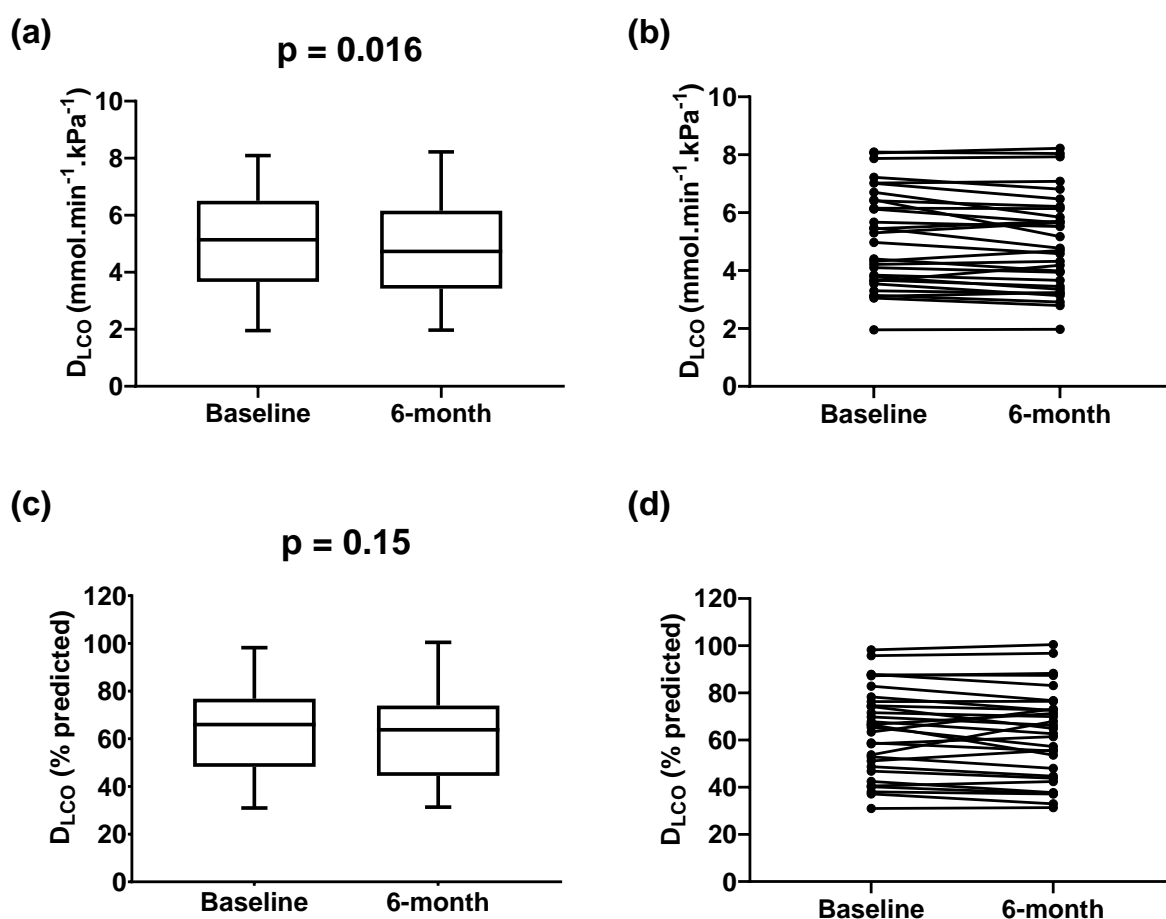


Figure 5.7. D_{LCO} (a-b) and D_{LCO}% (c-d) at baseline visit versus 6-month visit in the total study cohort (n=30). Statistical test: paired *t* test.

	Subjects 1 – 49	Subjects 19 – 49
K_{CO} (mmol.min⁻¹.kPa⁻¹L⁻¹)	1.08 ± 0.23	1.13 ± 0.25
K_{CO} change (mmol.min⁻¹.kPa⁻¹L⁻¹)	-0.04 ± 0.05	-0.05 ± 0.06
K_{CO} change (%)	-3.29 ± 4.68	-4.13 ± 4.57
K_{CO} (% predicted)	78.3 ± 16.9	82.1 ± 18.1
K_{CO}% absolute change (%)	-2.62 ± 3.99	-3.42 ± 4.30
K_{CO}% relative change (%)	-3.08 ± 4.68	-3.91 ± 4.58

K_{CO}: Carbon monoxide transfer coefficient.

Table 5.9. K_{CO} and K_{CO}% results at the **6-month visit**, and the longitudinal change in K_{CO} and K_{CO}% between the baseline and 6-month visits in the total study cohort (n=30) and subjects 19-49 (n=16). Results are presented as mean ± standard deviation.

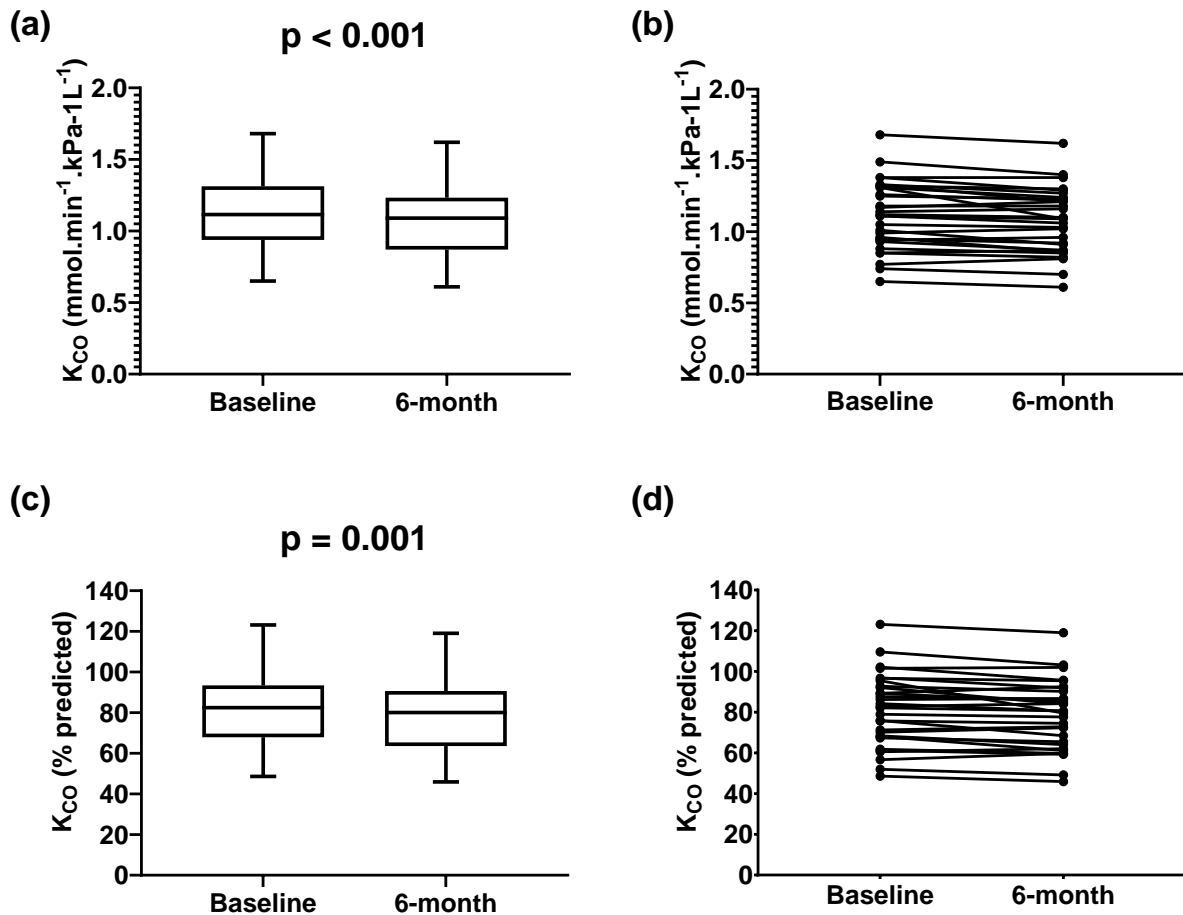


Figure 5.8. K_{CO} (a-b) and K_{CO}% (c-d) at baseline visit versus 6-month visit in the total study cohort (n=30). Statistical test: paired *t* test.

5.2.4 12-month visit

Between the baseline visit and the 12-month visit, there was no statistically significant PFT changes for both the total study cohort (n=33) and subjects 19-49 (n=20).

	Subjects 1 – 49	Subjects 19 – 49
FVC (L)	3.20 ± 0.84	3.36 ± 0.74
FVC change (L)	-0.12 ± 0.39	-0.06 ± 0.45
FVC change (%)	-2.98 ± 9.86	-0.65 ± 10.7
FVC (% predicted)	87.7 ± 18.5	92.8 ± 16.3
FVC% absolute change (%)	-1.89 ± 10.3	-0.49 ± 12.2
FVC% relative change (%)	-1.73 ± 10.0	-0.28 ± 11.0

FVC: Forced vital capacity.

Table 5.10. FVC and FVC% results at the **12-month visit**, and the longitudinal change in FVC and FVC% between the baseline and 12-month visits in the total study cohort (n=33) and subjects 19-49 (n=20). Results are presented as mean ± standard deviation.

	Subjects 1 – 49	Subjects 19 – 49
DL_{CO} (mmol.min⁻¹.kPa⁻¹)	5.07 ± 1.88	5.40 ± 1.93
DL_{CO} change (mmol.min⁻¹.kPa⁻¹)	-0.15 ± 0.66	-0.21 ± 0.70
DL_{CO} change (%)	-3.50 ± 14.9	-4.84 ± 16.1
DL_{CO} (% predicted)	65.3 ± 21.2	69.6 ± 20.9
DL_{CO}% absolute change (%)	-1.30 ± 8.64	-2.03 ± 9.21
DL_{CO}% relative change (%)	-2.85 ± 15.1	-4.13 ± 16.3

DL_{CO}: Diffusing capacity of the lung for carbon monoxide.

Table 5.11. DL_{CO} and DL_{CO}% results at the **12-month visit**, and the longitudinal change in DL_{CO} and DL_{CO}% between the baseline and 12-month visits in the total study cohort (n=33) and subjects 19-49 (n=20). Results are presented as mean ± standard deviation.

	Subjects 1 – 49	Subjects 19 – 49
K_{CO} (mmol.min⁻¹.kPa⁻¹L⁻¹)	1.12 ± 0.28	1.17 ± 0.30
K_{CO} change (mmol.min⁻¹.kPa⁻¹L⁻¹)	-0.02 ± 0.10	-0.03 ± 0.10
K_{CO} change (%)	-2.51 ± 10.4	-3.30 ± 10.5
K_{CO} (% predicted)	81.3 ± 20.3	84.8 ± 21.9
K_{CO}% absolute change (%)	-1.48 ± 7.52	-1.81 ± 7.10
K_{CO}% relative change (%)	-2.23 ± 10.4	-3.07 ± 10.5

K_{CO}: Carbon monoxide transfer coefficient.

Table 5.12. K_{CO} and K_{CO}% results at the **12-month visit**, and the longitudinal change in K_{CO} and K_{CO}% between the baseline and 12-month visits for the total study cohort (n=33) and subjects 19-49 (n=20). Results are presented as mean ± standard deviation.

5.2.5 Baseline, 3-month, 6-month and 12-month visits

PFT data was available at each of the baseline, 3-month, 6-month and 12-month visits in 12 subjects. There was a statistically significant decrease between the baseline and 3-month visits in FVC only (p=0.042) (Figure 5.9). There was a statistically significant decrease between the baseline visit and 6-month visits in K_{CO} (p=0.007) and K_{CO}% (p=0.009) (Figure 5.11). There was also a statistically significant decrease between the 3-month and 6-month visits in K_{CO} (p=0.014) and K_{CO}% (p=0.015).

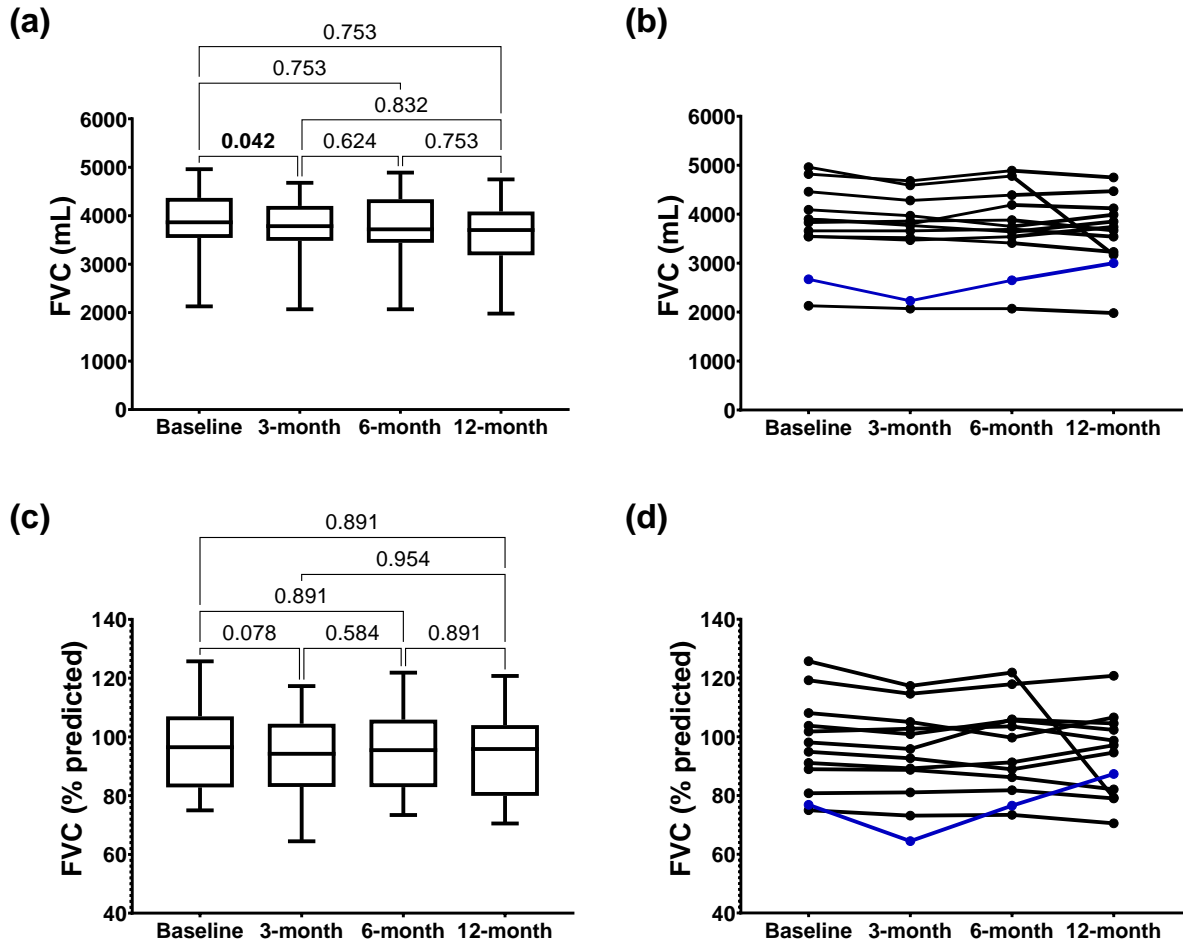


Figure 5.9. FVC (a-b) and FVC % predicted (c-d) at baseline, 3-month, 6-month and 12-month visits (n=12). The subject highlighted in blue commenced nintedanib approximately three months after the baseline study visit. Statistical test: one-way ANOVA.

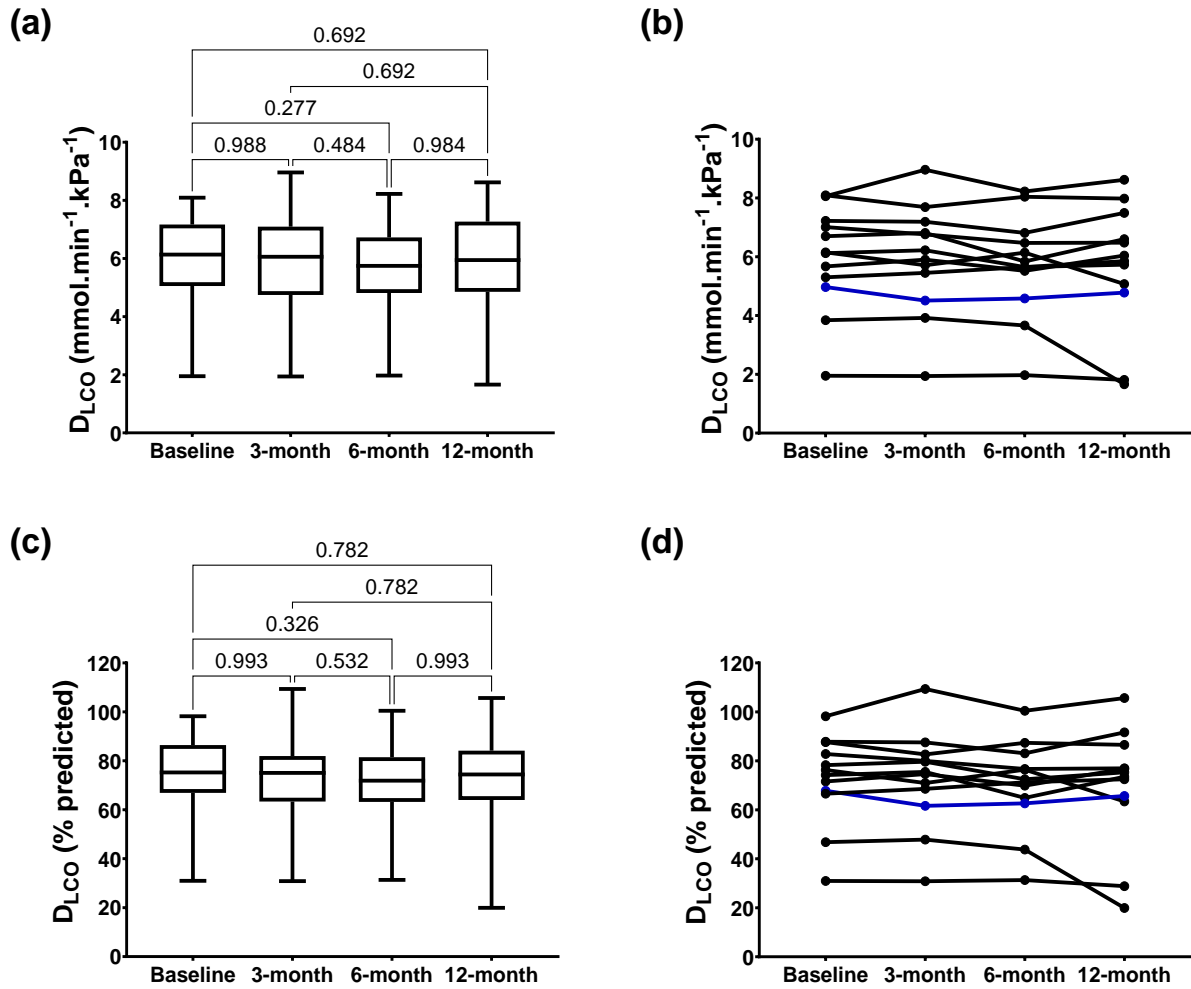


Figure 5.10. DLCO (a-b) and DLCO % predicted (c-d) at baseline, 3-month, 6-month and 12-month visits (n=12). The subject highlighted in blue commenced nintedanib approximately three months after the baseline study visit. Statistical test: one-way ANOVA.

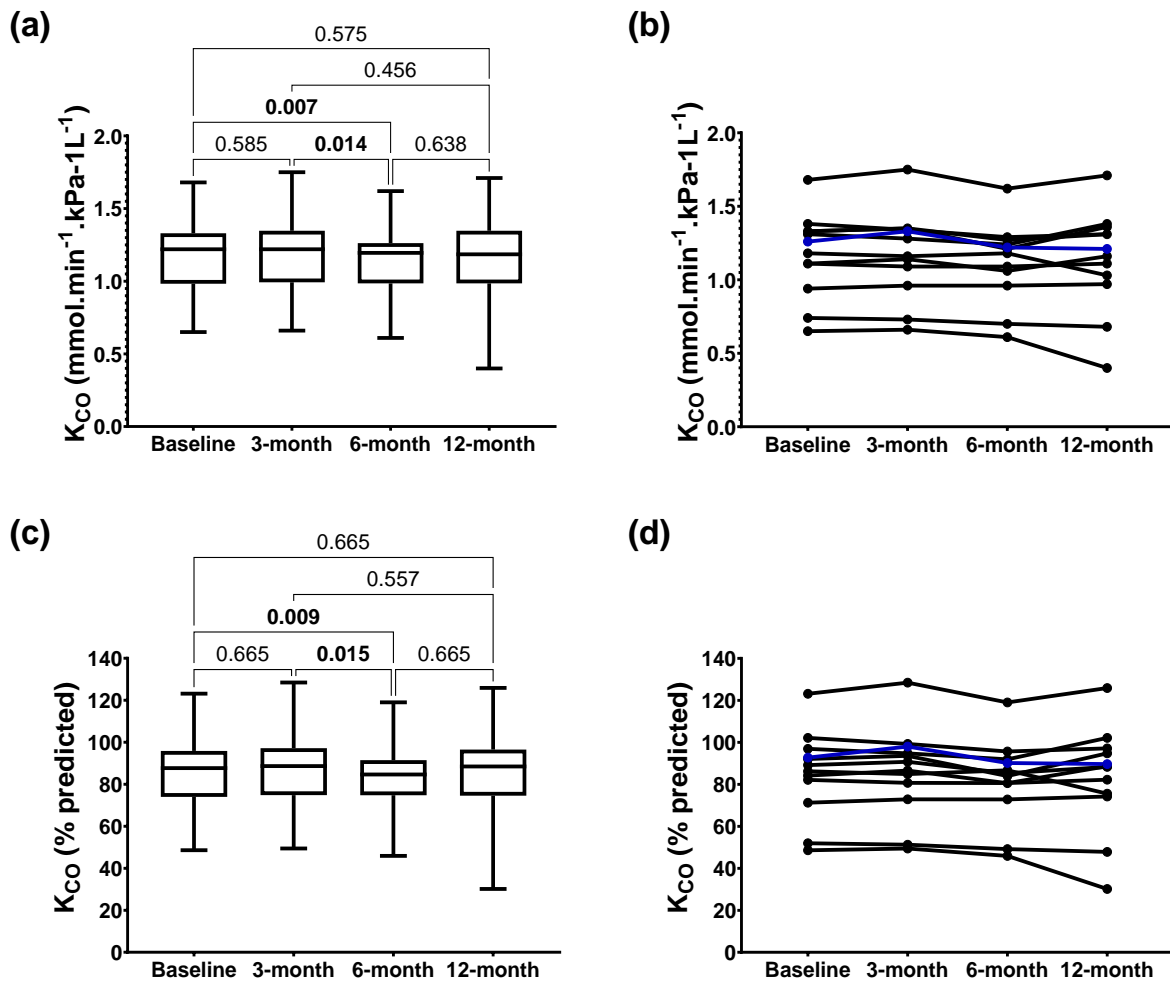


Figure 5.11. K_{CO} (a-b) and K_{CO} % predicted (c-d) at baseline, 3-month, 6-month and 12-month visits ($n=12$). The subject highlighted in blue commenced nintedanib approximately three months after the baseline study visit. Statistical test: one-way ANOVA.

5.2.6 Baseline, 6-month and 12-month visits in the total cohort

Out of the total study cohort, 27 subjects had standard PFTs performed at each of the baseline, 6-month and 12-month visits. There was a statistically significant decrease between the baseline and 6-month visits in FVC ($p=0.032$), FVC% ($p=0.046$), K_{CO} ($p=0.007$) and $K_{CO}\%$ ($p=0.014$) (Figures 5.12 and 5.16). There was a statistically significant decrease between the baseline and 12-month visits in FVC ($p=0.049$). Four subjects had been commenced on antifibrotic therapy prior to the baseline visit and an additional subject started nintedanib three months after the baseline visit (Figures 5.13, 5.15 and 5.17).

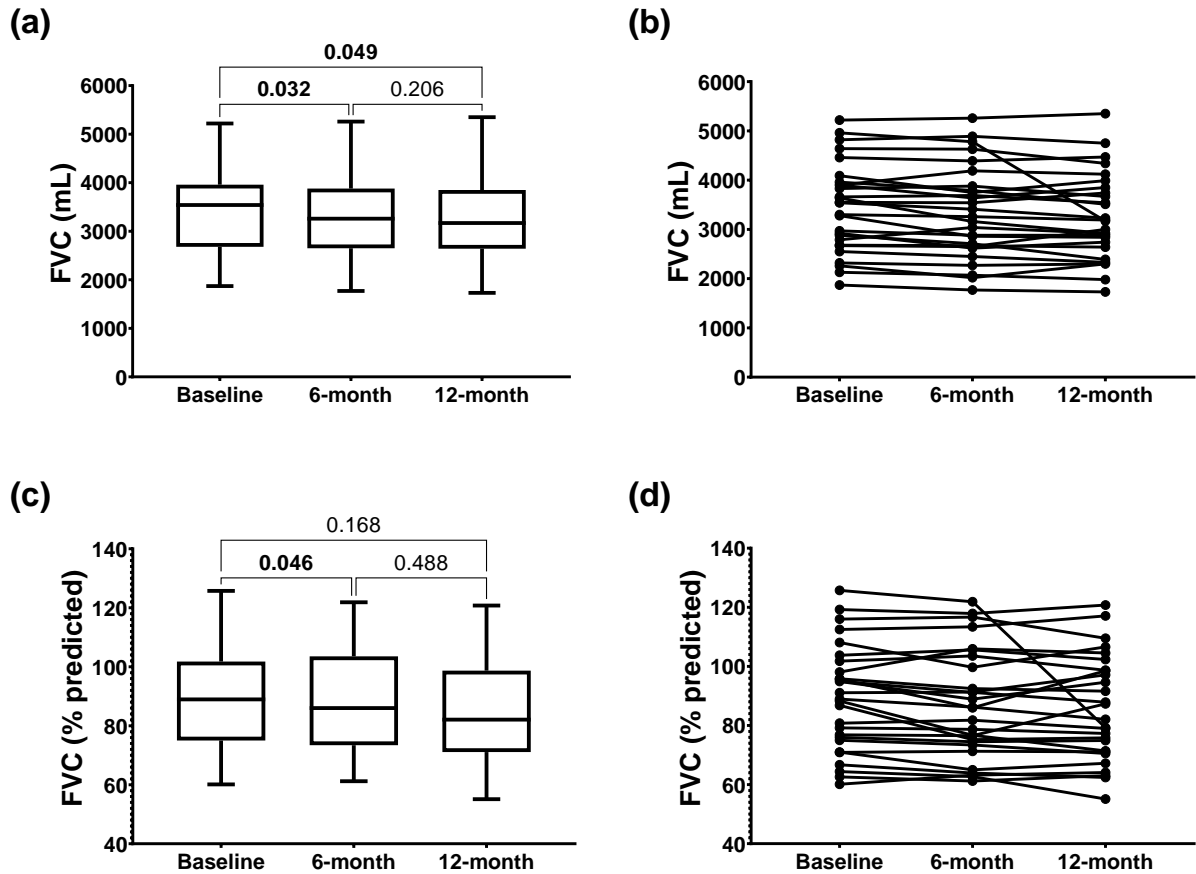


Figure 5.12. FVC (a-b) and FVC % predicted (c-d) at baseline, 6-month and 12-month visits (n=27). Statistical test: one-way ANOVA.

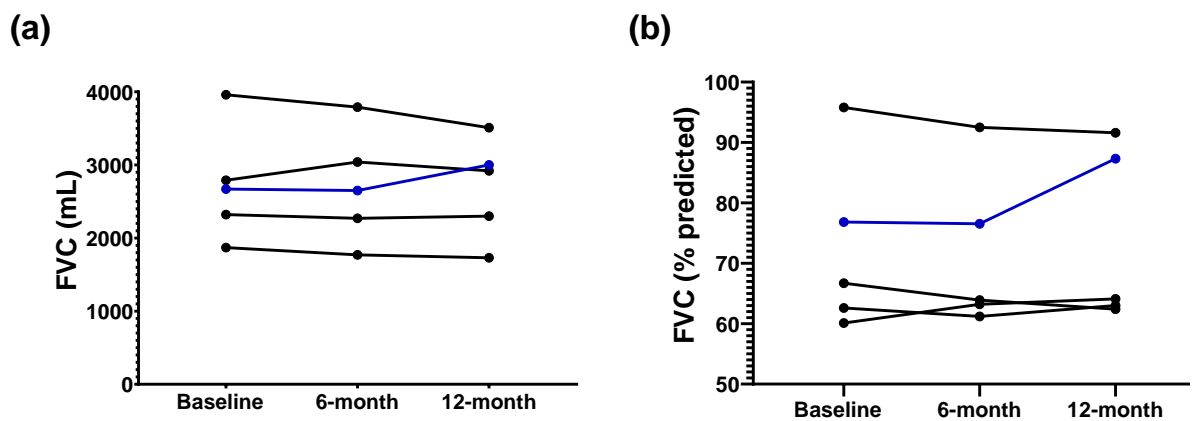


Figure 5.13. FVC (a-b) and FVC % predicted (c-d) at baseline, 6-month and 12-month visits in five subjects taking antifibrotic therapy during the study. The subject highlighted in blue commenced nintedanib approximately three months after the baseline study visit.

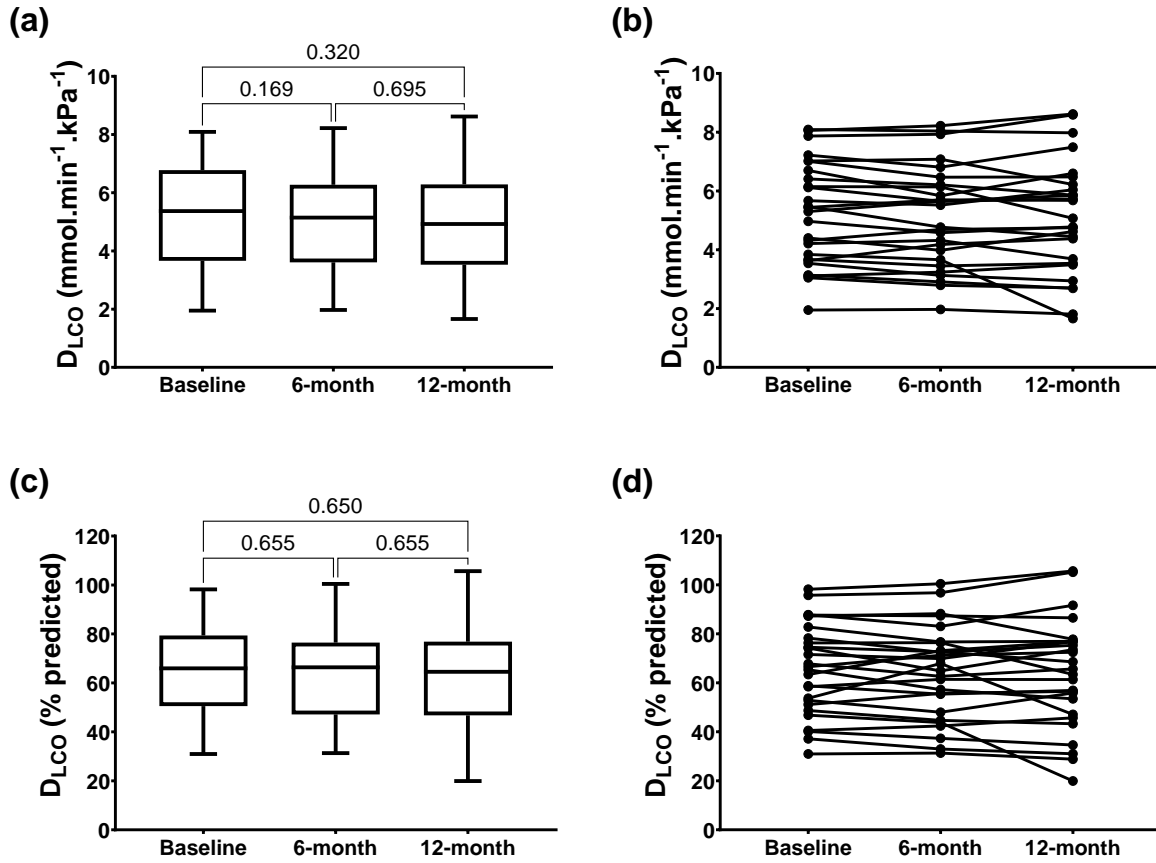


Figure 5.14. DLCO (a-b) and DLCO % predicted (c-d) at baseline, 6-month and 12-month visits (n=27). Statistical test: one-way ANOVA.

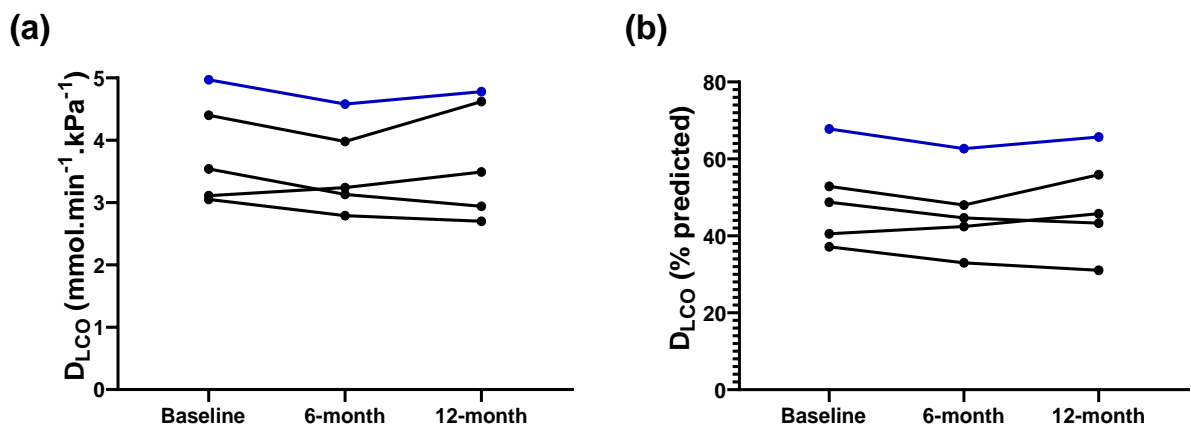


Figure 5.15. DLCO (a-b) and DLCO % predicted (c-d) at baseline, 6-month and 12-month visits in five subjects taking antifibrotic therapy during the study. The subject highlighted in blue commenced nintedanib approximately three months after the baseline study visit.

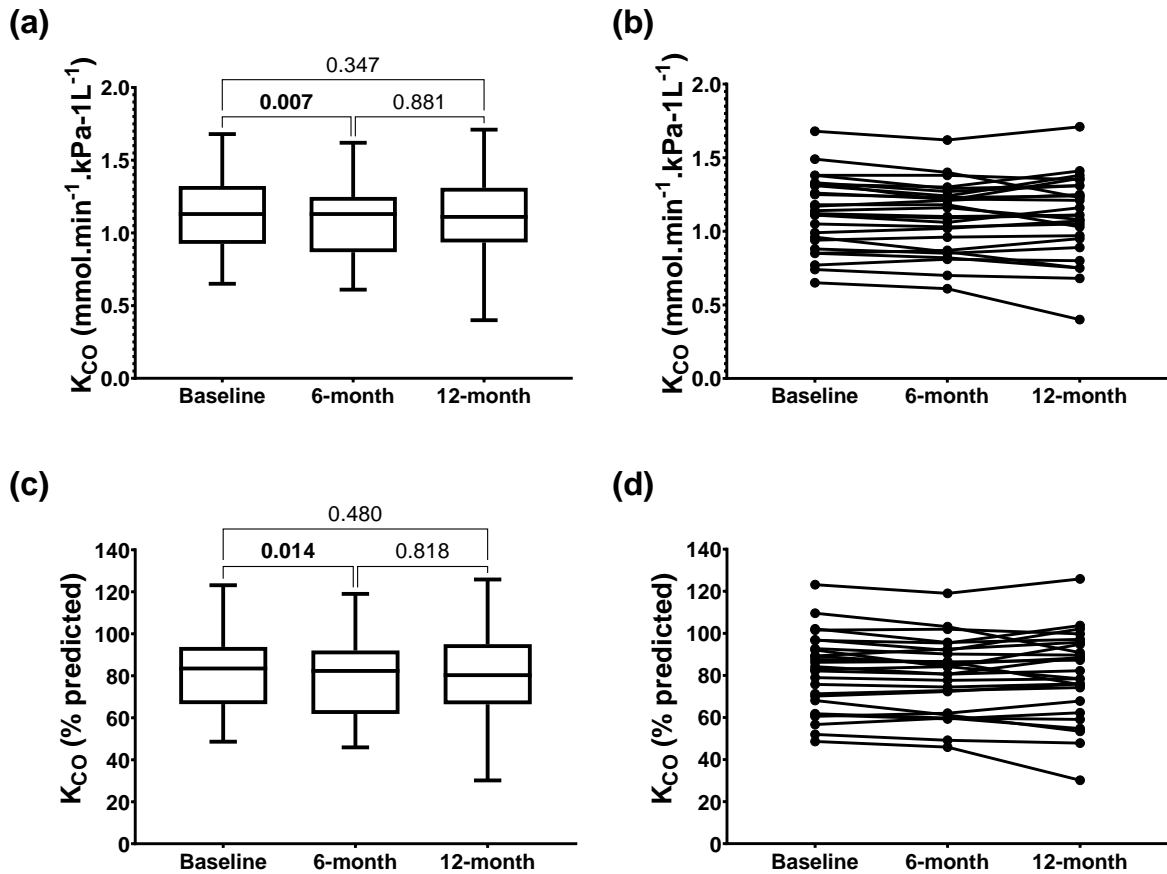


Figure 5.16. K_{CO} (a-b) and K_{CO} % predicted (c-d) at baseline, 6-month and 12-month visits ($n=27$). Statistical test: one-way ANOVA.

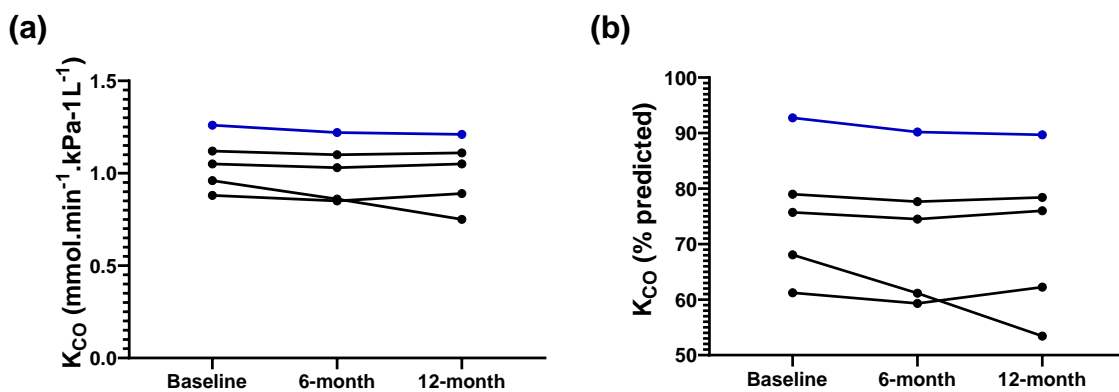


Figure 5.17. K_{CO} (a-b) and K_{CO} % predicted (c-d) at baseline, 6-month and 12-month visits in five subjects taking antifibrotic therapy during the study. The subject highlighted in blue commenced nintedanib approximately three months after the baseline study visit.

5.3 Dissolved ^{129}Xe MRI

5.3.1 Study visits

Due to changes in the spectroscopy sequence, 13 of the 49 subjects in the total study cohort had ^{129}Xe RBC:TP data analysed using a manual method. In this method, once both RBC and TP peaks were phased, points were manually selected where the spectra crossed the y axis at zero, each spectral curve was integrated, and then the RBC area was divided by the TP area to calculate the RBC:TP. The remaining 36 subjects had ^{129}Xe RBC:TP data analysed using a double Lorentzian, two peak automated method. However, the flip angle and repetition time in the spectroscopy sequence remained consistent for all 49 subjects. Bland-Altman statistical analysis demonstrated a negligible mean bias (-0.0076) between the manual versus the automated method of ^{129}Xe RBC:TP analysis (Figure 5.18), and hence the automated method was thereafter used throughout.

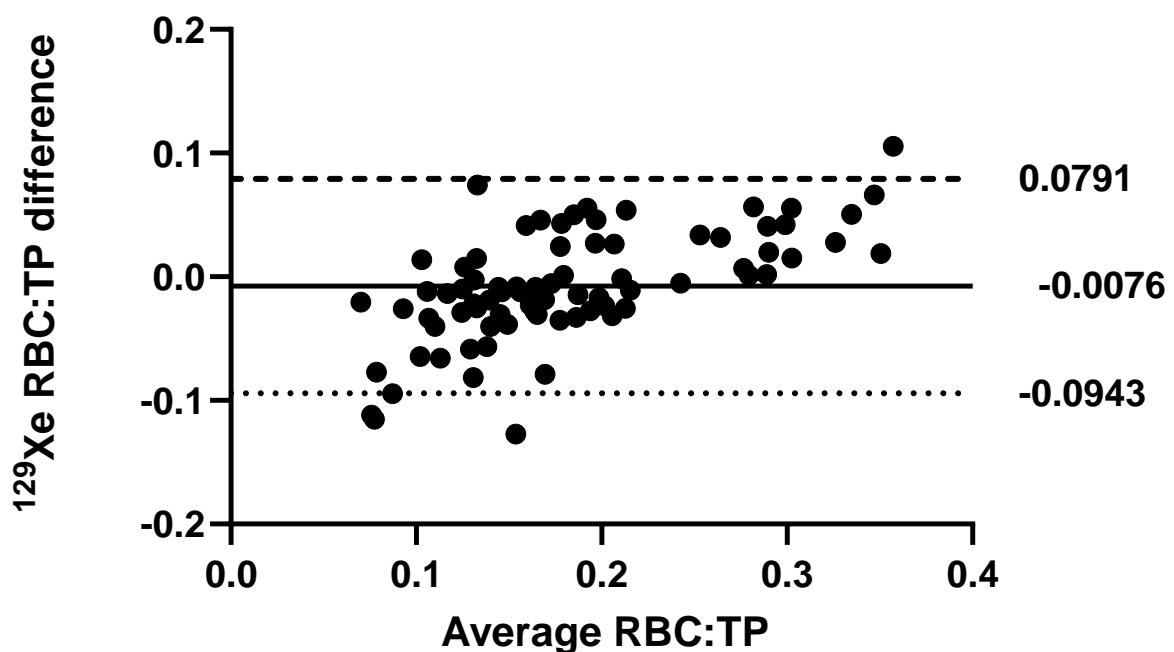


Figure 5.18. Bland-Altman statistical analysis of the manual versus the automated method of ^{129}Xe RBC:TP analysis.

In subjects 19-49, there was an error with the high-resolution dissolved phase spectroscopy in one of the baseline scans, one of the 3-month scans and two of the 12-month scans. The IDEAL technique was implemented in March 2019 and provided a regional measure of ^{129}Xe RBC:TP, RBC:Gas and TP:Gas, separated into upper, middle and lower zones, as well as central and peripheral zones. There was an error with the IDEAL spectroscopy in one baseline scans and one of the 6-month scans.

	High-resolution dissolved phase spectroscopy		IDEAL spectroscopy
	Subjects 1 – 49	Subjects 19 – 49	
Baseline visit, n	48	30	15
3-month visit, n	21	21	12
6-month visit, n	29	16	5
12-month visit, n	31	18	9
All 4 visits, n	10	10	5

IDEAL: iterative decomposition of water and fat with echo asymmetry and least squares estimation

Table 5.13. The number of subjects in which dissolved ^{129}Xe spectroscopy data was available for each study visit.

5.3.2 Baseline visit

5.3.2.1 High-resolution dissolved phase spectroscopy

At the baseline visit, the mean ^{129}Xe RBC:TP was 0.20 ± 0.08 for subjects 1-49 (n=48) and 0.18 ± 0.06 for subjects 19-49 (n=30).

5.7.2.2 IDEAL spectroscopic imaging technique

There was a statistically significant difference between the upper, middle and lower zones in ^{129}Xe RBC:TP ($p=0.003$; upper vs middle zone: $p=0.001$; upper vs lower zone: $p=0.008$) and ^{129}Xe RBC:Gas ($p<0.001$; upper vs middle zone: $p=0.002$; upper vs lower zone: $p=0.014$) at the baseline visit (Figure 5.19).

	RBC:TP	TP:Gas	RBC:Gas
Upper zone	0.24 (0.18 – 0.28)	0.0084 (0.0070 – 0.010)	0.0019 (0.0017 – 0.0023)
Middle zone	0.20 (0.17 – 0.27)	0.0084 (0.0067 – 0.0095)	0.0016 (0.0014 – 0.0018)
Lower zone	0.17 (0.16 – 0.22)	0.0088 (0.0073 – 0.0096)	0.0016 (0.0013 – 0.0017)
Central zone	0.21 (0.17 – 0.28)	0.0087 (0.0075 – 0.010)	0.0018 (0.0014 – 0.0024)
Peripheral zone	0.19 (0.17 – 0.23)	0.0088 (0.0072 – 0.0098)	0.0016 (0.0014 – 0.0020)

RBC: Red blood cell; TP: Tissue plasma.

Table 5.14. Regional ^{129}Xe RBC:TP, TP:Gas and RBC:Gas results at the baseline visit (n=15). Results are presented as median (interquartile range).

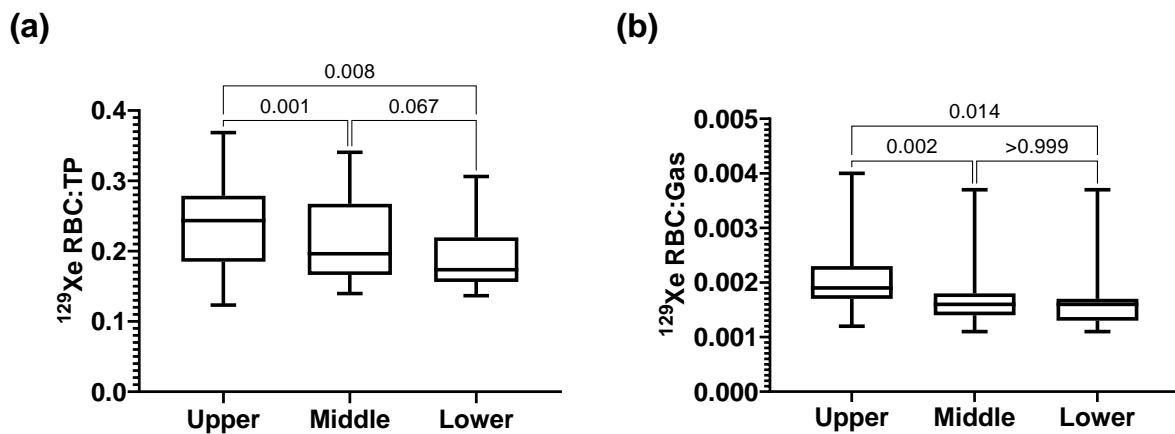


Figure 5.19. ^{129}Xe RBC:TP (a) and RBC:Gas (b) in the upper, middle and lower zones. Statistical test: Friedman test.

5.7.3 3-month visit

5.7.3.1 High-resolution dissolved phase spectroscopy

	Median	Interquartile range
RBC:TP	0.18	0.15 – 0.22
RBC:TP change	0.0057	-0.007 – 0.028
RBC:TP change (%)	3.43	-3.98 – 16.2

RBC: Red blood cell; TP: Tissue plasma.

Table 5.15. ^{129}Xe RBC:TP at the **3-month visit** (n=21), and the longitudinal change in ^{129}Xe RBC:TP between the baseline and 3-month visits (n=20).

5.7.3.2 IDEAL spectroscopic imaging technique

	RBC:TP change (%)	TP:Gas change (%)	RBC:Gas change (%)
Upper zone	8.81 (-3.81 – 24.0)	2.69 (-7.31 – 9.12)	12.7 (-16.6 – 30.0)
Middle zone	8.36 (-4.20 – 16.8)	3.56 (-2.44 – 5.34)	13.5 (-8.63 – 20.2)
Lower zone	11.1 (-0.86 – 17.6)	-0.82 (-3.50 – 3.48)	8.34 (-7.00 – 18.9)
Central zone	8.40 (-1.29 – 15.6)	-1.00 (-3.86 – 4.49)	10.3 (-6.87 – 16.8)
Peripheral zone	10.6 (0.84 – 21.3)	4.43 (-2.13 – 5.94)	11.3 (-10.6 – 19.9)

RBC: Red blood cell; TP: Tissue plasma.

Table 5.16. % change in regional ^{129}Xe RBC:TP, TP:Gas and RBC:Gas between the baseline and 3-month visits (n=12). Results presented as median (interquartile range).

5.3.4 6-month visit

5.3.4.1 High-resolution dissolved phase spectroscopy

	Subjects 1 – 49	Subjects 19 – 49
RBC:TP	0.18 (0.15 – 0.28)	0.18 (0.16 – 0.21)
RBC:TP change	-0.016 (-0.050 – 0.010)	-0.0045 (-0.032 – 0.031)
RBC:TP change (%)	-8.12 (-20.5 – 4.60)	-2.74 (-13.9 – 19.9)

RBC: Red blood cell; TP: Tissue plasma.

Table 5.17. ^{129}Xe RBC:TP at the **6-month visit**, and the longitudinal change in ^{129}Xe RBC:TP between the baseline and 6-month visits for the total study cohort (n=28) and subjects 19-49 (n=15). Results are presented as median (interquartile range).

In the total cohort (n=28), over the six months there was a statistically significant decrease in ^{129}Xe RBC:TP (mean: 0.23 ± 0.08 vs 0.21 ± 0.07 ; $p=0.049$) (Figure 5.20). However, in subjects 19-49 (n=15), there was no statistically significant change in ^{129}Xe RBC:TP between the baseline visit and the 6-month visit. The repeatability coefficient of ^{129}Xe RBC:TP was 0.09 in ten healthy volunteers using the same MRI protocol and performed at the University of Sheffield.

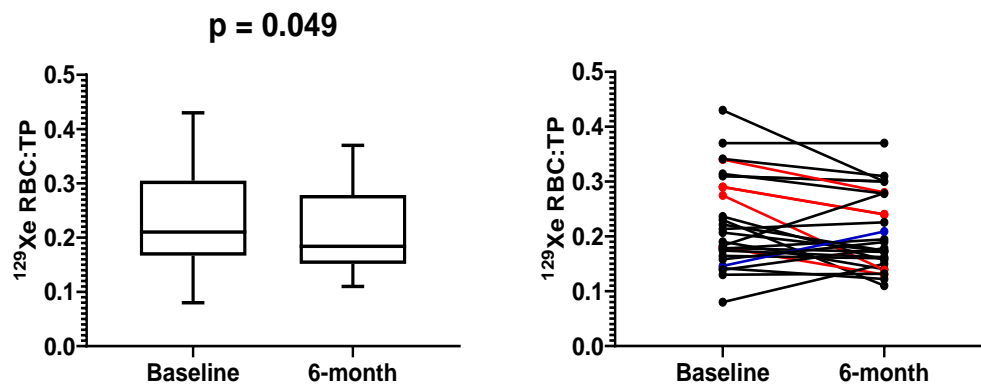


Figure 5.20. ^{129}Xe RBC:TP at baseline visit versus 6-month visit for the total study cohort (n=28). The subjects highlighted in red represent those taking antifibrotic therapy during the six-month period. The subject highlighted in blue commenced nintedanib approximately three months after the baseline study visit. Statistical test: paired *t* test.

5.3.4.2 IDEAL spectroscopic imaging technique

	RBC:TP change (%)	TP:Gas change (%)	RBC:Gas change (%)
Upper zone	-3.88 (-16.3 – 27.5)	9.65 (5.78 – 17.1)	14.0 (-5.66 – 34.4)
Middle zone	5.10 (-13.7 – 24.7)	10.2 (5.80 – 15.0)	14.5 (0.53 – 32.0)
Lower zone	14.2 (-13.4 – 26.6)	10.5 (1.02 – 11.3)	25.9 (-4.01 – 31.8)
Central zone	-0.36 (-10.6 – 22.0)	9.46 (5.03 – 13.5)	7.26 (0.01 – 33.3)
Peripheral zone	8.43 (-17.9 – 28.4)	12.5 (3.36 – 16.0)	23.4 (-3.16 – 31.5)

RBC: Red blood cell; TP: Tissue plasma.

Table 5.18. % change in regional ^{129}Xe RBC:TP, TP:Gas and RBC:Gas between the baseline and 6-month visits (n=5). Results are presented as median (interquartile range).

5.3.5 12-month visit

5.3.5.1 High-resolution dissolved phase spectroscopy

In the total cohort (n=31), over the 12 months there was a statistically significant decrease in ^{129}Xe RBC:TP (mean: 0.22 ± 0.09 vs 0.18 ± 0.06 ; $p=0.008$) (Figure 5.21). However, in subjects 19-49 (n=18), there was no statistically significant change in ^{129}Xe RBC:TP between the baseline visit and the 12-month visit. The repeatability coefficient of ^{129}Xe RBC:TP was 0.09 in ten healthy volunteers using the same MRI protocol and performed at the University of Sheffield.

	Subjects 1 – 49	Subjects 19 – 49
RBC:TP	0.18 (0.15 – 0.25)	0.17 (0.15 – 0.20)
RBC:TP change	-0.023 (-0.060 – 0.014)	-0.004 (-0.024 – 0.020)
RBC:TP change (%)	-10.3 (-21.0 – 8.52)	-2.23 (-10.7 – 13.2)

RBC: Red blood cell; TP: Tissue plasma.

Table 5.19. ^{129}Xe RBC:TP at the **12-month visit**, and the longitudinal change in ^{129}Xe RBC:TP between the baseline and 12-month visits for the total study cohort (n=31) and subjects 19-49 (n=18). Results are presented as median (interquartile range).

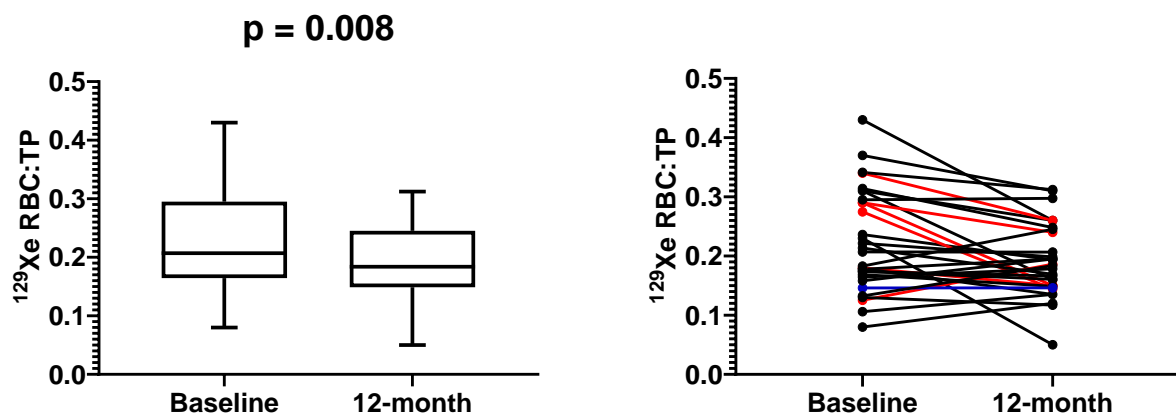


Figure 5.21. ^{129}Xe RBC:TP at baseline visit versus 12-month visit for the total study cohort (n=31). The subjects highlighted in red represent those taking antifibrotic therapy during the 12-month period. The subject highlighted in blue commenced nintedanib approximately three months after the baseline study visit. Statistical test: paired t test.

5.3.5.2 IDEAL spectroscopic imaging technique

	RBC:TP change (%)	TP:Gas change (%)	RBC:Gas change (%)
Upper zone	6.34 (-5.79 – 29.1)	-5.68 (-13.3 - -0.58)	5.07 (-11.5 – 15.4)
Middle zone	6.67 (-5.35 – 37.9)	-2.77 (-9.85 – 2.01)	11.3 (-7.76 – 29.3)
Lower zone	7.68 (-8.73 – 37.4)	-3.64 (-11.8 - -1.73)	2.87 (-9.16 – 30.9)
Central zone	9.67 (-4.77 – 37.2)	-3.90 (-12.3 – 2.61)	10.0 (-5.47 – 23.8)
Peripheral zone	7.11 (-6.34 – 37.9)	-4.04 (-10.6 – 1.39)	6.93 (-8.80 – 26.6)

RBC: Red blood cell; TP: Tissue plasma.

Table 5.20. % change in regional ^{129}Xe RBC:TP, TP:Gas and RBC:Gas between the baseline and 12-month visits (n=9). Results are presented as median (interquartile range).

5.3.6 Baseline, 3-month, 6-month and 12-month visits

High-resolution dissolved phase spectroscopy

^{129}Xe RBC:TP data were available at each of the baseline, 3-month, 6-month and 12-month visits in a subset of 10 subjects (Figure 5.22).

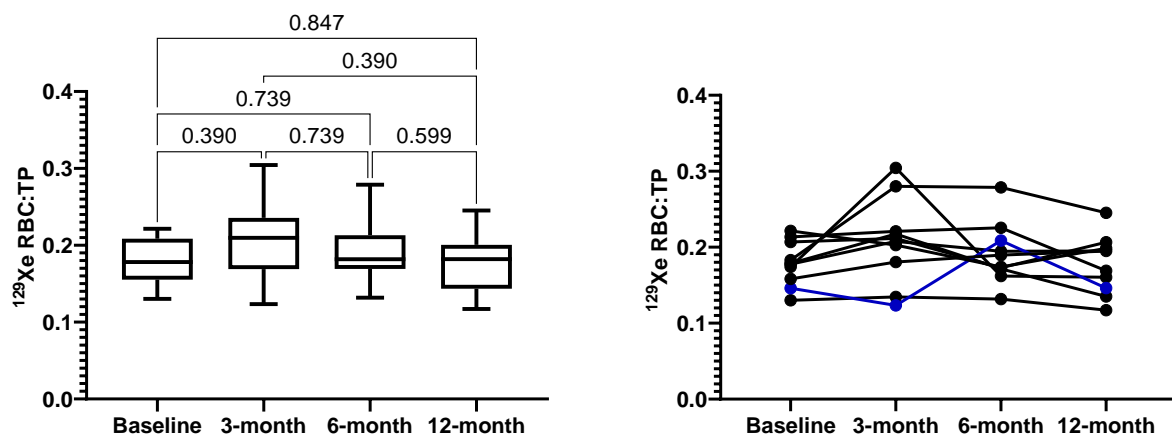


Figure 5.22. ^{129}Xe RBC:TP at baseline, 3-month, 6-month and 12-month visits (n=10). The subject highlighted in blue commenced nintedanib approximately three months after the baseline study visit. Statistical test: one-way ANOVA.

5.3.7 Baseline, 6-month and 12-month visits in the total cohort

High-resolution dissolved phase spectroscopy

Out of a total study cohort of 49 subjects, 22 had high-resolution dissolved phase ^{129}Xe spectroscopy performed successfully at baseline, 6-month and 12-month visits. There was a statistically significant decrease in ^{129}Xe RBC:TP between the baseline and 6-month visits ($p=0.045$), and between the baseline and 12-month visits ($p=0.045$) (Figure 5.21a-b). In the same 22 subjects, there were no statistically significant differences in FVC, FVC%, D_{LCO} or $D_{\text{LCO}}\%$ between any of the study visits. Between the baseline and 6-month visits, there was a statistically significant decrease in K_{CO} ($p=0.002$) and $K_{\text{CO}}\%$ ($p=0.003$) (Figure 5.23c-d). However, there was no statistically significant change in K_{CO} or $K_{\text{CO}}\%$ between the baseline and 12-month visits.

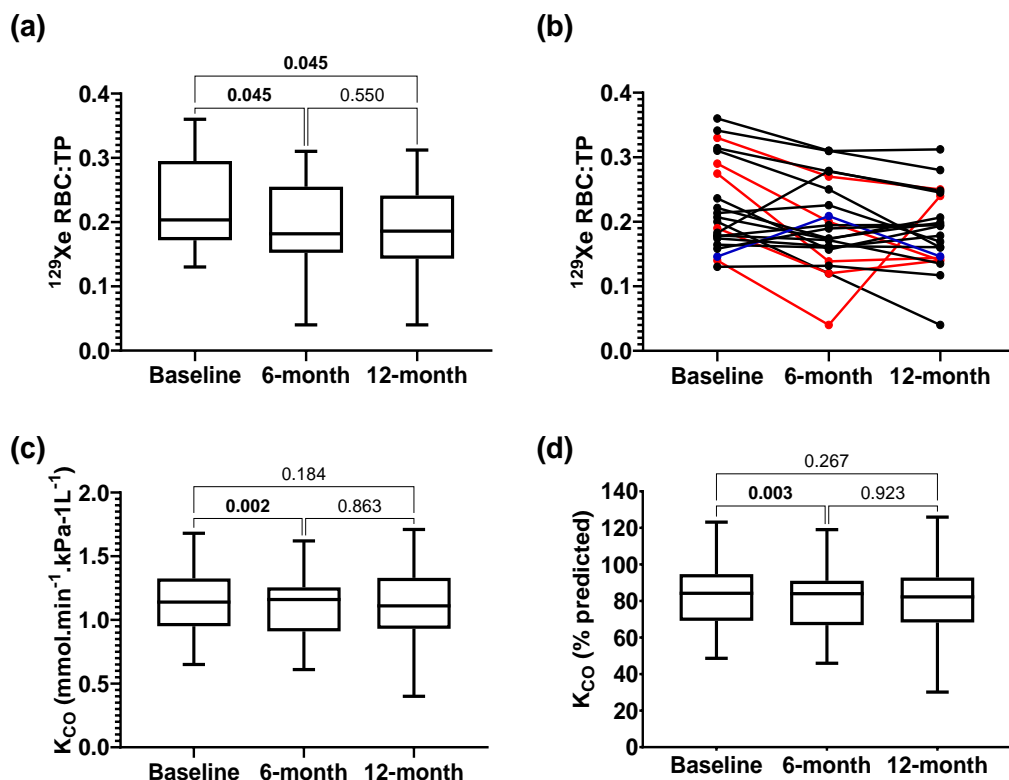


Figure 5.23. ^{129}Xe RBC:TP (a-b), K_{CO} (c) and $K_{\text{CO}}\%$ (d) at baseline, 6-month and 12-month visits ($n=22$). The subjects highlighted in red were taking antifibrotic therapy throughout the study. The subject highlighted in blue commenced nintedanib approximately three months after the baseline study visit. Statistical test: one-way ANOVA.

5.4 Diffusion-weighted MRI (airway microstructure)

Out of a total study cohort of 49 subjects, all had DW-MRI scans performed successfully at the baseline visit. However, DW-MRI was performed using ^3He instead of ^{129}Xe in subjects 1-18. Only the Lm_D data could be combined for subjects 1-18 and subjects 19-49. 13 study visit datasets were available for subjects that had both ^3He and ^{129}Xe DW-MRI performed and after Bland-Altman statistical analysis, there was a mean bias of $-40\mu\text{m}$ towards ^{129}Xe Lm_D (Figure 5.24). Therefore, the ^3He Lm_D values were corrected by $-40\mu\text{m}$ when combined with the ^{129}Xe Lm_D values.

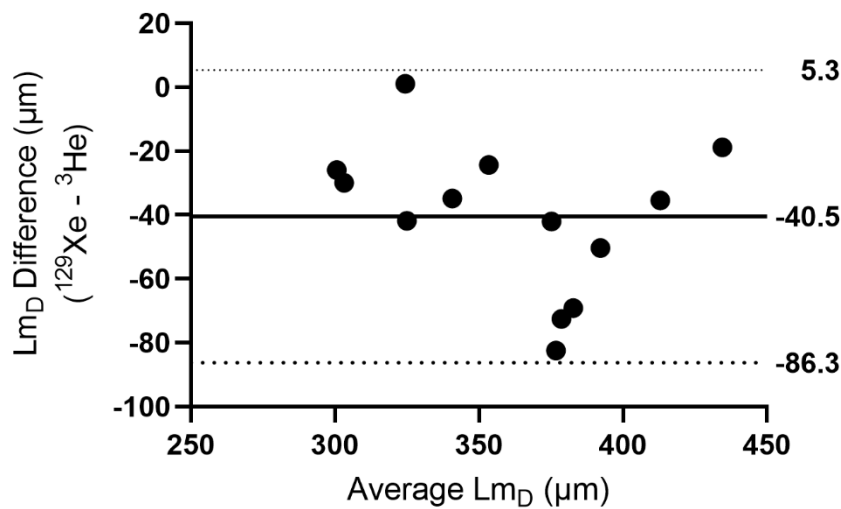


Figure 5.24. Bland-Altman statistical analysis of ^{129}Xe versus ^3He Lm_D .

5.4.1 Baseline visit

At the baseline visit, the mean global Lm_D was $329\mu\text{m} \pm 33.5 \mu\text{m}$ for the total cohort (n=49).

	Mean	Standard deviation	Range
ADC (cm^2/s)	0.044	0.007	0.034 – 0.065
Lm_D (μm)	324	27.4	279 – 395

ADC: Apparent diffusion coefficient; Lm_D : mean diffusive length scale.

Table 5.21. Global ^{129}Xe ADC and Lm_D at the baseline visit in subjects 19-49 (n=31).

	ADC (cm ² /s)	Lm _D (μm)
Upper zone	0.042 (0.037 – 0.045)	318 (296 – 327)
Middle zone	0.045 (0.040 – 0.049)	332 (305 – 346)
Lower zone	0.043 (0.037 – 0.049)	318 (290 – 348)
Central zone	0.045 (0.040 – 0.050)	327 (304 – 355)
Peripheral zone	0.043 (0.037 – 0.046)	321 (292 – 331)

ADC: Apparent diffusion coefficient; Lm_D: mean diffusive length scale.

Table 5.22. Regional ¹²⁹Xe ADC and Lm_D results at the baseline visit in subjects 19-49 (n=31). Results are presented as median (interquartile range).

There was a statistically significant difference between the upper, middle and lower zones in ¹²⁹Xe ADC (p=0.002; upper vs middle zone: p=0.001) and ¹²⁹Xe Lm_D (p<0.001; upper vs middle zone: p<0.001; middle vs lower zone: p=0.033) at the baseline visit (Figure 5.25a-b). There was also a statistically significant difference between the central and peripheral zones in ¹²⁹Xe ADC (p<0.001) and ¹²⁹Xe Lm_D (p<0.001) at the baseline visit (Figure 5.25c-d).

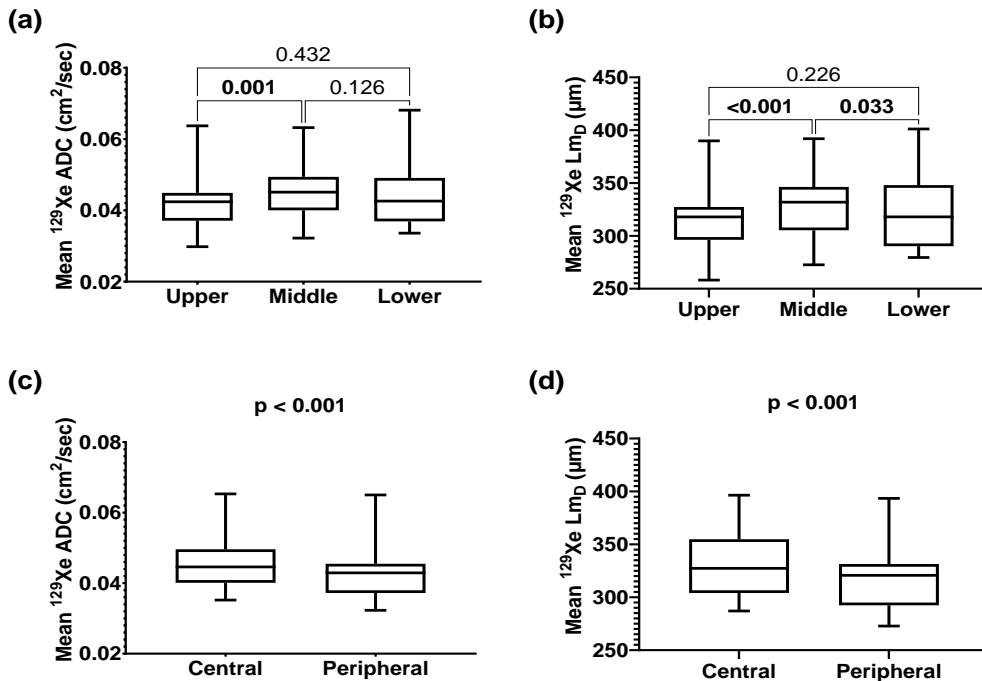


Figure 5.25. ¹²⁹Xe ADC (a) and Lm_D (b) in the upper, middle and lower zones. ¹²⁹Xe ADC (c) and Lm_D (d) in the central and peripheral zones. Statistical tests: Friedman test and Wilcoxon test (n=31).

5.4.2 3-month visit

	Mean	Standard deviation	Range
ADC (cm²/s)	0.044	0.007	0.032 – 0.065
ADC change (cm²/s)	0.0002	0.003	-0.005 – 0.005
ADC change (%)	0.39	6.09	-10.2 – 10.3
Lm_D (µm)	322	30.9	270 – 403
Lm_D change (µm)	0.97	12.5	-25.9 – 21.0
Lm_D change (%)	0.27	3.86	-7.65 – 6.28

ADC: Apparent diffusion coefficient; Lm_D: mean diffusive length scale.

Table 5.23. Global ¹²⁹Xe ADC and Lm_D at the **3-month visit** (n=22), and the longitudinal change in global ¹²⁹Xe ADC and Lm_D between the baseline and 3-month visits (n=22).

	ADC change (%)	Lm _D change (%)
Upper zone	0.73 (-8.02 – 6.15)	0.66 (-3.52 – 2.73)
Middle zone	1.68 (-5.25 – 5.43)	1.67 (-3.18 – 3.24)
Lower zone	1.77 (-4.14 – 5.71)	0.15 (-2.87 – 4.33)
Central zone	1.25 (-5.77 – 5.93)	2.60 (-5.92 – 3.78)
Peripheral zone	2.30 (-5.63 – 4.40)	0.95 (-3.99 – 2.66)

ADC: Apparent diffusion coefficient; Lm_D: mean diffusive length scale.

Table 5.24. % change in regional ¹²⁹Xe ADC and Lm_D between the baseline and 3-month visits (n=22). Results are presented as median (interquartile range).

5.4.3 6-month visit

	Subjects 1 – 49 (n=30)	Subjects 19 – 49 (n=16)
ADC (cm²/s)	NA	0.045 ± 0.009
ADC change (cm²/s)	NA	0.001 ± 0.002
ADC change (%)	NA	2.29 ± 5.50
Lm_D (µm)	330 ± 33.5	327 ± 35.7
Lm_D change (µm)	5.64 ± 11.7	4.96 ± 9.41
Lm_D change (%)	1.72 ± 3.65	1.46 ± 3.00

ADC: Apparent diffusion coefficient; Lm_D: mean diffusive length scale; NA: Not applicable.

Table 5.25. Global ADC and Lm_D at the **6-month visit** and the longitudinal change in global ADC and Lm_D between the baseline and 6-month visits. Results are presented as mean ± standard deviation.

In subjects 19-49, there was no statistically significant change between the baseline visit and the 6-month visit in global ^{129}Xe ADC or L_{mD} ($n=16$). However, there was a statistically significant increase in global L_{mD} between the baseline and 6-month visits (mean (μm): 326 ± 34.9 vs 332 ± 37.2 ; $p=0.013$) in the total study cohort ($n=30$) (Figure 5.26). The repeatability coefficient of ^{129}Xe ADC and L_{mD} was 0.002 and 11.3 respectively in ten healthy volunteers using the same MRI protocol and performed at the University of Sheffield.

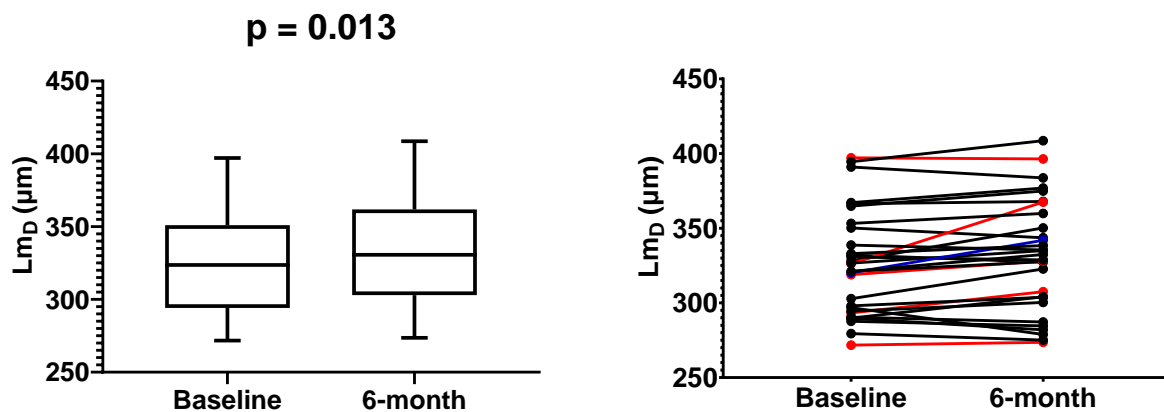


Figure 5.26. Global L_{mD} at baseline visit versus 6-month visit for the total study cohort ($n=30$). The subjects highlighted in red represent those taking antifibrotic therapy during the six-month period. The subject highlighted in blue commenced nintedanib approximately three months after the baseline study visit. Statistical test: paired t test.

	ADC change (%)	L_{mD} change (%)
Upper zone	0.92 (-4.58 – 2.59)	0.08 (-1.16 – 2.66)
Middle zone	3.13 (-0.34 – 5.95)	2.22 (-0.15 – 2.84)
Lower zone	4.05 (-2.01 – 9.48)	4.27 (-1.45 – 6.39)
Central zone	4.13 (-1.09 – 6.52)	1.74 (-0.83 – 5.28)
Peripheral zone	1.80 (-1.55 – 6.98)	0.79 (-0.74 – 3.29)

ADC: Apparent diffusion coefficient; L_{mD} : mean diffusive length scale.

Table 5.26. % change in regional ^{129}Xe ADC and L_{mD} between the baseline and 6-month visits ($n=16$). Results are presented as median (interquartile range).

There was a statistically significant increase in ^{129}Xe L_{mD} between the baseline visit and the 6-month visit in the middle zone (mean (μm): 327 ± 30.0 vs 333 ± 34.5 ; $p=0.044$) and the central zone (mean (μm): 329 ± 30.8 vs 335 ± 36.4 ; $p=0.030$) (Figure 5.27).

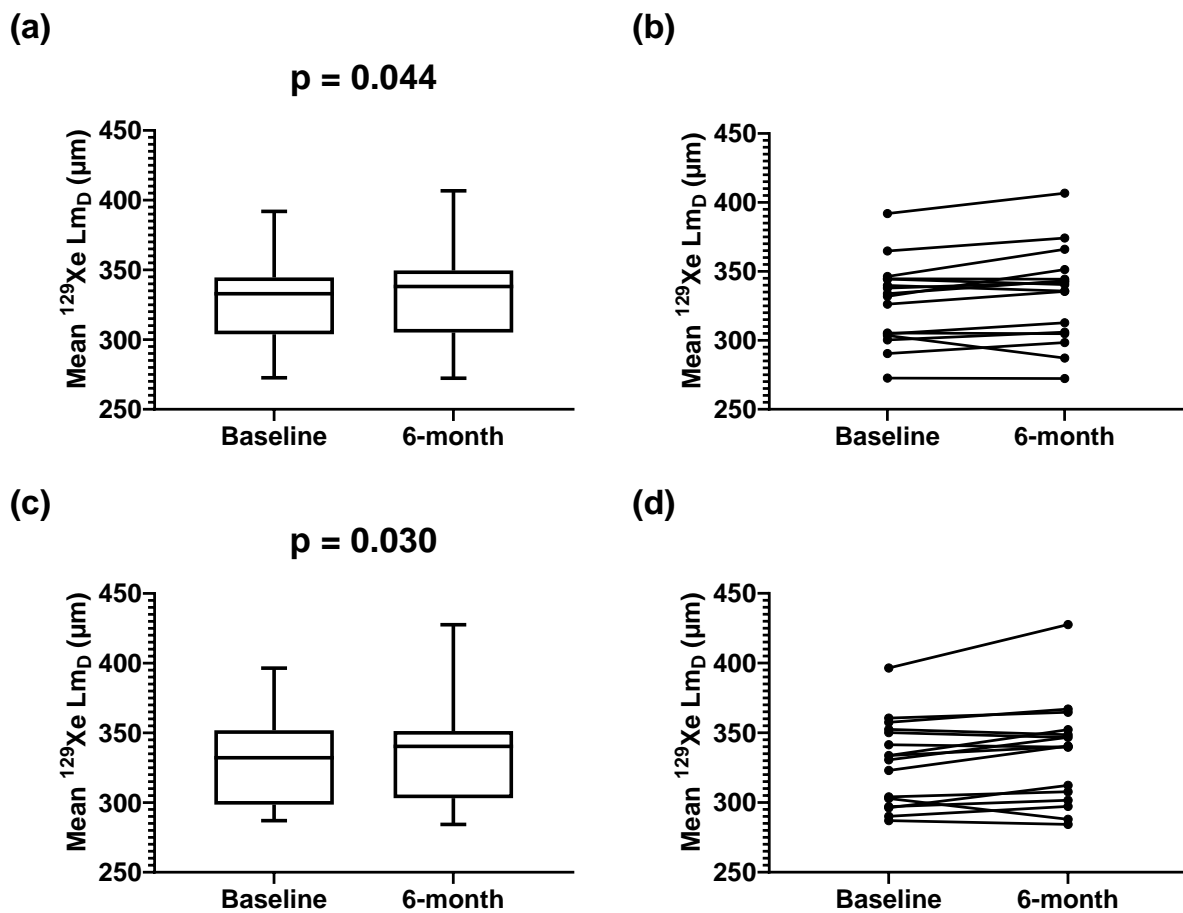


Figure 5.27. ^{129}Xe L_{mD} at the baseline visit versus the 6-month visit in the middle zone (a-b) and central zone (c-d). Statistical test: paired t test ($n=16$).

5.4.4 12-month visit

Figures 5.28 and 5.29 are examples of ^{129}Xe ADC and L_{mD} maps at the baseline visit compared to the 12-month visit in one of the subjects in the study.

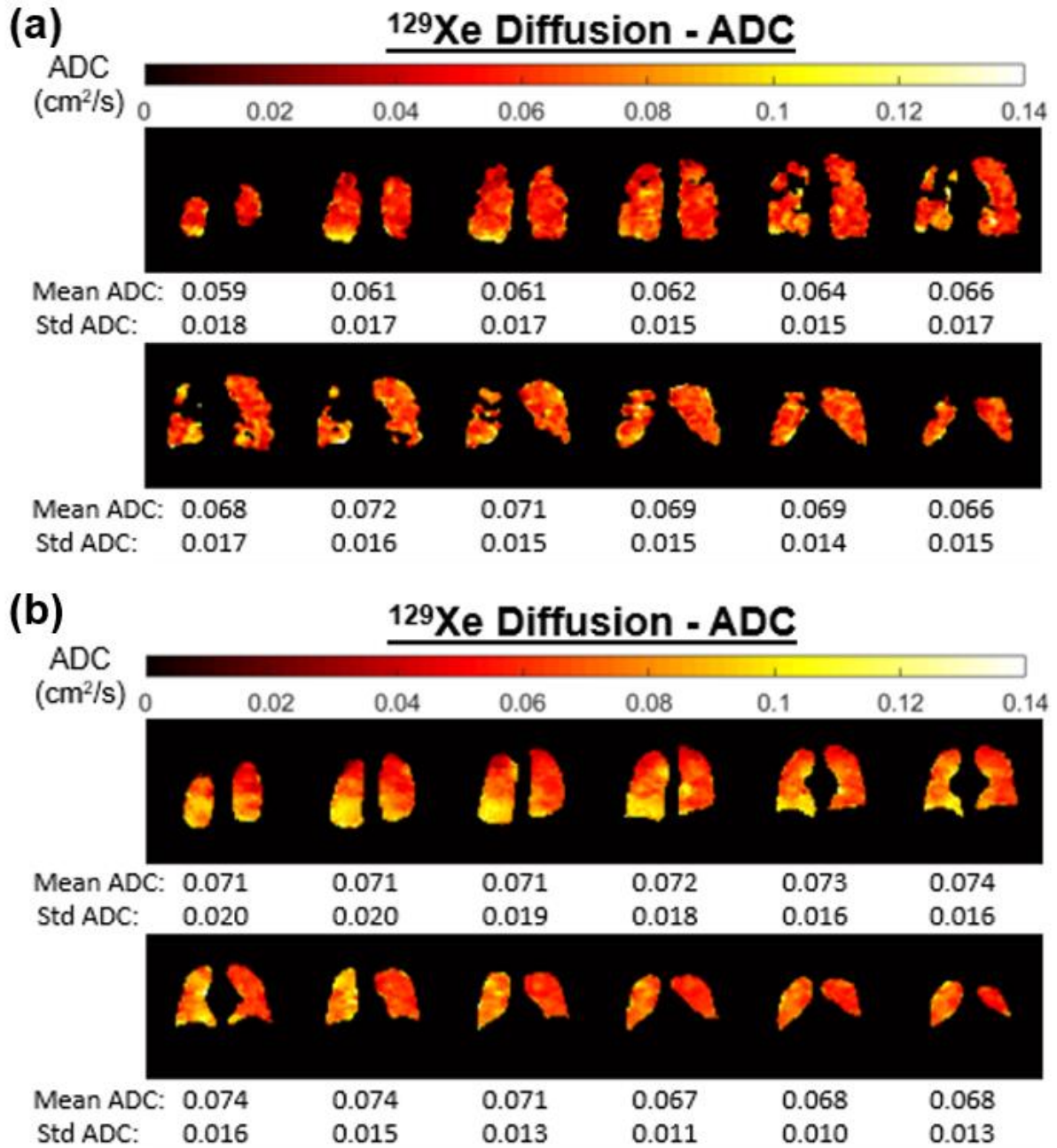


Figure 5.28. Example of ^{129}Xe ADC maps at the baseline visit (a) and 12-month visit (b) in the same IPF subject.

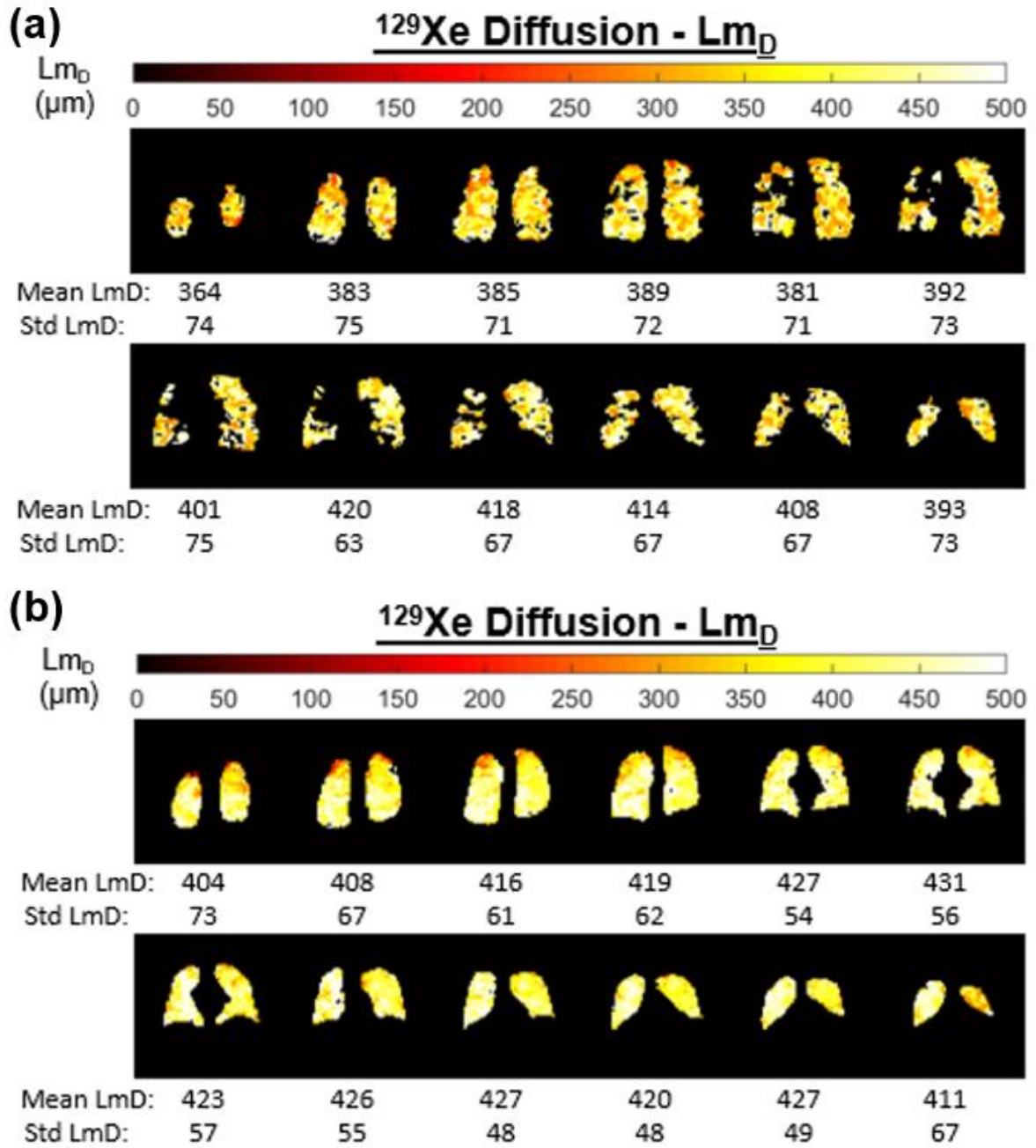


Figure 5.29. Example of ^{129}Xe Lm_D maps at the baseline visit (a) and 12-month visit (b) in the same IPF subject.

	Subjects 1 – 49 (n=33)	Subjects 19 – 49 (n=20)
ADC (cm ² /s)	NA	0.045 ± 0.009
ADC change (cm ² /s)	NA	0.001 ± 0.003
ADC change (%)	NA	2.74 ± 6.41
Lm _D (μm)	331 ± 39.7	325 ± 36.6
Lm _D change (μm)	7.33 ± 13.7	5.18 ± 12.7
Lm _D change (%)	2.19 ± 4.25	1.50 ± 3.97

ADC: Apparent diffusion coefficient; Lm_D: mean diffusive length scale; NA: Not applicable.

Table 5.27. Global ADC and Lm_D at the **12-month visit** and the longitudinal change in global ADC and Lm_D between the baseline and 12-month visits. Results are presented as mean ± standard deviation.

In subjects 19-49, there was a statistically significant increase in global ¹²⁹Xe ADC between the baseline and the 12-month visits (mean (cm²/s): 0.043 ± 0.008 vs 0.045 ± 0.009; p=0.044) (Figure 5.30), with no statistically significant change in PFTs over 12 months. There was no statistically significant change in global ¹²⁹Xe Lm_D between the baseline and the 12-month visits in subjects 19-49. However, there was a statistically significant increase in global Lm_D between the baseline and the 12-month visits (mean (μm): 324 ± 34.2 vs 331 ± 39.7; p=0.004) in the total study cohort (n=33) (Figure 5.31), with no statistically significant change in PFTs over 12 months. These results suggest that ¹²⁹Xe DW-MRI measurements are more sensitive to early progression of microstructural changes in IPF compared to PFTs. The repeatability coefficient of ¹²⁹Xe ADC and Lm_D was 0.002 and 11.3 respectively in ten healthy volunteers using the same MRI protocol and performed at the University of Sheffield.

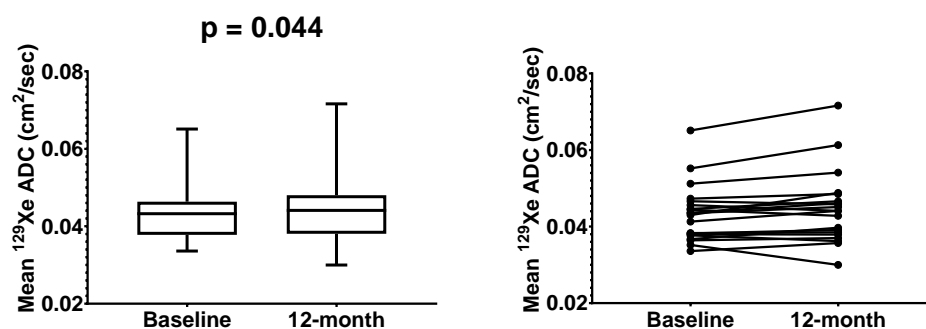


Figure 5.30. Global ¹²⁹Xe ADC at the baseline visit versus the 12-month visit (n=20). Statistical test: paired *t* test.

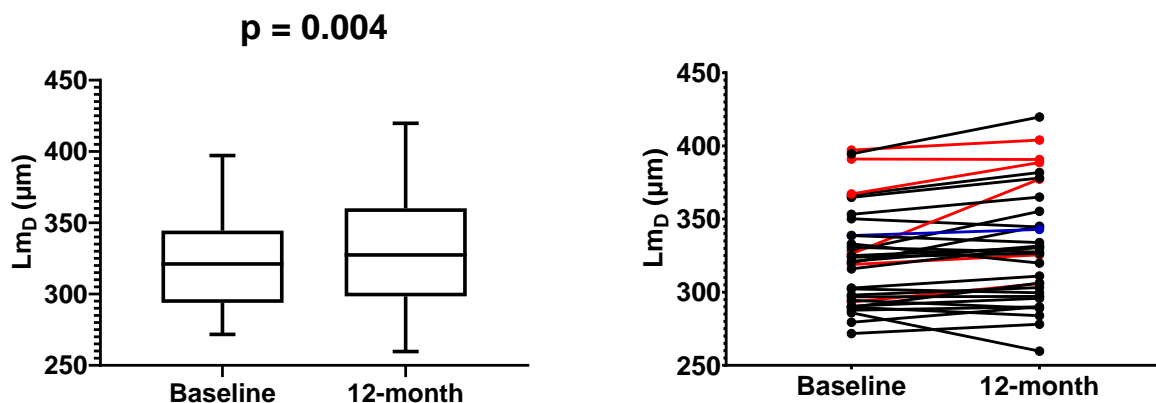


Figure 5.31. Global L_{mD} at baseline visit versus 12-month visit for the total study cohort ($n=33$). The subjects highlighted in red represent those taking antifibrotic therapy during the 12-month period. The subject highlighted in blue commenced nintedanib approximately three months after the baseline study visit. Statistical test: paired t test.

	ADC change (%)	L_{mD} change (%)
Upper zone	1.08 (-4.85 – 8.96)	0.90 (-4.73 – 6.04)
Middle zone	3.03 (-2.58 – 8.25)	1.55 (-1.52 – 5.09)
Lower zone	5.89 (-3.90 – 12.9)	2.68 (-2.10 – 9.04)
Central zone	3.85 (-2.88 – 7.96)	2.76 (-1.35 – 5.16)
Peripheral zone	2.41 (-0.75 – 7.99)	0.89 (-0.62 – 9.71)

ADC: Apparent diffusion coefficient; L_{mD} : mean diffusive length scale.

Table 5.28. % change in regional ^{129}Xe ADC and L_{mD} between the baseline and 12-month visits ($n=20$). Results are presented as median (interquartile range).

There was a statistically significant increase in ^{129}Xe ADC between the baseline and 12-month visits in the lower zone (median (cm^2/s): 0.039 (0.037 – 0.045) vs 0.043 (0.037 – 0.048); $p=0.027$) and the peripheral zone (median (cm^2/s): 0.042 (0.037 – 0.045) vs 0.043 (0.037 – 0.048); $p=0.041$) (Figure 5.32). There was also a statistically significant increase in ^{129}Xe L_{mD} between the baseline and 12-month visits in the lower zone (median (μm): 302 (290 – 331) vs 320 (297 – 343); $p=0.033$) (Figure 5.33).

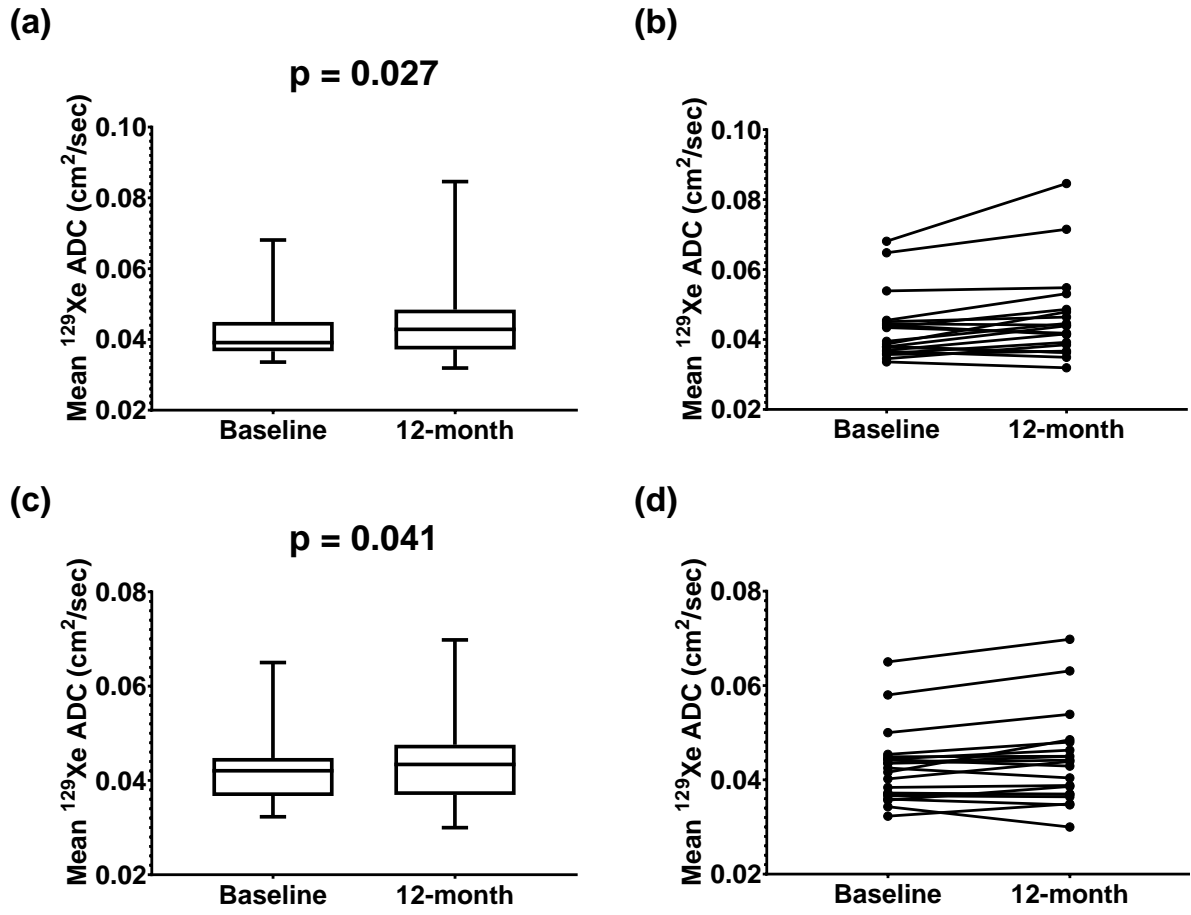


Figure 5.32. ^{129}Xe ADC at the baseline visit versus the 12-month visit in the lower zone (a-b) and peripheral zone (c-d) (n=20). Statistical test: Wilcoxon test.

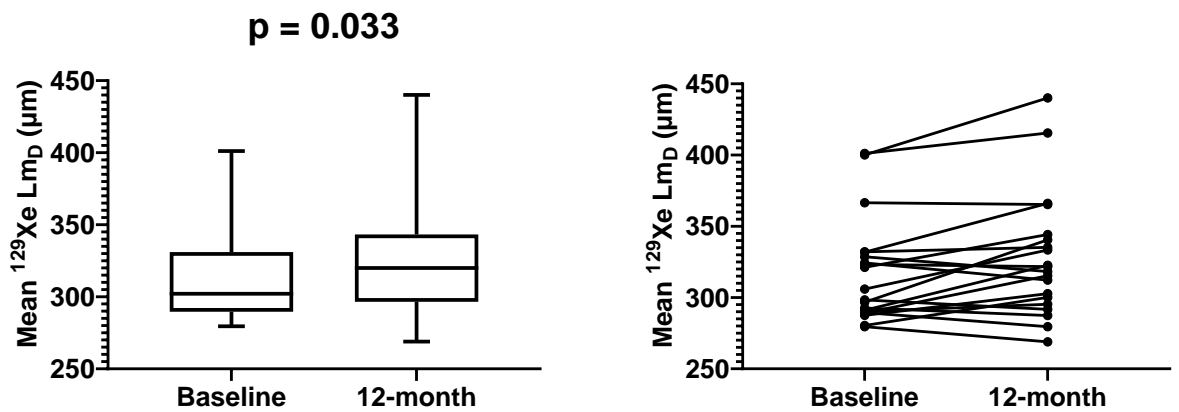


Figure 5.33. ^{129}Xe L_{mD} at the baseline visit versus the 12-month visit in the lower zone (n=20). Statistical test: Wilcoxon test.

5.4.5 Baseline, 3-month, 6-month and 12-month visits

^{129}Xe ADC and Lm_D data were available at each of the baseline, 3-month, 6-month and 12-month visits in 12 subjects. There were no statistically significant differences in global ^{129}Xe ADC or Lm_D between any of the study visits. For the same 12 subjects, there was a statistically significant decrease between the baseline and 3-month visits in FVC ($p=0.042$), between the baseline visit and 6-month visits in K_{CO} ($p=0.007$) and $\text{K}_{\text{CO}}\%$ ($p=0.009$), and between the 3-month and 6-month visits in K_{CO} ($p=0.014$) and $\text{K}_{\text{CO}}\%$ ($p=0.015$), as presented in Figures 5.9 and 5.11 in section 5.2.5. In the middle zone, there were statistically significant differences in ^{129}Xe ADC between the study visits ($p=0.022$; 3-month visit vs 12-month visit: $p=0.049$) (Figure 5.34). However, there were no statistically significant differences in regional ^{129}Xe Lm_D between any of the study visits.

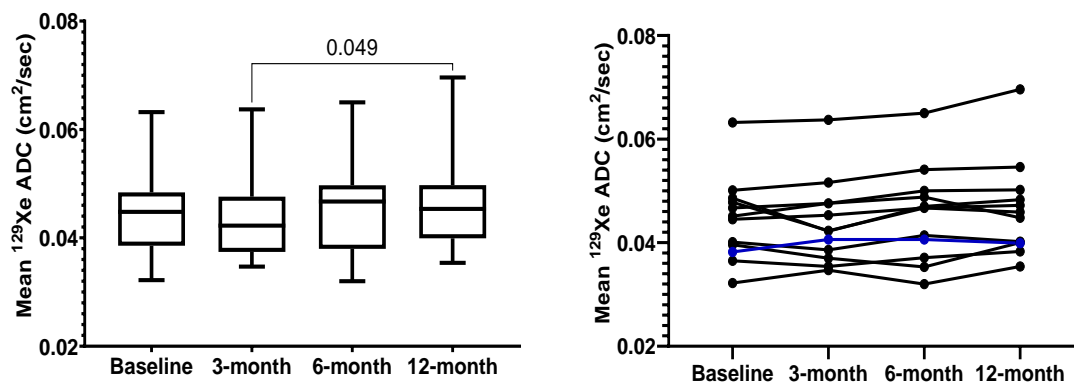


Figure 5.34. ^{129}Xe ADC at baseline, 3-month, 6-month and 12-month visits in the middle zone ($n=12$). The subject highlighted in blue commenced nintedanib approximately three months after the baseline study visit. Statistical test: one-way ANOVA.

5.4.6 Baseline, 6-month and 12-month visits in the total cohort

Out of the total study cohort ($n=49$), 27 subjects had DW-MRI data available at the baseline, 6-month and 12-month visits. There were statistically significant differences in Lm_D between the study visits ($p<0.001$; baseline vs 6-month: $p=0.047$; baseline vs 12-month: $p=0.003$; 6-month vs 12-month: $p=0.047$) (Figure 5.35).

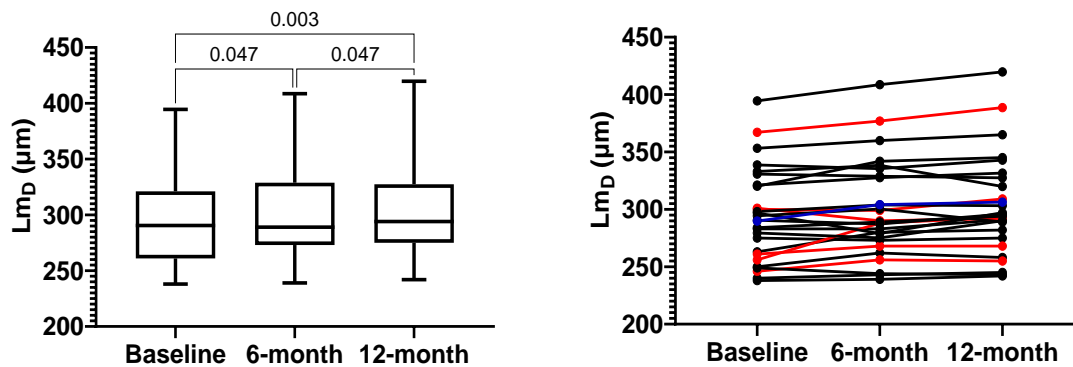


Figure 5.35. Lm_D at baseline, 6-month and 12-month visits ($n=27$). Subjects highlighted in red were taking antifibrotic therapy throughout the study. The subject highlighted in blue commenced nintedanib approximately three months after the baseline visit. Statistical test: one-way ANOVA.

In the same 27 subjects, between the baseline and 6-month visits, there was a statistically significant decrease in FVC ($p=0.032$), FVC% ($p=0.046$), K_{CO} ($p=0.007$) and $K_{CO}\%$ ($p=0.014$) (Figures 5.12 and 5.16 in section 5.2.6). There was also a statistically significant decrease in FVC between the baseline and 12-month visits ($p=0.049$) (Figure 5.12a-b in section 5.2.6).

5.5 Dynamic contrast enhanced MRI

22 (16.4%) of DCE-MRI scans were not of sufficient quality to perform accurate analysis.

	Subjects 1 – 49	Subjects 19 – 49
Baseline visit, n	40	28
3-month visit, n	20	20
6-month visit, n	27	16
12-month visit, n	25	16
All 4 visits, n	9	9

Table 5.29. The number of subjects in which DCE-MRI data was available for each study visit in the total study cohort and subjects 19-49.

5.5.1 Baseline visit

	Subjects 1 – 49	Subjects 19 – 49
FWHM (s)	7.04 (6.39 – 8.01)	7.08 (6.48 – 8.11)
MTT (s)	14.5 (13.1 – 15.9)	15.2 (13.5 – 17.1)
PBF (ml.mm³.s⁻¹)	38.4 (26.3 – 50.4)	42.6 (29.9 – 57.3)
PBV (ml.mm³)	9.04 (5.67 – 11.9)	10.8 (8.4 – 13.5)

FWHM: Full width of half maximum; MTT: Mean transit time; PBF: Pulmonary blood flow; PBV: Pulmonary blood volume.

Table 5.30. Global DCE-MRI results at the baseline visit in the total cohort (n=40) and subjects 19-49 (n=28). Results are presented as median (interquartile range).

	Subjects 1 – 49	Subjects 19 – 49
Full width of half maximum (s)		
Upper zone	7.10 (5.97 – 7.83)	7.13 (6.19 – 8.15)
Middle zone	6.87 (6.39 – 7.98)	6.88 (6.42 – 8.10)
Lower zone	7.61 (7.03 – 8.66)	7.77 (7.05 – 9.11)
Central zone	6.82 (6.19 – 7.99)	6.86 (6.28 – 7.97)
Peripheral zone	7.23 (6.37 – 8.17)	7.28 (6.70 – 8.29)
Mean transit time (s)		
Upper zone	14.1 (12.9 – 15.7)	15.0 (13.3 – 16.5)
Middle zone	14.3 (13.0 – 15.8)	14.9 (13.3 – 16.8)
Lower zone	15.2 (13.4 – 16.9)	15.7 (14.3 – 17.7)
Central zone	14.3 (12.7 – 15.6)	14.7 (12.9 – 16.7)
Peripheral zone	14.9 (13.5 – 16.4)	15.5 (13.9 – 17.3)
Pulmonary blood flow (ml.mm³.s⁻¹)		
Upper zone	34.3 (22.7 – 43.8)	41.5 (26.9 – 47.3)
Middle zone	39.1 (26.6 – 54.9)	42.4 (28.9 – 59.3)
Lower zone	45.4 (31.7 – 52.7)	47.7 (37.8 – 59.6)
Central zone	40.2 (26.7 – 52.8)	47.9 (32.5 – 58.3)
Peripheral zone	35.0 (24.5 – 45.6)	41.3 (29.1 – 56.6)
Pulmonary blood volume (ml.mm³)		
Upper zone	8.03 (4.83 – 10.9)	9.52 (6.93 – 11.0)
Middle zone	9.23 (5.70 – 13.1)	10.6 (8.36 – 14.0)
Lower zone	12.0 (7.45 – 13.7)	12.6 (11.3 – 15.9)
Central zone	9.63 (5.70 – 12.4)	10.8 (9.45 – 14.6)
Peripheral zone	9.23 (5.63 – 11.8)	10.5 (8.17 – 13.6)

Table 5.31. Regional DCE-MRI results at the baseline visit in the total cohort (n=40) and subjects 19-49 (n=28). Results are presented as median (interquartile range).

In the total cohort (n=40), there was a statistically significant difference between the upper, middle and lower zones in FWHM ($p < 0.001$; upper vs lower zone: $p < 0.001$; middle vs lower zone: $p < 0.001$), MTT ($p < 0.001$; upper vs lower zone: $p < 0.001$; middle vs lower zone: $p < 0.001$), PBF ($p < 0.001$; upper vs middle zone: $p < 0.001$; upper vs lower zone: $p < 0.001$) and PBV ($p < 0.001$; upper vs middle zone: $p < 0.001$; upper vs lower zone: $p < 0.001$; middle vs lower zone: $p < 0.001$) (Figures 5.36 and 5.37). There was also a statistically significant difference between the central and peripheral zones in FWHM ($p < 0.001$), MTT ($p < 0.001$), PBF ($p < 0.001$) and PBV ($p = 0.046$) (Figures 5.36 and 5.37).

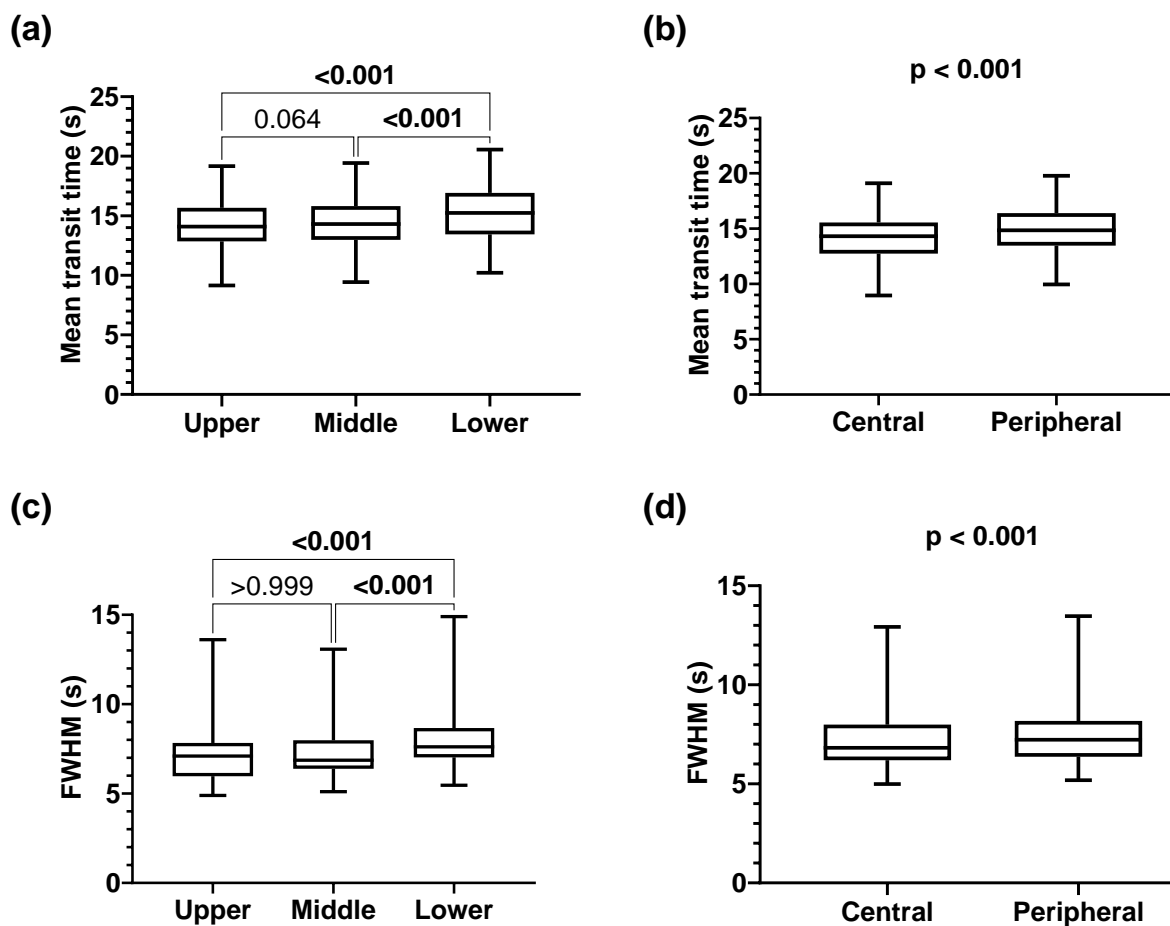


Figure 5.36. Regional differences in MTT (a-b) and FWHM (c-d) at the baseline visit (n=40). Statistical tests: one-way ANOVA (a), paired *t* test (b), Friedman test (c) and Wilcoxon test (d).

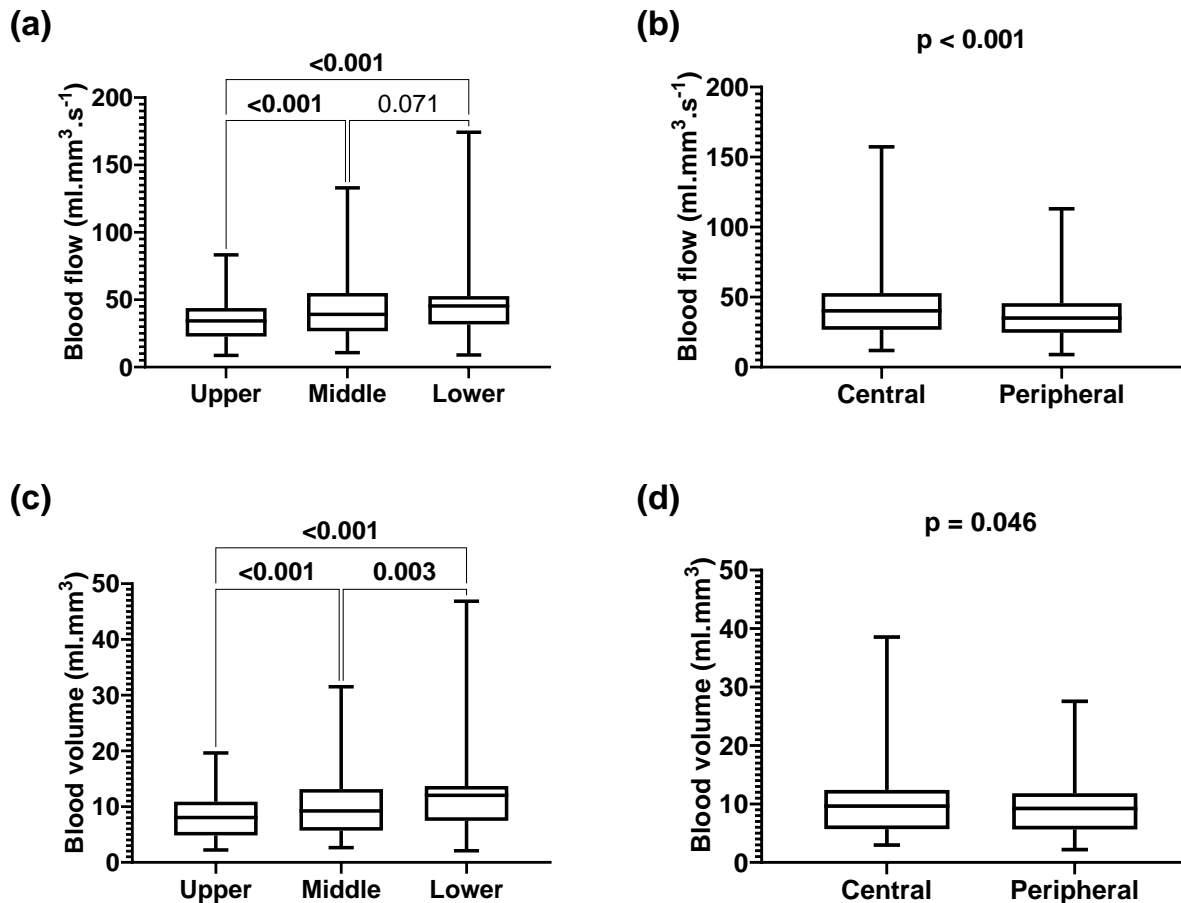


Figure 5.37. Regional differences in PBF (a-b) and PBV (c-d) at the baseline visit (n=40). Statistical tests: Friedman test and Wilcoxon test.

In subjects 19-49 (n=28), there was a statistically significant difference between the upper, middle and lower zones in FWHM ($p < 0.001$; upper vs lower zone: $p = 0.004$; middle vs lower zone: $p = 0.005$), MTT ($p < 0.001$; upper vs lower zone: $p < 0.001$; middle vs lower zone: $p < 0.001$), PBF ($p < 0.001$; upper vs middle zone: $p < 0.001$; upper vs lower zone: $p < 0.001$) and PBV ($p < 0.001$; upper vs middle zone: $p = 0.003$; upper vs lower zone: $p < 0.001$; middle vs lower zone: $p = 0.010$). There was also a statistically significant difference between the central and peripheral zones in FWHM ($p < 0.001$), MTT ($p < 0.001$) and PBF ($p = 0.001$).

5.5.2 3-month visit

	Median	Interquartile range
FWHM (s)	8.44	6.53 – 9.60
FWHM change (s)	0.15	-1.23 – 1.96
FWHM change (%)	1.72	-14.5 – 27.3
MTT (s)	16.2	13.7 – 18.1
MTT change (s)	0.42	-0.61 – 2.36
MTT change (%)	2.78	-3.64 – 14.3
PBF (ml.mm³.s⁻¹)	47.4	34.3 – 72.0
PBF change (ml.mm³.s⁻¹)	0.30	-20.4 – 29.0
PBF change (%)	0.73	-35.4 – 83.8
PBV (ml.mm³)	11.3	9.32 – 17.3
PBV change (ml.mm³)	-0.54	-4.26 – 7.86
PBV change (%)	-4.56	-28.2 – 89.5

FWHM: Full width of half maximum; MTT: Mean transit time; PBF: Pulmonary blood flow; PBV: Pulmonary blood volume.

Table 5.32. Global DCE-MRI results at the **3-month visit**, and the longitudinal change in global FWHM, MTT, PBF and PBV between the baseline and 3-month visits (n=20).

5.5.3 6-month visit

	Subjects 1 – 49	Subjects 19 – 49
FWHM (s)	6.87 (6.28 – 8.33)	7.13 (6.38 – 8.44)
FWHM change (s)	-0.11 (-1.37 – 1.03)	-0.32 (-1.36 – 1.07)
FWHM change (%)	-1.61 (-17.2 – 19.5)	-4.96 (-22.3 – 15.1)
MTT (s)	14.7 (13.2 – 16.0)	14.6 (13.5 – 16.8)
MTT change (s)	0.72 (-0.67 – 1.65)	0.36 (-0.88 – 1.50)
MTT change (%)	5.11 (-4.71 – 12.6)	2.62 (-7.05 – 10.1)
PBF (ml.mm³.s⁻¹)	31.2 (22.0 – 57.3)	50.0 (38.1 – 58.7)
PBF change (ml.mm³.s⁻¹)	-8.83 (-13.3 – 4.97)	-8.40 (-15.6 – 9.76)
PBF change (%)	-22.0 (-32.2 – 14.5)	-16.2 (-31.2 – 18.4)
PBV (ml.mm³)	8.57 (5.70 – 14.5)	13.4 (9.17 – 15.6)
PBV change (ml.mm³)	-1.57 (-2.27 – 1.34)	-1.74 (-4.00 – 3.53)
PBV change (%)	-15.2 (-25.3 – 20.4)	-16.9 (-24.9 – 35.6)

FWHM: Full width of half maximum; MTT: Mean transit time; PBF: Pulmonary blood flow; PBV: Pulmonary blood volume.

Table 5.33. Global DCE-MRI results at the **6-month visit**, and the longitudinal change in global FWHM, MTT, PBF and PBV between the baseline and 6-month visits in the total study cohort (n=27) and subjects 19-49 (n=16). Results are presented as median (interquartile range).

5.5.4 12-month visit

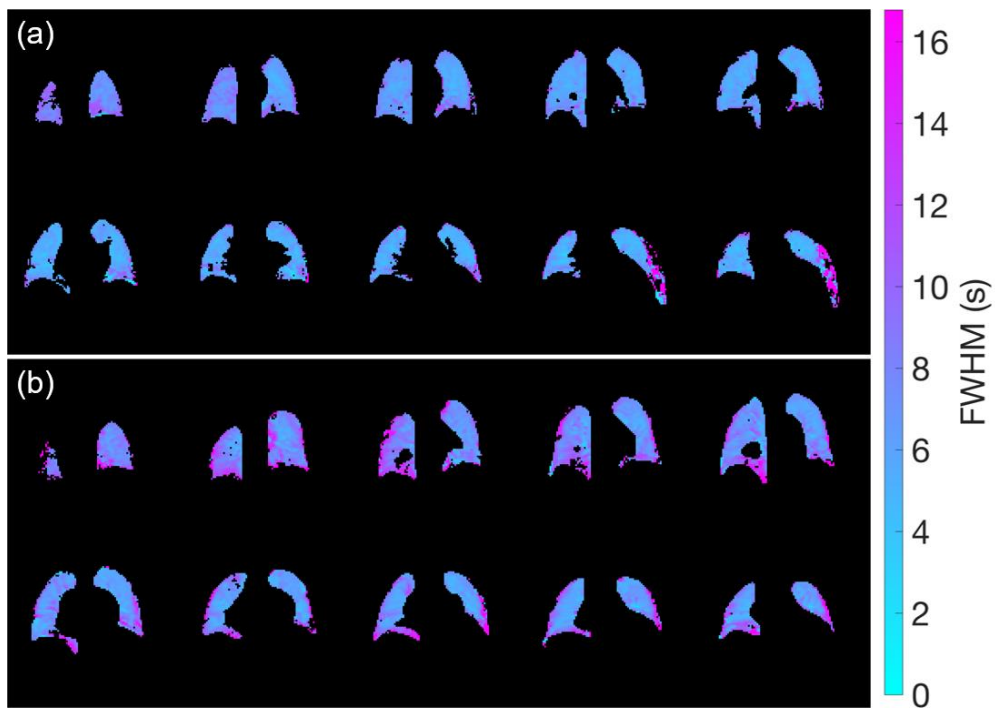


Figure 5.38. Example of FWHM maps at the baseline visit (a) and 12-month visit (b) in the same IPF subject.

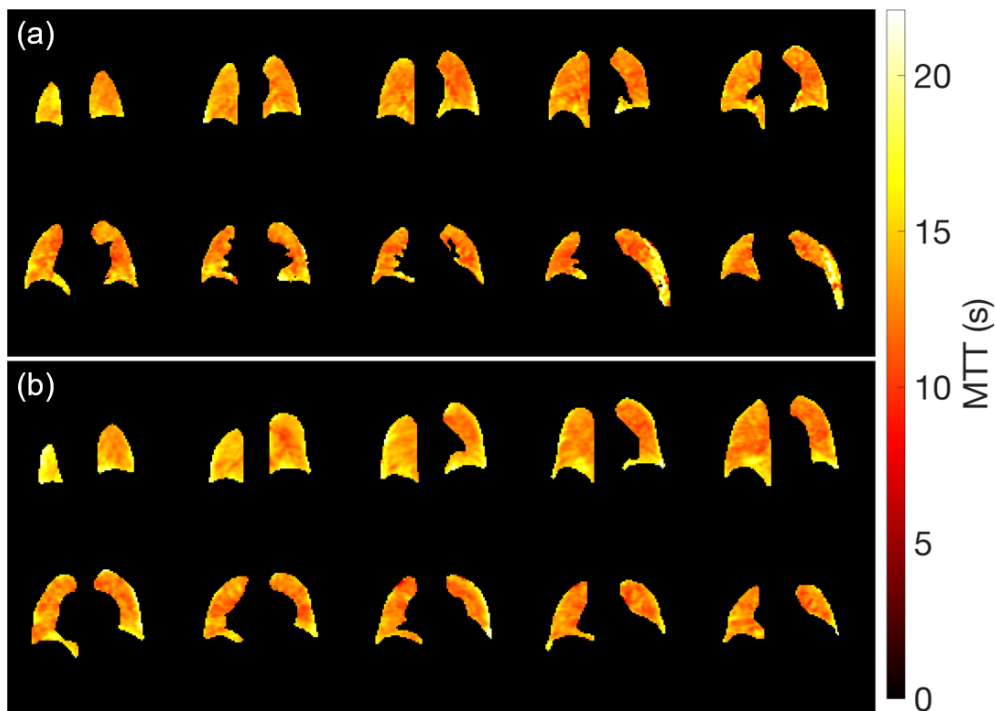


Figure 5.39. Example of MTT maps at the baseline visit (a) and 12-month visit (b) in the same IPF subject.

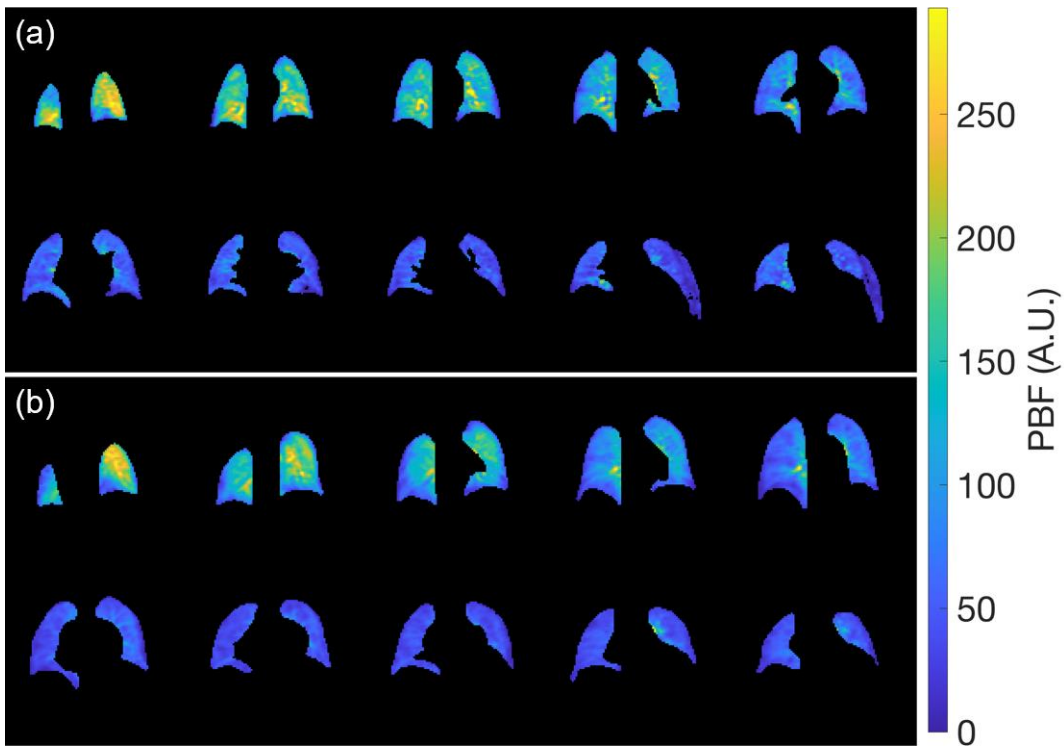


Figure 5.40. Example of PBF maps at the baseline visit (a) and 12-month visit (b) in the same IPF subject.

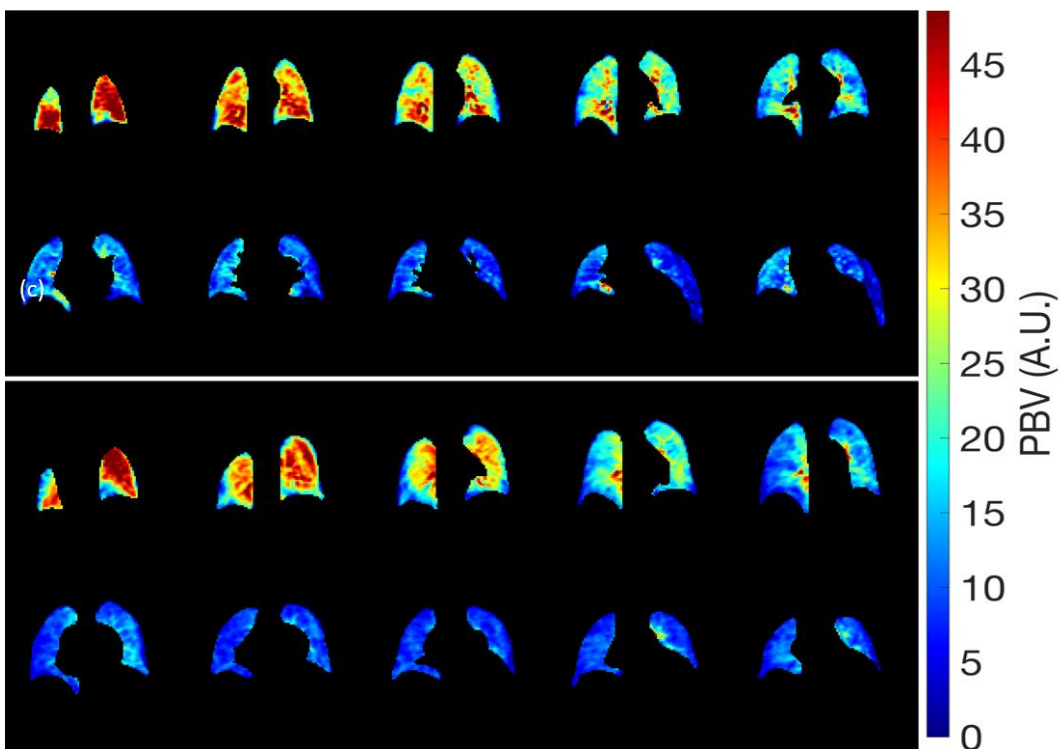


Figure 5.41. Example of PBV maps at the baseline visit (a) and 12-month visit (b) in the same IPF subject.

	Subjects 1 – 49	Subjects 19 – 49
FWHM (s)	6.62 (6.05 – 7.96)	6.56 (5.97 – 8.88)
FWHM change (s)	0.04 (-0.68 – 1.12)	-0.19 (-2.02 – 1.91)
FWHM change (%)	0.58 (-9.92 – 17.0)	-3.05 (-25.6 – 24.5)
MTT (s)	14.1 (12.9 – 15.7)	14.1 (12.7 – 17.1)
MTT change (s)	0.86 (-1.33 – 2.09)	0.54 (-3.55 – 3.60)
MTT change (%)	7.26 (-9.53 – 17.5)	3.99 (-20.6 – 27.6)
PBF (ml.mm³.s⁻¹)	39.3 (29.3 – 59.0)	54.8 (38.2 – 79.3)
PBF change (ml.mm³.s⁻¹)	2.43 (-8.31 – 24.2)	11.7 (-10.8 – 36.1)
PBF change (%)	6.54 (-19.5 – 58.1)	30.9 (-19.6 – 68.8)
PBV (ml.mm³)	11.1 (5.97 – 12.8)	12.4 (11.2 – 18.2)
PBV change (ml.mm³)	0.81 (-1.51 – 7.01)	3.58 (-3.10 – 7.73)
PBV change (%)	10.5 (-18.5 – 70.8)	40.4 (-22.8 – 105)

FWHM: Full width of half maximum; MTT: Mean transit time; PBF: Pulmonary blood flow; PBV: Pulmonary blood volume.

Table 5.34. Global DCE-MRI results at the **12-month visit**, and the longitudinal change in global FWHM, MTT, PBF and PBV between the baseline and 12-month visits in the total study cohort (n=25) and subjects 19-49 (n=16). Results are presented as median (interquartile range).

5.5.5 Baseline, 3-month, 6-month and 12-month visits

DCE-MRI data were available at each of the baseline, 3-month, 6-month and 12-month visits in 9 subjects. There were no statistically significant differences in global FWHM, MTT, PBF or PBV between any of the study visits. For the same 9 subjects, there was a statistically significant decrease between the baseline and 6-month visits in K_{co} ($p=0.011$) and K_{co} % predicted ($p=0.013$).

5.5.6 Baseline, 6-month and 12-month visits in the total cohort

Out of the total study cohort (n=49), 20 subjects had DCE-MRI data available at the baseline, 6-month and 12-month visits. There were no statistically significant differences in global FWHM, MTT, PBF or PBV between any of the study visits. For the same 20 subjects, there was a statistically significant decrease between the baseline and 6-month visits in K_{co} ($p=0.008$) and K_{co} % predicted ($p=0.013$).

In the lower zone, there were statistically significant differences in PBV between the study visits ($p=0.024$; 6-month visit vs 12-month visit: $p=0.023$) (Figure 5.42).

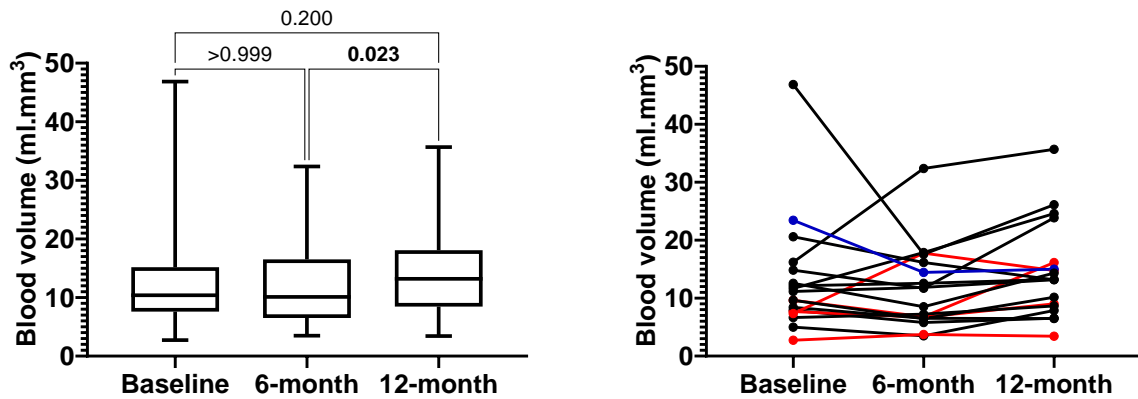


Figure 5.42. PBV at baseline, 6-month and 12-month visits in the lower zone (n=20). The subjects highlighted in red represent those taking antifibrotic therapy during the 12-month period. The subject highlighted in blue commenced nintedanib approximately three months after the baseline study visit. Statistical test: Friedman test.

5.6 CALIPER CT analysis

CALIPER CT analysis was performed on all available HRCT scans which provided both a global and regional measure of ground glass, honeycomb, reticular and VRS. Honeycomb and reticular measurements were combined and termed fibrosis. Ground glass, honeycomb and reticular measurements were also combined and termed ILD.

5.6.1 Study visits

In six subjects, the baseline visit CT was insufficient (not volumetric or contrast enhanced) for accurate CALIPER analysis and were not included in the dataset. Therefore, at the baseline visit, 43 out of the total study cohort of 49 subjects (27 out of 31 in subjects 19-49) were included in the CALIPER CT dataset. Only 20 of the 33 subjects in the total study cohort that completed the study had a CT performed at the 12-month study visit. Of the 20 subjects that had a CT performed at the 12-month study visit, in eight subjects the CT was insufficient (not volumetric or contrast enhanced) for accurate CALIPER analysis and were not included in the dataset. Therefore, at the 12-month visit, only 12 out of 33 subjects in the total study cohort (eight out of 20 in subjects 19-49) were included in the CALIPER CT dataset.

5.6.2 Baseline visit

	Subjects 1 – 49	Subjects 19 – 49
Fibrosis %	2.59 (1.46 – 5.84)	2.24 (1.38 – 5.06)
Ground glass %	4.04 (1.35 – 12.4)	2.27 (1.23 – 6.51)
Honeycomb %	0.09 (0.03 – 0.46)	0.09 (0.04 – 0.55)
ILD %	7.60 (3.40 – 19.4)	4.76 (3.27 – 11.5)
Reticular %	2.16 (1.43 – 4.57)	1.81 (1.32 – 4.51)
Vessel related structures %	2.88 (2.17 – 4.65)	2.57 (2.16 – 3.51)

Table 5.35. Global CALIPER CT results at the baseline visit in the total study cohort (n=43) and subjects 19-49 (n=27). Results are presented as median (interquartile range).

In the total study cohort (n=43), at the baseline visit there was a statistically significant difference ($p < 0.001$) between the upper and middle zones, upper and lower zones, and middle and lower zones in fibrosis %, ground glass %, honeycomb %, ILD %, and reticular %, as well as a statistically significant difference ($p < 0.001$) between the upper and middle zones, and upper and lower zones in VRS % (Figure 5.43). In the total study cohort (n=43), at the baseline visit there was a statistically significant difference between the central and peripheral zones in fibrosis % ($p < 0.001$), ground glass % ($p < 0.001$), honeycomb % ($p = 0.019$), ILD % ($p < 0.001$), reticular % ($p < 0.001$) and VRS % ($p < 0.001$) (Figure 5.44).

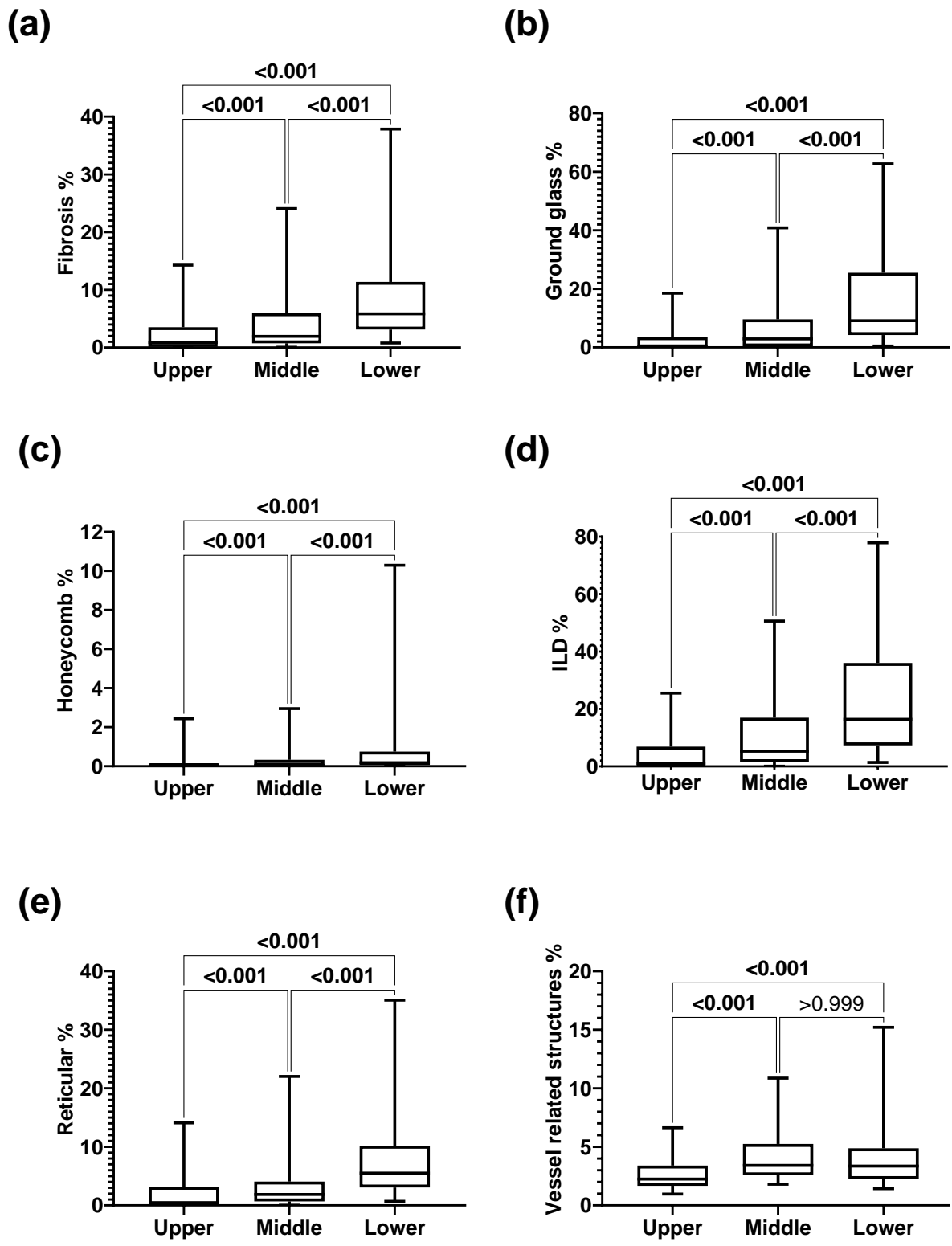


Figure 5.43. CALIPER fibrosis % (a), ground glass % (b), honeycomb % (c), ILD % (d), reticular % (e), VRS % (f) in the upper, middle and lower zones at baseline visit (n=43). Statistical test: Friedman test.

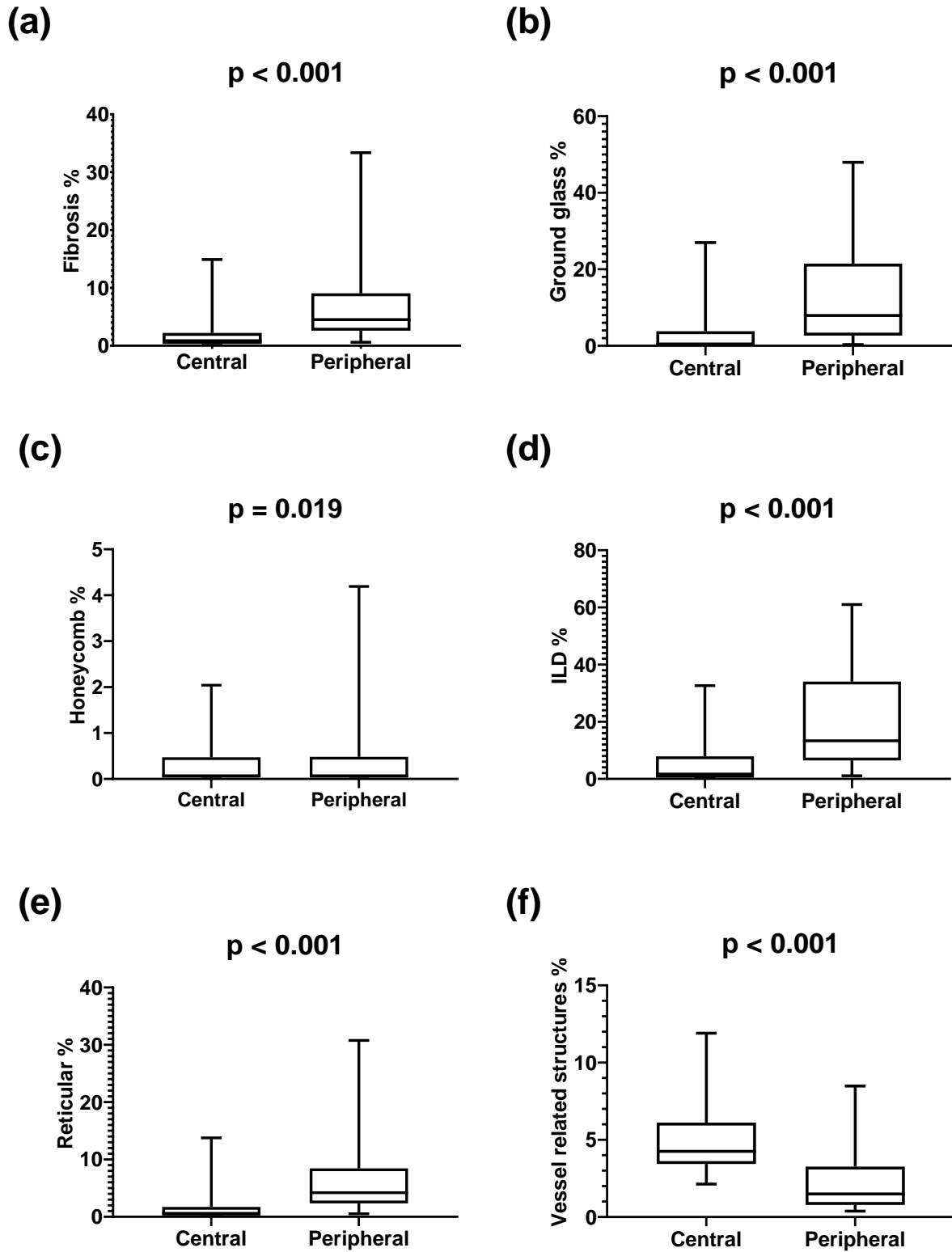


Figure 5.44. CALIPER fibrosis % (a), ground glass % (b), honeycomb % (c), ILD % (d), reticular % (e), VRS % (f) in the central and peripheral zones at the baseline visit (n=43). Statistical test: Wilcoxon test.

	Subjects 1 – 49	Subjects 19 – 49
Fibrosis %		
Upper zone	0.86 (0.12 – 3.52)	0.44 (0.03 – 1.44)
Middle zone	1.94 (0.74 – 5.94)	1.50 (0.59 – 4.26)
Lower zone	5.85 (3.12 – 11.4)	5.68 (3.14 – 12.0)
Central zone	0.86 (0.31 – 2.21)	0.54 (0.31 – 1.86)
Peripheral zone	4.50 (2.59 – 9.06)	3.83 (2.59 – 9.06)
Ground glass %		
Upper zone	0.28 (0.01 – 3.50)	0.10 (0.00 – 1.44)
Middle zone	2.92 (0.34 – 9.63)	1.29 (0.30 – 6.75)
Lower zone	9.14 (4.23 – 25.5)	6.58 (2.80 – 12.7)
Central zone	0.30 (0.08 – 3.81)	0.23 (0.04 – 0.82)
Peripheral zone	7.91 (2.67 – 21.5)	4.66 (2.65 – 13.2)
Honeycomb %		
Upper zone	0.01 (0.00 – 0.14)	0.01 (0.00 – 0.35)
Middle zone	0.05 (0.02 – 0.33)	0.05 (0.02 – 0.33)
Lower zone	0.18 (0.07 – 0.75)	0.24 (0.09 – 0.84)
Central zone	0.07 (0.03 – 0.47)	0.09 (0.03 – 0.51)
Peripheral zone	0.07 (0.03 – 0.48)	0.12 (0.03 – 0.62)
ILD %		
Upper zone	1.04 (0.19 – 6.88)	0.63 (0.03 – 3.85)
Middle zone	5.28 (1.46 – 16.9)	3.48 (0.68 – 9.57)
Lower zone	16.4 (7.33 – 36.0)	12.6 (7.31 – 24.7)
Central zone	1.69 (0.44 – 7.87)	0.73 (0.37 – 2.67)
Peripheral zone	13.3 (6.47 – 34.0)	8.74 (6.25 – 21.1)
Reticular %		
Upper zone	0.47 (0.11 – 3.16)	0.39 (0.03 – 1.42)
Middle zone	1.87 (0.69 – 4.07)	1.50 (0.56 – 3.70)
Lower zone	5.51 (3.06 – 10.2)	4.16 (3.06 – 10.2)
Central zone	0.59 (0.23 – 1.72)	0.45 (0.23 – 1.41)
Peripheral zone	4.21 (2.34 – 8.44)	3.62 (2.52 – 8.44)
Vessel related structures %		
Upper zone	2.25 (1.67 – 3.40)	1.86 (1.66 – 2.30)
Middle zone	3.42 (2.57 – 5.25)	2.87 (2.46 – 4.22)
Lower zone	3.36 (2.25 – 4.88)	3.15 (2.22 – 4.20)
Central zone	4.25 (3.43 – 6.11)	3.85 (3.39 – 4.63)
Peripheral zone	1.49 (0.78 – 3.26)	1.29 (0.69 – 2.71)

Table 5.36. Regional CALIPER CT results at the baseline visit in the total study cohort (n=43) and subjects 19-49 (n=27). Results are presented as median (interquartile range).

5.6.3 12-month visit

	Subjects 1 – 49	Subjects 19 – 49
Fibrosis %	3.96 (1.20 – 6.17)	3.96 (1.46 – 14.2)
Fibrosis % change	0.45 (-0.03 – 2.08)	0.82 (-0.03 – 2.08)
Ground glass %	3.27 (0.84 – 7.83)	2.23 (0.54 – 7.47)
Ground glass % change	0.66 (-0.16 – 4.14)	-0.12 (-0.22 – 3.44)
Honeycomb %	0.14 (0.03 – 0.76)	0.36 (0.05 – 3.25)
Honeycomb % change	0.03 (-0.02 – 0.56)	0.08 (-0.02 – 1.56)
ILD %	7.54 (2.00 – 19.0)	7.43 (2.00 – 19.0)
ILD % change	2.12 (-0.09 – 4.51)	0.62 (-0.41 – 6.44)
Reticular %	3.92 (1.07 – 5.56)	3.92 (1.17 – 7.75)
Reticular % change	0.03 (-0.40 – 2.37)	0.00 (-0.40 – 2.37)
Vessel related structures %	3.21 (2.34 – 4.81)	3.21 (2.46 – 4.71)
Vessel related structures % change	0.30 (0.06 – 1.19)	0.09 (-0.12 – 0.90)

Table 5.37. Global CALIPER CT results at the **12-month visit** and the change in the global CALIPER CT measurements between the baseline and 12-month visits in the total study cohort (n=12) and subjects 19-49 (n=8). Results are presented as median (interquartile range).

There was no statistically significant change in global CALIPER CT measurements between the baseline and 12-month visits in the total study cohort or subjects 19-49. In the total study cohort (n=12), between the baseline and 12-month visits there was a statistically significant increase in ground glass % (median (%): 0.24 (0.01 – 1.33) vs 0.61 (0.17 – 3.52); p=0.024), honeycomb % (median (%): 0.01 (0.00 – 0.28) vs 0.03 (0.00 – 0.43); p=0.033) and VRS % (median (%): 2.19 (1.69 – 2.71) vs 2.83 (1.75 – 3.67); p=0.042) in the upper zone (Figure 5.42). There was also a statistically significant increase in ground glass % (median (%): 0.21 (0.02 – 0.52) vs 0.61 (0.04 – 3.06); p=0.034) and ILD % (median (%): 0.82 (0.37 – 2.08) vs 2.44 (0.37 – 12.2); p=0.012) in the central zone (Figure 5.43). In the same 12 subjects, between the baseline and 12-month visits there was a statistically significant decrease in FVC (p=0.043) and FVC % predicted (p=0.007). It is possible that the increase in CALIPER ground glass % in the central and upper zones represent early fine fibrosis which may progress to reticulation over time and it is conceivable that regions of emphysema in the upper zone of IPF subjects were incorrectly classified as honeycombing.

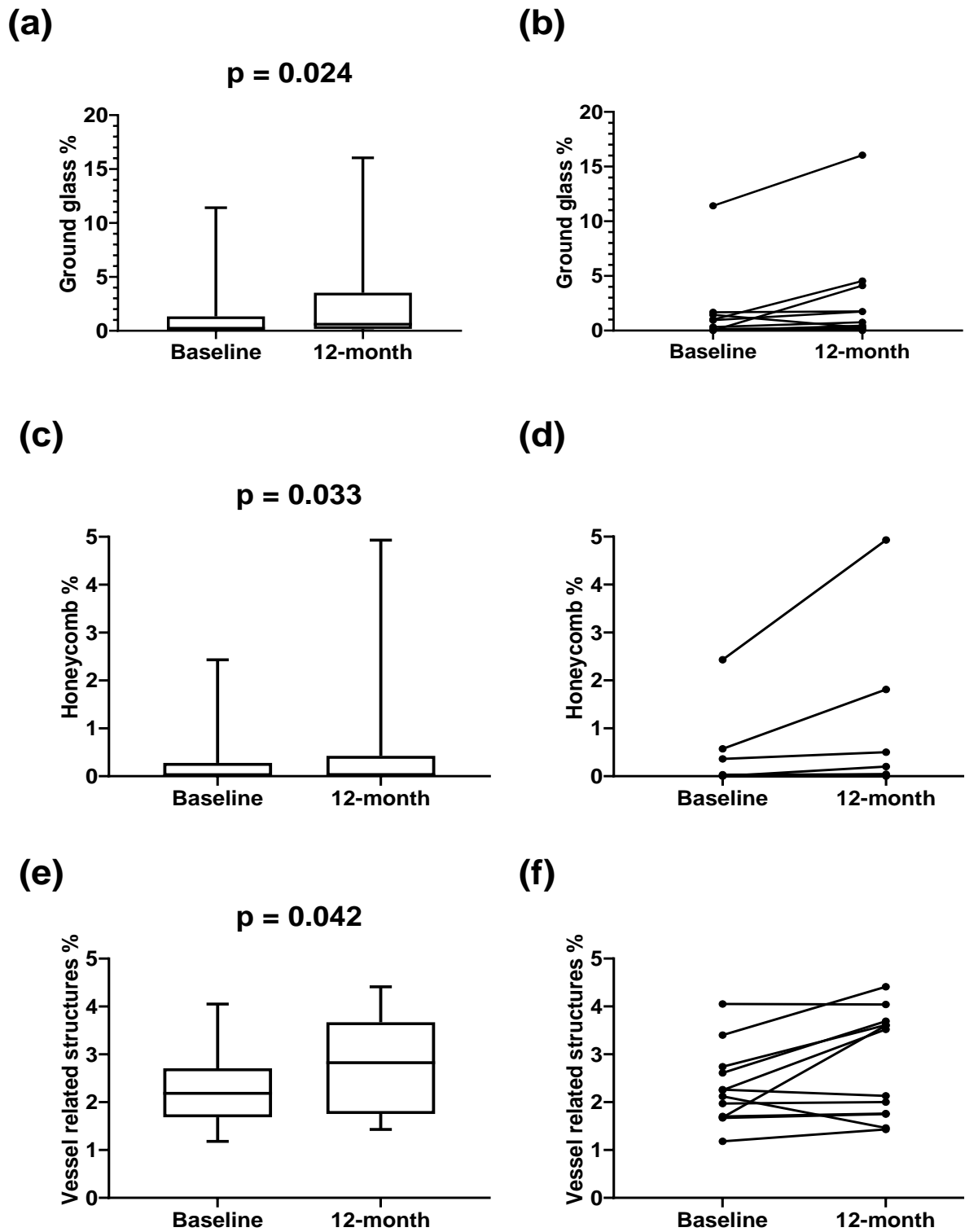


Figure 5.45. Upper zone ground glass % (a-b), honeycomb % (c-d) and VRS % (e-f) change between the baseline and 12-month visits in the total study cohort (n=12). Statistical test: Wilcoxon test.

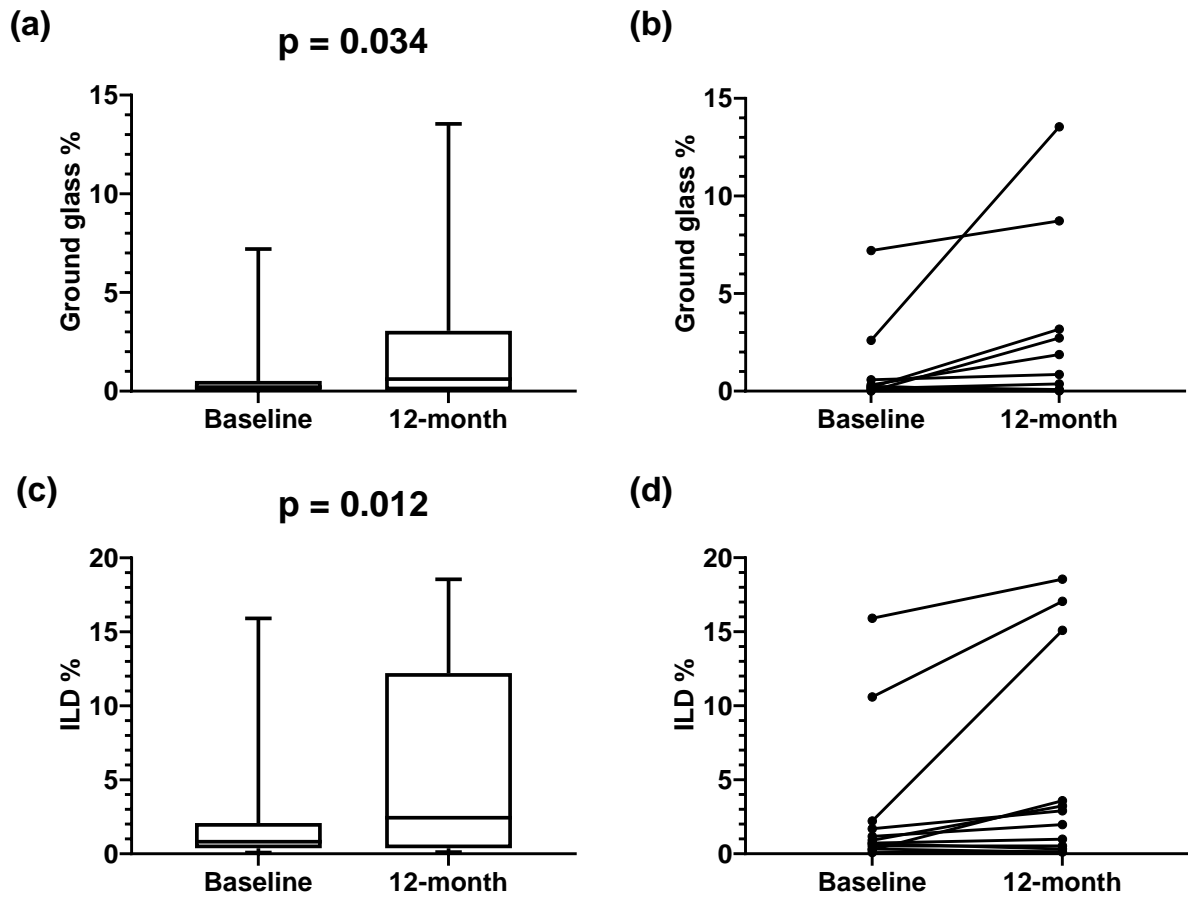


Figure 5.46. Central zone ground glass % (a-b) and ILD % (c-d) change between the baseline and 12-month visits in the total study cohort (n=12). Statistical test: Wilcoxon test.

	Subjects 1 – 49	Subjects 19 – 49
Fibrosis % change		
Upper zone	0.15 (-0.10 – 1.15)	0.11 (-0.10 – 2.12)
Middle zone	0.27 (-0.31 – 2.23)	0.84 (-0.31 – 2.32)
Lower zone	1.45 (-0.24 – 3.30)	1.48 (-0.10 – 3.30)
Central zone	0.37 (-0.11 – 0.92)	0.59 (0.00 – 1.08)
Peripheral zone	0.60 (-0.10 – 3.45)	0.88 (-0.10 – 3.45)
Ground glass % change		
Upper zone	0.29 (0.03 – 2.85)	0.09 (0.00 – 2.76)
Middle zone	0.94 (-0.04 – 4.10)	0.34 (-0.36 – 3.18)
Lower zone	1.52 (-0.40 – 7.45)	-0.33 (-1.88 – 2.98)
Central zone	0.26 (-0.02 – 2.43)	0.14 (-0.11 – 1.54)
Peripheral zone	1.26 (-0.31 – 5.80)	-0.15 (-1.52 – 5.12)
Honeycomb % change		
Upper zone	0.01 (0.00 – 0.18)	0.03 (0.00 – 0.97)
Middle zone	0.03 (-0.02 – 0.65)	0.03 (-0.05 – 1.52)
Lower zone	0.02 (-0.05 – 0.85)	0.20 (-0.05 – 1.00)
Central zone	0.04 (-0.01 – 0.47)	0.10 (-0.03 – 1.28)
Peripheral zone	0.05 (-0.02 – 0.66)	0.10 (-0.02 – 1.80)
ILD % change		
Upper zone	0.55 (-0.02 – 2.25)	0.34 (-0.02 – 4.24)
Middle zone	2.19 (-0.20 – 4.36)	1.61 (-0.77 – 5.04)
Lower zone	3.72 (-1.12 – 12.3)	0.28 (-1.97 – 11.3)
Central zone	1.00 (0.03 – 3.14)	0.74 (0.03 – 2.56)
Peripheral zone	0.41 (-0.52 – 6.98)	-0.10 (-0.90 – 11.3)
Reticular % change		
Upper zone	0.04 (-0.14 – 0.65)	0.02 (-0.14 – 0.95)
Middle zone	-0.03 (-0.41 – 2.15)	-0.10 (-0.41 – 2.37)
Lower zone	0.89 (-0.36 – 3.75)	0.93 (-0.36 – 3.75)
Central zone	0.07 (-0.18 – 0.70)	0.07 (-0.14 – 1.17)
Peripheral zone	0.22 (-0.69 – 3.65)	0.05 (-0.69 – 3.65)
Vessel related structures % change		
Upper zone	0.18 (0.00 – 1.06)	0.06 (-0.10 – 1.17)
Middle zone	0.49 (-0.07 – 1.00)	0.12 (-0.16 – 0.90)
Lower zone	0.26 (-0.18 – 1.28)	0.12 (-0.30 – 0.81)
Central zone	0.50 (-0.12 – 1.39)	0.10 (-0.36 – 1.27)
Peripheral zone	0.17 (0.02 – 0.92)	0.15 (-0.08 – 0.62)

Table 5.38. Change in regional CALIPER CT measurements between the baseline visit and the 12-month visit in the total study cohort (n=12) and subjects 19-49 (n=8). Results are presented as median (interquartile range).

5.7 Visual CT scoring

Visual CT scoring was performed by two consultant thoracic radiologists on all available CT scans. This provided global and regional ground glass, honeycomb and reticular scores. As with the CALIPER CT data, honeycomb and reticular scores were combined and termed fibrosis score. Also, ground glass, honeycomb and reticular scores were combined and termed ILD score.

5.7.1 Study visits

Visual CT score data was available for each subject that completed the baseline visit and for each subject that had a CT scan performed at the 12-month visit. At the 12-month visit, the visual CT scoring dataset included 20 subjects in the total study cohort and ten in subjects 19-49.

5.7.2 Baseline visit

	Subjects 1 – 49	Subjects 19 – 49
Fibrosis score	8.00 (5.00 – 13.50)	8.00 (4.00 – 11.00)
Ground glass score	1.00 (0.00 – 4.00)	2.00 (0.00 – 6.00)
Honeycomb score	0.00 (0.00 – 4.50)	0.00 (0.00 – 1.00)
ILD score	12.00 (6.50 – 16.00)	11.00 (6.00 – 16.00)
Reticular score	8.00 (5.00 – 10.00)	6.00 (4.00 – 8.00)

Table 5.39. Global visual CT scores at the baseline visit in the total study cohort (n=49) and subjects 19-49 (n=31). Results are presented as median (interquartile range).

In the total study cohort (n=49), at the baseline visit there was a statistically significant difference ($p<0.001$) between the upper and lower zones, and between the middle and lower zones in fibrosis score, ILD score and reticular score (Figure 5.47). In subjects 19-49 (n=31), at the baseline visit there was also a statistically significant difference ($p<0.001$) between the upper and lower zones, and between the middle and lower zones in fibrosis score, ILD score and reticular score.

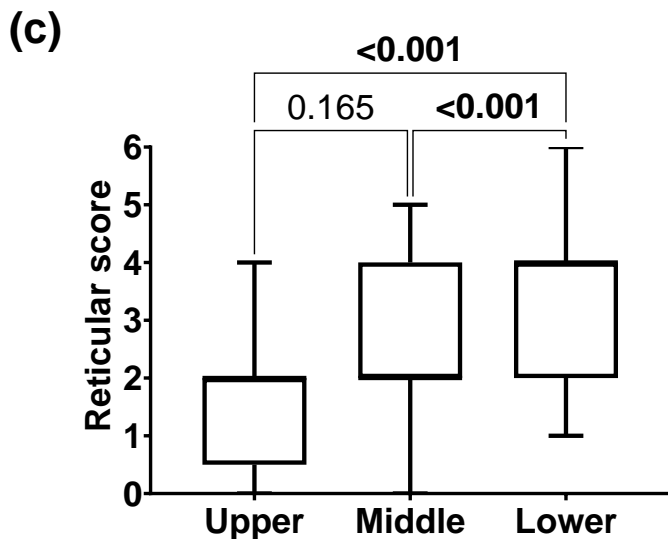
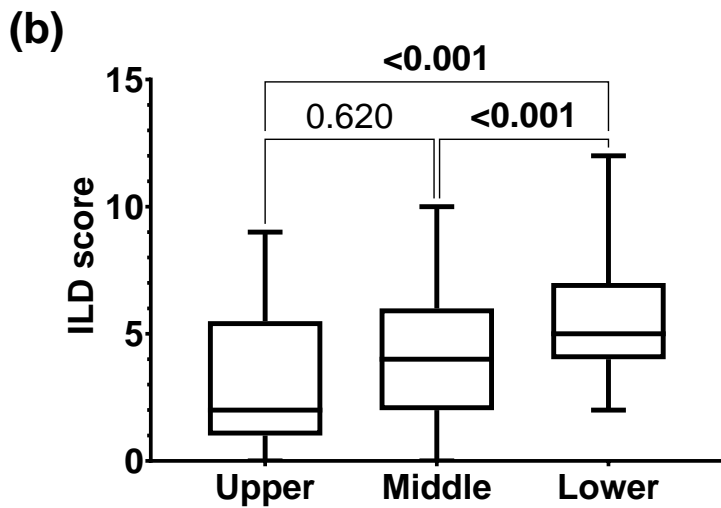
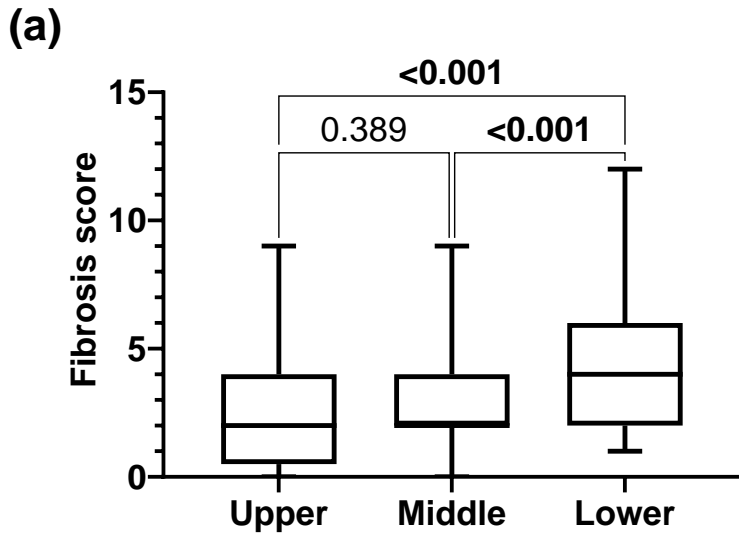


Figure 5.47. Visual CT fibrosis score, ILD score (b) and reticular score (c) in the upper, middle and lower zones at the baseline visit in the total study cohort (n=49). Statistical test: Friedman test.

	Subjects 1 – 49	Subjects 19 – 49
Fibrosis score		
Upper zone	2.00 (0.50 – 4.00)	2.00 (0.00 – 3.00)
Middle zone	2.00 (2.00 – 4.00)	2.00 (2.00 – 4.00)
Lower zone	4.00 (2.00 – 6.00)	4.00 (2.00 – 5.00)
Ground glass score		
Upper zone	0.00 (0.00 – 2.00)	0.00 (0.00 – 2.00)
Middle zone	0.00 (0.00 – 2.00)	0.00 (0.00 – 2.00)
Lower zone	0.00 (0.00 – 2.00)	2.00 (0.00 – 2.00)
Honeycomb score		
Upper zone	0.00 (0.00 – 1.00)	0.00 (0.00 – 0.00)
Middle zone	0.00 (0.00 – 1.50)	0.00 (0.00 – 0.00)
Lower zone	0.00 (0.00 – 2.00)	0.00 (0.00 – 1.00)
ILD score		
Upper zone	2.00 (1.00 – 5.50)	2.00 (0.00 – 5.00)
Middle zone	4.00 (2.00 – 6.00)	2.00 (2.00 – 4.00)
Lower zone	5.00 (4.00 – 7.00)	4.00 (4.00 – 7.00)
Reticular score		
Upper zone	2.00 (0.50 – 2.00)	2.00 (0.00 – 2.00)
Middle zone	2.00 (2.00 – 4.00)	2.00 (2.00 – 2.00)
Lower zone	4.00 (2.00 – 4.00)	4.00 (2.00 – 4.00)

Table 5.40. Regional visual CT scores at the baseline visit in the total study cohort (n=49) and subjects 19-49 (n=31). Results are presented as median (interquartile range).

5.7.3 12-month visit

There was no statistically significant change in any global or regional visual CT scores between the baseline visit and the 12-month visit in the total study cohort or subjects 19-49.

	Subjects 1 – 49	Subjects 19 – 49
Fibrosis score	10.00 (6.25 – 12.75)	9.50 (4.75 – 11.50)
Fibrosis score change	0.00 (0.00 – 0.00)	0.00 (0.00 – 0.00)
Ground glass score	0.00 (0.00 – 5.75)	2.50 (0.00 – 6.00)
Ground glass score change	0.00 (0.00 – 0.00)	0.00 (0.00 – 0.00)
Honeycomb score	1.50 (0.00 – 5.75)	2.00 (0.00 – 5.50)
Honeycomb score change	0.00 (0.00 – 0.00)	0.00 (0.00 – 0.00)
ILD score	12.50 (8.00 – 15.75)	12.50 (6.50 – 15.25)
ILD score change	0.00 (0.00 – 0.00)	0.00 (-2.00 – 0.00)
Reticular score	8.00 (5.25 – 8.00)	6.00 (4.00 – 8.00)
Reticular score change	0.00 (0.00 – 0.00)	0.00 (0.00 – 0.00)

Table 5.41. Global visual CT scores at the **12-month visit** and the change in the global visual CT scores between the baseline and 12-month visits in the total study cohort (n=20) and subjects 19-49 (n=10). Results are presented as median (interquartile range).

5.8 Summary of the imaging outcomes in the IPF study

The key imaging outcomes which demonstrated statistical significance were:

- 1) In the total study cohort, there was a decrease in global ^{129}Xe RBC:TP and an increase in global Lm_D between the baseline and 6-month visits, and between the baseline and 12-month visits. There was a statistically significant decrease in FVC, FVC % predicted, D_{LCO} , K_{CO} and K_{CO} % predicted between the baseline and 6-month visits, but not between the baseline and 12-month visits.
- 2) In subjects 19-49, there was an increase in global ^{129}Xe ADC between the baseline and 12-month visits, whereas there was no statistically significant change in PFTs over the same time period. There was also an increase in ^{129}Xe ADC in the lower and peripheral zones, and an increase in ^{129}Xe Lm_D in the lower zone between the baseline and 12-month visits.
- 3) In subjects 19-49, there was an increase in ^{129}Xe ADC in the middle and central zones between the baseline and 6-month visits. There was a statistically significant decrease in D_{LCO} , K_{CO} and K_{CO} % predicted over the six months.

- 4) In 12 subjects out of the total cohort, between the baseline and 12-month visits there was an increase in CALIPER CT ground glass %, honeycomb % and VRS % in the upper zone, and an increase in CALIPER CT ground glass % and ILD % in the central zone.

5.9 Correlations

Correlation analysis involving data from PFTs, global MRI measurements and global CT measurements were performed for each study visit in the total study cohort. Data from each study visit for each type of measurement was also combined. The same approach was taken for the regional MRI and CT data to perform correlation analysis. In addition to this, correlation analysis of the longitudinal change in the various measurements was performed.

5.9.1 Very strong correlations ($r = 0.80 - 0.99$)

At the 12-month visit, there were very strong negative correlations between CALIPER ILD % and K_{CO} ($r=-0.81$; $p=0.002$), and between ^{129}Xe DW-MRI measurements and K_{CO} (Figure 5.48).

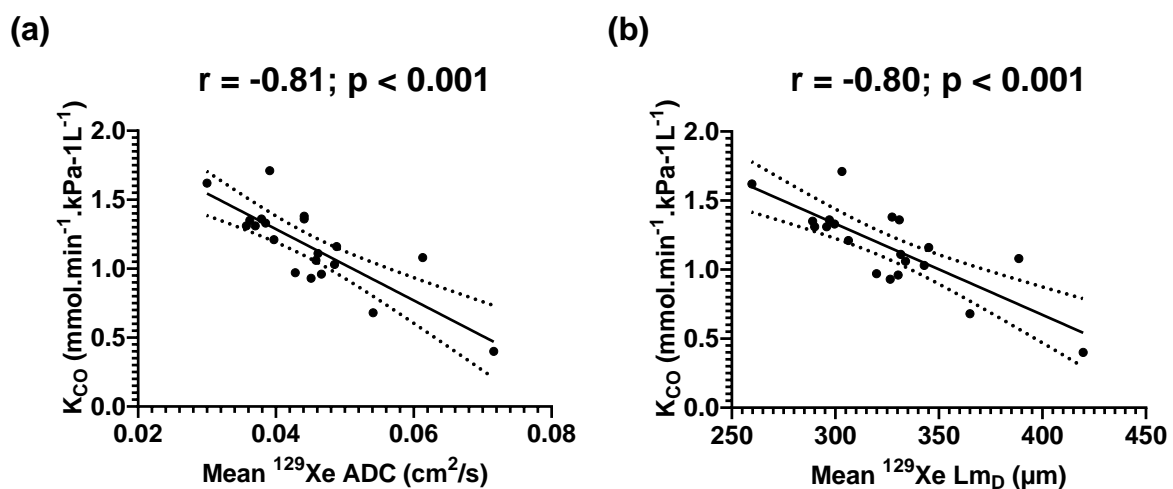


Figure 5.48. Correlation between K_{CO} and ^{129}Xe ADC (a), and between K_{CO} and ^{129}Xe L_{mD} (b) at the 12-month visit ($n=20$). Statistical test: Pearson correlation coefficient.

CALIPER CT measurement	Visual CT score(s)	Visit(s)
Honeycomb %	Honeycomb	12-month
ILD %	Fibrosis & ILD	12-month
Vessel related structures %	Fibrosis	Baseline; 12-month; baseline & 12-month combined
	ILD	12-month

CALIPER: Computer-Aided Lung Informatics for Pathology Evaluation and Rating; CT: Computed tomography; ILD: Interstitial lung disease.

Table 5.42. Very strong correlations between global CALIPER CT measurements and visual CT scores.

In the lower zone, there was a very strong correlation between the change in ^{129}Xe RBC:Gas and the change in PBF between the baseline and 12-month visits ($r=-0.90$; $p=0.028$). In the peripheral zone, very strong correlations were found between the change in CALIPER honeycomb % and the change in ^{129}Xe DW-MRI measurements between the baseline and 12-month visits (Figure 5.49).

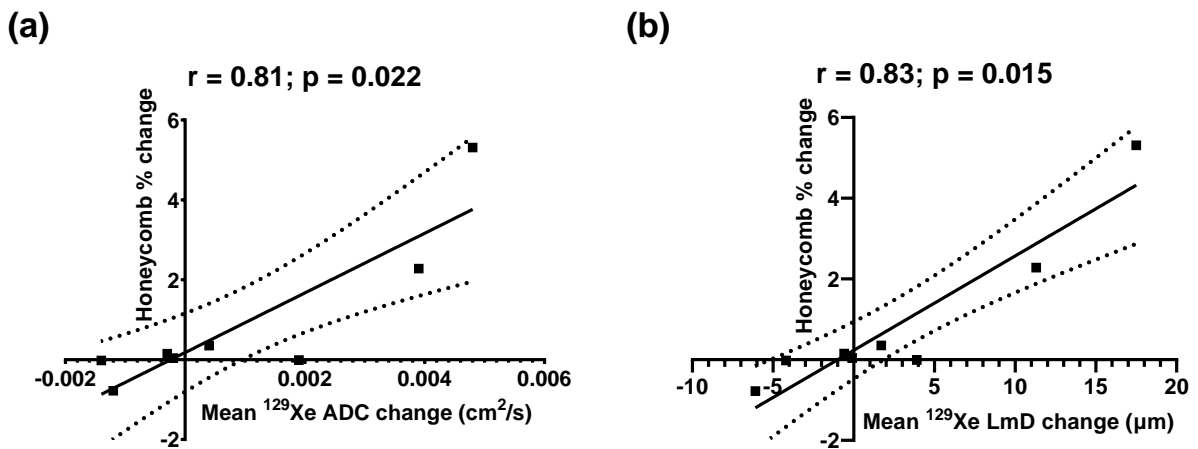


Figure 5.49. Correlations between the change in CALIPER honeycomb % and the change in ^{129}Xe ADC (a) and LmD (b) between the baseline and 12-month visits (n=8). Statistical test: Spearman's rank correlation.

5.9.2 Strong correlations (r = 0.60 – 0.79)

¹²⁹ Xe MRI measurement	PFT	Visit(s)
ADC	D _{LCO}	6-month; 12-month; 4 visits combined
	D _{LCO} %	Baseline; 3-month; 12-month
	K _{CO}	Baseline; 6-month; 4 visits combined
	K _{CO} %	Baseline; 3-month; 6-month; 12-month; 4 visits combined
L _{mD}	D _{LCO}	3-month; 6-month; 12-month; 4 visits combined
	D _{LCO} %	Baseline; 3-month; 12-month
	K _{CO}	Baseline; 6-month; 4 visits combined
	K _{CO} %	Baseline; 3-month; 6-month; 12-month; 4 visits combined
RBC:TP	FVC	3-month
	D _{LCO}	3-month & 12-month
	D _{LCO} % & K _{CO} %	12-month

ADC: Apparent diffusion coefficient; D_{LCO}: Diffusing capacity of the lung for carbon monoxide; FVC: Forced vital capacity; K_{CO}: Carbon monoxide transfer coefficient; L_{mD}: Mean diffusive length scale; MRI: Magnetic resonance imaging; PFT: Pulmonary function test; RBC: Red blood cell; TP: Tissue plasma; ¹²⁹Xe: 129-xenon.

Table 5.43. Strong correlations between global ¹²⁹Xe MRI measurements and PFTs.

CALIPER CT measurement	Visual CT score(s)	Visit(s)
Ground glass %	Fibrosis	Baseline; 12-month; baseline & 12-month combined
	ILD	12-month; baseline & 12-month combined
	Reticular	Baseline; baseline & 12-month combined
Fibrosis %	Fibrosis & ILD	Baseline; 12-month; baseline & 12-month combined
	Honeycomb	12-month; baseline & 12-month combined
	Reticular	Baseline; baseline & 12-month combined
Honeycomb %	Honeycomb	Baseline; baseline & 12-month combined
ILD %	Fibrosis; ILD	Baseline; baseline & 12-month combined
	Honeycomb	12-month
	Reticular	Baseline; 12-month; baseline & 12-month combined
Reticular %	Fibrosis & ILD	Baseline; 12-month; baseline & 12-month combined
	Honeycomb	12-month
	Reticular	Baseline; baseline & 12-month combined
VRS %	Honeycomb & reticular	Baseline; 12-month; baseline & 12-month combined
	ILD	Baseline; baseline & 12-month combined

CALIPER: Computer-Aided Lung Informatics for Pathology Evaluation and Rating; CT: Computed tomography; ILD: Interstitial lung disease; VRS: Vessel related structures.

Table 5.44. Strong correlations between global CALIPER CT measurements and global visual CT scores.

CALIPER CT measurement	PFT	Visit(s)
Fibrosis %	FVC; K _{CO} ; K _{CO} %	12-month
	FVC%	Baseline & 12-month
	D _{LCO} & D _{LCO} %	Baseline; 12-month; baseline & 12-month combined
Ground glass %	FVC	12-month; baseline & 12-month combined
	FVC% & D _{LCO}	Baseline; baseline & 12-month combined
	D _{LCO} %	Baseline; 12-month; baseline & 12-month combined
	K _{CO} & K _{CO} %	12-month
Honeycomb %	FVC%	12-month
ILD %	FVC	Baseline; baseline & 12-month combined
	FVC%; D _{LCO} ; D _{LCO} %	Baseline; 12-month; baseline & 12-month combined
	K _{CO} %	12-month
Reticular %	FVC	Baseline
	FVC%	Baseline; baseline & 12-month combined
	D _{LCO} & D _{LCO} %	Baseline; 12-month; baseline & 12-month combined
	K _{CO} & K _{CO} %	12-month
VRS %	FVC	Baseline
	FVC%; D _{LCO} ; D _{LCO} %	Baseline; 12-month; baseline & 12-month combined
	K _{CO} & K _{CO} %	12-month

CPI: Composite physiologic index; D_{LCO}: Diffusing capacity of the lung for carbon monoxide; FVC: Forced vital capacity; ILD: Interstitial lung disease; K_{CO}: Carbon monoxide transfer coefficient; PFT: Pulmonary function test; VRS: Vessel related structures.

Table 5.45. Strong correlations between global CALIPER CT measurements and PFT.

Visual CT score	PFT	Visit(s)
Fibrosis	D _{LCO}	Baseline
	D _{LCO} %	Baseline; baseline & 12-month combined
Honeycomb	D _{LCO} %	12-month
ILD	D _{LCO} %	Baseline

CPI: Composite physiologic index; CT: Computed tomography; D_{LCO}: Diffusing capacity of the lung for carbon monoxide; ILD: Interstitial lung disease; PFT: Pulmonary function test.

Table 5.46. Strong correlations between global visual CT scores and PFTs.

There was a strong correlation between global FWHM and CALIPER reticular % ($r=0.76$; $p=0.015$) at the 12-month visit. Between the baseline and 12-month visits, a strong negative correlation was seen between the change in global ¹²⁹Xe RBC:TP and ADC ($r=-0.64$; $p=0.005$), between the change in global ¹²⁹Xe ADC and K_{CO} ($r=-0.64$; $p=0.002$), between the change in global ¹²⁹Xe L_{MD} and K_{CO} ($r=-0.62$; $p=0.004$), and between the change in CALIPER VRS % and PFTs (FVC, D_{LCO} and K_{CO}). The change in CALIPER ILD % also correlated strongly with D_{LCO} and K_{CO} between the baseline and 12-month visits.

¹²⁹ Xe IDEAL spectroscopic imaging measurement	Other MRI measurement(s)	Zone(s)	Visit
TP:Gas	ADC & L _{mD}	Lower & peripheral	12-month
	PBF	Middle & central	3-month
RBC:Gas	L _{mD}	Lower	12-month
	PBF	Central	3-month

ADC: Apparent diffusion coefficient; IDEAL: Iterative decomposition of water and fat with echo asymmetry and least-squares estimation; L_{mD}: Mean diffusive length scale; MRI: Magnetic resonance imaging; PBF: Pulmonary blood flow; RBC: Red blood cell; TP: Tissue plasma; ¹²⁹Xe: 129-xenon.

Table 5.47. Strong correlations between regional ¹²⁹Xe IDEAL spectroscopic imaging measurements and other regional MRI measurements.

MRI measurement	CALIPER CT measurement(s)	Zone(s)	Visit
FWHM	Fibrosis % & honeycomb %	Upper	12-month
	Fibrosis % & reticular %	Peripheral	12-month
¹²⁹ Xe TP:Gas	Ground glass %	Upper & peripheral	Baseline
¹²⁹ Xe RBC:Gas	Honeycomb %	Middle	Baseline
	Vessel related structures %	Middle & lower	Baseline
¹²⁹ Xe RBC:TP	Vessel related structures %	Upper; middle; central; peripheral	Baseline

CALIPER: Computer-Aided Lung Informatics for Pathology Evaluation and Rating; CT: Computed tomography; FWHM: Full width of half maximum; MRI: Magnetic resonance imaging; RBC: Red blood cell; TP: Tissue plasma; ¹²⁹Xe: 129-xenon.

Table 5.48. Strong correlations between regional MRI measurements and regional CALIPER CT measurements.

MRI measurement	Visual CT score	Visit	Zone
FWHM	Honeycomb	12-month	Middle
MTT	Honeycomb	12-month	Middle
¹²⁹ Xe ADC	Ground glass	12-month	Lower
¹²⁹ Xe RBC:TP	ILD	Baseline	Middle

ADC: apparent diffusion coefficient; CT: Computed tomography; FWHM: Full width of half maximum; MRI: Magnetic resonance imaging; MTT: Mean transit time; RBC: Red blood cell; TP: Tissue plasma; ¹²⁹Xe: 129-xenon.

Table 5.49. Strong correlations between regional MRI measurements and regional visual CT measurements.

5.9.3 Moderate correlations (r = 0.40 – 0.59)

MRI measurements		Visit
¹²⁹ Xe ADC	¹²⁹ Xe RBC:TP	12-month
	PBF & PBV	Baseline
¹²⁹ Xe Lm _D	¹²⁹ Xe RBC:TP	12-month
	PBF & PBV	Baseline
	MTT	3-month
¹²⁹ Xe RBC:TP	MTT	Baseline

ADC: Apparent diffusion coefficient; Lm_D: Mean diffusive length scale; MRI: Magnetic resonance imaging; MTT: Mean transit time; PBF: Pulmonary blood flow; PBV: Pulmonary blood volume; RBC: Red blood cell; TP: Tissue plasma; ¹²⁹Xe: 129-xenon.

Table 5.50. Moderate correlations between different global MRI measurements.

MRI measurement	PFT	Visit(s)
¹²⁹ Xe ADC	D _{LCO}	Baseline & 3-month
	D _{LCO} %	6-month & 4 visits combined
¹²⁹ Xe Lm _D	D _{LCO}	Baseline
	D _{LCO} %	6-month & 4 visits combined
¹²⁹ Xe RBC:TP	FEV ₁ & FVC%	3-month
	FVC	12-month & 4 visits combined
	D _{LCO}	6-month & 4 visits combined
	D _{LCO} %	3-month; 6-month; 4 visits combined
	K _{CO}	12-month
MTT	K _{CO} & K _{CO} %	3-month
PBF	D _{LCO} & D _{LCO} %	Baseline
PBV	D _{LCO} ; D _{LCO} %; K _{CO} ; K _{CO} %	Baseline

ADC: Apparent diffusion coefficient; D_{LCO}: Diffusing capacity of the lung for carbon monoxide; FEV₁: Forced expiratory volume in 1 second; FVC: Forced vital capacity; K_{CO}: Carbon monoxide transfer coefficient; Lm_D: Mean diffusive length scale; MRI: Magnetic resonance imaging; MTT: Mean transit time; PBF: Pulmonary blood flow; PBV: Pulmonary blood volume; PFT: Pulmonary function test; RBC: Red blood cell; TP: Tissue plasma ratio.

Table 5.51. Moderate correlations between global MRI measurements and PFTs.

CALIPER CT measurement	Visual CT score(s)	Visit(s)
Ground glass %	Honeycomb	Baseline; baseline & 12-month combined
	ILD	Baseline
Fibrosis %	Honeycomb	Baseline
Honeycomb %	Fibrosis & ILD	Baseline; baseline & 12-month combined
ILD %	Honeycomb	Baseline; baseline & 12-month combined
Reticular %	Honeycomb	Baseline; baseline & 12-month combined

CALIPER: Computer-Aided Lung Informatics for Pathology Evaluation and Rating; CT: Computed tomography.

Table 5.52. Moderate correlations between global CALIPER CT measurements and global visual CT scores.

CALIPER CT measurement	PFT	Visit(s)
Fibrosis %	FVC	Baseline; baseline & 12-month combined
	FVC%; K _{CO} ; K _{CO} %	Baseline & 12-month combined
Ground glass %	FEV ₁ ; FEV ₁ %; K _{CO} %	Baseline; baseline & 12-month combined
	FVC	Baseline
	D _{LCO}	12-month
	K _{CO}	Baseline & 12-month combined
ILD %	FEV ₁ ; FEV ₁ %; K _{CO} ; K _{CO} %	Baseline; baseline & 12-month combined
	FVC	12-month
Reticular %	FEV ₁	Baseline; baseline & 12-month combined
	FEV ₁ %; FVC; K _{CO} ; K _{CO} %	Baseline & 12-month combined
VRS %	FEV ₁ & FEV ₁ %	Baseline; baseline & 12-month combined
	FVC	Baseline & 12-month combined

CALIPER: Computer-Aided Lung Informatics for Pathology Evaluation and Rating; CT: Computed tomography; D_{LCO}: Diffusing capacity of the lung for carbon monoxide; FVC: Forced vital capacity; ILD: Interstitial lung disease; K_{CO}: Carbon monoxide transfer coefficient; PFT: Pulmonary function test; VRS: Vessel related structures.

Table 5.53. Moderate correlations between global CALIPER CT measurements and PFTs.

Visual CT score	PFT	Visit(s)
Fibrosis	FVC%; K _{CO} ; K _{CO} %	Baseline; 12-month; baseline & 12-month combined
	D _{LCO}	12-month; baseline & 12-month combined
	D _{LCO} %	12-month
Honeycomb	FVC% & D _{LCO}	Baseline; 12-month; baseline & 12-month combined
	D _{LCO} %	Baseline; baseline & 12-month combined
	K _{CO} & K _{CO} %	12-month
ILD	FVC%	Baseline; 12-month; baseline & 12-month combined
	D _{LCO}	Baseline; baseline & 12-month combined
	D _{LCO} %	12-month; baseline & 12-month combined
	K _{CO} & K _{CO} %	Baseline
Reticular	FVC%	Baseline; 12-month; baseline & 12-month combined
	D _{LCO} & D _{LCO} %	Baseline; baseline & 12-month combined

CPI: Composite physiologic index; CT: Computed tomography; D_{LCO}: Diffusing capacity of the lung for carbon monoxide; ILD: Interstitial lung disease; PFT: Pulmonary function test.

Table 5.54. Moderate correlations between global visual CT scores and PFTs.

At the 12-month visit, there was a moderate negative correlation between global ^{129}Xe RBC:TP and CALIPER ILD % ($r=-0.59$; $p=0.049$), and between global ^{129}Xe RBC:TP and visual CT honeycomb score ($r=-0.48$; $p=0.044$). At the baseline visit, moderate negative correlations were seen between global CALIPER ground glass % and both PBF ($r=-0.40$; $p=0.019$) and PBV ($r=-0.41$; $p=0.015$).

Between the baseline and 12-month visits, a moderate negative correlation was seen between the change in global ^{129}Xe RBC:TP and ^{129}Xe L_{mD} ($r=-0.59$; $p=0.010$) and between the change in global ^{129}Xe ADC and D_{LCO} ($r=-0.50$; $p=0.026$).

^{129}Xe IDEAL spectroscopic imaging measurement	CALIPER CT measurement(s)	Zone
RBC:TP	Fibrosis % & ILD %	Middle
	Ground glass % & ILD %	Peripheral
	Vessel related structures %	Lower
TP:Gas	Ground glass % & reticular %	Central
	ILD %	Upper

CALIPER: Computer-Aided Lung Informatics for Pathology Evaluation and Rating; CT: Computed tomography; IDEAL: Iterative decomposition of water and fat with echo asymmetry and least-squares estimation; ILD: Interstitial lung disease; RBC: Red blood cell; TP: Tissue plasma; ^{129}Xe : 129-xenon.

Table 5.55. Moderate correlations between regional ^{129}Xe IDEAL spectroscopic imaging measurements and CALIPER CT measurements at the baseline visit.

^{129}Xe MRI measurement	Visual CT score(s)	Zone
ADC	Fibrosis; honeycomb; ILD	Lower
L_{mD}	Fibrosis; honeycomb; ILD	Lower
RBC:Gas	Fibrosis & reticular	Lower
RBC:TP	Fibrosis; ground glass; reticular	Middle
TP:Gas	Ground glass & ILD	Upper

ADC: Apparent diffusion coefficient; CT: Computed tomography; ILD: Interstitial lung disease; L_{mD} : Mean diffusive length scale; MRI: Magnetic resonance imaging; RBC: Red blood cell; TP: Tissue plasma; ^{129}Xe : 129-xenon.

Table 5.56. Moderate correlations between regional ^{129}Xe MRI measurements and visual CT scores at the baseline visit.

¹²⁹ Xe DW-MRI measurement	Other MRI measurement(s)	Zone(s)	Visit(s)
ADC	¹²⁹ Xe TP:Gas	Middle; lower; peripheral	4 visits combined
	MTT	Upper & central	3-month
	PBF & PBV	Upper; middle; central; peripheral	Baseline
	PBF & PBV	Lower	Baseline & 12-month
Lm _D	¹²⁹ Xe TP:Gas	Middle; lower; peripheral	4 visits combined
	MTT	Upper & peripheral	3-month
	PBF & PBV	Upper; middle; lower central; peripheral	Baseline

ADC: Apparent diffusion coefficient; DW-MRI: Diffusion weighted magnetic resonance imaging; Lm_D: mean diffusive length scale; MRI: Magnetic resonance imaging; MTT: mean transit time; PBF: pulmonary blood flow; PBV: pulmonary blood volume; TP: tissue plasma; ¹²⁹Xe: 129-xenon.

Table 5.57. Moderate correlations between regional ¹²⁹Xe DW-MRI measurements and other regional MRI measurements.

¹²⁹ Xe DW-MRI measurement	DCE-MRI measurement(s)	Zone
ADC change	Change in: MTT & PBV	Peripheral
Lm _D change	Change in: MTT & PBF	Peripheral
	PBV change	Middle

ADC: apparent diffusion coefficient; DCE-MRI: dynamic contrast enhanced magnetic resonance imaging; DW-MRI: diffusion weighted magnetic resonance imaging; Lm_D: mean diffusive length scale; MTT: mean transit time; PBF: pulmonary blood flow; PBV: pulmonary blood volume; ¹²⁹Xe: 129-xenon.

Table 5.58. Moderate correlations between the change in regional ¹²⁹Xe DW-MRI measurements and the change in regional DCE-MRI measurements between the baseline and 6-month visits.

5.10 Variables that predict disease progression

Univariate logistic regression analysis was performed to identify any variables that were able to predict disease progression. The cohort included a total of 37 IPF subjects in which data was available to determine whether disease progression had occurred between the baseline visit and the 12-month visit. Disease progression was defined as death, lung transplantation, ≥10% absolute reduction in FVC% and/or ≥15% absolute reduction in DL_{CO}%.

The following variables were investigated:

- Age
- Gender
- Ever smoker
- BMI
- Antifibrotic therapy during study
- Baseline visit oxygen saturations
- Baseline visit PFTs (FEV₁, FEV₁%, FVC, FVC%, DLCO, DLCO%, Kco and Kco%), and the change between baseline and 3-month visits, and between baseline and 6-month visits.
- Baseline visit global ¹²⁹Xe RBC:TP, and the change between baseline and 3-month visits, and between baseline and 6-month visits.
- Baseline visit regional ¹²⁹Xe RBC:TP, TP:Gas and RBC:Gas, and the change between baseline and 3-month visits, and between baseline and 6-month visits.
- Baseline visit ¹²⁹Xe ADC and Lm_D (global and regional), and change between baseline and 3-month visits, and between baseline and 6-month visits.
- Baseline visit FWHM, MTT, PBF and PBV (global and regional), and change between baseline and 3-month visits, and between baseline and 6-month visits.
- Baseline visit CALIPER CT measurements (global and regional).
- Baseline visit visual CT scores (global and regional).

Variable	Odds ratio	95% confidence interval	P value
Baseline oxygen saturations	0.68	0.44 – 0.96	0.042
Baseline GAP stage	8.37	2.17 – 56.2	0.007
Baseline D _{LCO}	0.47	0.21 – 0.84	0.031
Baseline D _{LCO} %	0.93	0.87 – 0.98	0.012
Baseline K _{CO}	0.006	5.17e-005 – 0.24	0.016
Baseline K _{CO} %	0.94	0.88 – 0.98	0.020
Baseline global L _{mD}	1.03	1.01 – 1.07	0.019
Baseline global CALIPER CT fibrosis %	1.24	1.05 – 1.62	0.037
Baseline global CALIPER CT ILD %	1.08	1.01 – 1.17	0.026
Baseline global CALIPER CT reticular %	1.25	1.05 – 1.64	0.036
Baseline global visual CT fibrosis score	1.23	1.08 – 1.47	0.006
Baseline visual CT fibrosis score (upper zone)	1.91	1.28 – 3.40	0.007
Baseline visual CT fibrosis score (middle zone)	1.80	1.19 – 3.08	0.012
Baseline visual CT fibrosis score (lower zone)	1.44	1.07 – 2.06	0.023
Baseline global visual CT honeycomb score	1.24	1.04 – 1.52	0.020
Baseline visual CT honeycomb score (upper zone)	1.97	1.20 – 3.68	0.015
Baseline visual CT honeycomb score (middle zone)	2.01	1.03 – 3.66	0.045
Baseline visual CT honeycomb score (lower zone)	1.52	1.01 – 2.38	0.049
Baseline global visual CT ILD score	1.25	1.09 – 1.51	0.006
Baseline visual CT ILD score (upper zone)	1.81	1.26 – 2.94	0.004
Baseline visual CT ILD score (middle zone)	1.89	1.25 – 3.28	0.007
Baseline visual CT ILD score (lower zone)	1.42	1.06 – 2.03	0.029
Baseline global visual CT reticular score	1.91	1.28 – 3.45	0.009
Baseline visual CT reticular score (upper zone)	6.92	2.03 – 49.9	0.013
Baseline visual CT reticular score (middle zone)	2.95	1.39 – 7.46	0.010
Baseline visual CT reticular score (lower zone)	2.71	1.21 – 9.21	0.039
FVC change (baseline – 6-month visits)	0.99	0.98 – 1.00	0.043
FVC% absolute change (baseline – 6-month)	0.75	0.54 – 0.96	0.042
FVC% relative change (baseline – 6-month)	0.78	0.58 – 0.98	0.048

CALIPER: Computer-Aided Lung Informatics for Pathology Evaluation and Rating; CT: Computed tomography; D_{LCO}: Diffusing capacity of the lung for carbon monoxide; FVC: Forced vital capacity; GAP: Gender-age-physiology; K_{CO}: Carbon monoxide transfer coefficient; L_{mD}: mean diffusive length scale.

Table 5.59. Variables with a statistically significant odds ratio for predicting disease progression using univariate logistic regression analysis.

All of the variables in Table 5.59 still had a statistically significant odds ratio for predicting disease progression when age was added to the logistic regression model.

Imaging variable	Odds ratio	95% confidence interval	P value
Baseline ¹²⁹ Xe ADC (lower zone)	2.38e+046	2.803-005 – 8.66e+10	0.088
Baseline global ¹²⁹ Xe RBC:TP	2.83e-005	1.14e-011 – 1.46	0.098
Baseline global CALIPER CT GG %	1.08	0.99 – 1.20	0.083
Baseline global CALIPER CT VRS%	1.50	0.99 – 2.51	0.078
Global ¹²⁹ Xe ADC % change (baseline – 3-month visits)	1.38	1.03 – 2.26	0.095
¹²⁹ Xe ADC % change (lower zone) (baseline – 3-month visits)	1.33	1.03 – 2.09	0.086
Global Lm _D change (baseline – 3-month visits)	1.28	1.05 – 1.87	0.072
Global Lm _D % change (baseline – 3-month visits)	2.06	1.14 – 5.90	0.071
Lm _D change (lower zone) (baseline – 3-month visits)	1.36	1.07 – 2.28	0.095
Lm _D change (peripheral zone) (baseline – 3-month visits)	1.21	1.03 – 1.58	0.070
Lm _D % change (peripheral zone) (baseline – 3-month visits)	1.73	1.08 – 3.86	0.077
Global FWHM % change (baseline – 3-month visits)	0.91	0.78 – 0.99	0.081
FWHM % change (middle zone) (baseline – 3-month visits)	0.90	0.77 – 0.98	0.079
FWHM % change (central zone) (baseline – 3-month visits)	0.90	0.78 – 0.99	0.074
FWHM % change (peripheral zone) (baseline – 3-month visits)	0.92	0.80 – 0.99	0.094
PBF % change (lower zone) (baseline – 3-month visits)	1.02	1.00 – 1.05	0.076

ADC: apparent diffusion coefficient; CALIPER: Computer-Aided Lung Informatics for Pathology Evaluation and Rating; CT: Computed tomography; FWHM: Full width of half maximum; GG: Ground glass; Lm_D: mean diffusive length scale; PBF: Pulmonary blood flow; RBC: Red blood cell; TP: Tissue plasma; VRS: Vessel related structures; ¹²⁹Xe: 129-xenon.

Table 5.60. Imaging variables that had odds ratios with p values 0.05 – 0.10 for predicting disease progression using univariate logistic regression analysis.

5.11 Summary

The results reported in this chapter expands upon previous work involving novel MRI techniques in IPF. Novel findings include a statistically significant change in global Lm_D and ¹²⁹Xe RBC:TP over both six and 12 months, despite relatively stable PFTs. Also, there was evidence that DW-MRI measurements may have utility in the monitoring and prediction of disease progression in IPF.

Chapter 6: The Assessment of Interstitial Lung Disease Using Imaging Biomarkers – Discussion of Two Longitudinal Studies

6.1 Imaging outcomes

The results outlined in the previous two chapters builds on previously published work regarding the assessment of IPF using ^{129}Xe MRI and DCE-MRI techniques, and the evaluation of ILD patients with CALIPER CT analysis. The TRISTAN-ILD study demonstrates the first known application of ^{129}Xe MRI and DCE-MRI in subjects with a variety of different ILD subtypes, rather than focusing only on IPF.

This section of the discussion chapter will summarise the clinical outcomes from the TRISTAN-ILD and IPF studies and further explore the different imaging modalities in the context of previously published work.

6.1.1 Summary of the imaging outcomes in the TRISTAN-ILD study

Tables 6.1 and 6.2 provide a summary of the results from the global imaging measurements investigated in the TRISTAN-ILD study. The key imaging outcomes which demonstrated statistical significance were:

1. A difference in global ^{129}Xe ADC and L_{mD} between the ILD subtypes, and between the fibrotic and inflammation groups, with higher values seen in IPF versus HP, and in the fibrotic versus inflammation groups.
2. A decrease in global ^{129}Xe RBC:TP and an increase in global CALIPER CT VRS % in the IPF group over six months, with no statistically significant PFT change over the same time period.
3. An increase in global ^{129}Xe ADC and L_{mD} over six weeks in the DI-ILD group, with no statistically significant PFT change over the same time period.
4. A decrease in global MTT and increase in global PBF over six weeks in the HP group, with no statistically significant PFT change over the same time period.
5. A decrease in global CALIPER CT fibrosis %, ground glass %, ILD % and reticular % between visits 1 and 2 in the inflammation group, with no statistically significant PFT change over the same time period.

	¹²⁹ Xe spectroscopy	¹²⁹ Xe DW-MRI	¹²⁹ Xe ventilation	DCE-MRI
Differences between ILD subtypes	No	ADC and L _{mD} at visits 1 and 2 (higher in IPF vs HP group)	No	No
Difference between fibrotic & inflammation groups	No	ADC and L _{mD} at visits 1 and 2 (higher in fibrotic group)	No	No
Change between visit 1 & visit 2	Decrease in RBC:TP in IPF and fibrotic groups	Increase in ADC and L _{mD} in DI-ILD group	No	Decrease in MTT and increase in PBF in HP group
Correlations between MRI measurements	Moderate: ¹²⁹ Xe RBC:TP with PBV (r=0.56); ¹²⁹ Xe ADC and L _{mD} with VV%.			
Correlations with CT measurements	No	Strong: Visual CT fibrosis score (ADC and L _{mD}). Moderate: CALIPER honeycomb % (ADC and L _{mD}). Visual CT fibrosis, honeycomb, ILD and reticular scores (ADC and L _{mD}).	No	Moderate: PBV with CALIPER honeycomb %. MTT change with visual CT fibrosis score change. PBF change with change in visual CT fibrosis and honeycomb scores.
Correlations with PFTs	Moderate: D _{LCO} and D _{LCO} %.	Moderate: ADC and L _{mD} with D _{LCO} %.	No	Moderate: MTT change with FEV ₁ change. PBF change with D _{LCO} change.
Predictor of disease progression	No (close to statistical significance; p=0.075)	No	No	No

ADC: apparent diffusion coefficient; CALIPER: Computer-Aided Lung Informatics for Pathology Evaluation and Rating; CT: Computed tomography; DCE-MRI: Dynamic contrast enhanced magnetic resonance imaging; DI-ILD: Drug induced interstitial lung disease; D_{LCO}: Diffusing capacity of the lung for carbon monoxide; DW-MRI: Diffusion weighted magnetic resonance imaging; FEV₁: Forced expiratory volume in one second; HP: Hypersensitivity pneumonitis; ILD: Interstitial lung disease; IPF: Idiopathic pulmonary fibrosis; L_{mD}: mean diffusivity length scale; MTT: Mean transit time; PBF: Pulmonary blood flow; PBV: Pulmonary blood volume; PFT: Pulmonary function test; RBC: Red blood cell; TP: Tissue plasma; VV: Ventilated volume; ¹²⁹Xe: 129-xenon.

Table 6.1. Summary of the global MRI results in the TRISTAN-ILD study.

	CALIPER CT analysis	Visual CT scoring
Differences between ILD subtypes	No	Higher fibrosis score and lower ground glass score in IPF group vs HP group at visit 1.
Difference between fibrotic & inflammation groups	Higher ground glass % and ILD % in inflammation group at visit 1. Higher honeycomb % in fibrotic group at visit 1 and visit 2. Higher fibrosis %, ground glass %, honeycomb %, ILD %, reticular % and VRS % in fibrotic group at visit 3.	Higher fibrosis, honeycomb and reticular scores, and lower ground glass score in fibrotic group at visits 1, 2 and 3. Higher ILD score in fibrotic group at visit 3.
Change between visits	Increase in honeycomb % between visits 1 and 3 in DI-ILD group. Increase in VRS % between visits 1 and 2 in IPF group. Increase in VRS % between visits 1 and 3 in IPF & fibrotic groups. Decrease in fibrosis %, ground glass %, ILD % and reticular % between visits 1 and 2 in inflammation group. Decrease in fibrosis %, ground glass %, ILD %, reticular % and VRS % between visits 1 and 3 in inflammation group.	Decrease in ground glass score between visits 1 and 3 in inflammation group.
Correlations between CT measurements	<p>Strong: CALIPER honeycomb % with visual CT fibrosis, honeycomb and ILD scores. CALIPER VRS % with visual CT fibrosis and ILD scores.</p> <p>Moderate: CALIPER fibrosis % with visual CT fibrosis, honeycomb and reticular scores. CALIPER ground glass % with visual CT ground glass score. CALIPER honeycomb % with visual CT reticular score. CALIPER ILD % with visual CT ground glass score. CALIPER reticular % with visual CT fibrosis score. CALIPER VRS % with visual CT honeycomb and reticular scores.</p>	
Correlations (strong only) with PFTs	Fibrosis % with FEV ₁ , FVC, FVC%, DLCO, DLCO%. Reticular % with FVC, FVC%, DLCO, DLCO%. VRS % with FVC%, DLCO and DLCO%.	Fibrosis with DLCO%. Honeycomb and ILD with DLCO%.
Predictor of disease progression	No (CALIPER VRS % close to statistical significance; p=0.088)	No

CALIPER: Computer-Aided Lung Informatics for Pathology Evaluation and Rating; CT: Computed tomography; DI-ILD: Drug induced interstitial lung disease; DLCO: Diffusing capacity of the lung for carbon monoxide; FEV₁: Forced expiratory volume in one second; FVC: Forced vital capacity; HP: Hypersensitivity pneumonitis; ILD: Interstitial lung disease; IPF: Idiopathic pulmonary fibrosis; PFT: Pulmonary function test; VRS: Vessel related structures.

Table 6.2. Summary of the global CT results in the TRISTAN-ILD study.

6.1.2 Summary of the imaging outcomes in the IPF study

Tables 6.3 and 6.4 provide a summary of the results from the global imaging measurements investigated in the IPF study. The key imaging outcomes which demonstrated statistical significance were:

- 1) Several imaging variables at the baseline visit were predictors of disease progression over 12 months including:
 - a) Global LmD (OR 1.03).
 - b) Global CALIPER CT fibrosis % (OR 1.24), ILD % (OR 1.08) and reticular % (OR 1.25).
 - c) Global visual CT fibrosis (OR 1.23), honeycomb (OR 1.24), ILD (OR 1.25) and reticular (OR 1.91) scores.
 - d) Visual CT fibrosis, honeycomb, ILD and reticular scores in the upper, middle and lower zones.
- 2) In the total study cohort, there was a decrease in global ^{129}Xe RBC:TP and an increase in global LmD between the baseline and 6-month visits, and between the baseline and 12-month visits. There was a statistically significant decrease in FVC, FVC%, DLCO, KCO and KCO% between the baseline and 6-month visits, but not between the baseline and 12-month visits.
- 3) In subjects 19-49, there was an increase in global ^{129}Xe ADC between the baseline and 12-month visits, with no statistically significant change in PFTs over the same time period. There was also an increase in ^{129}Xe ADC in the lower and peripheral zones, and an increase in ^{129}Xe LmD in the lower zone between the baseline and 12-month visits.
- 4) In subjects 19-49, there was an increase in ^{129}Xe ADC in the middle and central zones between the baseline and 6-month visits, with a statistically significant decrease in DLCO, KCO and KCO % predicted over the same time period.
- 5) In 12 subjects out of the total cohort, between the baseline and 12-month visits there was an increase in CALIPER CT ground glass %, honeycomb % and VRS % in the upper zone, and an increase in CALIPER CT ground glass % and ILD % in the central zone.

	¹²⁹ Xe spectroscopy	DW-MRI	DCE-MRI
Change between visits	Total cohort: Decrease in RBC:TP between baseline and 6-month visits, and between baseline and 12-month visits.	Total cohort: Increase in L _{mD} between baseline and 6-month visits, and baseline and 12-month visits. Subjects 19-49: Increase in ¹²⁹ Xe ADC between baseline and 12-month visits.	No
Correlations between MRI measurements	Strong: ¹²⁹ Xe RBC:TP change with ¹²⁹ Xe ADC change over 12 months (r=-0.64). Moderate: ¹²⁹ Xe RBC:TP with ¹²⁹ Xe ADC, ¹²⁹ Xe L _{mD} and MTT. ¹²⁹ Xe ADC with PBF and PBV. ¹²⁹ Xe L _{mD} with MTT, PBF and PBV. ¹²⁹ Xe RBC:TP change with ¹²⁹ Xe L _{mD} change over 12 months (r=-0.59).		
Correlations with CT measurements	Moderate: CALIPER CT ILD % (r=-0.59). Visual CT honeycomb score (r=-0.48).	No	Strong: FWHM with CALIPER reticular % (r=0.76) Moderate: PBF and PBV with CALIPER ground glass %.
Correlations with PFTs	Strong: FVC, D _{LCO} , D _{LCO} %, and K _{CO} %. Moderate: FEV ₁ , FVC% and K _{CO} .	Very strong: ¹²⁹ Xe ADC and L _{mD} with K _{CO} . Strong: ¹²⁹ Xe ADC and L _{mD} with D _{LCO} , D _{LCO} %, K _{CO} and K _{CO} %. Change in ¹²⁹ Xe ADC and L _{mD} with change in K _{CO} and K _{CO} % over 12 months.	Moderate: MTT with K _{CO} and K _{CO} %. PBF with D _{LCO} and D _{LCO} %. PBV with D _{LCO} , D _{LCO} %, K _{CO} and K _{CO} %.
Predictor of disease progression	No	Baseline visit global L _{mD} (OR 1.03; p=0.019)	No

ADC: apparent diffusion coefficient; CALIPER: Computer-Aided Lung Informatics for Pathology Evaluation and Rating; CT: Computed tomography; DCE-MRI: Dynamic contrast enhanced magnetic resonance imaging; D_{LCO}: Diffusing capacity of the lung for carbon monoxide; DW-MRI: Diffusion weighted magnetic resonance imaging; FEV₁: Forced expiratory volume in one second; FVC: Forced vital capacity; FWHM: Full width of half maximum; K_{CO}: carbon monoxide transfer coefficient; L_{mD}: mean diffusive length scale; MRI: Magnetic resonance imaging; MTT: Mean transit time; OR: Odds ratio; PBF: Pulmonary blood flow; PBV: Pulmonary blood volume; PFT: Pulmonary function test; RBC: Red blood cell; TP: Tissue plasma; ¹²⁹Xe: 129-xenon.

Table 6.3. Summary of the global MRI results in the IPF study.

	CALIPER CT analysis	Visual CT scoring
Change between baseline and 12-month visits	No	No
Correlations between CT measurements (very strong and strong included only)	<p>Very strong: CALIPER Honeycomb % with visual CT honeycomb score. CALIPER ILD % with visual CT fibrosis and ILD scores. CALIPER VRS% with visual CT fibrosis and ILD scores.</p> <p>Strong: CALIPER fibrosis % with visual CT fibrosis, honeycomb, ILD & reticular scores. CALIPER ground glass % with visual CT fibrosis, ILD and reticular scores. CALIPER ILD % with visual CT honeycomb and reticular scores. CALIPER reticular % with visual CT fibrosis, honeycomb, ILD & reticular scores. CALIPER VRS% with visual CT honeycomb and reticular scores.</p>	
Correlations with PFTs (very strong and strong included only)	<p>Very strong: ILD % with K_{CO}.</p> <p>Strong: Fibrosis % with FVC, FVC%, DL_{CO}, DL_{CO}%, K_{CO}, K_{CO}%. Ground glass % with FVC, FVC%, DL_{CO}, DL_{CO}%, K_{CO}, K_{CO}%. Honeycomb % with FVC%. ILD % with FVC, FVC%, DL_{CO}, DL_{CO}%, K_{CO}%. Reticular % with FVC, FVC%, DL_{CO}, DL_{CO}%, K_{CO}, K_{CO}%. VRS % with FVC, FVC%, DL_{CO}, DL_{CO}%, K_{CO}, K_{CO}%.</p>	<p>Strong: Fibrosis score with DL_{CO} and DL_{CO}%. Honeycomb and ILD scores with DL_{CO}%.</p>
Predictors of disease progression	<p>Baseline visit: fibrosis % (OR 1.24; p=0.037), ILD % (OR 1.08; p=0.026), reticular % (OR 1.25; p=0.036).</p>	<p>Baseline visit: fibrosis (OR 1.23), honeycomb (OR 1.24), ILD (OR 1.25), reticular (OR 1.91)</p>

CALIPER: Computer-Aided Lung Informatics for Pathology Evaluation and Rating; CT: Computed tomography; DL_{CO}: Diffusing capacity of the lung for carbon monoxide; FVC: Forced vital capacity; ILD: Interstitial lung disease; K_{CO}: carbon monoxide transfer coefficient; OR: Odds ratio; PFT: Pulmonary function test; VRS: Vessel related structures.

Table 6.4. Summary of the global CT results in the IPF study.

6.1.3. Dissolved ¹²⁹Xe MRI

In the TRISTAN-ILD study, there was a statistically significant decrease in global ¹²⁹Xe RBC:TP in the IPF group over six months, with no statistically significant change in FVC, FVC%, DL_{CO} or DL_{CO}% over the same time period. Similarly, there was also a statistically significant decrease in global ¹²⁹Xe RBC:TP over six months and 12 months in the total study cohort of the IPF study. In these subjects there was a statistically significant decrease in FVC, FVC%, DL_{CO}, K_{CO} and K_{CO}% between the baseline and 6-month visits, but not between the baseline and 12-month visits. These findings suggest that global ¹²⁹Xe RBC:TP is more sensitive to early disease progression in IPF when compared to PFTs.

6.1.4. Diffusion weighted MRI

One of the novel findings from the TRISTAN-ILD study was the statistically significant difference in global ^{129}Xe ADC and Lm_D between the ILD subtypes and between the fibrotic and inflammation groups, with higher values seen in IPF versus HP and in the fibrotic versus inflammation groups. This suggests that ^{129}Xe DW-MRI has value in differentiating between the pathological processes that cause the physiological abnormalities in the various ILD subtypes. ^{129}Xe DW-MRI also provides unique information regarding microstructural changes, especially in fibrotic ILD. This is supported by the regional variation found between ILD subtypes. For example, higher ^{129}Xe ADC and Lm_D in the middle zone versus the lower zone in HP subjects, compared to higher ^{129}Xe Lm_D in the lower zone versus the upper zone, and the lower zone versus the middle zone in IPF subjects. There was a statistically significant increase in global ^{129}Xe ADC and Lm_D over six weeks in the DI-ILD group, with no statistically significant PFT change over the same time period. Although the increase in ^{129}Xe ADC and Lm_D occurred over a short period of time, it is possible that these findings were due to fibrotic microstructural changes. This is supported by the statistically significant increase in CALIPER honeycomb % between visits 1 and 3 in the DI-ILD group.

There were statistically significant longitudinal changes in global and regional ^{129}Xe DW-MRI measurements in the IPF study, as described in section 6.1.2. These results suggests that ^{129}Xe DW-MRI measurements are more sensitive to early progression of microstructural changes in IPF compared to PFTs. These findings build upon the ^3He DW-MRI results found in subjects 1-18, that showed a statistically significant increase in Lm_D over 12 months, whereas ADC, FVC and DLCO were not statistically different over the same time period (240).

6.1.5. Dynamic contrast enhanced MRI

Another novel finding from the TRISTAN-ILD study was a statistically significant decrease in global MTT and increase in global PBF over six weeks in the HP group, whereas there was no statistically significant change in FVC, FVC%, DLCO or $\text{DLCO}\%$ over the same time period. 10 out of the 13 subjects with HP were categorised into the inflammation group (visual CT ground glass score ≥ 2). Therefore, it is possible that

the decrease in MTT and increase in PBF was associated with a reduction in inflammation due to a response to steroids and/or antigen avoidance. This suggests that DCE-MRI measurements may be sensitive imaging biomarkers in subjects with inflammation predominant ILD. There were moderate correlations between the change in MTT and FEV₁, ($r=-0.40$; $p=0.033$), and between the change in PBF and DLCO ($r=0.44$; $p=0.018$) in the total study cohort. It is therefore possible that an improvement in gas exchange in ILD is associated with increased perfusion to regions of the lung previously affected by significant inflammation.

In the total cohort of the IPF study, none of the global DCE-MRI measurements demonstrated a statistically significant change between visits. This is in contrast to the findings of a statistically significant increase in FWHM over six months in a recent publication by Weatherley *et al*, which included 19 subjects from the IPF study (211). The majority of these 19 subjects were recruited between February 2016 and February 2018 by Dr Weatherley. Only 9.7% of subjects 19-49 experienced disease progression, whereas disease progression occurred in 21.6% of the total cohort. Therefore, it is likely that subjects 19-49 had more stable disease than the 19 subjects that demonstrated the FWHM change over six months. In the total cohort of the IPF study there was a statistically significant increase in PBV between the 6-month and 12-month visits in the lower zone which is consistent with the predominant location of fibrotic changes (UIP) seen on CT in IPF. Therefore, regional changes in PBV, and perhaps other DCE-MRI measurements, could provide useful information in the assessment of early perfusion changes in IPF.

6.1.6. CALIPER CT analysis

In the IPF group of the TRISTAN-ILD study, there was a statistically significant increase in global CALIPER VRS % between the baseline HRCT scan and the HRCT scan at six months. In the same subjects, there was no statistically significant change in FVC, FVC%, DLCO or DLCO% over 6 months. This suggests that CALIPER VRS % is more sensitive to early disease progression in IPF compared to PFTs. However, the HRCT scan used for the baseline visit scan was performed up to 12 months before the first study visit and therefore the increase in global CALIPER VRS % would have occurred over a period of more than six months.

In the IPF study, 12 subjects out of the total cohort had CALIPER CT data available at both the baseline and 12-month visits. In these subjects, there was an increase in CALIPER ground glass %, honeycomb % and VRS % in the upper zone, and an increase in CALIPER ground glass % and ILD % in the central zone. In the same 12 subjects, over the 12-months there was a statistically significant decrease in FVC and FVC%, but no statistically significant change in D_{LCO} , $D_{LCO}\%$, K_{CO} or $K_{CO}\%$. The regional changes in CALIPER ground glass %, honeycomb % and ILD % are surprising as the characteristic UIP pattern involves fibrotic changes at the bases and periphery of the lungs. It is possible that the increase in CALIPER ground glass % in the central and upper zones represent early fine fibrosis which may progress to reticulation over time and it is conceivable that regions of emphysema in the upper zone of IPF subjects were incorrectly classified as honeycombing.

CALIPER VRS % in the upper zones of IPF patients has previously been reported as the strongest predictor of disease progression ($\geq 10\%$ FVC decline or death at 12 months) when compared to other regional CALIPER CT measurements and PFTs (169). The pathophysiological mechanism associated with CALIPER VRS is not fully understood. However, it has been suggested that in patients with fibrotic ILD, high negative intrathoracic pressures produced during breathing may increase with disease progression and that this could lead to more blood being diverted into the lungs (176). It has also been proposed that destruction of the capillary bed in areas of the lung with advanced fibrosis and localised raised pulmonary arterial pressure, may divert blood flow to regions without significant fibrosis, such as the upper zones in IPF (168). Therefore, these theories may explain the longitudinal change in CALIPER VRS % in the upper zone seen in the IPF study.

6.1.7. Visual CT scores

In the inflammation group of the TRISTAN-ILD study, there was a statistically significant decrease in the global visual CT ground glass score between visits 1 and 3, whereas there was no statistically significant change in PFTs over the same study visit period. This suggests that the semi-quantitative assessment of GGO on HRCT by radiologists may be useful to determine response to immunosuppressant treatment in inflammation predominant ILD, before significant physiological changes are identified.

The sensitivity of visual CT ground glass score to longitudinal change was inferior to CALIPER CT fibrosis %, ground glass %, ILD % and reticular %, as the statistically significant decrease in these measurements occurred between visits 1 and 2, as well as between visits 1 and 3.

6.1.8 Correlations – TRISTAN-ILD study

^{129}Xe RBC:TP correlated strongly with CALIPER CT fibrosis % and reticular % in the peripheral zone, ground glass % in the upper and middle zones, and ILD % in the upper zone. These regional correlations suggest that reduced ^{129}Xe RBC:TP is associated with CT features of inflammation and/or fine fibrosis (CALIPER ground glass %), in addition to fibrotic CT features.

It is likely that increased ^{129}Xe ADC and LmD is a result of reduced acinar integrity as a consequence of fibrotic changes in the lung, such as honeycombing and possibly traction bronchiectasis. This is supported by the findings of a strong correlation between global ^{129}Xe DW-MRI measurements and visual CT fibrosis score, and a moderate correlation between global ^{129}Xe DW-MRI measurements and CALIPER CT honeycomb %, as well as visual CT fibrosis, ILD and reticular scores. ^{129}Xe ADC was also strongly correlated with visual CT fibrosis, honeycomb, ILD and reticular scores in the lower zone, and ^{129}Xe DW-MRI measurements were moderately correlated with CALIPER CT honeycomb %, reticular % and VRS % in the lower and peripheral zones.

A moderate negative correlation was seen between PBV and CALIPER CT honeycomb % in the TRISTAN-ILD study. Also, MTT change was correlated with visual CT fibrosis score change, and PBF change was negatively correlated with change in the visual CT fibrosis and honeycomb scores. These findings suggest associations between pulmonary perfusion and fibrotic changes in the lung. It is therefore likely that decreased pulmonary perfusion is associated with the pathophysiological abnormalities seen with progression of fibrotic ILD.

6.1.9 Correlations – IPF study

^{129}Xe RBC:TP was negatively correlated with ^{129}Xe ADC, ^{129}Xe L_{MD} and MTT. Between the baseline and 12-month visits, the change in ^{129}Xe RBC:TP correlated negatively with the change in ^{129}Xe ADC and ^{129}Xe L_{MD} . These global correlations suggest that reduced ^{129}Xe RBC:TP in ILD is associated with pulmonary perfusion limitation, and increased Brownian gas diffusion in the acinar airways as a result of microstructural changes (reflected by ^{129}Xe DW-MRI changes).

In addition to the correlations between ^{129}Xe RBC:TP and other MRI measurements, there is evidence that ^{129}Xe RBC:TP is related to the extent of disease on CT scans. Moderate negative correlations were seen between ^{129}Xe RBC:TP and CALIPER CT ILD %, and between ^{129}Xe RBC:TP and visual CT honeycomb score. These findings are in contrast to a study which found no correlation between ^{129}Xe RBC:TP and visual CT fibrosis score in subjects with IPF (229).

^{129}Xe RBC:TP correlated strongly with FVC, D_{LCO} , $D_{\text{LCO}}\%$ and $K_{\text{CO}}\%$. The correlation between ^{129}Xe RBC:TP and D_{LCO} is consistent with findings by Kaushik *et al* in a study involving six IPF subjects (230). A more recent study by the same group which included 12 patients with IPF (229), also reported a correlation between ^{129}Xe RBC:TP and D_{LCO} ($r=0.94$; $p<0.01$), as well as a correlation between Xe RBC:TP and FVC ($r=0.75$; $p<0.01$).

The change in CALIPER CT honeycomb % was very strongly correlated with the change in ^{129}Xe ADC and L_{MD} in the peripheral zone. This suggests that in IPF, the longitudinal changes in ^{129}Xe ADC and L_{MD} are due to increased ^{129}Xe diffusion secondary to enlarged and/or increased numbers of honeycomb cysts.

^{129}Xe DW-MRI measurements correlated with D_{LCO} , $D_{\text{LCO}}\%$, K_{CO} and $K_{\text{CO}}\%$. These correlations suggest that the elevated ^{129}Xe DW-MRI measurements are associated with decreased gas exchange in the alveoli due to a reduction in the alveolar surface area and are in keeping with correlations seen between ^3He DW-MRI and the gas exchange measurements D_{LCO} and K_{CO} (240). Results from the IPF study also demonstrated that the change in ^{129}Xe DW-MRI measurements were strongly correlated with the change in K_{CO} and $K_{\text{CO}}\%$.

There were strong negative correlations between global CALIPER CT measurements (fibrosis %, ground glass %, ILD %, reticular % and VRS %) and PFT values (FVC, FVC%, D_{LCO} , $D_{LCO}\%$, K_{CO} and $K_{CO}\%$), as well as a strong negative correlation between CALIPER honeycomb % and FVC%. The negative correlation of FVC with CALIPER ILD % and VRS % has been reported in two retrospective studies involving patients with IPF (167, 248). In one of these studies, D_{LCO} was also negatively correlated with CALIPER ILD % and VRS % (167).

6.1.10. Predictors of disease progression

In the TRISTAN-ILD study, using univariate logistic regression analysis, none of the global or regional imaging biomarkers were statistically significant predictors of disease progression, with baseline global ^{129}Xe RBC:TP being the closest to reaching statistical significance ($p=0.075$). It is possible that logistic regression analysis involving a larger number of subjects and/or subjects with more advanced disease would have resulted in the successful detection of ILD predictive imaging biomarkers.

In the IPF study, univariate logistic regression analysis identified several global CALIPER CT measurements (fibrosis %, ILD % and reticular %), global visual CT scores (fibrosis, honeycomb, ILD and reticular) and regional visual CT scores (fibrosis, honeycomb, ILD and reticular scores in the upper, middle and lower zones) that were statistically significant predictors of disease progression when the values at the baseline visit were used. Also, baseline visit global LmD was shown to be a predictor of disease progression (OR 1.03; 95% CI 1.01-1.07; $p=0.019$). All of these imaging biomarkers continued to have a statistically significant odds ratio for predicting disease progression when age was added to the logistic regression model. Visual CT reticular score at the baseline visit was the strongest global predictor of disease progression (OR 1.91; 95% CI 1.28-3.45; $p=0.009$) and baseline visual CT reticular score in the upper zone was the strongest regional predictor of disease progression (OR 6.92; 95% CI 2.03-49.9; $p=0.013$). The finding that upper zone fibrosis in IPF is a significant predictor of disease progression is likely a result of advanced disease. As IPF is characteristically basal predominant, the presence of upper zone fibrosis may be related to late presentation or aggressive disease.

Several CALIPER CT measurements have demonstrated utility as predictors of mortality and/or disease progression in IPF. In a study by Jacob *et al*, univariate Cox regression analysis demonstrated that all baseline global CALIPER CT measurements (ground glass %, ILD %, honeycomb % reticular % and PVV %) and corresponding visual CT scores were predictive of mortality to a 0.01 level of statistical significance (168). Following multivariate Cox regression analysis, CALIPER PVV % (HR 1.53; 95% CI 1.41-1.66; $p < 0.001$) and honeycombing % (HR 1.12; 95% CI 1.04-1.21; $p = 0.004$) were the strongest predictors of death. Following on from this study, the same group found that global CALIPER VRS %, as well as VRS % in the upper and middle zones were the strongest predictors of disease progression ($\geq 10\%$ FVC decline or death at 12 months), and that global VRS % and VRS % in the upper zone also strongly predicted mortality (169). CALIPER variables of ILD % extent $> 20\%$ and VRS % score $> 5\%$ have also been associated with reduced survival in IPF (248). A study by Maldonado *et al*, reported that short-term (3-15 months) changes in global CALIPER reticular % were associated with survival after a median follow-up of 2.4 years on both univariate (HR 1.38; 95% CI 1.03-1.84; $p = 0.032$) and multivariate analysis (HR 1.93; 95% CI 1.30-2.89; $p = 0.001$) (165).

Multiple visual CT scores have been reported as predictors of mortality in IPF, as shown in Table 2.3 in section 2.3.1. In IPF, fibrosis score has been associated with progression free survival (284) and visual GGR score (combination of ground glass and reticulation) has been found to be predictive of disease progression (157).

6.2. Limitations

6.2.1 Sample size

The main limitation of the work presented is the relatively small number of subjects in the studies. However, the total number of subjects in each of the two studies is more than previously published prospective ^{129}Xe MRI studies in IPF. Also, ILD studies demonstrating CALIPER CT measurements and visual CT scores as predictive biomarkers have been retrospective studies and thereby have larger numbers of subjects, as the CTs will generally have been performed initially for clinical purposes.

The power calculation for the TRISTAN-ILD study proposed 15 subjects in each ILD subgroup. At baseline, this was achieved in the HP group (n=15), in the IPF group (n=19), and almost in the DI-ILD group (n=13). However, recruitment of CTD-ILD patients proved to be a challenge and only five of these patients entered the study. Following amendments to the study, recruitment of iNSIP patients commenced in June 2019 and was progressing reasonably well with three of these patients having entered the study by the time all recruitment was suspended in March 2020 due to COVID-19 restrictions. Therefore, the study was only powered to detect a difference in biomarkers between the HP and IPF groups at the baseline visit. It is hoped that recruitment into the study will be able to restart soon, now that COVID-19 restrictions are beginning to be removed. There was further reduction to the statistical power of the longitudinal changes as data from follow-up visits were missing in multiple subjects either due to death (n=7), withdrawal from the study (n=4) or missed visits due to COVID-19 restrictions (n=13). As a result, only 31 of the 55 (56.4%) subjects recruited completed all study visits. Less than 15 subjects from each ILD subtype group completed visits 1 and 2, or all study visits. Therefore, the study was not powered to detect longitudinal changes in the biomarkers when ILD subtype groups were analysed separately, thereby increasing the risk of type 2 errors. When the total study cohort was stratified into fibrotic and inflammation groups, the study was powered for longitudinal changes between visits 1 and 2 as there were more than 15 subjects in each of these two groups at both visits. However, only 12 subjects in the inflammation group completed the study, whereas 19 subjects in the fibrotic group completed the study.

The power calculation for the IPF study proposed a further recruitment of 32 patients, in addition to the 21 that had been recruited by Dr Weatherley between February 2016 and February 2018. 30 IPF patients were recruited by myself between November 2018 and November 2019 but two of them did not complete the baseline MRI scan due to claustrophobia. As mentioned above, study visits were suspended in March 2020 due to COVID-19 restrictions, which resulted in the recruitment target not being achieved, as well as one 3-month visits being missed and nine 6-month visits being missed before follow-up study visits could resume again in October 2020. This missing data prevented the comparison of the change in biomarkers over multiple time points in these subjects. In ten subjects, the COVID-19 restrictions led to a delay of up to six

months in the 12-month visit which may have affected the results of longitudinal change in biomarkers between the baseline and 12-month visits. Despite these limitations, the power calculation stated a minimum of 15 subjects to complete all study visits, which was achieved.

6.2.2 Timing of follow-up study visits

In the TRISTAN-ILD study the timing of the follow-up study visits was determined by the ILD subtype. In the DI-ILD, HP and iNSIP subjects, the follow-up visits occurred at two weeks (visit 1A – introduced in June 2019), six weeks (visit 2) and six months (visit 3). In the CTD-ILD and IPF subjects, the follow-up visits occurred at three months (visit 1A), six months (visit 2) and 12 months (visit 3). The reason for this was that DI-ILD, HP and iNSIP subjects were expected to improve within six months, whereas improvements or progression of disease in CTD-ILD and IPF were expected to occur over longer periods of time. However, one could challenge the validity of the comparison of longitudinal changes in biomarkers between ILD subtypes that have different follow-up visit timepoints. This could also be the case when comparing between the fibrotic and inflammation groups, and especially when evaluating the longitudinal change in biomarkers in these two groups separately as they comprise of ILD subtypes with inconsistent follow-up visit timepoints

6.2.3 Imaging methodology and biomarkers

The CT scan used for clinical diagnostic purposes was also used as the baseline CT scan in both studies. The reason for this was to limit the radiation exposure for subjects. These CT scans could have been performed up to 12 months prior to the baseline study visit, and therefore the time period for the longitudinal changes in the CALIPER CT measurements and the visual CT scores varied between subjects. One could therefore argue the validity of comparing the longitudinal changes in these CT biomarkers with the MRI biomarkers performed in the study. It is also likely that this had an effect on the correlation at baseline between the CT biomarkers and other types of biomarkers which could have been performed several months apart.

In the IPF study, the 12-month CT scan dataset was incomplete, with only 20 of the 33 subjects who completed the 12-month MRI study visit also having a CT scan performed. In subjects 19-49, in which I was present at the 12-month MRI study visit, the reason for not having a CT scan performed was due to COVID-19 restrictions on the use of the NHS radiology department for research purposes. Of the 20 subjects that had both baseline and 12-month CT scans, only 12 were suitable at both timepoints for accurate CALIPER CT analysis. Problems mainly occurred in subjects 1-18 due to some CT scans being contrast enhanced or non-volumetric.

There were inconsistencies in the technical CT parameters (e.g. reconstruction and slice thickness) between subjects and at different time points in the same subject, due to different scanners used in a variety of hospitals. However, similar issues would likely occur in real-world application of QCT software, and it is debatable if these technical differences would have significantly altered the results of the CALIPER CT measurements. If QCT software becomes used clinically for routine monitoring of ILD patients in the future then it is possible that the technical CT parameters may require standardisation across different types of scanners to ensure reliable outcomes. Some of the subjects in the IPF study had relatively high CALIPER ground glass % results which may have been a consequence of the reconstruction parameters used. In this study, of all the CALIPER CT measurements, ground glass % was the only one that did not have a strong or very strong correlation with the corresponding visual CT score.

A significant limitation was the technical problems experienced with DCE-MRI scans. There were several occasions in both studies when DCE-MRI measurements could not be reliably produced. This was mainly due to contrast bolus not reaching the pulmonary vessels in time for accurate assessment, and/or registration failures due to poor quality images. Some of the issues with the image quality were a result of motion artefact, which may have been due to some subjects having difficulty with breath hold manoeuvres. Another limitation was that there were differences in the methodology of DCE-MRI analysis between the TRISTAN-ILD study (performed by Bioxydyn Limited) and the IPF study (performed at the University of Sheffield). These differences included the arterial input function definition and the threshold value used in the deconvolution analysis (see appendix 1 for a detailed technical explanation). Therefore, the DCE-MRI measurements cannot be directly compared between the two studies.

Subjects 1-13 of the IPF study had ^{129}Xe RBC:TP data analysed using a manual method (described in section 5.7), rather than the automated double Lorentzian, two peak method (230) used in subjects 14-49. However, the flip angle and TR remained consistent. Therefore, the slightly different methods are unlikely to have affected results. This is supported by Bland-Altman statistical analysis of the data from subjects that had both methods performed which demonstrated a mean bias of -0.0076 which is negligible. Also, there was a consistent outcome in both studies in terms of a statistically significant decrease in ^{129}Xe RBC:TP over six months in IPF subjects.

Subjects 1-18 of the IPF study had DW-MRI performed using ^3He instead of ^{129}Xe . Only the L_{M_D} data could be combined for subjects 1-18 and subjects 19-49. 13 study visit datasets were available for subjects that had both ^3He and ^{129}Xe DW-MRI performed and after Bland-Altman statistical analysis, there was a mean bias of $-40\mu\text{m}$ towards ^{129}Xe L_{M_D} . Therefore, the ^3He L_{M_D} values were corrected by $-40\mu\text{m}$ when combined with the ^{129}Xe L_{M_D} values.

The ^{129}Xe MRI sequences involve breath hold manoeuvres performed at FRC plus one litre of gas, although there is likely to be a degree of variability due to lack of spirometric control. In theory, this could alter the alveolar inflation which could in turn affect DW-MRI measurements. However, this is unlikely to be significant, especially given the high degree of same day reproducibility previously demonstrated with the use of ^3He DW-MRI in IPF (240). Unpublished data from 10 healthy volunteers as part of the TRISTAN-ILD study has also shown excellent repeatability in ^{129}Xe ADC (ICC=0.98), ^{129}Xe L_{M_D} (ICC=0.97) and ^{129}Xe RBC:TP (ICC=0.95).

Inconsistency in HRCT lung volume data could have affected some of the findings, as inspiratory volume can have a significant effect on the characterisation of QCT features in particular. In the TRISTAN-ILD study a QA process was implemented to ensure consistent imaging acquisition but this was not the case in the IPF study. Potential inconsistency in inspiratory volume could have been reduced with the use of standardised breathing instructions. However, this was not possible as the CT scans were performed by different radiographers and different sites. A potential method to improve reproducibility of HRCT lung volume data is the use of spirometric control. However, this would not have been feasible in the studies as the majority of the baseline scans were performed clinically for diagnostic purposes prior to recruitment.

6.2.4 Treatment effects

In both studies, several subjects were already taking antifibrotic therapy at the time of recruitment and a few subjects commenced nintedanib after the baseline study visit (2 subjects in the TRISTAN-ILD study and one in the IPF study). It is difficult to determine if antifibrotic therapy had an effect on the longitudinal changes in biomarkers due to the small sample size. It would be interesting to incorporate the MRI and QCT biomarkers into future randomised antifibrotic trials to investigate the treatment effects.

A limitation of the TRISTAN-ILD study was the non-standardised approach in the management of the non-IPF subjects and the timing between their management and the baseline study visit. Of the DI-ILD subjects that were recruited from Manchester, four were taking prednisolone at some point during the study, whereas all except one of the DI-ILD subjects recruited from Sheffield had relatively mild disease with the management plan involving withdrawal of the causative drug only. Also, the timing of the baseline study visits in relation to the management of non-IPF subjects varied between the two centres. In the subjects recruited from Sheffield, the ILD management (commencing prednisolone or stopping drugs causing DI-ILD) mainly occurred within a week of the baseline study visit. However, this was not generally the case in the subjects recruited from Manchester, with some of them having commenced immunosuppressants or stopped medication weeks prior to the baseline study visit, and in some cases, prednisolone was commenced weeks after the baseline study visit. It is possible that the variation in the management of the non-IPF subjects in the TRISTAN-ILD study could have had an effect on the longitudinal changes in the biomarkers and that a more standardised approach may have resulted in different outcomes.

6.2.5 Confounding effects of emphysema and pulmonary hypertension

The baseline CT scans were screened for significant emphysema prior to recruitment. This was done subjectively using the CT report and/or in the ILD MDT meeting. It is possible that some of the subjects may have had a significant amount of emphysema that was under-reported. Therefore, it is possible that emphysema could have had a confounding effect on FVC and ^{129}Xe DW-MRI measurements in some subjects.

PH can have a confounding effect on D_{LCO} , DCE-MRI measurements and ^{129}Xe RBC:TP. In the IPF study, the echocardiogram report at baseline (performed for clinical purposes) was used to screen subjects for significant PH with only one subject having evidence of significant PH (estimate systolic pulmonary artery pressure 53-58mmHg). In the TRISTAN-ILD study PH was not screened for. Therefore, it is possible that some of the subjects in the TRISTAN-ILD study could have had significant PH.

6.2.6 Interpretation of findings when multiple outcome measures are used

The statistical analysis performed in the two studies did not involve any adjustment of p-values when multiple outcome measures were investigated (such as several imaging metrics being compared between the same groups). Therefore, one may question the interpretation of these findings due to the increased risk of type I errors (false positives). However, although p-value adjustments would have reduced the possibility of type I errors occurring, this would have increased the risk of type II errors (false negatives) as the chances of these two types of errors happening are inversely proportional.

6.3. Future work

Mortality data from the subjects in the TRISTAN-ILD study will be collected for up to three years following the first study visit. It will be interesting to use this data in the future to assess the biomarkers as predictors of mortality rather than disease progression only.

In the IPF study, the plan is to continue recruitment, and in the future, mortality data could be used to determine which imaging biomarkers can predict survival. It is possible that a larger sample size would allow multivariate predictive models of mortality and/or disease progression to be assessed using the various biomarkers. A larger sample size could also enable the estimation of the minimal clinically important difference of each of the imaging biomarkers.

Advanced image registration techniques developed within the pulmonary imaging department at the University of Sheffield have enabled regional microstructural changes in the lung of ILD subjects to be accurately mapped between ^{129}Xe DW-MRI and CALIPER CT. This has already been done in a small sample of TRISTAN-ILD study subjects which has identified elevated ^{129}Xe ADC and LmD values within regions of the lung with a normal CALIPER CT classification. Future work in this will hopefully be achieved with the remaining dataset and it is possible that it could also be applied to the IPF study dataset. It should also be possible to use similar registration techniques to compare regionally between CALIPER CT and other MRI measurements, and possibly between different MRI metrics.

6.4. Conclusion

Despite evidence that hyperpolarised ^{129}Xe MRI combined with proton MRI, is able to provide both structural and functional data, its clinical application has been relatively limited in the field of ILD. However, following reduction in the cost of ^{129}Xe and improvements in the availability of polarisers over the last several years it is hoped that hyperpolarised ^{129}Xe MRI will become more widely accessible in the future. The insensitivity of PFTs in early disease, and the ability of hyperpolarised ^{129}Xe MRI to assess regional lung function makes it an appealing tool to explore in the diagnosis and monitoring of ILD. However, the transition from research into clinical practice remains a significant challenge.

CT involves ionising radiation and is unable to provide functional data. However, it has some advantages over MRI in terms of its speed, image contrast and spatial resolution. Various automated, computer based, QCT analysis methods have been reported in ILD. There is evidence that texture analysis techniques are superior to visual CT scores performed by radiologists. QCT variables such as CALIPER VRS are particularly interesting but will likely require validation in a large prospective study to confirm its superiority in predicting prognosis compared to visual CT scores and FVC. It has also been suggested that the various types of QCT software currently available should be compared against each other prospectively to identify a standard technology that can be widely implemented in clinical practice (285).

Despite the multiple individual predictors of survival and the numerous mortality prediction models that have been developed in ILD, it remains unclear as to how they should be implemented in routine clinical practice to stage disease and predict prognosis. The optimal mortality prediction model for IPF has not yet been defined and none have been included in clinical guidelines. Currently, FVC is the most widely used single prognostic variable as a result of its availability, ease of measurement and consistent performance in studies evaluating prognosis. However, there is potential for combining novel imaging biomarkers with routine clinical findings in future research to optimise ILD management and improve prediction of disease progression and mortality. As new drug treatments are developed, the ability to quantify subtle changes using QCT and MRI could be particularly valuable.

It is anticipated that MRI techniques, especially hyperpolarised ^{129}Xe MRI, as well as QCT, could play an important future role as objective, reproducible and sensitive imaging biomarkers in the monitoring of ILD progression, assessment of response to treatment and prediction of prognosis. In addition, it is hoped that they will be able to perform accurate staging at baseline and identify subgroups of patients with ILD that are most likely to benefit from lung transplantation or a particular drug treatment.

The findings reported in this thesis represent the first known longitudinal data combining hyperpolarised ^{129}Xe MRI (dissolved and diffusion weighted) and DCE-MRI with CALIPER CT measurements and visual CT scores alongside PFTs in a cohort of various ILD subtypes. It also expands upon previous work involving these novel MRI techniques in IPF, demonstrating the potential of imaging biomarkers as sensitive modalities in assessing disease progression. However, before these imaging biomarkers can be implemented into routine clinical practice, they will require technical validation and will likely need to demonstrate utility as surrogate endpoints in future multicentre ILD drug trials.

References

1. Guler SA, Ellison K, Algamdi M, Collard HR, Ryerson CJ. Heterogeneity in Unclassifiable Interstitial Lung Disease. A Systematic Review and Meta-Analysis. *Ann Am Thorac Soc*. 2018;15(7):854-63.
2. Mueller-Mang C, Grosse C, Schmid K, Stiebellehner L, Bankier AA. What every radiologist should know about idiopathic interstitial pneumonias. *Radiographics*. 2007;27(3):595-615.
3. Raghu G, Remy-Jardin M, Myers JL, Richeldi L, Ryerson CJ, Lederer DJ, et al. Diagnosis of Idiopathic Pulmonary Fibrosis. An Official ATS/ERS/JRS/ALAT Clinical Practice Guideline. *Am J Respir Crit Care Med*. 2018;198(5):e44-e68.
4. Hansell DM, Bankier AA, MacMahon H, McLoud TC, Muller NL, Remy J. Fleischner Society: glossary of terms for thoracic imaging. *Radiology*. 2008;246(3):697-722.
5. Glaspole I, Goh NS. Differentiating between IPF and NSIP. *Chron Respir Dis*. 2010;7(3):187-95.
6. Tsubamoto M, Muller NL, Johkoh T, Ichikado K, Taniguchi H, Kondoh Y, et al. Pathologic subgroups of nonspecific interstitial pneumonia: differential diagnosis from other idiopathic interstitial pneumonias on high-resolution computed tomography. *J Comput Assist Tomogr*. 2005;29(6):793-800.
7. Travis WD, Hunninghake G, King TE, Jr., Lynch DA, Colby TV, Galvin JR, et al. Idiopathic nonspecific interstitial pneumonia: report of an American Thoracic Society project. *Am J Respir Crit Care Med*. 2008;177(12):1338-47.
8. Flaherty KR, Brown KK, Wells AU, Clerisme-Beaty E, Collard HR, Cottin V, et al. Design of the PF-ILD trial: a double-blind, randomised, placebo-controlled phase III trial of nintedanib in patients with progressive fibrosing interstitial lung disease. *BMJ Open Respir Res*. 2017;4(1):e000212.
9. Wells AU, Brown KK, Flaherty KR, Kolb M, Thannickal VJ, Group IPFCW. What's in a name? That which we call IPF, by any other name would act the same. *Eur Respir J*. 2018;51(5).
10. Cottin V, Hirani NA, Hotchkiss DL, Nambiar AM, Ogura T, Otaola M, et al. Presentation, diagnosis and clinical course of the spectrum of progressive-fibrosing interstitial lung diseases. *Eur Respir Rev*. 2018;27(150).
11. Olson AL, Gifford AH, Inase N, Fernandez Perez ER, Suda T. The epidemiology of idiopathic pulmonary fibrosis and interstitial lung diseases at risk of a progressive-fibrosing phenotype. *Eur Respir Rev*. 2018;27(150).
12. Flaherty KR, Wells AU, Cottin V, Devaraj A, Walsh SLF, Inoue Y, et al. Nintedanib in Progressive Fibrosing Interstitial Lung Diseases. *N Engl J Med*. 2019;381(18):1718-27.
13. American Thoracic S, European Respiratory S. American Thoracic Society/European Respiratory Society International Multidisciplinary Consensus Classification of the Idiopathic Interstitial Pneumonias. This joint statement of the American Thoracic Society (ATS), and the European Respiratory Society (ERS) was adopted by the ATS board of directors, June 2001 and by the ERS Executive Committee, June 2001. *Am J Respir Crit Care Med*. 2002;165(2):277-304.
14. Travis WD, Costabel U, Hansell DM, King TE, Jr., Lynch DA, Nicholson AG, et al. An official American Thoracic Society/European Respiratory Society statement: Update of the international multidisciplinary classification of the idiopathic interstitial pneumonias. *Am J Respir Crit Care Med*. 2013;188(6):733-48.
15. Nadrous HF, Myers JL, Decker PA, Ryu JH. Idiopathic pulmonary fibrosis in patients younger than 50 years. *Mayo Clin Proc*. 2005;80(1):37-40.
16. Lynch DA, Sverzellati N, Travis WD, Brown KK, Colby TV, Galvin JR, et al. Diagnostic criteria for idiopathic pulmonary fibrosis: a Fleischner Society White Paper. *Lancet Respir Med*. 2018;6(2):138-53.
17. Lederer DJ, Martinez FJ. Idiopathic Pulmonary Fibrosis. *N Engl J Med*. 2018;378(19):1811-23.
18. Khor YH, Ng Y, Barnes H, Goh NSL, McDonald CF, Holland AE. Prognosis of idiopathic pulmonary fibrosis without anti-fibrotic therapy: a systematic review. *Eur Respir Rev*. 2020;29(157).

19. Jo HE, Glaspole I, Grainge C, Goh N, Hopkins PM, Moodley Y, et al. Baseline characteristics of idiopathic pulmonary fibrosis: analysis from the Australian Idiopathic Pulmonary Fibrosis Registry. *Eur Respir J*. 2017;49(2).
20. Guenther A, Krauss E, Tello S, Wagner J, Paul B, Kuhn S, et al. The European IPF registry (eurIPFreg): baseline characteristics and survival of patients with idiopathic pulmonary fibrosis. *Respir Res*. 2018;19(1):141.
21. Wu X, Kim GH, Salisbury ML, Barber D, Bartholmai BJ, Brown KK, et al. Computed Tomographic Biomarkers in Idiopathic Pulmonary Fibrosis. The Future of Quantitative Analysis. *Am J Respir Crit Care Med*. 2019;199(1):12-21.
22. Ley B, Collard HR, King TE, Jr. Clinical course and prediction of survival in idiopathic pulmonary fibrosis. *Am J Respir Crit Care Med*. 2011;183(4):431-40.
23. National Institute for Health and Care Excellence (2018) Pirfenidone for treating idiopathic pulmonary fibrosis (Technology appraisal guidance TA504). Available at: <https://www.nice.org.uk/guidance/ta504>
24. National Institute for Health and Care Excellence (2016) Nintedanib for treating idiopathic pulmonary fibrosis (Technology appraisal guidance TA379). Available at: <https://www.nice.org.uk/guidance/TA379>.
25. King TE, Jr., Bradford WZ, Castro-Bernardini S, Fagan EA, Glaspole I, Glassberg MK, et al. A phase 3 trial of pirfenidone in patients with idiopathic pulmonary fibrosis. *N Engl J Med*. 2014;370(22):2083-92.
26. Richeldi L, du Bois RM, Raghu G, Azuma A, Brown KK, Costabel U, et al. Efficacy and safety of nintedanib in idiopathic pulmonary fibrosis. *N Engl J Med*. 2014;370(22):2071-82.
27. Walsh SLF, Wells AU, Desai SR, Poletti V, Piciucchi S, Dubini A, et al. Multicentre evaluation of multidisciplinary team meeting agreement on diagnosis in diffuse parenchymal lung disease: a case-cohort study. *Lancet Respir Med*. 2016;4(7):557-65.
28. Raghu G, Collard HR, Anstrom KJ, Flaherty KR, Fleming TR, King TE, Jr., et al. Idiopathic pulmonary fibrosis: clinically meaningful primary endpoints in phase 3 clinical trials. *Am J Respir Crit Care Med*. 2012;185(10):1044-8.
29. King TE, Jr., Albera C, Bradford WZ, Costabel U, du Bois RM, Leff JA, et al. All-cause mortality rate in patients with idiopathic pulmonary fibrosis. Implications for the design and execution of clinical trials. *Am J Respir Crit Care Med*. 2014;189(7):825-31.
30. Collard HR, Brown KK, Martinez FJ, Raghu G, Roberts RS, Anstrom KJ. Study design implications of death and hospitalization as end points in idiopathic pulmonary fibrosis. *Chest*. 2014;146(5):1256-62.
31. Nathan SD, Albera C, Bradford WZ, Costabel U, du Bois RM, Fagan EA, et al. Effect of continued treatment with pirfenidone following clinically meaningful declines in forced vital capacity: analysis of data from three phase 3 trials in patients with idiopathic pulmonary fibrosis. *Thorax*. 2016;71(5):429-35.
32. Russell A-M, Adamali H, Molyneaux PL, Lukey PT, Marshall RP, Renzoni EA, et al. Daily Home Spirometry: An Effective Tool for Detecting Progression in Idiopathic Pulmonary Fibrosis. *American Journal of Respiratory and Critical Care Medicine*. 2016;194(8):989-97.
33. Johannson KA, Vittinghoff E, Morisset J, Lee JS, Balmes JR, Collard HR. Home monitoring improves endpoint efficiency in idiopathic pulmonary fibrosis. *Eur Respir J*. 2017;50(1).
34. Kligerman SJ, Groshong S, Brown KK, Lynch DA. Nonspecific interstitial pneumonia: radiologic, clinical, and pathologic considerations. *Radiographics*. 2009;29(1):73-87.
35. Belloli EA, Beckford R, Hadley R, Flaherty KR. Idiopathic non-specific interstitial pneumonia. *Respirology*. 2016;21(2):259-68.
36. Jegal Y, Kim DS, Shim TS, Lim CM, Do Lee S, Koh Y, et al. Physiology is a stronger predictor of survival than pathology in fibrotic interstitial pneumonia. *Am J Respir Crit Care Med*. 2005;171(6):639-44.

37. Antoniou KM, Margaritopoulos G, Economidou F, Siafakas NM. Pivotal clinical dilemmas in collagen vascular diseases associated with interstitial lung involvement. *Eur Respir J.* 2009;33(4):882-96.
38. Kinder BW, Collard HR, Koth L, Daikh DI, Wolters PJ, Elicker B, et al. Idiopathic nonspecific interstitial pneumonia: lung manifestation of undifferentiated connective tissue disease? *Am J Respir Crit Care Med.* 2007;176(7):691-7.
39. Tansey D, Wells AU, Colby TV, Ip S, Nikolakoupolou A, du Bois RM, et al. Variations in histological patterns of interstitial pneumonia between connective tissue disorders and their relationship to prognosis. *Histopathology.* 2004;44(6):585-96.
40. Kim EJ, Elicker BM, Maldonado F, Webb WR, Ryu JH, Van Uden JH, et al. Usual interstitial pneumonia in rheumatoid arthritis-associated interstitial lung disease. *Eur Respir J.* 2010;35(6):1322-8.
41. Vasakova M, Morell F, Walsh S, Leslie K, Raghu G. Hypersensitivity Pneumonitis: Perspectives in Diagnosis and Management. *Am J Respir Crit Care Med.* 2017;196(6):680-9.
42. Lacasse Y, Girard M, Cormier Y. Recent advances in hypersensitivity pneumonitis. *Chest.* 2012;142(1):208-17.
43. Raghu G, Remy-Jardin M, Ryerson CJ, Myers JL, Kreuter M, Vasakova M, et al. Diagnosis of Hypersensitivity Pneumonitis in Adults. An Official ATS/JRS/ALAT Clinical Practice Guideline. *Am J Respir Crit Care Med.* 2020;202(3):e36-e69.
44. Lacasse Y, Selman M, Costabel U, Dalphin JC, Ando M, Morell F, et al. Clinical diagnosis of hypersensitivity pneumonitis. *Am J Respir Crit Care Med.* 2003;168(8):952-8.
45. Selman M, Pardo A, King TE, Jr. Hypersensitivity pneumonitis: insights in diagnosis and pathobiology. *Am J Respir Crit Care Med.* 2012;186(4):314-24.
46. Pereira CA, Gimenez A, Kuranishi L, Storrer K. Chronic hypersensitivity pneumonitis. *J Asthma Allergy.* 2016;9:171-81.
47. Lima MS, Coletta EN, Ferreira RG, Jasinowodolinski D, Arakaki JS, Rodrigues SC, et al. Subacute and chronic hypersensitivity pneumonitis: histopathological patterns and survival. *Respir Med.* 2009;103(4):508-15.
48. Dias OM, Baldi BG, Pennati F, Aliverti A, Chate RC, Sawamura MVY, et al. Computed tomography in hypersensitivity pneumonitis: main findings, differential diagnosis and pitfalls. *Expert Rev Respir Med.* 2018;12(1):5-13.
49. Silva CI, Muller NL, Lynch DA, Curran-Everett D, Brown KK, Lee KS, et al. Chronic hypersensitivity pneumonitis: differentiation from idiopathic pulmonary fibrosis and nonspecific interstitial pneumonia by using thin-section CT. *Radiology.* 2008;246(1):288-97.
50. Morell F, Roger A, Reyes L, Cruz MJ, Murio C, Munoz X. Bird fancier's lung: a series of 86 patients. *Medicine (Baltimore).* 2008;87(2):110-30.
51. Tateishi T, Ohtani Y, Takemura T, Akashi T, Miyazaki Y, Inase N, et al. Serial high-resolution computed tomography findings of acute and chronic hypersensitivity pneumonitis induced by avian antigen. *J Comput Assist Tomogr.* 2011;35(2):272-9.
52. Chung JH, Montner SM, Adegunsoye A, Oldham JM, Husain AN, Vij R, et al. CT findings associated with survival in chronic hypersensitivity pneumonitis. *Eur Radiol.* 2017;27(12):5127-35.
53. Salisbury ML, Gross BH, Chughtai A, Sayyouh M, Kazerooni EA, Bartholmai BJ, et al. Development and validation of a radiological diagnosis model for hypersensitivity pneumonitis. *Eur Respir J.* 2018;52(2).
54. Schwaiblmair M, Behr W, Haeckel T, Markl B, Foerg W, Berghaus T. Drug induced interstitial lung disease. *Open Respir Med J.* 2012;6:63-74.
55. Skeoch S, Weatherley N, Swift AJ, Oldroyd A, Johns C, Hayton C, et al. Drug-Induced Interstitial Lung Disease: A Systematic Review. *J Clin Med.* 2018;7(10).
56. Amar RK, Jick SS, Rosenberg D, Maher TM, Meier CR. Drug-/radiation-induced interstitial lung disease in the United Kingdom general population: incidence, all-cause mortality and characteristics at diagnosis. *Respirology.* 2012;17(5):861-8.

57. Delaunay M, Cadranel J, Lusque A, Meyer N, Gounant V, Moro-Sibilot D, et al. Immune-checkpoint inhibitors associated with interstitial lung disease in cancer patients. *Eur Respir J*. 2017;50(2):1700050.
58. Sears CR, Peikert T, Possick JD, Naidoo J, Nishino M, Patel SP, et al. Knowledge Gaps and Research Priorities in Immune Checkpoint Inhibitor-related Pneumonitis. An Official American Thoracic Society Research Statement. *Am J Respir Crit Care Med*. 2019;200(6):e31-e43.
59. Matsuno O. Drug-induced interstitial lung disease: mechanisms and best diagnostic approaches. *Respir Res*. 2012;13(1):39.
60. Kudoh S, Kato H, Nishiwaki Y, Fukuoka M, Nakata K, Ichinose Y, et al. Interstitial lung disease in Japanese patients with lung cancer: a cohort and nested case-control study. *Am J Respir Crit Care Med*. 2008;177(12):1348-57.
61. Kenmotsu H, Naito T, Kimura M, Ono A, Shukuya T, Nakamura Y, et al. The risk of cytotoxic chemotherapy-related exacerbation of interstitial lung disease with lung cancer. *J Thorac Oncol*. 2011;6(7):1242-6.
62. Johkoh T, Sakai F, Kusumoto M, Arakawa H, Harada R, Ueda M, et al. Association between baseline pulmonary status and interstitial lung disease in patients with non-small-cell lung cancer treated with erlotinib--a cohort study. *Clin Lung Cancer*. 2014;15(6):448-54.
63. Kobayashi H, Naito T, Omae K, Omori S, Nakashima K, Wakuda K, et al. ILD-NSCLC-GAP index scoring and staging system for patients with non-small cell lung cancer and interstitial lung disease. *Lung Cancer*. 2018;121:48-53.
64. Gyotoku H, Yamaguchi H, Ishimoto H, Sato S, Taniguchi H, Senju H, et al. Prediction of Anti-Cancer Drug-Induced Pneumonia in Lung Cancer Patients: Novel High-Resolution Computed Tomography Fibrosis Scoring. *J Clin Med*. 2020;9(4).
65. Nishino M, Giobbie-Hurder A, Hatabu H, Ramaiya NH, Hodi FS. Incidence of Programmed Cell Death 1 Inhibitor-Related Pneumonitis in Patients With Advanced Cancer: A Systematic Review and Meta-analysis. *JAMA Oncol*. 2016;2(12):1607-16.
66. Naidoo J, Wang X, Woo KM, Iyriboz T, Halpenny D, Cunningham J, et al. Pneumonitis in Patients Treated With Anti-Programmed Death-1/Programmed Death Ligand 1 Therapy. *J Clin Oncol*. 2017;35(7):709-17.
67. Flaherty KR, King TE, Jr., Raghu G, Lynch JP, 3rd, Colby TV, Travis WD, et al. Idiopathic interstitial pneumonia: what is the effect of a multidisciplinary approach to diagnosis? *Am J Respir Crit Care Med*. 2004;170(8):904-10.
68. Thomeer M, Demedts M, Behr J, Buhl R, Costabel U, Flower CD, et al. Multidisciplinary interobserver agreement in the diagnosis of idiopathic pulmonary fibrosis. *Eur Respir J*. 2008;31(3):585-91.
69. Walsh SLF. Multidisciplinary evaluation of interstitial lung diseases: current insights: Number 1 in the Series "Radiology" Edited by Nicola Sverzellati and Sujal Desai. *Eur Respir Rev*. 2017;26(144).
70. Flaherty KR, Andrei AC, King TE, Jr., Raghu G, Colby TV, Wells A, et al. Idiopathic interstitial pneumonia: do community and academic physicians agree on diagnosis? *Am J Respir Crit Care Med*. 2007;175(10):1054-60.
71. Sumikawa H, Johkoh T, Ichikado K, Taniguchi H, Kondoh Y, Fujimoto K, et al. Usual interstitial pneumonia and chronic idiopathic interstitial pneumonia: analysis of CT appearance in 92 patients. *Radiology*. 2006;241(1):258-66.
72. Salisbury ML, Xia M, Murray S, Bartholmai BJ, Kazerooni EA, Meldrum CA, et al. Predictors of idiopathic pulmonary fibrosis in absence of radiologic honeycombing: A cross sectional analysis in ILD patients undergoing lung tissue sampling. *Respir Med*. 2016;118:88-95.
73. Kazerooni EA, Martinez FJ, Flint A, Jamadar DA, Gross BH, Spizarny DL, et al. Thin-section CT obtained at 10-mm increments versus limited three-level thin-section CT for idiopathic pulmonary fibrosis: correlation with pathologic scoring. *AJR Am J Roentgenol*. 1997;169(4):977-83.
74. Ebner L, Kammerman J, Driehuys B, Schiebler ML, Cadman RV, Fain SB. The role of hyperpolarized (129)xenon in MR imaging of pulmonary function. *Eur J Radiol*. 2017;86:343-52.

75. Wells AU. High-resolution computed tomography and scleroderma lung disease. *Rheumatology (Oxford)*. 2008;47 Suppl 5:v59-61.
76. Wells AU, Hansell DM, Corrin B, Harrison NK, Goldstraw P, Black CM, et al. High resolution computed tomography as a predictor of lung histology in systemic sclerosis. *Thorax*. 1992;47(9):738-42.
77. Remy-Jardin M, Giraud F, Remy J, Copin MC, Gosselin B, Duhamel A. Importance of ground-glass attenuation in chronic diffuse infiltrative lung disease: pathologic-CT correlation. *Radiology*. 1993;189(3):693-8.
78. Aziz ZA, Wells AU, Hansell DM, Bain GA, Copley SJ, Desai SR, et al. HRCT diagnosis of diffuse parenchymal lung disease: inter-observer variation. *Thorax*. 2004;59(6):506-11.
79. Walsh SL, Calandriello L, Sverzellati N, Wells AU, Hansell DM, Consort UIPO. Interobserver agreement for the ATS/ERS/JRS/ALAT criteria for a UIP pattern on CT. *Thorax*. 2016;71(1):45-51.
80. MacDonald SL, Rubens MB, Hansell DM, Copley SJ, Desai SR, du Bois RM, et al. Nonspecific interstitial pneumonia and usual interstitial pneumonia: comparative appearances at and diagnostic accuracy of thin-section CT. *Radiology*. 2001;221(3):600-5.
81. Flaherty KR, Thwaite EL, Kazerooni EA, Gross BH, Toews GB, Colby TV, et al. Radiological versus histological diagnosis in UIP and NSIP: survival implications. *Thorax*. 2003;58(2):143-8.
82. Elliot TL, Lynch DA, Newell JD, Jr., Cool C, Tuder R, Markopoulou K, et al. High-resolution computed tomography features of nonspecific interstitial pneumonia and usual interstitial pneumonia. *J Comput Assist Tomogr*. 2005;29(3):339-45.
83. Silva CI, Muller NL, Hansell DM, Lee KS, Nicholson AG, Wells AU. Nonspecific interstitial pneumonia and idiopathic pulmonary fibrosis: changes in pattern and distribution of disease over time. *Radiology*. 2008;247(1):251-9.
84. Hunninghake GW, Lynch DA, Galvin JR, Gross BH, Muller N, Schwartz DA, et al. Radiologic findings are strongly associated with a pathologic diagnosis of usual interstitial pneumonia. *Chest*. 2003;124(4):1215-23.
85. Raghu G, Mageto YN, Lockhart D, Schmidt RA, Wood DE, Godwin JD. The accuracy of the clinical diagnosis of new-onset idiopathic pulmonary fibrosis and other interstitial lung disease: A prospective study. *Chest*. 1999;116(5):1168-74.
86. Hunninghake GW, Zimmerman MB, Schwartz DA, King TE, Jr., Lynch J, Hegele R, et al. Utility of a lung biopsy for the diagnosis of idiopathic pulmonary fibrosis. *Am J Respir Crit Care Med*. 2001;164(2):193-6.
87. Aalokken TM, Naalsund A, Mynarek G, Berstad AE, Solberg S, Strom EH, et al. Diagnostic accuracy of computed tomography and histopathology in the diagnosis of usual interstitial pneumonia. *Acta Radiol*. 2012;53(3):296-302.
88. Assayag D, Elicker BM, Urbania TH, Colby TV, Kang BH, Ryu JH, et al. Rheumatoid arthritis-associated interstitial lung disease: radiologic identification of usual interstitial pneumonia pattern. *Radiology*. 2014;270(2):583-8.
89. Yagihashi K, Huckleberry J, Colby TV, Tazelaar HD, Zach J, Sundaram B, et al. Radiologic-pathologic discordance in biopsy-proven usual interstitial pneumonia. *Eur Respir J*. 2016;47(4):1189-97.
90. Plantier L, Cazes A, Dinh-Xuan AT, Bancal C, Marchand-Adam S, Crestani B. Physiology of the lung in idiopathic pulmonary fibrosis. *Eur Respir Rev*. 2018;27(147).
91. Esam H, Alhamad JPL, Fernando J, Martinez. Pulmonary Function Tests In Interstitial Lung Disease: What Role Do They Have? *Clin Chest Med*. 2001;22(4):715-50.
92. Buzan MT, Pop CM. State of the art in the diagnosis and management of interstitial lung disease. *Clujul Med*. 2015;88(2):116-23.
93. Blakemore WS, Forster RE, Morton JW, Ogilvie CM. A standardized breath holding technique for the clinical measurement of the diffusing capacity of the lung for carbon monoxide. *J Clin Invest*. 1957;36(1 Part 1):1-17.

94. Graham BL, Brusasco V, Burgos F, Cooper BG, Jensen R, Kendrick A, et al. 2017 ERS/ATS standards for single-breath carbon monoxide uptake in the lung. *Eur Respir J*. 2017;49(1):1600016.
95. Frans A, Nemery B, Veriter C, Lacquet L, Francis C. Effect of alveolar volume on the interpretation of single breath DLCO. *Respir Med*. 1997;91(5):263-73.
96. Wallaert B, Wemeau-Stervinou L, Salleron J, Tillie-Leblond I, Perez T. Do we need exercise tests to detect gas exchange impairment in fibrotic idiopathic interstitial pneumonias? *Pulm Med*. 2012;2012:657180.
97. Cottin V, Wollin L, Fischer A, Quaresma M, Stowasser S, Harari S. Fibrosing interstitial lung diseases: knowns and unknowns. *Eur Respir Rev*. 2019;28(151).
98. Bodlet A, Maury G, Jamart J, Dahlqvist C. Influence of radiological emphysema on lung function test in idiopathic pulmonary fibrosis. *Respir Med*. 2013;107(11):1781-8.
99. Wells AU. Interstitial lung disease in systemic sclerosis. *Presse Med*. 2014;43(10 Pt 2):e329-43.
100. Schmidt SL, Tayob N, Han MK, Zappala C, Kervitsky D, Murray S, et al. Predicting pulmonary fibrosis disease course from past trends in pulmonary function. *Chest*. 2014;145(3):579-85.
101. Wells AU, Desai SR, Rubens MB, Goh NS, Cramer D, Nicholson AG, et al. Idiopathic pulmonary fibrosis: a composite physiologic index derived from disease extent observed by computed tomography. *Am J Respir Crit Care Med*. 2003;167(7):962-9.
102. Collins FS, Varmus H. A new initiative on precision medicine. *N Engl J Med*. 2015;372(9):793-5.
103. Spagnolo P, Tzouvelekis A, Maher TM. Personalized medicine in idiopathic pulmonary fibrosis: facts and promises. *Curr Opin Pulm Med*. 2015;21(5):470-8.
104. Goldin JG. Computed tomography as a biomarker in clinical trials imaging. *J Thorac Imaging*. 2013;28(5):291-7.
105. Silva M, Milanese G, Seletti V, Ariani A, Sverzellati N. Pulmonary quantitative CT imaging in focal and diffuse disease: current research and clinical applications. *Br J Radiol*. 2018;91(1083):20170644.
106. Hansell DM, Goldin JG, King TE, Jr., Lynch DA, Richeldi L, Wells AU. CT staging and monitoring of fibrotic interstitial lung diseases in clinical practice and treatment trials: a position paper from the Fleischner Society. *Lancet Respir Med*. 2015;3(6):483-96.
107. Lynch DA, Godwin JD, Safrin S, Starko KM, Hormel P, Brown KK, et al. High-resolution computed tomography in idiopathic pulmonary fibrosis: diagnosis and prognosis. *Am J Respir Crit Care Med*. 2005;172(4):488-93.
108. Goldin J, Elashoff R, Kim HJ, Yan X, Lynch D, Strollo D, et al. Treatment of scleroderma-interstitial lung disease with cyclophosphamide is associated with less progressive fibrosis on serial thoracic high-resolution CT scan than placebo: findings from the scleroderma lung study. *Chest*. 2009;136(5):1333-40.
109. Sundaram B, Gross BH, Oh E, Muller N, Myles JD, Kazerooni EA. Reader accuracy and confidence in diagnosing diffuse lung disease on high-resolution computed tomography of the lungs: impact of sampling frequency. *Acta Radiol*. 2008;49(8):870-5.
110. Siemienowicz ML, Kruger SJ, Goh NS, Dobson JE, Spelman TD, Fabiny RP. Agreement and mortality prediction in high-resolution CT of diffuse fibrotic lung disease. *J Med Imaging Radiat Oncol*. 2015;59(5):555-63.
111. Walsh SL, Sverzellati N, Devaraj A, Keir GJ, Wells AU, Hansell DM. Connective tissue disease related fibrotic lung disease: high resolution computed tomographic and pulmonary function indices as prognostic determinants. *Thorax*. 2014;69(3):216-22.
112. Watadani T, Sakai F, Johkoh T, Noma S, Akira M, Fujimoto K, et al. Interobserver variability in the CT assessment of honeycombing in the lungs. *Radiology*. 2013;266(3):936-44.
113. Chong DY, Kim HJ, Lo P, Young S, McNitt-Gray MF, Abtin F, et al. Robustness-Driven Feature Selection in Classification of Fibrotic Interstitial Lung Disease Patterns in Computed Tomography Using 3D Texture Features. *IEEE Trans Med Imaging*. 2016;35(1):144-57.

114. Newell JD, Jr., Sieren J, Hoffman EA. Development of quantitative computed tomography lung protocols. *J Thorac Imaging*. 2013;28(5):266-71.
115. Obuchowski NA, Reeves AP, Huang EP, Wang XF, Buckler AJ, Kim HJ, et al. Quantitative imaging biomarkers: a review of statistical methods for computer algorithm comparisons. *Stat Methods Med Res*. 2015;24(1):68-106.
116. Mascalchi M, Camiciottoli G, Diciotti S. Lung densitometry: why, how and when. *J Thorac Dis*. 2017;9(9):3319-45.
117. Washko GR, Parraga G, Coxson HO. Quantitative pulmonary imaging using computed tomography and magnetic resonance imaging. *Respiology*. 2012;17(3):432-44.
118. Kim HJ, Brown MS, Chong D, Gjertson DW, Lu P, Kim HJ, et al. Comparison of the quantitative CT imaging biomarkers of idiopathic pulmonary fibrosis at baseline and early change with an interval of 7 months. *Acad Radiol*. 2015;22(1):70-80.
119. Beinert T, Behr J, Mehnert F, Kohz P, Seemann M, Rienmuller R, et al. Spirometrically controlled quantitative CT for assessing diffuse parenchymal lung disease. *J Comput Assist Tomogr*. 1995;19(6):924-31.
120. Beinert T, Kohz P, Seemann M, Egge T, Reiser M, Behr J. Spirometrically controlled high resolution computed tomography - quantitative assessment of density distribution in patients with diffuse fibrosing alveolitis. *Eur J Med Res*. 1996;1(6):269-72.
121. Sverzellati N, Zompatori M, De Luca G, Chetta A, Bna C, Ormitti F, et al. Evaluation of quantitative CT indexes in idiopathic interstitial pneumonitis using a low-dose technique. *Eur J Radiol*. 2005;56(3):370-5.
122. Sverzellati N, Calabro E, Chetta A, Concari G, Larici AR, Mereu M, et al. Visual score and quantitative CT indices in pulmonary fibrosis: Relationship with physiologic impairment. *Radiol Med*. 2007;112(8):1160-72.
123. Camiciottoli G, Diciotti S, Bartolucci M, Orlandi I, Bigazzi F, Matucci-Cerinic M, et al. Whole-lung volume and density in spirometrically-gated inspiratory and expiratory CT in systemic sclerosis: correlation with static volumes at pulmonary function tests. *Sarcoidosis Vasc Diffuse Lung Dis*. 2013;30(1):17-27.
124. Cetincakmak MG, Goya C, Hamidi C, Tekbas G, Abakay O, Batmaz I, et al. Quantitative volumetric assessment of pulmonary involvement in patients with systemic sclerosis. *Quant Imaging Med Surg*. 2016;6(1):50-6.
125. Do KH, Lee JS, Colby TV, Kitaichi M, Kim DS. Nonspecific interstitial pneumonia versus usual interstitial pneumonia: differences in the density histogram of high-resolution CT. *J Comput Assist Tomogr*. 2005;29(4):544-8.
126. Sumikawa H, Johkoh T, Yamamoto S, Oota M, Ueguchi T, Ogata Y, et al. Volume histogram analysis for lung thin-section computed tomography: differentiation between usual interstitial pneumonia and nonspecific interstitial pneumonia. *J Comput Assist Tomogr*. 2007;31(6):936-42.
127. Tanizawa K, Handa T, Nagai S, Hirai T, Kubo T, Oguma T, et al. Clinical impact of high-attenuation and cystic areas on computed tomography in fibrotic idiopathic interstitial pneumonias. *BMC Pulm Med*. 2015;15:74.
128. Iwasawa T, Takemura T, Okudera K, Gotoh T, Iwao Y, Kitamura H, et al. The importance of subpleural fibrosis in the prognosis of patients with idiopathic interstitial pneumonias. *Eur J Radiol*. 2017;90:106-13.
129. Best AC, Lynch AM, Bozic CM, Miller D, Grunwald GK, Lynch DA. Quantitative CT indexes in idiopathic pulmonary fibrosis: relationship with physiologic impairment. *Radiology*. 2003;228(2):407-14.
130. Nakagawa H, Nagatani Y, Takahashi M, Ogawa E, Tho NV, Ryujin Y, et al. Quantitative CT analysis of honeycombing area in idiopathic pulmonary fibrosis: Correlations with pulmonary function tests. *Eur J Radiol*. 2016;85(1):125-30.

131. Ohkubo H, Kanemitsu Y, Uemura T, Takakuwa O, Takemura M, Maeno K, et al. Normal Lung Quantification in Usual Interstitial Pneumonia Pattern: The Impact of Threshold-based Volumetric CT Analysis for the Staging of Idiopathic Pulmonary Fibrosis. *PLoS One*. 2016;11(3):e0152505.
132. Iwasawa T, Kanauchi T, Hoshi T, Ogura T, Baba T, Gotoh T, et al. Multicenter study of quantitative computed tomography analysis using a computer-aided three-dimensional system in patients with idiopathic pulmonary fibrosis. *Jpn J Radiol*. 2016;34(1):16-27.
133. Ash SY, Harmouche R, Vallejo DL, Villalba JA, Ostridge K, Gunville R, et al. Densitometric and local histogram based analysis of computed tomography images in patients with idiopathic pulmonary fibrosis. *Respir Res*. 2017;18(1):45.
134. Rea G, De Martino M, Capaccio A, Dolce P, Valente T, Castaldo S, et al. Comparative analysis of density histograms and visual scores in incremental and volumetric high-resolution computed tomography of the chest in idiopathic pulmonary fibrosis patients. *Radiol Med*. 2020.
135. Iwasawa T, Asakura A, Sakai F, Kanauchi T, Gotoh T, Ogura T, et al. Assessment of prognosis of patients with idiopathic pulmonary fibrosis by computer-aided analysis of CT images. *J Thorac Imaging*. 2009;24(3):216-22.
136. Colombi D, Dinkel J, Weinheimer O, Obermayer B, Buzan T, Nabers D, et al. Visual vs Fully Automatic Histogram-Based Assessment of Idiopathic Pulmonary Fibrosis (IPF) Progression Using Sequential Multidetector Computed Tomography (MDCT). *PLoS One*. 2015;10(6):e0130653.
137. Orlandi I, Camiciottoli G, Diciotti S, Bartolucci M, Cavigli E, Nacci F, et al. Thin-section and low-dose volumetric computed tomographic densitometry of the lung in systemic sclerosis. *J Comput Assist Tomogr*. 2006;30(5):823-7.
138. Camiciottoli G, Orlandi I, Bartolucci M, Meoni E, Nacci F, Diciotti S, et al. Lung CT densitometry in systemic sclerosis: correlation with lung function, exercise testing, and quality of life. *Chest*. 2007;131(3):672-81.
139. Marten K, Dicken V, Kneitz C, Hoehmann M, Kenn W, Hahn D, et al. Computer-assisted quantification of interstitial lung disease associated with rheumatoid arthritis: preliminary technical validation. *Eur J Radiol*. 2009;72(2):278-83.
140. Marten K, Dicken V, Kneitz C, Hohmann M, Kenn W, Hahn D, et al. Interstitial lung disease associated with collagen vascular disorders: disease quantification using a computer-aided diagnosis tool. *Eur Radiol*. 2009;19(2):324-32.
141. Ariani A, Silva M, Bravi E, Saracco M, Parisi S, De Gennaro F, et al. Operator-independent quantitative chest computed tomography versus standard assessment of interstitial lung disease related to systemic sclerosis: A multi-centric study. *Mod Rheumatol*. 2015;25(5):724-30.
142. Ninaber MK, Stolk J, Smit J, Le Roy EJ, Kroft LJ, Bakker ME, et al. Lung structure and function relation in systemic sclerosis: application of lung densitometry. *Eur J Radiol*. 2015;84(5):975-9.
143. Salaffi F, Carotti M, Bosello S, Ciapetti A, Gutierrez M, Bichisecchi E, et al. Computer-aided quantification of interstitial lung disease from high resolution computed tomography images in systemic sclerosis: correlation with visual reader-based score and physiologic tests. *Biomed Res Int*. 2015;2015:834262.
144. Salaffi F, Carotti M, Di Donato E, Di Carlo M, Ceccarelli L, Giuseppetti G. Computer-Aided Tomographic Analysis of Interstitial Lung Disease (ILD) in Patients with Systemic Sclerosis (SSc). Correlation with Pulmonary Physiologic Tests and Patient-Centred Measures of Perceived Dyspnea and Functional Disability. *PLoS One*. 2016;11(3):e0149240.
145. Bocchino M, Bruzzese D, D'Alto M, Argiento P, Borgia A, Capaccio A, et al. Performance of a new quantitative computed tomography index for interstitial lung disease assessment in systemic sclerosis. *Sci Rep*. 2019;9(1):9468.
146. Guisado-Vasco P, Silva M, Duarte-Millan MA, Sambataro G, Bertolazzi C, Pavone M, et al. Quantitative assessment of interstitial lung disease in Sjogren's syndrome. *PLoS One*. 2019;14(11):e0224772.
147. Ufuk F, Demirci M, Altinisik G, Karasu U. Quantitative analysis of Sjogren's syndrome related interstitial lung disease with different methods. *Eur J Radiol*. 2020;128:109030.

148. Ariani A, Carotti M, Gutierrez M, Bichisecchi E, Grassi W, Giuseppetti GM, et al. Utility of an open-source DICOM viewer software (OsiriX) to assess pulmonary fibrosis in systemic sclerosis: preliminary results. *Rheumatol Int.* 2014;34(4):511-6.
149. Ariani A, Lumetti F, Silva M, Santilli D, Mozzani F, Lucchini G, et al. Systemic sclerosis interstitial lung disease evaluation: comparison between semiquantitative and quantitative computed tomography assessments. *J Biol Regul Homeost Agents.* 2014;28(3):507-13.
150. Nguyen-Kim TDL, Maurer B, Suliman YA, Morsbach F, Distler O, Frauenfelder T. The impact of slice-reduced computed tomography on histogram-based densitometry assessment of lung fibrosis in patients with systemic sclerosis. *J Thorac Dis.* 2018;10(4):2142-52.
151. Best AC, Meng J, Lynch AM, Bozic CM, Miller D, Grunwald GK, et al. Idiopathic pulmonary fibrosis: physiologic tests, quantitative CT indexes, and CT visual scores as predictors of mortality. *Radiology.* 2008;246(3):935-40.
152. Kloth C, Maximilian Thaiss W, Preibsch H, Mark K, Kotter I, Hetzel J, et al. Quantitative chest CT analysis in patients with systemic sclerosis before and after autologous stem cell transplantation: comparison of results with those of pulmonary function tests and clinical tests. *Rheumatology (Oxford).* 2016;55(10):1763-70.
153. Yabuuchi H, Matsuo Y, Tsukamoto H, Horiuchi T, Sunami S, Kamitani T, et al. Evaluation of the extent of ground-glass opacity on high-resolution CT in patients with interstitial pneumonia associated with systemic sclerosis: comparison between quantitative and qualitative analysis. *Clin Radiol.* 2014;69(7):758-64.
154. Kloth C, Henes J, Xenitidis T, Thaiss WM, Blum AC, Fritz J, et al. Chest CT texture analysis for response assessment in systemic sclerosis. *Eur J Radiol.* 2018;101:50-8.
155. Salaffi F, Carotti M, Tardella M, Di Carlo M, Fraticelli P, Fischetti C, et al. Computed tomography assessment of evolution of interstitial lung disease in systemic sclerosis: Comparison of two scoring systems. *Eur J Intern Med.* 2020;76:71-5.
156. Koyama H, Ohno Y, Yamazaki Y, Nogami M, Kusaka A, Murase K, et al. Quantitatively assessed CT imaging measures of pulmonary interstitial pneumonia: effects of reconstruction algorithms on histogram parameters. *Eur J Radiol.* 2010;74(1):142-6.
157. Salisbury ML, Lynch DA, van Beek EJ, Kazerooni EA, Guo J, Xia M, et al. Idiopathic Pulmonary Fibrosis: The Association between the Adaptive Multiple Features Method and Fibrosis Outcomes. *Am J Respir Crit Care Med.* 2017;195(7):921-9.
158. Uppaluri R, Hoffman EA, Sonka M, Hartley PG, Hunninghake GW, McLennan G. Computer recognition of regional lung disease patterns. *Am J Respir Crit Care Med.* 1999;160(2):648-54.
159. Uppaluri R, Hoffman EA, Sonka M, Hunninghake GW, McLennan G. Interstitial lung disease: A quantitative study using the adaptive multiple feature method. *Am J Respir Crit Care Med.* 1999;159(2):519-25.
160. Iwasawa T, Ogura T, Sakai F, Kanauchi T, Komagata T, Baba T, et al. CT analysis of the effect of pirfenidone in patients with idiopathic pulmonary fibrosis. *Eur J Radiol.* 2014;83(1):32-8.
161. Kim HG, Tashkin DP, Clements PJ, Li G, Brown MS, Elashoff R, et al. A computer-aided diagnosis system for quantitative scoring of extent of lung fibrosis in scleroderma patients. *Clin Exp Rheumatol.* 2010;28(5 Suppl 62):S26-35.
162. Kim HJ, Brown MS, Elashoff R, Li G, Gjertson DW, Lynch DA, et al. Quantitative texture-based assessment of one-year changes in fibrotic reticular patterns on HRCT in scleroderma lung disease treated with oral cyclophosphamide. *Eur Radiol.* 2011;21(12):2455-65.
163. Kim HJ, Tashkin DP, Gjertson DW, Brown MS, Kleerup E, Chong S, et al. Transitions to different patterns of interstitial lung disease in scleroderma with and without treatment. *Ann Rheum Dis.* 2016;75(7):1367-71.
164. Goldin JG, Kim GHJ, Tseng CH, Volkmann E, Furst D, Clements P, et al. Longitudinal Changes in Quantitative Interstitial Lung Disease on Computed Tomography after Immunosuppression in the Scleroderma Lung Study II. *Ann Am Thorac Soc.* 2018;15(11):1286-95.

165. Maldonado F, Moua T, Rajagopalan S, Karwoski RA, Raghunath S, Decker PA, et al. Automated quantification of radiological patterns predicts survival in idiopathic pulmonary fibrosis. *Eur Respir J*. 2014;43(1):204-12.
166. Bartholmai BJ, Raghunath S, Karwoski RA, Moua T, Rajagopalan S, Maldonado F, et al. Quantitative computed tomography imaging of interstitial lung diseases. *J Thorac Imaging*. 2013;28(5):298-307.
167. Jacob J, Bartholmai BJ, Rajagopalan S, Kokosi M, Nair A, Karwoski R, et al. Automated Quantitative Computed Tomography Versus Visual Computed Tomography Scoring in Idiopathic Pulmonary Fibrosis: Validation Against Pulmonary Function. *J Thorac Imaging*. 2016;31(5):304-11.
168. Jacob J, Bartholmai BJ, Rajagopalan S, Kokosi M, Nair A, Karwoski R, et al. Mortality prediction in idiopathic pulmonary fibrosis: evaluation of computer-based CT analysis with conventional severity measures. *Eur Respir J*. 2017;49(1).
169. Jacob J, Bartholmai BJ, Rajagopalan S, van Moorsel CHM, van Es HW, van Beek FT, et al. Predicting Outcomes in Idiopathic Pulmonary Fibrosis Using Automated Computed Tomographic Analysis. *Am J Respir Crit Care Med*. 2018;198(6):767-76.
170. Jacob J, Bartholmai BJ, Rajagopalan S, Kokosi M, Egashira R, Brun AL, et al. Serial automated quantitative CT analysis in idiopathic pulmonary fibrosis: functional correlations and comparison with changes in visual CT scores. *Eur Radiol*. 2018;28(3):1318-27.
171. De Giacomo F, Raghunath S, Karwoski R, Bartholmai BJ, Moua T. Short-term Automated Quantification of Radiologic Changes in the Characterization of Idiopathic Pulmonary Fibrosis Versus Nonspecific Interstitial Pneumonia and Prediction of Long-term Survival. *J Thorac Imaging*. 2018;33(2):124-31.
172. Crews MS, Bartholmai BJ, Adegunsoye A, Oldham JM, Montner SM, Karwoski RA, et al. Automated CT Analysis of Major Forms of Interstitial Lung Disease. *J Clin Med*. 2020;9(11).
173. Jacob J, Bartholmai BJ, Rajagopalan S, Brun AL, Egashira R, Karwoski R, et al. Evaluation of computer-based computer tomography stratification against outcome models in connective tissue disease-related interstitial lung disease: a patient outcome study. *BMC Med*. 2016;14(1):190.
174. Ungprasert P, Wilton KM, Ernste FC, Kalra S, Crowson CS, Rajagopalan S, et al. Novel Assessment of Interstitial Lung Disease Using the "Computer-Aided Lung Informatics for Pathology Evaluation and Rating" (CALIPER) Software System in Idiopathic Inflammatory Myopathies. *Lung*. 2017;195(5):545-52.
175. Jacob J, Bartholmai BJ, Brun AL, Egashira R, Rajagopalan S, Karwoski R, et al. Evaluation of visual and computer-based CT analysis for the identification of functional patterns of obstruction and restriction in hypersensitivity pneumonitis. *Respirology*. 2017;22(8):1585-91.
176. Jacob J, Bartholmai BJ, Egashira R, Brun AL, Rajagopalan S, Karwoski R, et al. Chronic hypersensitivity pneumonitis: identification of key prognostic determinants using automated CT analysis. *BMC Pulm Med*. 2017;17(1):81.
177. Jacob J, Bartholmai BJ, Rajagopalan S, Karwoski R, Mak SM, Mok W, et al. Automated computer-based CT stratification as a predictor of outcome in hypersensitivity pneumonitis. *Eur Radiol*. 2017;27(9):3635-46.
178. Humphries SM, Yagihashi K, Huckleberry J, Rho BH, Schroeder JD, Strand M, et al. Idiopathic Pulmonary Fibrosis: Data-driven Textural Analysis of Extent of Fibrosis at Baseline and 15-Month Follow-up. *Radiology*. 2017;285(1):270-8.
179. Humphries SM, Swigris JJ, Brown KK, Strand M, Gong Q, Sundry JS, et al. Quantitative high-resolution computed tomography fibrosis score: performance characteristics in idiopathic pulmonary fibrosis. *Eur Respir J*. 2018;52(3).
180. Park SO, Seo JB, Kim N, Lee YK, Lee J, Kim DS. Comparison of usual interstitial pneumonia and nonspecific interstitial pneumonia: quantification of disease severity and discrimination between two diseases on HRCT using a texture-based automated system. *Korean J Radiol*. 2011;12(3):297-307.

181. Kazantzi A, Costaridou L, Skiadopoulou S, Korfiatis P, Karahaliou A, Daoussis D, et al. Automated 3D interstitial lung disease extent quantification: performance evaluation and correlation to PFTs. *J Digit Imaging*. 2014;27(3):380-91.
182. Martyanov V, Kim GJ, Hayes W, Du S, Ganguly BJ, Sy O, et al. Novel lung imaging biomarkers and skin gene expression subsetting in dasatinib treatment of systemic sclerosis-associated interstitial lung disease. *PLoS One*. 2017;12(11):e0187580.
183. Yoon RG, Seo JB, Kim N, Lee HJ, Lee SM, Lee YK, et al. Quantitative assessment of change in regional disease patterns on serial HRCT of fibrotic interstitial pneumonia with texture-based automated quantification system. *Eur Radiol*. 2013;23(3):692-701.
184. Park HJ, Lee SM, Song JW, Lee SM, Oh SY, Kim N, et al. Texture-Based Automated Quantitative Assessment of Regional Patterns on Initial CT in Patients With Idiopathic Pulmonary Fibrosis: Relationship to Decline in Forced Vital Capacity. *AJR Am J Roentgenol*. 2016;207(5):976-83.
185. Tashkin DP, Volkmann ER, Tseng CH, Kim HJ, Goldin J, Clements P, et al. Relationship between quantitative radiographic assessments of interstitial lung disease and physiological and clinical features of systemic sclerosis. *Ann Rheum Dis*. 2016;75(2):374-81.
186. Clukers J, Lanclus M, Mignot B, Van Holsbeke C, Roseman J, Porter S, et al. Quantitative CT analysis using functional imaging is superior in describing disease progression in idiopathic pulmonary fibrosis compared to forced vital capacity. *Respir Res*. 2018;19(1):213.
187. Maher TM, van der Aar EM, Van de Steen O, Allamassey L, Desrivot J, Dupont S, et al. Safety, tolerability, pharmacokinetics, and pharmacodynamics of GLPG1690, a novel autotaxin inhibitor, to treat idiopathic pulmonary fibrosis (FLORA): a phase 2a randomised placebo-controlled trial. *Lancet Respir Med*. 2018;6(8):627-35.
188. McLellan T, George PM, Ford P, De Backer J, Van Holsbeke C, Mignot B, et al. Idiopathic pulmonary fibrosis: airway volume measurement identifies progressive disease on computed tomography scans. *ERJ Open Res*. 2020;6(1).
189. Walsh SLF, Calandriello L, Silva M, Sverzellati N. Deep learning for classifying fibrotic lung disease on high-resolution computed tomography: a case-cohort study. *Lancet Respir Med*. 2018;6(11):837-45.
190. Rea G. Magnetic resonance imaging in the evaluation of idiopathic pulmonary fibrosis: a real possibility, or an attractive challenge? *Quant Imaging Med Surg*. 2016;6(3):331-3.
191. Kruger SJ, Nagle SK, Couch MJ, Ohno Y, Albert M, Fain SB. Functional imaging of the lungs with gas agents. *J Magn Reson Imaging*. 2016;43(2):295-315.
192. McFadden RG, Carr TJ, Wood TE. Proton magnetic resonance imaging to stage activity of interstitial lung disease. *Chest*. 1987;92(1):31-9.
193. Müller NL, Mayo JR, Zwirer CV. Value of MR imaging in the evaluation of chronic infiltrative lung diseases: comparison with CT. *AJR Am J Roentgenol*. 1992;158(6):1205-9.
194. Pinal-Fernandez I, Pineda-Sanchez V, Pallisa-Nunez E, Simeon-Aznar CP, Selva-O'Callaghan A, Fonollosa-Pla V, et al. Fast 1.5 T chest MRI for the assessment of interstitial lung disease extent secondary to systemic sclerosis. *Clin Rheumatol*. 2016;35(9):2339-45.
195. Ohno Y, Nishio M, Koyama H, Takenaka D, Takahashi M, Yoshikawa T, et al. Pulmonary MR imaging with ultra-short TEs: utility for disease severity assessment of connective tissue disease patients. *Eur J Radiol*. 2013;82(8):1359-65.
196. Ohno Y, Koyama H, Yoshikawa T, Seki S, Takenaka D, Yui M, et al. Pulmonary high-resolution ultrashort TE MR imaging: Comparison with thin-section standard- and low-dose computed tomography for the assessment of pulmonary parenchyma diseases. *J Magn Reson Imaging*. 2016;43(2):512-32.
197. Lutterbey G, Gieseke J, von Falkenhausen M, Morakkabati N, Schild H. Lung MRI at 3.0 T: a comparison of helical CT and high-field MRI in the detection of diffuse lung disease. *Eur Radiol*. 2005;15(2):324-8.

198. Lutterbey G, Grohe C, Gieseke J, von Falkenhausen M, Morakkabati N, Wattjes MP, et al. Initial experience with lung-MRI at 3.0T: Comparison with CT and clinical data in the evaluation of interstitial lung disease activity. *Eur J Radiol.* 2007;61(2):256-61.
199. Primack SL, Mayo JR, Hartman TE, Miller RR, Muller NL. MRI of infiltrative lung disease: comparison with pathologic findings. *J Comput Assist Tomogr.* 1994;18(2):233-8.
200. Saunders LC, Eaden JA, Bianchi SM, Swift AJ, Wild JM. Free breathing lung T1 mapping using image registration in patients with idiopathic pulmonary fibrosis. *Magn Reson Med.* 2020.
201. Benlala I, Albat A, Blanchard E, Macey J, Raheison C, Benkert T, et al. Quantification of MRI T2 Interstitial Lung Disease Signal-Intensity Volume in Idiopathic Pulmonary Fibrosis: A Pilot Study. *J Magn Reson Imaging.* 2020.
202. Buzan MT, Eichinger M, Kreuter M, Kauczor HU, Herth FJ, Warth A, et al. T2 mapping of CT remodelling patterns in interstitial lung disease. *Eur Radiol.* 2015;25(11):3167-74.
203. Buzan MTA, Wetscherek A, Heussel CP, Kreuter M, Herth FJ, Warth A, et al. Texture analysis using proton density and T2 relaxation in patients with histological usual interstitial pneumonia (UIP) or nonspecific interstitial pneumonia (NSIP). *PLoS One.* 2017;12(5):e0177689.
204. Montesi SB, Caravan P. Novel Imaging Approaches in Systemic Sclerosis-Associated Interstitial Lung Disease. *Curr Rheumatol Rep.* 2019;21(6):25.
205. Gordon Y, Partovi S, Muller-Eschner M, Amarteifio E, Bauerle T, Weber MA, et al. Dynamic contrast-enhanced magnetic resonance imaging: fundamentals and application to the evaluation of the peripheral perfusion. *Cardiovasc Diagn Ther.* 2014;4(2):147-64.
206. Jaspers K, Leiner T, Dijkstra P, Oostendorp M, van Golde JM, Post MJ, et al. Optimized pharmacokinetic modeling for the detection of perfusion differences in skeletal muscle with DCE-MRI: effect of contrast agent size. *Med Phys.* 2010;37(11):5746-55.
207. Walker-Samuel S, Leach MO, Collins DJ. Evaluation of response to treatment using DCE-MRI: the relationship between initial area under the gadolinium curve (IAUGC) and quantitative pharmacokinetic analysis. *Phys Med Biol.* 2006;51(14):3593-602.
208. Pack NA, DiBella EV. Comparison of myocardial perfusion estimates from dynamic contrast-enhanced magnetic resonance imaging with four quantitative analysis methods. *Magn Reson Med.* 2010;64(1):125-37.
209. Lin YR, Tsai SY, Huang TY, Chung HW, Huang YL, Wu FZ, et al. Inflow-weighted pulmonary perfusion: comparison between dynamic contrast-enhanced MRI versus perfusion scintigraphy in complex pulmonary circulation. *J Cardiovasc Magn Reson.* 2013;15(1):21.
210. Fink C, Ley S, Risse F, Eichinger M, Zaporozhan J, Buhmann R, et al. Effect of inspiratory and expiratory breathhold on pulmonary perfusion: assessment by pulmonary perfusion magnetic resonance imaging. *Invest Radiol.* 2005;40(2):72-9.
211. Weatherley ND, Eaden JA, Hughes PJC, Austin M, Smith L, Bray J, et al. Quantification of pulmonary perfusion in idiopathic pulmonary fibrosis with first pass dynamic contrast-enhanced perfusion MRI. *Thorax.* 2020.
212. Yi CA, Lee KS, Han J, Chung MP, Chung MJ, Shin KM. 3-T MRI for differentiating inflammation- and fibrosis-predominant lesions of usual and nonspecific interstitial pneumonia: comparison study with pathologic correlation. *AJR Am J Roentgenol.* 2008;190(4):878-85.
213. Mirsadraee S, Tse M, Kershaw L, Semple S, Schembri N, Chin C, et al. T1 characteristics of interstitial pulmonary fibrosis on 3T MRI-a predictor of early interstitial change? *Quant Imaging Med Surg.* 2016;6(1):42-9.
214. Lavelle LP, Brady D, McEvoy S, Murphy D, Gibney B, Gallagher A, et al. Pulmonary fibrosis: tissue characterization using late-enhanced MRI compared with unenhanced anatomic high-resolution CT. *Diagn Interv Radiol.* 2017;23(2):106-11.
215. Montesi SB, Rao R, Liang LL, Goulart HE, Sharma A, Digumarthy SR, et al. Gadofosveset-enhanced lung magnetic resonance imaging to detect ongoing vascular leak in pulmonary fibrosis. *Eur Respir J.* 2018;51(5).

216. Tsuchiya N, Ayukawa Y, Murayama S. Evaluation of hemodynamic changes by use of phase-contrast MRI for patients with interstitial pneumonia, with special focus on blood flow reduction after breath-holding and bronchopulmonary shunt flow. *Jpn J Radiol.* 2013;31(3):197-203.
217. Tsuchiya N, Yamashiro T, Murayama S. Decrease of pulmonary blood flow detected by phase contrast MRI is correlated with a decrease in lung volume and increase of lung fibrosis area determined by computed tomography in interstitial lung disease. *Eur J Radiol.* 2016;85(9):1581-5.
218. Muller CJ, Schwaiblmair M, Scheidler J, Deimling M, Weber J, Loffler RB, et al. Pulmonary diffusing capacity: assessment with oxygen-enhanced lung MR imaging preliminary findings. *Radiology.* 2002;222(2):499-506.
219. Ohno Y, Hatabu H. Basics concepts and clinical applications of oxygen-enhanced MR imaging. *Eur J Radiol.* 2007;64(3):320-8.
220. Molinari F, Eichinger M, Risse F, Plathow C, Puderbach M, Ley S, et al. Navigator-triggered oxygen-enhanced MRI with simultaneous cardiac and respiratory synchronization for the assessment of interstitial lung disease. *J Magn Reson Imaging.* 2007;26(6):1523-9.
221. Ohno Y, Nishio M, Koyama H, Yoshikawa T, Matsumoto S, Seki S, et al. Oxygen-enhanced MRI for patients with connective tissue diseases: comparison with thin-section CT of capability for pulmonary functional and disease severity assessment. *Eur J Radiol.* 2014;83(2):391-7.
222. Marinelli JP, Levin DL, Vassallo R, Carter RE, Hubmayr RD, Ehman RL, et al. Quantitative assessment of lung stiffness in patients with interstitial lung disease using MR elastography. *J Magn Reson Imaging.* 2017;46(2):365-74.
223. Mammarrappallil JG, Rankine L, Wild JM, Driehuys B. New Developments in Imaging Idiopathic Pulmonary Fibrosis With Hyperpolarized Xenon Magnetic Resonance Imaging. *J Thorac Imaging.* 2019;34(2):136-50.
224. Norquay G, Collier GJ, Rao M, Stewart NJ, Wild JM. ^{129}Xe -Rb Spin-Exchange Optical Pumping with High Photon Efficiency. *Phys Rev Lett.* 2018;121(15):153201.
225. Couch MJ, Blasiak B, Tomanek B, Ouriadov AV, Fox MS, Dowhos KM, et al. Hyperpolarized and inert gas MRI: the future. *Mol Imaging Biol.* 2015;17(2):149-62.
226. Fain SB, Korosec FR, Holmes JH, O'Halloran R, Sorkness RL, Grist TM. Functional lung imaging using hyperpolarized gas MRI. *J Magn Reson Imaging.* 2007;25(5):910-23.
227. Mugler JP, 3rd, Altes TA. Hyperpolarized ^{129}Xe MRI of the human lung. *J Magn Reson Imaging.* 2013;37(2):313-31.
228. Cleveland ZI, Cofer GP, Metz G, Beaver D, Nouls J, Kaushik SS, et al. Hyperpolarized Xe MR imaging of alveolar gas uptake in humans. *PLoS One.* 2010;5(8):e12192.
229. Wang JM, Robertson SH, Wang Z, He M, Virgincar RS, Schrank GM, et al. Using hyperpolarized ^{129}Xe MRI to quantify regional gas transfer in idiopathic pulmonary fibrosis. *Thorax.* 2018;73(1):21-8.
230. Kaushik SS, Freeman MS, Yoon SW, Liljeroth MG, Stiles JV, Roos JE, et al. Measuring diffusion limitation with a perfusion-limited gas--hyperpolarized ^{129}Xe gas-transfer spectroscopy in patients with idiopathic pulmonary fibrosis. *J Appl Physiol (1985).* 2014;117(6):577-85.
231. Stewart NJ, Leung G, Norquay G, Marshall H, Parra-Robles J, Murphy PS, et al. Experimental validation of the hyperpolarized ^{129}Xe chemical shift saturation recovery technique in healthy volunteers and subjects with interstitial lung disease. *Magn Reson Med.* 2015;74(1):196-207.
232. Weatherley ND, Stewart NJ, Chan HF, Austin M, Smith LJ, Collier G, et al. Hyperpolarised xenon magnetic resonance spectroscopy for the longitudinal assessment of changes in gas diffusion in IPF. *Thorax.* 2019;74(5):500-2.
233. Hahn AD, Kammerman J, Evans M, Zha W, Cadman RV, Meyer K, et al. Repeatability of regional pulmonary functional metrics of Hyperpolarized ^{129}Xe dissolved-phase MRI. *J Magn Reson Imaging.* 2019;50(4):1182-90.
234. Kaushik SS, Robertson SH, Freeman MS, He M, Kelly KT, Roos JE, et al. Single-breath clinical imaging of hyperpolarized ^{129}Xe in the airspaces, barrier, and red blood cells using an interleaved 3D radial 1-point Dixon acquisition. *Magn Reson Med.* 2016;75(4):1434-43.

235. Wang Z, Robertson SH, Wang J, He M, Virgincar RS, Schrank GM, et al. Quantitative analysis of hyperpolarized (129) Xe gas transfer MRI. *Med Phys*. 2017;44(6):2415-28.
236. Bier EA, Robertson SH, Schrank GM, Rackley C, Mammarrappallil JG, Rajagopal S, et al. A protocol for quantifying cardiogenic oscillations in dynamic (129) Xe gas exchange spectroscopy: The effects of idiopathic pulmonary fibrosis. *NMR Biomed*. 2019;32(1):e4029.
237. Wang Z, Bier EA, Swaminathan A, Parikh K, Nouls J, He M, et al. Diverse cardiopulmonary diseases are associated with distinct xenon magnetic resonance imaging signatures. *Eur Respir J*. 2019;54(6).
238. Liu Z, Araki T, Okajima Y, Albert M, Hatabu H. Pulmonary hyperpolarized noble gas MRI: recent advances and perspectives in clinical application. *Eur J Radiol*. 2014;83(7):1282-91.
239. Kaushik SS, Cleveland ZI, Cofer GP, Metz G, Beaver D, Nouls J, et al. Diffusion-weighted hyperpolarized 129Xe MRI in healthy volunteers and subjects with chronic obstructive pulmonary disease. *Magn Reson Med*. 2011;65(4):1154-65.
240. Chan HF, Weatherley ND, Johns CS, Stewart NJ, Collier GJ, Bianchi SM, et al. Airway Microstructure in Idiopathic Pulmonary Fibrosis: Assessment at Hyperpolarized (3)He Diffusion-weighted MRI. *Radiology*. 2019;291(1):223-9.
241. Chan HF, Stewart NJ, Norquay G, Collier GJ, Wild JM. 3D diffusion-weighted (129) Xe MRI for whole lung morphometry. *Magn Reson Med*. 2018;79(6):2986-95.
242. Kirby M, Svenningsen S, Owrangi A, Wheatley A, Farag A, Ouriadov A, et al. Hyperpolarized 3He and 129Xe MR imaging in healthy volunteers and patients with chronic obstructive pulmonary disease. *Radiology*. 2012;265(2):600-10.
243. Kirby M, Heydarian M, Svenningsen S, Wheatley A, McCormack DG, Etemad-Rezai R, et al. Hyperpolarized 3He magnetic resonance functional imaging semiautomated segmentation. *Acad Radiol*. 2012;19(2):141-52.
244. Svenningsen S, Kirby M, Starr D, Leary D, Wheatley A, Maksym GN, et al. Hyperpolarized (3) He and (129) Xe MRI: differences in asthma before bronchodilation. *J Magn Reson Imaging*. 2013;38(6):1521-30.
245. Loeh B, Brylski LT, von der Beck D, Seeger W, Krauss E, Bonniaud P, et al. Lung CT Densitometry in Idiopathic Pulmonary Fibrosis for the Prediction of Natural Course, Severity, and Mortality. *Chest*. 2019;155(5):972-81.
246. Ariani A, Silva M, Seletti V, Bravi E, Saracco M, Parisi S, et al. Quantitative chest computed tomography is associated with two prediction models of mortality in interstitial lung disease related to systemic sclerosis. *Rheumatology (Oxford)*. 2017;56(6):922-7.
247. Fraioli F, Lyasheva M, Porter JC, Bomanji J, Shortman RI, Endozo R, et al. Synergistic application of pulmonary (18)F-FDG PET/HRCT and computer-based CT analysis with conventional severity measures to refine current risk stratification in idiopathic pulmonary fibrosis (IPF). *Eur J Nucl Med Mol Imaging*. 2019;46(10):2023-31.
248. Romei C, Tavanti LM, Taliani A, De Liperi A, Karwoski R, Celi A, et al. Automated Computed Tomography analysis in the assessment of Idiopathic Pulmonary Fibrosis severity and progression. *Eur J Radiol*. 2020;124:108852.
249. Hosein KS, Sergiacomi G, Zompatori M, Mura M. The CALIPER-Revised Version of the Composite Physiologic Index is a Better Predictor of Survival in IPF than the Original Version. *Lung*. 2020;198(1):169-72.
250. Sverzellati N, Silva M, Seletti V, Galeone C, Palmucci S, Piciocchi S, et al. Stratification of long-term outcome in stable idiopathic pulmonary fibrosis by combining longitudinal computed tomography and forced vital capacity. *Eur Radiol*. 2020;30(5):2669-79.
251. Kim GHJ, Weigt SS, Belperio JA, Brown MS, Shi Y, Lai JH, et al. Prediction of idiopathic pulmonary fibrosis progression using early quantitative changes on CT imaging for a short term of clinical 18-24-month follow-ups. *Eur Radiol*. 2020;30(2):726-34.

252. Nakano A, Ohkubo H, Taniguchi H, Kondoh Y, Matsuda T, Yagi M, et al. Early decrease in erector spinae muscle area and future risk of mortality in idiopathic pulmonary fibrosis. *Sci Rep*. 2020;10(1):2312.
253. Walsh SL, Sverzellati N, Devaraj A, Wells AU, Hansell DM. Chronic hypersensitivity pneumonitis: high resolution computed tomography patterns and pulmonary function indices as prognostic determinants. *Eur Radiol*. 2012;22(8):1672-9.
254. Goh NS, Desai SR, Veeraraghavan S, Hansell DM, Copley SJ, Maher TM, et al. Interstitial lung disease in systemic sclerosis: a simple staging system. *Am J Respir Crit Care Med*. 2008;177(11):1248-54.
255. Moore OA, Goh N, Corte T, Rouse H, Hennessy O, Thakkar V, et al. Extent of disease on high-resolution computed tomography lung is a predictor of decline and mortality in systemic sclerosis-related interstitial lung disease. *Rheumatology (Oxford)*. 2013;52(1):155-60.
256. Shin KM, Lee KS, Chung MP, Han J, Bae YA, Kim TS, et al. Prognostic determinants among clinical, thin-section CT, and histopathologic findings for fibrotic idiopathic interstitial pneumonias: tertiary hospital study. *Radiology*. 2008;249(1):328-37.
257. Lee HY, Lee KS, Jeong YJ, Hwang JH, Kim HJ, Chung MP, et al. High-resolution CT findings in fibrotic idiopathic interstitial pneumonias with little honeycombing: serial changes and prognostic implications. *AJR Am J Roentgenol*. 2012;199(5):982-9.
258. Mooney JJ, Elicker BM, Urbania TH, Agarwal MR, Ryerson CJ, Nguyen MLT, et al. Radiographic fibrosis score predicts survival in hypersensitivity pneumonitis. *Chest*. 2013;144(2):586-92.
259. Bax S, Jacob J, Ahmed R, Bredy C, Dimopoulos K, Kempny A, et al. Right Ventricular to Left Ventricular Ratio at CT Pulmonary Angiogram Predicts Mortality in Interstitial Lung Disease. *Chest*. 2020;157(1):89-98.
260. Hanak V, Golbin JM, Hartman TE, Ryu JH. High-resolution CT findings of parenchymal fibrosis correlate with prognosis in hypersensitivity pneumonitis. *Chest*. 2008;134(1):133-8.
261. Chung JH, Zhan X, Cao M, Koelsch TL, Manjarres DCG, Brown KK, et al. Presence of Air Trapping and Mosaic Attenuation on Chest Computed Tomography Predicts Survival in Chronic Hypersensitivity Pneumonitis. *Ann Am Thorac Soc*. 2017;14(10):1533-8.
262. Salisbury ML, Gu T, Murray S, Gross BH, Chughtai A, Sayyoub M, et al. Hypersensitivity Pneumonitis: Radiologic Phenotypes Are Associated With Distinct Survival Time and Pulmonary Function Trajectory. *Chest*. 2019;155(4):699-711.
263. Sumikawa H, Johkoh T, Colby TV, Ichikado K, Suga M, Taniguchi H, et al. Computed tomography findings in pathological usual interstitial pneumonia: relationship to survival. *Am J Respir Crit Care Med*. 2008;177(4):433-9.
264. Ley B, Elicker BM, Hartman TE, Ryerson CJ, Vittinghoff E, Ryu JH, et al. Idiopathic pulmonary fibrosis: CT and risk of death. *Radiology*. 2014;273(2):570-9.
265. Tossier C, Dupin C, Plantier L, Leger J, Flament T, Favelle O, et al. Hiatal hernia on thoracic computed tomography in pulmonary fibrosis. *Eur Respir J*. 2016;48(3):833-42.
266. Sin S, Lee KH, Hur JH, Lee SH, Lee YJ, Cho YJ, et al. Impact of mediastinal lymph node enlargement on the prognosis of idiopathic pulmonary fibrosis. *PLoS One*. 2018;13(7):e0201154.
267. Takei R, Arita M, Kumagai S, Ito Y, Tokioka F, Koyama T, et al. Radiographic fibrosis score predicts survival in systemic sclerosis-associated interstitial lung disease. *Respirology*. 2018;23(4):385-91.
268. Akira M, Inoue Y, Arai T, Okuma T, Kawata Y. Long-term follow-up high-resolution CT findings in non-specific interstitial pneumonia. *Thorax*. 2011;66(1):61-5.
269. Taha N, D'Amato D, Hosein K, Ranalli T, Sergiacomi G, Zompatori M, et al. Longitudinal functional changes with clinically significant radiographic progression in idiopathic pulmonary fibrosis: are we following the right parameters? *Respir Res*. 2020;21(1):119.
270. Oda K, Ishimoto H, Yatera K, Naito K, Ogoshi T, Yamasaki K, et al. High-resolution CT scoring system-based grading scale predicts the clinical outcomes in patients with idiopathic pulmonary fibrosis. *Respir Res*. 2014;15:10.

271. Jacob J, Aksman L, Mogulkoc N, Procter AJ, Gholipour B, Cross G, et al. Serial CT analysis in idiopathic pulmonary fibrosis: comparison of visual features that determine patient outcome. *Thorax*. 2020;75(8):648-54.
272. Song JW, Do KH, Kim MY, Jang SJ, Colby TV, Kim DS. Pathologic and radiologic differences between idiopathic and collagen vascular disease-related usual interstitial pneumonia. *Chest*. 2009;136(1):23-30.
273. Gemma A, Kudoh S, Ando M, Ohe Y, Nakagawa K, Johkoh T, et al. Final safety and efficacy of erlotinib in the phase 4 POLARSTAR surveillance study of 10 708 Japanese patients with non-small-cell lung cancer. *Cancer Sci*. 2014;105(12):1584-90.
274. Enomoto N, Suda T, Kono M, Kaida Y, Hashimoto D, Fujisawa T, et al. Amount of elastic fibers predicts prognosis of idiopathic pulmonary fibrosis. *Respir Med*. 2013;107(10):1608-16.
275. Song JW, Do KH, Jang SJ, Colby TV, Han S, Kim DS. Blood biomarkers MMP-7 and SP-A: predictors of outcome in idiopathic pulmonary fibrosis. *Chest*. 2013;143(5):1422-9.
276. Doubkova M, Svancara J, Svoboda M, Sterclova M, Bartos V, Plackova M, et al. EMPIRE Registry, Czech Part: Impact of demographics, pulmonary function and HRCT on survival and clinical course in idiopathic pulmonary fibrosis. *Clin Respir J*. 2018;12(4):1526-35.
277. Adegunsoye A, Oldham JM, Bonham C, Hrusch C, Nolan P, Klejch W, et al. Prognosticating Outcomes in Interstitial Lung Disease by Mediastinal Lymph Node Assessment. An Observational Cohort Study with Independent Validation. *Am J Respir Crit Care Med*. 2019;199(6):747-59.
278. Winstone TA, Hague CJ, Soon J, Sulaiman N, Murphy D, Leipsic J, et al. Oesophageal diameter is associated with severity but not progression of systemic sclerosis-associated interstitial lung disease. *Respirology*. 2018;23(10):921-6.
279. Choi JS, Lee SH, Leem AY, Song JH, Chung KS, Jung JY, et al. Prognostic impact of the ratio of the main pulmonary artery to that of the aorta on chest computed tomography in patients with idiopathic pulmonary fibrosis. *BMC Pulm Med*. 2019;19(1):81.
280. Shin S, King CS, Puri N, Shlobin OA, Brown AW, Ahmad S, et al. Pulmonary artery size as a predictor of outcomes in idiopathic pulmonary fibrosis. *Eur Respir J*. 2016;47(5):1445-51.
281. Enomoto Y, Takemura T, Hagiwara E, Iwasawa T, Fukuda Y, Yanagawa N, et al. Prognostic factors in interstitial lung disease associated with primary Sjogren's syndrome: a retrospective analysis of 33 pathologically-proven cases. *PLoS One*. 2013;8(9):e73774.
282. Alhamad EH, Al-Kassimi FA, Alboukai AA, Raddaoui E, Al-Hajjaj MS, Hajjar W, et al. Comparison of three groups of patients with usual interstitial pneumonia. *Respir Med*. 2012;106(11):1575-85.
283. Moon SW, Choi JS, Lee SH, Jung KS, Jung JY, Kang YA, et al. Thoracic skeletal muscle quantification: low muscle mass is related with worse prognosis in idiopathic pulmonary fibrosis patients. *Respir Res*. 2019;20(1):35.
284. Umeda Y, Demura Y, Morikawa M, Anzai M, Kadowaki M, Ameshima S, et al. Prognostic Value of Dual-Time-Point 18F-FDG PET for Idiopathic Pulmonary Fibrosis. *J Nucl Med*. 2015;56(12):1869-75.
285. Ley B. A Glimpse into the Future: Automated Quantitative Computed Tomography as a Biomarker in Idiopathic Pulmonary Fibrosis. *Am J Respir Crit Care Med*. 2017;195(7):850-2.
286. Richeldi L, Ryerson CJ, Lee JS, Wolters PJ, Koth LL, Ley B, et al. Relative versus absolute change in forced vital capacity in idiopathic pulmonary fibrosis. *Thorax*. 2012;67(5):407-11.
287. Noble PW, Albera C, Bradford WZ, Costabel U, Glassberg MK, Kardatzke D, et al. Pirfenidone in patients with idiopathic pulmonary fibrosis (CAPACITY): two randomised trials. *Lancet*. 2011;377(9779):1760-9.
288. Caminati A, Bianchi A, Cassandro R, Mirenda MR, Harari S. Walking distance on 6-MWT is a prognostic factor in idiopathic pulmonary fibrosis. *Respir Med*. 2009;103(1):117-23.
289. Sharp C, Adamali HI, Millar AB. A comparison of published multidimensional indices to predict outcome in idiopathic pulmonary fibrosis. *ERJ Open Res*. 2017;3(1).
290. Goh NS, Veeraraghavan S, Desai SR, Cramer D, Hansell DM, Denton CP, et al. Bronchoalveolar lavage cellular profiles in patients with systemic sclerosis-associated interstitial lung disease are not predictive of disease progression. *Arthritis Rheum*. 2007;56(6):2005-12.

291. Goh NS, Hoyles RK, Denton CP, Hansell DM, Renzoni EA, Maher TM, et al. Short-Term Pulmonary Function Trends Are Predictive of Mortality in Interstitial Lung Disease Associated With Systemic Sclerosis. *Arthritis & Rheumatology*. 2017;69(8):1670-8.
292. Zamora AC, Hoskote SS, Abascal-Bolado B, White D, Cox CW, Ryu JH, et al. Clinical features and outcomes of interstitial lung disease in anti-Jo-1 positive antisynthetase syndrome. *Respir Med*. 2016;118:39-45.
293. Park JH, Kim DS, Park IN, Jang SJ, Kitaichi M, Nicholson AG, et al. Prognosis of fibrotic interstitial pneumonia: idiopathic versus collagen vascular disease-related subtypes. *Am J Respir Crit Care Med*. 2007;175(7):705-11.
294. King TE, Jr., Schwarz MI, Brown K, Tooze JA, Colby TV, Waldron JA, Jr., et al. Idiopathic pulmonary fibrosis: relationship between histopathologic features and mortality. *Am J Respir Crit Care Med*. 2001;164(6):1025-32.
295. Hallstrand TS, Boitano LJ, Johnson WC, Spada CA, Hayes JG, Raghu G. The timed walk test as a measure of severity and survival in idiopathic pulmonary fibrosis. *Eur Respir J*. 2005;25(1):96-103.
296. Jeon K, Chung MP, Lee KS, Chung MJ, Han J, Koh WJ, et al. Prognostic factors and causes of death in Korean patients with idiopathic pulmonary fibrosis. *Respir Med*. 2006;100(3):451-7.
297. Han MK, Murray S, Fell CD, Flaherty KR, Toews GB, Myers J, et al. Sex differences in physiological progression of idiopathic pulmonary fibrosis. *Eur Respir J*. 2008;31(6):1183-8.
298. Fell CD, Liu LX, Motika C, Kazerooni EA, Gross BH, Travis WD, et al. The prognostic value of cardiopulmonary exercise testing in idiopathic pulmonary fibrosis. *Am J Respir Crit Care Med*. 2009;179(5):402-7.
299. Lee SH, Kim SY, Kim DS, Kim YW, Chung MP, Uh ST, et al. Predicting survival of patients with idiopathic pulmonary fibrosis using GAP score: a nationwide cohort study. *Respir Res*. 2016;17(1):131.
300. Bahmer T, Kirsten AM, Waschki B, Rabe KF, Magnussen H, Kirsten D, et al. Prognosis and longitudinal changes of physical activity in idiopathic pulmonary fibrosis. *BMC Pulm Med*. 2017;17(1):104.
301. Snyder L, Neely ML, Hellkamp AS, O'Brien E, de Andrade J, Conoscenti CS, et al. Predictors of death or lung transplant after a diagnosis of idiopathic pulmonary fibrosis: insights from the IPF-PRO Registry. *Respir Res*. 2019;20(1):105.
302. Nurmi HM, Purokivi MK, Karkkainen MS, Kettunen HP, Selander TA, Kaarteenaho RL. Are risk predicting models useful for estimating survival of patients with rheumatoid arthritis-associated interstitial lung disease? *BMC Pulm Med*. 2017;17(1):16.
303. Wallaert B, Monge E, Le Rouzic O, Wemeau-Stervinou L, Salleron J, Grosbois JM. Physical activity in daily life of patients with fibrotic idiopathic interstitial pneumonia. *Chest*. 2013;144(5):1652-8.
304. Paterniti MO, Bi Y, Rekić D, Wang Y, Karimi-Shah BA, Chowdhury BA. Acute Exacerbation and Decline in Forced Vital Capacity Are Associated with Increased Mortality in Idiopathic Pulmonary Fibrosis. *Ann Am Thorac Soc*. 2017;14(9):1395-402.
305. Soares MR, Pereira C, Ferreira R, Nei Aparecida Martins Coletta E, Silva Lima M, Muller Storrer K. A score for estimating survival in idiopathic pulmonary fibrosis with rest SpO₂>88. *Sarcoidosis Vasc Diffuse Lung Dis*. 2015;32(2):121-8.
306. Sokai A, Tanizawa K, Handa T, Kanatani K, Kubo T, Ikezoe K, et al. Importance of serial changes in biomarkers in idiopathic pulmonary fibrosis. *ERJ Open Res*. 2017;3(3).
307. Zamora-Legoff JA, Krause ML, Crowson CS, Ryu JH, Matteson EL. Patterns of interstitial lung disease and mortality in rheumatoid arthritis. *Rheumatology (Oxford)*. 2017;56(3):344-50.
308. Morisset J, Vittinghoff E, Elicker BM, Hu X, Le S, Ryu JH, et al. Mortality Risk Prediction in Scleroderma-Related Interstitial Lung Disease: The SADL Model. *Chest*. 2017;152(5):999-1007.
309. Ikeda K, Shiratori M, Chiba H, Nishikiori H, Yokoo K, Saito A, et al. Serum surfactant protein D predicts the outcome of patients with idiopathic pulmonary fibrosis treated with pirfenidone. *Respir Med*. 2017;131:184-91.

310. Jo HE, Glaspole I, Moodley Y, Chapman S, Ellis S, Goh N, et al. Disease progression in idiopathic pulmonary fibrosis with mild physiological impairment: analysis from the Australian IPF registry. *BMC Pulm Med.* 2018;18(1):19.
311. Schmidt SL, Nambiar AM, Tayob N, Sundaram B, Han MK, Gross BH, et al. Pulmonary function measures predict mortality differently in IPF versus combined pulmonary fibrosis and emphysema. *European Respiratory Journal.* 2010;38(1):176-83.
312. Salisbury ML, Xia M, Zhou Y, Murray S, Tayob N, Brown KK, et al. Idiopathic Pulmonary Fibrosis. *Chest.* 2016;149(2):491-8.
313. Manali ED, Stathopoulos GT, Kollintza A, Kalomenidis I, Emili JM, Sotiropoulou C, et al. The Medical Research Council chronic dyspnea score predicts the survival of patients with idiopathic pulmonary fibrosis. *Respir Med.* 2008;102(4):586-92.
314. Kurashima K, Takayanagi N, Tsuchiya N, Kanauchi T, Ueda M, Hoshi T, et al. The effect of emphysema on lung function and survival in patients with idiopathic pulmonary fibrosis. *Respirology.* 2010;15(5):843-8.
315. Cai M, Zhu M, Ban C, Su J, Ye Q, Liu Y, et al. Clinical features and outcomes of 210 patients with idiopathic pulmonary fibrosis. *Chin Med J (Engl).* 2014;127(10):1868-73.
316. Moua T, Zamora Martinez AC, Baqir M, Vassallo R, Limper AH, Ryu JH. Predictors of diagnosis and survival in idiopathic pulmonary fibrosis and connective tissue disease-related usual interstitial pneumonia. *Respir Res.* 2014;15(1):154.
317. Fernandez Perez ER, Swigris JJ, Forssen AV, Tourin O, Solomon JJ, Huie TJ, et al. Identifying an inciting antigen is associated with improved survival in patients with chronic hypersensitivity pneumonitis. *Chest.* 2013;144(5):1644-51.
318. Long X, He X, Ohshimo S, Griese M, Sarria R, Guzman J, et al. Serum YKL-40 as predictor of outcome in hypersensitivity pneumonitis. *Eur Respir J.* 2017;49(2).
319. Gimenez A, Storrer K, Kuranishi L, Soares MR, Ferreira RG, Pereira CAC. Change in FVC and survival in chronic fibrotic hypersensitivity pneumonitis. *Thorax.* 2018;73(4):391-2.
320. Fujisawa T, Hozumi H, Kono M, Enomoto N, Hashimoto D, Nakamura Y, et al. Prognostic factors for myositis-associated interstitial lung disease. *PLoS One.* 2014;9(6):e98824.
321. Nishiyama O, Taniguchi H, Kondoh Y, Kimura T, Kataoka K, Nishimura K, et al. Health-related quality of life does not predict mortality in idiopathic pulmonary fibrosis. *Sarcoidosis Vasc Diffuse Lung Dis.* 2012;29(2):113-8.
322. Lee KJ, Chung MP, Kim YW, Lee JH, Kim KS, Ryu JS, et al. Prevalence, risk factors and survival of lung cancer in the idiopathic pulmonary fibrosis. *Thorac Cancer.* 2012;3(2):150-5.
323. Kimura M, Taniguchi H, Kondoh Y, Kimura T, Kataoka K, Nishiyama O, et al. Pulmonary hypertension as a prognostic indicator at the initial evaluation in idiopathic pulmonary fibrosis. *Respiration.* 2013;85(6):456-63.
324. Dai J, Cai H, Li H, Zhuang Y, Min H, Wen Y, et al. Association between telomere length and survival in patients with idiopathic pulmonary fibrosis. *Respirology.* 2015;20(6):947-52.
325. Furukawa T, Taniguchi H, Ando M, Kondoh Y, Kataoka K, Nishiyama O, et al. The St. George's Respiratory Questionnaire as a prognostic factor in IPF. *Respir Res.* 2017;18(1):18.
326. Serajeddini H, Rogliani P, Mura M. Multi-dimensional Assessment of IPF Across a Wide Range of Disease Severity. *Lung.* 2018;196(6):707-13.
327. Akiyama N, Hozumi H, Isayama T, Okada J, Sugiura K, Yasui H, et al. Clinical significance of serum S100 calcium-binding protein A4 in idiopathic pulmonary fibrosis. *Respirology.* 2020;25(7):743-9.
328. Nolan CM, Maddocks M, Maher TM, Banya W, Patel S, Barker RE, et al. Gait speed and prognosis in patients with idiopathic pulmonary fibrosis: a prospective cohort study. *Eur Respir J.* 2019;53(2).
329. Mejia M, Carrillo G, Rojas-Serrano J, Estrada A, Suarez T, Alonso D, et al. Idiopathic pulmonary fibrosis and emphysema: decreased survival associated with severe pulmonary arterial hypertension. *Chest.* 2009;136(1):10-5.

330. du Bois RM, Weycker D, Albera C, Bradford WZ, Costabel U, Kartashov A, et al. Ascertainment of individual risk of mortality for patients with idiopathic pulmonary fibrosis. *Am J Respir Crit Care Med.* 2011;184(4):459-66.
331. du Bois RM, Albera C, Bradford WZ, Costabel U, Leff JA, Noble PW, et al. 6-Minute walk distance is an independent predictor of mortality in patients with idiopathic pulmonary fibrosis. *Eur Respir J.* 2014;43(5):1421-9.
332. Corte TJ, Wort SJ, MacDonald PS, Edey A, Hansell DM, Renzoni E, et al. Pulmonary function vascular index predicts prognosis in idiopathic interstitial pneumonia. *Respirology.* 2012;17(4):674-80.
333. Peelen L, Wells AU, Prijs M, Blumenthal JP, Van Steenwijk RP, Jonkers RE, et al. Fibrotic idiopathic interstitial pneumonias: Mortality is linked to a decline in gas transfer. *Respirology.* 2010;15(8):1233-43.
334. Reichmann WM, Yu YF, Macaulay D, Wu EQ, Nathan SD. Change in forced vital capacity and associated subsequent outcomes in patients with newly diagnosed idiopathic pulmonary fibrosis. *BMC Pulm Med.* 2015;15:167.
335. Durham MT, Collard HR, Roberts RS, Brown KK, Flaherty KR, King TE, Jr., et al. Association of hospital admission and forced vital capacity endpoints with survival in patients with idiopathic pulmonary fibrosis: analysis of a pooled cohort from three clinical trials. *Lancet Respir Med.* 2015;3(5):388-96.
336. Novelli F, Tavanti L, Cini S, Aquilini F, Melosini L, Romei C, et al. Determinants of the prognosis of idiopathic pulmonary fibrosis. *Eur Rev Med Pharmacol Sci.* 2014;18(6):880-6.
337. Raghu G, Ley B, Brown KK, Cottin V, Gibson KF, Kaner RJ, et al. Risk factors for disease progression in idiopathic pulmonary fibrosis. *Thorax.* 2020;75(1):78-80.
338. Song JW, Song JK, Kim DS. Echocardiography and brain natriuretic peptide as prognostic indicators in idiopathic pulmonary fibrosis. *Respir Med.* 2009;103(2):180-6.
339. Collard HR, Bradford WZ, Cottin V, Flaherty KR, King TE, Jr., Koch GG, et al. A new era in idiopathic pulmonary fibrosis: considerations for future clinical trials. *Eur Respir J.* 2015;46(1):243-9.
340. Cottin V, Hansell DM, Sverzellati N, Weycker D, Antoniou KM, Atwood M, et al. Effect of Emphysema Extent on Serial Lung Function in Patients with Idiopathic Pulmonary Fibrosis. *Am J Respir Crit Care Med.* 2017;196(9):1162-71.
341. Tiev KP, Hua-Huy T, Kettaneh A, Gain M, Duong-Quy S, Toledano C, et al. Serum CC chemokine ligand-18 predicts lung disease worsening in systemic sclerosis. *Eur Respir J.* 2011;38(6):1355-60.
342. Lee YS, Kim HC, Lee BY, Lee CK, Kim MY, Jang SJ, et al. The Value of Biomarkers as Predictors of Outcome in Patients with Rheumatoid Arthritis-Associated Usual Interstitial Pneumonia. *Sarcoidosis Vasc Diffuse Lung Dis.* 2016;33(3):216-23.
343. Zappala CJ, Latsi PI, Nicholson AG, Colby TV, Cramer D, Renzoni EA, et al. Marginal decline in forced vital capacity is associated with a poor outcome in idiopathic pulmonary fibrosis. *Eur Respir J.* 2010;35(4):830-6.
344. Ryerson CJ, Abbritti M, Ley B, Elicker BM, Jones KD, Collard HR. Cough predicts prognosis in idiopathic pulmonary fibrosis. *Respirology.* 2011;16(6):969-75.
345. Ooi GC, Mok MY, Tsang KW, Wong Y, Khong PL, Fung PC, et al. Interstitial lung disease in systemic sclerosis. *Acta Radiol.* 2003;44(3):258-64.
346. Rossi SE, Erasmus JJ, McAdams HP, Sporn TA, Goodman PC. Pulmonary drug toxicity: radiologic and pathologic manifestations. *Radiographics.* 2000;20(5):1245-59.
347. Johnson KM, Fain SB, Schiebler ML, Nagle S. Optimized 3D ultrashort echo time pulmonary MRI. *Magn Reson Med.* 2013;70(5):1241-50.
348. Tofts PS, Brix G, Buckley DL, Evelhoch JL, Henderson E, Knopp MV, et al. Estimating kinetic parameters from dynamic contrast-enhanced T(1)-weighted MRI of a diffusible tracer: standardized quantities and symbols. *J Magn Reson Imaging.* 1999;10(3):223-32.
349. Ostergaard L, Weisskoff RM, Chesler DA, Gyldensted C, Rosen BR. High resolution measurement of cerebral blood flow using intravascular tracer bolus passages. Part I: Mathematical approach and statistical analysis. *Magn Reson Med.* 1996;36(5):715-25.

350. Zhang WJ, Niven RM, Young SS, Liu YZ, Parker GJ, Naish JH. Dynamic oxygen-enhanced magnetic resonance imaging of the lung in asthma -- initial experience. *Eur J Radiol.* 2015;84(2):318-26.
351. Dietrich O, Gaass T, Reiser MF. T1 relaxation time constants, influence of oxygen, and the oxygen transfer function of the human lung at 1.5T-A meta-analysis. *Eur J Radiol.* 2017;86:252-60.
352. Stewart NJ, Norquay G, Griffiths PD, Wild JM. Feasibility of human lung ventilation imaging using highly polarized naturally abundant xenon and optimized three-dimensional steady-state free precession. *Magn Reson Med.* 2015;74(2):346-52.
353. Hughes PJC, Horn FC, Collier GJ, Biancardi A, Marshall H, Wild JM. Spatial fuzzy c-means thresholding for semiautomated calculation of percentage lung ventilated volume from hyperpolarized gas and (1) H MRI. *J Magn Reson Imaging.* 2018;47(3):640-6.
354. Woodhouse N, Wild JM, Paley MN, Fichelle S, Said Z, Swift AJ, et al. Combined helium-3/proton magnetic resonance imaging measurement of ventilated lung volumes in smokers compared to never-smokers. *J Magn Reson Imaging.* 2005;21(4):365-9.
355. Wiesinger F, Weidl E, Menzel MI, Janich MA, Khagai O, Glaser SJ, et al. IDEAL spiral CSI for dynamic metabolic MR imaging of hyperpolarized [1-13C]pyruvate. *Magn Reson Med.* 2012;68(1):8-16.
356. Collier GJ, Eaden JA, Hughes PJC, Bianchi SM, Stewart NJ, Weatherley ND, et al. Dissolved (129) Xe lung MRI with four-echo 3D radial spectroscopic imaging: Quantification of regional gas transfer in idiopathic pulmonary fibrosis. *Magn Reson Med.* 2020.
357. Quanjer PH, Stanojevic S, Cole TJ, Baur X, Hall GL, Culver BH, et al. Multi-ethnic reference values for spirometry for the 3-95-yr age range: the global lung function 2012 equations. *Eur Respir J.* 2012;40(6):1324-43.
358. Stewart NJ, Horn FC, Norquay G, Collier GJ, Yates DP, Lawson R, et al. Reproducibility of quantitative indices of lung function and microstructure from (129) Xe chemical shift saturation recovery (CSSR) MR spectroscopy. *Magn Reson Med.* 2017;77(6):2107-13.
359. Behr J, Kreuter M, Hoepfer MM, Wirtz H, Klotsche J, Koschel D, et al. Management of patients with idiopathic pulmonary fibrosis in clinical practice: the INSIGHTS-IPF registry. *Eur Respir J.* 2015;46(1):186-96.
360. Vaz S, Falkmer T, Passmore AE, Parsons R, Andreou P. The case for using the repeatability coefficient when calculating test-retest reliability. *PLoS One.* 2013;8(9):e73990.
361. Ohno Y, Hatabu H, Murase K, Higashino T, Kawamitsu H, Watanabe H, et al. Quantitative assessment of regional pulmonary perfusion in the entire lung using three-dimensional ultrafast dynamic contrast-enhanced magnetic resonance imaging: Preliminary experience in 40 subjects. *J Magn Reson Imaging.* 2004;20(3):353-65.
362. Levin DL, Chen Q, Zhang M, Edelman RR, Hatabu H. Evaluation of regional pulmonary perfusion using ultrafast magnetic resonance imaging. *Magnetic Resonance in Medicine: An Official Journal of the International Society for Magnetic Resonance in Medicine.* 2001;46(1):166-71.
363. Wu O, Østergaard L, Weisskoff RM, Benner T, Rosen BR, Sorensen AG. Tracer arrival timing-insensitive technique for estimating flow in MR perfusion-weighted imaging using singular value decomposition with a block-circulant deconvolution matrix. *Magnetic Resonance in Medicine: An Official Journal of the International Society for Magnetic Resonance in Medicine.* 2003;50(1):164-74.
364. Gaa T, Neumann W, Sudarski S, Attenberger UI, Schönberg SO, Schad LR, et al. Comparison of perfusion models for quantitative T1 weighted DCE-MRI of rectal cancer. *Sci Rep.* 2017;7(1):1-9.

Appendix 1: Differences in DCE-MRI calculations between TRISTAN-ILD study and IPF study data (written by Paul Hughes)

One obvious difference in the work presented in this thesis is the DCE-MRI values seen in patients analysed at the University of Sheffield when compared to those analysed by Bioxydyn Ltd as part of the TRISTAN-ILD study. The primary cause for these differences is the semi-quantitative and quantitative approaches employed as explained below.

Firstly, data from the University of Sheffield does not make use of native T1 and proton spin density to calculate contrast agent concentration whereas the data as part of the TRISTAN-ILD study is converted from signal values (in arbitrary units) to contrast concentration in mmol/L (361). To account for signal changes, the data at the University of Sheffield was transformed to a pseudo concentration by subtracting the first baseline point from every time course (362). Secondly, a deconvolution analysis was employed in the TRISTAN-ILD data (363), which is not employed in the University of Sheffield IPF study data (this is in part due to the uncertainty caused in the deconvolution by the lack of signal normalisation to density).

Therefore, in this work the mean transit time (MTT) is described by: $MTT = \int \frac{t(S(t)-S(0))}{S(t)-S(0)}$ for the University of Sheffield data where S is the signal at time t , whereas the TRISTAN-ILD data has MTT defined by: $MTT = \int \frac{tI(t)}{\max(I)}$ where I is the result of the deconvolution of a lung voxel time course signal curve and the arterial input (after conversion to contrast concentration).

Put simply this means that the areas over which MTT are defined are going to be different as not only will deconvolution reduce the amplitude of the measured curve, but it will also impact the shape (example shown below – all normalised to range 0-1 for illustration and shown with maximum values).

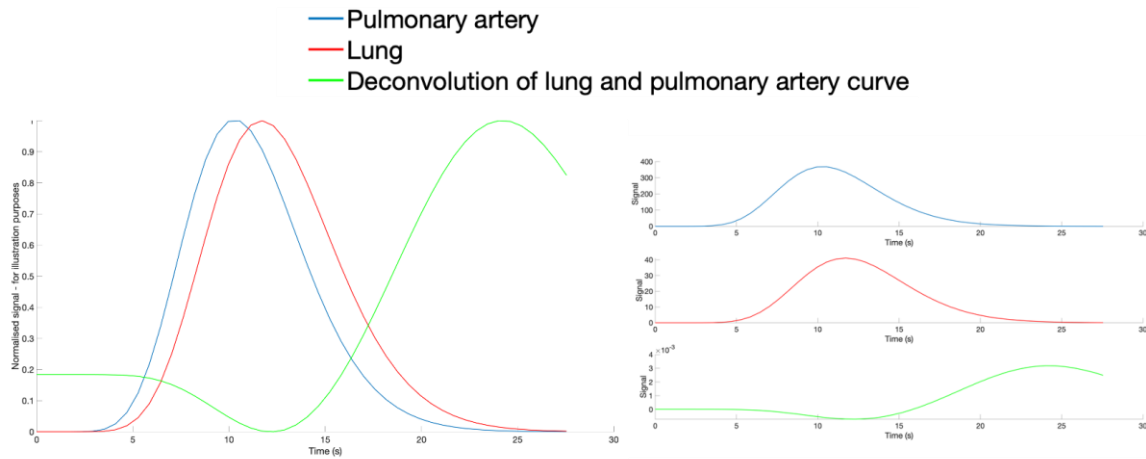


Figure 1: Example curves from a patient showing the normalised curves (left) and the original curves (right). As can be seen there is a distinct difference in the values seen and the shape of the deconvolved curve.

Deconvolution was also applied to the data where contrast was estimated by subtraction of the baseline signal only. Given the linear correlations seen in Figure 2, it is clear that a difference in analysis methodology can lead to fairly large variations in the outcomes when considering DCE-MRI in the lungs of patients as has been shown in previous work comparing the numerous models available (364).

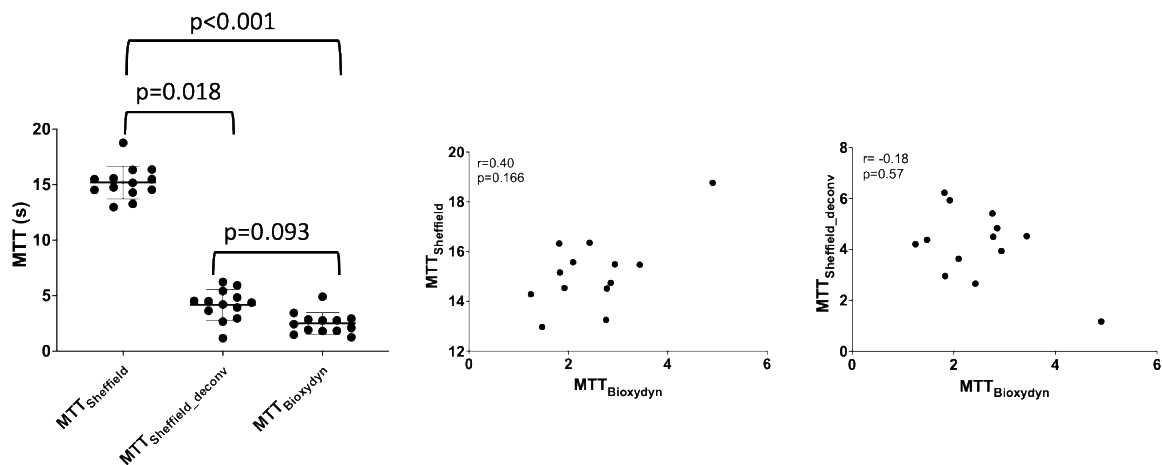


Figure 2: Differences in MTT between the DI-ILD patients in the TRISTAN-ILD study analysed (pared t-test) using the aforementioned techniques and the correlation between the values obtained.

Appendix 2: Research Output

Research papers published as first author in peer reviewed journals during the PhD (not directly related to this thesis)

1. Eaden JA, Skeoch S, Waterton JC, Chaudhuri N, Bianchi SM. How consistently do physicians diagnose and manage drug-induced interstitial lung disease? Two surveys of European ILD specialist physicians. *ERJ Open Research*. 2020, 6 (1) 00286-2019.
2. Eaden JA, Barber CM, Renshaw SA, Chaudhuri N, Bianchi SM. Real world experience of response to pirfenidone in patients with idiopathic pulmonary fibrosis: a two-centre retrospective study. *Sarcoidosis Vasculitis and Diffuse Lung Diseases*. 2020;37(2):218-24.

Research papers published as second author in peer reviewed journals during the PhD

1. Weatherley ND, Eaden JA, Stewart NJ, Bartholmai BJ, Swift AJ, Bianchi SM, Wild JM. Experimental and quantitative imaging techniques in interstitial lung disease. *Thorax*. 2019;74(6):611-619.
2. Saunders LC, Eaden JA, Bianchi SM, Swift AJ, Wild JM. Free breathing lung T₁ mapping using image registration in patients with idiopathic pulmonary fibrosis. *Magnetic Resonance in Medicine*. 2020; 84(6):3088-3102.
3. Collier G, Eaden J, Hughes P, Bianchi S, Stewart N, Weatherley N, Norquay G, Schulte R, Wild J. Dissolved 129Xe lung MRI with four-echo 3D radial spectroscopic imaging: quantification of regional gas transfer in idiopathic pulmonary fibrosis. *Magnetic Resonance in Medicine*. 2020; 85(5):2622-2633.
4. Weatherley ND, Eaden JA, Hughes PJC, Austin M, Smith L, Bray J, Marshall H, Renshaw S, Bianchi SM, Wild JM. Quantification of pulmonary perfusion in idiopathic pulmonary fibrosis with first pass dynamic contrast-enhanced perfusion MRI. *Thorax*. 2021;76(2):144-151.

Conference abstract proceedings and presentations as first author during the PhD

1. International Society of Magnetic Resonance in Medicine 28th Annual Meeting, May 2019: Powerpitch and E-poster.
 - a. Hyperpolarised xenon-129 MR spectroscopy and diffusion-weighted xenon-129 MRI at baseline in patients with interstitial lung disease.
2. European Respiratory Society International Congress, September 2019, Madrid, Spain: Traditional poster.
 - a. Hyperpolarised 129-xenon diffusion-weighted MRI in interstitial lung disease.
 - b. Longitudinal change in hyperpolarised 129-xenon MR spectroscopy in interstitial lung disease.
3. British Thoracic Society Winter Meeting, December 2019, London, UK: Oral presentation.
 - a. Quantitative CT and hyperpolarised 129-xenon diffusion-weighted MRI in interstitial lung disease.
4. International Society of Magnetic Resonance in Medicine 27th Annual Meeting, August 2020: E-poster.
 - a. Regional hyperpolarised 129-xenon MR spectroscopy and diffusion-weighted MRI in patients with idiopathic pulmonary fibrosis.
5. European Respiratory Society International Congress, September 2020: Oral presentation.
 - a. Regional hyperpolarised 129-xenon diffusion-weighted MRI in patients with IPF.
6. British Thoracic Society Winter Meeting, February 2021: Oral presentation.
 - a. Hyperpolarised 129-xenon MRI in differentiating between fibrotic and inflammatory interstitial lung disease and assessing longitudinal change.

Awards

The International Society of Magnetic Resonance in Medicine Annual Meeting Summa Cum Laude Merit Award for the work presented at the ISMRM 27th Annual Meeting, May 2019.

Appendix 3: Participant Information Sheets

TRISTAN-ILD study: DI-ILD, HP or iNSIP patients

Invitation

Thank you for taking the time to read this information sheet. We would like to invite you to take part in our research study about lung imaging. Before you decide whether to take part, we would like you to understand why the research is being done and what it would involve for you. Talk to other people about the study if you wish. Please ask us if there is anything that is not clear. A member of the team will go through this information sheet with you and answer any questions you have.

Why are we doing this research?

Interstitial lung disease (ILD) is a condition where inflammation and scarring occurs in the lungs, making patients breathless. It can occur in patients who have started certain medications such as cancer or arthritis drugs. It can also be as a result of conditions such as rheumatoid arthritis or as a reaction to something in the environment. When developing new medications it is important to be able to identify if the new drug could harm the lungs causing ILD in which case it may not be further developed.

At the moment the tests we use do not always accurately pick up ILD in the early stages or detect improvements. In some patients it can be difficult to tell if the ILD has occurred due to a condition such as rheumatoid arthritis or whether the drugs used to treat the condition are in fact harming the lungs.

Advances in the way we take pictures of the lungs may provide an opportunity to improve the way we diagnose and monitor ILD.

What is the purpose of this study?

We would like to test whether newly developed lung MRI and CT scans can be used to diagnose ILD and monitor patient who have ILD. In particular we would like to see if the new scans are better at detecting and monitoring ILD compared with the current tests we use. We want to see if the scans can be used to decide if the ILD is due to reaction to medication rather than another condition.

As a result of this study we hope to go on to develop a new type of test for diagnosing and monitoring ILD patients and which can be used to assess safety of new drugs and to assess ILD patients in clinic.

Why have I been asked to take part?

You have been asked to take part as you have ILD or your doctor suspects you might have ILD.

What will happen to me if I take part?

We will ask you undertake some extra visits to the hospital to have some blood tests, breathing tests and scans of the lungs. We would like to see you 3 times over a 6 month period. We will try to arrange the visits for when you would be coming to see your lung doctor anyway.

The picture on the next gives an overview of what the study involves and further details of each visit are described on the next page in the picture.

Visit 1- attend the Hospital (either Royal Hallamshire or Northern General)

- Doctor and nurse review
- Blood tests
- Breathing tests
- MRI scan of the lungs



Visit 2- 6 weeks later at the same hospital

- Doctor and nurse review
- Blood tests
- Breathing tests
- CT scan of the lungs
- MRI scan of the lungs



Visit 3- 6 months after visit 1 at the same hospital

- Doctor and nurse review
- Blood tests
- Breathing tests
- CT scan of the lungs

Visit One

If you agree to take part, you will be asked to visit either the Northern General Hospital or the Royal Hallamshire Hospital in Sheffield. You will be seen by a doctor who is a specialist in ILD. We will ask you questions about your health and examine you. After this you will have blood tests and breathing tests done which are described below. This visit will likely take approximately 5 hours including lunch, although it may take longer if a lot of breaks are taken during the MRI scan. Free refreshments will be provided.

Blood test: a blood sample (approximately 3.5 table spoonfuls of blood) will be taken.

Breathing tests: You will be asked to breath in and out several times into a tube which is attached to a machine called a spirometer. We will then ask you to breath in harmless gas that helps us measure how well the lung absorbs oxygen. These breathing tests are used in the clinic to diagnose ILD and you may already have performed these tests at your own doctor's request. We like to repeat them in our own department as it is more accurate if to use the same spirometry machine for each visit.

MRI scan: The medical team will discuss the scan with you. They will then ask you to lie down on a bed in the MRI scanner and a cannula will be inserted in the vein in your arm. This is a small plastic tube which allows us to give you an injection during the scan. During the scan you will be asked to breath in a harmless gas which allows us to measure how well oxygen and other gases can move in and out of your lungs. We will also give you an injection through the cannula which allows us to see how well the blood flows into the lungs. This type of injection is used commonly in the NHS when performing MRI scans.

The total time in the MRI scanner will be around 90 minutes but this will be broken up into smaller periods of time and you can get up and walk around in these rest periods. We expect that in total the scan will take around 2 hours but it could be longer if you need more breaks between these scanning periods and we can discuss with you what you would prefer when you visit. After the scan we will arrange for a taxi to take you home. If there any problems that mean you cannot complete the MRI scan you may not need to come back for any further visits.

We will ask you to complete a short patient satisfaction survey after the MRI scan (this can be done over the phone at a later time if preferred). This is to help us find out how you find the process of having the scan and how we can make any possible suggested improvements in the experience in future.

Most patients have CT scans performed when the diagnosis of ILD is first suspected. Therefore rather than asking you to have another CT scan when you first join the study, we would like to examine the scan you have already had through your regular doctor. With your permission we will arrange for the pictures from the previous CT scans to be anonymised and transferred to our research team. If this scan is not of a high quality we might ask you to have an extra CT scan at the same time as you have your 1st MRI scan.

Visit 2

6 weeks later we will invite you back to the hospital. We will repeat the assessments, breathing tests and take another blood sample. We will also repeat the MRI scan.

During the visit we will also arrange for you to have a CT scan of your lungs. The scan performed at this visit will be exactly the same type of scan that your own doctor would have arranged when they first thought you might have ILD. You will be asked to lie down on the scanner bed which will then move through the doughnut shaped scanner. No injection is required and it usually only takes 15-30 minutes. If your own doctor has already arranged another CT scan as part of your routine care we will not need to repeat the CT scan during your visit.

Visit 3

6 months after you first started the study we will invite you back for a final visit to the hospital. You will be seen by the doctor and nurse and have a blood test, breathing tests and CT scan repeated (if you have not had a scan within the last 2 months as part of your normal care).

If during the study period, you have a procedure called a bronchoscopy, as part of your routine clinical care, we would like to keep a sample taken during this procedure for research purposes. This will not require anything extra from you in regard to time or procedures. We would only keep a sample if you are having the procedure done anyway. If you would prefer us not to keep a sample you can just let us know and it will not impact on your involvement in the study or your care. When you have finished the visits we would like to ask your own doctor to update us on how your health is. This will help us understand how well the tests perform in predicting long term problems in patients with ILD. You will not need to provide any information but we will ask for your consent to contact your GP/specialist for further information about your health for up to 2 and a half years after you have completed the study.

Do I have to take part?

No, if you decide not to take part, you do not have to give a reason for this. If you agree to take part, you will be asked to sign a consent form and you are free to withdraw at any time without giving a reason. If you decide not to take part, or to withdraw, this ***will not affect the treatment you receive.***

If you wish to withdraw from the study you can decide if you would also like to withdraw any data or samples already collected. You may wish for the data and samples to be used in the research or in future research. You can discuss this with the research team should you wish to withdraw.

What are the possible risks of taking part?

The risks of MRI scanning are very small. Safety is our first concern and we will give you a questionnaire to complete to make sure there is no significant risk of placing you into the

magnetic field of the scanner. If we find any reason for the scanner to cause harm, we will not perform the scan and you will not be able to take part in the study.

Inhaling xenon gas has previously been shown to be safe and well tolerated in people with lung disease. However, you may find you become light-headed, drowsy or feel sick for a few seconds. Holding your breath can cause a brief decrease in blood oxygen levels, which reverses on breathing normally and is not harmful. We will closely monitor your oxygen levels throughout the study.

Sometimes, the contrast that is injected into the vein (gadolinium) can cause dizziness and light-headedness. Rarely, blood pressure can fall, which can be treated immediately with a drip (fluid through the cannula). Very rarely (less than one in 1000 people) an allergic reaction to the contrast is seen. This usually includes skin rash and itchy eyes for a short time, but more severe reactions have been reported, which result in shortness of breath. In the unlikely event of a severe reaction, medical staff are on site and will be able to deal with this quickly.

If you take part in this study you will have Chest CT scans, some of which may be extra to those that you would have if you did not take part. These procedures use ionising radiation to form images of your body and provide your doctor with clinical information. Ionising radiation can cause cell damage that may, after many years or decades, turn cancerous.

We are all at risk of developing cancer during our lifetime. The normal risk is that this will happen to about 50% of people at some point in their life. Taking part in this study will increase the chances of this happening to you from 50% to up to 50.15 %.

Results

It may be that some of the tests are relevant to your clinical care and we pass results of blood tests and breathing tests on to your doctor at their request. If any unexpected results come up we will inform you as soon as possible and also inform your GP and/or your hospital doctor who can arrange any further management.

What are the possible benefits of taking part?

You may not receive any direct personal benefit from taking part in this study. However we may assess your breathing in more detail than is done as part of routine practice. You may have tests done which pick up health problems at an earlier stage which could lead to earlier treatment. Some of the tests performed during the study such as the CT scans may be useful to your own doctor for guiding treatment of your lung disease.

You will also be contributing to medical science, helping us develop better ways to identify and monitor ILD and develop drugs in a safer way.

Will I be paid for taking part?

No, you will not be paid for helping us with this study, although we will reimburse reasonable travel expenses including taxi fares, train tickets or mileage and we can arrange overnight accommodation if required. We will also provide a £15 gift voucher for each visit as recognition of you giving up your time to the study.

What will happen to the blood samples and scans?

The samples will be gifted to medical research and will be stored in a secure laboratory at The University of Manchester. The samples will be anonymised so your personal details will not be stored with the samples. We would be able to link the blood to other anonymised information you have given us such as health conditions and medications that you are taking. However, only authorised personnel will have access to the samples and information.

The blood samples will be tested for proteins and markers associated with rheumatology and lung conditions. On one of the blood tests will check for the presence of specific genes that are associated with ILD. This may help us understand why some people are more at risk of developing ILD. We will not test any genes associated with other conditions. We would like to retain the blood samples at the end of the study. They may be valuable in future research into ILD. However, if we were to use the samples in the future we would seek further ethical approval as necessary. We may send the samples to be tested at other specialist laboratories. However these laboratories would not receive any of your personal identifiable information and would only perform tests that have been approved by an ethics committee.

All your lung scans will be anonymised and transferred securely to Bioxydyn Limited, an imaging company based in Manchester who is a partner in the research group. Some blood tests results that help with interpreting the scans will also be transferred but none of your personal details will be included. The scans will be analysed by Bioxydyn Scientists and also Scientists at the University of Sheffield. Some of the results may be analysed by researcher at The University of Sheffield and University of Leeds. However none of your personal information will be transferred with the scans or blood results.

What if there is a problem?

If you have a concern about any aspect of this study, you should ask to speak to the researchers who will do their best to answer your questions.

Minor complaints: If you have a minor complaint then you need to contact the researcher(s) in the first instance. You can contact Fiona Stirling on 0161 275 5504

Formal complaint: If you wish to make a formal complaint or if you are not satisfied with the response you have gained from the researchers in the first instance then please contact the Research Governance and Integrity Manager, Research Office, Christie Building, University of Manchester, Oxford Road, Manchester, M13 9PL, by emailing: research.complaints@manchester.ac.uk or by telephoning 0161 275 2674 or 275 2046.

You may also talk to patient advice and liaison service (PALS) staff within the hospital (contact Patient Services Team, pst@sth.nhs.uk or Tel: 0114 2712400. They may be able to resolve your concerns on the spot or can provide you with details of how to make an official complaint.

Statement on Harm

In the event that something does go wrong and you are harmed during the research you may have grounds for a legal action for compensation against the University of Manchester or NHS Trust but you may have to pay your legal costs. The normal National Health Service complaints mechanisms will still be available to you.

Will my taking part in this study be kept confidential?

Information collected from you will be sent to The University of Manchester where it will be stored securely under conditions in keeping with the Data Protection Act 1998. Your name and any other personal information from which you could be identified will be kept separately from any research data. Only individuals directly involved with the study will have access to this information. The anonymised MRI and CT scans will be stored securely with Bioxydyn Limited, Manchester.

After the study has finished the anonymised data will be kept securely at the University for up to 25 years but your personal details will be destroyed. A copy of your consent form will be kept securely in the long term and will be placed in your hospital records. The anonymised scans and results will be also be archived at The European Organisation for Research and Treatment of Cancer, who are responsible for safely storing all the data generated from this

and other associated imaging studies. None of your personal information will be transferred for archiving, all the data will be anonymised.

During the study some parts of your medical records will be looked at by responsible individuals from the University of Manchester, the NHS Trusts and Regulatory Authorities. This is necessary to make sure that the study is being carried out correctly. Research and clinical team members may also look at your notes to check for information about your health condition or treatment which might be relevant for the study. All individuals involved will have a duty of confidentiality to you as a research participant and will never reveal your identity to anyone who is not directly involved with the study.

What will happen to the results of the study?

The results of this study will be published in a professional medical journal. Your name, or any details that could be used to identify you, will not be used in any such publications.

We will also arrange a feedback day for patients taking part in the study, to explain what we have found and if you are not able to make this we can send you a summary of the results of the study.

You have the right to request information about any personal data that we hold on you, or to request that any inaccuracies be corrected. To make such a request you should contact your rheumatologist or research nurse.

We may use the data in future studies or share it with other researchers working interested in imaging and lung disease. All of the data anonymous before it is shared or used for future research so no-one will be able to identify you and there will be a vetting process to ensure the data is used for valid research purposes.

Who is organising and funding the research?

This research study has been organised by members of the respiratory (lung) and rheumatology teams and researchers in Manchester, Sheffield and Leeds. We are part of a bigger research group investigating the use of scans to detect drug toxicity in different parts of the body which includes researchers from across Europe. The funding for the study has been provided by Innovative Medicines Initiative which is a partnership between the European Union and the Pharmaceutical Industry Association (EFPIA).

Who has reviewed and approved the study?

This research has been approved by the North West Research Ethics Committee and also the hospital research departments.

What do I do now?

We would be happy to discuss the details of the study further with you but if you would like to do away and think about the study more, you can contact us later on the details below.

Contact details

For further advice regarding this study you can contact:

Dr James Eaden

Department of Academic Radiology

C Floor, Royal Hallamshire Hospital

Sheffield

S10 2JF

email: j.a.eaden@sheffield.ac.uk

TRISTAN-ILD study: CTD-ILD or IPF patients

Invitation

Thank you for taking the time to read this information sheet. We would like to invite you to take part in our research study about lung imaging. Before you decide whether to take part, we would like you to understand why the research is being done and what it would involve for you. Talk to other people about the study if you wish. Please ask us if there is anything that is not clear. A member of the team will go through this information sheet with you and answer any questions you have.

Why are we doing this research?

Interstitial lung disease (ILD) is a condition where inflammation and scarring occurs in the lungs, making patients breathless. It can occur in patients who have started certain medications such as cancer or arthritis drugs. It can also be as a result of conditions such as rheumatoid arthritis or as a reaction to something in the environment. When developing new medications it is important to be able to identify if the new drug could harm the lungs causing ILD in which case it may not be further developed.

At the moment the tests we use do not always accurately in pick up ILD in the early stages or detect improvements. In some patients it can be difficult to tell if the ILD has occurred due to a condition such as rheumatoid arthritis or whether the drugs used to treat the condition are in fact harming the lungs.

Advances in the way we take pictures of the lungs may provide an opportunity to improve the way we diagnose and monitor ILD.

What is the purpose of this study?

We would like to test whether newly developed lung MRI and CT scans can be used to diagnose ILD and monitor patient who have ILD. In particular we would like to see if the new scans are better at detecting and monitoring ILD compared with the current tests we use. We want to see if the scans can be used to decide if the ILD is due to reaction to medication rather than another condition.

As a result of this study we hope to go on to develop a new type of test for diagnosing and monitoring ILD patients and which can be used to assess safety of new drugs and to assess ILD patients in clinic.

Why have I been asked to take part?

You have been asked to take part as you have ILD or your doctor suspects you might have ILD.

What will happen to me if I take part?

We will ask you undertake some extra visits to the hospital to have some blood tests, breathing tests and scans of the lungs. We would like to see you 3 times over a 12 month period. We will try to arrange the visits for when you would be coming to see your lung doctor anyway.

The picture below gives an overview of what the study involves and further details of each visit are described in the picture on the next page.

Visit 1- attend the Hospital (either Royal Hallamshire or Northern General)

- Doctor and nurse review
- Blood tests
- Breathing tests
- MRI scan of the lungs



Visit 2- 6 Months later at the same hospital

- Doctor and nurse review
- Blood tests
- Breathing tests
- CT scan of the lungs
- MRI scan of the lungs



Visit 3- 12 months after visit 1 at the same hospital

- Doctor and nurse review
- Blood tests
- Breathing tests
- CT scan of the lungs

Visit One

If you agree to take part, you will be asked to visit either the Northern General Hospital or the Royal Hallamshire Hospital in Sheffield. You will be seen by a doctor who is a specialist in ILD. We will ask you questions about your health and examine you. After this you will have blood tests and breathing tests done which are described below. This visit will likely take approximately 5 hours including lunch, although it may take longer if a lot of breaks are taken during the MRI scan. Free refreshments will be provided. Free refreshments will be provided.

Blood test: a blood sample (approximately 3.5 table spoonfuls of blood) will be taken.

Breathing tests: You will be asked to breath in and out several times into a tube which is attached to a machine called a spirometer. We will then ask you to breath in harmless gas that helps us measure how well the lung absorbs oxygen. These breathing tests are used in the clinic to diagnose ILD and you may already have performed these tests at your own doctor's request. We like to repeat them in our own department as it is more accurate if to use the same spirometry machine for each visit.

MRI scan: The medical team will discuss the scan with you. They will then ask you to lie down on a bed in the MRI scanner and a cannula will be inserted in the vein in your arm. This is a small plastic tube which allows us to give you an injection during the scan. During the scan you will be asked to breath in a harmless gas which allows us to measure how well oxygen and other gases can move in and out of your lungs. We will also give you an injection through the cannula which allows us to see how well the blood flows into the lungs. This type of injection is used commonly in the NHS when performing MRI scans.

The total time in the MRI scanner will be around 90 minutes but this will be broken up into smaller periods of time and you can get up and walk around in these rest periods. We expect that in total the scan will take around 2 hours but it could be longer if you need more breaks between these scanning periods and we can discuss with you what you would prefer when you visit. After the scan we will arrange for a taxi to take you home. If there any problems that mean you cannot complete the MRI scan you may not need to come back for any further visits.

We will ask you to complete a short patient satisfaction survey after the MRI scan (this can be done over the phone at a later time if preferred). This is to help us find out how you find the process of having the scan and how we can make any possible suggested improvements in the experience in future.

Most patients have CT scans performed when the diagnosis of ILD is first suspected. Therefore rather than asking you to have another CT scan when you first join the study, we would like to examine the scan you have already had through your regular doctor. With your permission we will arrange for the pictures from the previous CT scans to be anonymised and transferred to our research team. If this scan is not of a high quality we might ask you to have an extra CT scan at the same time as you have your 1st MRI scan.

Visit 2

6 months later we will invite you back to the hospital. We will repeat the assessments, breathing tests and take another blood sample. We will also repeat the MRI scan.

During the visit we will also arrange for you to have a CT scan of your lungs. The scan performed at this visit will be exactly the same type of scan that your own doctor would have arranged when they first thought you might have ILD. You will be asked to lie down on the scanner bed which will then move through the doughnut shaped scanner. No injection is required and it usually only takes 15-30 minutes. If your own doctor has already arranged another CT scan as part of your routine care we will not need to repeat the CT scan during your visit.

Visit 3

12 months after you first started the study we will invite you back for a final visit to the hospital. You will be seen by the doctor and nurse and have a blood test, breathing tests and CT scan repeated (if you have not had a scan within the last 2 months as part of your normal care).

If during the study period, you have a procedure called a bronchoscopy, as part of your routine clinical care, we would like to keep a sample taken during this procedure for research purposes. This will not require anything extra from you in regard to time or procedures. We would only keep a sample if you are having the procedure done anyway. If you would prefer us not to keep a sample you can just let us know and it will not impact on your involvement in the study or your care. When you have finished the visits we would like to ask your own doctor to update us on how your health is. This will help us understand how well the tests perform in predicting long term problems in patients with ILD. You will not need to provide any information but we will ask for your consent to contact your GP/specialist for further information about your health for up to 2 years after you have completed the study.

Do I have to take part?

No, if you decide not to take part, you do not have to give a reason for this. If you agree to take part, you will be asked to sign a consent form and you are free to withdraw at any time without giving a reason. If you decide not to take part, or to withdraw, this ***will not affect the treatment you receive.***

If you wish to withdraw from the study you can to decide if you would also like to withdraw any data or samples already collected. You may wish for the data and samples to be used in the research or in future research. You can discuss this with the research team should you wish to withdraw.

What are the possible risks of taking part?

The risks of MRI scanning are very small. Safety is our first concern and we will give you a questionnaire to complete to make sure there is no significant risk of placing you into the magnetic field of the scanner. If we find any reason for the scanner to cause harm, we will not perform the scan and you will not be able to take part in the study.

Inhaling xenon gas has previously been shown to be safe and well tolerated in people with lung disease. However, you may find you become light-headed, drowsy or feel sick for a few seconds. Holding your breath can cause a brief decrease in blood oxygen levels, which reverses on breathing normally and is not harmful. We will closely monitor your oxygen levels throughout the study.

Sometimes, the contrast that is injected into the vein (gadolinium) can cause dizziness and light-headedness. Rarely, blood pressure can fall, which can be treated immediately with a drip (fluid through the cannula). Very rarely (less than one in 1000 people) an allergic reaction to the contrast is seen. This usually includes skin rash and itchy eyes for a short time, but more severe reactions have been reported, which result in shortness of breath. In the unlikely event of a severe reaction, medical staff are on site and will be able to deal with this quickly.

If you take part in this study you will have Chest CT scans, some of which may be extra to those that you would have if you did not take part. These procedures use ionising radiation to form images of your body and provide your doctor with clinical information. Ionising radiation can cause cell damage that may, after many years or decades, turn cancerous.

We are all at risk of developing cancer during our lifetime. The normal risk is that this will happen to about 50% of people at some point in their life. Taking part in this study will increase the chances of this happening to you from 50% to up to 50.15 %.

Results

It may be that some of the tests are relevant to your clinical care and we pass results of blood tests and breathing tests on to your doctor at their request. If any unexpected results come up we will inform you as soon as possible and also inform your GP and/or your hospital doctor who can arrange any further management.

What are the possible benefits of taking part?

You may not receive any direct personal benefit from taking part in this study. However we may assess your breathing in more detail than is done as part of routine practice. You may have tests done which pick up health problems at an earlier stage which could lead to earlier treatment. Some of the tests performed during the study such as the CT scans may be useful to your own doctor for guiding treatment of your lung disease.

You will also be contributing to medical science, helping us develop better ways to identify and monitor ILD and develop drugs in a safer way.

Will I be paid for taking part?

No, you will not be paid for helping us with this study, although we will reimburse reasonable travel expenses including taxi fares, train tickets or mileage and we can arrange overnight accommodation if required. We will also provide a £15 gift voucher for each visit as recognition of you giving up your time to the study.

What will happen to the blood samples and scans?

The samples will be gifted to medical research and will be stored in a secure laboratory at The University of Manchester. The samples will be anonymised so your personal details will not be stored with the samples. We would be able to link the blood to other anonymised

information you have given us such as health conditions and medications that you are taking. However, only authorised personnel will have access to the samples and information.

The blood samples will be tested for proteins and markers associated with rheumatology and lung conditions. On one of the blood tests will check for the presence of specific genes that are associated with ILD. This may help us understand why some people are more at risk of developing ILD. We will not test any genes associated with other conditions. We would like to retain the blood samples at the end of the study. They may be valuable in future research into ILD. However, if we were to use the samples in the future we would seek further ethical approval as necessary. We may send the samples to be tested at other specialist laboratories. However these laboratories would not receive any of your personal identifiable information and would only perform tests that have been approved by an ethics committee.

All your lung scans will be anonymised and transferred securely to Bioxydyn Limited, an imaging company based in Manchester who is a partner in the research group. Some blood tests results that help with interpreting the scans will also be transferred but none of your personal details will be included. The scans will be analysed by Bioxydyn Scientists and also Scientists at the University of Sheffield. Some of the results may be analysed by researchers at The University of Sheffield and University of Leeds. However none of your personal information will be transferred with the scans or blood results.

What if there is a problem?

If you have a concern about any aspect of this study, you should ask to speak to the researchers who will do their best to answer your questions.

Minor complaints: If you have a minor complaint then you need to contact the researcher(s) in the first instance. You can contact Fiona Stirling on 0161 275 5504

Formal complaint: If you wish to make a formal complaint or if you are not satisfied with the response you have gained from the researchers in the first instance then please contact the Research Governance and Integrity Manager, Research Office, Christie Building, University of Manchester, Oxford Road, Manchester, M13 9PL, by emailing: research.complaints@manchester.ac.uk or by telephoning 0161 275 2674 or 275 2046.

You may also talk to patient advice and liaison service (PALS) staff within the hospital. They may be able to resolve your concerns on the spot or can provide you with details of how to make an official complaint.

Statement on Harm

In the event that something does go wrong and you are harmed during the research you may have grounds for a legal action for compensation against the University of Manchester or NHS Trust but you may have to pay your legal costs. The normal National Health Service complaints mechanisms will still be available to you.

Will my taking part in this study be kept confidential?

Information collected from you will be sent to The University of Manchester where it will be stored securely under conditions in keeping with the Data Protection Act 1998. Your name and any other personal information from which you could be identified will be kept separately from any research data. Only individuals directly involved with the study will have access to this information. The anonymised MRI and CT scans will be stored securely with Bioxydyn Limited, Manchester.

After the study has finished the anonymised data will be kept securely at the University for up to 25 years but your personal details will be destroyed. A copy of your consent form will be kept securely in the long term and will be placed in your hospital records. The anonymised

scans and results will be also be archived at The European Organisation for Research and Treatment of Cancer, who are responsible for safely storing all the data generated from this and other associated imaging studies. None of your personal information will be transferred for archiving, all the data will be anonymised.

During the study some parts of your medical records will be looked at by responsible individuals from the University of Manchester, the NHS Trusts and Regulatory Authorities. This is necessary to make sure that the study is being carried out correctly. Research and clinical team members may also look at your notes to check for information about your health condition or treatment which might be relevant for the study. All individuals involved will have a duty of confidentiality to you as a research participant and will never reveal your identity to anyone who is not directly involved with the study.

What will happen to the results of the study?

The results of this study will be published in a professional medical journal. Your name, or any details that could be used to identify you, will not be used in any such publications.

We will also arrange a feedback day for patients taking part in the study, to explain what we have found and if you are not able to make this we can send you a summary of the results of the study.

You have the right to request information about any personal data that we hold on you, or to request that any inaccuracies be corrected. To make such a request you should contact your rheumatologist or research nurse.

We may use the data in future studies or share it with other researchers working interested in imaging and lung disease. All of the data anonymous before it is shared or used for future research so no-one will be able to identify you and there will be a vetting process to ensure the data is used for valid research purposes.

Who is organising and funding the research?

This research study has been organised by members of the respiratory (lung) and rheumatology teams and researchers in Manchester, Sheffield and Leeds. We are part of a bigger research group investigating the use of scans to detect drug toxicity in different parts of the body which includes researchers from across Europe. The funding for the study has been provided by Innovative Medicines Initiative which is a partnership between the European Union and the Pharmaceutical Industry Association (EFPIA).

Who has reviewed and approved the study?

This research has been approved by the North West Research Ethics Committee and also the hospital research departments.

What do I do now?

We would be happy to discuss the details of the study further with you but if you would like to do away and think about the study more, you can contact us later on the details below.

Contact details

For further advice regarding this study you can contact:

Dr James Eaden

Department of Academic Radiology

C Floor

Royal Hallamshire Hospital

Sheffield

S10 2JF

email: j.a.eaden@sheffield.ac.uk

IPF study

Short study title:

Assessing lung fibrosis with magnetic resonance imaging.

Invitation:

Thank you for taking the time to read this information sheet. We would like to invite you to take part in our research study about lung imaging. Before you decide whether to take part, we would like you to understand why the research is being done and what it would involve for you. Talk to other people about the study if you wish. Please ask us if there is anything that is not clear. **A member of the team will go through this information sheet with you and answer any questions you have.**

Why have I been invited?

You have a condition known as idiopathic pulmonary fibrosis (IPF), which causes lung scarring. We would like to discover more about the role of Magnetic Resonance Imaging (MRI) in IPF.

MRI is a type of scan which uses magnets to take images of the lungs. It may have a role in looking at several lung diseases. In particular, we are interested to see if MRI can discover more about what is happening to the lungs of patients with IPF. We are testing new techniques, which improves the pictures received from the scanner by breathing in harmless gas (xenon) during the scan.

At the moment, the tools we have to tell us if the health of patients with IPF is getting worse or is likely to get worse in the future are not ideal. MRI may help us to assess the disease process and may also help us to research treatments for the disease in the future.

Do I have to take part?

No. It is up to you to decide whether or not to take part in this study. If you decide to take part, you will be given this information sheet to keep and asked to sign a consent form before

the first scan. If you choose not to take part or you want to later withdraw from the study, you do not need to give a reason and your medical care will not be affected in any way.

What will happen to me if I take part?

If you choose to take part, we will show you around the MRI department at the Royal Hallamshire Hospital, Sheffield, and a doctor will check that you are well enough to be in the study by asking a few questions about your health. We will need to put a cannula (thin tube) into a vein.

You will then have a series of scans. The first two scans will happen on the same day. Further scans will then take place after another 3, 6 and 12 months. The visits will each take 2 to 3 hours.

During each scan, we will ask you to lie still for periods of time, while monitoring your heart rate and blood oxygen level. The scans take around an hour to complete, though we can give you breaks during the scan to get up and walk around or have a drink.

At certain points during the scan, we will ask you to breathe in gas from a bag (containing xenon) and hold your breath for up to 15 seconds. After the short breath-hold, you can breathe again normally. At one stage of the scan, we will inject gadolinium contrast into the cannula to look at the flow of blood through your lung. A dedicated radiographer or physicist with experience in doing this will talk you through the whole process before and during the scans.

During your study visit, we will ask you to have a lung function test (breathing test) . You will likely have undergone a similar set of tests in chest clinic at the request of your doctor. In addition we would like to perform a further breathing test looking at how well your lungs transfer gases, such as oxygen and carbon dioxide, using a special gas mixture. To allow comparisons to the measurements taken during the MRI scan this test will be performed both lying down as well as sitting down.

We will provide lunch and transport to and from the department for each visit.

You will have had a CT scan to determine the diagnosis and severity of your lung condition and your doctor may ask you to have another CT scan in 12 months time, as part of a routine assessment. If you don't have another CT scan in 12 months time as part of routine clinical assessment, we will ask you to undertake one specifically as part of this research study. These scans will be looked at by the study team for comparison with the MRI images.

When do I have to decide?

We would prefer that you make a decision about taking part within two weeks of receipt of this letter. However, we are very happy to discuss the study further and you can have more time to think about it if needed.

Will this affect my existing treatment?

No. You will see a doctor and can continue, start or stop treatments as you usually would. These treatments make no difference to our study.

What are the possible disadvantages and risks of taking part?

The risks of MRI scanning are very small. Safety is our first concern and we will give you a questionnaire to complete to make sure there is no significant risk of placing you into the magnetic field of the scanner. If we find any reason for the scanner to cause harm, we will not perform the scan and you will not be able to take part in the study.

Lying in the scanner can be difficult for people who dislike being in small spaces. It can be noisy at times, but we will provide you with ear defenders to reduce the noise.

Inhaling xenon gas has previously been shown to be safe and well tolerated in people with lung disease. However, you may find you become light-headed, drowsy or feel sick for a few seconds. Holding your breath can cause a brief decrease in blood oxygen levels, which reverses on breathing normally and is not harmful. We will closely monitor your oxygen levels throughout the study.

Sometimes, the contrast that is injected into the vein (gadolinium) can cause dizziness and light-headedness. Rarely, blood pressure can fall, which can be treated immediately with a

drip (fluid through the cannula). Very rarely (less than one in 1000 people) an allergic reaction to the contrast is seen. This usually includes skin rash and itchy eyes for a short time, but more severe reactions have been reported, which result in shortness of breath.

In the unlikely event of a severe reaction, medical staff are on site and will be able to deal with this quickly.

If you take part in this study you will have CT Chest scans. These procedures use ionising radiation to form images of your body and provide your doctor with clinical information. Ionising radiation can cause cell damage that may, after many years or decades, turn cancerous.

In some cases you might have the CT Chest scans anyway as part of your normal clinical care. If you do have an additional CT scan that is not part of your normal clinical care, the additional risk of developing cancer as a consequence of the study is estimated as 0.02 % (1 in every 2000 people). For comparison, the natural lifetime cancer incidence in the general population is about 50% (i.e. around half of the general population will develop some form of cancer over their lifetime).

What are the possible benefits of taking part?

While the study is not designed for the benefit of individual participants, we are happy to discuss the research and the MRI with you further. We will provide you with a lay summary of the findings after completing the study, for your interest. Unfortunately, we won't be able to show you your own scans.

How long will this study last?

12 months.

Will my taking part in the study be kept confidential?

Yes. It will be governed by the General Data Protection Regulation and Data Protection Act (2018) and has Research Ethics Committee approval. Information will be anonymised before analysis or publication.

Our administration staff will have access to your contact details in order to arrange future scans. Physicists and radiographers will require your name and date of birth in order to perform and analyse the scans.

Information that can identify you personally will **never** be given to anyone else or published. Only doctors involved in the study, regulatory authorities, or your NHS Trust will look at only sections of your medical notes that are relevant to this study. Personal data will only be stored on NHS password protected computers and when this is partially anonymised the identification list will be located on a separate NHS system.

What will happen if I don't want to carry on with the study?

You can leave the study at any time in the future without giving a reason. If you withdraw your consent to take part, or become unable to give informed consent, any information collected up to that point will remain and be used in the study. No further information will be collected and a record will be kept that you withdrew consent or were unable to continue to provide consent.

Your medical care will **not** be affected if you withdraw from the study.

What if there is a problem?

Any complaints about the way you have been dealt with or ill effects you might suffer during the study will be addressed by people outside of the research team. Information on who to contact is given at the end of this information sheet.

What will happen to the results of the research study?

These will be analysed by the research team to look for information that will help us understand more about the role of MRI in IPF. We will share information with other scientists and doctors by publishing the information in journals, so that we can better understand this form of lung disease. Any information we share will not identify your personal information.

What if we find an unexpected abnormality?

If we find an abnormality that wasn't expected and requires attention, we will either arrange to contact your GP for follow up, or one of our doctors will arrange for you to be seen by a hospital doctor.

Will my general practitioner (GP) be contacted?

Yes. We will tell your GP that you have chosen to be a part of this study. We will also need to contact you and your GP if we find out any new information that affects your health during the process of this study.

Who is organising and funding the research?

This research has been jointly organised by members of the respiratory (lung) team and academic radiology (MRI specialist) team at Sheffield Teaching Hospitals. The National Institute for Health Research has provided money for our department to perform these scans.

Who has reviewed the study?

All research in the NHS is looked at by an independent group of people, called a Research Ethics Committee, to protect your interests. This study has been reviewed and given favourable opinion by North West Research Ethics Committee and the Sheffield Teaching Hospitals NHS Foundation Trust Research and Development Department (Clinical Research Office).

Thank you for taking the time to read this information sheet and to consider whether to take part in this study.

Further information and contact details:

If you would like:

- Further information about the research
- To confirm that you would like to take part
- To withdraw from the study, or withdraw your interest
- To express a complaint

Then please contact:

Leanne Armstrong

Research Administrator

0114 215 9603

Alt 0114 215 9595

If you have any complaints that you would like to be dealt with independently please contact:

The Patient Services Team

Email: pst@sth.nhs.uk

Telephone: 0114 2712400

Or write to: The Medical Director

Sheffield Teaching Hospitals

8 Beech Hill Rd

Sheffield

S10 2SB